Mahidol University
Faculty of Environment
and Resource Studies

ENRIC 2021

The 4th Environment and Natural Resources International Conference

Challenges, Innovations and Transformations for Environmental Sustainability

December 16, 2021

01 Natural Resources Management

02 Science, Engineering and Energy Technology

03 Climate Change, COVID-19 and Risk Management

04 21st Century Industry

Plenary Speech on

"From Policy to Practice: How Thailand Deal with Climate Change and Environment Crisis?"

Wijarn Simachaya, Ph.D.
President of Thai Environment Institute (TEI), the Secretary-General of Thailand Business Council for Sustainable Development (TBCSD), and Chairman of Thai Sustainable Consumption and Production Association and Network

Dr. Wijarn Simachaya is the current President of Thai Environment Institute (TEI) and the Secretary-General of Thailand Business Council for Sustainable Development (TBCSD). He is a chairman of the Circular Economy under Bio-Circular-Green Economy Model, current national agenda. His various responsibilities in the past were natural resources and environmental plans, strategy development, pollution control plans as well as international cooperation on natural resources and environment issues. He was also a representative of the ministry of various UN, Sub-regional, and ASEAN / ASEAN Plus 3 forums. Under the ASEAN Framework, he had played an important role to develop the ASEAN Haze-Free Road Map by 2020, and Bangkok Declaration on Combating Marine Plastic Debris in ASEAN region, endorsed by ASEAN Summit in June, 2019. He worked as a leader of green growth and government reform strategy development for Thailand. Besides, he served as a chairman of the long-term national strategy (20-year plan) on natural resources and environmental management, including water resources and sustainable forest management, together with pollution control and environmental governance for the Ministry. He currently works with various government agencies, international organizations, public-private agencies, civil societies and communities on the ground to develop environmental management models for the country, and moving toward sustainable development.

Dr. Wijarn joined the Office of Environmental Policy and Planning Board in 1984 and Pollution Control Department in 1992. He used to serve as a director of the Environment Division of the Mekong River Commission Secretariat (International Organization) in Lao PDR during 1997-1998. He served as several high ranking positions in the Ministry, including Inspector-General and

Deputy Permanent Secretary of the Ministry of Natural Resources and Environment, Director-General of the Pollution Control Department for 2 times and the Secretary-General of the Office of Natural Resources and Environmental Policy and Planning. His last position with government was the Permanent Secretary of the Ministry of Natural Resources and Environment until his retirement, 30 September, 2019.

Dr. Wijarn Simachaya holds 2 Bachelor's degrees in Chemical Education and Laws from Chiang Mai University and Ramkhamhaeng University, respectively, a Master's in Environmental Science from Kasetsart University and a Graduate Diploma in Sanitary Engineering from Chulalongkorn University. His highest degree is a Doctorate in Philosophy (Ph.D.) in Environmental Engineering from University of Guelph, Canada in 1990. He also received honorary doctoral degrees in Environmental Science, Environmental Management, and Environmental Education from 7 universities in Thailand.

Plenary Speech on

"Pathways to Sustaining Natural Resources in Asia: Challenges and Opportunities"

Dindo Campilan, Ph.D.
Regional Director for Asia & Hub Director for Oceania
International Union for Conservation of Nature (IUCN)
Bangkok, Thailand

IUCN (since March 2021)

Manages IUCN's conservation-for-development regional agenda, strategy and operations in Asia- Oceania – covering 49 countries through a network of 11 offices and 250+ staff members.

CGIAR (1999-2020)

Over 20 years with the CGIAR, the largest global partnership in agricultural research for development. Senior scientist and science-for-development manager of Asia-wide regional programmes in agriculture-food-environment; served on the global management team for CGIAR centres with Colombia and Peru HQs. Posted in the Philippines, China, India and Vietnam.

- ***Director for Asia***, International Center for Tropical Agriculture (CIAT), 2014-2020
  Managed 18-country portfolio covering: inclusive markets and food systems, climate-smart agricultural policies and investments, and sustainable agricultural landscapes/ecosystem services. Served as senior thematic expert on climate-smart agri-food systems.
- ***Regional leader and senior scientist Asia***, International Potato Center (CIP), 1999-2014
  Managed 15-country portfolio from East Asia and the Pacific to Central and West Asia covering: Crop improvement and management, sustainable natural resources and agricultural value chains. Served as senior thematic expert on agri-food value chains and community-based NRM.

UN International Labour Organization (2020-2021)

- *Senior programme and operations officer/chief technical adviser*, Sustainable Enterprises Department. Based in Vietnam/Myanmar.
  Managed small and medium enterprise (SME) support in Myanmar, including for the ILO/UN- wide Covid-19 rapid response and recovery in-country efforts.

Other Institutional Affiliations and Short-term Professional Assignments

- *Affiliate scientist:* International Rice Research Institute (IRRI), International Crops Research Institute for Semi-Arid Tropics (ICRISAT)
- *Commissioned expert:* International Fund for Agricultural Development (IFAD), United Nations Development Programme (UNDP), Food and Agriculture Organization (FAO)

Other Countries of Professional Experience

- Asia: Australia, Bangladesh, Bhutan, Cambodia, Japan, Indonesia, Lao PDR, Malaysia, Maldives, Nepal, Pakistan, Sri Lanka, Thailand, Uzbekistan
- Other Regions: Canada, Colombia, Ghana, Italy, Kenya, Peru, The Netherlands, USA

Education PhD in Agricultural and Environmental Sciences, Wageningen University, The Netherlands **Country of Nationality** Philippines

Chair of the Conference

Professor Suvaluck Satumanatpan, Ph.D.

Faculty of Environment and Resource Studies, Mahidol University, Thailand

Board Advisor

1. Associate Professor Kampanad Bhaktikul, Ph.D.	Mahidol University, Thailand
2. Associate Professor Kitikorn Charmondusit, Ph.D.	Mahidol University, Thailand
3. Associate Professor Sura Pattanakiat, Ph.D.	Mahidol University, Thailand

Editorial Team

1. Professor Anthony SF Chiu, Ph.D.	De La Salle University-Manila, Philippines
2. Professor Dokrak Marod, Ph.D.	Kasetsart University, Thailand
3. Professor Hideki Nakayama, Ph.D.	Nagasaki University, Japan
4. Professor Mark G. Robson, Ph.D.	Rutgers University, USA
5. Professor Tamao Kasahara, Ph.D.	Kyushu University, Japan
6. Professor Wisakha Phoochinda, Ph.D.	National Institute of Development Administration (NIDA), Thailand
7. Associate Professor Benjaphorn Prapagdee, Ph.D.	Mahidol University, Thailand
8. Associate Professor Naiyanan Ariyakanon, Ph.D.	Chulalongkorn University, Thailand
9. Associate Professor Nathsuda Pumijumnong, Ph.D.	Mahidol University, Thailand
10. Associate Professor Sate Sampattagul, Ph.D.	Chiang Mai University, Thailand
11. Associate Professor Shimpei Iwasaki, Ph.D.	Fukuoka women's University, Japan
12. Associate Professor Thamasak Yeemin, Ph.D.	Ramkhamhaeng University, Thailand
13. Assistant Professor Anukul Buranaprapteprat, Ph.D.	Burapha University, Thailand
14. Assistant Professor Devi N. Choesin, Ph.D.	Institut Teknologi Bandung (ITB), Indonesia
15. Assistant Professor Said Munir, Ph.D.	Umm Al-Qura University, Saudi Arabia
16. Kitsanai Charoenjit, Ph.D.	Burapha University, Thailand
17. Merry Krisdawati Sipahutar, Ph.D.	Universitas Balikpapan, Indonesia
18. Mohamed Fassy Yassin, Ph.D.	University of Kuwait, Kuwait
19. Nguyen Thanh Giao, Ph.D.	Can Tho University, Vietnam
20. Poonperm Vardhanabindu, Ph.D.	Mahidol University, Thailand

HOME

Conference Committee

1. Assistant Professor Achara Ussawarujikulchai, Ph.D.	Mahidol University, Thailand
2. Assistant Professor Monthira Yuttitham, Ph.D.	Mahidol University, Thailand
3. Assistant Professor Noppol Arunrat, Ph.D.	Mahidol University, Thailand
4. Assistant Professor Paramita Punwong, Ph.D.	Mahidol University, Thailand
5. Assistant Professor Thamarat Phutthai, Ph.D.	Mahidol University, Thailand
6. Allan Sriratana Tabucanon, Ph.D.	Mahidol University, Thailand
7. Chitsanupong Prathum, Ph.D.	Mahidol University, Thailand
8. Kamalaporn Kanongdate, Ph.D.	Mahidol University, Thailand
9. Thomas Neal Stewart, Ph.D.	Mahidol University, Thailand
10. Witchaya Rongsayamanont, Ph.D.	Mahidol University, Thailand

Organizing Committee

1. Apirom Angsurat	2. Chardaporn Prasoptin
3. Chutintorn Moonthongnoi	4. Isaree Apinya
5. Panee Nakraikhing	6. Parynya Chwawiwathana
7. Sawatdirak Saingam	8. Sirinapat Charmondusit
9. Supalak Wattanachalarmyot	10. Suphawadee Jampala
11. Sureekarn Totaiya	12. Varong Boonchirdchoo
13. Vilinthorn Xuto	14. Thanchanok Onlamool
15. Wantanee Poklang	16. Yupa Viriyalai

Tentative Program

December 16th, 2021 (Thursday)

TIME	EVENT
08.00 – 09.00	Registration
09.00 – 09.30	**OPENING CEREMONY**
	Conference Reported by **Professor Dr. Suvaluck Satumanatpan,** Conference Chair
	Welcome Remarks and Conference Opening Remarks by **Associate Professor Dr. Sura Pattanakiat,** Dean of the Faculty of Environment and Resource Studies, Mahidol University
09.30 – 10.00	**KEYNOTE SPEAKER**
	"From Policy to Practice: How Thailand Deal with Climate Change and Environment Crisis?" By **Dr. Wijarn Simachaya** President of Thai Environment Institute (TEI), the Secretary-General of Thailand Business Council for Sustainable Development (TBCSD) and chairman of the Circular Economy under Bio-Circular-Green Economy Model, current national agenda
10.00 – 10.15	**BREAK**
10.15 – 10.45	**"Pathways to Sustaining Natural Resources in Asia: Challenges and Opportunities"** By Dr. Dindo Campilan Regional Director for IUCN Asia and Hub Director for Oceania

TIME	EVENT		
10.45 – 11.00	**BREAK**		
11.00 – 11.30	**POSTER SESSION**		
	Topic 1: Natural Resources Management **Chair: Asst. Prof. Dr. Thamarat Phutthai** **Co-chair: Dr. Kamalaporn Kanongdate**	**Topic 2: Science, Engineering and Energy Technology** **Chair: Assoc. Prof. Dr. Benjaphorn Prapagdee** **Co-chair: Prof. Dr. Hideki Nakayama and Dr. Witchaya Rongsayamanont**	**Topic 3: Climate Change, COVID-19 and Risk Management** **Chair: Assoc. Prof. Dr. Sunhee Suk** **Co-chair: Asst. Prof. Dr. Monthira Yuttitham Asst. Prof. Dr. Noppol Arunrat**
	No. 2021-04 Restoring Seaweed Beds by Changing Sea Urchin Foraging Behavior Dominic F.C. Belleza*, Takeshi Urae, Shinichiro Tanimae, Hiroto Tateishi, Makoto Kabeyama, Shigetaka Matsumuro, and Gregory N. Nishihara	No. 2021-11 Phosphorus Recovery and Bioavailability from Chemical Extraction of Municipal Wastewater Treatment's Waste Activated Sludge: A Case of Bangkok Metropolis, Thailand Kay Thi Khaing and Chongchin Polprasert*	No. 2021-30 A Study on the Coupling Coordination Between Tourism Economy and Ecological Environment Yiming Liu, Taro Nishizawa, Yanning Cai, Shanshan Wang, and Sunhee Suk*
	No. 2021-20 Is Species Richness of Macroalgae Related to Wave Exposure and Water Temperature in Arikawa Bay? Shinichiro Tanimae, Dominic F.C. Belleza, and Gregory N. Nishiharaa*		

TIME	EVENT		
	No. 2021-38 Community Structure of Meiofauna in Coral Reefs at Mu Ko Similan National Park, the Andaman Sea Nachaphon Sangmanee*, Makamas Sutthacheep, Laongdow Jungrak, Sirirat Jaihan, Suphakarn Paoduang, Prarop Plangngan, and Thamasak Yeemin		
11.30 – 13.00	**LUNCH**		
13.00 – 17.00	**ORAL PRESENTATION**		
	Topic 1: Natural Resources Management **Chair: Asst. Prof. Dr. Thamarat Phutthai** **Co-chair: Dr. Kamalaporn Kanongdate**	**Topic 2: Science, Engineering and Energy Technology** **Chair: Assoc. Prof. Dr. Benjaphorn Prapagdee** **Co-chair: Prof. Dr. Hideki Nakayama and Dr. Witchaya Rongsayamanont**	**Topic 3: Climate Change, COVID-19 and Risk Management** **Chair: Assoc. Prof. Dr. Sunhee Suk** **Co-chair: Asst. Prof. Dr. Monthira Yuttitham Asst. Prof. Dr. Noppol Arunrat**
13.00 – 13.15	No. 2021-44 Consumption Patterns on Food Waste Behavior: A Case Study in Nong Chok District, Bangkok Suchanat Aneknopparat and Apichaya Lilavanichakul*	No. 2021-06 Rhizo-mineralization of Manganese Oxides by a Halophyte *Salicornia europaea* Pulla Kaothien-Nakayama, Yoshiki Ohgi, Yu-Shan Wu, and Hideki Nakayama*	No. 2021-07 Carbon Footprint in the Faculty of Public Health, Mahidol University During Lockdown and Non-Lockdown Periods N. Chareonwimonruk, W. Patthanaissaranukool, T. Neamhom, and S. Polprasert*

TIME	EVENT		
13.15 – 13.30	No. 2021-01 The Evaluations of Land Use, Land Cover Changes and the Impacts to Ecosystem Services Values in Northeast Thailand Kousiki Lalatika Patnaik*, Noppol Arunrat, Sukanya Sereenonchai, Poonperm Vardhanabindu, and Winai Chaowiwat	No. 2021-08 Color Removal of Pulp and Paper Mill Wastewater by the Residual Eucalyptus Wood Kanjana Yupin, Thanakrit Neamhom, Chatchawal Singhakant, Sirenee Sreesai, and Supawadee Polprasert*	No. 2021-32 Slope Stability Analysis to Evaluate Slope Failure in Northern Thailand by Standard Penetration Test Patthranit Payaksiri*, Sayam Aroonsrimorakot, Pet Pakchotanon, and Bunlur Emaruchi
13.30 – 13.45	No. 2021-02 Evaluation of Petroleum Distribution Based on Well Logging and 3D Seismic Data of Ban Thi Oil Field in Fang Basin, Northern Thailand Chanin Pattarakamolsen and Kannipa Motanated*	No. 2021-13 Regeneration Heat Duty of Novel AMP-MPDL Solvent for CO_2 capture Rattanaporn Apaiyakul, Ratana Jiraratananon, Paitoon Tontiwachwuthikul, and Teerawat Sema*	
13.45 – 14.00	No. 2021-05 The Comparative Compressive Strength Study between Hand Cut Waste PET Bottles Fiber Concrete and Standard Concrete Surada Chundasutathanakul and Norlabodee Supatchapichai*	No. 2021-16 Effects of Steam Activated Chars from Bamboo and Palm Kernel Shell on Biocrude Production from Bagasse by Hydrothermal Liquefaction Natchanon Nilon and Prapan Kuchonthara*	**Topic 4: 21st Century Industry** **Chair: Dr. Poonperm Vardhanabindu** **Co-chair: Dr.Thomas Neal Stewart** No. 2021-10 Nanomechanical Property of Podoviruses for Biocontrol Agents of Bacterial Wilt Disease Udom Sae-Ueng*

TIME	EVENT		
14.00 – 14.15	No. 2021-19 The distribution of marine debris within a small *Zostera marina* meadow Gregory N. Nishihara*, Makoto Kabeyama, Dominic F. C. Belleza, and Makoto Ehama	No. 2021-18 Ammonia Effects on Reproductivity of the Marine Rotifer *Brachionus rotundiformis* Chengyan Han*, Hee-Jin Kim, Yoshitaka Sakakura, and Atsushi Hagiwara	No. 2021-15 Study of Using Natural Rubber Latex as a Filtrate Loss Prevention Additive for API Class G Cement Pattariya Aksornnarong* and Akkapun Wannnakomol
14.15 – 14.30	No. 2021-22 The Spatiotemporal Change Features of Groundwater Nitrogen Content in Miyakonojo River Basin, South Japan Zhi-Qiang Yu, Kei Nakagawa*, Ronny Berndtsson, Toru Hiraoka, and Yoshihiro Suzuki	No. 2021-23 Indoor Air Quality in Public Health Centers: A Case Study of Public Health Centers Located on Main and Secondary Roadside, Bangkok Natlada Boonphikham, Chatchawal Singhakant*, Suwimon Kanchanasuta, Withida Patthanaissaranukool, and Tawach Prechthai	No. 2021-31 Citizen-led Renewable Energy Implementation: A case study of Nagasaki Prefecture in Japan Taro Nishizawa and Sunhee Suk*
14.30 – 14.45	No. 2021-25 Efficiency of Di-(2-Ethylhexyl) Phthalate Degrading Bacteria Isolated from Mangrove Sediment and Landfill Soil Kanphorn Saengkla, Onruthai Pinyakong, and Prinpida Sonthiphand*	No. 2021-24 Enhancement of Sulfate Removal Efficiency Using Ettringite Precipitation at High Temperature Pullop Treerasaeng, Yothin Chimupala, and Pimluck Kijjanapanich*	No. 2021-51 An Innovative Toxic Heavy Metals Monitoring Product Development for a Sustainable Industry: A Case Study of Smartphone-Based Electrochemical Analytical Device Wasapon Thanabodypath*, Kingkan Pungjunun, Sudkate Chaiyo, Achara Chandrachai, and Orawon Chailapakul

TIME	EVENT		
14.45 – 15.15	**BREAK**		
	Topic 1: Natural Resources Management **Chair: Asst. Prof. Dr. Thamarat Phutthai** **Co-chair: Dr. Kamalaporn Kanongdate**	**Topic 2: Science, Engineering and Energy Technology** **Chair: Assoc. Prof. Dr. Benjaphorn Prapagdee** **Co-chair: Prof. Dr. Hideki Nakayama and Dr. Witchaya Rongsayamanont**	**Topic 4: 21st Century Industry** **Chair: Dr. Poonperm Vardhanabindu** **Co-chair: Dr.Thomas Neal Stewart**
15.15 – 15.30	No. 2021-26 The Diversity of Small Mammals in Natural and Recovery Forests in Mae Rim District, Chiang Mai Province Palita Kunchorn*, Pimonrat Tiansawat, and Alice Sharp	No. 2021-29 Ambient Noise Levels at an Urban Recreational Lake Park: A Case Study of Ampang Hilir Lake Park Nazatul Syadia Zainordin*, Muhammad Adib Azahar, Nur Izzati Zulkifli, Nurshahira Osmadi and Nur Aina Kamilia Othman	No. 2021-21 Operationalizing One Health for the Survival of the Planet and Humanities Boripat Siriaroonrat*
15.30 – 15.45	No. 2021-27 Comparative Study on Seed Dispersal and Tree Seedling Diversity Between a Natural Forest and a Restored Forest Area in Mae Rim District, Chiang Mai Atcharawan Saeaiew, Titaree Yamsri, Chrismas Kerdsak*, Alice Sharp, and Pimonrat Tiansawat	No. 2021-33 Analysis of Microplastics (MPs) Pollution in Wastewater Treatment Plant (WWTP) and Study on Microplastics Removal Efficiency Chutinat Boonwattana*, Pumis Tubtimdang, and Alice Sharp	

TIME	EVENT		
15.45 – 16.00	No. 2021-37 Seasonal Changes in Vertical Stratification of Moth Diversity in Tropical Rainforests of Thailand Ronnarot Taveesri*, Akihiro Nakamura, Ekgachai Jeratthitikul, and Alyssa B. Stewart	No. 2021-40 Decolorization of Reactive Red 239 by Activated Sludge Immobilized in Calcium Alginate Beads Sitanan Norkaew, Kulapa Chanawanno, and Pumis Thuptimdang*	
16.00 – 16.15	No. 2021-34 The Evolution of Hybrid Modes in Water and Agriculture: Case Study of Vietnamese Mekong Delta Linh Nguyen*, Keichiro Iguchi, Hironori Hamasaki, and Dang Kieu Nhan	No. 2021-41 Effect of Sludge Addition on the Biodegradation Efficiency of Diclofenac in Wastewater from Chiang Mai University Wastewater Treatment Plant Piriyakorn Injai, Kullapa Chanawanno, Pumis Thuptimdang*	
16.15 – 16.30	No. 2021-46 Water Footprint Assessment of Durian Monthong Before Harvesting and the Harvesting Period in Rayong Province Suphawadee Jampala*, Nathsuda Pumijumnong, Achara Ussawarujikulchai, and Noppol Arunrat	No. 2021-48 Potential of Ethanol-to-jet (ETJ) in Accordance with Carbon Offsetting and Reduction Scheme for International Aviation (CORSIA) Tadpong Ratanasoponchai*, Weerin Wangjiraniran	

TIME	EVENT		
16.30 -16.45	No. 2021-17 Harnessing Water Quality Management through Environmental Education Approach (Case Study of LERD Project, Phetchaburi-Thailand) Doris Ifeoma Ogueri*, Surat Bualert, Kasem Chunkao, and Onanong Phewnil	No. 2021-50 Site Selection for Feasibility Study of Pump-Storage Hydropower Project in the Philippines Sornsawan Utthakrue* and Thitisak Boonpramote	
16.45 – 17.00		No. 2021-11 Phosphorus Recovery and Bioavailability from Chemical Extraction of Municipal Wastewater Treatment's Waste Activated Sludge: A Case of Bangkok Metropolis, Thailand Kay Thi Khaing and Chongchin Polprasert*	
17.00 – 17.15	**CLOSING CEREMONY**		
	Conference Overall Conclusions Reported by **Dr. Suvaluck Satumanatpan,** Conference Chair Occasion - Presentation of Certificate to Chair and Co-chair Session - Outstanding Oral Presentation Certificate - Best Paper Award Closing Speech by **Associate Professor Dr. Sura Pattanakiat,** Dean of the Faculty of Environment and Resource Studies, Mahidol University		

***Remarkable: Bangkok Time (Bangkok, GMT+07:00)**

Table of content

The Evaluations of Land Use, Land Cover Changes and the Impacts to Ecosystem Services Values in Northeast Thailand

Kousiki Lalatika Patnaik[a*], Noppol Arunrat[a], Sukanya Sereenonchai[a], Poonperm Vardhanabindu[a], and Winai Chaowiwat[b]

[a]*Faculty of Environment and Resource Studies, Mahidol University, Nakhon Pathom 73170, Thailand*
[b]*Hydro-Informatics Innovation Division, Hydro Informatics Institute, Bangkok 10400, Thailand*

Abstract

Fluctuations in land use land cover (LULC) induces destruction of green cover, changes in nature, and pollution of water resources hence it disturbs ecosystem service values (ESVs). Objectives of the study were (1) to extract LULC status (from secondary data) and its change during the year 2008, 2013, 2018; (2) to assess LULC change impact on ecosystem service standards between 2008 and 2018. Therefore, to get status of LULC type, data of 2008, 2013, 2018 were classified from SERVIR-Mekong website under the Regional Land Cover Monitoring System (RLCMS). Ecosystem services (ESs) from the derived LULC data through simple benefit transfer method were then evaluated. Northeast Thailand was divided into three sections of big, medium and small provinces in terms of population density per area for a better comparison and analysis. Results revealed that cropland areas significantly decreased while forest land areas increased remarkably over the decade for all three sections. Whereas total ESVs increased for all sections from about 22837 million USD in 2008 to 23346 million USD in 2018 for the region. The impact that LULC changes had on ESVs remarkably fluctuated among the LULC categories according to the area and ESVs for individual LULC division over the decade. In conclusion, increase in ESV suggest that the region has great potential for land use and city planners to optimize the effect of LULC change on ESVs during the planning process.

Keyword: Land use land cover/ Ecosystem service values/ Ecosystem services/ Benefit transfer/ Northeast Thailand

---

*Corresponding Author: Kousiki Lalatika Patnaik
E-mail address: kousikilalatika.pat@student.mahidol.ac.th

1. Introduction

The development of urban parts and the outcome of social actions on ecosystems have remained leading concerns of environmental attention. According to "World urbanisation prospects: The 2009 revision population database" by United Nations (2010), it is estimated that more than 50% of the worldwide populace are living in cities, and this fraction will reach to about 69.6% by end of 2050. Even though the total urban area resolves only a minor portion of the global surface (Grimm et al., 2000; Zhang et al., 2013), presently, urbanisation is informed to be the most authoritative influencer of climate change (Mccarthy et al., 2010). Exhaustive and accelerated urbanisation is an instance of human-induced land use/land cover (LULC) alteration, which has deteriorated the constant effects that affect the climate system (Jin et al., 2005).

The fluctuations in LULC induces destruction of green cover, changes in nature, and pollution of water resources (Billa et al., 2013). Escalating urban growth and LULC surges pressures on human welfare and the natural environment and have become a universal apprehension. Accelerated urban development typically occurs next to the expense of major cultivated land, with the forfeiture of open public space and natural landscape (Ongsomwang et al., 2019). The land use land cover (LULC) pattern of an area can be dependant by the socioeconomic and natural factors and their consumption by humans in space and time (Shiferaw & Singh, 2011; Showqi et al., 2014). The exterior of the ground has altered significantly over the last five decades by human activities particularly through intensive agricultural practices, desertification and urbanisation. Deviations in LULC are amid

the utmost significant variations on the earth's surface (Showqi et al., 2014) The change of forest, woods and savannah into pasture and cropland through the previous decades has increased dramatically in the tropics (Lambin et al., 2003; Shiferaw & Singh, 2011). The dominant LULC change and quick urbanisation that are taking place in emergent nations such as Turkey, India, Thailand, Pakistan and other Latin American nations have been a growing consideration (Dewan & Yamaguchi, 2009; Geymen & Baz, 2008; Henríquez et al., 2006; Kumar et al., 2007; López et al., 2001).

The notion of ecosystem service can be well-defined as "the circumstances and procedures through which naturally occurring ecosystems, and the concurrent species that make them up, sustain and accomplish anthropoid life" (Luederitz et al., 2015; Ongsomwang et al., 2019). Ecosystem service is fatal to sustaining natural life and stable ecosystem. In recent years, ecosystem services research has become extremely significant. The number of researches focussing on ecosystem services is progressing exponentially and the consequence of the notion is perceived by the book of the Millennium Ecosystem Assessment (MEA), an outstanding work that comprises contribution of about 1300 researchers. One of the vital outcomes of the MEA was the discovery that universally 15 of the 24 ecosystem investigated are waning out, which will lead to a considerable and damaging effect on subsequent human well-being (Fisher et al., 2009; Millennium Ecosystem Assessment (MEA), 2005; Ongsomwang et al., 2019). MEA (2005) classified ecosystem facilities into four groups: (1) regulating services which are profits from the regulation of ecosystems such as flood control, purification of water, or readjustment of the climate through carbon sequestration; (2) provisioning amenities which are the product from the ecosystems like timber or food; (3) supporting services which are required for the manufacture of supplementary services for instance soil development and nutrient cycling; and (4) cultural services which help people from ecosystems through intellectual development, spiritual enrichment, aesthetic experiences, recreation and reflection (Ongsomwang et al., 2019).

Alternatively, the approach of ecosystem package valuation has been largely divided into three categories: economic, ecological and socio-cultural value (Ongsomwang et al., 2019). Ecosystem service values (ESVs) are specified evaluations of natural possessions and services, which show economic significance including the wellbeing and status of an ecosystem (Costanza, 2012; Johnston & Russell, 2011; Peng et al, 2015; Sannigrahi et al, 2018; Sannigrahi et al., 2020; Sannigrahi, Chakraborti, et al., 2019; Sannigrahi, Joshi, et al., 2019; Yan et al., 2016). Most of the studies on appraisal of ecosystems services is concentrated on assessing and monetizing definitive Ecosystem-Service Values (ESVs) at a particular juncture (Costanza et al., 1997; Li & Fang, 2014; Li et al., 2016).

Therefore, this research aims to apply geoinformatics technology and land us land cover change (LULCC) model to judge the impact of LULCC on ecosystem service standards in the North-eastern region of Thailand. Northeast Thailand was selected as the study region because it encompasses a total area of more than 170,000 square kilometres and is known for its vast agricultural growth potential for Thailand. The region covers one third of the country and for several years, North-eastern Thailand has had the major rural population growth (Ratanopad & Kainz, 2012).

The objectives of the study were (1) to extract LULC status (from secondary data) and its change during the year 2008, 2013, 2018; and (2) to assess LULC change impact on ecosystem service standards between 2008 and 2018. This research will focus on the years from 2008 to 2018 as the secondary data of LULC map is available only till the year 2018. Land cover map for 2019 and 2020 is still not available. This research also aims at a bigger picture by taking the entire region of Northeast Thailand instead of sticking to a particular province. This research can be a guideline for land use and city planners to give an optimum LULC scenario for balancing the economic development and ecosystem health in future for the entire region altogether.

2. Methodology

2.1 Study Area

Northeast Thailand (NET) (Figure 1) encompasses an overall area of more than 170,000 km^2 which inhabits one third of the country and is home to around 21 million people and it is the largest region in Thailand (Lacombe et al., 2017; Ratanopad & Kainz, 2012). The region is better known as Isan for the Thai people and it consists of 20 provinces. NET is situated on the Khorat Plateau, bounded by the border of the Sankamphaeng Range south of Nakhon Ratchasima, by Cambodia to the southeast and by Laos and Mekong River to the north and east. To the west it is divided from northern and central Thailand by the Phetchabun Mountains ("Isan", n.d.). The region is primarily a sandstone plateau gently undulating between 100 and 500 m above sea level (Lacombe et al., 2017), tilting from the Phetchabun Mountains in the west down toward the Mekong River.

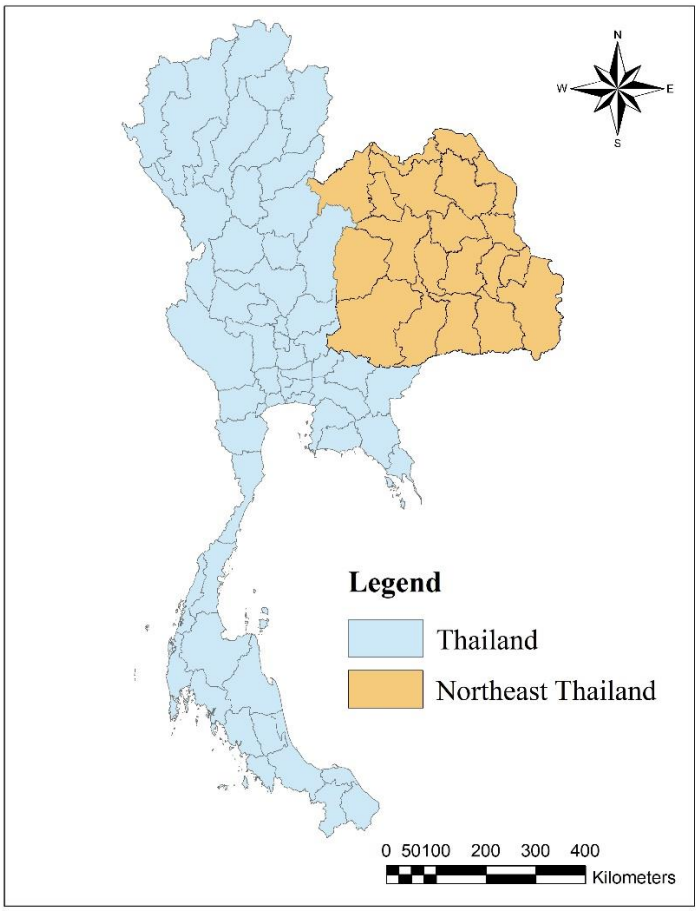

Figure 1. Map of Northeast Thailand

The region's average temperature is from 19.6°C to 30.2°C. Typically, the region has unpredictable rainfall but is intense from May to October during the rainy season. Average annual precipitation ranges from 1,270 mm in the southwestern provinces of Buriram, Chaiyaphum, Nakhon Ratchasima, Maha Sarakham and Khon Kaen to 2,000 mm in some other areas. The hot season is generally from February to May with the highest temperatures in April and the cool season from October to February ("Isan", n.d.). Approximately 80% of the population live in rural areas, mainly from agriculture and payments acknowledged from lots of permanent and seasonal migrants (Lacombe et al., 2017). The region also consists numerous national parks and possesses high biodiversity and several native species.

The development plans of Thailand don't always cover regions in particular, it focusses on

small sections of areas for example the Eastern Economic Corridor (EEC) or the lower Chao Phraya area and so on. As NET is a very big region, calculating the entire region's land use land cover values and the ecosystem services values altogether might result in giving a biased outcome; therefore, it is better to divide the region into different sections of big provinces, medium provinces and smaller provinces in terms of population density per area (Figure 2). The population density per area has been divided in a range from 200-150/km^2 for big provinces, 150-100/km^2 for medium sized provinces and 100-50/km^2 for small provinces.

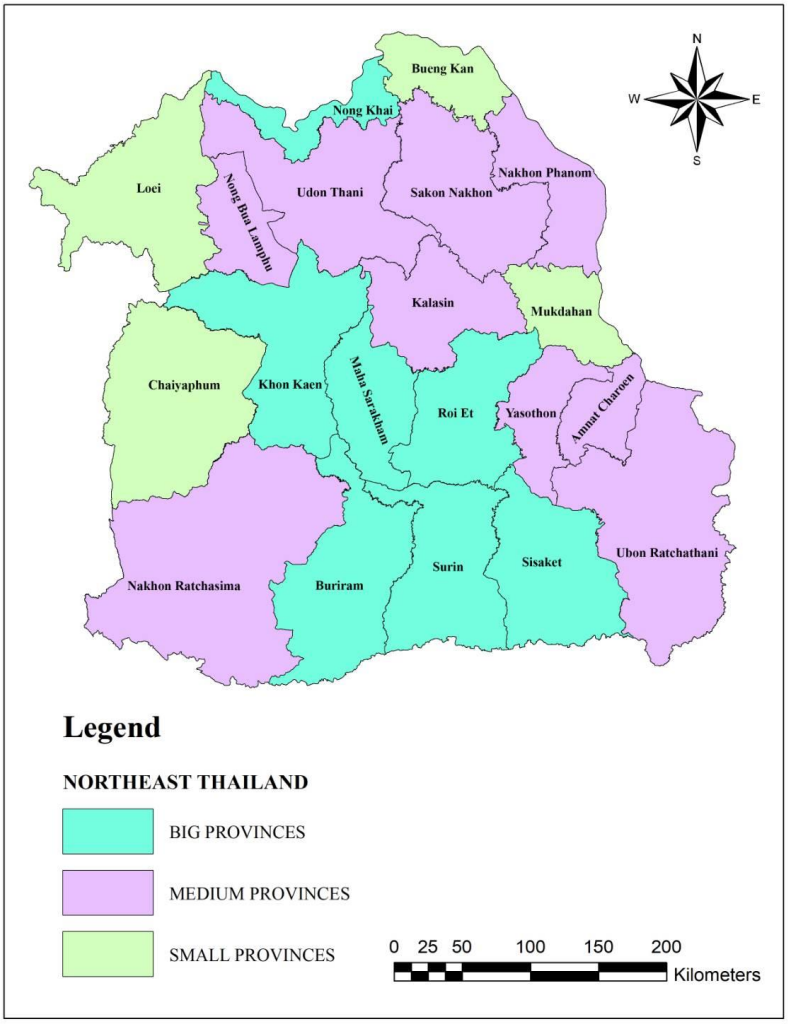

Figure 2. Big, Medium and Small Provinces of NET

2.2 Data Collection and Analysis

2.2.1 LULC Assessment

In order to get the area as well as the change of the LULC type, first, the old and recent LULC in 2008, 2013, 2018 was classified from the SERVIR-Mekong website (SERVIR Mekong, n.d.) under the Regional Land Cover Monitoring System (RLCMS). SEVIR-Mekong is a geospatial data-for-development program that responds to the needs of Lower Mekong countries. SERVIR-Mekong is mobilizing space technology and open data to help focus on challenges related to a changing climate, through a unique partnership between the U.S. Agency for International Development (USAID) and the U.S. National Aeronautics and Space Agency (NASA). It works in partnership with these leading organizations to assist the five countries in the Lower Mekong Region (Myanmar, Lao PDR, Cambodia, Vietnam and Thailand) to use information provided by geospatial technologies and Earth observing satellites to manage climate risks.

Under this program is the Regional Land Cover Monitoring System (RLCMS) which

produces high-quality regional land cover maps and identifies annual land cover changes in the Lower Mekong region. It uses well documented, transparent open-source technique. It also consists of quality assurance/ quality control approaches that combines information from multiple sources (Regional Land Cover Monitoring System Methodology, n.d.). The process in which the land cover map was produced is the following: once the map of Northeast Thailand (NET) was downloaded, LULC classification was done by using the typology values from RLCMS. In this study, the LULC classification system comprised of (1) Barren Land (bare land, abandoned land, landfills and pits); (2) Cropland; (3) Forest Land; (4) Marsh and Swamp; (5) Rangeland; (6) Surface Water; and (7) Urban and Built-up Area which was altered from the standard land use classification system in Thailand by the Land Development Department. Once the classification was done, the area of each LULC type was calculated using the ArcGIS software.

2.2.2 Ecosystem Service Evaluation (240 words)

Once the LULC status assessment data is created, the next phase of the research consists of evaluating the ecosystem services. ESVs were quantified using a simple benefit transfer method, which is used to calculate economic values for ecosystem services by substituting existing data from the previous study of Ongsomwang et al. (2019) to the present study region, since this technique is an instantaneous and a lower cost approach to assessing ecosystem valuation. Moreover, benefit values of separate LULC types with regard to ecosystem service was inaccessible. The LULC data that was derived between 2008, 2013 and 2018 was used to calculate ESVs determined from the simple benefit transfer method (Costanza et al., 1997) as:

$$ESV = \sum (VC_k \times A_k) \quad (1)$$

Where, ESV signifies the entire value of ecosystem service, while VC_k and A_k represent the coefficient value in USD/ha/year (Table 1) (which were assigned to each LULC type according to the value used by Ongsomwang et al., (2019)) and the area in ha for LULC type 'k', respectively. Proceeding, ESV change was evaluated by comparing the results of one dataset with the equivalent result of the second dataset in each time period. Therefore, the ESV changes were calculated (Kindu, Schneider, Teketay, & Knoke, 2016) as:

$$\text{ESV change} = \text{ESV final year} - \text{ESV initial year} \quad (2)$$

To calculate the percentage ESV changes the following equation was used (Kindu et al., 2016):

$$\%\ \text{ESV change} = [(\text{ESV final year} - \text{ESV initial year}) / (\text{ESV initial year})] \times 100 \quad (3)$$

Furthermore, to calculate estimated values of services provided by each ecosystem functions within the study area, the following equation was taken:

$$ESV_f = \sum (VC_{fk} \times A_k) \quad (4)$$

Where, ESV_f signifies calculated ecosystem service value of function 'f', VC_{fk} is the value coefficient of function 'f' (USD/ha/year) for LULC type 'k' and A_k is the area (ha).

3. Results and Discussion

3.1 LULC Status

In 2008, 2013 and 2018, the top three dominant LULC types for all three sections of Isan were cropland, forest-land and surface water. For big provinces the three dominant LULC types covered 83.86% (cropland), 12.78% (forest-land), and 1.51% (surface water) of the total area; for medium provinces they covered 76.15% (cropland), 20.45% (forest-land), and 1.86% (surface water) of the total area; for small provinces they covered 53.30% (cropland), 44.39% (forest-land), and 0.96% (surface water) of the total area (Figures 3 (a)-(c), Figures 4 (a)-(c), Figures 5 (a)-(c)). In these periods, forest-land areas notably increased from 6190.17 km^2 in 2008 to 7808.05 km^2 in 2018 for big provinces; from 15384.21 km^2 in 2008 to 17528.37 km^2 in 2018 for medium provinces and from 12837.80 km^2 in 2008 to 14847.13 km^2 in 2018 for small

provinces. However, cropland and surface water exceptionally decreased from 48107.85 km^2 in 2008 to 46398.47 km^2 in 2018 for big provinces; from 64515.42 km^2 in 2008 to 62236.57 km^2 in 2018 for medium provinces and from 18186.82 km^2 in 2008 to 16131.92 km^2 in 2018 for small provinces (Figure 3 (d), Figure 4 (d), Figure 5 (d)). Among the three divisions in the region, medium provinces have the highest area of LULC covering 243231.15 km^2.

Table 1. Coefficient value for different LULC types for ESV estimation

Ecosystem services category	Ecosystem services function	Ecosystem service value of each LULC type (USD/ha/year)						
		Urban and Built-up Area	Cropland	Forest Land	Surface Water	Marsh and Swamp	Range Land	Barren Land
Regulating services	1) Gas regulation	0	74.7	299.4	0	268.9	104	4.2
	2) Climate regulation	0	133	282.1	68.7	2,554.7	108	9.0
	3) Waste Treatment	0	245	119.2	2,719.0	2,716.0	91.5	18.0
Supporting services	1) Soil formation	0	218.1	278.6	1.5	255.5	155	11.8
	2) Biodiversity protection	0	106.1	312.6	372	373.5	130	27.7
Provision Services	1) Water supply	0	89.6	283.5	3047.7	2 315.6	105	4.8
	2) Food production	0	149.4	22.9	14.9	44.8	29.8	1.4
	3) Raw materials	0	14.9	206.5	1.5	10.5	25	2.8
Cultural services	1) Recreation and culture	12.7	1.5	144.2	648.4	829.2	60.3	16.6
Total		12.7	1,032.30	1,949.00	6,873.70	9,368.70	808.6	96.3

Source: Modified from (Mamat et al., 2018; Ongsomwang et al., 2019)

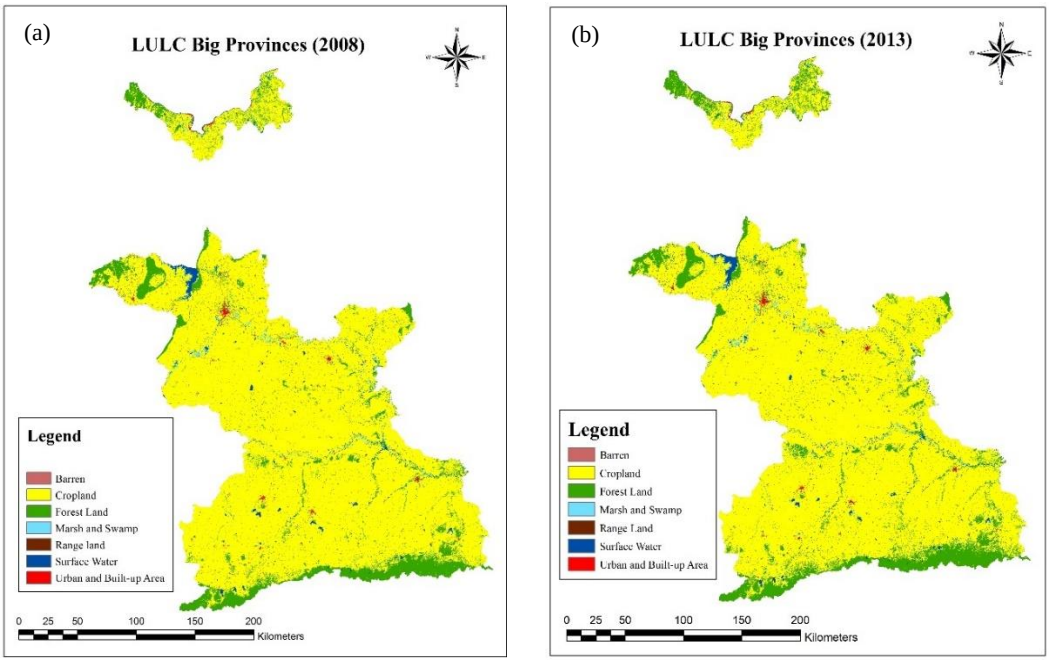

Figure 3. Spatial distribution of LULC data for big provinces in three years (a), (b), (c) and (d) comparison of LULC area in 2008, 2013, and 2018

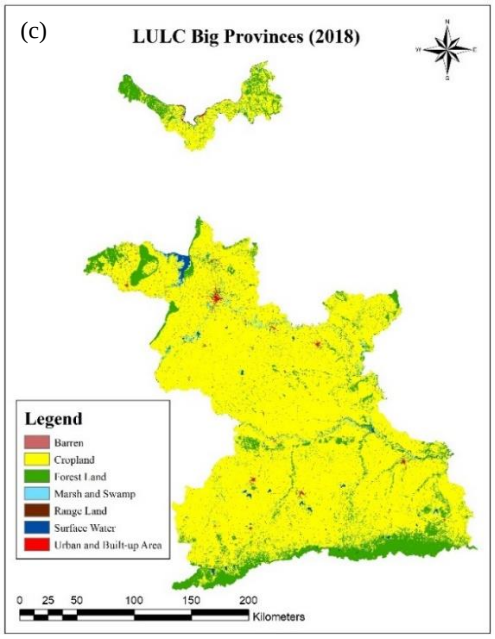

(d)

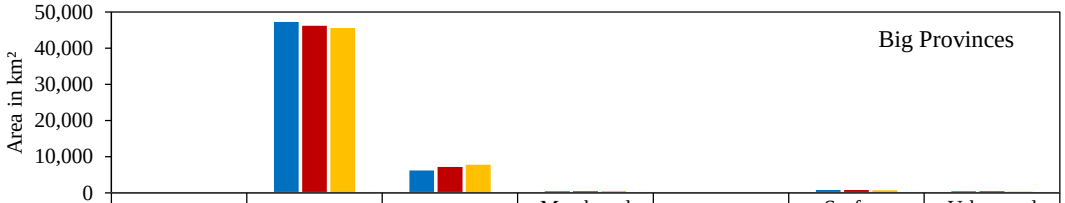

	Barren	Cropland	Forest Land	Marsh and Swamp	Range Land	Surface Water	Urban and Built-up Area
2008	33.42	47233.80	6190.17	455.50	14.20	874.05	473.24
2013	29.42	46218.12	7199.62	490.31	21.61	838.67	476.50
2018	35.51	45613.64	7808.05	576.69	35.92	784.83	420.01

Figure 3. Spatial distribution of LULC data for big provinces in three years (a), (b), (c) and (d) comparison of LULC area in 2008, 2013, and 2018 (cont.)

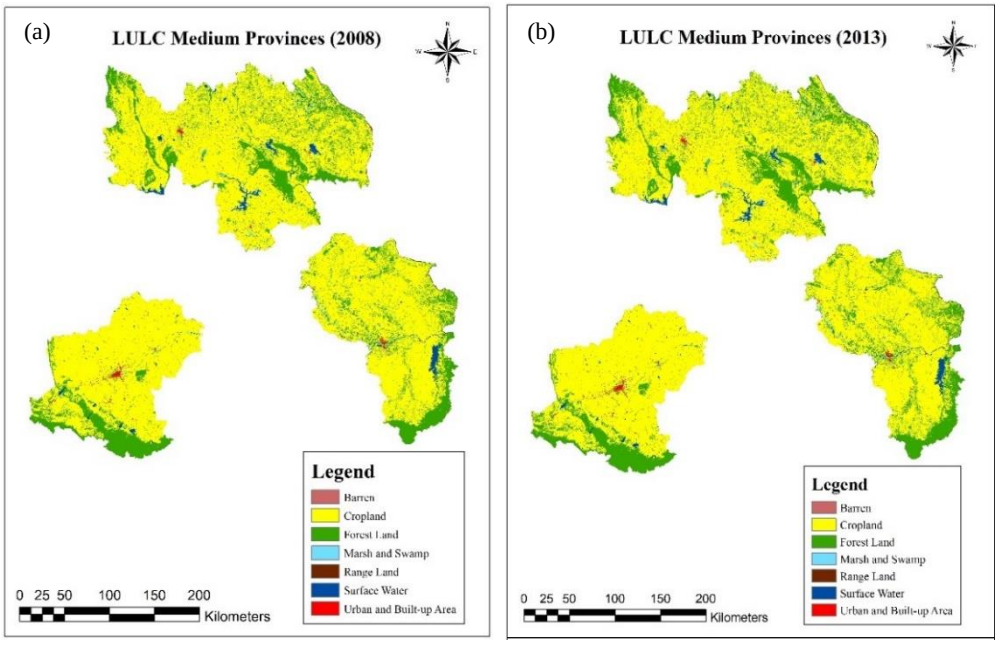

Figure 4. Spatial distribution of LULC data for medium provinces in three years (a), (b), (c) and (d) comparison of LULC area in 2008, 2013, and 2018

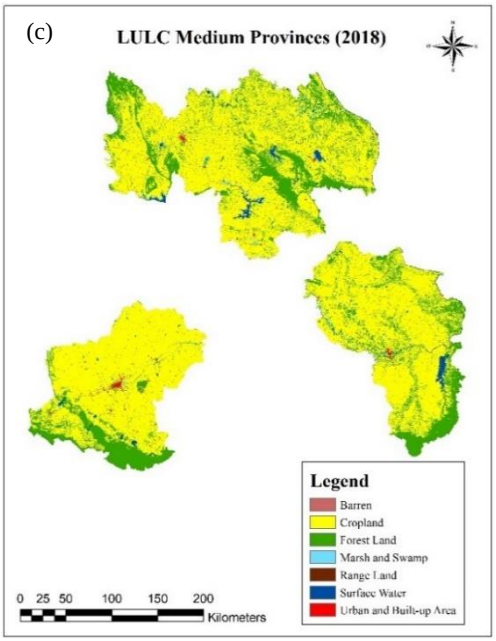

(d)

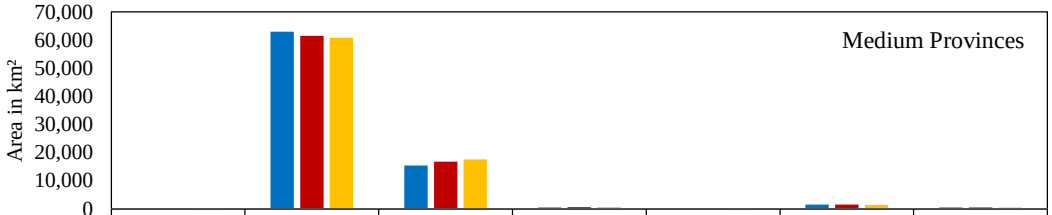

	Barren	Cropland	Forest Land	Marsh and Swamp	Range Land	Surface Water	Urban and Built-up Area
2008	50.37	62964.92	15384.21	535.68	33.73	1550.50	557.67
2013	53.60	61499.01	16827.62	590.35	47.13	1496.30	562.93
2018	63.83	60764.16	17528.37	661.47	79.22	1472.41	507.68

Figure 4. Spatial distribution of LULC data for medium provinces in three years (a), (b), (c) and (d) comparison of LULC area in 2008, 2013, and 2018 (cont.)

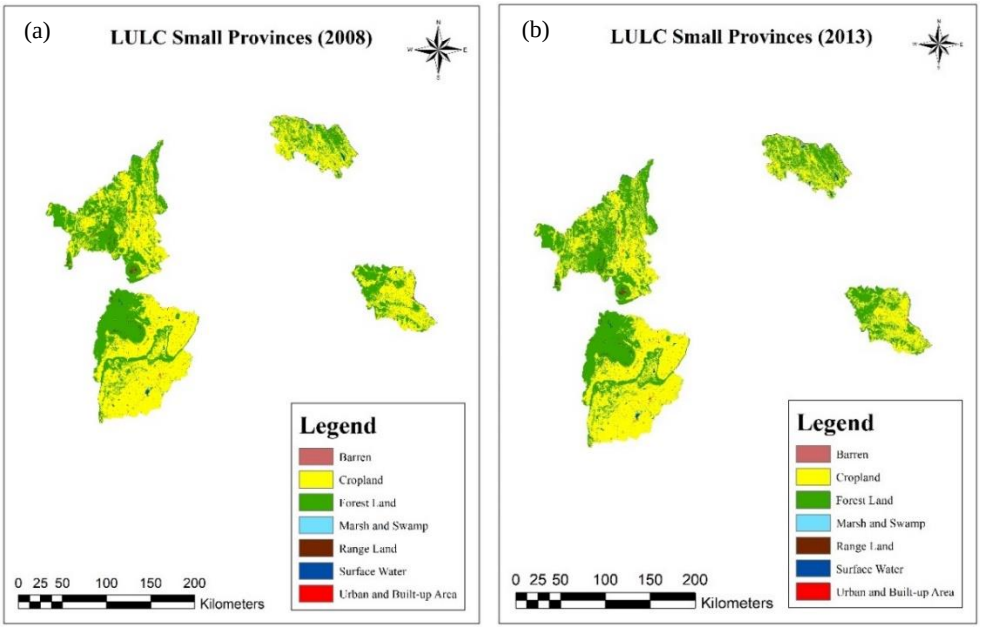

Figure 5. Spatial distribution of LULC data for small provinces in three years (a), (b), (c) and (d) comparison of LULC area in 2008, 2013, and 2018

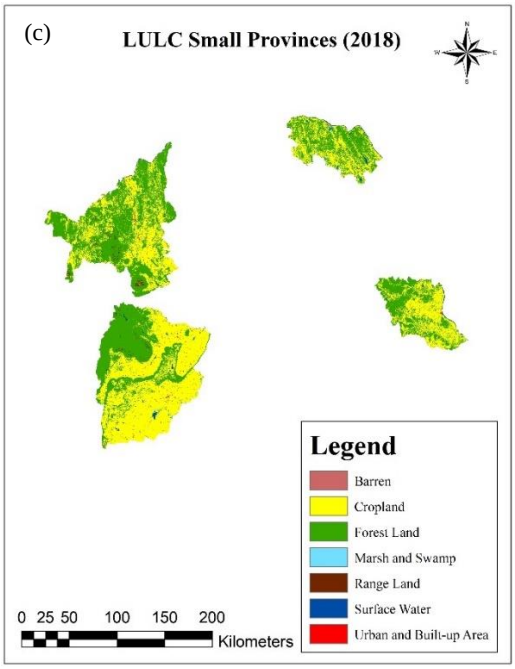

(d)

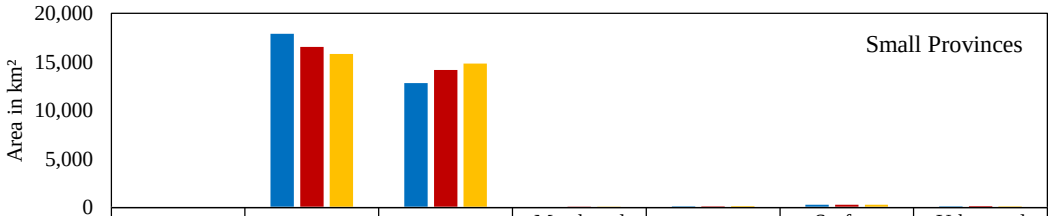

	Barren	Cropland	Forest Land	Marsh and Swamp	Range Land	Surface Water	Urban and Built-up Area
2008	7.45	17881.76	12837.80	91.47	148.06	305.07	158.19
2013	9.08	16538.55	14168.46	96.18	156.45	300.76	160.29
2018	12.09	15834.31	14847.13	110.47	184.30	297.62	144.04

Figure 5. Spatial distribution of LULC data for small provinces in three years (a), (b), (c) and (d) comparison of LULC area in 2008, 2013, and 2018 (cont.)

3.2 Ecosystem Service Values Estimation

The ESV estimations according to LULC types (Tables 2 (a)-(c)) revealed that the top four predominant LULC types for all three divisions were cropland, forest land, surface water, and marsh and swamp. They contributed ESVs in 2008, 2013, and 2018 around 99.97%, 99.96% and 99.95% of total ESVs for big provinces, about 99.96%, 99.96% and 99.93% of total ESVs for medium provinces, and approximately 99.74%, 99.73% and 99.66% of total ESVs for small provinces, respectively.

Table 2. Ecosystem Service values estimation according to LULC type for big (a), medium (b), and small (c) provinces

(a) Big Provinces

	ESVs in Million USD					
LULC type	2008		2013		2018	
	ESV	%	ESV	%	ESV	%
Barren	0.32	0.005	0.28	0.004	0.34	0.005
Cropland	4875.94	68.559	4771.10	66.148	4708.70	64.379
Forest Land	1206.46	16.964	1403.21	19.454	1521.79	20.806
Marsh and Swamp	426.74	6.000	459.35	6.369	540.29	7.387
Range Land	1.15	0.016	1.75	0.024	2.90	0.040

Table 2. Ecosystem Service values estimation according to LULC type for big (a), medium (b), and small (c) provinces (cont.)

	ESVs in Million USD					
LULC type	2008		2013		2018	
	ESV	%	ESV	%	ESV	%
Surface Water	600.80	8.448	576.48	7.992	539.47	7.376
Urban and Built-up Area	0.60	0.008	0.61	0.008	0.53	0.007
Total	7112.02	100.000	7212.77	100.000	7314.02	100.000

(b) Medium Provinces

	ESVs in Million USD					
LULC type	2008		2013		2018	
	ESV	%	ESV	%	ESV	%
Barren	0.49	0.004	0.52	0.005	0.61	0.005
Cropland	6499.87	58.717	6348.54	56.608	6272.68	56.108
Forest Land	2998.38	27.086	3279.70	29.244	3416.28	30.558
Marsh and Swamp	501.86	4.534	553.08	4.932	470.97	4.213
Range Land	2.73	0.025	3.81	0.034	6.41	0.057
Surface Water	1065.77	9.628	1028.51	9.171	1012.09	9.053
Urban and Built-up Area	0.71	0.006	0.71	0.006	0.64	0.006
Total	11069.80	100.000	11214.88	100.000	11179.69	100.000

(c) Small Provinces

	ESVs in Million USD					
LULC type	2008		2013		2018	
	ESV	%	ESV	%	ESV	%
Barren	0.07	0.002	0.09	0.002	0.12	0.002
Cropland	1845.93	39.649	1707.27	35.735	1634.58	33.683
Forest Land	2502.09	53.743	2761.43	57.800	2893.71	59.630
Marsh and Swamp	85.69	1.841	90.11	1.886	103.49	2.133
Range Land	11.97	0.257	12.65	0.265	16.13	0.332
Surface Water	209.69	4.504	205.77	4.307	204.57	4.216
Urban and Built-up Area	0.20	0.004	0.20	0.004	0.18	0.004
Total	4655.65	100.000	4777.53	100.000	4852.77	100.000

Furthermore, the input of ESVs by ecosystem service functions (ESFs) throughout the study period affirmed that the top four principle ESFs were waste treatment, soil formation, water supply, and climate regulation for all three parts. Amongst these four functions, ESV of waste treatment declined, whereas surprisingly, ESV of both soil formation and water supply improved over the decade (Figures 6 (a)-(c), Figures 7 (a)-(c), Figures 8 (a)-(c)). For example, ESVs of waste treatment dropped from 1592.57 million USD in 2008 to 1581.02 million USD in 2018 for big provinces, from 2293.49 million USD in 2008 to 2278.51 million USD in 2018 for medium provinces, and from 700.29 million USD in 2008 to 677.55 million USD in 2018 for small provinces. Contrarily, ESVs of soil formation increased from 1214.66 million USD in 2008 to 1227.82 million USD in 2018 for big provinces, from 1816.37 million USD in 2008 to 1832.03 million USD in 2018 for medium provinces, from 752.35 million USD in 2008 to 764.73 million USD in 2018 for small provinces. In the same way, ESVs of water supply rose from 970.73 million USD in 2008 to 1003.18 million USD in 2018 for big provinces, from 1597.27 million USD in 2008 to 1644.16 million USD in 2018 for medium provinces, from 639.89 million USD in 2008 to 681.02 million USD in 2018 for small provinces.

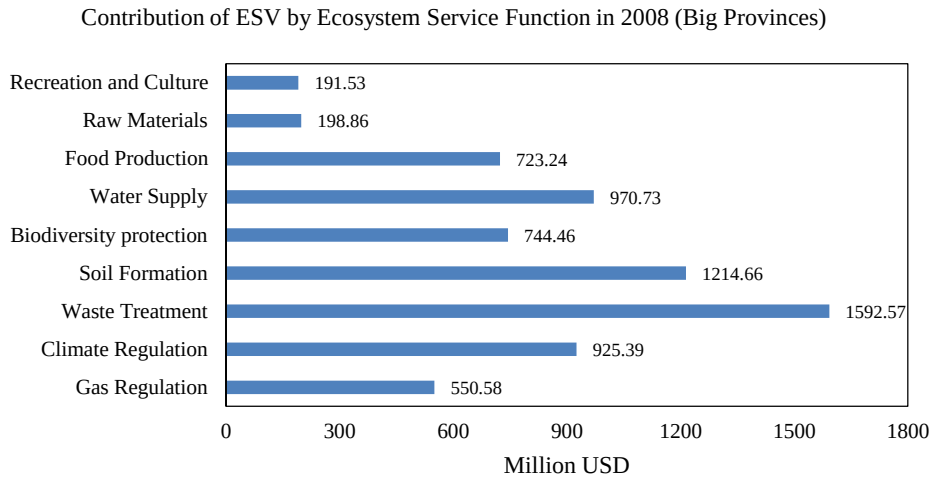

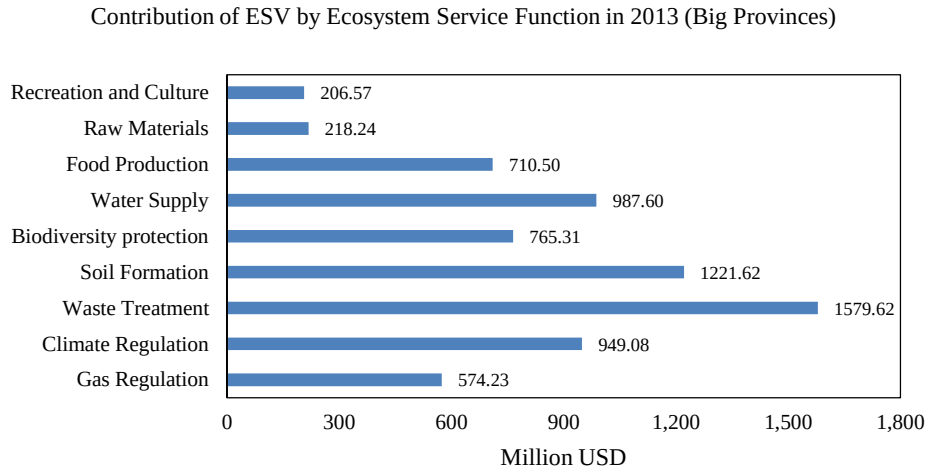

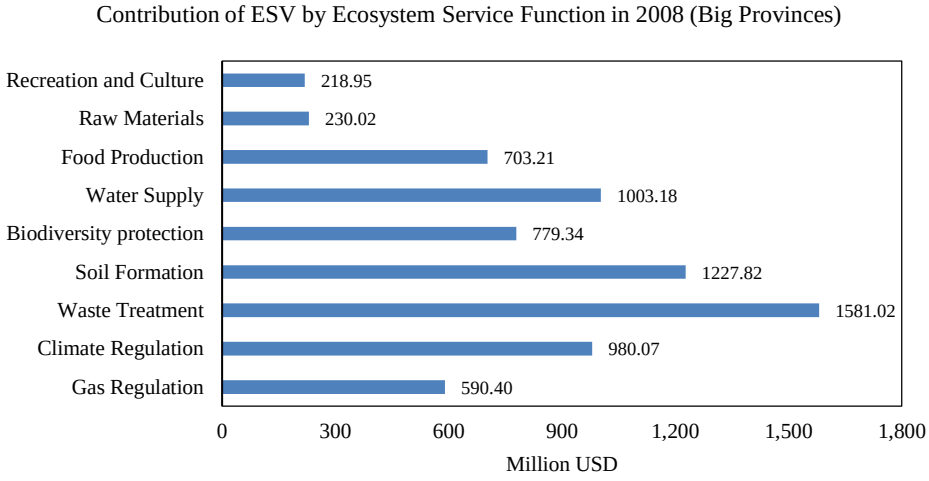

Figure 6. Ecosystem service value contribution by its function from 2008 to 2018 for big provinces

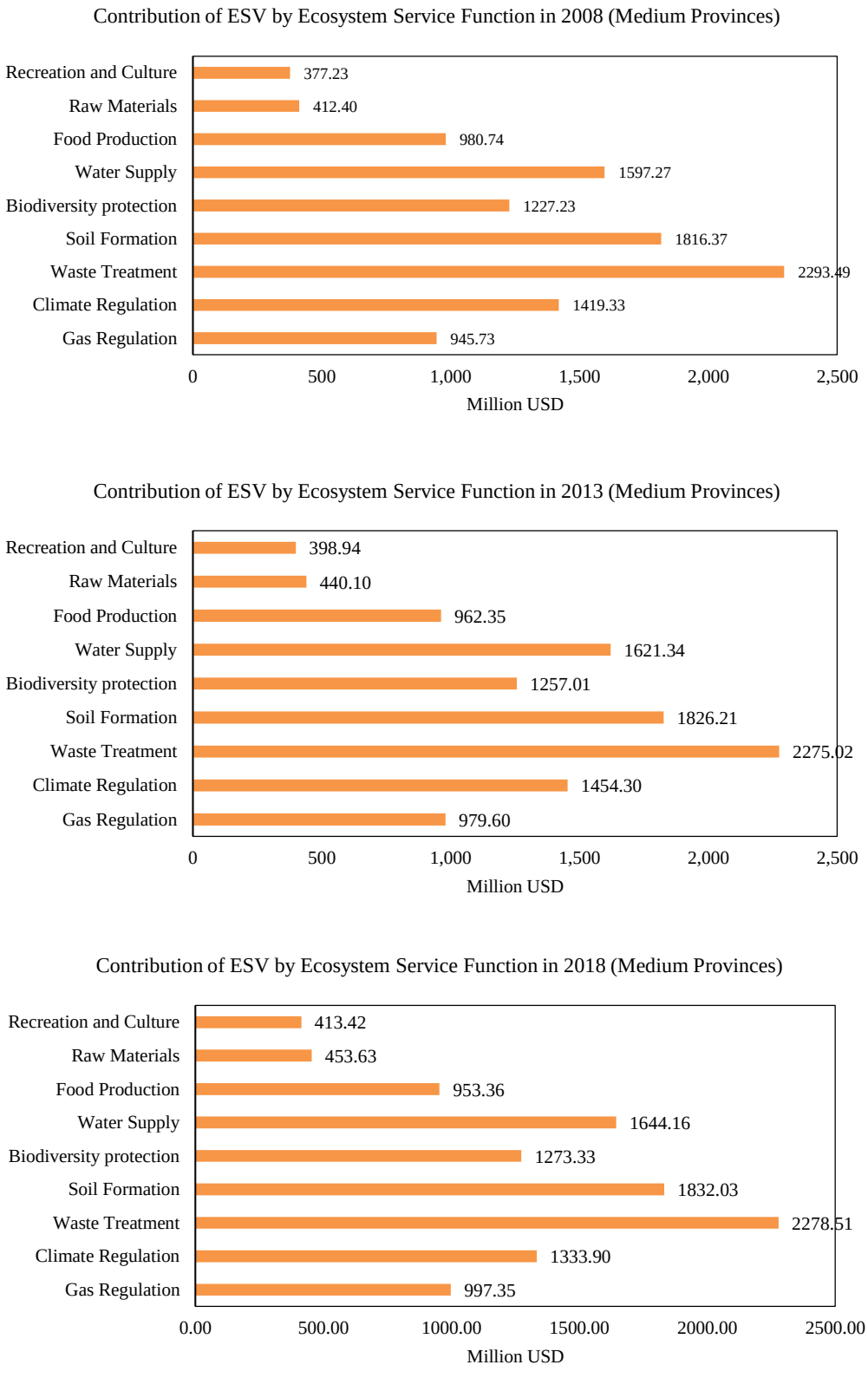

Figure 7. Ecosystem service value contribution by its function from 2008 to 2018 for medium provinces

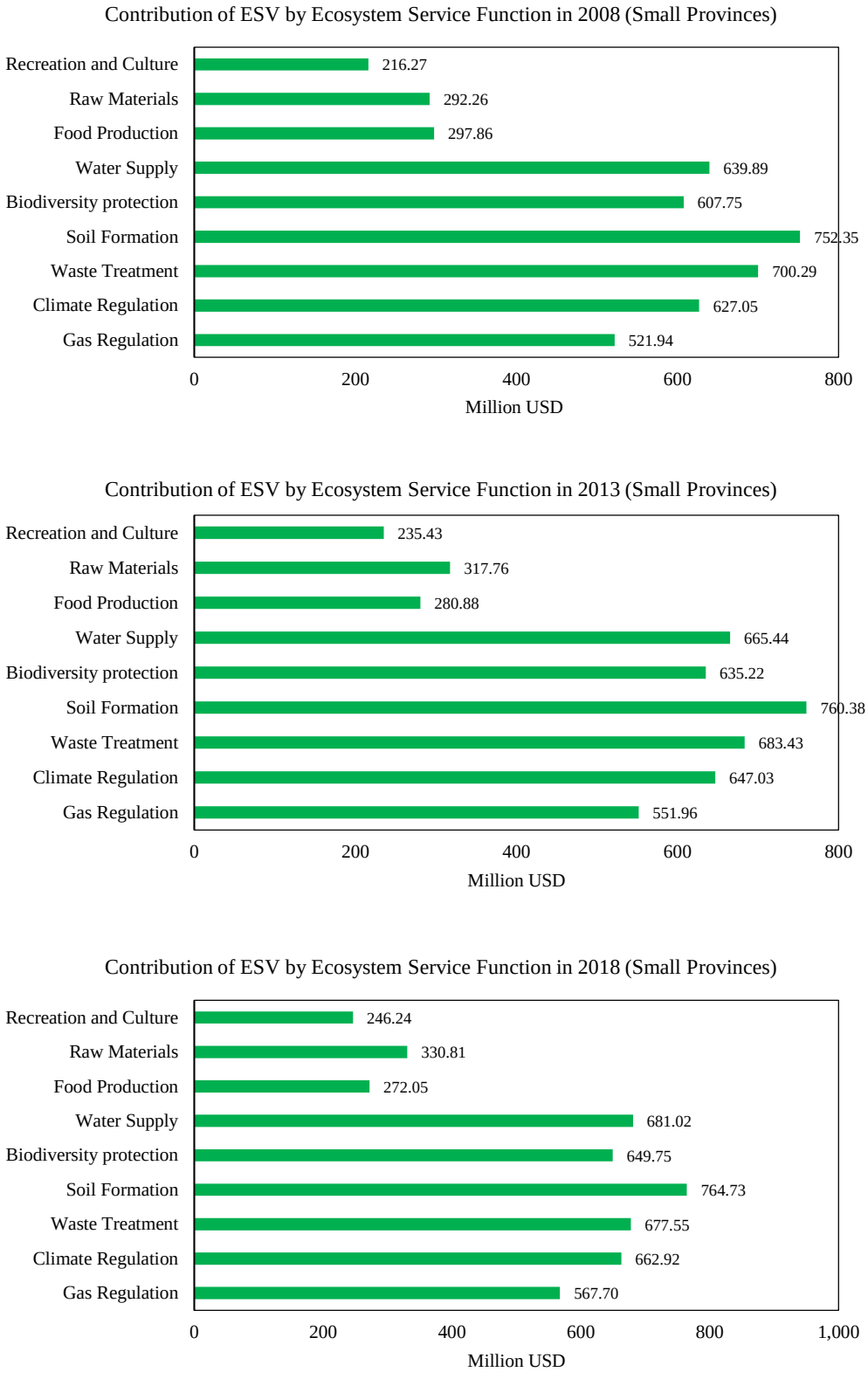

Figure 8. Ecosystem service value contribution by its function from 2008 to 2018 for small provinces

3.3 Changes in Ecosystem Service Values

The changes in ESVs revealed a noteworthy increase in the total ESVs over the study period (Tables 3 (a)-(c)). The overall ESVs fluctuations for big provinces from 2008 to 2013 was 100.75 million USD or 58.68% of the entire price in 2008 and it further increased from 2013 to 2018 with an amount of 101.25 million USD

or 93.44% of the total value in 2013. Meanwhile, for medium provinces the summation number of changes of ESVs from 2008 to 2013 was 145.08 million USD or 60.85% of the over-all amount in 2008 and from 2013 to 2018 the ESV change was of 35.19 million USD or 63.83% of the total value in 2013. This entails that the change in ESV from 2013 to 2018 was smaller than during the year 2008 to 2013. In a similar manner, for small provinces the total variation in ESVs from 2008 to 2013 was 121.88 million USD or 34.90% of the sum value in 2008. From 2013 to 2018, for small provinces, the entire ESV change was of 75.24 million USD or 65.31% of the entire value in 2013. This finding indicates that the change in ESV from 2013 to 2018 was smaller than during the year 2008 to 2013 just like for medium provinces.

Table 3. Ecosystem services values changes for big (a), medium (b), and small (c) provinces

(a) Big Provinces

LULC type	2008-2013		2013-2018	
	Million USD	Proportion (%)	Million USD	Proportion (%)
Barren	-0.04	-11.97	0.06	20.69
Cropland	-104.85	-2.15	-62.40	-1.31
Forest Land	196.74	16.31	118.58	8.45
Marsh and Swamp	32.61	7.64	80.93	17.62
Range Land	0.60	52.21	1.16	66.26
Surface Water	-24.32	-4.05	-37.00	-6.42
Urban and Built-up Area	0.00	0.69	-0.07	-11.85
Total	100.75	58.68	101.25	93.44

(b) Medium Provinces

LULC type	2008-2013		2013-2018	
	Million USD	Proportion (%)	Million USD	Proportion (%)
Barren	0.03	6.41	0.10	19.09
Cropland	-151.33	-2.33	-75.86	-1.19
Forest Land	281.32	9.38	136.58	4.16
Marsh and Swamp	51.22	10.21	-82.11	-14.85
Range Land	1.08	39.73	2.59	68.07
Surface Water	-37.25	-3.50	-16.42	-1.60
Urban and Built-up Area	0.01	0.94	-0.07	-9.82
Total	145.08	60.85	-35.19	63.86

(c) Small Provinces

LULC type	2008-2013		2013-2018	
	Million USD	Proportion (%)	Million USD	Proportion (%)
Barren	0.02	21.76	0.03	33.17
Cropland	-138.66	-7.51	-72.70	-4.26
Forest Land	259.35	10.37	132.27	4.79
Marsh and Swamp	4.42	5.16	13.38	14.85
Range Land	0.68	5.66	3.48	27.48
Surface Water	-3.92	-1.87	-1.20	-0.58
Urban and Built-up Area	0.00	1.33	-0.02	-10.14
Total	121.88	34.90	75.24	65.31

Additionally, the changes in ESVs revealed a significant increase or decrease in ESVs from varied LULC types in different periods for all three sections of provinces (see Table 3). As shown, for big provinces, the increment of ESVs between 2008 and 2013 was mainly characterized by forest land, marsh and swamp and rangeland that calculated to be 229.95 million USD, while the decrease of ESVs in the same period signified by cropland and surface water summed up to be 129.17 million USD. Likewise, between 2013 and 2018, the increase and decrease of ESVs was represented by the same LULC types, i.e., forest land, marsh and swamp and rangeland, and cropland and surface water respectively. Meanwhile for medium provinces, the surge in ESVs between 2008 and 2013 was represented by forest land, marsh and swamp and rangeland that accounted for 333.62 million USD, while the decline of ESVs in the same period characterised by cropland and surface water summed up to be 188.58 million USD. But surprisingly, between 2013 and 2018, the increase of ESVs was characterised by forest land and rangeland, whereas the decrease was represented by cropland, marsh and swamp and surface water. Moving onto the small provinces, the increase of ESVs between 2008 and 2013 was mostly represented by forest land, marsh and swamp and rangeland that summed to be 264.44 million USD, while the decrease of ESVs in the same period signified by cropland and surface water accounted for 142.58 million USD. Similarly, between 2013 and 2018, the increase of ESVs was represented by the same LULC types and also for the decrease of ESVs, the same LULC types were defined that is cropland and surface water.

Moreover, the fluctuations in ESVs by ESFs revealed a considerable increase of nearly all functions except waste treatment under regulating services and food production under provision services in all periods for all three sections of provinces (Tables 4 (a)-(c)), with the exception of climate regulation under regulating services for medium provinces. As an outcome, for big provinces, climate regulation under regulating services had considerably increased from 23.69 million USD in the 2008-2013 time period to 30.98 million USD in the 2013-2018 time period. While soil formation under supporting services increased from 6.97 million USD in the 2008-2013 timeframe to 6.20 million USD in the 2013-2018 timeframe, describing that the changes during 2013-2018 was less than during 2008-2013. Likewise, water supply under provision services increased from 16.87 million USD in the period of 2008-2013 to 15.58 million USD in the period of 2013-2018 and recreation and culture under culture services boosted from 15.04 million USD between 2008 and 2013 to 12.38 million USD between 2013 and 2018. Both these functions show that the changes during 2013-2018 was less than during 2008-2013. Further, waste treatment under regulating services declined from 12.96 million USD in the 2008-2013 time period to 1.41 million USD in the 2013-2018 time period and food production under provision services deteriorated from 12.74 million USD in the timeframe of 2008-2013 to 7.29 million USD in the timeframe of 2013-2018.

In the meantime, for medium provinces, climate regulation under regulating services, saw an increase between the years 2008-2013 with an amount of 34.96 million USD, whereas it decreased significantly between the years 2013-2018 with an amount of 120.39 million USD. While soil formation under supporting services surged from 9.84 million USD in the 2008-2013 time period to 5.82 million USD in the 2013-2018 time period, suggesting that the changes during 2013-2018 was less than during 2008-2013. Similarly, water supply under provision services rose from 24.07 million USD in the timeframe of 2008-2013 to 22.81 million USD in the timeframe of 2013-2018 and recreation and culture under culture services increased from 21.71 million USD between 2008 and 2013 to 14.48 million USD between 2013 and 2018. Both these functions indicate that the 2013-2018 changes were less than the 2008-2013 changes. To the contrary, waste treatment under regulating services saw a decrease between the years 2008-2013 with an amount of 18.47 million USD, whereas it increased slightly between the years 2013-2018 with an amount of 3.48 million USD; and food production under provision services deteriorated from 18.39 million USD in the period of 2008-2013 to 8.99 million USD in the period of 2013-2018.

Table 4. Ecosystem services values changes by ecosystem service function for big (a), medium (b), and small (c) provinces

(a) Big Provinces

Ecosystem services function	2008	2013	2018	2008-2013		2008-2013	
	Million USD	Million USD	Million USD	Million USD	%	Million USD	%
Regulating services							
Gas Regulation	550.58	574.23	590.40	23.65	4.29	16.18	2.82
Climate Regulation	925.39	949.08	980.07	23.69	2.56	30.98	3.26
Waste Treatment	1592.57	1579.62	1581.02	-12.96	-0.81	1.41	0.09
Supporting services							
Soil Formation	1214.66	1221.62	1227.82	6.97	0.57	6.20	0.51
Biodiversity protection	744.46	765.31	779.34	20.85	2.80	14.03	1.83
Provision services							
Water Supply	970.73	987.60	1003.18	16.87	1.74	15.58	1.58
Food Production	723.24	710.50	703.21	-12.74	-1.76	-7.29	-1.03
Raw Materials	198.86	218.24	230.02	19.38	9.75	11.78	5.40
Cultural services							
Recreation and Culture	191.53	206.57	218.95	15.04	7.85	12.38	5.99
Total	7112.02	7212.77	7314.02	100.75	26.99	101.25	20.46

(b) Medium Provinces

Ecosystem services function	2008	2013	2018	2008-2013		2008-2013	
	Million USD	Million USD	Million USD	Million USD	%	Million USD	%
Regulating services							
Gas Regulation	945.73	979.60	997.35	33.88	3.58	17.74	1.81
Climate Regulation	1419.33	1454.30	1333.90	34.96	2.46	-120.39	-8.28
Waste Treatment	2293.49	2275.02	2278.51	-18.47	-0.81	3.48	0.15
Supporting services							
Soil Formation	1816.37	1826.21	1832.03	9.84	0.54	5.82	0.32
Biodiversity protection	1227.23	1257.01	1273.33	29.78	2.43	16.32	1.30
Provision services							
Water Supply	1597.27	1621.34	1644.16	24.07	1.51	22.81	1.41
Food Production	980.74	962.35	953.36	-18.39	-1.88	-8.99	-0.93
Raw Materials	412.40	440.10	453.63	27.71	6.72	13.53	3.07
Cultural services							
Recreation and Culture	377.23	398.94	413.42	21.71	5.75	14.48	3.63
Total	11069.80	11214.88	11179.69	145.08	20.31	-35.19	2.48

Table 4. Ecosystem services values changes by ecosystem service function for big (a), medium (b), and small (c) provinces (cont.)

(c) Small Provinces

Ecosystem services function	2008	2013	2018	2008-2013		2008-2013	
	Million USD	Million USD	Million USD	Million USD	%	Million USD	%
Regulating services							
Gas Regulation	521.94	551.96	567.70	30.02	5.75	15.73	2.85
Climate Regulation	627.05	647.03	662.92	19.98	3.19	15.90	2.46
Waste Treatment	700.29	683.43	677.55	-16.86	-2.41	-5.88	-0.86
Supporting services							
Soil Formation	752.35	760.38	764.73	8.03	1.07	4.35	0.57
Biodiversity protection	607.75	635.22	649.75	27.47	4.52	14.53	2.29
Provision services							
Water Supply	639.89	665.44	681.02	25.56	3.99	15.57	2.34
Food Production	297.86	280.88	272.05	-16.98	-5.70	-8.82	-3.14
Raw Materials	292.26	317.76	330.81	25.50	8.73	13.05	4.11
Cultural services							
Recreation and Culture	216.27	235.43	246.24	19.15	8.86	10.81	4.59
Total	4655.65	4777.53	4852.77	121.88	27.99	75.24	15.20

Proceeding to small provinces, climate regulation under regulating services rose from 19.98 million USD in the period of 2008-2013 to 15.90 million USD in the period of 2013-2018. This data indicates that the changes during 2013-2018 was less than the changes during 2008-2013. While soil formation under supporting services increased from 8.03 million USD in the 2008-2013 timeframe to 4.35 million USD in the 2013-2018 timeframe, signifying that the fluctuations during 2013-2018 was less than the fluctuations during 2008-2013. Similarly, water supply under provision services upscaled from 25.56 million USD in the period of 2008-2013 to 15.57 million USD in the period of 2013-2018 and recreation and culture under culture services increased from 19.15 million USD between 2008 and 2013 to 10.81 million USD between 2013 and 2018. Both these functions point to the fact that 2013-2018 changes were less than 2008-2013 changes. Besides, waste treatment under regulating services declined from 16.86 million USD in the 2008-2013 time period to 5.88 million USD in the 2013-2018 time period and food production under provision services deteriorated from 16.98 million USD in the timeframe of 2008-2013 to 8.82 million USD in the timeframe of 2013-2018.

3.4 LULC change impact on ecosystem service values

The effect of LULC change on ESVs clearly had a fluctuation between the LULC categories as noticed in the inputs of the area and ESV for specific LULC group over the time periods for all three groups of provinces (Figures 9 (a)-(c)). Especially, for big provinces, the forest land increased about 6190.17 km^2 (11.19%) in 2008 to 7808.05 km^2 (14.12%) in 2018 and marsh and swamp increased from about 455.50 km^2 (0.82%) in 2008 to 576.69 km^2 (1.04%) in 2018. (See Figure 3 (d)). And because of this increase, the total ESVs essentially increased over the decade. The ESV of forest land significantly increased from 196.74 million USD in 2008 to 118.58 million USD in 2018. Likewise, the ESV of marsh and swamp increased from 32.61 million USD in 2008 to 80.93 million USD in 2018. For big provinces, mainly the changes in these two LULC type (forest land and marsh and swamp) suggestively affected the changes in the total ESVs throughout the decade. Herein, the

total ESVs of these two LULC increased by 199.52 million USD from 2013-2018 while the total ESVs in the study area increased by 101.25 million USD (Table 3 (a)). Contrarily, cropland areas repetitively decreased over the time period. It deteriorated from around 47233.80 km^2 (85.45%) in 2008 to 45613.64 km^2 (82.52%) in 2018, and its corresponding ESV showed a decrease from 104.85 million USD in 2008 to 62.4 million USD in 2018.

Meanwhile for medium provinces, the forest land increased about 15384.21 km^2 (18.97%) in 2008 to 17528.37 km^2 (21.62%) in 2018 and marsh and swamp increased from about 535.68 km^2 (0.66%) in 2008 to 661.47 km^2 (0.81%) in 2018. (See Figure 4 (d)). And because of this increase, the total ESVs essentially increased as well. The ESV of forest land significantly increased from 281.32 million USD in 2008 to 136.58 million USD in 2018. Whereas, the ESV of marsh and swamp increased in 2008 by 51.22 million USD but surprisingly decreased to 82.11 million USD in 2018. For medium provinces, mainly the changes in forest land significantly affected the changes in the total ESVs throughout the decade. Herein, the total ESVs of forest land increased by 136.58 million USD from 2013-2018 while the total ESVs in the study area from 2013-2018 became 35.19 million USD (Table 3 (b)). This data is mainly suggesting that the change from 2008-2013 was way higher than the change from 2013-2018, even-though the total ESV of medium provinces increased (Table 2 (b)). Furthermore, cropland areas constantly decreased over the time period. It reduced from approximately 62964.92 km^2 (77.66%) in 2008 to 60764.16 km^2 (74.95%) in 2018, and its corresponding ESV showed a decrease from 151.33 million USD in 2008 to 75.86 million USD in 2018.

Additionally, for small provinces, the forest land rose from about 12837.80 km^2 (40.85%) in 2008 to 14847.13 km^2 (47.24%) in 2018 and marsh and swamp increased from about 91.47 km^2 (0.29%) in 2008 to 110.47 km^2 (0.35%) in 2018. (See Figure 5 (d)). And because of this increase, the total ESVs significantly increased over the decade. The ESV of forest land significantly increased from 259.35 million USD in 2008 to 132.27 million USD in 2018. Likewise, the ESV of marsh and swamp increased from 4.42 million USD in 2008 to 13.38 million USD in 2018. For small provinces, mainly the changes in these two LULC type (forest land and marsh and swamp) prominently affected the changes in the total ESVs throughout the study period. Herein, the total ESVs of these two LULC increased by 145.65 million USD from 2013-2018 while the total ESVs in the study area increased by 75.24 million USD (Table 3 (c)). While, cropland areas continually decreased over the time period. It worsened from around 17881.76 km^2 (56.89%) in 2008 to 15834.31 km^2 (50.38%) in 2018, and its corresponding ESV showed a decrease from 138.66 million USD in 2008 to 72.7 million USD in 2018.

Therefore, depending on the simple benefit transfer method of Costanza et al. (1997) with the altered coefficient of ESVs from Ongsomwang et al. (2019), the general tendency of ESVs as an outcome of changes in LULC were similar (Figures 9 (a)-(c)).

3.5 Discussion

Ecosystem services are encountering extensive pressure due to climate change and mainly human activities as chief contributors who are changing the ecosystem services through LULC changes, and it is likely to continue to rise (Wang at al., 2014). LULC changes are the essential motive of deviations in the ecosystem function assessment, the land-use formation, and the compelling developments of landscapes around the world and they disturb ecosystem services by animal husbandry, agricultural actions, mining, developed areas and human settlements (Mamat et al., 2018). Ecosystem services are not given too much importance in policy decisions because they are not entirely 'occupied' in profitable markets or sufficiently calculated in terms similar with manufactured capital (Costanza et al., 1997). This indifference will eventually weaken the sustainability of individuals in the environment. The savings of the Earth would come to a standstill without the facilities of ecological life-support structures (Costanza et al., 1997); in other words one can tell that their overall worth to the economy is endless. Human beings along with other organisms profit directly as well as indirectly in

several aspects from the environment's ecosystems, for instance by the arrangement of food and resources, air purification, storing carbon, pharmaceuticals, the regulation of local climates and biodiversity protection; and understanding the various benefits contributed by these ecosystems is becoming gradually critical (Chuai et al., 2016; R-Q. Li et al., 2007; Mamat et al., 2018; Sawut et al., 2013).

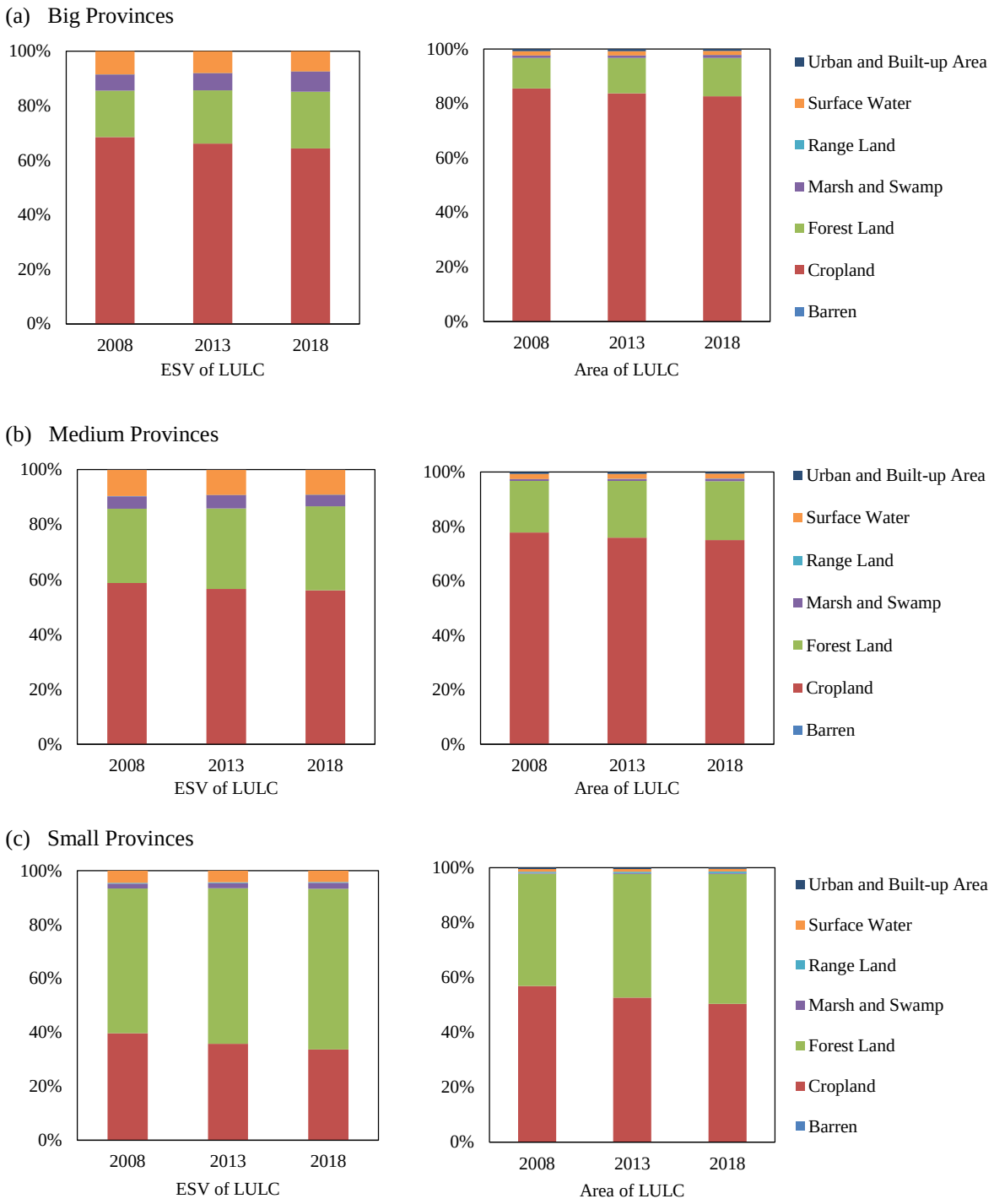

Figure 9. Ecosystem services value and area contribution of LULC categories in different years for big (a), medium (b), and small (c) provinces

Most of the studies on valuation of ecosystems services is concentrated on assessing and monetizing definitive ESVs at any particular stage (Costanza et al., 1997; G. Li & Fang, 2014;

G. Li et al., 2016). Even though time-based fluctuations in ESVs are equally important, observing alterations over an extended time period has hardly ever been done on regional, nationwide or global scales; still, this subject has fascinated intellectual consideration recently (Costanza et al., 2014; G. Li et al., 2016). Perhaps, Costanza et al. calculated that the worldwide damage of ESV since 1997 to 2011 triggered by land-use changes was US$4.3–20.2 trillion/year (Costanza et al., 2014). Su et al. (2012) researched that significant urban development caused a forfeiture of 8.5 billion RMB Yuan ecosystem-service amount per year since 1994 and 2003 in the Hang-Jia-Hu part of China (Su et al., 2012). Kreuter et al. (2001) testified a 4% total drop in the assessed yearly cost of ecosystem services amid 1976 and 1991 in San Antonio, the USA (Kreuter et al., 2001). Additionally, the amount of research based on this subject has increased quickly (Hu et al., 2008; G. Li et al., 2016; R.-Q. Li et al., 2007; Mamat et al., 2018; Ongsomwang et al., 2019; Sannigrahi et al., 2020; Zhao et al., 2004).

Northeast Thailand consists numerous national parks and possesses high biodiversity and native species (Lacombe et al., 2017). According to the LULC data gathered, it was found that areas of forest land increased in the ten years of the study period for all three sections, which mainly suggests that the entire region of Northeast Thailand saw an increase in forest land. Whereas in the study of Ratanopad and Kainz (2012) results showed that forest land had decreased. It can be argued that this study only focused on one province of the entire region of NET, making the results quite specific. While this study looked at a larger picture and therefore giving results that are slightly dissimilar. Additionally, from the LULC data, it was reported that cropland areas decreased overall for all three groups, suggesting that NET's cropland fell over the decade. Approximately 80% of the population of NET live in rural areas, mainly from agriculture and payments acknowledged from lots of permanent and seasonal migrants (Lacombe et al., 2017). This indicates that as majority of the population depend on agricultural land, and cropland being one of the main sources, it is quite likely that cropland areas might be exploited.

Moreover, the changes in ESVs of the land use categories varied according to their fluctuations in area. As the forest land area increased, its corresponding ESV value increased and similarly as cropland area decreased, its corresponding ESV value decreased. According to the data calculated the total ESV for all three sections increased from 2008 to 2018, meaning that ESV increased for entire NET. It was observed that the main LULCs that were responsible for the increase in ESVs were forest land and marsh and swamp. This was because of their high coefficient value in the region. Even though, cropland area was bigger than the area of forest land and marsh and swamp combined, its coefficient value was dramatically less than the other two LULC types combined (forest land and marsh and swamp). Since the coefficient value for forest land and marsh and swamp was high and their area as well increased over the study period, they eventually contributed more to the overall ESV.

A limitation from this study was the LULC information as it was derived from secondary data. The information given were restricted in terms of LULC classification, if they were given in more details, perhaps the data calculated could have been even more precise. In this study, ESV that were calculated surprisingly increased over the time period but it should be noted that the timeframe was only of ten years. Most of the other studies had a longer timeframe, therefore resulting in a decreasing ESV. Further studies can potentially elaborate on the year factor and then calculate ESVs to compare from this study. Additionally, the coefficient value of ecosystem services was taken from secondary data as well leading for the ESV data to have rough estimations. The coefficient value of ecosystem services for the particular region should be surveyed with more specification for individual LULC category when ESVs were calculated depending on the simple benefit transfer method.

Even with these limitations, according to the results found from this study, the increase in ESV suggest that the entire region has a great potential for land use and city planners to optimize the effect of LULC change on ESVs

during the planning process. If needed, they can divide the region into smaller sections so that planning process can be made easier with smaller areas. The planning should maintain a stability between ecosystem health and economic development so that ESVs should not decrease.

4. Conclusions

This study used the technology of geoinformatics to classify LULC data for calculating the LULC variation impact on ESVs in the entire region of Northeast Thailand. The impact that LULC changes had on ESVs remarkably fluctuated among the LULC categories according to the area and ESVs for individual LULC division over the decade from 2008 to 2018 for all three groups: big provinces, medium provinces and small provinces. It reported that for all three sections, areas of forest land increased remarkably: for big provinces from 6190.17 km^2 (11.19%) in 2008 to 7808.05 km^2 (14.12%) in 2018, for medium provinces from 15384.21 km^2 (18.97%) in 2008 to 17528.37 km^2 (21.62%) in 2018, and for small provinces from 12837.80 km^2 (40.85%) in 2008 to 14847.13 km^2 (47.24%) in 2018. Whereas, areas of cropland significantly reduced for all three groups: for big provinces from 47233.80 km^2 (85.45%) in 2008 to 45613.64 km^2 (82.52%) in 2018, for medium provinces from 62964.92 km^2 (77.66%) in 2008 to 60764.16 km^2 (74.95%) in 2018, and for small provinces from 17881.76 km^2 (56.89%) in 2008 to 15834.31 km^2 (50.38%) in 2018.

The total ESVs measurably increased over the decade for all three sections. For big and small provinces, the change in forest land and marsh and swamp greatly influenced the changes in the total ESVs in the study region. Their ESVs increased significantly: for big provinces, by approximately 200 million USD, while the overall ESVs increased by 101 million USD; for small provinces, by approximately 146 million USD, while the overall ESVs increased by 75 million USD. Whereas for medium provinces, the change in forest land alone greatly influenced the changes in the total ESVs in the study region. To conclude, the increase in ESV suggest that the entire region has a great potential for land use and city planners to optimize the effect of LULC change on ESVs during the planning process. Further studies would be suggested to discover future opportunities and include involvement strategies for a bigger study period.

Acknowledgements

This research project is supported by Mahidol University and the study was approved by the Institutional Review Board of Institute for Population and Social Research, Mahidol University (IPSR-IRB). The authors express their sincere gratitude to the Faculty of Graduate Studies and Graduate Studies of Mahidol University Alumni Association for partially funding the research. Furthermore, the authors would like to thank the reviewers for their valuable comments to improve the manuscript.

References

Al-Shalabi, M., Billa, L., Pradhan, B., Mansor, S., & Al-Sharif, A. A. A. (2013). Modelling urban growth evolution and land-use changes using GIS based cellular automata and SLEUTH models: the case of Sana'a metropolitan city, Yemen. *Environmental Earth Sciences*, *70*(1), 425-437.

Chuai, X., Huang, X., Wu, C., Li, J., Lu, Q., Qi, X., … Lu, J. (2016). Land use and ecosystems services value changes and ecological land management in coastal Jiangsu, China. *Habitat International*, *57*, 164–174.

Costanza, R. (2012). Ecosystem health and ecological engineering. *Ecological Engineering*, *45*, 24-29.

Costanza, R., D'Arge, R., De Groot, R., Farber, S., Grasso, M., Hannon, B., … Van Den Belt, M. (1997). The value of the world's ecosystem services and natural capital. *Nature*, *387*(6630), 253-260.

Costanza, R., De Groot, R., Sutton, P., Van Der Ploeg, S., Anderson, S. J., Kubiszewski, I., … Turner, R. K. (2014). Changes in the global value of ecosystem services. *Global Environmental Change*, *26*, 152–158.

Dewan, A. M., & Yamaguchi, Y. (2009). Land use and land cover change in Greater Dhaka, Bangladesh: Using remote sensing to promote sustainable urbanization. *Applied Geography*, *29*(3), 390-401.

Fisher, B., Turner, R. K., & Morling, P. (2009). Defining and classifying ecosystem services for decision making. *Ecological Economics*, *68*(3), 643-653.

Geymen, A., & Baz, I. (2008). Monitoring urban growth and detecting land-cover changes on the Istanbul metropolitan area. *Environmental Monitoring and Assessment*, *136*(1–3), 449-459.

Grimm, N. B., Morgan Grove, J., Pickett, S. T. A., & Redman, C. L. (2000). Integrated Approaches to Long-TermStudies of Urban Ecological Systems. *BioScience*, *50*(7), 571.

Henríquez, C., Azócar, G., & Romero, H. (2006). Monitoring and modeling the urban growth of two mid-

sized Chilean cities. *Habitat International*, *30*(4), 945-964.

Hu, H., Liu, W., & Cao, M. (2008). Impact of land use and land cover changes on ecosystem services in Menglun, Xishuangbanna, Southwest China. *Environmental Monitoring and Assessment*, *146*(1–3), 147–156.

Isan. (n.d.). In *Wikipedia*. Retrieved from https://en.wikipedia.org/wiki/Isan

Jin, M., Dickinson, R. E., & Zhang, D. L. (2005). The footprint of urban areas on global climate as characterized by MODIS. *Journal of Climate*, *18*(10), 1551–1565.

Johnston, R. J., & Russell, M. (2011). An operational structure for clarity in ecosystem service values. *Ecological Economics*, *70*(12), 2243-2249.

Kindu, M., Schneider, T., Teketay, D., & Knoke, T. (2016). Changes of ecosystem service values in response to land use/land cover dynamics in Munessa–Shashemene landscape of the Ethiopian highlands. *Science of The Total Environment*, *547*, 137-147.

Kreuter, U. P., Harris, H. G., Matlock, M. D., & Lacey, R. E. (2001). Change in ecosystem service values in the San Antonio area, Texas. *Ecological Economics*, *39*(3), 333–346.

Kumar, J. A. V., Pathan, S. K., & Bhanderi, R. J. (2007). *Spatio-temporal analysis for monitoring urban growth – a case study of Indore City*. *35*(1), 11-20.

Lacombe, G., Polthanee, A., & Trébuil, G. (2017). Long-term change in rainfall distribution in Northeast Thailand: Will cropping systems be able to adapt? *Cahiers Agricultures*, *26*(2).

Lambin, E. F., Geist, H. J., & Lepers, E. (2003). DYNAMICS OFLAND-USE ANDLAND-COVERCHANGE INTROPICALREGIONS. *Annual Review of Environment and Resources*, *28*(1), 205-241.

Li, G., & Fang, C. (2014). Global mapping and estimation of ecosystem services values and gross domestic product: A spatially explicit integration of national 'green GDP' accounting. *Ecological Indicators*, *46*, 293–314.

Li, G., Fang, C., & Wang, S. (2016). Exploring spatiotemporal changes in ecosystem-service values and hotspots in China. *Science of The Total Environment*, *545–546*, 609-620.

Li, R.-Q., Dong, M., Cui, J.-Y., Zhang, L.-L., Cui, Q.-G., & He, W.-M. (2007). Quantification of the Impact of Land-Use Changes on Ecosystem Services: A Case Study in Pingbian County, China. *Environmental Monitoring and Assessment*, *128*(1–3), 503–510.

López, E., Bocco, G., Mendoza, M., & Duhau, E. (2001). Predicting land-cover and land-use change in the urban fringe. *Landscape and Urban Planning*, *55*(4), 271-285.

Luederitz, C., Brink, E., Gralla, F., Hermelingmeier, V., Meyer, M., Niven, L., … Von Wehrden, H. (2015). A review of urban ecosystem services: six key challenges for future research. *Ecosystem Services*, *14*, 98-112.

Mamat, A., Halik, Ü., & Rouzi, A. (2018). Variations of Ecosystem Service Value in Response to Land-Use Change in the Kashgar Region, Northwest China. *Sustainability*, *10*(1), 200.

Mccarthy, M. P., Best, M. J., & Betts, R. A. (2010). Climate change in cities due to global warming and urban effects. *Geophysical Research Letters*, *37*(9), n/a-n/a.

Millennium Ecosystem Assessment (MA). (2005). *Ecosystem and Human Well-being: Synthesis*. Washington DC: Island Press.

Ongsomwang, S., Pattanakiat, S., & Srisuwan, A. (2019). Impact of Land Use and Land Cover Change on Ecosystem Service Values: A Case Study of Khon Kaen City, Thailand. *Environment and Natural Resources Journal*, *17*(4), 43-58.

Peng, J., Liu, Y., Wu, J., Lv, H., & Hu, X. (2015). Linking ecosystem services and landscape patterns to assess urban ecosystem health: A case study in Shenzhen City, China. *Landscape and Urban Planning*, *143*, 56-68.

Ratanopad, S., & Kainz, W. (2012). Land Cover Classification and Monitoring in Northeast Thailand Using Landsat 5 Tm Data. *International Archives of Photogrammetry, Remote Sensing, and Spatial Information Sciences*, *36*(2), 137–144.

Regional Land Cover Monitoring System Methodology [Online]. (n.d.). Retrieved from https://rlcms-servir.adpc.net/en/method/

Sannigrahi, S., Bhatt, S., Rahmat, S., Paul, S. K., & Sen, S. (2018). Estimating global ecosystem service values and its response to land surface dynamics during 1995–2015. *Journal of Environmental Management*, *223*, 115-131.

Sannigrahi, S., Chakraborti, S., Joshi, P. K., Keesstra, S., Sen, S., Paul, S. K., … Dang, K. B. (2019). Ecosystem service value assessment of a natural reserve region for strengthening protection and conservation. *Journal of Environmental Management*, *244*, 208-227.

Sannigrahi, S., Joshi, P. K., Keesstra, S., Paul, S. K., Sen, S., Roy, P. S., … Bhatt, S. (2019). Evaluating landscape capacity to provide spatially explicit valued ecosystem services for sustainable coastal resource management. *Ocean and Coastal Management*, *182*(February), 104918.

Sannigrahi, S., Zhang, Q., Joshi, P. K., Sutton, P. C., Keesstra, S., Roy, P. S., … Sen, S. (2020). Examining effects of climate change and land use dynamic on biophysical and economic values of ecosystem services of a natural reserve region. *Journal of Cleaner Production*, *257*, 120424.

Sawut, M., Eziz, M., & Tiyip, T. (2013). The effects of land-use change on ecosystem service value of desert oasis: a case study in Ugan-Kuqa River Delta Oasis, China. *Canadian Journal of Soil Science*, *93*(1), 99–108.

SERVIR Mekong. (n.d.). *Connecting Space to Village in the Lower Mekong Region* [Online]. Retrieved from https://servir.adpc.net/

Shiferaw, A., & Singh, K. . (2011). Evaluating The Land Use And Land Cover Dynamics In Borena Woreda South Wollo Highlands, Ethiopia. *Journal of Sustainable Development in Africa*, *2*(1).

Showqi, I., Rashid, I., & Romshoo, S. A. (2014). Land use land cover dynamics as a function of changing demography and hydrology. *GeoJournal*, *79*(3), 297–307.

Su, S., Xiao, R., Jiang, Z., & Zhang, Y. (2012). Characterizing landscape pattern and ecosystem service

value changes for urbanization impacts at an eco-regional scale. *Applied Geography, 34,* 295–305.

United Nations. (2010). *World urbanization prospects: The 2009 revision population database.* http://esa.un.org/unpd/wup/index.htm.

Wang, S., Wu, B., & Yang, P. (2014). Assessing the changes in land use and ecosystem services in an oasis agricultural region of Yanqi Basin, Northwest China. *Environmental Monitoring and Assessment*, *186*(12), 8343-8357.

Yan, Y., Zhao, C., Wang, C., Shan, P., Zhang, Y., & Wu, G. (2016). Ecosystem health assessment of the Liao River Basin upstream region based on ecosystem services. *Acta Ecologica Sinica*, *36*(4), 294-300.

Zhang, H., Qi, Z. fang, Ye, X. yue, Cai, Y. bin, Ma, W. chun, & Chen, M. nan. (2013). Analysis of land use/land cover change, population shift, and their effects on spatiotemporal patterns of urban heat islands in metropolitan Shanghai, China. *Applied Geography*, *44*, 121-133.

Zhao, B., Kreuter, U., Li, B., Ma, Z., Chen, J., & Nakagoshi, N. (2004). An ecosystem service value assessment of land-use change on Chongming Island, China. *Land Use Policy*, *21*(2), 139–148.

Evaluation of Petroleum Distribution Based on Well Logging and 3D Seismic Data of Ban Thi Oil Field in Fang Basin, Northern Thailand

Chanin Pattarakamolsen[a,b] and Kannipa Motanated[b*]

[a]*Northern Petroleum Development Centre, Fang, Chiang Mai 50110, Thailand*
[b]*Department of Geological Sciences, Faculty of Science, Chiang Mai University, Chiang Mai 50200, Thailand*

Abstract

Fang basin is the first oil field of Thailand located in Fang district, Chiang Mai province, northern Thailand. The basin can be divided into three zones, northern, central, and southern zones. Ban Thi oil field is in the central zone. The petroleum distribution of the field is evaluated from isoparametric maps. The reservoir layers are in Mae Sod formation, which is sandstone interbedded with shale and coal beds. Hydrocarbon appears in the sandstone under the coal bed. The well logging data (gamma-ray, resistivity, neutron porosity, and bulk density) are from five boreholes. The isoparametric maps are constructed from the pay thickness, shale volume (V_{sh}), total porosity (ϕt), effective porosity (ϕeff), hydrocarbon saturation (S_h), and water saturation (S_w) calculated from the well logging data. The boundary of the hydrocarbon zone is interpreted from 3D seismic data. From the isoparametric maps, wells located in the northwestern and southwestern zones have higher hydrocarbon saturation than those in the central zone. These findings correspond with the interpretation of hydrocarbon boundary from the seismic data. The total reservoir area is 1,144.422 acres (4.63 square kilometers), and the hydrocarbon-bearing reservoirs are distributed in the northwestern and southwestern zone. Therefore, the litho-saturation cross-plots and the isoparametric maps can be used to assess the hydrocarbon boundary, which is essential for well planning during the exploration and production phases.

Keyword: Isoparametric maps/ Hydrocarbon saturation/ Well logging/ 3D seismic

---

*Corresponding Author: Kannipa Motanated, Tel: +66-5394-3417
E-mail: kannipa.motanated@cmu.ac.th

1. Introduction

The geologic components and processes required for hydrocarbon generation and storage are different from one oil field to the others. As a result, the distribution of petroleum in an oil field depends on many factors such as rock and fluid properties and reservoir structure. The distribution of petroleum reservoir and reservoir boundary must be defined to have an economically efficient well planning and design (Ashraf, 2021). In the petroleum industry, the combination of well logging and 3D seismic data has been used to assess the reservoir characteristics and evaluate the petroleum potential (Anees and Ashraf, 2019). The reservoir quality could be determined from the volume of shale, total and effective porosity, hydrocarbon, and water saturation derived from well logging data (Ali, 2020 and Ali, 2021). The boundary of the hydrocarbon zone can be interpreted from 3D seismic data along with well log data.

This study aims to construct the isoparametric maps depicting the distribution of hydrocarbon zone and interpret the boundary of the hydrocarbon zone of the Ban Thi oil field in Fang basin. The previous study of Charoensrisomboon and Jankaew (2009) and Kongurai (2013) studied the geology of Fang basin including the lithostratigraphy using cutting and well log data in Mae sod formation and sedimentary facies in San Sai oil field by core and cutting data, respectively and Nantajun (2009) studied seismic stratigraphy in Mae Soon oil field by 3D seismic data. This study area is chosen because this oil field's hydrocarbon reservoir distribution and boundary have not previously been determined. The isoparametric maps depicting the distribution of hydrocarbon and the boundary of the hydrocarbon zone are useful for well design and drilling plans during the exploration and production phases.

Fang oil field located in Fang basin is the first oil field of Thailand. The Northern Petroleum Development Center, Defense Energy Department, Ministry of Defense is currently being explored and produced. The Fang basin is initiated by the collision between Shan-Thai and Indochina in Tertiary (Bunopas and Vella, 1983). Fang basin is a rift basin formed as a half-graben; a large fault line bounds the western rim of the basin. The basin is oriented in the NNE-SSW direction, 60 kilometers wide and 18 kilometers long, and the deepest part is around 2 kilometers (Settakul, 2009). The Fang basin was deposited in a fluvial-lacustrine environment. There are two main source rocks, one feeds Mae Soon and San Sai oil fields, and the other feeds Ban Thi and Pong Nok oil fields (Petersen, 2007). The Fang basin is divided into three zones, northern, central, and southern. The central zone has the highest production and contains eight oil fields, Mae Soon, Pong Nok, Nong Yao, San Sai, Ban Rai, Sam Jang, Pong Sai Kham, and Ban Thi. The study area is in the Ban Thi oil field located on the eastern side of the Fang basin (Figure 1).

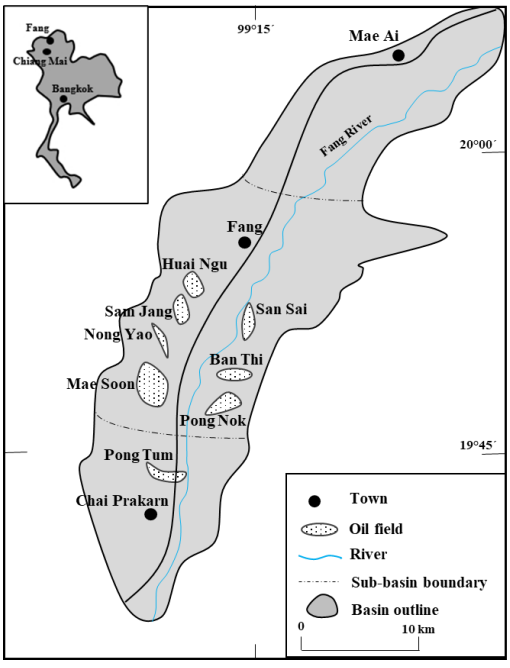

Figure 1. Lithostratigraphic column of BanThi oil field

The Ban Thi oil field is around 5 square kilometers and has two formations (Figure 2). The upper formation is the Mae Fang formation which is mostly unconsolidated sediments. The underlying formation is the Mae Sod formation which is interbedded sandstones and shale. Hydrocarbon is in the sandstone beneath the coal seam located at a depth of approximately 3,700 to 3,900 feet (Figure 2).

2. Methodology

This research aims to construct isoparametric maps from five borehole logging data (BT10, BT11, BT12, MP7, and MP8 boreholes) of the Ban Thi oil field and interpret hydrocarbon closure area 3D seismic data of Fang Basin. The methodology employed in this research is illustrated in the flowchart, as shown in Figure 3. The lateral distribution of hydrocarbon occurrence in the reservoir horizon will be studied and described through the isoparametric maps. The petrophysical parameters, including the pay thickness (ft), shale volume (V_{sh}), total porosity (ϕt), effective porosity (ϕeff), hydrocarbon saturation (S_h) and water saturation (S_w), will be calculated from well logging data (gamma-ray, resistivity, neutron porosity and bulk density) as explained in section 2.1. The volume of shale depicts the distribution of potential reservoir (sandstone reservoir). Moreover, the total porosity and effective porosity can indicate pore volume. Furthermore, the water saturation and hydrocarbon saturation refer to the hydrocarbon zones, which indicate whether an area is a good or bad reservoir. The zone of hydrocarbon distribution will be identified through the combination of these isoparametric maps.

The litho-saturation cross-plots (CPI) is a vertical distribution that presents the pay zone of hydrocarbon and water saturation in the reservoirs. The seismic horizons of interest are tracked to create a time structural map. Faults are indicated by breaks or abrupt termination of seismic reflection. The geometry and location of seismic markers (horizons and fault) combined with the vertical and lateral distribution of hydrocarbon zones could be used to identify the hydrocarbon boundary in the Ban Thi area.

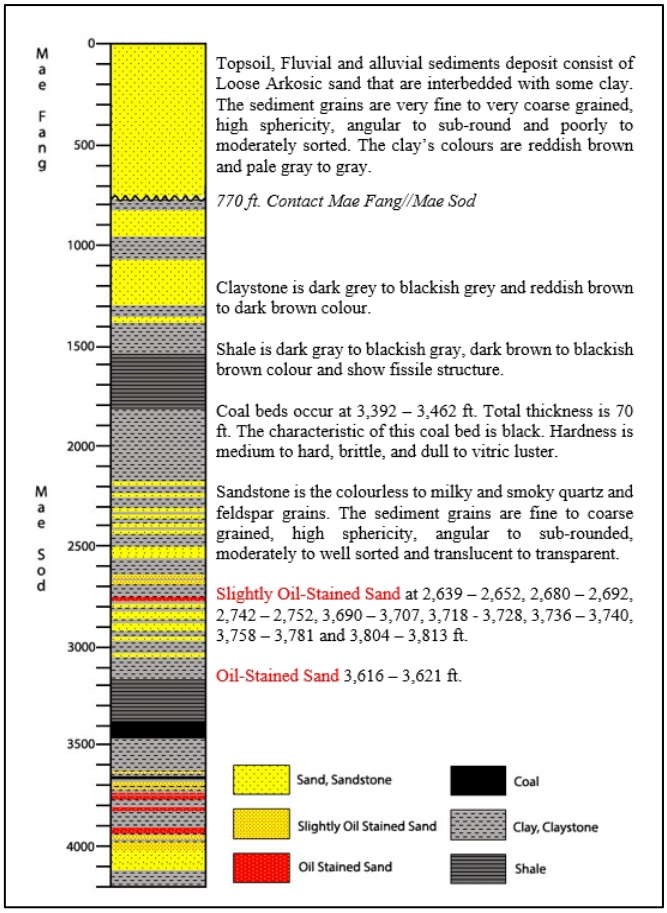

Figure 2. Central Fang oil field (Modified from Foopatthanakamol, 2008).

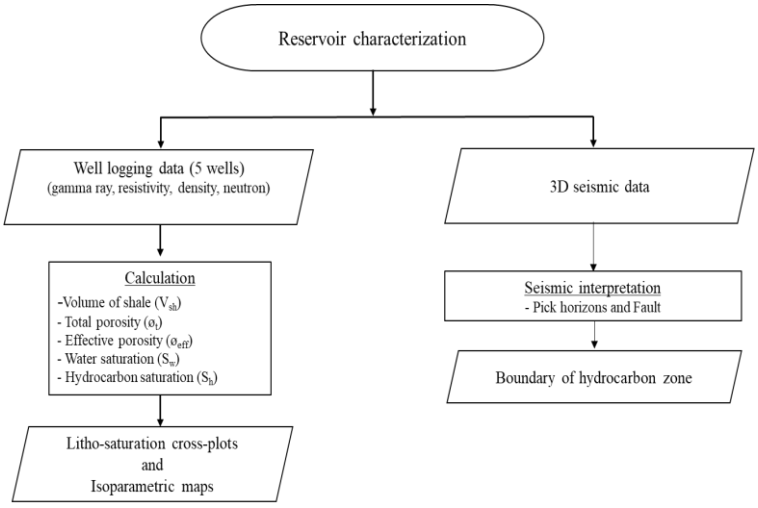

Figure 3. Methodology workflow

2.1. Lateral distribution of the petrophysical parameter

2.1.1 Shale volume (V_{sh})

Shale volume (V_{sh}) is a petrophysical parameter that can analyze the reservoir potential by distinguishing reservoirs from non-reservoir rocks. The following shale volume equation is determined by Larionov (1969):

$$V_{sh} = 0.083\left[2^{(3.7IGR)} - 1\right] \qquad (2.1)$$

$$IGR = \frac{GR_{log} - GR_{min}}{GR_{max} - GR_{min}} \quad (2.2)$$

IGR is the gamma-ray index. GR_{log} is the gamma-ray reading from the log, GR_{min} is the gamma-ray value of clean formation, and GR_{max} is the gamma-ray value of shale.

2.1.2 Determination of porosities (ϕ)

Porosity is the volume ratio of pore space to total volume in the formation. It means the hydrocarbon or other fluid fill in the pore of the formation. The porosity can be calculated from density porosity and neutron porosity.

2.1.2.1 Density porosity (ϕD)

The density porosity measures bulk density, which includes the density of rock and fluids enclosed in each formation's pore space. In clean and shaly formations, the density porosity can be determined by using the equation from Wyllie et al. (1958). The calculation of clean formations, the porosity value from density log (ϕD) is computed from the formula:

$$\emptyset D = \frac{\rho_{ma} - \rho_b}{\rho_{ma} - \rho_f} \quad (2.3)$$

Where; ρ_b is the formation bulk density, ρ_f is the fluid density (1.1 for salt mud, 1.0 for fresh mud, and 0.7 for gas), and ρ_{ma} is the matrix density (sandstone is 2.65 g/cm^3, limestone is 2.71 g/cm^3 and dolomite is approximately 2.87 g/cm^3). The calculation of shaly formations derived from the correction term is corrected for the presentation of shale.

$$\emptyset D = \left[\frac{\rho_{ma} - \rho_b}{\rho_{ma} - \rho_f}\right] \times V_{sh} \left[\frac{\rho_{ma} - \rho_{sh}}{\rho_{ma} - \rho_f}\right] \quad (2.4)$$

Where; ρ_{sh} is the density of shale.

2.1.2.2 Neutron porosity (ϕN)

Neutron logs detect the concentration of hydrogen, which is the composition of water, oil, and gas in pore spaces in the formation. Therefore, the neutron log is related to the porosity of the formation. In clean formation, porosity is filled with water or hydrocarbon, and the neutron log directly gives the porosity values (ϕN), which can be read directly from the well log data. In shaly formation, neutron porosity must be corrected by the shale effect. The neutron corrected can be computed using the equation from Allen et al. (1965):

$$\emptyset NC = \emptyset N_{log} - V_{sh} \times \emptyset_{sh} \quad (2.5)$$

Where; ϕNC is the neutron porosity corrected from shale effect, ϕ_{sh} is the neutron porosity for shale, V_{sh} is the volume of shale, and ϕN_{log} is the neutron porosity from the log. The crossover between density and neutron logs is commonly used to classify the zone of hydrocarbon and gas. Moreover, the crossplots between these two logs can be used to interpret the formation's lithology and mineral composition.

2.1.3 Total porosity (ϕt) and effective porosity (ϕeff)

The total porosity is the total void space, including isolated pores and the space occupied by clay-bound water. It is the pore volume per unit volume of rock measured in volume by volume, percent or porosity units. The total porosity (ϕt) is calculated by averaging the density porosity and neutron porosity (Allen et al., 1965):

$$\emptyset t = (\emptyset N + \emptyset D)/2 \quad (2.6)$$

Effective porosity determines the total volume of rock having connected void space, allowing the pore-filling fluids to flow into the drilling wells. The effective porosity is calculated by Allen's equation (1965) as follows:

$$\emptyset eff = \emptyset t \times (1 - V_{sh}) \quad (2.7)$$

2.1.4 Fluid saturation

The pore volume fractions occupied by water and hydrocarbon are termed water saturation and hydrocarbon saturation, respectively. Archie's formula (1942) is generally used to determine the water saturation (S_w) as follows:

$$S_w = \left(\frac{a}{\emptyset_t^m} \times \frac{R_w}{R_t}\right)^{1/n} \quad (2.8)$$

Where; ϕt is the formation porosity, a is the tortuosity exponent (1 for carbonate and 0.62 for sandstone). m is the cementation factor (2.0 for clean, 1.7-2.0 for shaly formation, and 2.0-2.5 for vuggy porosity). n is the saturation exponent (2.0 in clean and 1.8 (or less) for rocks with clayey matrix or fractures). R_w is the water resistivity and R_t is the formation resistivity. The Hydrocarbon saturation (S_h) is the reciprocal of water saturation, which is used to calculate oil or gas reserves. The total hydrocarbon saturation was determined as follows:

$$S_h = 1 - S_w \quad (2.9)$$

2.2 Litho-saturation cross-plot

The litho-saturation cross-plots are an indication of the vertical distribution of lithology and petrophysics parameters in each borehole. It was used to determine the accumulation zone of hydrocarbon that fills in the reservoir rock. The result from the petrophysics parameter (gamma-ray, resistivity, neutron porosity, and bulk density) will demonstrate the hydrocarbon saturation. For instance, the presence of hydrocarbon in most of each zone will show high r esistivity, more porosity, and low gamma-ray value that refer to the good reservoir zone.

2.3 Seismic interpretation

Seismic interpretation can depict the subsurface formations to extract and gain a better understanding of a basin's geological structure and stratigraphy, such as a fault trap, gas or oil pockets, salt dome, and structure termination style (onlap, toplap, downlap and offlap). After the reservoirs have been identified from the litho-saturation cross-plot, the reservoir formation is picked and traced on the seismic reflection data. The Ban Thi oil field has 50 inlines and 50 crosslines with 25 meters inline and crossline intervals and 4-millisecond sample intervals covering the study area of about 5 square kilometers. The locations of wells BT10, BT11, BT12, MP7, and M P8 are shown in Figure 4.

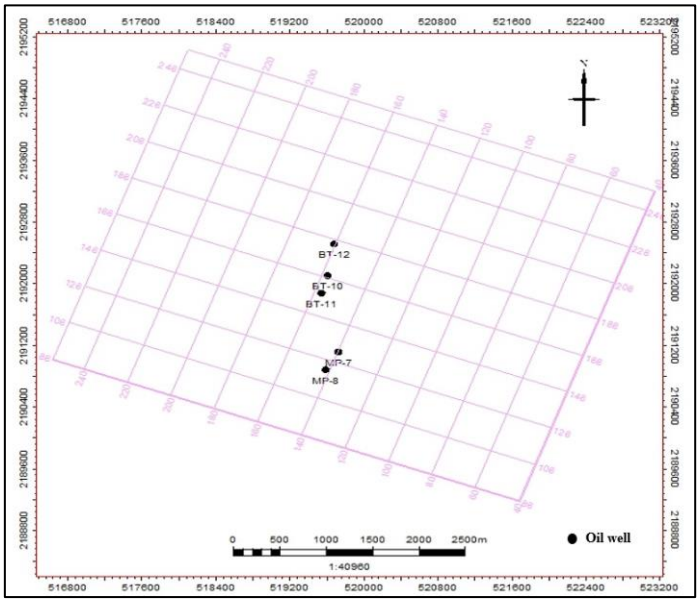

Figure 4. Base map of well locations in seismic line of Ban Thi Oil Field

3. Results

3.1 Lithology-saturation cross-plot

Lithology-saturation cross-plot shows the vertical lithology, water saturation, and hydrocarbon saturation of the Mae Sod formation. Figure 5 shows the cross-plots of BT10, BT11, BT12, MP7, and MP8 wells. The lower part of the Mae Sod formation below the coal bed has sandstone interbedded with shale. It is the main reservoir. The upper part of the Mae Sod formation consists of shale and less sandstone, but this zone's hydrocarbon saturation is negligible. The lithologic cross-section from the gamma-ray logs in the lower part of the Mae Sod formation shows the

intercalation of sandstone and shale. The low gamma-ray value refers to the thickness of the main reservoir in BT10, BT11, BT12, and MP7 wells as greater than MP8 wells. The high resistivity value and crossover of density and neutron show the hydrocarbon saturation.

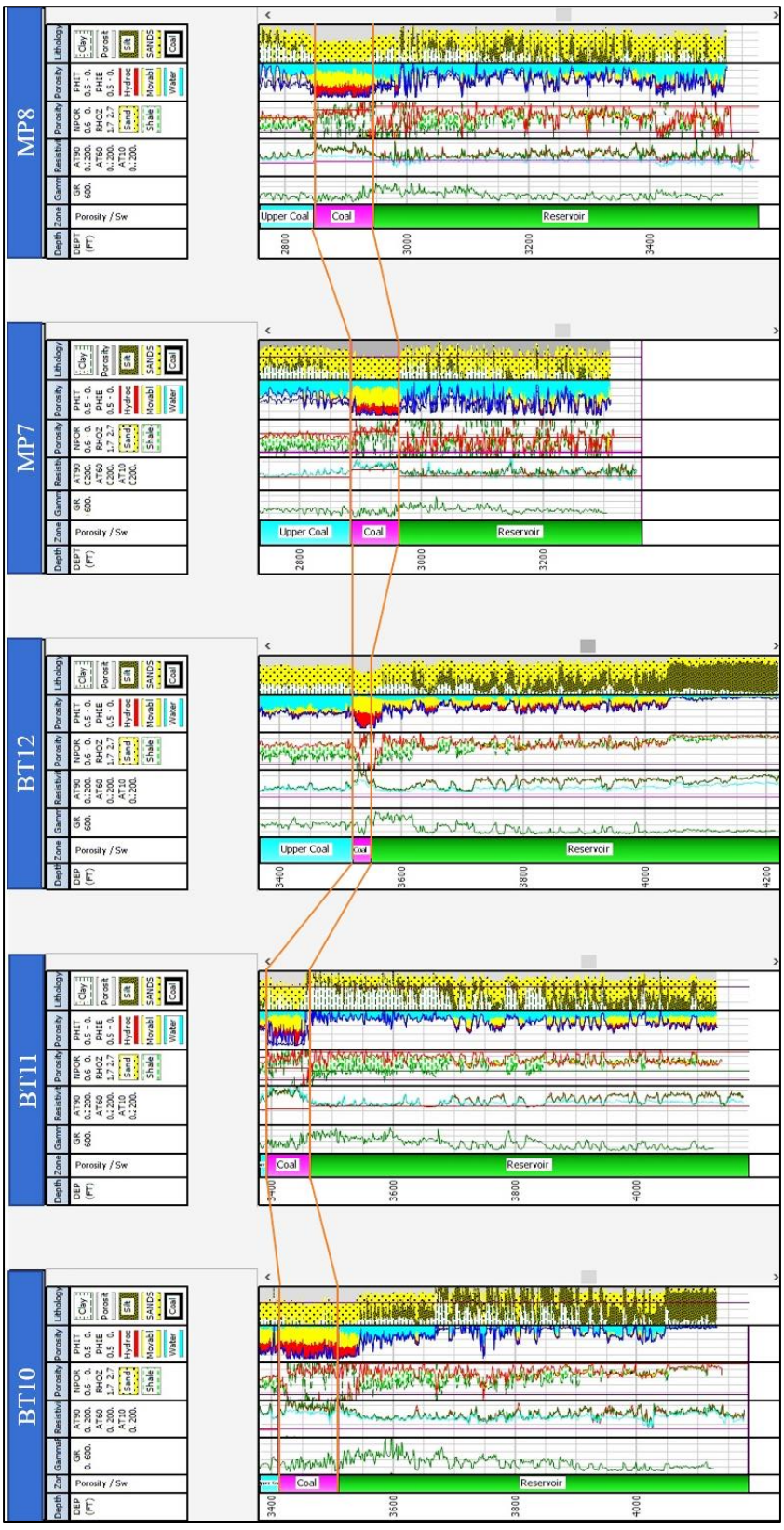

Figure 5. Lithology-saturation cross-plot of the study area

3.2 Formation evaluation

The pay thickness, shale volume (V_{sh}), total porosity (ϕt), effective porosity (ϕeff), hydrocarbon saturation (S_h) and water saturation (S_w) of all five wells are shown in Table 1. The isoparametric map illustrates the distribution of each parameter in this study area.

3.2.1 Pay thickness distribution map

The pay thickness distribution map of the Mae Sod formation reveals that the maximum thickness is 417.75 feet found in the BT12 well located in the northern zone, and the minimum thickness is 135 feet found in the BT10 well (Figure 6a). The thickness of the Mae Sod formation generally increases northwards.

3.2.2 Shale content

The shale content is highest in the northern zone at BT12 well, approximately 10.40% and the lowest shale content is 3.20% at BT10 well (Figure 6b). The shale content is generally increasing northwards and southwards from BT10 well.

Table 1. Pay thickness (ft) and averages shale volume (V_{sh}), total porosity (ϕt), effective porosity (ϕeff), hydrocarbon saturation (S_h), and water saturation (S_w) computed from the pay zone of each well.

Well	Pay thickness (ft)	V_{sh}	ϕt	ϕeff	S_w	S_h
BT-10	135	0.032	0.265	0.256	0.420	0.580
BT-11	269.75	0.038	0.213	0.205	0.213	0.787
BT-12	417.75	0.104	0.185	0.166	0.246	0.754
MP-7	135.25	0.100	0.344	0.310	0.344	0.656
MP-8	221.5	0.080	0.284	0.261	0.284	0.716

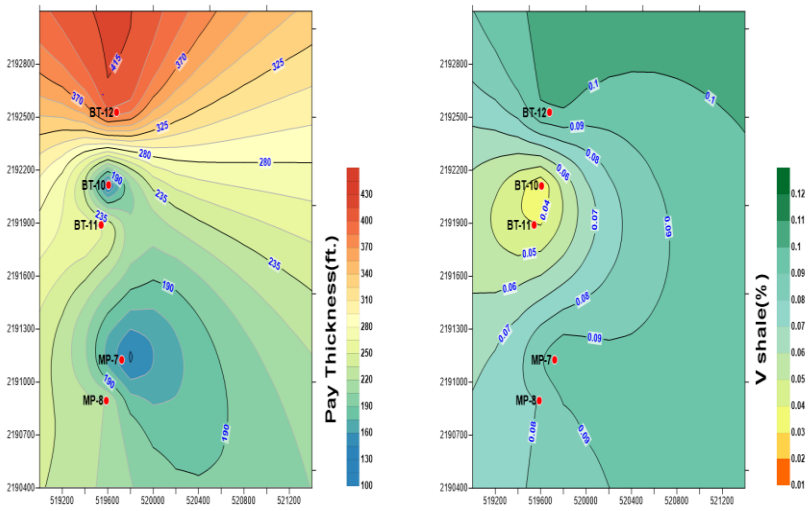

Figure 6. The pay thickness distribution map (a) and average shale content distribution map (b)

3.2.3 Porosity distribution map

Figure 7a shows the total porosity in the study area. The highest total porosity is 34.40%, found in the MP7 well located in the central zone. The northern zone has the lowest total porosity of 18.50% at BT12 well. The porosity in the southern zone in MP7 and MP8 wells is 34.40% and 28.40%, respectively. The effective porosity distribution is illustrated in Figure 7b, and the distributions of the total and effective porosities are similar. The maximum and minimum effective porosities are 31.10% in MP7 wells and 16.60% in BT12 wells.

3.2.4 Hydrocarbon saturation and water saturation distribution map

Figure 8 shows the distribution of hydrocarbon saturation and water saturation. The high-value hydrocarbon saturation is 78.70% found in BT11 well and 75.40% found in BT12 well. In the southern zone, there is still quite high saturation in MP7, and MP8 wells are

65.60% and 71.60%, respectively. In contrast, The BT10 well is a relatively lower hydrocarbon saturation than the other well is 58% which is the highest water saturation, 42%. The other well is quite low similar water saturation range from BT11, BT12, MP8, and MP7 are 21.30%, 24.60%. 28.40% and 31%, respectively.

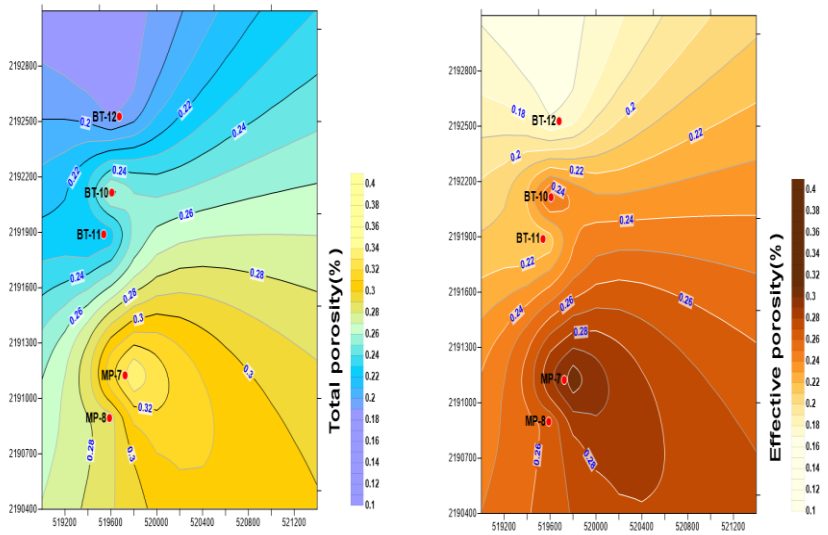

Figure 7. Total porosity (a) and effective porosity (b) distribution map

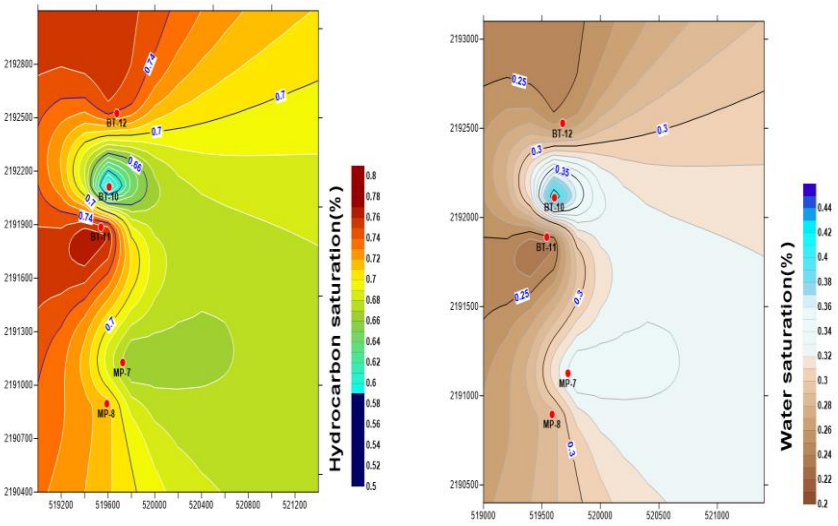

Figure 8. Average hydrocarbon saturation (a) and water saturation distribution map (b)

3.3 Seismic interpretation

An example of the seismic profile is shown in Figure 9. The pay horizon (red line) in the lower part of the Mae Sod formation is below the coal bed (blue). The time structural map is shown in Figure 10. The reservoir in the western part of the study area is deeper than the eastern part. Multiple faults are in the western and central parts; petroleum accumulation has filled near the fault lines, which is the nature of fault traps. However, the hydrocarbon is stratigraphically trapped in the eastern part, and the fault is rarely found. The distribution of petroleum proportion is 92.60% of Ban Thi oil field and 0.81% of Fang basin.

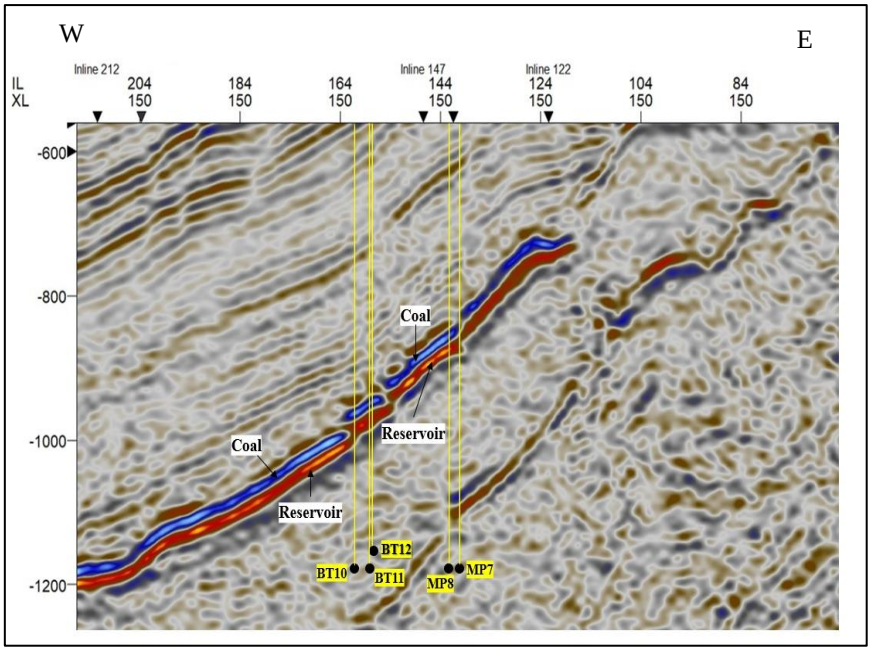

Figure 9. Seismic profile shows the well location, coal bed (blue) and reservoir (red) that present hydrocarbon accumulation of Ban Thi oil field.

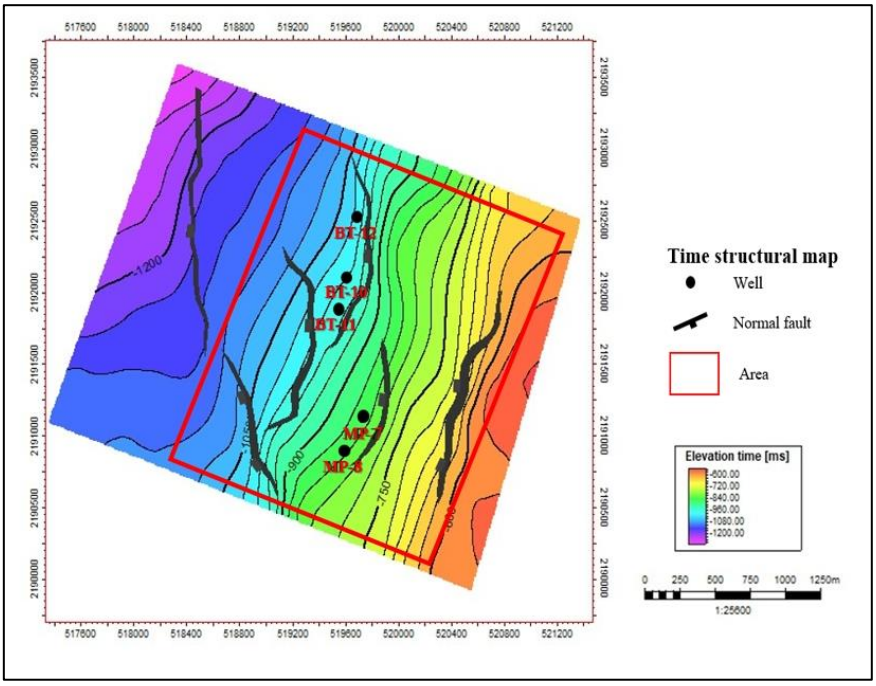

Figure 10. Time structural map of Ban Thi oil field (1,144.422 acres or 4.63 square kilometers).

4. Discussions

The litho-saturation cross-plots and the isoparametric maps show the distribution of the hydrocarbon zone. The boundary of the hydrocarbon zone is delineated from the seismic interpretation. The litho-saturation cross-plots show vertical distribution of rock which consists of unconsolidated sediment in the Mae Fang formation and show the reservoir zone in the Mae Sod formation. The hydrocarbon zone is in the lower Mae sod formation because of the high resistivity value and crossing over between density line and neutron line, which indicate hydrocarbon. The appearance of the hydrocarbon zone is under the coal bed, which

could indicate that the coal bed is the seal rock preventing further hydrocarbon migration.

The pay thickness is based on the shale content. When the shale content increases, the pay thickness decreases because it is the volume of shale in the formation; if the formation contains less shale, it becomes sandier. For instance, the pay thickness of the MP7 well located in the southern zone is 135.25 feet and has 10% shale content, and the MP8 well contains slightly less shale volume (8%) and has a thicker pay thickness (221.5 ft). This observation found in this study is not always true in all basins because the pay thickness depends on the total thickness related to the sedimentation rate. The water saturation is an important factor for the analysis of hydrocarbon zone because it distinguishes hydrocarbon zone from water zone.

The water saturation is influenced by two factors, including formation resistivity and porosity. The resistivity tends to show high values in the hydrocarbon zone and low values in the water zone. Besides, the fluid can accumulate in the pore space, so rock formation with high porosity has more space for fluid than those with lower porosity. On the seismic profiles, the reservoir horizon is the hydrocarbon zone under the coal bed. The depth of the hydrocarbon zone interpreted from the litho-saturation cross-plots from well-logging data has been converted to time (ms) to cross-check the hydrocarbon zone's depth determined from two types of data.

Combining the seismic data with the litho-saturation cross-plots and the isoparametric map can determine the boundary and distribution of the hydrocarbon, which are critical for well planning during the exploration and production phases. The northwestern and southwestern zones have high hydrocarbon saturation and faults that can trap the hydrocarbon. The future production wells should be in the southwestern zone around the MP08 well and the northwestern zone around BT12 well. In addition, the eastern zone of the study area should have more exploration wells to verify the existence of the hydrocarbon because there is one extensive fault line in this zone that could be a hydrocarbon trap.

5. Conclusions

The litho-saturation cross-plots of Ban Thi oil field in Fang basin show the hydrocarbon saturation under the coal bed in Mae sod formation. The petrophysics calculation can construct the isoparametric maps of the pay thickness, shale volume (V_{sh}), total porosity (ϕt), effective porosity (ϕeff), hydrocarbon saturation (S_h), and water saturation (S_w) and litho-saturation cross-plots. These are promising the good reservoir located in the northwestern and southwestern zones of the study area. The time structural map from the 3D seismic interpretation shows more fault structure traps in the west zone which the hydrocarbon can fill near the fault lines. The western area is a possibly new prospect for well drilling which has more saturation of hydrocarbon and good structure for hydrocarbon accumulation than the eastern area.

Acknowledgement

The Ministry of Defense of Thailand funds this research. We want to thank Petroleum Science and Technology Section, Petroleum Exploration and Production Division, Northern Petroleum Development Centre, Defense Energy Department for the data.

References

Ali, M., Jiang, R., Ma, H., Pan, H., Abbas, K., Ashraf, U., & Ullah, J. (2021). Machine learning-A novel approach of well logs similarity based on synchronization measures to predict shear sonic logs. Journal of Petroleum Science and Engineering, 203, 108602.

Ali, M., Ma, H., Pan, H., Ashraf, U., & Jiang, R. (2020). Building a rock physics model for the formation evaluation of the Lower Goru sand reservoir of the Southern Indus Basin in Pakistan. Journal of Petroleum Science and Engineering, 107,461.

Allen, L.S., Mills, W.R., and Goldwell, R.I. (1965). The effect of fluid invasion in pulsed neutron logging. Journal of Geophysics, 30, 339-449.

Anees, A., Wanzhong, S., Ashraf, U., Qinghai, X. (2019). Channel identification using 3D seismic attributes in lower Shihezi Formation of Hangjinqi area, northern Ordos Basin, China. Journal of Apply Geophysics, 63, 139-150.

Archie, G.E. (1942). The electrical resistivity log as an aid in determining some reservoir characteristics. Journal of Petroleum Technology, 5, 54-62.

Ashraf, U., Zhang, H., Anees, A., Mangi, H. N., Ali, M., Zhang, X., Imraz, M., Abbasi, S., Abbas, A., Ullah, Z., and Tan, S. (2021). A Core Logging, Machine Learning

and Geostatistical Modeling Interactive Approach for Subsurface Imaging of Lenticular Geobodies in a Clastic Depositional System, SE Pakistan. Natural Resources Research, 30, 2087-2830.

Ashraf, U., Zhu, P., Yasin, Q., Anees, A., Imraz, M., Mangi, H. N., & Shakeel, S. (2019). Classification of reservoir facies using well log and 3D seismic attributes for prospect evaluation and field development: A case study of Sawan gas field, Pakistan. Journal of Petroleum Science and Engineering, 175, 338-351.

Bunopas, S., and Vella, P. (1983). Opening of the gulf of Thailand: rifting of continental S.E. Asia and Late Cenozoic Tectonics; Journal of Geological Society. Thailand, 6, 1-12.

Charoensrisomboon, S., and Jankaew, K. (2009). Lithostratigraphy of Mae Sod Formation, Fang Basin, Changwat Chaing Mai. BEST, 2, 87-89.

Foopatthanakamol, A., Ratanasthien, B., Petersen, H. I., Wongpornchai, P., and Utamo, W. (2008). Composition and petroleum potential of lake facies in the FA-MA-48-73 well Mae Soon structure, Fang oilfield, Northern Thailand. Journal of Petroleum Geology, 31, 317-326.

Kongurai, P. 2013. Sedimentary facies and evolution of San Sai Oil Field, Fang Basin. M.S. dissertation, Suranaree University of Technology.

Larionov, V.V. 1969. Borehole radiometry. Moscow: Nedra.

Nuntajun, R. (2009). Seismic Stratigraphy of the Fang Basin, Chiang Mai, Thailand. Chiang Mai Journal of Science, 36, 77-82.

Petersen, H.I., Nytoft, H.P., Ratanasthien, B., and Foopatthanakamol, A. (2007). Oils from Cenozoic rift-basins in central and northern Thailand. Journal of Petroleum Geology, 40, 59-78.

Settakul, N. (2009). Fang Oilfield Development. Walailak Journal of Science and Technology, 6, 1-15.

Harnessing Water Quality Management through Environmental Education Approach (Case Study of LERD Project, Phetchaburi-Thailand)

Doris Ifeoma Ogueri*, Surat Bualert, Kasem Chunkao, and Onanong Phewnil

Department of Environmental Science, Faculty of Environment, Kasetsart University, Bangkok 10900, Thailand

Abstract

Although water is known as an integral part of the ecosystem with enormous importance to both flora and fauna, its pollution still remains one of the most predominant environmental issues globally with much emphasis in Thailand. Above all, water contamination is also associated with health impacts such as cholera, hepatitis A, dysentery among others. Therefore, the call for effective water management cannot be over-emphasized in order to facilitate the achievement of SDG 6 (to ensure the availability and sustainable management of water and sanitation for all by 2030). As a result of the aforementioned, this work focuses on the application of oxidation pond method of municipal wastewater treatment combined with environmental education in the management and improvement of water resources in Thailand. The LERD Project which was established by Late HRM King Bhumibol in Phetchaburi province of Thailand uses locally available resources in the treatment of municipal wastewater which results in efficiency rate of 50-70% with the capacity of treating 10,000cm^3 of wastewater daily. As a means to propagate the in-depth knowledge of this successful project to a wider audience and to achieve behavioral change, selected international school students and teachers were used as target group. The findings indicate that there was a significant difference in the students' environmental knowledge, attitudes, skills and behavior prior and after the program while the control group recorded no significant difference with p values of 0.569, 0.097, 0.250, and 0.864 respectively. 89% of the participants believe that environmental education is effective in water quality management.

Keyword: Environmental education/ Oxidation pond/ Wastewater/ Sustainable development goals/ Integrated approach/ Water quality

---

*Corresponding Author: Doris Ifeoma Ogueri
E-mail address: dorisogueri6@gmail.com

1. Introduction

The only known planet that can supports life is earth due to its availability of the basic requirements needed for adequate survival of living things such as water, carbon dioxide, oxygen and other gases. The depletion of earth's natural resources such as water, air, soil, trees, among others are therefore a major concern and mostly caused by man and its uncontrolled activities. However, water pollution has been identified as one of the most prevalent environmental problem especially in Thailand and its cause has been linked to over-population, lack of or inadequate wastewater treatment among others. This is in line with the report of UN-Water (2010) which indicates that in most low- and middle-income countries, wastewater is discharged directly into the sea or rivers without treatment. Another report by UNDP (2019) also states that 80 percent of wastewater goes into waterways without adequate treatment (UNDP, 2019). In congruence with the aforementioned, Sateinpong et al., (2014) identify the relationship between Thailand's water pollution problem with municipal wastewater generated from both daily domestic and industrial activities.

Notwithstanding the recent advancements made in wastewater treatment technologies globally, the ineffective and difficulty in implementation of theme still remain a huge concern. This is mostly associated to the high cost, lack of technical know-how as well as lack of maintenance. As a result of this, the decentralized, low-cost and natural processes have been proposed as alternatives to the modern sophisticated treatment processes (Giri et al., 2006). The Late King Bhumibol consequently established The King's Royally Initiated Laem Pak Bia Environmental Research

and Development (LERD) project which is located at Phetchaburi province to help in solving the environmental problems of solid waste and wastewater within the area. The knowledge was subsequently extended to other provinces as a result of its recorded success. The amount of daily water consumption in Phetchaburi Municipality is estimated as 60.55 liters per person and it was revealed that almost 95.06% of the wastewater is released into the water body which is the main cause of pollution in the Phetchaburi River (Sateinpong et al., 2014). The LERD project uses environmental-friendly methods known as nature-by-nature process to rehabilitate deteriorated natural resources (Kasem et al., 2014; LERD, 2019).

On the other hand, recent studies have highlighted the contribution of man's lack of knowledge of the consequences of his uncontrolled activities on the environment. Environmental education (EE) is therefore seen as a useful tool in eradicating some of the causes of environmental degradation. It is simply "a process that gives the public opportunity to explore environmental problems, engage in problem solving as well as participate in its improvement" (Alexandar & Poyyamoli, 2014; EPA, 2017). The awareness and sensitivity of the people towards environment and environmental problems will therefore promote making decisions that will protect the environment rather than hurting it. In order to meet up with the achievement of United Nations Sustainable Development Goal 6 (clean water and sanitation) which aims at ensuring availability and sustainable management of water and sanitation for all by the year 2030, a lot actions need to be carried out by all concerned. As a result of this, this study projects the harnessing of water quality improvement through combined approaches of wastewater treatment and environmental education (EE). To contribute effectively to this call to action, the LERD project therefore needs to be propagated to different target groups for proper understanding of wastewater, its suitable treatment method and contribution to water quality improvement.

2. Methodology

2.1 Study Location

The King's Royally Initiated Laem Phak Bia Environmental Research and Development (LERD) Project site is located at Laem Phak Bia sub-district, Ban Laem district of Phetchaburi province, west of Thailand near the Gulf of Thailand (latitude 130 02′40″ to 130 03′20″ N; longitude 1000 05′10″ to 1000 06′05″ E or UTM 1442240 to 1443480 N and 0617780 to 0619271 E). The 7,500 hectares project site was established in 1991 by the late King of Thailand, H.M. Bhumibol Adulyadej to help in solving the environmental problems of solid waste and wastewater within the area. The oxidation pond treatment system consists of a series of five shallow ponds occupying a land area of 154,178.5 m^2 with a total wastewater storage capacity of 20,000 m^3/day (Chaichana and Dampin, 2016; Kasem et al., 2014).

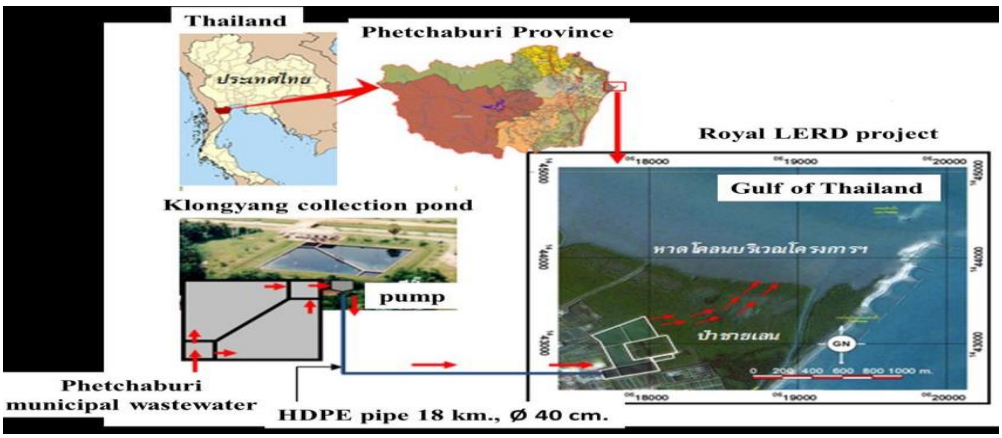

Figure 1. Laem Phak Bia Environmental and Research Development (LERD) Project site location (Source: Kasem et al., 2014).

2.2 Oxidation Pond System

The LERD oxidation pond system is arranged in series of five large, shallow earthen basins: one sedimentation pond, three oxidation ponds and one stabilization pond. The municipal wastewater (influent) from different point sources within Phetchaburi is discharged through the municipal sewerage to four different pumping stations, and then to Klongyang collection ponds. It is subsequently pumped through high density poly-ethylene (HDPE) pipe to cover a distance of 18.5km into the LERD site where it is drained into two separate lines; one to small wetlands and the other to 5-consecutive ponds. Importantly, the organic load of the wastewater is reduced during the transfer through the HDPE pipe by anaerobic organic digestion process (Kasem et al., 2014; LERD, 2019). An approximate of 10,000 m^3 of municipal wastewater is received by LERD daily. The natural purification processes occur in the pond within the 21-28 days retention period after which it is discharged after meeting up with the National wastewater quality standards.

2.3 Environmental Education Program

The environmental education program delivery was carried out in an international school located in the Lat Phrao District of Bangkok, Thailand (latitude: 13.8242°N and longitude: 100.6087°E or UTM 673760.92783706E and 1526575.1365599N). The first phase of the study was the assessment of LERD project oxidation pond process materials and other reviewed literature to identify the in-depth knowledge and derivation of the key principles. The second phase involved the assessment of the science curriculum of the study school. The in-depth knowledge analysis of the science curriculum helped to determine the suitable topics to fit in the program. Content analysis approach which is used in research to draw out desired words, variables or topics from texts as described by (Ozdashli, 2015) was applied to determine the related topics from the curriculum. Subsequently, the key findings extracted from the first phase were infused into the related water quality topics in the school curriculum to develop the instructional materials. Finally, assessment of the environmental awareness level of the students and their knowledge of wastewater treatment was carried out through a questionnaire approach prior to the program implementation.

The environmental education program was later delivered to the students by workshop, discussion and observation and PowerPoint presentation approaches. A total of 50 students aged between 11 to 15 years (Grades 6 to 8) participated in the study and posttest survey was conducted at the end of the program which lasted for 5 days (5 hours in all). In conclusion, descriptive statistical analysis was applied to extract the program impacts on the students.

3. Results

3.1 Simplification of the oxidation pond process key ideas

Some of the key ideas extracted from the in-depth analysis of the LERD oxidation pond knowledge includes the following; water pollution, community wastewater treatment, oxidation pond process and water quality improvement (Figure 2). They were used in the formulation of the environmental education program.

The results of the wastewater quality parameters analyzed at various stages of the treatment process are shown on Table 1.

3.2 Content analysis of the school's science curriculum

Through content analysis of the in-depth knowledge of the science curriculum of the international school, the key topics that have environmental contents were extracted. Fifteen different environmental topics were identified such as biodiversity, scientific processes, natural resources and others. The program perfectly fit into "water quality", "human impacts on the environment", "human use of water" topics, hence, the lesson was planned around them putting into consideration the age, cultural diversity, prior knowledge to science and other factors to achieve an effective and positive outcome at the end of the program.

Figure 2. Key ideas extracted from the oxidation pond process

Table 1. Water quality parameters of the oxidation pond system (Source: Kasem et al., 2014)

Ponds	Sample Stations	Water Quality Indicator (mg/L)							
		BOD	SS	Nitrate	Nitrite	Ammonia	TKN	Phosphate	Potassium
Klongyang	input	31.20	12.80	<0.01	0.013	<0.05	1.930	1.10	14.10
Collection Pond	output	45.07	17.73	0.067	0.013	<0.05	<0.05	3.03	15.77
Sedimentation	input	42.20	16.40	0.037	0.003	<0.05	0.657	2.27	10.57
Pond	output	21.50	21.87	0.153	<0.002	2.437	5.647	2.77	15.87
Oxidation Pond No.1	output	7.33	59.00	0.380	0.297	<0.05	<0.05	1.37	23.10
Oxidation Pond No.2	output	10.87	65.10	0.397	<0.002	<0.05	<0.05	1.37	18.87
Oxidation Pond No.3	output	8.50	38.17	0.137	0.018	<0.05	<0.05	1.07	22.87
Polishing Pond	output	16.40	54.90	0.177	0.006	<0.05	<0.05	0.43	26.60

3.3 Pre-Environmental Education Phase

This phase was to determine the level of environmental awareness, knowledge, attitude, skills and behavior among the students from the chosen school. Figure 3 shows the responses of the participants to the question, "who is responsible for taking care of the environment?"

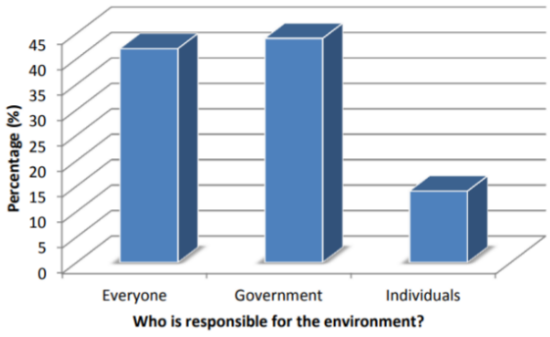

Figure 3. Who is responsible for taking care of the environment?

Figure 4 further shows their level of concern towards the state of the environment. A wide range of opinions from good to bad were recorded.

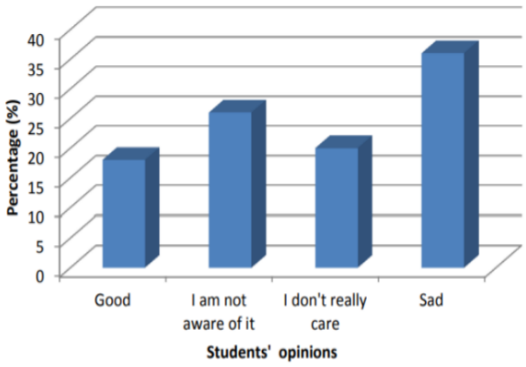

Figure 4. Students' opinions about the environmental issues

In order to ascertain the level of knowledge of the respondents towards wastewater prior to the program, questions about

the meaning of wastewater and its sources of generation were asked. Figure 5 shows the students; responses when asked if wastewater generated from their residential areas is treated. In general, the findings from the surveys carried out on the students prior to the program indicate that their environmental awareness, knowledge, attitudes, skills and behavior levels were low.

3.4 Post-Environmental Education Phase

Figure 6 indicates an improvement in all the environmental education objectives prior to and after the program. A high positive environmental learning impact was recorded at the end of the environmental education program. Majority of the students also reported that water quality can be improved through environmental education.

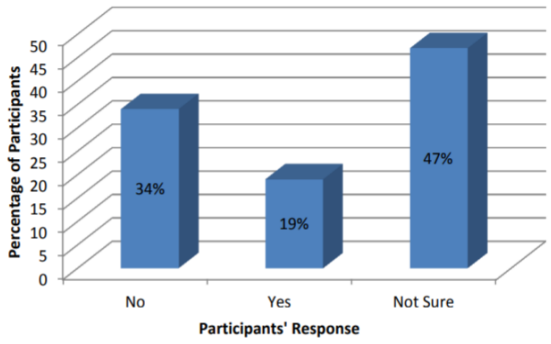

Figure 5. Awareness of the respondents on wastewater treatment within their area of residence

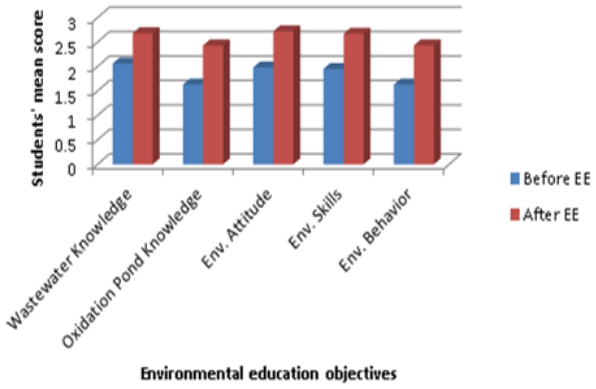

Figure 6. Comparison of Environmental Objectives' levels of the participants before and after the program

On the other hand, the results from the ten students who were used as the control group for the study and exempted from participating in the program indicate that there was no significant difference between the students' environmental knowledge, attitudes, skills and behavior prior and after the program. The recorded p values were all >0.05; environmental attitude, p=0.097; environmental skills, p=0.250; oxidation pond knowledge, p=0.569; wastewater knowledge, p=0.864 and environmental behavior, p=0.186.

4. Discussion

Some scientific topics like wastewater treatment are known to be abstract, complicated and therefore difficult to understand. As a result of this, the simplification of the oxidation pond method of municipal wastewater treatment is needed for easy understanding by the students and for attainment of learning outcomes. Most importantly, the integration of environmental education into existing subjects in the curriculum rather that teaching it as a separate subject is beneficial as indicated by Siddqui and Khan (2015). To buttress this point, Gunjan and Poonam (2017) emphasize that integration of environmental education into school curriculum by addressing respective topics through the lenses of different subjects is the most effective method of teaching environmental education in schools. This approach therefore offers a holistic opportunity in achieving effective understanding and experiences. Increase in environmental awareness, knowledge and attitudes among the students are more assured through this approach. As a result of the above mentioned, the integration of the extracted key ideas from the LERD oxidation pond process into the related environmental topics in the curriculum helped in the successful achievement of the environmental education program goals.

It is worthy to note that the efficiency rate of 50 to 70% (Table 1) was achieved at the end of the oxidation pond wastewater treatment process which is in accordance with the national wastewater quality standard. The Biological Oxygen Demand (BOD) concentration of the municipal wastewater was decreased by anaerobic organic digestion while the oxygen needed for the treatment processes in the ponds was supplied through both photosynthetic and thermo-siphon processes (Kasem et al., 2014). Therefore, knowledge of the LERD oxidation

pond project is very important as it is also an environmentally friendly method which utilizes the microbial communities of bacteria, viruses, fungi and protozoa to operate (Butler et al., 2017). However, the positive effects of the wastewater treatment include health, economic and environmental benefits. For instance, the project has helped in the improvement of the water quality of Phetchaburi River basin which on the other hand contributed to improved aquatic lives and livelihood of the people in general. According to Sateinpong et al. (2014), there is improved yield recorded by the fishermen and overall biodiversity richness. Hence, the approach of making the students to understand the meaning, causes and consequences of water pollution before going into details of how to treat wastewater by oxidation pond method and finally what roles they can play to contribute to water quality improvement is imperative. This concept made them to feel at home and well engaged with the topic. They were also able to relate it to their daily activities easily.

It can be clearly seen that there was no significant difference between the before and after data generated from the students' control group so it can be inferred that without the exposure to the program, the students' environmental attitudes, knowledge, skills and behavior levels remained unchanged. However, the significant difference recorded among the participants' group support the idea that environmental knowledge and awareness promote environmental behavior (Geiger et al., 2018; Hoang & Kato, 2016; Otto & Pensini, 2017). It can hence be deduced that it is a powerful tool to use in promotion of environmental knowledge and awareness and aids in promoting environmental protection.

5. Conclusions

The integrative approach was used in the delivery of the environmental education program of transferring the knowledge of oxidation pond method of wastewater treatment to international school students from a selected school in Thailand. As Loubser et al. (2014) argued, integration of environmental education in school subjects helps in achievement of long-term program outcome among learners. In line with this study, the program was therefore successfully integrated into the science subject by identifying water quality related topics. In this regard, the findings revealed there were significant improvements among the students after the program. The knowledge and importance of oxidation pond method was easily understood by the participants and their respective roles in water quality improvement was clearly understood. Most importantly, the eagerness to help propagate the knowledge among their families and friends was inspired through this program. Therefore, water quality management can be harnessed globally and in Thailand in particular by combined approach of environmental education and wastewater treatment for more effective outcome and achievement of United Nations Sustainable Development Goal 6 (Clean water and sanitation for all).

Acknowledgement

The authors wish to thank the Department of Environmental Science, Kasetsart University, Bangkok, Thailand and most especially The King's Royally Initiated Laem Pak Bia Environmental Research and Development (LERD) project, Thailand for sponsoring this work.

References

Alexandar, R., & Poyyamoli, G. (2014). The effectiveness of environmental education for sustainable development based on active teaching and learning at high school level-a case study from Puducherry and Cuddalore regions, India. The Journal of Sustainability Education, 7.

Butler E., Hung, Y., Al Ahmad. M., Yeh, R., Liu, R. & Fu, Y. (2017). Oxidation pond for municipal wastewater treatment. Applied Water Science, 7:31-51.

Chaichana, R., & Dampin, R. (2016). Unialgal Blooms of Cyanobacteria in Oxidation Ponds of the King's Royally Initiated Laem Phak Bia Environmental Research and Development Project, Thailand, Environment Asia, 9(2).

EPA. (2017). United States Environmental Protection Agency. Available: https://www.epa.gov/education/what-environmental-education [Accessed on 20th Nov. 2021].

Geiger, S., Dombois, C., & Funke, J. (2018). The Role of Environmental Knowledge and Attitude: Predictors for Ecological Behavior Across Cultures? An Analysis of

Argentinean and German Students. Umweltpsychologie, 22(1), 69-87.

Giri, R., Takeuchi, J. & Ozaki, H. (2006). Biodegradation of domestic wastewater under the simulated conditions of Thailand. Water and Environment Journal, 20(3), 169-176.

Hoang, T., & Kato, T. (2016). Measuring the effect of environmental education for sustainable development at elementary schools: A case study in Da Nang city, Vietnam. Sustainable Environment Research 2, 26(6).

Kasem C., Wit T.; Paiboon P., Onanong P., Surat B., Kittichai D., Thanit P. & Chatri N. (2014). The King's Royally Initiated LERD Project on Community Wastewater Treatment through Small Wetlands and Oxidation Pond in Phetchaburi, Thailand. Modern Applied Science, Vol. 8, No. 5.

LERD. (2019). The King's Royally Initiated Laem Phak Bia Environmental Research and Development (LERD) Project Handbook, Phetchaburi Province, Thailand.

Loubser, C., Azlin, Y., Dreyer, J., & Azyyati, A. (2014). The effectiveness of environmental education workshops for teachers, learners and schools in Malaysia. Environmental Development Sustainability, 16, 1163-1176.

Otto, S., & Pensini, P. (2017). Nature-based environmental education of children: Environmental knowledge and connectedness to nature, together, are related to ecological behavior. Global Environmental Change, 47, 88-94.

Özdaşli, K. (2015). Positioning in Business Administration Education at Universities Established in 2006: A Content Analysis on Strategic Drivers and Curriculum. Procedia - Social and Behavioral Sciences, 174, 2926-2933.

Sateinpong, K., Wasin, I., Onanong, P., Anukorn, B., & Kasem, C. (2014). The Coastal Water Quality Change by Effluent Discharging from Phetchaburi Municipal Wastewater Treatment System: The King's Royally Initiated Environmental Research and Development Project, Phetchaburi province, Thailand. Environment and Natural Resources, 12(2), 56-65.

Siddqui, T., & Khan, A. (2015). Environmental education: An Indian perspective. Research Journal of Chemical Sciences, 5(1), 1-6.

UN-Water. (2010). Water quality and sanitation. UN-Water Decade Program on Advocacy and Communication. Available: https://www.un.org/waterforlifedecade/swm_cities_zaragoza_2010/pdf/01_water_quality_and_sanitation.pdf [Accessed on 10th Nov. 2021].

UNDP. (2019). United Nations Development Program [Online]. Available: https://www.undp.org/content/undp/en/home/sustainable-development-goals/goal-6-clean-water-and-sanitation.html [Accessed on 13th Nov. 2021].

The Distribution of Marine Debris within a Small *Zostera marina* Meadow

Gregory N. Nishihara[a,b*], Makoto Kabeyama[c], Dominic F. C. Belleza[d], and Makoto Ehama[e]

[a]*Organization for Marine Science and Technology, Nagasaki University, Japan*
[b]*Institute for East China Sea Research, Nagasaki University, Japan*
[c]*Faculty of Fisheries Science, Nagasaki University, Japan*
[d]*Graduate School of Fisheries and Environmental Sciences, Nagasaki University, Japan*
[e]*Fisheries Division, Shinkamigoto Town Office, Japan*

Abstract

Marine debris, which includes plastic debris and lost or abandoned fishing gear, has been negatively affecting coastal ecosystems for more than 50 years. We have been closely examining a seagrass ecosystem in Arikawa Bay, Nakadori Island, Nagasaki, Japan by collecting marine debris found within the seagrass meadow and in the barren sand surrounding the meadow. Over the course of the study period (2021 May to November), 117.2 $g \cdot m^{-2}$ of marine debris was collected, of which only 5.4% was collected from within the meadow. A multinomial analysis indicates that marine debris affects the coverage of seagrass and the probability of low coverage increases in the presence of marine debris. We hypothesize that the presence of marine debris is an additional factor that can lead to the degradation of seagrass ecosystems. We recommend that more research is needed to reveal the impacts of marine debris on seagrass ecosystems, given the sparsity of information regarding this environmental issue.

Keyword: Marine plastic/ Macrophyte/ Seagrass/ Coastal pollution /Marine litter/ Benthic ecosystems

---

*Corresponding Author: Gregory N. Nishihara
E-mail address: greg@nagasaki-u.ac.jp

1. Introduction

Marine pollution can be roughly divided into three categories; radioactive pollution, chemical pollution, and pollution caused by the release of solid objects into the ocean; mostly plastics such as containers and fishing gear (Kennish 1997). Marine debris, such as plastic debris and lost or abandoned fishing gear remains a contemporary topic. However, it is relevant to note that the negative effects that marine debris causes in the marine ecosystem was pointed out more than 50 years ago. One of the first reports that suggested the negative effects of plastic debris in marine ecosystems was Carpenter and Smith (1972), which demonstrated that small plastic particles occurred in the Atlantic Ocean (i.e., Sargasso Sea) and suggested the potential harm to marine organisms. By the late 1970s, the wide- ranging dispersal of marine debris was reported in the Pacific and Antarctic Oceans, and studies described how entanglement and ingestion of plastics caused death in many marine mammals and birds (Merrel 1980, Slip and Burton 1991). Although the effect of marine debris, especially plastic debris, on megafauna has been the focus of many studies (e.g., Roman et al. 2021), lost and abandoned fishing gear has been shown to entangle benthic primary producers (Angiolillo and Fortibuoni 2020) and micro plastics are suggested to negatively affect the growth of microalgae (Gao et al. 2021). Indeed, microplastics have been found to accumulate in seagrass meadows (Sanchez-Vidal et al. 2021) and plastic debris accumulate within the coastal mangrove forests (Martin et al. 2019, Kesavan et al. 2021) and we are only just beginning to examine the impacts of these materials on marine benthic ecosystems.

Seagrass ecosystems are widespread coastal ecosystems that provide a wide variety of ecosystem services, such as carbon absorption, sediment stabilization, and fisheries production (Deyanova et al. 2017, Duarte et al. 2013, Unsworth et al. 2019). Along the coastal regions of Southeast Asia, seagrasses such as *Thalassia hemprichii* and *Cymodocea serrulata* and *C. rotundata* are abundant (Fortes et al. 2018). Further north, along the Ryukyu Archipelago

(i.e., the islands extending from the southern tip of Kyushu Island to Yonaguni Island) seagrass taxa similar to those in Southeast Asia can be observed, although it remains the northern distributional limit for many taxa, especially *Enhalus acoroides*, *T. hemprichii*, *C. serrulata*, and *C. Rotundata* (Kuo et al. 2006). In the main islands of Japan, *Zostera marina* is the most frequently encountered species (Tanaka et al. 2009).

Throughout the world, seagrass ecosystems loss is accelerating (Waycot et al. 2009) with some species under the threat of extinction (Short et al. 2001). Although fine-scale maps of seagrass ecosystems in Southeast Asia are available (e.g., Fortes et al. 2018) information regarding the distribution of seagrasses in Japan remain vague at best (Tanaka et al. 2009). Nevertheless, the extent of seagrass (i.e., *Z. marina*) distribution in Japan is decreasing and the declines have been attributed to climate change as well as coastal water pollution (Terawaki et al. 2003). There is some progress in research regarding seagrass restoration in Japan; the management of environmental conditions, such as light and water quality and sand and water motion, are prerequisites for the expansion of seagrass meadows in Japan (Hiraoka et al. 2006).

Since May 2021, we have been investigating the effects of marine debris on the coverage of a small (ca. 1470 m^2) patch of seagrass (*Z. marina*) in Arikawa Bay, Nakadori Island, Nagasaki, Japan. We are interested in examining the negative effects of marine debris on seagrass ecosystems, since marine debris was hypothesized to increase stress and mortality of mangroves (Martin et al. 2019), and because southwestern Japan is a sink for a large quantity of marine debris that originates from the East China Sea (Lee et al. 2006, Kuroda et al. 2020). Although Sanchez-Vidal et al. (2021) show that seagrasses can trap marine debris, especially small plastic debris, and remove it from the water column, we hypothesized that through entrapment and removal of marine debris, seagrasses succumb to negative effects caused by entanglement, scouring and smothering. Therefore, as a first step into understanding the mechanisms that cause negative effects on seagrass ecology by marine debris, we examine the hypothesis that marine debris can influence the distribution of seagrasses in a well-defined coastal ecosystem.

2. Methodology

The study site is located in a small cove in Arikawa Bay, Nakadori Island, Nagasaki, Japan (32.9883°N, 129.1180°E). It is a small area well protected from wave energy by a seawall on its western edge. Surveys of marine debris and seagrass coverage were conducted once a month from 2021 May to November by skin-diving. Each monthly survey commenced by preparing 5 transects running north-south across the seagrass meadow during the first month (May) and increased to 11 transects thereafter. Each transects was 10 m apart during the first survey and 5 m apart thereafter. Photo quadrats were taken at 2 m intervals along each transect and the coverage of seagrass was given a rank of A to E, where A was for coverage estimated to range from 71% to 100%, B was for the range 41% to 70%, C was for the range 11 to 40%, D was for the range 1 to 11%, and E indicated no seagrass coverage (McKenzie, 2003). The result of this survey was modeled with a generalized additive model (GAM), assuming a multinomial distribution, and by applying a probit link-function. The response variable was the coverage rank and the predictors were the spatial coordinates of the quadrats.

Next, a survey independent of the transect surveys was conducted to assess the coverage of seagrass in the presence of marine debris. At most, five photo quadrats were taken in a haphazardly chosen location of the seagrass meadow, in areas of sand in the presence of marine debris, and in areas of the seagrass meadow in the presence of marine debris. The probability of seagrass coverage rank with respect to the type of marine debris was also analyzed assuming a multinomial distribution. In this case, the coverage rank was the response variable and type of marine debris was the predictor. The link-function was the probit function. The effect of the presence of marine debris on the probability of coverage rank was assessed using the difference in the expected log predictive probabilities (ELPD) of the model tested against the null model (Vehtari et al. 2017).

Finally, all observable marine debris were collected and classified into six categories: plastics, ropes and nets, metal debris, rubber debris, glass and ceramics, and textiles. Marine debris that was collected from the survey site were transported to the field lab, cleaned of organic matter, separated and dried prior to classification and measurement. Debris was measured to the nearest gram using an electronic scale and the density of marine debris found during the survey period is expressed with respect to the area of the seagrass meadow or sand.

All statistical analyses were done in R version 4.1.2 (R Core Team 2021) using Bayesian methods. A Student's t- distribution with 3 degrees-of-freedom, a location of 0, and a scale of 2.5, was used as the prior distribution for all parameters in the model. Four Markov chains were generated to produce at least 1000 effective samples. The chains and posterior distributions of all models were visually assessed.

3. Results

The total area of the survey site was 3740 m^2 and seagrass was detected in approximately 1470 m^2. The mean and standard deviation of spatial area for each coverage rank was, 35±19 m^2 for rank A, 110±34 m^2 for rank B, 216±97 m^2 for rank C, 664±158 m^2 for rank D, and 2534±484 m^2 for rank E. The multinomial GAM also indicated that the most likely rank to be observed at the study site was E and the next highest was D (Figure 1). Indeed, most of the seagrass were concentrated in the center of the survey site.

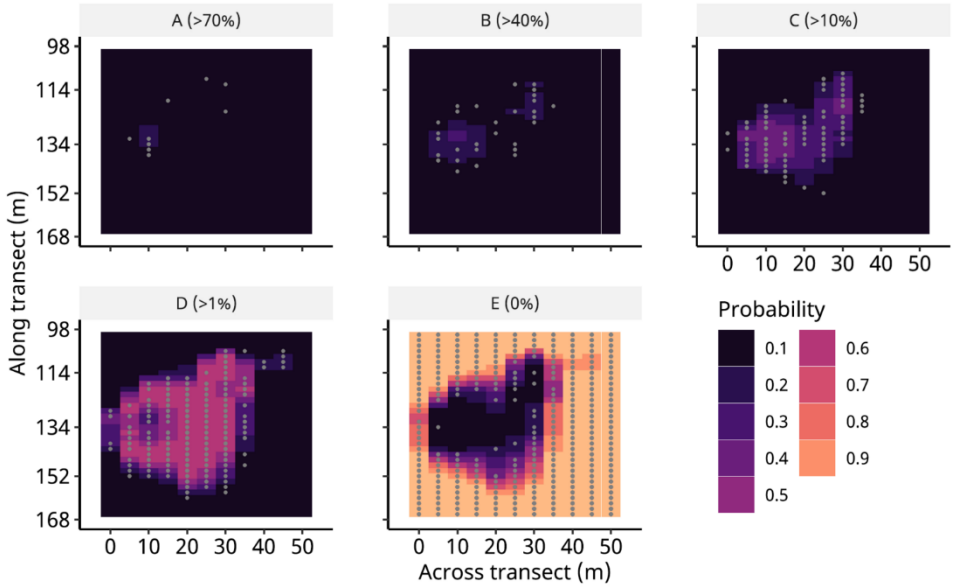

Figure 1. Multinomial model of seagrass coverage in a small *Zostera marina* meadow in Arikawa Bay, Nakadori Is., Nagasaki, Japan**.** Grey dots indicate a single quadrat with the appropriate coverage rank.

Over the survey period a total of 117.2 $g \cdot m^{-2}$ of marine debris was collected. A total of 110.7 $g \cdot m^{-2}$ was collected from the sand surrounding the seagrass meadow and only 6.5 $g \cdot m^{-2}$ was collected from within the meadow. Rope and nets associated with fishing gear was the most abundant type of marine debris (Figure 2) by mass. A total of 87.2 $g \cdot m^{-2}$ was collected from the study site, with the majority found in coverage rank E (i.e., sand). The next most abundant type of marine debris were glass and ceramics with a density of 10.1 $g \cdot m^{-2}$. Plastics debris, which includes plastic bags, plastic bottles, and large plastic fragments from household goods were the next most common type of debris in coverage rank E and the total density of plastics was 10.0 $g \cdot m^{-2}$. Metal debris, rubber debris, and discarded textiles were relatively less abundant by mass and ranged from 1.7 $g \cdot m^{-2}$ to 4.4 $g \cdot m^{-2}$

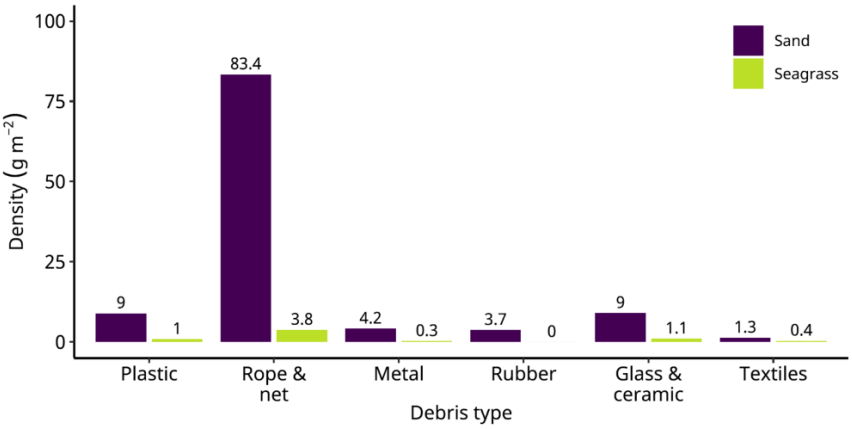

Figure 2. The total density of marine debris collected from the survey site during 2021 May to November.

A multinomial analysis of the transect-independent photo quadrat surveys revealed that at total of 133 pieces of debris were collected over the survey period (Figure 3A). Among which, plastics were the most common type of debris (71 items) while rope and nets (i.e., fisheries gear related debris) were the second most common (47 items). The model indicated that marine debris was an important factor that influenced coverage score (ΔELPD = -44.9±8.6) and that the probability of observing any type of marine debris was highest in coverage rank E (i.e., sand; Figure 3B). This contrasts with areas where no marine debris were observed, where coverage rank E occurred at relatively low probabilities.

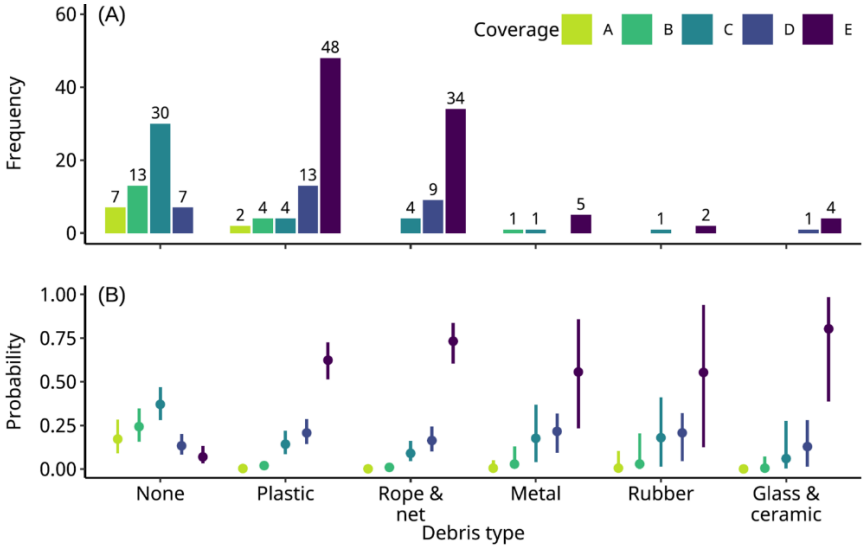

Figure 3. The (A) frequency of items observed in the survey site and (B) the multinomial model of the probability of coverage rank with respect to the presence of marine debris. None indicates no marine debris. The dots indicate the expected value and the vertical lines indicate the 95% highest density credible interval.

4. Discussion

The marine debris collected in and around the seagrass meadow of Arikawa Bay, Nagasaki, Japan was exclusively anthropogenic in origin. Approximately 86.1% of the collected marine debris by mass was plastic (i.e., plastic and rope and nets) or rubber, since the ropes and nets were all made of synthetic materials. It is difficult to compare our findings with past studies, since most studies of marine debris in coastal areas rely on the collection and identification of debris that are cast-up on shore (e.g., Fauziah et al. 2015) or focuses on the impact of microplastics on the benthos (e.g., Thushari et al. 2017). The

frequency of plastics observed in the seagrass meadow in our study, were similar to that of an intertidal coastal area in False Bay, South Africa, where plastics accounted for 31% to 78% by mass (Weiderman et al. 2020). Plastics were also the most common type of marine debris trapped by mangrove forests along the coastal areas of the Arabian Gulf (Martin et al. 2019) and in the mangrove regions of Mumbai, India where 62% of the trapped marine debris were plastic (Kesavan et al. 2021).

Nets and rope were the most abundant marine debris by mass and generally occurred in the areas where seagrasses were not found (i.e., coverage rank E), ropes and nets were also the most abundant type of debris found in areas where seagrasses were present, however there was one order of magnitude less material within the meadow (Figure 2). Indeed, there was systematically less marine debris within the seagrass meadow when compared to the adjacent barren areas of sand. Therefore, unlike Sanchez-Vidal et al. (2021), where seagrasses were effective in trapping micro-size plastic particles, macro-plastic debris and any other large debris in general are unlikely to be able to penetrate the canopy of a seagrass meadow, since the hydrodynamic regime can abruptly change near the vicinity of the canopy (Inoue et al. 2019). Near the canopy, water motion is deflected and reduced by canopy drag, and can lead to the settlement of large objects prior to entering the canopy interior (Abdolahpour et al. 2018). We can only speculate that marine debris can also cause seagrass loss in our study site because of the lack of historical data on the extent of seagrass cover in Arikawa Bay prior to the deposition of marine debris. A long term study would be needed to elucidate the mechanisms through which marine debris affects the seagrass meadow at our study site. However, manipulative experiments and field studies elsewhere have demonstrated the negative impacts of plastics on the surface of seagrass bed through shading (Fitzpatrick and Kirkman, 1995), facilitate the spread of invasive species (Menicagli et al. 2021) or by altering biogeochemical processes when buried in the sediment (Green et al. 2015, Balestri et al. 2017). Nevertheless, our analysis indicates that in the presence of marine debris, the probability that seagrasses are present is low (Figure 2 and Figure 3). Here, we provide a few hypotheses that remain to be explored.

The presence of nets, ropes, and plastic bags may interfere with seagrass shoot expansion, rooting of new seedlings, and nutrient flux to and from the sediment by preventing the ingress of rhizoids into barrens sandy areas and preventing the flow of materials to and from the sediment surface. The mechanisms through which marine debris, especially that of plastic bags and nets, affect seagrass ecology can be inferred from the use of plastic films (i.e., plastic mulch) used by the agricultural industry. Plastic films are widely used in the agriculture industry to prevent the growth of weeds through a combination of smothering and blocking sunlight, increasing soil temperature, and providing soil stabilization (Sintim and Flury 2017). We hypothesize that plastic bags and other plastic debris in a seagrass meadow can likewise prevent material flux and interfere with rhizoid expansion. Indeed, *Z. marina* rhizoids were often observed at the edges of buried nets but were not detected within net masses during our study. The effect of smothering and shading by plastic debris is supported by evidence that plastic accumulation in the root zone of mangroves causes stress and negatively affects tree survival (van Bijsterveldt et al. 2021). Alternatively, the removal of marine debris on the surface and those buried in the sediments can lead to the recovery and facilitate the expansion of seagrasses.

Marine debris especially ropes and plastic bags can also cause entanglement. Entanglement can increase the drag experienced by individuals and elevate the risk of dislodgement and structural failure. Discarded and abandoned fishing debris was shown to negatively impact benthic animal and coral communities (Yoshikawa and Asoh 2004, Angiolillo and Fortibuoni 2020), leading to necrosis and breakage. Although we did not conduct experiments to directly assess the effects of smothering or entanglement on seagrasses, the high probability of a rank E coverage in the presence of marine debris supports our belief that large marine debris can lead to the degradation of seagrass ecosystems.

5. Conclusion

More than 60% of marine debris is plastic (World Economic Forum 2016) and the economic cost of marine plastics on ecosystem services is believed to range from 3300 to 33,000 USD $ton^{-1}year^{-1}$ (Beaumont et al. 2019). Although research regarding the effect of microplastics on our ecosystems and the effects on marine debris on megafauna are increasing, very little is known about how plastics will affect the state of seagrass, mangrove, coral, and macroalgal ecosystems. Our study on the distribution of marine debris in a small seagrass meadow suggests that the accumulation of marine debris, especially persistent non-degradable plastics can be one factor in the degradation of these ecosystems.

We recommend that research regarding the impacts of marine debris on benthic ecosystems intensify and expand, so that we can continue to benefit from these important and productive coastal ecosystems.

Acknowledgement

We would like to thank Mr. Hamamura of the Arikawa Fisheries Cooperative for help in safely running the field work at Arikawa Bay. We would also like to thank the members in the Laboratory of Aquatic Plant Ecology for all of their hard-work in the field. This project was partially supported by the Grant-in-Aid for Scientific Research (B) JSPS KAKENHI Grant Number JP20H03076.

References

Abdolahpour, M., Ghisalberti, M., McMahon, K. and Lavery, P. S. 2018. The impact of flexibility on flow, turbulence, and vertical mixing in coastal canopies. Limnology and Oceanography (63), 2777–2792.

Aleksandarov, B. G., Minicheva, G. G., Strikalenko, T. V. 2002. Ecological aspects of artificial reef construction using scrap tires. Russian Journal of Marine Biology (28), 120–126.

Angiolillo, M. & Fortibuoni, T. 2020. Impacts of marine litter on Mediterranean reef systems: From shallow to deep waters. Frontiers in Marine Science (7), 581966.

Balestri, E., Menicagli, V., Vallerini, F., Lardicci, C. 2017. Biodegradable plastic bags oon the seafloor: A future threat for seagrass meadows? Science of the Total Environment (605-606), 755-763.

Beaumont, N.J., Aanesen, M., Austen, M.C., Börger, T., Clark, J.R., Cole, M., Hooper, T., Lindeque, P.K., Pascoe, C., Wyles, K.J., 2019. Global ecological, social and economic impacts of marine plastic. Marine Pollution Bulletin (142), 189–195.

van Bijsterveldt, C. E. J., van Wesenbeeck, B. K., Ramadhani, S., Raven, O. V., van Gool, F. E., Pribadi, R., Bouma, T. J. 2021. Does plastic waste kill mangroves? A field experiment to assess the impact of macro plastics on mangrove growth, stress response and survival. Science of The Total Environment (756), 142826.

Carpenter, E., & Smith, K. 1972. Plastics on the Sargasso Sea surface. Science (175), 1240-1241.

Deyanova, D., Gullström, M., Lyimo, L.D., Dahl, M., Hamisi, M.I., Mtolera, M. S. P., & Björk, M. 2017. Contribution of seagrass plants to CO_2 capture in a tropical seagrass meadow under experimental disturbance. PLOS ONE (12), e0181386.

Duarte, C. M., Losada, I. J., Hendriks, I. E., Mazarrasa, I. & Marba, N. 2013. The role of coastal plant communities for climate change mitigation and adaptation. Nature Climate Change (3), 961–968.

Fitzpatrick, J. & Kirkman, H. 1995. Effects of prolonged shading stress on growth and survival of seagrass *Posidonia australis* in Jervis Bay, New South Wales, Australia. Marine Ecology Progress Series (127), 279-289.

Fauziah, S.H., Liyana, I.A., & Agamuthu, P. 2015. Plastic debris in the coastal environment: The invincible threat? Abundance of buried plastic debris on Malaysian beaches. Waste Management & Research (33), 812–821.

Fortes, M. D., Ooi, J. L. S., Tan, Y.-M., Prathep, A., Bujang, J. Si., & Yaakub, S. M. 2018. Seagrass in Southeast Asia: a review of status and knowledge gaps, and a road map for conservation. Botanica Marina (61), 269-288.

Green, D. S., Boots, B., Blockley, D. J., Rocha, C., Thompson, R. 2015. Impacts of discarded plastic bags on marine assemblages and ecosystem functioning. Environmental Science and Technology (49), 5380-5389.

Gao, G., Zhao, X., Jin, P., Gao, K., & Beardall, J. 2021. Current understanding and challenges for aquatic primary producers in a world with rising micro- and nano-plastic levels. Journal of Hazardous Materials (406), 124685.

Hiraoka, K., Sugimoto, K., Miura, H., Terawaki, T., & Okada, M. 2006. Study on eelgrass (*Zostera marina* L.) bed restoration based on literatures and field experiment. Environmental Science (19), 241-248. in Japanese.

Inoue, Y., Terada R., Belleza, D. F. C., Nishihara G. N. 2020. Effect of water velocity on the physiology of a collapsing *Sargassum siliquastrum* canopy under a controlled environment. Phycological Research (68), 313-322.

Kennish, M. J. 1997. Practical Handbook of Estuarine and Marine Pollution. CRC Press, Bota Raton. pp. 554.

Kesavan, S., Xaiver, K. A. M., Deshmukhe, G., Jaiswar, A. K., Bhusan, S., Shukla, S. P. 2021. Anthropogenic pressure on mangrove ecosystems: Quantification and source identification of surficial and trapped debris. Science of the Total Environment (794), 148677.

Kuroda, M., Ichida, K., Tokai, T., Miyamoto, Y., Imai, K., Yagi, M., Yamanaka, Y., Mituhashi, T. 2020. The

current state of marine debris on the seafloor in offshore area around Japan. Marine Pollution Bulletin (161), 111670.

Lee, D.-I., Cho, H.-S., Jeong, S.-B. 2006. Distribution characteristics of marine litter on the sea bed of the East China Sea and the South Sea of Korea. Estuarine, Coastal and Shelf Science (70), 187-194.

Martin, C., Almahasheer, H., Duarte, C. M. 2019. Mangrove forests as traps for marine litter. Environmental Pollution (247), 499-508.

McKenzie, L. J. 2003. Guidelines for the rapid assessment and mapping of tropical seagrass habitats. (QFS, NFC, Cairns), 46 pp.

Menicagli, V., Balestri, E., Vallerini, F., De Battisti, D., Lardicci, C. 2021. Plastics and sedimentation foster the spread of non-native macroalga on seagrass meadows. Science of the Total Environment (757), 143812.

Merrell, T. 1980. Accumulation of plastic litter on beaches of Amchitka Island, Alaska. Marine Environmental Research (3), 171-184.

Roman, L., Schuyler, Q.,Wilcox, C., & Hardesty, B. D. 2021. Plastic pollution is killing marine megafauna, but how do we prioritize policies to reduce mortality? Conservation Letters (14), e12781.

R Core Team. 2021. R: A language and environment for statistical computing. R Foundation for Statistical Computing, Vienna, Austria. URL https: / / www. R-project.org/.

Sanchez-Vidal, A., Canals, M., de Haan, W.P., Romero, J., & Veny, M. 2021. Seagrasses provide a novel ecosystem service by trapping marine plastics. Scientific Reports (11), 254.

Sintim, H. Y. & Flury, M. 2017. Is biodegradable plastic mulch the solution to agriculture' s plastic problem? Environmental Science & Technology (51), 1068-1069.

Slip, D., & Burton, H. 1991. Accumulation of fishing debris, plastic litter, and other artefacts, on Heard and Macquarie Islands in the Southern Ocean. Environmental Conservation (18), 249-254.

Tanaka, N., Aida, S., Akaike, S., Aramaki, H., Chiyukubo, T., Chow, S., Fujii, A., Fujiwara, M., Ikeuchi, H., Ishii, M., Ishikawa, R., Ito, H., Kudo, T., Muraoka, D., Nagahama, T., Nambu, T., Okumura, H., Oshino, A., Saigusa, M., Shimizu, Y., Suwa, T., Suzuki, K., Takeda, K., Tanada, N., Tanimoto, T., Tsuda, F., Urabe, S., Yatsuya, K., Yoshida, G., Yoshimatsu, T., Yoshimitsu, S., Yoshimura, K., Morita, K., Saitoh, K.. 2009. Distribution of Zostera species in Japan. I. *Zostera marina* L. (Zosteraceae). Bulletin of the National Museum of Nature and Science. Series B (35), 23-40.

Terawaki, T., Yoshikawa, K., Yoshida, G., Uchimura, M., Iseki, K. 2003. Ecology and restoration techniques for *Sargassum* beds in the Seto Inland Sea, Japan. Marine Pollution Bulletin (47), 198-201.

Thushari, G. G. N., Senevirathna, J. D. M., Yakupitiyage, A., & Chavanich, S. 2017. Effects of microplastics on sessile invertebrates in the eastern coast of Thailand: An approach to coastal zone conservation. Marine Pollution Bulletin (124), 349–355.

Unsworth, R. K. F., Nordlund, L. M. & Cullen-Unsworth, L. C. 2019. Seagrass meadows support global fisheries production. Conservation Letters (12), e12566.

Vehtari, A., Gelman, A., and Gabry, J. 2017. Practical Bayesian model evaluation using leave-one-out cross-validation and WAIC. Statistics and Computing (27), 1413–1432.

Weideman, E. A., Perold, V., Omardien, A., Smyth, L. K., Ryan, P. G. 2020. Quantifying temporal trends in anthropogenic litter in a rocky intertidal habitat. Marine Pollution Bulletin (160), 111543.

World Economic Forum, 2016. Ellen MacArthur Foundation and McKinsey & Company, The New Plastics Economy - Rethinking the Future of Plastics.

Yoshikawa, T. & Asoh, K. 2004. Entanglement of monofilament fishing lines and coral death. Biological Conservation, (117), 557-560.

The Spatiotemporal Change Features of Groundwater Nitrogen Content in Miyakonojo River Basin, South Japan

Zhi-Qiang Yu[a], Kei Nakagawa[*b], Ronny Berndtsson[c], Toru Hiraoka[d], and Yoshihiro Suzuki[e]

[a]Graduate School of Fisheries and Environmental Sciences, Nagasaki University, 1-14 Bunkyo-machi, Nagasaki 852-8521, Japan
[b]Institute of Integrated Science and Technology, Nagasaki University,1-14 Bunkyo-machi, Nagasaki 852-8521, Japan
[c]Division of Water Resources Engineering & Centre for Advanced Middle Eastern Studies, Lund University, Box 118, SE-221 00 Lund, Sweden
[d]Department of Information Systems, University of Nagasaki,1-1-1, Manabino, Nagayo-chou, Nishisonogi-gun, Nagasaki-ken 851-2195, Japan
[e]Department of Civil and Environmental Engineering, University of Miyazaki,Gakuen Kibanadai-Nishi 1-1, Miyazaki 889-2192, Japan

Abstract

For preserving good status of groundwater in Miyakonojo river basin, the Nitrate-Nitrogen Reduction Plan has been implemented since 2004. However, the effects of Nitrate-Nitrogen Reduction Plan have not yet been quantitively evaluated. For this purpose, we used groundwater nitrogen data for 21 years (1996-2016) from groundwater observation wells (486-584) for spatial times series analyses (e.g., Mann-Kendall and Spearman's Rho test). Results show that the number of observation wells with decreasing nitrogen trend (statistically significant level, $p \leq 0.05$) increased from 100 to 200 from 2004 to 2016. However, the number of observation wells with increasing nitrogen trend ($p \leq 0.05$) increased to 60 wells up to 2012, and thereafter, levelled off little by little with time. The nitrogen change rate for annual groundwater samples was calculated ($p \leq 0.05$) based on Sens`s slope. The results show that annual change rate of groundwater nitrogen decreased slowly with time. Thus, there are statistical evidence of improvements from the Nitrate-Nitrogen Reduction Plan based on observations at the regional river basin scale.

Keyword: Groundwater nitrogen content/ Mann-Kendall test/ Spearman's Rho test

---

*Corresponding Author: Kei Nakagawa, Tel: +81 95 819 2763
E-mail address: kei-naka@nagasaki-u.ac.jp.

1. Introduction

Nitrogen contamination of groundwater have generally occurred in many countries, due to human activities such as sewage discharge, agriculture and livestock production. This pollution have caused the risk of human health and even some diseases. At the same time, groundwater-dependent ecosystems were also affected at some areas (Hansen et al., 2017). In order to solve the above issues, there are a series of policies of water recources management (Nitrate-Nitrogen Reduction Plan, Water Cycle Act, as well as Water Pollution Prevention Law) that have been established in Japan (Yu et al., 2021).

Miyakonojo river basin is one of major agricultural production area in south Japan. Due to intensive agricultural farming, groundwater bodies have been seriously polluted by excessive nitrogen emissions in this basin. Because of this, the Nitrate-Nitrogen Reduction Plan have been implemented in the Miyakonojo river basin since 2004. The main regulations have taken measures to reduce nitrogen release from livestock waste, synthetic chemical fertilizers and municipal wastewater. On the basis of these measures, water resource manager try to preserve the good status of groundwater quality (Matsunaga et al., 2015; Yu et al., 2021). However, what extent it has improved to groundwater status over time in the regional groundwater basin. The effects of Nitrate-Nitrogen Reduction Plan need to be further quantitively assessed. For this purpose, we have gathered a mass of groundwater nitrogen data for 21 years (1996-2016) from groundwater observation wells (486-584). Then, we used the methods of spatial time-series analysis to disuss

the spatiotemporal change features of groundwater nitrogen content in the Miyakonojo river basin.

2. Methodology

The non-parametric statistical test such as Mann-Kendall test and Spearman's Rho test have extensively applied to hydro-meteorological time series trend analysis (e.g., water quality, rainfall and streamflow). Based on the above two statistical tests, the time-series trend detection of groundwater nitrogen content have been performed (start:1996-2003 yr, end:1996-2016 yr). Then the statistical significane (p-value) has been calculated for data of each invegtigated well, therein, these observation wells ($p \leq 0.05$) are further computed the time-series change rate of nitrogen based on Sen`s slope estimator (Yue et al., 2002). The statistical tools such as Excel (XLSTAT), and JMP were applied during analysis the time-series features of groundwater nitrogen data. At the same time, the change for spatial, time-series features of groundwater nitrogen content were described by QGIS.

3. Results and Discussion

The results of Mann-Kendall test have been summarized in Figure 1. The number of observation wells with increasing nitrogen trend ($p \leq 0.05$) increases to 60 wells up to 2012, and thereafter, levelled off little by little with time. Though the Nitrate-Nitrogen Reduction Plan have been performed since 2004, the number of observation wells with increasing nitrogen trend ($p \leq 0.05$) were still growing until the peak occurred between 2009 to 2012. In other words, groundwater nitrogen response to regional Nitrate-Nitrogen Reduction Plan have time delay, due to slow groundwater flow velocity across the vadose zone. The number of observation wells which contain increasing nitrogen trend ($p > 0.05$) and decreasing nitrogen trend ($p > 0.05$) have both clearly declined with time. However, the number of observation wells with decreasing nitrogen trend ($p \leq 0.05$) have increased approximately from 100 to 200 for the year 2004 to 2016. The effects of Nitrate-Nitrogen Reduction Plan is obvious in these observation wells. Likewise, the results of Spearman`s Rho test is basically consistent with the results of Mann-Kenall test.

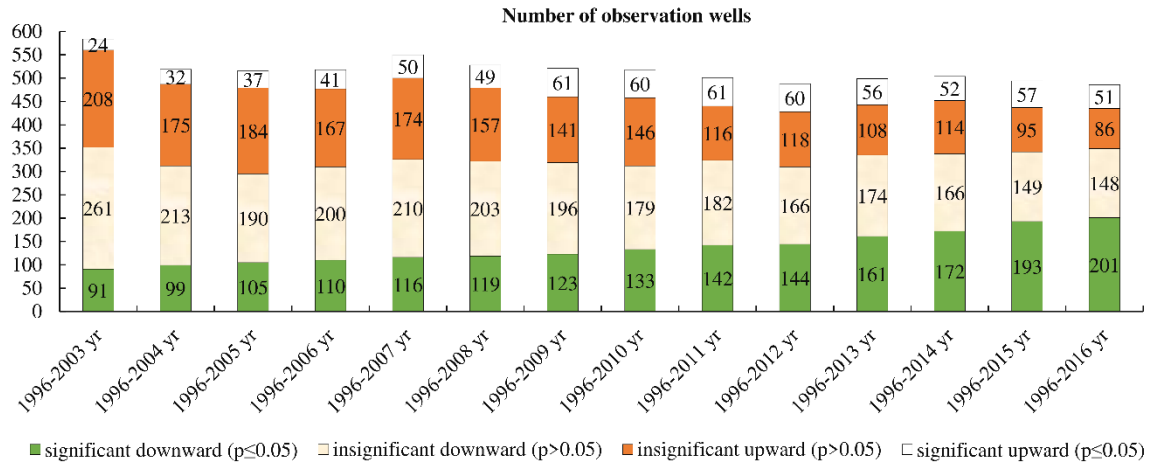

Figure 1. Results of Mann-Kendall test

In addition, the annual change rate of nitrogen from these observation wells ($p \leq 0.05$) have been calculated on the basis of Sen`s slope estimator. The mean and median values of annual change rate of nitrogen are depicted in Figure 2. As for the observation wells with increasing nitrogen trend in Figure 2(a), the annual change rate of nitrogen has decreased with time. This implies that the growth rate of groundwater nitrogen content has reduced over time, even groundwater nitrogen concentration was still growing in these observation wells. Meanwhile, as for the observation wells with decreasing nitrogen trend in Figure 2(b), the

annual change rate of nitrogen has also reduced with time, as well as groundwater nitrogen concentration has begun to decline in these observation wells. Besides, nitrogen loads in vadose zone has reduced within the influence area of these observation wells. The spatial change features of groundwater nitrogen content were also described by QGIS based on the results of statistical analysis. The observation wells with decreasing nitrogen trend are mainly distributed in urban areas and specific agricultural farming areas in this region.

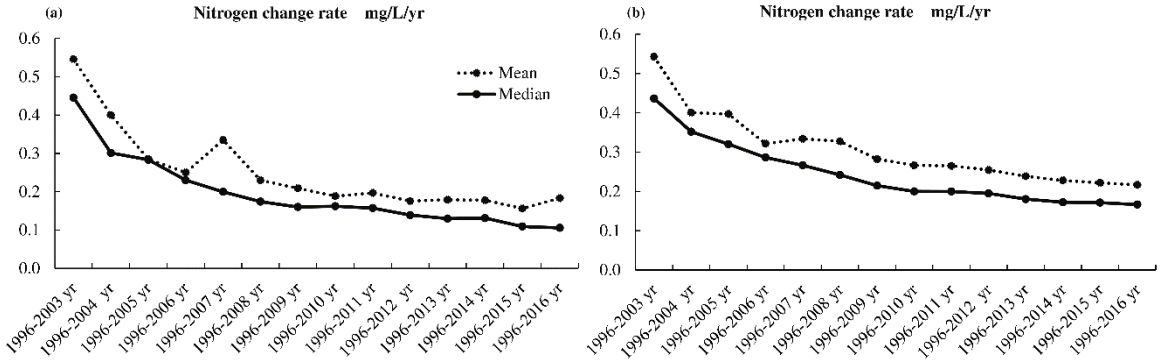

Figure 2. The mean and median values of annual change rate of nitrogen based on Sen`s slope (a) The observation wells with the increasing nitrogen trend ($p \leq 0.05$) (b) The observation wells with the decreasing nitrogen trend ($p \leq 0.05$)

4. Conclusions

The analysis results of Mann-Kendall test and Spearman`s Rho test are basically consistent. The effects of Nitrate-Nitrogen Reduction Plan are efficient in the regional basin. Especially, the number of observation wells with decreasing nitrogen trend have increased from 100 to 200 for the year 2004 to 2016. These observation wells are primarily distributed at the urban areas and specific agricultural production areas.

References

Hansen, B., Thorling, L., Schullehner, J., Termansen, M., Dalgaard, T., 2017. Groundwater nitrate response to sustainable nitrogen management. Sci. Rep. 7.

Matsunaga, M., Shimada, J., Hosono, T., Tawara, Y., Iwasa, K., 2015. Visualization of nitrate behavior by using 3D groundwater flow simulation in the Miyakonojo Basin. J Groundw Hydrol 57, 495-513. (in Japanese with English abstract).

Yue, S., Pilon, P., Cavadias, G., 2002. Power of the Mann-Kendall and Spearman's rho tests for detecting monotonic trends in hydrological series. J Hydrol 259, 254-271.

Yu, Z.Q., Nakagawa, K., Berndtsson, R., Hiraoka, T., Suzuki, Y., 2021. Groundwater nitrogen response to regional land-use management in South Japan. Environ. Earth Sci. 80, 1-18.

Efficiency of Di-(2-Ethylhexyl) Phthalate Degrading Bacteria Isolated fom Mangrove Sediment and Landfill Soil

Kanphorn Saengkla[a], Onruthai Pinyakong[b], and Prinpida Sonthiphand[a*]

[a]Department of Biology, Faculty of Science, Mahidol University, Thailand
[b]Department of Microbiology, Faculty of Science, Chulalongkorn University, Thailand

Abstract

Phthalate esters (PAEs) are widely used as plasticizers to improve plasticity and flexibility of polymeric materials. Di-(2-ethylhexyl) phthalate (DEHP), one of the commonly used PAEs in plastic industries, has been ranked the top priority pollutants by the United States Environmental Protection Agency (USEPA). Biodegradation is considered a promising technology for DEHP removal. Consequently, the objectives of this study were to isolate efficient DEHP-degrading bacteria from contaminated mangrove sediment and landfill soil. The efficiencies of DEHP-degrading activities among the isolated bacteria were subsequently compared. The mangrove sediment and landfill soil samples were respectively collected from Samut Prakan and Rayong provinces, Thailand. Both locations have chronic exposure to plastic waste. In this study, five and seven DEHP-degrading bacterial isolates were obtained from mangrove sediment and landfill soil, respectively, by enrichment approach. For each isolate, the degradation efficiencies of 200 mg/l DEHP were monitored after 7 days. The DEHP degradation efficiencies of those retrieved from mangrove sediment (SPK) and landfill soil (RY) ranged from 71.34% to 96.70% and 9.19% to 30.65%, respectively. The results indicated that DEHP-degrading bacteria isolated from mangrove sediment were able to more efficiently degrade DEHP than those obtained from landfill soil. Mangrove sediment impacted by plastic pollution could provide a valuable source of efficient DEHP-degrading bacteria. Further study will focus on the development of DEHP-degrading bacterial consortium composing of a variety of bacterial characteristics, including the ability to degrade other PAEs. Bioremediation technology for plastic waste can be built upon initial findings gained from this study.

Keyword: Di-(2-ethylhexyl) phthalate (DEHP)/ Biodegradation/ DEHP-degrading bacteria/ Mangrove sediment/ Landfill soil/ Plastic waste

---

*Corresponding Author: Prinpida Sonthiphand
E-mail address: prinpida.son@mahidol.ac.th

1. Introduction

The worldwide production of plastic waste significantly increased over recent decades (Akhbarizadeh et al., 2020). Phthalate esters (PAEs) are known as plasticizers which are a composition of plastic. PAEs are widely used in plastic industries to improve plasticity, versatility, fluidity, malleability and flexibility of several materials, such as polyvinylchloride (PVC). Due to the lack of chemical bonding between the plasticizer and the polymer chain, PAEs can be easily discharged into the environment during manufacture, weathering, evaporating, and disposal processes. Consequently, PAEs can be found in soil, sediments, waters, and air (Fernández et al., 2012).

Di-(2-ethylhexyl) phthalate (DEHP) is one of the most commonly used plasticizers and it is mainly used in the production of PVC plastics. DEHP has been detected in drinking water, surface water, ground water, sludge, soil, and sediments. Consequently, humans potentially exposure to DEHP via ingestion, inhalation and dermal absorption (Malem et al., 2019; Zhu et al., 2020). Numerous toxicological studies have demonstrated that DEHP are endocrine disrupting chemicals (EDCs). Due to its toxicity such as carcinogenic, estrogenic, hepatotoxic agents, and contributors to chronic health effects, DEHP has been classified as a priority pollutant by the United States Environmental Protection Agency (USEPA), the European Union (EU) and the Chinese National Environmental Monitoring Center (CNEMC) (Hu et al., 2021; Lu et al.,

2020; Wang et al., 2020; Yuan et al., 2010). Previous studied reported that the concentration of DEHP at Pradu Bay, Rayong province, Thailand was 0.31-0.91 µg/l in seawater but it was below detection limit to 1.65 µg/g in sediment samples (Malem et al., 2019). Another study reported that the concentrations of DEHP in urban soil and agricultural soils collected from Guangzhou, China, were 264 µg/g dw and 29.4 µg/g dw, respectively (Zhu et al., 2020). The prevalence of DEHP in environments are now received high attention because it is relevant to health problems.

The PAEs can be degraded by both biotic and abiotic processes (Meng et al., 2015). Biodegradation is more likely to be the most effective process to remove PAEs from the environments due to its prominent advantages, including the complete degradation and the less production of environmental disturbance (Fernández et al., 2012; Hu et al., 2021). Numerous studies have revealed that microorganisms such as bacteria, yeast, and fungi were able to degrade DEHP under aerobic or anaerobic conditions. Bacterial strains isolated from various environments, including *Rhodococcus jostii* (Annamalai & Vasudevan, 2020), *Rhodococcus rhodochrous* (Chao & Cheng, 2007), *Bacillus subtilis* (Quan et al., 2005), *Pseudomonas fluorescens* (Xu et al., 2007), *Sphigomonas* sp. and *Corynebacterium* sp. (Chang et al., 2004) were capable of degrading PAEs. Previous studies reported that *Rhodococcus pyridinivorans* XB isolated from activated sludge degraded high-concentration of DEHP (200 mg/l) with a degradation efficiency of 98% within 48 hours (Zhao et al., 2018). Thus, the ability of microorganisms in degrading DEHP has high potential for the development of bioremediation technology. Although previous studies mostly focused on the degradation of DEHP using pure bacterial culture, bacterial consortium showed better adaption to harsh environments (Chang et al., 2004). Bacterial consortium also exhibited more efficient metabolisms. There have been several reports about the complete mineralization of specific PAEs by a mixed culture consortium (Wang et al., 2004; Wu et al., 2010). The halotolerant bacterial consortium LF1 enriched from activated sludge contained *Gordonia* sp., *Rhodococcus* sp.and *Achromobacter* sp. as predominant species could degrade 93.84% of 1000 mg/l DEHP after 48 hours incubation (Li et al., 2018). However, more information on the degradation of DEHP by bacterial consortium is still needed.

This study aims 1) to compare the efficiencies of DEHP-degrading activities among isolated bacterial strains and 2) to verify the DEHP-degrading activity of bacterial consortium. DEHP-degrading bacteria were enriched and isolated from mangrove sediment and landfill soil. Mangrove sediment was collected from Ban Seelong coastal area connected to the Gulf of Thailand in Bang Bo District, Samut Prakan, Thailand. Landfill soil was collected from Mueang Rayong District, Rayong, Thailand. Both sampling locations have been impacted by plastic wastes, including plastic bottle, plastic bag and food packaging. The concentration of DEHP used in this study was 200 mg/l, representing the impact of high levels of the pollutant. The knowledge obtained from this study will provide the information for the development of in situ remediating of PAEs from a contaminated environment.

2. Methodology

2.1 Enrichment media

A modified mineral salt medium (MSM) was applied for the bacterial enrichment contains the following ingredients (all concentrations in gram per litter): KH_2PO_4, 2.2; $Na_2HPO_4 \cdot 12H_2O$, 0.8; NH_4Cl, 3; $CaCl_2 \cdot 2H_2O$ 0.05, 0.1; $MgSO_4 \cdot 7H_2O$, 0.1; and $FeCl_3 \cdot 6H_2O$, 0.05 (Yuan et al., 2010). The pH of the medium was adjusted to 7 before autoclaving at 121 ^oC. DEHP with >98% purity was purchased from Applied Chemical and Instrument Co., Ltd. (Bangkok, Thailand). A stock solution of DEHP was prepared by dissolving the DEHP in dichloromethane to a concentration of 10,000 mg/l. Then, it was subsequently diluted with dichloromethane to a final concentration of 200 mg/l prior to use.

2.2 Sampling site description and sample collection

The mangrove forest area located in Ban Seelong coastal area near the Gulf of Thailand in

Bang Bo District, Samut Prakan, Thailand (13.48105ºN, 100.84848ºE). This sampling site is a small fishing community with the abundance of shrimp, crabs, fish and various aquatic animals. This area used to be a plentiful mangrove forest. Later the plastic pollution occurred by the accumulation of waste from the ocean. A lot of plastic wastes especially plastic bottles and food packaging have been found around the sampling site (Figure 1). So, the mangrove sediment likely has been exposed to chronic contamination of PAEs, including DEHP.

Landfill soil was collected from a landfill area from Mueang Rayong District, Rayong, Thailand (12.668819ºN, 101.250638ºE). The landfill has been operated by the local administrative organizations since 1995. The total amount of waste received is 3,600 tons/month (ONEP). A lot of wastes, including plastic material, have been found around the sampling site. So, the landfill soil may also expose to chronic contamination of PAEs, including DEHP.

The mangrove sediment and landfill soil samples used in the present study were randomly collected around the sampling site. The sediment samples and landfill soil samples were pooled on site and kept in a sterile Ziplock bag. The samples were kept on ice during transportation.

Figure 1. The mangrove forest area located in Bang Bo District, Samut Prakan, Thailand.

2.3 Enrichment of DEHP-degrading bacteria

DEHP-degrading bacteria from the mangrove sediment (SPK) and landfill soil (RY) were separately enriched. Five grams of sediment or soil sample were inoculated into the 250-ml Erlenmeyer flask containing 100 ml of the MSM supplement with DEHP at the concentration of 50 mg/l as the sole carbon and energy sources (Yuan et al., 2010). The suspension was incubated aerobically on an orbital shaker (200 rpm) in the dark at room temperature (30 ºC) for 7 days. One ml of the enrichment culture was serially transferred to 100 ml of fresh MSM with 100, 150, and 200 mg/l DEHP and incubated aerobically on an orbital shaker (200 rpm) in the dark at room temperature (30 ºC) for 7 days. Control cultures lacking a carbon source was performed under the same conditions.

2.4 Isolation of DEHP-degrading bacteria

After the enrichment was sub-cultured for four times, DEHP-degrading bacteria were isolated using a MSM agar plates containing 200 mg/l DEHP. The agar plates were incubated at room temperature (30 ºC) in the dark for 7 days. Colonies of candidate DEHP-degrading bacteria were picked up based on the differences in the colony morphology (i.e., sizes, shapes, margins and colors). Potential degraders were isolated and purified by repetitive streaking on MSM agar plates containing 200 mg/l DEHP. Bacterial strains SPK were isolated from mangrove sediment and bacterial strains RY were isolated from landfill soil. The characteristics of an individual colony of bacteria growing on MSM agar were observed based on their colony morphology (i.e., form, size, elevation, margin, surface, opacity, and color). The isolated strains

on MSM that were able to utilize DEHP for their growth were selected for further study.

2.5 Identification of DEHP-degrading bacteria

The identification of the isolates was based on 16S ribosomal RNA (rRNA) gene sequence analysis. The service of DNA extraction, purifying and sequencing was provided by Bionics in Korea. PCR of 16S rRNA gene amplicon was performed using 27F and 1492R primers, and sequencing was conducted using 518F and 800R primers. Finally, the Bioedit software was used to create a consensus DNA sequence from forward and reverse sequences. The similarity of the nucleotide sequence was determined by BLAST search against the National Center for Biotechnology Information databases (NCBI).

2.6 Verification of DEHP-degrading activity by isolated bacteria

All purified strains were tested for DEHP-degrading ability. The isolated strains were grown in the flask containing 50 ml of the 0.5X LB broth. Each flask was incubated aerobically on an orbital shaker (200 rpm) at room temperature (30 ºC) for 24 hr. Then, each culture was diluted to optical density approximately 1.0 with MSM. The microbial cell was centrifuged and washed three times with MSM before using as cell suspension for the biodegradation test. Microbial cell was resuspended with MSM. Then, 5 ml of cell suspension were transferred into a test tube and spiked with 200 mg/l DEHP. Sterile controls were prepared by autoclaving before the DEHP addition. The added DEHP was filtered through a PTFE filter sterile 0.22 µm membrane. All experiments were conducted in triplicate. Each flask was incubated aerobically on an orbital shaker (200 rpm) at room temperature (30 ºC) for 7 days. At day 0 and 7, the cultures were taken for the measurements of DEHP concentration.

2.7 Verification of DEHP-degrading activity by microbial consortia

The biodegradation of DEHP by mixed cultures was investigated. Four microbial consortia were formulated by mixing equal proportions of pure bacterial cultures that were isolated from mangrove sediment and landfill soil. The strains were selected based on their growth in MSM supplement with DEHP and their efficiency in degrading DEHP. Consortium 1 consisted of RY-01 and RY-04. Consortium 2 consisted of RY-01 and SPK-13. Consortium 3 consisted of RY-04 and SPK-12. Consortium 4 consisted of SPK-12 and SPK-13. The concentration of DEHP for the biodegradation test was 200 mg/l. All treatments were conducted in triplicate. Each flask was incubated aerobically on an orbital shaker (200 rpm) at room temperature (30 ºC) for 7 days. At days 0 and 7, the cultures were taken for measurement of DEHP concentration.

2.8 Analysis of DEHP concentration

Residual DEHP contents in culture media were determined according to previously published protocol (Chao, Lin, Shiung, & Kuo, 2006; Zhu et al., 2018). An equal volume of dichloromethane (5 ml) was added directly to each flask, followed by vortexing for 1 min. Dichloromethane layer was transferred into a new tube and the aqueous phase was further extracted with dichloromethane (5 ml, 2X). After the solvent being dried by left in the fume hood, the DEHP residues were eluted with 1 ml of dichloromethane. Then, the solution was passed through a 0.2-µm membrane filter into the GC vial and analyzed using a gas chromatograph equipped with flame ionization detector (GC-FID, Agilent USA).

2.9 Statistical analysis

A t-test was conducted to compare the significant differences ($p<0.05$) of the reduction of DEHP concentrations between the experimental treatments and controls (Excel software, Microsoft).

3. Results and Discussion

3.1 Biodegradation of DEHP by bacteria isolated from mangrove sediment

The results show that five DEHP-degrading bacterial isolates, SPK-03G, SPK-05, SPK-08, SPK-12, and SPK-13, were obtained from the mangrove sediment (Figure 2). The DEHP-degrading activities of these five isolates were monitored at days 0 and 7. The DEHP

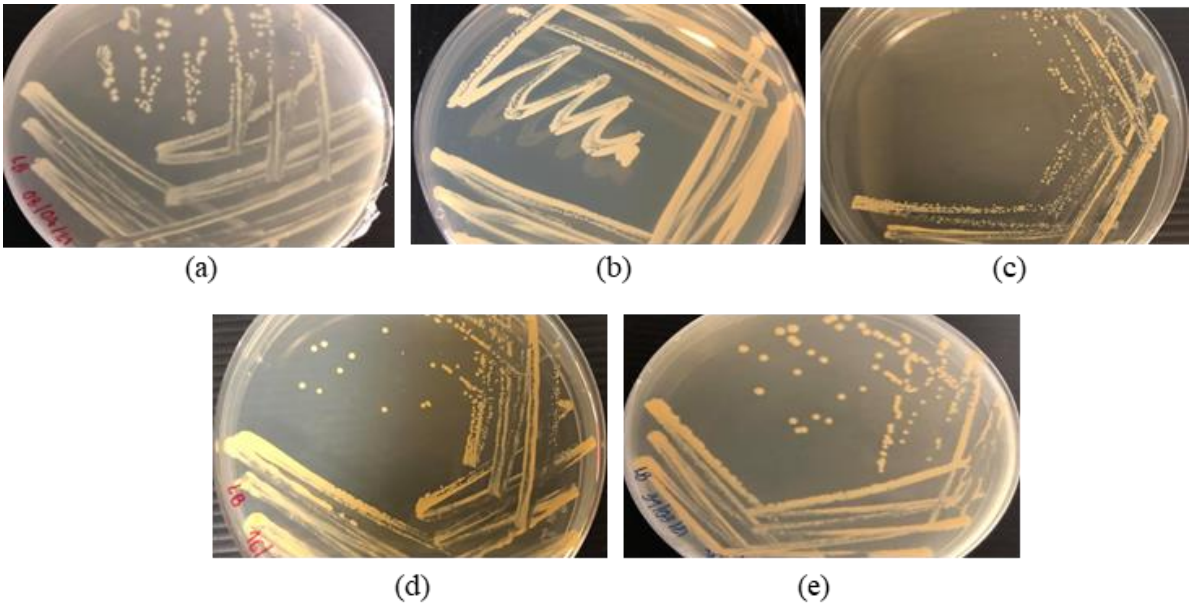

Figure 2. Five DEHP-degrading bacteria isolated from mangrove sediment on LB agar plate after incubated at room temperature in the dark for 2 days. SPK-03G (a), SPK-05 (b), SPK-08 (c), SPK-12 (d), and SPK-13 (e).

degradation efficiencies of all isolates obtained from the mangrove sediment were 71.34% to 96.70% (Table 1). Among the obtained isolates, only one isolate can be identified and it was closely related to *Bacillus megaterium* strain AK4. A previous study showed that *Bacillus* sp. was the dominant bacteria found in the mangrove sediment responsible for PAE aerobic degradation. A previous study also demonstrated that DEHP-degrading bacteria isolated from mangrove sediment were associated with *Bacillus pumilus*, *Bacillus catenulatus*, and *Bacillus amyloliquefaciens* (Yuan et al., 2010).

Our results also revealed that the SPK-12 and SPK-13, mixed culture, showed the very high efficiencies of the DEHP-degradation (Table 1). Both enrichment cultures may contain cooperative DEHP-degrading bacteria. However, both SPK-12 and SPK-13 will be further isolated and identified. The relationship among the cooperative DEHP-degrading bacteria will also be further investigated.

3.2 Biodegradation of DEHP by bacteria isolated from landfill soil

In this study, seven DEHP-degrading bacterial isolates, RY-01, RY-02, RY-03, RY-04, RY-06, RY-08, and RY-09, were obtained from the landfill soil (Figure 3). The isolated bacteria were monitored their DEHP-degrading activities at days 0 and 7 (Table 1). The results showed that DEHP-degrading bacteria obtained from the landfill soil were able to degrade DEHP ranged from 9.19% to 30.65%. The isolated RY-01, closely related to *Bartonella* sp. B43870, showed the highest DEHP-degradation efficiency (Table 1). The majority of the isolates (RY-03, RY-06, RY-08, and RY-09) was closely related to *Luteimicrobium* sp. G6 and another was affiliated with *Rhodococcus hoagii* RYA5. Overall, the obtained isolates showed relatively low DEHP degradation efficiency. Previously identified DEHP-degrading bacteria isolated from landfill or activated sludge were *Rhodococcus pyridinivorans* XB (an initial concentration = 200 mg/l DEHP, degradation efficiency = 98% within 2 days; Zhao et al., 2018), *Microbacterium* sp. J-1 (an initial concentration = 200 mg/l DEHP, degradation efficiency =96% within 5 days; Zhao et al., 2017), and *Agromyces* sp. MT-O (an initial concentration = 200 mg/l DEHP, degradation efficiency =90% within 4 days; Zhao et al., 2016). Overall, the DEHP degradation efficiencies shown by previous studies are higher than those obtained by this study. Enrichment conditions will be further optimized to enhance the growth of DEHP-degrading bacteria in the analyzed landfill soil.

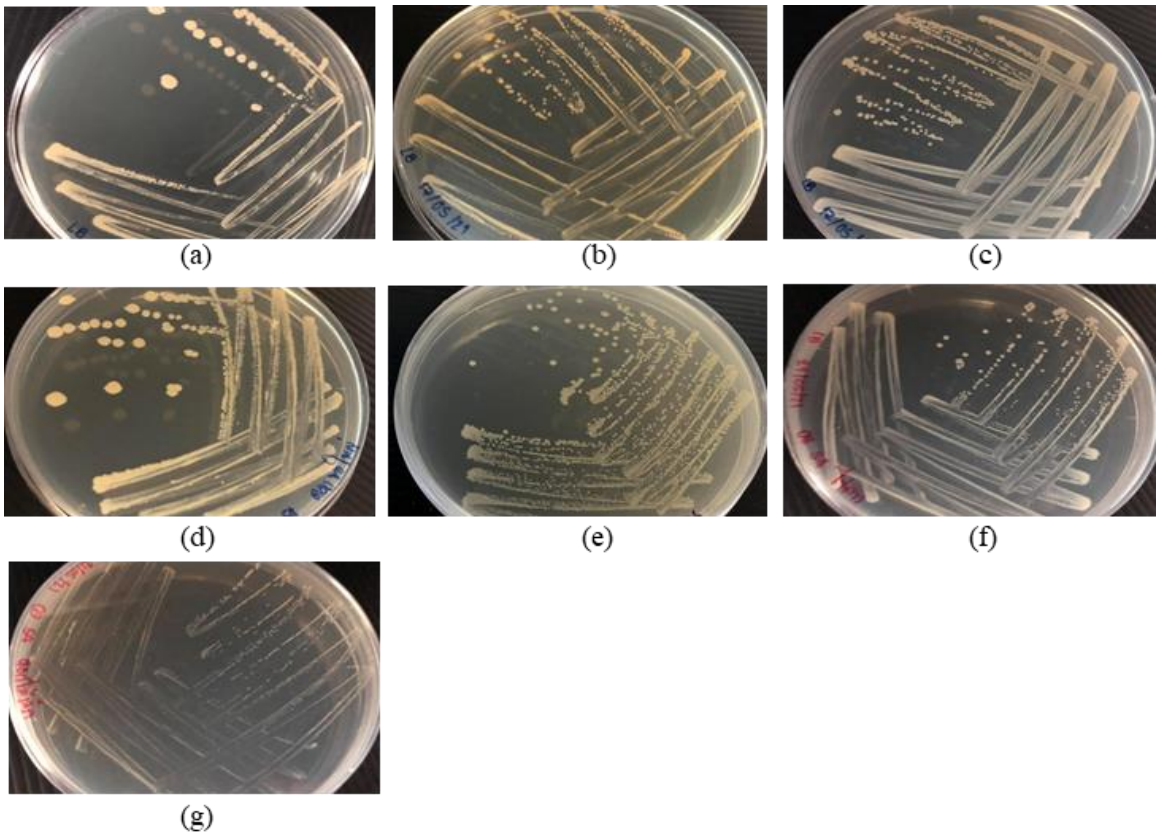

Figure 3. DEHP-degrading bacteria isolated from landfill soil on LB agar plate after incubated at room temperature in the dark for 2 days. RY-01 (a), RY-02 (b), RY-03 (c), RY-04 (d), RY-06 (e), RY-08 (f), and RY-09 (g).

Table 1: DEHP degrading activity of bacteria isolated from mangrove sediment and landfill soil.

Isolate	Degradation efficiency (%)	Closely related bacteria	Similarity (%)	Length (bp)	Accession
Mangrove sediment					
SPK-03G	75.93 ± 1.63	Unidentified	N/A	N/A	N/A
SPK-05	71.34 ± 2.09	Unidentified	N/A	N/A	N/A
SPK-08	77.43 ± 2.24	*Bacillus megaterium* strain AK4	99.93%	1383	MK966390
SPK-12	91.00 ± 2.34	Mixed	N/A	N/A	N/A
SPK-13	96.70 ± 0.47	Mixed	N/A	N/A	N/A
Landfill soil					
RY-01	30.65 ± 2.83	*Bartonella* sp. strain B43870	95.54%	830	MN504692
RY-02	28.02 ± 2.26	*Rhodococcus hoagii* strain RYA5	100.00%	1352	MT549098
RY-03	16.23 ± 4.28	*Luteimicrobium* sp. strain G6	100.00%	1363	MT993404
RY-04	28.55 ± 3.56	Mixed	N/A	N/A	N/A
RY-06	16.78 ± 5.94	*Luteimicrobium* sp. strain G6	100.00%	1348	MT993404
RY-08	9.19 ± 2.39	*Luteimicrobium* sp. strain G6	100.00%	1362	MT993404
RY-09	22.73 ± 4.90	*Luteimicrobium* sp. strain G6	100.00%	1366	MT993404

N/A: Not available

3.3 Comparison of DEHP degradation efficiency

The DEHP degradation efficiencies among the isolated bacteria obtained from mangrove sediment and landfill soil were compared (Table 1 and Figure 4). The DEHP degradation efficiencies of bacteria retrieved from the mangrove sediment were higher than those obtained from the landfill soil. Each ecosystem may contain unique microbial communities, including DEHP-degrading microorganisms. The mangrove sediment analyzed in this study has been influenced by the long-term contamination of plastic pollution. Therefore, plastic pollution could enhance the activity of DEHP-degrading bacteria. Indigenous bacteria in the impacted mangrove sediment may well adapt to use DEHP for their growth. Furthermore, the incubation condition conducted in this study (i.e., pH, DEHP concentration, and temperature) might be more suitable for promoting DEHP-degrading bacteria in the mangrove sediment than those in the landfill soil.

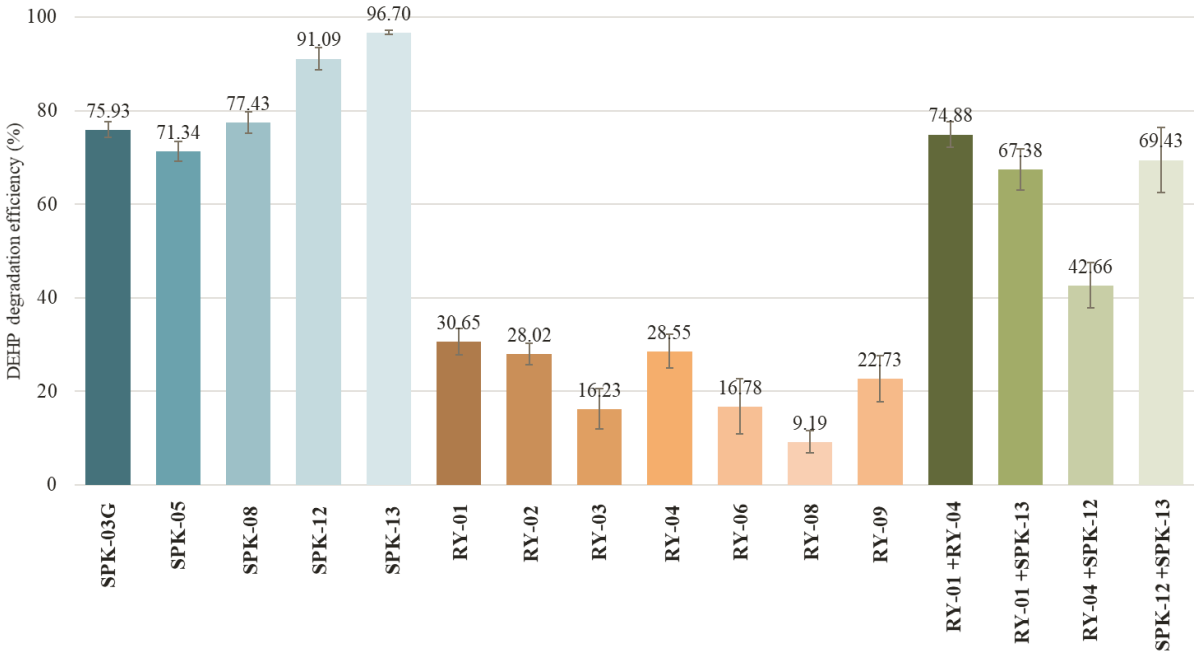

Figure 4. Comparison of DEHP degradation efficiencies among the isolated and mixed bacterial cultures.

3.4 Biodegradation of DEHP by bacterial consortium

Based on their efficiency in degrading DEHP, four bacterial isolates were selected to construct 4 bacterial consortia. Consortium 1 that was composed of RY-01 and RY-04 showed the highest DEHP-degrading efficiency (Figure 4). Although RY-01 and RY-04 solely exhibited low DEHP-degradation efficiency (Table 1), the combination of RY-01 and RY-04 increased the DEHP-degradation efficiency. This is possibly due to synergetic interaction and enzymatic system of bacteria in the Consortium 1. Individual microorganism can degrade only a limited range of hydrocarbon substrates, so mixed microorganisms with multiple metabolic capacities may increase relevant catabolic pathways associated with biodegradation (Naloka et al., 2021; Wanapaisan et al., 2018).

However, the Consortium 2 (RY-01 and SPK-13), Consortium 3 (RY-04 and SPK-12), and Consortium 4 (SPK-12 and SPK-13) could not enhance the DEHP-degradation efficiency compare to the individuals (Table 1 and Figure 4). It is possible that toxic intermediates produced by one DEHP-degrading bacteria are harmful to others (Wu et al. 2010). Shariati et al. (2021) reported that the consortium An6 (*Pseudomonas putida* ShA and *Gordonia alkanivorans* Sh6) could degrade 97.65%% of 500 mg/l DEHP within 3 days. The halotolerant bacterial consortium LF1 (*Gordonia* sp., *Rhodococcus* sp.

and *Achromobacter* sp.) enriched from activated sludge could degrade 93.84% of DEHP (1000 mg/l) after 48-hour incubation (Li et al., 2018). Further investigation on bacterial characteristics and physiological functions and an optimal ratio of inocula is needed for the construction of highly efficient DEHP-degrading bacterial consortium.

4. Conclusions

Five and seven DEHP-degrading bacterial isolates were retrieved from the mangrove sediment and the landfill soil, respectively. Although the landfill soil was a potential source of DEHP-degrading bacteria, the mangrove sediment impacted by plastic pollution was considered the valuable source of highly efficient DEHP-degrading bacteria. Among the obtained cultures, the SPK-12 and SPK-13 showed the particularly high degradation efficiencies of DEHP at 200 mg/l within 7 days. The results suggested that the SPK-12 and SPK-13 can be used as potential candidates for further development of bioremediation technology for DEHP removal. Although each isolate obtained from the landfill soil showed low DEHP degradation efficiencies, the combination of RY-01 and RY-04 enhanced the DEHP degradation efficiency. Further study will focus on the development of DEHP-degrading bacterial consortium composing of a variety of bacterial characteristics, including the ability to degrade other PAEs.

Acknowledgement

This research was supported by the CIF and CNI grant, Faculty of Science, Mahidol University. Nuntanat Kitisrivorapan of the Central Instrument Facility (CIF), Faculty of Science, Mahidol University was thankful for valuable instrument suggestions. Parichaya Tiralerdpanich, Natthariga Laothamteep, and Adisan Rungsihiranrut provided constructive comments.

References

Akhbarizadeh, R., Dobaradaran, S., Schmidt, T. C., Nabipour, I., & Spitz, J. (2020). Worldwide bottled water occurrence of emerging contaminants: A review of the recent scientific literature. *Journal of Hazardous Materials, 392*, 122271.

Annamalai, J., & Vasudevan, N. (2020). Enhanced biodegradation of an endocrine disrupting micro-pollutant: Di (2-ethylhexyl) phthalate using biogenic self-assembled monolayer of silver nanoparticles. *Science of The Total Environment, 719*, 137115.

Chang, B. V., Yang, C. M., Cheng, C. H., & Yuan, S. Y. (2004). Biodegradation of phthalate esters by two bacteria strains. *Chemosphere, 55*(4), 533-538.

Chao, W. L., & Cheng, C. Y. (2007). Effect of introduced phthalate-degrading bacteria on the diversity of indigenous bacterial communities during di-(2-ethylhexyl) phthalate (DEHP) degradation in a soil microcosm. *Chemosphere, 67*(3), 482-488.

Fernández, M. A., Gómara, B., & González, M. J. (2012). Occurrence of Phthalates and Their Metabolites in the Environment and Human Health Implications. In D. Barceló (Ed.), *Emerging Organic Contaminants and Human Health* (pp. 307-336). Berlin, Heidelberg: Springer Berlin Heidelberg.

He, Z., Xiao, H., Tang, L., Min, H., & Lu, Z. (2013). Biodegradation of di-n-butyl phthalate by a stable bacterial consortium, HD-1, enriched from activated sludge. *Bioresource Technology, 128*, 526-532.

Hu, R., Zhao, H., Xu, X., Wang, Z., Yu, K., Shu, L., . . . Wang, C. (2021). Bacteria-driven phthalic acid ester biodegradation: Current status and emerging opportunities. *Environment International, 154*, 106560.

Li, F., Liu, Y., Wang, D., Zhang, C., Yang, Z., Lu, S., & Wang, Y. (2018). Biodegradation of di-(2-ethylhexyl) phthalate by a halotolerant consortium LF. *PLOS ONE, 13*(10), e0204324.

Lu, M., Jiang, W., Gao, Q., Zhang, M., & Hong, Q. (2020). Degradation of dibutyl phthalate (DBP) by a bacterial consortium and characterization of two novel esterases capable of hydrolyzing PAEs sequentially. *Ecotoxicology and Environmental Safety, 195*, 110517.

Malem, F., Soonthondecha, P., Khawmodjod, P., Chunhakorn, V., Whitlow, H. J., & Chienthavorn, O. (2019). Occurrence of phthalate esters in the eastern coast of Thailand. *Environmental Monitoring and Assessment, 191*(10), 627.

Meng, X., Niu, G., Yang, W., & Cao, X. (2015). Di(2-ethylhexyl) phthalate biodegradation and denitrification by a Pseudoxanthomonas sp. strain. *Bioresource Technology, 180*, 356-359.

Naloka, K., Polrit, D., Muangchinda, C., Thoetkiattikul, H., & Pinyakong, O. (2021). Bioballs carrying a syntrophic Rhodococcus and Mycolicibacterium consortium for simultaneous sorption and biodegradation of fuel oil in contaminated freshwater. *Chemosphere, 282*, 130973.

Office Of Natural Resources and Environmental Policy and Planning (ONEP). Retrived October 26, 2021, from http://waste.onep.go.th/projectdetail.php?id=123.

Quan, C. S., Liu, Q., Tian, W. J., Kikuchi, J., & Fan, S. D. (2005). Biodegradation of an endocrine-disrupting chemical, di-2-ethylhexyl phthalate, by Bacillus subtilis No. 66. *Applied Microbiology and Biotechnology, 66*(6), 702-710.

Wanapaisan, P., Laothamteep, N., Vejarano, F., Chakraborty, J., Shintani, M., Muangchinda, C., . . . Pinyakong, O. (2018). Synergistic degradation of pyrene

by five culturable bacteria in a mangrove sediment-derived bacterial consortium. *Journal of Hazardous Materials, 342*, 561-570.

Wang, Q., Jiang, L., Fang, C., & Chen, L. (2020). Effects of di-n-butyl phthalate and di-2-ethylhexyl phthalate on pollutant removal and microbial community during wastewater treatment. *Ecotoxicology and Environmental Safety, 198*, 110665.

Wang, Y., Fan, Y., & Gu, J.-D. (2004). Dimethyl phthalate ester degradation by two planktonic and immobilized bacterial consortia. *International Biodeterioration & Biodegradation, 53*(2), 93-101.

Wu, X., Liang, R., Dai, Q., Jin, D., Wang, Y., & Chao, W. (2010). Complete degradation of di-n-octyl phthalate by biochemical cooperation between Gordonia sp. strain JDC-2 and Arthrobacter sp. strain JDC-32 isolated from activated sludge. *Journal of Hazardous Materials, 176*(1), 262-268.

Xu, X.-R., Li, H.-B., & Gu, J.-D. (2007). Metabolism and biochemical pathway of n-butyl benzyl phthalate by Pseudomonas fluorescens B-1 isolated from a mangrove sediment. *Ecotoxicology and Environmental Safety, 68*(3), 379-385.

Yang, J., Guo, C., Liu, S., Liu, W., Wang, H., Dang, Z., & Lu, G. (2018). Characterization of a di-n-butyl phthalate-degrading bacterial consortium and its application in contaminated soil. *Environmental Science and Pollution Research, 25*(18), 17645-17653.

Yuan, S.-Y., Huang, I. C., & Chang, B.-V. (2010). Biodegradation of dibutyl phthalate and di-(2-ethylhexyl) phthalate and microbial community changes in mangrove sediment. *Journal of Hazardous Materials, 184*(1), 826-831.

Zhao, H.-M., Du, H., Lin, J., Chen, X.-B., Li, Y.-W., Li, H., . . . Wong, M.-H. (2016). Complete degradation of the endocrine disruptor di-(2-ethylhexyl) phthalate by a novel Agromyces sp. MT-O strain and its application to bioremediation of contaminated soil. *Science of The Total Environment, 562*, 170-178.

Zhao, H.-M., Hu, R.-W., Chen, X.-X., Chen, X.-B., Lü, H., Li, Y.-W., . . . Wong, M.-H. (2018). Biodegradation pathway of di-(2-ethylhexyl) phthalate by a novel Rhodococcus pyridinivorans XB and its bioaugmentation for remediation of DEHP contaminated soil. *Science of The Total Environment, 640-641*, 1121-1131.

Zhao, H.-M., Hu, R.-W., Huang, H.-B., Wen, H.-F., Du, H., Li, Y.-W., . . . Wong, M.-H. (2017). Enhanced dissipation of DEHP in soil and simultaneously reduced bioaccumulation of DEHP in vegetable using bioaugmentation with exogenous bacteria. *Biology and Fertility of Soils, 53*(6), 663-675.

Zhu, F., Doyle, E., Zhu, C., Zhou, D., Gu, C., & Gao, J. (2020). Metagenomic analysis exploring microbial assemblages and functional genes potentially involved in di (2-ethylhexyl) phthalate degradation in soil. *Science of The Total Environment, 715*, 137037.

The Diversity of Small Mammals in Natural and Recovery Forests in Mae Rim District, Chiang Mai Province

Palita Kunchorn[a*], Pimonrat Tiansawat[a], and Alice Sharp[a,b]

[a]Department of Biology, Faculty of Science, Chiang Mai University, Mueang Chiang Mai, Chiang Mai 50200, Thailand
[b]Environmental Science Research Center, Faculty of Science, Chiang Mai University, Mueang Chiang Mai, Chiang Mai 50200, Thailand

Abstract

Forest areas in Mae Rim District, Chiang Mai Province, have been converted to farmlands, causing the area to deteriorate and affecting wildlife habitats. Various organizations are working to restore the area. The effectiveness of the restoration program must then be monitored. The purpose of this study was to investigate and compare the diversity of small mammals and their frequency of detection (FD) in natural and restored forests in Mae Rim District, Chiang Mai Province. From February to August 2021, three camera traps were installed at each site to detect mammals that are active on the ground. There was in total 531 traps-night per forest. Nine mammal species from six families and two orders were discovered in the natural forest. The Large Indian Civet (*Viverra zibetha*) had the highest FD value of 4.14, followed by the Small Indian Civet (*Viverricula indica*) (FD = 2.82) and Leopard Cat (*Prionailurus bengalensis*) (FD = 1.13). There were five species from four families and one order recorded in the restored forest. The Leopard Cat (*Prionailurus bengalensis*) had the highest frequency of entering with an FD of 0.94, followed by the Small Indian Civet (*Viverricula indica*) with an FD of 0.56. Leopard Cats are carnivores, while civets are omnivores and potential seed dispersers. The similarity of mammal species found in both locations was 71%. The findings show that forest restoration provides habitats for local mammals, and the presence of seed dispersers implies the area's potential to undergo natural regeneration.

Keyword: Mammal diversity/ Camera trapping/ Forest restoration/ Chiang Mai

---

*Corresponding Author: Palita Kunchorn, +6-684-173-8076
E-mail address: palita_kunchorn@cmu.ac.th

1. Introduction

Based on Thailand's forest area data in 2020, Chiang Mai Province covers an area of 22,135.35 square kilometers, and the forest area is accounted for 15,337.97 square kilometers or 69.29 percent of the total area. It is the third-largest forest area in the northern provinces. On the other hand, the provincial forest area has continued to decline, from 75.62 percent in 1988 to 71.72 percent, 69.90 percent, and 69.29 percent in 1993, 2017, and 2020, respectively (Royal Forest Department, 2020).

Illegal logging, deforestation, forest fires, and encroachment on arable land contribute to Thailand's shrinking forest area. As a result, the soil surface at watershed areas has been destroyed. It also devastates plants and wildlife habitats, resulting in lower biological diversity (Ratchapruek Institute Foundation, 2021). Reduced forest cover impacts the area's ecosystem and increases greenhouse gas emissions into the atmosphere, exacerbating the problem of climate change. It is estimated that forest area loss from 2000 to 2010 accounted for 68.1Mt CO_2eq of greenhouse gas emissions (Global Forest Watch, 2021).

As a result of this issue, various environmental agencies and organizations are taking steps to restore forest areas that have been destroyed or disturbed by human activity. Forest restoration can be accomplished in a variety of ways. Conventionally, forest restoration was frequently used to select fast-growing plants, regardless of whether the seedlings were native or not. As a result, the cost of restoring such forests is often prohibitively high. In addition, seedlings take longer to grow because they are not native plants in rehabilitation areas. Furthermore, the biodiversity of recovery areas has decreased (FORRU, 2006).

The Forest Restoration Research Unit (FORRU), Faculty of Science, Chiang Mai University, restore forests through native plant structures. The Unit also carried out studies to compare various restoration techniques and processes. Following up on forest restoration is therefore critical. For example, to assess the study area's success in terms of biodiversity. In addition, the return of wildlife in recovery areas can be a good indicator of biodiversity. Additionally, local animal populations play different roles in ecosystems, particularly those that disperse seeds, which can help increase the area's biodiversity (FORRU, 2006). On the other hand, seed predators may destroy seeds that enter an area and thus act as a limiting factor in this regard.

This study investigates the diversity of mammals in natural forests and rehabilitation forests in Mae Rim District, Chiang Mai Province. The species richness and the frequency of detection between the two areas can be compared by installing automatic cameras.

2. Methodology

2.1 Study site

This study was carried out in a natural forest area (latitude 18.937, longitude 98.819) and a 9-year-old reforestation area (latitude 18.938, longitude 98.821) in Doi Suthep-Pui National Park, Chiang Mai Province (Figure 1). The area is known for its moist evergreen forest (1,300 – 1,420 m), with an average year-round temperature of around 23.0 degrees Celsius and an annual rainfall of 1,312 mm. The natural forest study plot area was 3,277.57 square meters, and the reforestation plot area was 1,178.90 square meters.

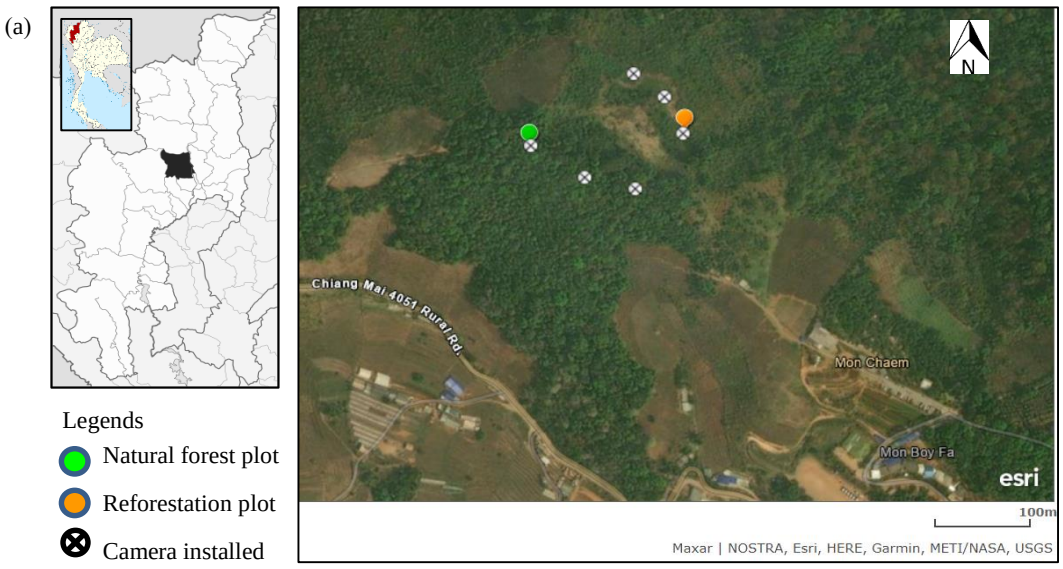

Figure 1. Study area. (a) map of the study area, (b) natural forest plot, and (c) reforestation plot.

2.2 Camera Trapping

From February to August 2021, images of small mammals were captured using the HC-801A Infrared trail camera in six locations, divided into three locations at the natural forest area and three at the reforested area. This equates to 531 trap nights per area. The camera installation location was chosen by surveying the animal tracks to determine the area that represented the forest—using a Line transect survey. Automatic cameras were installed at three locations at least 50 meters apart. The cameras were installed around a strong tree by positioning the camera about 40 centimeters above the ground (Jiménez et al., 2010). Thus, the camera should face toward an open, grass-free area. If the grass grows, mow it down to keep the camera's sensor from capturing unwanted motion. Next, insert an SD card, 8 AA alkaline batteries into the camera, and set the camera to continuous mode (three snapshots per detection). The SD card and batteries were replaced once a month. Data in the SD card were taken for analysis.

Small mammals are classified according to their species and genus. "A Naturalist's Guide to the Mammals of Thailand and Southeast Asia" (Shepherd and Shepherd, 2012) was used. When a single species appeared in photographs taken more than 30 minutes apart, the two subjects were treated as separate individuals (O'Brien et al., 2003). Data were examined for the Frequency of Detection, Species Richness, and Similarity Index. For each parameter, the calculation method is described as follows.

- Frequency of Detection (FD) was calculated using the same formula as in the Relative Abundance Index (RAI) = (E/TN) * 100, where E is the number of events or photographs taken and TN is the total number of trap nights. The relative abundance reveals how common or rare a species is relative to other species in a defined location or community. However, in this study, the term frequency of detection is used instead of relative abundance to avoid misleading the audience as the data may not conclude the abundance of a species. Although popular among wildlife camera trapping studies, the calculation of RAI is influenced by sampling-related factors that can bias the results and thus their interpretations (Sollmann et al., 2012). Those sampling-related factors include the home range of animals, the size of the sampling area, the location of the camera installed, etc.
- Species Richness (S) is the number of species recorded within a defined area.
- Similarity index was calculated based on the Sorensen index for presence-absence data (Krebs, 1999) where Ss = (2Wx100)/ (A+B). In this equation, W is the number of species present in both study sites, A is the number of species present only in the natural forest plot, and B is the number of species found only in the reforestation plot.

3. Results and Discussion

3.1 Species richness and detection frequency

Ninety-three images were captured by camera traps, with 72 percent (n=67) from the natural forest plot and 28 percent (n=26) from the reforestation plot. There were 90 percent (n= 84) of these that could be identified. Due to inadequate focus, lighting, or angle, the remaining shots were unidentifiable. Mammals and birds were among the animals taken.

In the natural forest, nine mammal species were found from two genera of the six families (Table 1). With a frequency of detection (FD) of 4.14, the Large Indian Civet (*Viverra zibetha*) had the highest frequency. The FD values of the Small Indian Civet (*Viverricula indica*) and the Leopard Cat (*Prionailurus bengalensis*) were 2.82 and 1.13, respectively. As for the reforestation area, five mammal species were found from one genus and four families (Table 2). The Leopard Cat (*Prionailurus bengalensis*) had the highest detection frequency, with an FD of 0.94. The second highest FD of 0.56 was of Small Indian Civet (*Viverricula indica*). Figure 2 depicts a photograph of mammals detected in this study. The limitation in analyzing camera trap data is that the data obtained can determine the

number of species discovered. Still, it cannot be used to calculate the population density of the animals. The animals photographed at different times may be the same individual and cannot be distinguished from the photographs.

3.2 Similarity between sites

The study found mammals such as Large Indian Civet, Small Indian Civet, Leopard Cat, Crab-eating Mongoose, Hog Badger, Masked Palm Civet, Shortridge's Mouse, Small Asian Mongoose and squirrel in the natural forest area. While in the reforestation plot, the study found Large Indian Civet, Small Indian Civet, Hog Badger, Leopard Cat, and Crab-eating Mongoose. The similarity of mammal species found in the natural forest and reforestation area equals 71%. The result demonstrated the return of mammals to the degraded forests. Furthermore, the presence of seed dispersal species in the reforestation area suggests that seeds from the natural forest may be dispersed into the area. In addition, some of the predator species such as Leopard cat and Crab-eating mongoose found in the reforestation plot may also help control the population of seed predators, thus promoting the regeneration of forest area.

Table 1. List of species captured and frequency of detection of wild mammals in the natural forest plot.

Scientific name	Common name	No. of photo taken (pictures)	Frequency of Detection
Viverra zibetha	Large Indian Civet	22	4.14
Viverricula indica	Small Indian Civet	15	2.82
Prionailurus bengalensis	Leopard Cat	6	1.13
Herpestes urva	Crab-eating Mongoose	5	0.94
Arctonyx collaris	Hog Badger	4	0.75
Paguma larvata	Masked Palm Civet	2	0.38
Mus shortridgei	Shortridge's Mouse	2	0.38
Herpestes javanicus	Small Asian Mongoose	2	0.38
Sundasciurus sp.	Squirrel	1	0.19
Total photographs		59	

Table 2. List of species captured and frequency of detection of wild mammals in the reforestation plot

Scientific name	Common name	No. of photo taken (pictures)	Frequency of detection
Prionailurus bengalensis	Leopard Cat	5	0.94
Viverricula indica	Small Indian Civet	3	0.56
Arctonyx collaris	Hog Badger	1	0.19
Viverra zibetha	Large Indian Civet	1	0.19
Herpestes urva	Crab-eating Mongoose	1	0.19
Total photographs		11	

3.3 Ecological roles

We discovered one Large Indian Civet (*Viverra zibetha*), an omnivore listed as Near Threatened on The IUCN Red List of Threatened Species (Bista et al., 2012). The Large Indian Civet is an essential species for secondary seed dispersal (FORRU, 2006). In addition, we discovered small mammal species that live in a variety of habitats, such as the Leopard Cat (*Prionailurus bengalensis*) (Ross et al., 2015), hog badger (Arctonyx collaris) (Ross et al., 2015; Duckworth et al., 2016) Table 3 summarize ecological roles of each species detected.

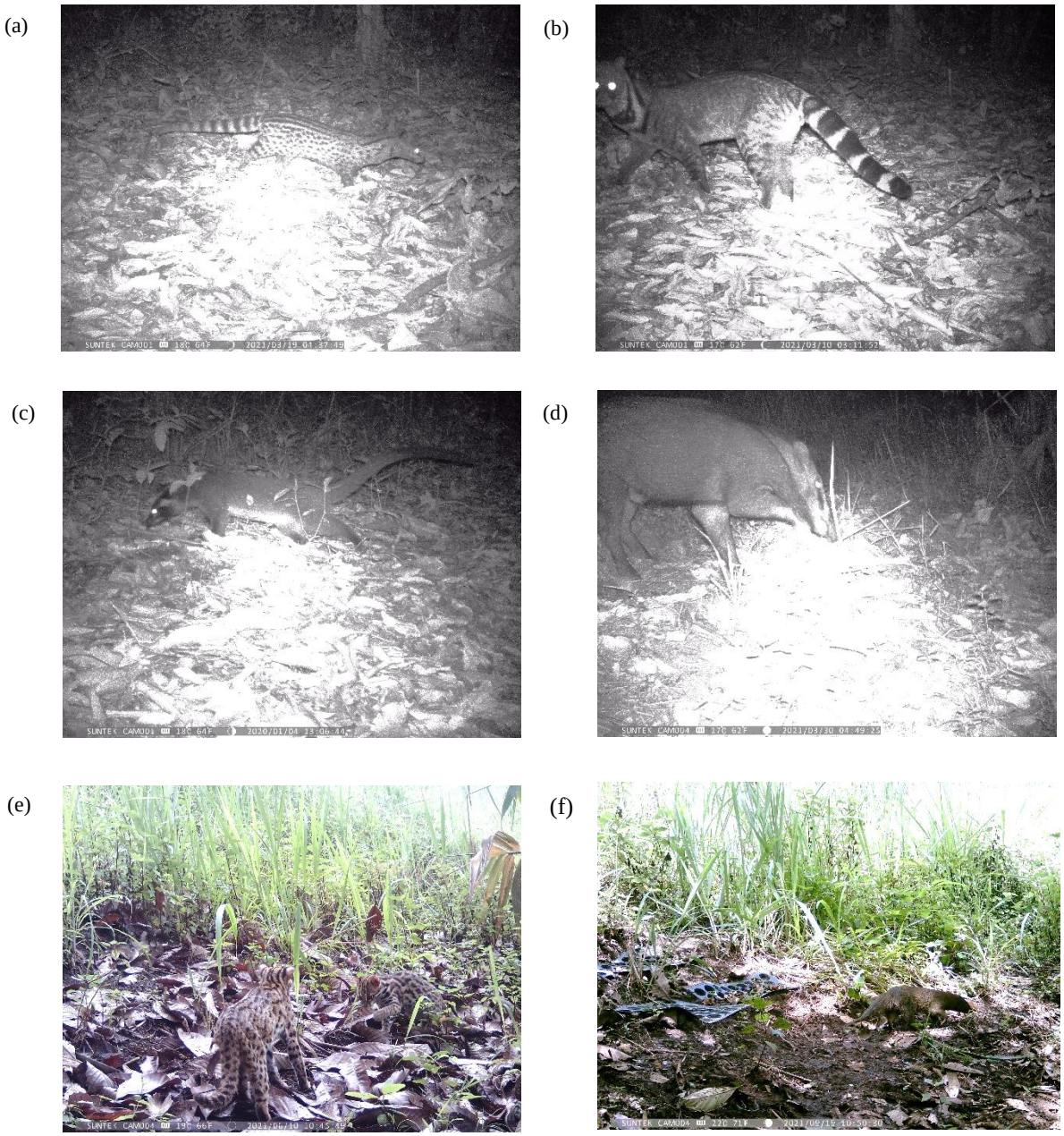

Figure 2. Examples of small mammal photos taken from the study sites. (a) Small Indian Civet (*Viverricula indica*), (b) Large Indian Civet (*Viverra zibetha*), (c) Masked Palm Civet (*Paguma larvata*), (d) Hog Badger (*Arctonyx collaris*), (e) Leopard Cat (*Prionailurus bengalensis*), and (f) Small Asian Mongoose (*Herpestes javanicus*)

4. Conclusions

Based on the research findings, the number of animal species found in natural and rehabilitated forest areas can be determined. The study demonstrates the advantages of forest restoration in terms of increasing ecosystem biodiversity. The findings of this study can be used to gather information about mammals that play an essential role in ecosystems and aid in forest restoration efforts to increase biodiversity in the long run. Further study of factors affecting forest regeneration, such as seed predation and seed dispersion, can also be studied.

Table 3. Summary of species' ecological roles.

No.	Species	Conservation Status	Sites found	Ecological roles
1	Large Indian Civet (Viverra zibetha)	Near Threatened	Both	Secondary seed dispersal species
2	Shortridge's mouse (*Mus* sp.)	Least concerned	Only in natural forest	Seed predator
3	Small Indian Civet (*Viverricula indica*)	Least concerned	Both	Secondary seed dispersal species, control rodent populations
4	Leopard cat (*Prionailurus bengalensis*)	Least concerned	Both	Predator species, control rodent populations which are seed predators.
5	Crab-eating mongoose (*Herpestes urva*)	Least concerned	Both	Control rodent populations
6	Masked palm civet (*Paguma larvata*)	Least concerned	Only in natural forest	Secondary seed dispersal species
7	Small Asian mongoose (*Herpestes javanicus*)	Least concerned	Only in natural forest	Control rodent populations
8	Hog badger (*Arctonyx collaris*)	Near Threatened	Both	Secondary seed dispersal species creates habitat soil aeration
9	Squirrel (*Sundasciurus sp.*)	-	Only in natural forest	secondary seed dispersal species

Acknowledgement

The research was partially supported by The Forest Restoration Research Unit (FORRU), Faculty of Science, Chiang Mai University.

References

Bista, A., Chanchani, P., Warrier, R., Mann, R., Gupta, M. and Vattakavan, J. 2012. Detection of large indian civet *Viverra zibetha* in camera-trap surveys in and around Dudhwa National Park in the Terai Region of North India. Small Carnivore Conservation 47: 54–57.

Duckworth, J.W., Timmins, R., Chutipong, W., Gray, T.N.E., Long, B., Helgen, K., Rahman, H., Choudhury, A. and Willcox, D.H.A. 2016. Arctonyx collaris. The IUCN red list of threatened species 2016. Available from: http://dx.doi.org/10.2305/IUCN.UK.2016-1.RLTS.T70205537A45209459.en. Downloaded on 05 October 2016

FORRU. 2006. Planting trees. In: Elliott, S., Blakesley, D., Maxwell, J.F., Doust and Suwannaratana. S. How to plant a forest: the principles and practices of restoring tropical forests. Biology Department, Science Faculty, Chiang Mai University, Chiang Mai p. 103–132.

Jiménez, C. F., Quintana, H., Pacheco, V., Melton, D., Torrealva, J., & Tello, G. (2010). Camera trap survey of medium and large mammals in a montane rainforest of northern Peru. Revista peruana de Biología, 17(2), 191-196.

Krebs, C. J. (1999). Ecological methodology (2nd ed.). California: Addison Wesley Longman.

O'Brein, T., G'Kinnarid, M.F. and Wibisono, H.T. 2003: Crouching tigers, hidden prey: Sumatran tiger and prey populations in a tropical forest landscape. – Animal Conservation 6: 131–139.

Rabinowitz, A. 1991. Behaviour and movements of sympatric civet species in Huni Kha Khaeng Wildlife Sanctuary, Thailand. Journal of Zoology, 223(2): 281-298.

Ross, J., Brodie, J., Cheyne, S., Hearn, A., Izawa, M., Loken, B., Lynam, A., McCarthy, J., Mukherjee, S., Phan, C., Rasphone, A. & Wilting, A. 2015. Prionailurus bengalensis. The IUCN Red List of Threatened Species 2015. Available from: http://dx.doi.org/10.2305/IUCN.UK.2015-4.RLTS. Downloaded on 05 October 2016.

Royal Forest Department. (2020). Forestry Statistics Data 2020.

Shepherd, C.R. and Shepherd, L.A. 2012. A naturalist's guide to the mammals of Thailand and Southeast Asia. Asia Books Co.,Ltd 176 pp.

Sollmann, R., Mohamed, A., Samejima, H., & Wilting, A. (2013). Risky business or simple solution–Relative abundance indices from camera-trapping. Biological Conservation, 159, 405-412.

The 4G GIVE GREEN GET GREEN project is green all over Thailand. Retrieved November 1, 2021, from THE RAJAPRUEK INSTITUTE FOUNDATION Web site: https://rajapruek.org/th/foundation-project/research-and-forest-restoration/item/22-4g-give-green-get-green.html

Comparative Study on Seed Dispersal and Tree Seedling Diversity Between a Natural Forest and a Restored Forest Area in Mae Rim District, Chiang Mai

Atcharawan Saeaiew[a], Titaree Yamsri[a], Chrismas Kerdsak[a*], Alice Sharp[b], and Pimonrat Tiansawat[a]

[a]Department of Biology, Chiang Mai University, 239, Huaykeaw Road, Suthep Sub-District, Muang District, Chiang Mai 50200, Thailand
[b]Environmental Science Research Center, Chiang Mai University 239, Huaykeaw Road, Suthep Sub-District, Muang District, Chiang Mai 50200, Thailand

Abstract

Accelerating forest regeneration in degraded areas is one of the essential tasks to mitigating global climate change. Natural regeneration can occur if seeds from the neighboring forest disperse to degraded areas, germinate, and thrive. The study compared seed rain and tree seedling diversity in natural and adjacent5-year-old restored forests in Mae Rim District, Chiang Mai. From January to September 2021, to ensure that data collection covers both wet and dry seasons, ten hanging-mesh seed traps were installed in each site, and seeds deposited in the traps were collected and identified once a month. Tree seedling diversity was carried out by establishing three 10-m-diameter circular plots in each site. Natural seedlings ranging in height from 10 to 100 cm were recorded and identified. The seed trap experiment shows seeds of eight tree species in the natural forest and two species in the restored forest. Similarity seeds found in both sites show that 20% of the seed species can disperse from natural forests to neighboring areas. The study of seedlings in both sites revealed 23 species in the natural forest and 11 species in the restored forest. When the species found in seed traps and seedling surveys were compared, six species were the same in the natural forest and one in the restoration plot, resulting in a 30% and 15% similarity index, respectively. These findings imply that natural regeneration in restoration forests is slower and less diverse than natural forests. As a result, additional intervention such as planting native tree seedlings and regular weeding may be required to speed up the regeneration process.

Keyword: Forest restoration/ Seed dispersal/ Seedling/ Seed trap/ Similarity index/ Circular plot

---

*Corresponding Author: Chrismas Kerdsak, Tel: +66854747259
E-mail address: chrismas_k@cmu.ac.th

1. Introduction

Agricultural expansion is the primary cause of forest destruction and degradation, causing forest biodiversity to decline (FAO, 2020). Chiang Mai Province is still dealing with deforestation to convert the land for occupations and residence. Some communities in Chiang Mai Province's Mae Rim District, for example, burn down forests and encroach on arable land. Consequently, the forest area has been significantly reduced. As a result, the forest must be restored (Ratchapruek Institute Foundation, 2012). Forest restoration aims to restore biomes, biodiversity, and ecological processes (Silva et al., 2015).

One of the most critical factors in biodiversity conservation is seed dispersion (Traveset et al., 2008). Also, seed production, germination, and seedling survival are essential in maintaining plant populations (Almeida and Galetti 2007; Harper 1977; Hille Ris Lambers and Clark 2003; Jordano 2000; Levine and Murrell 2003). Plants develop various mechanisms for dispersing seeds from the parent plant. These are wind-dispersed, water-dispersed, gravity-dispersed, explosion-dispersed, and zoochory-dispersed (Stoner & Henry, 2005). These mechanisms allow seeds to disperse directly into appropriate locations (Wenny and Levey, 1998).

The goal of this study was to compare seed and seedling distribution in natural and rehabilitation forests. In addition, the study aims

to determine whether the environment in the disturbed area is capable of natural regeneration.

2. Methodology

The study was carried out in the Mon Jam area (18°56'16.8" N, 98°49'12.0" E), Mae Rim District, Chiang Mai Province. The forest in this area is an evergreen forest. The site is 1,300-1,420 meters above sea level, with an average temperature of about 23 degrees Celsius all year and an average rainfall of 1,314 millimeters per year (Nong Hoi Royal Project Development Center, 2019). The natural forest plot and reforestation plot are adjacent with an area of 3,277 and 1,058 square meters, respectively. Figure 1 depicts the location of the study sites and their characteristics.

Figure 1. Location of study sites. (a) Map of Mae Rim District; (b) natural forest; and (c) reforestation area.

2.1 Seed dispersal

Place ten seed traps in each area. The seed trap used is a hanging mesh trap with a seed receiving area of 50×50 cm nylon net. The legs were constructed from 100 cm long PVC pipes (Figure 2). In each area, seed traps were placed 5 meters apart. The GPS coordinates were saved. Once a month, seeds deposited in the trap were removed for laboratory analysis.

Figure 2. Hanging mesh seed trap

2.2 Tree seedling

A Circular Sampling Unit (CSU) was used to collect seedling data. Each area has three CSUs. Each CSU had a diameter of 10 m. (5 m radius). The seedlings that germinated naturally in each circular plot were identified, and their heights were measured. The seedlings must be between 10 and 100 centimeters in height.

2.3 Data analysis

2.3.1 Similarity index

The Sorensen's Similarity Coefficient (Krebs, 1999) was used to calculate the similarity index. The formula is as follows.

$$\text{Sorensen Coefficient} = 2C \times 100 / A + B$$

Where; A=No. of species found in area 1; B=No. of species found in area 2; C=No. of species found in both areas

2.3.2 Seedling density, D

The total number of seedlings counted is divided by the total area surveyed to determine the mean seedling density.

2.3.3 Seed and seedling identification

Seeds and seedlings were identified following the "Tree Seeds and Seedlings for Restoring Forests in Northern Thailand" (FORRU, 2000) and "A Field Guide to Forest Trees of Northern Thailand" (Gardner et al., 2007).

3. Results and Discussion

According to the seed dispersal and seedling survey, a total of 8 seeds species and 26 seedling species were discovered in the natural forest area. A total of 2 species of seeds and 11 species of seedlings were found in the reforestation area. Seed dispersal results can be found in Table 1.

Table 1. Seed species found in seed traps.

Species found in natural forest	Species found in the restoration area	Similarity
Schima wallichii	*Prunus cerasoides*	Sorensen Coefficient=20%
Dalbergia cultrata	*Engelhardia spicata*	
Castanopsis diversifolia		
Engelhardia spicata		
Lithocarpus polystachyus		
Lannea coromandelica		
Phoebe lanceolata (Wall. ex Nees) Nees		
Quercus lamellosa		

Eight types of seeds were found in the natural forests, two in the reforestation area. Only one species can be found on both sites, *Engelhardia spicata*. Seeds of *Engelhardia spicata* are wind-dispersed. Therefore, it is possible that the seeds were dispersed from the nearby natural forest into the restoration area. When comparing the seed dispersal similarity between the two forests, the two sites have a similarity coefficient of 20%.

The results of the tree seedlings study in both forest areas revealed that 270 seedlings from 23 species were found in the natural forest area, while 134 seedlings from 11 species were found in the restored forest area. In terms of seedling density, a natural forest has 1.145 seedlings per square meter, while a restored area has 0.568 trees per square meter. When comparing the similarity index of the two forests' seedlings, the seedling species discovered had a similarity index of 55 percent. The seedling species found in both areas are shown in Table 2. Most of the seedlings found in the natural forest can thrive and grow well. Appropriate physical conditions include temperature, light, hydrology (such as rainfall and soil moisture), and infrequent events that reshape ecological systems, such as fires and storms, encourage seedling growth.

The comparison between seed and tree seedlings found in each site revealed that six species were similar in the natural forest area and one in the restoration area, with the similarity index of 30 and 15 percent, respectively. The higher number of seeds/seedlings found in the natural forest may be due to the capacity to produce seeds together with the favorable physical conditions for seed germination and seedlings growth.

Table 2. Seedling species found in the study areas.

Species found in natural forest	Species found in the restoration area	Similarity
Schima wallichii	*Prunus cerasoides*	Sorensen Coefficient=33%
Dalbergia cultrata	*Litsea glutinosa (Lour.) C.B. Rob.*	
Castanopsis diversifolia	*Bauhinia variegata Linn.*	
Lithocarpus polystachyus	*Glochidion kerrii*	
Phoebe lanceolata (Wall. ex Nees) Nees	*Castanopsis diversifolia*	
Quercus lamellosa	*Michelia Floribunda*	
Aporusa villosa	*Phoebe lanceolata (Wall. Ex Ness)Ness*	
Helicia nilagirica	*Eurya acumminata*	
Wendlandia tinctoria	*Alangium kurzii*	
Antidesma bunius	*Eugenia fruticosa*	
Glochidion acuminatum	*Syzygium claviflorum (Roxb.) A.M.Cowan & Cowan*	
Castanopsis acuminatissima (Blume) A.DC.		
Lithocarpus elegans		
Castanopsis argyrophylla		
Prunus cerasoides		
Elaeocarpus lanceifolius		
Alstonia scholaris		
Anneskea fragrans		
Litsea glutinosa (Lour.) C.B. Rob.		
Syzygium claviflorum (Roxb.) A.M.Cowan & Cowan		
Gluta obovata Craib		
Eugenia fruticosa		
Decaspermum parviflorum		

4. Conclusions

Tree seeds can be dispersed to the adjacent area. However, the ability to disperse may be limited by several factors: distance from the forest's edge, the seed's shape, size, and dispersal mechanism. Even when the seed can disperse into the degraded area, it does not guarantee the germination and survival of seedlings. Other environmental factors may influence seedling germination and growth. More research should be done on the factors that limit seed germination and seedling growth. Climate, seed predators, seed dispersers, and seasonal influence may be investigated further. Additional intervention such as planting native tree seedlings and regular weeding may be required to speed up the restoration process.

Acknowledgement

The authors would like to express gratitude to the Forest Restoration Research Unit (FORRU), Faculty of Science, Chiang Mai University, for partially financing the research work and supporting the identification of seeds and seedlings by FORRU staff.

References

Almeida, L. B., & Galetti M. (2007). Seed dispersal and spatial distribution of *Attalae geraensis* (Arecaeae) in two remnants of Cerrado in Southeastern Brazil. Acta Oecolgica, 32,180-187.

Forest Restoration Research Unit, 2000. Tree Seeds and Seedlings for Restoring Forests in Northern Thailand.

Gardner, S., Sidisunthorn, P. & Anusarnsunthorn, V. (2007). A Field Guide to Forest Trees of Northern Thailand. Kobfai Publishing Project, Bangkok, Thailand.

Harper, J.L. (1997) Population Biology of Plants. London: Academic Press.

Lambers, J.H.R., & Clark, J.S. (2003). Effects of dispersal, shrubs, and density-dependent mortality on seed and seedling distributions in temperate forests. Canadian Journal of Forest Research. 33,783-795.

Jordano, P. (2000). Fruits and frugivory. In Fenner M (ed) Seeds: The Ecology of Regeneration in Plant

Communities 2nd Edition, Wallingford, UK: CAB International, 125-166.

Stoner, K.E., & Henry, M. (2005). Seed dispersal and frugivory in Tropical ecosystems. Tropical Biology and Conservation management.

Krebs, C.J. (1999). Ecological Methodology. 2nd Edition, Benjamin Cummings, Menlo Park, 620 p.

Levine, J. M., & Murrell, D. J. (2003). The community-level consequence of seed dispersal patterns. Annual Review of Ecology, Evolution, and Systematics, 34, 549-574.

Chen, L., Wang, L., Baiketuerhan, Y., Zhang, C., Zhao, X., & Gadow, K. (2013). Seed dispersal and seedling recruitment of trees at different successional stages in a temperate forest in northeastern China. Journal of Plant Ecology, (7)4, 337-346.

Silva, F.R.D., Montoya, D., Furtado, R., Memmott, J., Pizo, M., & Rodrigues, R. (2015). The restoration of tropical seed dispersal networks. Restoration Ecology, 23(6), 1-9.

Stone, J.L., Malloy, R., & Murray, G. 2017. Diversity of seeds captured by interception exceeds diversity of seed deposited in traps. Biotropica, 49(3), 1-6.

Wenny, D.G., & Levey, D.J. (1998). Directed Seed Dispersal by Bellbirds in a Tropical Cloud Forest. Proceedings of the National Academy of Sciences, 95(11), 6204-6207.

Seasonal Changes in Vertical Stratification of Moth Diversity in Tropical Rainforests of Thailand

Ronnarot Taveesri[a*], Akihiro Nakamura[b], Ekgachai Jeratthitikul[a], and Alyssa B. Stewart[c]

[a]Department of Biology, Faculty of Science, Mahidol University, Bangkok 10400, Thailand
[b]Xishuangbanna Tropical Botanical Garden, Chinese Academy of Sciences, China
[c]Department of Plant Science, Faculty of Science, Mahidol University, Bangkok 10400, Thailand

Abstract

Canopies of tropical rainforests present distinguished microclimates and habitats, creating vertically stratified forest biodiversity. Although distances from the ground to canopy layers are at most tens of meters, vertical turnover of communities are generally much greater than horizontal turnover which can stretch hundreds or thousands of meters. Insect diversity is stratified along vertical gradients, as insects, especially herbivorous insects, depend on various food resources and microhabitats provided by canopy trees. Although seasonal changes in insect community composition have been extensively documented, little attention has been paid to understand how vertical stratification of insects change across seasons. Here we investigated how moth diversity change vertically and horizontally across seasons in tropical rainforests located at different latitudes in Thailand. Moth samples were collected at Mo Singto (MS, 14º22′55″N 101º25′54″E) Khao Yai National Park, and Klong Naka Wildlife Sanctuary (KN, 9º27′34″N 98º30′15″E) in wet and dry seasons. At each site, moth samples were collected from the canopy and understory layers at a total of nine sampling plots established within a 300 m × 300 m grid. We identified moths to family as family level data can be compared across sites at different latitudes. The results showed that vertical stratification of moth diversity was more distinct in KN than MS plots, whereas seasonal change in moth diversity was more distinct in MS than KN. Our study suggests that vertical stratification of moth diversity is universal, as is suggested by other studies, but seasonal influence on vertical stratification may be highly variable across different latitudes.

Keyword: Lepidoptera/ Beta diversity/ Canopy layer/ Understory layer/ Seasonal variation

---

*Corresponding Author: Ronnarot Taveesri
E-mail address: ronnarot.tav@student.mahidoal.ac.th

1. Introduction

Tropical rainforests are heterogeneous in microclimate and other habitat conditions across landscapes. Such heterogeneity is generally viewed horizontally, but there is an additional dimension in which microclimate and other habitat conditions are stratified vertically from forest floor to the canopy. Forest canopies are generally covered by tree crowns that act as sunlight filter and temperature insulator (Frenne et al., 2019; Lowman & Moffett, 1993). Insect species are distributed across space according to their own physical tolerance, resource-requirements and behavior (Wardhaugh, 2014). Thus, insect communities have been observed to change along not only horizontally but also vertically within tropical rainforests (Basset et al., 2015).

In the last few decades, β-diversity has gained much attention to be used as a tools to understand the mechanisms underlying the community assembly (Mori et al., 2018). Although β-diversity has recently been studied in a variety of ecosystems, canopy organisms did not gain attention due to limited accessibility to the canopy and the untested assumption that forest communities are more or less homogeneous across vertical gradients (Basset et al., 2003; Lowman et al., 1992). This assumption has been defied by recent studies that presented high heterogeneity of organisms along vertical strata (Ashton et al. 2016, Basset et al. 2012). These studies found that vertical, rather than horizontal dimension, explained changes in forest community composition. Moreover, tropical canopy was reported to harbour more and unique

species than understory (Lowman et al., 2013; Nakamura et al., 2017).

Previous studies of vertical diversity, however, overlooked how seasonal variation may influence vertical stratification of forest biodiversity (Ashton et al., 2016; Basham et al., 2019). Populations of tropical insect species are highly dynamic with varying abundance and activity periods across seasons (Wardhaugh, 2014). Although, tropical rainforests are recognized as a seasonal forests, temperature and rainfall change across seasons and the magnitude of such changes escalates with increasing latitude within tropical areas (Denlinger, 1986). Wet seasons provide higher precipitation (rainfall) resulting in increasing plant resources for insects (Poulin et al., 1999). Thus, peaks in insect abundance generally coincide with wet seasons when production of new leaves and flowers by many plant species occur (Basset, 1991; Frith & Frith, 1985).

Insects were commonly used as ecological models in β-diversity studies because they are key drivers of many ecological processes and predictors of environmental changes (Ashton et al., 2016; Nakamura et al., 2017). In this study, we focus on moths - common nocturnal insects that belong to the order Lepidoptera. They are one of the most widespread and species-rich insect groups in the world (Gaston, 1991). Moths are chosen because of the following reasons: moths are abundant and diverse insects which provide reliable statistical analysis; moths can be collected by automated light traps; and their herbivore feeding that links moths with plant spatial and temporal dynamics (Ashton et al., 2015; Basset et al., 2012).

This study aims to investigate how moth diversity is vertically stratified and how vertical stratification changes across latitudes and seasons in tropical rainforests of Thailand. This study presented the results of the influence of vertical stratification on moth β-diversity with seasonal changes through similarity, dispersion and distance-decay relationship of moth assemblage between strata. further, to investigate the consistency of changes in assemblage composition, 2 sampling plots were established in Mo Singto plot of Khao Yai National Park and Klong Naka wildlife sanctuary.

2. Methodology

2.1 Study site

Moths were collected inside the two protected tropical forest locations of Thailand. First sampling location was established in Mo Singto, Khao Yai National Park (MS, 14º22′55″N 101º25′54″E), Nakhon Ratchasima Province of northeastern Thailand. Second location was established in Klong Naka Wildlife sanctuary (KN, 9º27′34″N 98º30′15″E), Ranong Province of southern Thailand. In each location, a total of nine sampling plots were arranged as 3 × 3 grid points which were separated by 150 meters from each other (Figure 1). Sampling was conducted in two seasons at each location: sampling in Mo Singto was conducted in June (wet season) and December 2019 (dry season); and sampling in Klong Naka was conducted in March (dry season) and September 2020 (wet season).

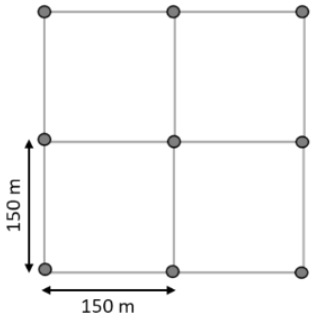

Figure 1. Diagram of the nine sampling plots established within each forest locations.

2.2 Sample collecting

Moths were collected using Pennsylvania-style light traps (Figure 2). At each sampling plot, moths were collected from the forest canopy and understory. One light trap was set immediately below the canopy surface at least 20 m above the ground but the height varied depending on the tree height (generally higher in KN than MS). Another trap was set two meters above the ground. Light traps were hoisted using a white rope which was suspended by the tree branches. For the canopy traps, we used a Big Shot Line Launcher (WesSpur Bellingham WA) to suspend the ropes over the tree branches.

Traps were running for a total of three nights during the sampling season but avoided seven days before and after full moon. Traps were retrieved next day of the light trapping and specimens were kept in the plastic containers (with tissue papers) and left in a deep freezer (-20°C). Temperature and light intensity (lux) were measured using HOBO pendant data loggers suspended in the canopy and understory at each plot for 3-6 months after moth sampling was completed. Canopy height was recorded using a handheld laser clinometer (HT-900A Compact).

Figure 2. Pennsylvania light traps with Philips TL 8W actinic BL light bulb

2.3 Sample processing

Macro-moths (>2 cm wing spans) were selected as target insects. All macro-moths were identified to family using morphological key of *The Moths of Borneo* (Holloway, 1983). Other non-target insects were preserved in 95% ethanol.

2.4 Statistical analysis

Macro-moth families and their abundances from each stratum (canopy or understory) at each sampling plot across two locations and seasons were used as sample unit used for statistical analysis. Three sampling nights from each sampling season were pooled. We therefore obtained a total of: 2 locations×2 seasons×9 sampling plots×2 strata=72 samples We first estimated sampling sufficiency and gamma diversity of moth families collected from different vertical strata and seasons in MS and KN locations by generating rarefaction curves using *iNEXT* package (Hsieh et al., 2016) in R program (Project R for Statistical Computing). We generated individual-based rarefaction curves by plotting family richness against a number of individuals. Extrapolation was also made by doubling the number of observed individuals to estimate moth family richness.

Beta diversities were calculated using Horn dissimilarity index. Horn dissimilarity index quantifies the overlap of species among sampling units which could reduce bias caused by rare or dominated species (Jost, 2007). To test the influence of three main factors (Vertical stratum, Seasonal changes and Forest type) and their interactions on moth assemblages, we ran PERMANOVA tests using *adonis2* function of *vegan* package with 9999 permutations of samples (Anderson, 2001; Oksanen et al., 2019). Then assemblages between canopies and understories were compared across different seasons and forests via post-hoc pairwise analysis using *pairwise.adonis* functions of *pairwiseAdonis* package (Oksanen et al., 2019). Additionally, as vertical stratification could differently affect moths in each family, we performed similarity percentages analysis using *SIMPER* of *vegan* package (Oksanen et al., 2019) to detect moth families that significantly changed their abundance and occurrence frequencies among groups of samples. NMDs plots were generated to visualize changes in moth assemblage composition between vertical strata and seasons. They were created by *metaMND* function of *vegan* package (Faith et al., 1987).

Horizontal beta diversity (measured as average distances of moth assemblage samples from the centroids of the group distances) in moth diversity was quantified within canopy and understory strata across two locations *beta.disper* function on *vegan* package and tested by ANOVA (Anderson, 2006). Distance-decay relationships (pair-wise horizontal distances plotted against pair-wise distance measures between samples) were investigated using *decay.model* function of *betapart* package (Nekola & Mcgill, 2014).

Variation portioning were analyzed to investigate how much variation in the moth

assemblage composition was explained by seasons, horizontal distance and vertical distance in MS and KN (two locations analyzed separately) using *varpart* function on vegan package (Borcard et al., 1992).

3. Results

3.1 Abundance and family richness

We collected a total of 13723 moths belonging to 13 families in this study. Mean abundance of wet season moth was higher than dry season in both Mo Singto (MS) and Klong Naka plot (KN). MS plot showed higher mean abundance of moth in canopy than understory in wet season with no difference in dry season. In contrast, KN plots showed higher mean abundance of moth in understory than canopy in wet season with no difference in dry season (Figure 3).

Individual-based rarefaction curves showed that MS plot had higher number of families in canopy than understory in wet season, but their 95% confidence intervals overlapped, suggesting that the differences were not significant. Similar trajectories were found in canopy and understory of dry season which showed lower than the wet season. Extrapolating to twice the number of individuals didn't present different trends (Figure 4a). In Klong Naka plot, although smaller number of individuals were collected in dry than wet seasons, both canopy and understory samples from wet and dry seasons showed similar trajectories with similar number of families, and extrapolating to twice the number of individuals did not change the observed trends (Figure 4b).

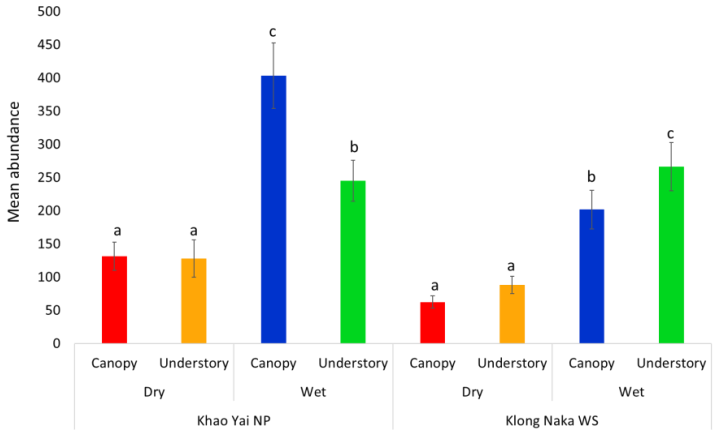

Figure 3. Mean abundance of moths in each vertical stratum and seasons in Mo Singto (MS) Khao Yai NP (left) and Klong Naka (KN) Wildlife Sancturat (right).

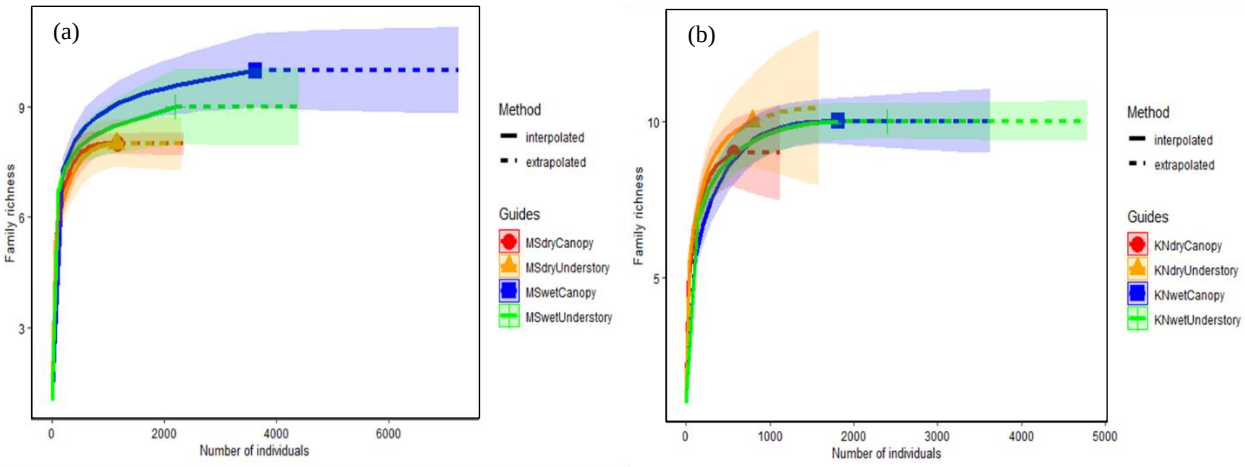

Figure 4. Individual-based rarefaction curves of moth family richness in canopy and understory samples collected in dry and wet seasons in: a=Mo Singto plots; and b=Klong Naka plots.

3.2 PERMANOVA

PERMANOVA analysis indicated that moth communities were significantly explained by vertical stratum, locations and seasons. Three-way interaction of those factors was observed (Table 1). Post-hoc PERMANOVA showed that vertical stratification of moth was influenced by sampling area and seasons with different pattern (Table 2).

Table 1. PERMANOVA results based on Horn dissimilarities using family data for moth community structure in relation to compartment for vertical stratum (canopy and understory), locations (Mo Singto and Klong Naka plot) and seasonality (wet and dry season).

Factor	Df	Sum of Sqs	R2	F	Pr(>F)	
Vertical	1	0.099	0.142	18.360	0.001	***
Location	1	0.089	0.127	16.467	0.002	**
Season	1	0.123	0.176	22.834	0.001	***
Vertical: Location	1	-0.030	-0.043	-5.584	1	
Vertical: Season	1	0.028	0.040	5.194	0.065	.
Vertical: Location: Season	1	0.039	0.055	7.150	0.018	*
Residual	65	0.352	0.502			
Total	71	0.701	1			

Significant codes: '***' = P>0.001; '**' = P>0.01; '*' = P>0.05; '.' = P>0.1; ' ' = P>1

Table 2. Post-hoc PERMANOVA results compared moth communities between canopy and understory.

Locations and seasons	Df	Sums Of Sqs	F.Model	R2	p.value	p.adjusted	
MS Wet	1	0.038	8.934	0.358	0.028	0.028	.
MS Dry	1	0.002	0.321	0.020	0.544	0.544	
KN Wet	1	0.007	20.231	0.558	0.001	0.001	**
KN Dry	1	0.097	30.523	0.656	0.001	0.001	**

Significant codes: '***' = P>0.001; '**' = P>0.01; '*' = P>0.05; '.' = P>0.1; ' ' = P>1

3.3 Similarity percentages of moth communities along vertical stratum

In MS wet season, similarity percentages showed that 5 of 10 moth families, namely Crambidae (P<0.001), Noctuidea (P<0.05), Cossidae (P<0.05), Erebidae (P<0.1) and Saturnidea (P<0.1) (Table 3), were vertically significantly different and higher in the canopy. In MS dry season, only Bombycidae was significantly higher in the canopy (P<0.1) (Table 4).

In KN wet season, similarity percentages showed that 4 of 11 moth families, namely Zygaenidea (P>0.001), Geometridae (P>0.01), Notodontidae (P>0.01) and Lasiocampidae (P>0.05) (Table 5), were vertically significantly different and greater in the understory. In KN dry season, 3 of 9 moth families, namely Erebidae (P>0.01), Geometridae (P>0.01) and Notodontidae (P>0.01) (Table 6), were greater in the understory.

Table 3. Similarity percentages of moth family communities between canopy and understory of Mo Singto wet season

Family	average	sd	ratio	canopy	understory	P-value	
Crambidae	0.160	0.074	2.158	172.556	75.889	0.001	***
Geometridae	0.079	0.061	1.291	89.556	82.222	0.999	
Noctuidea	0.055	0.039	1.413	59.556	27.667	0.03	*
Erebidae	0.044	0.028	1.567	64.444	44	0.055	.
Notodontidae	0.010	0.007	1.319	7.333	9	0.112	
Sphingidae	0.006	0.006	0.966	5.444	3.667	0.57	
Lasiocampidae	0.003	0.003	1.078	2.556	1.667	0.646	

Significant codes: '***' = P>0.001; '**' = P>0.01; '*' = P>0.05; '.' = P>0.1; ' ' = P>1

Table 3. Similarity percentages of moth family communities between canopy and understory of Mo Singto wet season (cont.)

Family	average	sd	ratio	canopy	understory	P-value	
Bombycidea	0.002	0.002	1.007	1	0.556	0.843	
Saturniidae	0.001	0.0008	0.878	0.444	0.111	0.079	.
Cossidae	0.0001	0.0004	0.348	0.111	0	0.015	*

Significant codes: '***' = P>0.001; '**' = P>0.01; '*' = P>0.05; '.' = P>0.1; ' ' = P>1

Table 4. Similarity percentages of moth family communities between canopy and understory of Mo Singto plot dry season

Family	average	sd	ratio	canopy	understory	P-value	
Crambidae	0.130	0.094	1.389	54.333	49.556	0.84	
Erebidae	0.114	0.080	1.419	39.556	42.667	0.945	
Geometridae	0.060	0.055	1.075	16.778	16.778	0.931	
Noctuidea	0.041	0.029	1.442	16.778	14.556	0.799	
Notodontidae	0.012	0.010	1.188	2.333	3.222	0.39	
Sphingidae	0.003	0.005	0.603	0.556	0.556	0.558	
Lasiocampidae	0.002	0.003	0.797	0.444	0.444	0.641	
Bombycidea	0.002	0.004	0.551	0.444	0	0.091	.
Zygaenidea	0.001	0.002	0.467	0	0.222	0.345	

Significant codes: '***' = P>0.001; '**' = P>0.01; '*' = P>0.05; '.' = P>0.1; ' ' = P>1

Table 5. Similarity percentages of moth family communities between canopy and understory of Klong Naka plot wet season

Family	average	sd	ratio	canopy	understory	P-value	
Crambidae	0.125	0.088	1.418	110.889	144.778	0.221	
Geometridae	0.061	0.038	1.621	19	45.333	0.005	**
Erebidae	0.052	0.036	1.447	56.444	51.778	1	
Noctuidea	0.016	0.014	1.148	11.222	13.444	0.647	
Notodontidae	0.008	0.007	1.225	1.667	5.333	0.006	**
Zygaenidea	0.005	0.004	1.318	0	2.667	0.001	***
Lasiocampidae	0.003	0.002	1.345	0.556	1.444	0.043	*
Delceridae	0.002	0.002	0.798	0.444	0.556	0.116	
Bombycidea	0.001	0.001	1.004	0.556	0.444	0.987	
Saturniidae	0.001	0.001	0.909	0.444	0.333	0.974	
Sphingidae	0.0005	0.001	0.495	0.222	0	0.473	

Significant codes: '***' = P>0.001; '**' = P>0.01; '*' = P>0.05; '.' = P>0.1; ' ' = P>1

Table 6. Similarity percentages of moth family communities between canopy and understory of Klong Naka plot dry season

Family	average	sd	ratio	canopy	understory	P-value	
Crambidae	0.110	0.078	1.407	32.444	30.444	0.994	
Erebidae	0.107	0.069	1.551	13.778	28.444	0.003	**
Geometridae	0.084	0.057	1.487	5.222	18	0.008	**
Noctuidea	0.034	0.027	1.254	8.667	7	0.635	
Notodontidae	0.012	0.008	1.472	0.333	2.111	0.009	**
Delceridae	0.007	0.006	1.024	0.778	0.667	0.263	
Bombycidea	0.005	0.006	0.850	0.444	0.556	0.923	
Lasiocampidae	0.004	0.004	0.954	0.444	0.444	0.922	
Sphingidae	0.001	0.003	0.615	0.111	0.222	0.501	
Limacodidae	0.0006	0.002	0.348	0	0.111	0.106	

Significant codes: '***' = P>0.001; '**' = P>0.01; '*' = P>0.05; '.' = P>0.1; ' ' = P>1

3.4 NMDs ordination

NMDs ordination showed that, in MS, moth assemblages between the canopy and understory in wet season trended to be more dissimilar than those between canopy and understory in dry season. Moth communities between wet and dry seasons were obviously separated. At KN, moth assemblages between understory and canopy separated, but dry season moth assemblages were similar to the canopy samples collected in wet season. In contrast, wet season understory moths assemblages were distinctively different from others (Figure 5).

3.5 Beta dispersion

Beta dispersion found no significant differences in dispersion between the canopy and understory strata (Table 7) across locations and seasons. Significant distance-decay relationship was found only in wet season of canopy moths in Mo Singto (P>0.01) (Figure 6).

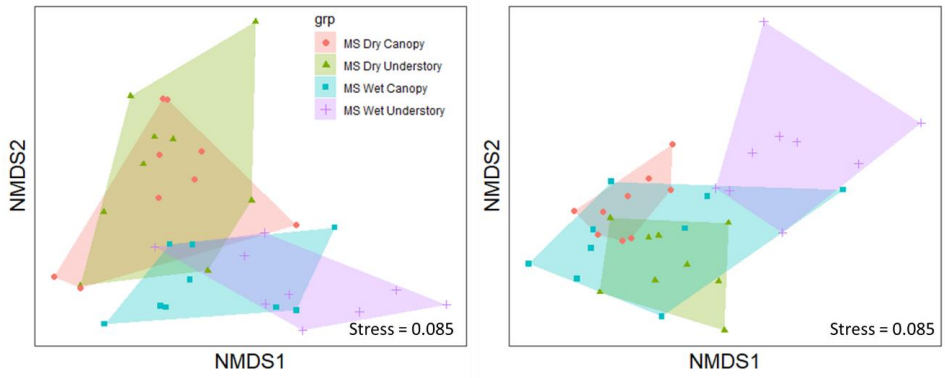

Figure 5. NMDs ordination of moth assemblages (based on Horn distance index) collected from the canopy and understory in wet and dry seasons. MS (left) and KN (right) locations were presented separately. Which points represented each community within their vertical layers and seasons.

Table 7. Beta dispersion of horizontal moth assemblage between canopy and understory.

Habitat		Df	Sum Sq	Mean Sq	F value	Pr(>F)
MS Wet	Groups	1	0.000319	0.000319	0.1709	0.6848
	Residuals	16	0.029821	0.001864		
MS Dry	Groups	1	0.000063	6.35E-05	0.0217	0.8848
	Residuals	16	0.046847	2.93E-03		
KN Wet	Groups	1	5.48E-05	5.48E-05	0.3061	0.5877
	Residuals	16	0.002864	1.79E-04		
KN Dry	Groups	1	0.000234	2.34E-04	0.1567	0.6974
	Residuals	16	0.023898	1.49E-03		

Significant codes: '***' = P>0.001; '**' = P>0.01; '*' = P>0.05; '.' = P>0.1; ' ' = P>1

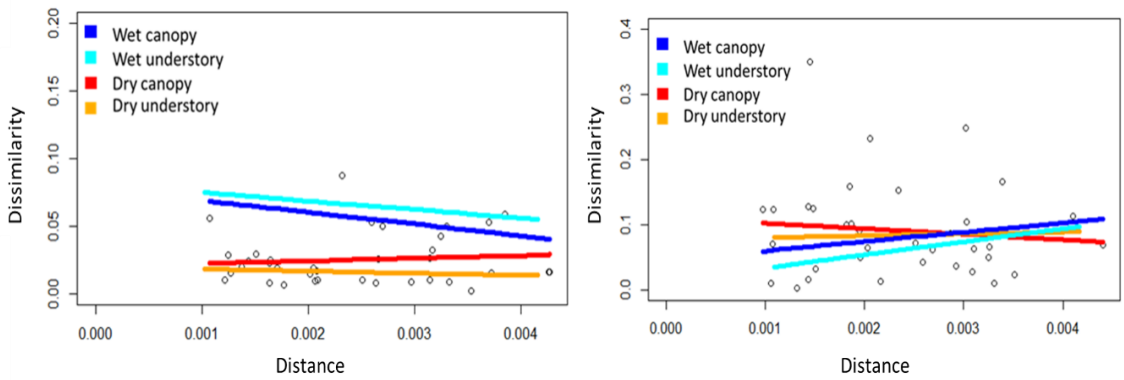

Figure 6. Distance-decay of moth communities along horizontal distance in each vertical Table stratum, sampling area and seasons.

3.6 Variation partitioning

In MS, moth assemblages were mostly explained by seasons (75.2%) and vertical distance (10.9%). In KN, assemblage variation was explained by vertical distance (23.2%) and seasons (16.5%). Very small proportions of moth assemblage composition were explained by horizontal distance in both Mo Singto (4.7%) and Klong Naka (4.2%). Note that more variation was explained in MS (45.4% residuals) than KN location (64.1% residuals) (Figure 7).

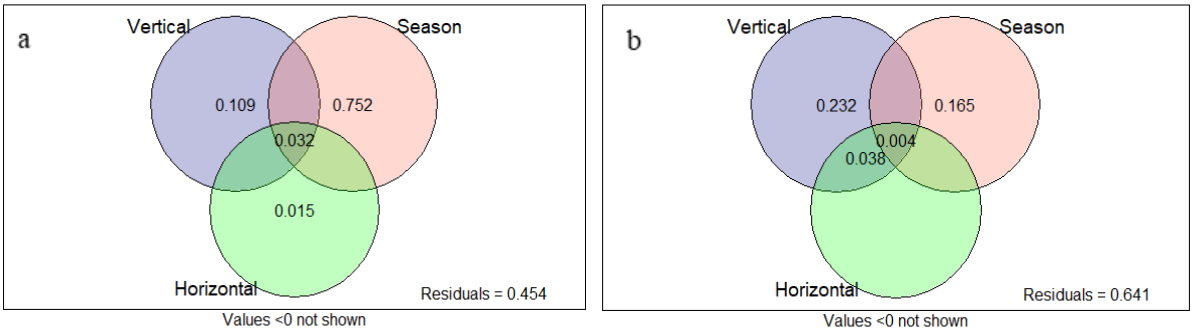

Figure 7. Venn diagram displaying proportions of variations in moth assemblage composition explained by seasons and vertical and horizontal distances in MS (a) and KN (b) locations. As Horn distance index was not Euclidean distances, some correlation coefficients returned negative values (not shown) and, as a result, explained variations and residuals do not add up to 1. (a=Mo Singto plot, b=Klong Naka plot)

4. Discussion

The results revealed the evidence that moth communities changed along vertical dimension and across seasons (Table 1). Vertical stratification was found in the results of moth community dissimilarity and characteristic moth families primarily found in the canopy or understory. Patterns in vertical stratification and seasonal influence were, however, different between the two locations (Table 2-6, Figure 5). Moth communities were explained by vertical distances and seasonal changes, whereas little variation was explained by horizontal distances (Figure 7). Moreover, moth assemblage dispersion and distance-decay relationships (both in horizontal dimension) were non-significant (Table 7 and Figure 6).

The results showed clear vertical stratification in moth communities. Canopy moth communities differed from understory moth communities, and the same patterns were found elsewhere (Nice et al., 2019). Forest canopies created different habitat structures, physical conditions and plant communities which vary through vertical gradients. Moths were influenced by forest structures and openness. Canopy gaps create space to access the food and provide mating resource which was important to rainforest lepidopterans (Delabye et al., 2021; Vlasanek et al., 2013). Plant diversity could play an important role for enhancing moth diversity. Indeed, previous studies showed that vertical stratification of plant species created vertical stratification of lepidopterans (Aduse-Poku et al., 2012).

Seasonal changes affected moth abundance and community composition. At Mo Singto, moth assemblages between seasons had low similarity. Wet season increased the magnitude of vertical stratification. Seasonal changes are associated with weather conditions such as rainfall, temperature, wind, radiation and plant phenology. Those factors may have had effects on the distribution of arthropods (Grimbacher & Stork, 2009; Poulin et al., 1999). However, this study only collected samples in only one months for each season and was not monthly surveys which could represent the gradual changes in moth community through time.

Mo Singto and Klong Naka locations were different in forest type, weather and unique species. Mo Singto is located in northern-east part of Thailand with seasonal evergreen forests. Due to northern-east weather condition, wet season is in summer (June to October) and dry

season in winter (November - February). Whereas, Klong Naka is located in southern Thailand which generaly has rainy season from May to October and dry season from November to April. Klong Naka forest had smaller seasonal changes in plant phenology and forest structures than Mo Singto. Therefore, seasonal influences are more pronounced in the Mo Singto than Klong Naka, as was seen in the results of variation partitioning (variation in moth assemblages explained by seasonal differences: MS, 75.9%; KN, 16.5%) (Figure 7). Moreover, Klong Naka plots showed greater magnitude of vertical stratification than Mo Singto (Table 2, Figure 5). Vertical stratification of diversity may increase with decreasing latitude, and this could be driven by increasing forest structural complexity, vegetation diversity and canopy height in the equatorial tropical rainforests (Lieberman et al., 1996).

Unfortunately, horizontal distance did not explain moth communities. Due to our taxonomic resolution at moth family and not species, it is possible that our limited taxonomic resolution could not be used to differentiate horizontal moth communities. On the other hand, our limited taxonomic resolution was still sufficient to detect vertical stratification and seasonal changes across the two locations at different latitudes.

5. Conclusions

Moth community was highly influenced by vertical stratum and seasonal changes, but the magnitude of differences depend on the forest type and latitude. Vertical stratification of moths was confirmed by community dissimilarity and some moth families unequally distributed along vertical strata. Seasonal differences were related to increasing vertical stratification of moth. This study represented the importance of seasonal variation and forest types on vertical stratification study in tropical rainforests.

Acknowledgement

I would like to thank Prof. Akihiro Nakamura of key laboratory of Tropical Forest Ecology, Xishuangbanna Tropical Botanical Garden, Chinese Academy of Sciences and Asst. Prof. Dr. Ekgachai Jeratthitikul of department of Biology, Faculty of Science, Mahidol University who teach and advice my research works. And also, Laksamee Punthuwat, Pattharawadee Waitayachart, Ponrujee Yongsiri, Achariyaporn and Koth Amratisha who help and co-work in field trips. This study was support by funding from Southeast Asia Biodiversity Research Institute (SEABRI).

References

Aduse-Poku, K., William, O., Oppong, S. K., Larsen, T., Ofori-Boateng, C., & Molleman, F. (2012). Spatial and temporal variation in butterfly biodiversity in a West African forest: Lessons for establishing efficient rapid monitoring programmes. *African Journal of Ecology*, *50*(3), 326-334.

Anderson, M. J. (2001). A new method for non-parametric multivariate analysis of variance. *Austral Ecology*, *26*, 32-46.

Anderson, M. J. (2006). Distance-based tests for homogeneity of multivariate dispersions. *Biometrics*, *62*(1), 245-253.

Ashton, L. A., Barlow, H. S., Nakamura, A., & Kitching, R. L. (2015). Diversity in tropical ecosystems: The species richness and turnover of moths in Malaysian rainforests. *Insect Conservation and Diversity*, *8*(2), 132-142.

Ashton, L. A., Nakamura, A., Basset, Y., Burwell, C. J., Cao, M., Eastwood, R., Odell, E., de Oliveira, E. G., Hurley, K., Katabuchi, M., Maunsell, S., Mcbroom, J., Schmidl, J., Sun, Z., Tang, Y., Whitaker, T., Laidlaw, M. J., Mcdonald, W. J. F., & Kitching, R. L. (2016). Vertical stratification of moths across elevation and latitude. *Journal of Biogeography*, *43*(1), 59-69.

Basham, E. W., Seidl, C. M., Andriamahohatra, L. R., Oliveira, B. F., & Scheffers, B. R. (2019). Distance–decay differs among vertical strata in a tropical rainforest. *Journal of Animal Ecology*, *88*(1), 114-124.

Basset, V., Cizek, L., Cuénoud, P., Didham, R. K., Guilhaumon, F., Missa, O., Novotny, V., Ødegaard, F., Roslin, T., Schmidl, J., Tishechkin, A. K., Winchester, N. N., Roubik, D. W., Aberlenc, H. P., Bail, J., Barrios, H., Bridle, J. R., Castaño-Meneses, G., Corbara, B., … Leponce, M. (2012). Arthropod diversity in a tropical forest. *Science*, *338*(6113), 1481-1484.

Basset, Y. (1991). The seasonality of arboreal arthropods foraging within an Australian rainforest tree. *Ecological Entomology*, *16*(3), 265-278.

Basset, Y., Cizek, L., Cuénoud, P., Didham, R. K., Novotny, V., Ødegaard, F., Roslin, T., Tishechkin, A. K., Schmidl, J., Winchester, N. N., Roubik, D. W., Aberlenc, H. P., Bail, J., Barrios, H., Bridle, J. R., Castaño-Meneses, G., Corbara, B., Curletti, G., Duarte Da Rocha, W., … Leponce, M. (2015). Arthropod distribution in a tropical rainforest: Tackling a four dimensional puzzle. *PLoS ONE*, *10*(12), 1-22.

Basset, Y., Hammond, P. M., Barrios, H., Holloway, J. D., & Miller, S. E. (2003). Vertical stratification of arthropod assemblages. In *Arthropods of tropical*

forests: spatio-temporal dynamics and resource use in the canopy.

Borcard, D., Legendre, P., & Drapeau, P. (1992). Partialling out the Spatial Component of Ecological Variation Author (s): Daniel Borcard , Pierre Legendre and Pierre Drapeau Published by : Ecological Society of America PARTIALLING OUT THE SPATIAL COMPONENT OF ECOLOGICAL VARIATION1. *Ecology*, *73*(3), 1045-1055.

de Frenne, P., Zellweger, F., Rodríguez-Sánchez, F., Scheffers, B. R., Hylander, K., Luoto, M., Vellend, M., Verheyen, K., & Lenoir, J. (2019). Global buffering of temperatures under forest canopies. *Nature Ecology and Evolution*, *3*(5), 744-749.

Delabye, S., Maicher, V., Sáfián, S., Doležal, J., Altman, J., Janeček, Š., Kobe, I. N., Murkwe, M., Šebek, P., & Tropek, R. (2021). Butterfly and moth communities differ in their response to habitat structure in rainforests of Mount Cameroon. *Biotropica*, *53*(2), 567-580.

Denlinger, D. L. (1986). Dormancy in tropical insects. *Annual Review of Entomology. Vol. 31*, 239-264.

Faith, D. P., Minchin, P. R., & Belbin, L. (1987). Compositional dissimilarity as a robust measure of ecological distance. *Vegetatio*, *69*(1–3), 57-68.

Frith, C. B., & Frith, D. W. (1985). Seasonality of insect abundance in an Australian upland tropical rainforest. *Australian Journal of Ecology*, *10*(3), 237–248.

Gaston, K. J. (1991). The Magnitude of Global Insect Species Richness. *Conservation Biology*, *5*(3), 283-296.

Grimbacher, P. S., & Stork, N. E. (2009). Seasonality of a diverse beetle assemblage inhabiting lowland tropical rain forest in australia. *Biotropica*, *41*(3), 328-337.

Holloway, J. D. (1983). *The Moths of Borneo: Key to families; families Cossidae, Metarbelidae, Ratardidae, Dudgeoneidae, Epipyropidae and Limacodidae*. Malaysian Nature Society.

Hsieh, T. C., Ma, K. H., & Chao, A. (2016). iNEXT: an R package for rarefaction and extrapolation of species diversity (Hill numbers). *Methods in Ecology and Evolution*.

Jost, L. (2007). Partitioning Diversity into Independent Alpha and Beta Components. *Ecology*, *88*(10), 2427–2439.

Lieberman, D., Lieberman, M., Peralta, R., & Hartshorn, G. S. (1996). Tropical Forest Structure and Composition on a Large-Scale Altitudinal Gradient in Costa Rica. *The Journal of Ecology*, *84*(2), 137.

Lowman, M., Devy, S., & Ganesh, T. (2013). Treetops at risk: Challenges of global canopy ecology and conservation. In *Treetops at Risk: Challenges of Global Canopy Ecology and Conservation*.

Lowman, M., & Moffett, M. (1993). The ecology of tropical rain forest canopies. *Trends in Ecology and Evolution*, *8*(3), 104-107.

Lowman, M., Taylor, P., & Block, N. (1992). Vertical stratification ofsmall mammals and insects in the canopy of a temperate deciduous forest: A reversal of tropical forest distribution? *Selbyana*, *14*, 25.

Mori, A. S., Isbell, F., & Seidl, R. (2018). β-Diversity, Community Assembly, and Ecosystem Functioning. *Trends in Ecology and Evolution*, *33*(7), 549-564.

Nakamura, A., Kitching, R. L., Cao, M., Creedy, T. J., Fayle, T. M., Freiberg, M., Hewitt, C. N., Itioka, T., Koh, L. P., Ma, K., Malhi, Y., Mitchell, A., Novotny, V., Ozanne, C. M. P., Song, L., Wang, H., & Ashton, L. A. (2017). Forests and Their Canopies: Achievements and Horizons in Canopy Science. *Trends in Ecology and Evolution*, *32*(6), 438-451.

Nekola, J. C., & Mcgill, B. J. (2014). Scale dependency in the functional form of the distance decay relationship. *Ecography*, *37*(4), 309-320.

Nice, C. C., Fordyce, J. A., Bell, K. L., Forister, M. L., Gompert, Z., & DeVries, P. J. (2019). Vertical differentiation in tropical forest butterflies: A novel mechanism generating insect diversity? *Biology Letters*, *15*(1).

Oksanen, A. J., Blanchet, F. G., Friendly, M., Kindt, R., Legendre, P., Mcglinn, D., Minchin, P. R., Hara, R. B. O., Simpson, G. L., Solymos, P., Stevens, M. H. H., & Szoecs, E. (2019). Vegan. *Encyclopedia of Food and Agricultural Ethics*, 2395-2396.

Poulin, B., Wright, S. J., Lefebvre, G., & Calderón, O. (1999). Interspecific synchrony and asynchrony in the fruiting phenologies of congeneric bird-dispersed plants in Panama. *Journal of Tropical Ecology*, *15*(2), 213-227.

Vlasanek, P., Sam, L., & Novotny, V. (2013). Dispersal of butterflies in a New Guinea rainforest: Using mark-recapture methods in a large, homogeneous habitat. *Ecological Entomology*, *38*(6), 560-569.

Wardhaugh, C. W. (2014). The spatial and temporal distributions of arthropods in forest canopies: Uniting disparate patterns with hypotheses for specialisation. *Biological Reviews*, *89*(4), 1021-1041.

Consumption Patterns on Food Waste Behavior: A Case Study in Nong Chok District, Bangkok

Suchanat Aneknopparat and Apichaya Lilavanichakul*

Department of Agro-Industrial Technology, Faculty of Agro-Industry, Kasetsart University, Bangkok, Thailand

Abstract

This study aimed to study the relationship between consumption patterns and food waste behavior at household level in Nong Chok district, Bangkok. The data were collected with 210 samples by using the questionnaire and analyzed by using descriptive statistics, factor analysis, and Pearson correlation coefficient. Findings showed that most respondents were aged at 46-60 years old and married (and have children). About 38.1% of total respondents have participated in waste separation campaign of the community. For food purchasing behavior and post-consumption management, about 39.0% of total respondents throw out the food surplus, followed by keeping food surplus for the next meals (38.8%), feeding animal (15.7%), and making compost at home (6.5%), respectively. The result of factor analysis can be divided into 5 factors that have unique characteristic. Findings on the relationship between consumption patterns and food waste behavior revealed that lifestyle for consumption pattern on leftover unconcerned, over-purchasing food preferred, and price and promotion conscious causing food leftovers statistically positively affected food waste generation (p-value < 0.01). Consumption patterns of respondents tend purchase foods over necessary causing food waste continue rising. Thus, promoting food waste reduction and creating awareness of food waste impact on the environment through marketing activities and driving food waste separation to all sectors should be encouraged.

Keyword: Food waste behavior/ Consumption patterns/ Community/ Household

---

*Corresponding Author: Apichaya Lilavanichakul
E-mail address: apichaya.l@ku.ac.th

1. Introduction

In the past 5 years, about one-third of the global food produced or approximately 1.3 billion tones has been lost or wasted, while 10.8% of the world population remains hungry and more than 62.5% of the world population are in Asia (FAO et al, 2019). In addition, food loss and food waste have led to a significant environmental impact on climate change and global warming, as well as healthy food system. Poor management at each level of food system contributes to food waste such as at the consumer level when consumers purchase more than they need and throw out leftover food, or at the production level where food is damaged during storage or transportation. Thus, reducing food waste is one of the 2030 Agenda for Sustainable Development Goals (SDGs), where goal 12 aims to ensure sustainable consumption and production patterns and target a 50% reduction of food waste by 2030 (United Nations, 2015).

Thailand is one of the countries that faces challenges on food waste generations and waste pollution. In Thailand, the actual amount of food waste has not been collected properly, but has inferred from the amount of organic waste, which are considered as a food waste. The report by Pollution Control Department (2017) revealed that about 17.56 tones or 64% of the total municipal solid waste in Thailand are organic waste, which almost 31% of total waste were disposed improperly (Pollution Control Department, 2021). Food waste management has been long-term problems because Thai consumers are lack of awareness on food waste reduction, waste utilization, and knowledge on proper waste separation. These result in high costs of food waste management after post-consumption and more complicated waste separation process on recycling and disposal. According to SDGs and Thailand's roadmap on the BCG economy, national waste management

plan (2016-2021) has become a direction for preventing food loss and waste with 3Rs concept (reduce, reuse, and recycle) and proper disposal methods among all sectors (NSTDA, 2020). However, the action on food waste management has been slowly implemented to each sector and require long time to adjust to a new behavior, especially at the household level. Some communities have launched a waste management campaign for promoting local food waste reduction, whereas households with various consumption patterns would generate food waste and participate in the campaign differently. Therefore, this study addresses the relationship between consumption patterns and food waste behavior at household level in order to provide strategies to promote food waste reduction and create awareness of food waste impact on the environment and communities.

2. Methodology

2.1 Questionnaire development

The questionnaire consisted of 3 sections. Section 1 included demographic characteristics of the participants (gender, age, marital status, level of education, monthly household income, household size, and person in charge of meal preparation or food purchase). Section 2 comprised of questions regarding food purchasing behavior and post-consumption management (frequency on grocery shopping, food expenditure, and self-reported amounts of leftover after meals). Section 3 related to consumption patterns which respondents were required to indicate their degree of agreement on a five-point Likert scale (1 = completely disagree; 5 = completely agree).

2.2 Data collection and analysis

A sample of 210 respondents in Nong Chok district were analyzed by using descriptive statistics to describe the demographic characteristics, food purchasing behavior and post-consumption management. For consumption patterns, the set of variables within each factor were identified by using factor analysis. The principal components analysis (PCA) is a technique for reducing the dimensionality of data set and compute the components or factors that perform the Kaiser-Meyer-Olkin (KMO) measure of sampling adequacy above 0.7 are desired (Hoelzle & Meyer, 2013) and the significance level from Bartlett's Test of sphericity below 0.05. Then, Pearson Correlation Coefficient was used to study the relationship between consumption pattern factors and food waste behavior.

3. Results and Discussions

The survey sample (n = 210) showed that 67.6% of respondents were female, in terms of age, most respondents aged 46-60 years old (48.1%), followed by 16-30 years old (29.0%). About 51.0% of total respondents have married (and have children) and half of total respondents (55.7%) have level of education below bachelor's degree. Majority of the respondents (54.8%) earned household income less than 20,000 Baht per month. The survey found that 41.4% of total respondents have household size more than 3 people, and 73.8% of total respondents are the primarily responsible for meal preparation or food purchase as showed in Table 1.

Findings on purchasing behavior and post-consumption management found that the frequency of buying raw food materials 1-2 days/week, average food expenditure 100-299 Baht/time. Majority of total respondents generate 10% of food leftover after meal and they choose to throw out unused food (39%), use leftover for the next meal (38.8%), and feed animals (15.7%), respectively. There was only 6.5% of total respondents who use leftover for composting as showed in Table 2.

Results from principal components analysis (PCA) with varimax rotation showed a total variance explained of 59.74%. The KMO achieved a value of 0.769, exceeding the recommended value, suggesting suitable components of 20 variables on consumption patterns. In addition, the Bartlett's test of sphericity was statistically significance ($p<0.05$), indicating the data's suitability for structural detection. Finally, all factor loadings of measured items that meet the guidance exceeding acceptable level of 0.40 (Williams et al., 2010). Rotated component matrix of five lifestyle for consumption pattern factors was showed in Table 3. Five factors consisted of food awareness and balance, leftover unconcerned, trendy and

Table 1. Demographic characteristics of sample n = 210 (number and (%))

Characteristics	Variable	Sample (% percentage)
Gender	Male	68 (32.4%)
	Female	142 (67.6%)
Age	16-30	61 (29.0%)
	31-45	33 (15.7%)
	46-60	101 (48.1%)
	> 60	15 (7.1%)
Marital status	Single	77 (36.7%)
	Married (and have children)	107 (51.0%)
	Married (with no children)	21 (10.0%)
	Divorced	5 (2.4%)
Level of education	Below a bachelor's degree	117 (55.7%)
	Bachelor's degree or higher	93 (44.3%)
Income (Baht/month)	< 20,000	115 (54.8%)
	20,000-55,000	70 (33.3%)
	> 55,000	25 (11.9%)
Household size (person)	1	30 (14.3%)
	2	44 (21.0%)
	3	49 (23.3%)
	>3	87 (41.4%)
Primarily responsible for meal preparation or food purchase	Yes	155 (73.8%)
	No	55 (26.2%)

Table 2. Purchasing behavior and post-consumption management n = 210 (number and (%))

Purchasing behavior and post-consumption management	Variable	Sample
Frequency of buying raw food materials (days/week)	Everyday	48 (22.9%)
	5-6 days	35 (16.7%)
	3-4 days	57 (27.1%)
	1-2 days	70 (33.3%)
Food expenditure (Baht/time)	<100	10 (4.7%)
	100-299	102 (48.6%)
	300-499	42 (20.0%)
	>500	56 (26.7%)
Food leftover	10%	120 (57.1%)
	20%	18 (8.6%)
	30%	19 (9.0%)
	40%	4 (1.9%)
	50%	9 (4.3%)
	No food leftover	40 (19.0%)
Post-consumption management (multiple choice)	Eat leftover	138 (38.8%)
	Trash	139 (39.0%)
	Feed animals	56 (15.7%)
	Composting	23 (6.5%)
Waste separation	Yes	80 (38.1%)
	No	130 (61.9%)

convenient preferred, over-purchasing food preferred, and price and promotion conscious. Each factor groups included specific lifestyle for consumption pattern. The first factor group, food awareness and balance contained planning household consumption, rearranging items in refrigerator, balancing raw materials with other foods, and controlling the amount of food meals. The second factor was leftover unconcerned, including having leftover due to over-ordering foods or controlling body weight, and throwing out unused food. Third factor of trendy and convenient preferred contained trying new products, purchase by following reviews and trends, and preferring food delivery. The fourth factor group was over-purchasing food preferred including buying near-expired food and buying food more than one time consumption. The last factor was price and promotion conscious consisting of buying cheap or discounted food. These factor groups were used to analyze the relationship between lifestyle for consumption pattern and food waste behavior by using Pearson correlation coefficient.

Table 3. Rotated Component Matrix

Variables	Factor				
	1	2	3	4	5
Factor 1: Food awareness and balance					
1. planning household consumption	.745				
2. rearranging items in refrigerator	.741				
3. Planning the amount of food to be suitable for consumption	.729				
4. Always check items in refrigerator	.722				
5. Read the label before buying	.695				
6. Buying food by choosing a package size to be suitable for consumption	.649				
7. Controlling the amount of food meals	.522				
8. Always finish their food	.471				
Factor 2: Leftover unconcerned					
1. Having leftover due to controlling body weight		.785			
2. Having leftover due to over-ordering foods		.762			
3. Throwing out unused food		.667			
4. Buying food more than the whole family's consumption.		.571			
Factor 3: Trendy and convenient preferred					
1. Trying new products			.824		
2. Purchase by following reviews and trends			.648		
3. Order food via delivery channel			.577		
Factor 4: Over purchasing food preferred					
1. Buying near-expired food				.705	
2. Buying food they do not particularly like				.646	
3. Buying food more than one time consumption				.564	
Factor 5: Price and promotion conscious					
1. Buying cheap food					.839
2. Buying discounted food					.524

Table 4 presented the correlation between lifestyle for consumption pattern factor groups and food waste behavior, four factor groups are statistically significant (p-value ≤ 0.05) including leftover unconcerned, trendy and convenient preferred, over-purchasing food preferred, and price and promotion conscious. Positive correlation coefficient indicated that lifestyle for consumption pattern factor groups statistically positive affected food waste generation. Correlation Matrix of food waste behavior with the correlation coefficient, r ranged between 0.137 to 0.384.

Overall, findings of this study supported Quested et al. (2013) who reported a positive association between over-purchasing and food waste behavior, consumers often rely on food shopping routines and admit to regularly buying more food than needed (Evan, 2011), thereby increasing possible food waste, as well as special offer or price promotion are positively related food waste (Stefan et al., 2013; Stancu et al.,

Table 4. Correlation Matrix

Lifestyle for consumption pattern factor groups	Food awareness and balance	Leftover unconcerned	Trendy and convenient behavior	Over-purchasing food preferred	Price and promotion conscious	Food waste behavior
Food awareness and balance	1	.000	.000	.000	.000	.096
Leftover unconcerned	.000	1	.000	.000	.000	.310**
Trendy and convenient behavior	.000	.000	1	.000	.000	-.182*
Over-purchasing food preferred	.000	.000	.000	1	.000	.137**
Price and promotion conscious	.000	.000	.000	.000	1	.384**
Food waste behavior	.096	.310**	-.182*	.137**	.384**	1

* p-value = 0.05, ** p-value = 0.01

2016) mainly associated with buying more than what can be consumed (e.g. due to promotions and discounts). According to Tsalis et al. (2021), some studies found that consumers buying price-promoted food products showed average or even lower levels of food waste. Leftover unconcerned statistically positively affected food waste generation. The significance negative association between trendy and convenient behavior and food waste, which is inconsistent with Glanz (2008) mentioned that consumers who bought food because of advertising or trying something new tended to be waste more than food.

4. Conclusions

Due to various lifestyle for food consumption patterns, this study explored the relationship between consumption patterns and food waste behavior at household level. Most respondents generate 10% of food leftover after meals and one-third of respondents choose to throw out unused food, while another one-third of respondents use leftover for the next meal. Results showed that lifestyle for food consumption patterns including leftover unconcerned, over-purchasing food preferred, and price and promotion conscious significantly positive influence on food waste generation. Therefore, it is vital to promote food waste reduction and food waste impact on the environment through marketing activities and social media. The government should cooperate with the retail businesses to communicate about food waste reduction and building awareness of the negative aspects of food waste. In addition, food waste separation should be encouraged to all sectors, especially at household and community level.

Acknowledgement

Faculty of Agro-Industry, Kasetsart University

References

FAO, IFAD, UNICEF, WFP WHO. (2019). The State of Food Security and Nutrition in the World 2019. In: FAO (Ed.), Safeguarding against economic slowdowns and downturns. FAO, Rome, Italy.

Glanz, R. (2008). Causes of Food Waste Generation in Households – An Empirical Analysis M.Sc. Thesis. University of Natural Resources and Applied Life Sciences, Vienna and Cranfield.

Hoelzle, J. B., & Meyer, G. J. (2013). Exploratory factor analysis: Basics and beyond. In Weiner, I. B., Schinka, J. A., Velicer, W. F. (Eds.), Handbook of psychology: Research methods in psychology (Vol. 2, 2nd ed., pp. 164-188). Hoboken, NJ: Wiley.

Pollution Control Department. (2017). Solid waste situation in the country [Online] Available: https://thaimsw.pcd.go.th/ [Accessed on 3 March 2021].

Pollution Control Department. (2021). Thailand State of Pollution Report 2020. Available: https://www.pcd.go.th/publication/14100/

Quested, T. E., Marsh, E., Stunell, D., & Parry, A. D. (2013). Spaghetti Soup:The Complex World of Food Waste

Behaviour. Resources, Conservation and Recycling, 79: 43–51.

Stancu, V., Haugaard, P., & Lähteenmäki, L. (2016). "Determinants of consumer food waste behaviour: two routes to food waste", Appetite, Vol. 96, pp. 7-17.

Stefan, V., van Herpen, E., Tudoran, A. A., & Lähteenmäki, L. (2013). Avoiding food waste by Romanian consumers: The importance of planning and shopping routines. Food Quality and Preference, 28(1), 375-381.

The National Science and Technology Development Agency (NSTDA). (2020). BCG in Action: Circular Economy [Online] Available: https://waa.inter.nstda.or.th [Accessed on 20 September 2021].

Tsalis, G., Jensen, B. B., Wakeman, S.W., & Aschemann-Witzel, J. (2021). Promoting Food for the Trash Bin? A Review of the Literature on Retail Price Promotions and Household-Level Food Waste. Sustainability 2021, 13, 4018.

United Nations. (2015). Transforming our world: the 2030 Agenda for Sustainable Development. [Online]. Available: https://sustainabledevelopment.un.org/post2015/transformingourworld. [Accessed on 1 December 2020].

Williams, B., Brown, T., & Onsman, A. (2010). Exploratory factor analysis: A five-step guide for novices. Australasian Journal of Paramedicine. 8(3):1-13.

Water Footprint Assessment of Durian Monthong Before Harvesting and the Harvesting Period in Rayong Province

Suphawadee Jampala*, Nathsuda Pumijumnong, Achara Ussawarujikulchai, and Noppol Arunrat

Faculty of Environment and Resource Studies, Mahidol University, Thailand

Abstract

This research analyzed the Water Footprint Assessment of Durian Monthong orchards before harvesting and during harvesting periods in Rayong Province. Analysis of data was done using the CROPWAT 8.0 program. The data was collected from responses to a questionnaire from 56 farmers in five districts of Rayong province. The data from the study area revealed that only five districts of Rayong had Durian Monthong orchards. Secondary data included climate data, rainfall data, crop water use, and soil series data.

The results of this study determined the volume of water used for cultivation from rainwater, water reservoirs, and open canals. Fertilizers and pesticides were used during the maintenance period. The crop water usage of Durian Monthong orchards before harvesting (1-5 years) showed that the crop water use (CWU_{proc}) was 4,672 m^3/rai, consisting of 1,029 m^3/rai of green water use (CWU_{green}), 1,372 m^3/rai of blue water use (CWU_{blue}), and 2,271 m^3/rai of gray water use (CWU_{gray}). The first harvesting period (6-10 years) indicated that the total water footprint (WF_{proc}) was 4,527 m^3/ton, consisting of 1,140 m^3/ton of green water footprint (WF_{green}), 1,520 m^3/ton of blue water footprint (WF_{blue}), and 1,867 m^3/ton of gray water footprint (WF_{gray}). In addition, the second harvesting period (11-20 years) showed that the water footprint (WF_{proc}) was 3,592 m^3/ton, consisting of 850 m^3/ton of green water footprint (WF_{green}), 1134 m^3/ton of blue water footprint (WF_{blue}) and 1,608 m^3/ton of gray water footprint (WF_{gray}). The results of this research could be used for managing the water used for agriculture.

Keyword: Water footprint/ Durian Monthong/ Before Harvest/ Harvesting Period

---

*Corresponding Author: Suphawadee Jampala
E-mail address: suphawad@gmail.com

1. Introduction

Global climate change causes several impacts to water cycles such as prolonged droughts or shortened rainy seasons. These impacts affect the water security of many countries (Vörösmarty et al., 2000; Hangermann et al., 2013). Thailand is one of the countries that is affected by the aforementioned impacts. Due to the change of climate and prolonged drought, some agricultural areas cannot perform agricultural activities as usual or have lower production yields compared to the past (Office of Agricultural Economics 7, 2016). Moreover, increasing global population leads to increasing demand of water usage for food, energy, and consumer goods production (Arnell, 2004). This water usage situation draws great attention to various industries since water resource is crucial for every production process. Similarly, agricultural industry is also emphasized on the water resource situation because water resource is a major factor in cultivation and has a direct effect on production yield (Wallcae, 2000).

Thailand is an agricultural country. Thailand exports various agricultural products to many different countries around the world. This can be compared to exporting water resource in a form of agriculture products (Office of Agricultural Economics 7, 2016). From the information of Thailand agricultural products export 2018, Thailand exported agricultural products worth 1,388,541 million baht, where fruit products are the top 10 exported products of Thailand with a value of 142,310 million baht. The most exported fruit is fresh durian worth 30,187 million baht (Centre for Agricultural Information, Office of Agricultural Economics, 2019). A durian species that is popular among farmers is Monthong, since Monthong has a color, odor, and taste that is preferred by consumers and favored by the exporting market (Johnny Sawangsrisakulpon, 2017).

The agricultural statistical data in Thailand from the Office of Agricultural Economics shows that, during 2017-2019, the eastern part of Thailand had the highest production of durian with 424,094 tons, 405,428 tons, and 497,851 tons, respectively. Rayong province has become a province of interest since it is the second highest durian production province in the eastern region and it is also a province in the Eastern Seaboard development project which will be a main economic community in the region. Due to this development project, Rayong has high urban expansion and increase in industrial area. According to the information from Land Development Department 2016 and 2018, agricultural land use in this type of orchard (durian) has a total area of 60,781 rai, which increased from 2016 by 16,340 rai. At the same time, community and buildings type of land use has also increased while many areas have changed to industrial area and households. In some areas, release of wastewater into agricultural water resources has become a problem, as well as water resource conflict between agricultural and industrial sectors which can cause impact on fruit plantation in the future (Agricultural Development Policy and Planning Division, Office of Agricultural and Economics, 2019).

From the above-mentioned statements, the study of water usage in agricultural activities is crucial and should be done urgently since the information can be used to estimate the water resources sufficiency in the area. Water footprint study is an important tool to evaluate water usage in agricultural industry. This method is the assessment of water usage from the beginning until the end of the production process (Hoekstra et al.,2011). This study will clearly demonstrate farmers' hidden water usage in the production process. Furthermore, this can evaluate impacts to water usage caused by the production process (Chapagain et al., 2006). The study of water footprint allows a better understanding of water scarcity problems in the area and leads to proper water management. For these reasons, the researcher aimed to study the water footprint assessment of Durian Monthong orchards before fruit can be harvested (1 to 5 years old trees) and during the harvesting period (6 to 20 years old trees) in Rayong province to have a better understanding on the actual water usage of Durian Monthong plantations for a better water management guideline in the area.

2. Methodology

2.1 Data collection

Data used in water footprint assessment of Durian Monthong before harvesting and the harvesting period in Rayong province was separated into two parts including primary data and secondary data. The details are as follows.

2.2.1 Primary data

Primary data is the data gathered in the study area via an in-depth interview with Durian Monthong plantation farmers both male and female. The 56 key informants from the in-depth interview in five districts of Rayong province are selected by specific criteria of 1) the farmers only plant Durian Monthong and 2) The age of durian plantation is the the range of 1-5 years, 6-10 years, and 11-20 years. All three age ranges needed to be in the same district of Rayong province. Three farmers were selected from each of the durian plantation age range from the names registered with the district agricultural office or provincial agricultural office. The researcher initially contacted the farmers that fit the criteria through phone call. If a farmer was willing to give information, the researcher made an appointment for data collection in the area. The questions include water usage data in Durian Monthong plantation, Durian Monthong yield in the past year, fertilizer or chemical usage in Durian Monthong plantation, and cost in planting Durian Monthong.

Furthermore, the questionnaire had been granted Ethical Approval by the Institutional Review Board, Institute for Population and Social Research, Mahidol University. The code was COA. No. 2020/07-346.

2.2.2. Secondary data

Secondary data is the data gathered from various agencies to use for water footprint assessment of Durian Monthong in the study area. The secondary data includes climate data, rainfall data, crop data, and soil data. Details about the secondary data are as follows. Climate

data uses an average climate data in the past 30 years (1989-2019), minimum and maximum temperature, humidity, wind speed, and amount of light from the Meteorological department, Rayong station. Rainfall data uses the average rainfall data in the past 30 years (1989-2019) from the Meteorological department, Rayong station. Crop data includes information on growth stages of crops which can be classified into four stages, initial stage, development stage, mid-season stage, and last stage, and information on crop coefficient (K_c) . Soil data is the data provided in CROPWAT 8.0 program which was chosen to suit with the study area. This data will include soil profile, maximum water seepage, soil humidity, and rooting depth.

2.2 CROPWAT 8.0 program calculation

The data usage in CROPWAT 8.0 program calculations included climate data, rainfall data, crop data, and soil data. Climate data consist of minimum and maximum temperature, humidity, wind speed, and amount of light. Rainfall data is the average twelve-month rainfall in the past 30 years. Crop data includes Durian Monthong growth stages and crop coefficient (K_c). Soil data provided in CROPWAT 8.0 program.

3. Results

3.1 Data from in-depth interview in the area

An In-depth interview questionnaire of water footprint assessment of Durian Monthong plantations before harvesting and during the harvesting period in Rayong province was done with 56 key informants from five districts of Rayong. The data from the study area revealed that only five districts of Rayong had Durian Monthong orchards. Moreover, from the interview, farmers in Ban Chang district, Pluak Daeng district, and Nikhom Phatthana district are not planting Durian Monthong, but the majority will plant pineapple, cassava, and rubber tree. The results showed that an average Durian Monthong plantation area is equal to 29 rai with the largest area of 120 rai and smallest area of 5 rai. In an area of 1 rai, farmers commonly plant 20 durians. The production yield from durian during year 6-10 is equal to 1.19 tons/rai, during year 11-20 is equal to 1.68 tons/rai, and during year 20 onward is equal to 1.44 tons/rai. The majority of farmers will do an annual maintenance of leaves, branches, and trunks of durian during May-October and will start to reduce watering of durian in November-December to induce flowering. They will return to normal watering of durian during January-April which is a young fruit development stage until the ripening stage of durian fruit. A length stage for durian plantation is approximately 365 days. Watering of durian is commonly done by sprinkler system which uses the water from surface water resources, such as ponds, though some farmers also use water from underground resource. Watering frequency of durian is around 6-15 times/month, depending on climate conditions of the plantation year. Furthermore, there are chemical fertilizer, organic fertilizer, and pesticide usage throughout the season.

The top three motives of Durian Monthong planation are the desirable breed of durian by the customers, the high value of product, and the preferable breed for exporting market, respectively. The farm gate price of durian is 128 baht/kilogram.

3.2 Water footprint value of Durian Monthong before harvesting and during the harvesting period in Rayong province.

From the assessments of water usage of Durian Monthong, it shows that crop water usage of Durian Monthong before harvesting (1-5 years) is equal to 4,673 cubic meters/ton, and the water footprints of Durian Monthong during the harvesting period years 6-10 and years 11-20 are equal to 4,528 cubic meters/ton, and 3,592 cubic meters/ton, respectively, as shown in Table 1.

The information in Table 2 was calculated by the statistic methodology; Analysis of variance test (ANOVA). The result showed that the average water footprints of Durian Monthong in the harvesting period of 6-10 years and 11-20 years have significantly different means at the alpha 0.05. The detail is shown in Table 3.

Table 1. Water footprint values of Durian Monthong before harvesting and the harvesting period in Rayong province.

Period	Year	Yield	CWU_{proc}	CWU_{green}	CWU_{blue}	CWU_{grey}
		(ton/rai)	(m^3/rai)	(m^3/rai)	(m^3/rai)	(m^3/rai)
Before harvesting period	1-5	0	*4,672	*1,029	*1,372	*2,271
Harvesting period	6-10	1.13	4,527	1,140	1,520	1,867
	11-20	1.60	3,592	850	1,134	1,608

Table 2. Water footprint calculation of Durian Monthong harvesting period in Rayong province

Code	Amount of Fertilize	Yield	WF_{green}	WF_{blue}	WF_{Grey}
	kg/rai	ton/rai	m^3/rai	m^3/rai	m^3/rai
6-10 years					
001	67.2	0.8	1,287	1,715	1,680
002	135.6	0.8	1,287	1,715	3,390
003	154.8	2.6	396	528	1,191
004	28.8	0.6	1,716	2,287	960
005	70.2	0.8	1,287	1,715	1,755
006	70.0	1.6	643	858	875
007	94.8	1.4	735	980	1,354
008	157.6	1.6	643	858	1,970
009	74.0	0.6	1,716	2,287	2,467
010	28.8	0.8	1,287	1,715	720
011	56.0	1.0	1,029	1,372	1,120
012	157.6	0.6	1,716	2,287	5,253
013	45.0	0.8	1,287	1,715	1,125
014	70.0	1.0	1,029	1,372	1,400
015	157.6	1.8	572	762	1,751
016	116.8	0.6	1,716	2,287	3,893
017	74.0	0.6	1,716	2,287	2,467
018	41.6	0.6	1,716	2,287	1,387
019	92.0	2.0	515	686	920
020	166.8	2.0	515	686	1,668
	Average		1,140	1,520	1,867
11-20 years					
001	67.6	0.8	1,287	1,715	1,690
002	157.6	0.8	1,287	1,715	3,940
003	94.8	1.4	735	980	1,354
004	41.6	1.0	1,029	1,372	832
005	192.8	3.0	343	457	1,285
006	166.8	2.0	515	686	1,668
007	198.8	3.4	303	404	1,169
008	154.8	3.0	343	457	1,032
009	107.0	1.2	858	1,144	1,783
010	45.0	0.8	1,287	1,715	1,125
011	70.2	1.0	1,029	1,372	1,404
012	116.8	0.8	1,287	1,715	2,920
013	28.8	0.8	1,287	1,715	720

Table 2. Water footprint calculation of Durian Monthong harvesting period in Rayong province (cont.)

Code	Amount of Fertilize	Yield	WF_{green}	WF_{blue}	WF_{Grey}
	kg/rai	ton/rai	m^3/rai	m^3/rai	m^3/rai
014	115.6	1.0	1,029	1,372	2,312
015	111.6	3.0	343	457	744
016	140.0	1.6	643	858	1,750
Average			850	1,134	1,608

Table 3. ANOVA test of average water footprints data of Durian Monthong in harvesting period.

SUMMARY				
Groups	*Count*	*Sum*	*Average*	*Variance*
6-10 years	20	90551.98	4527.599	3810333
11-20 years	16	57470.68	3591.917	2203169

ANOVA						
Source of Variation	*SS*	*df*	*MS*	*F*	*P-value*	*F crit*
Between Groups	7,782,219	1	7,782,219	2.509	0.122	4.130
Within Groups	105,443,868	34	3,101,290			
Total	113,226,086	35				

4. Discussion

From the calculation of crop water use of Durian Monthong before harvesting and the water footprint of Durian Monthong during the harvesting period in Rayong province, the results show that before harvesting period (year 1-5) has a total crop water use in plantation process, green, blue, and grey crop water use of 4,673 m^3/rai, 1,029 m^3/rai, 1,372 m^3/rai, and 2,271 m^3/rai as maximum values, respectively. For the plantation of Durian Monthong during harvesting period year 6-10, the total water footprint, green water footprint, blue water footprint, and grey water footprint are equal to 4,528 m^3/ton, 1,140 m^3/ton, 1,520 m^3/ton, and 1,867 m^3/ton, respectively. During the harvesting period year 11-20, the total water footprint, green water footprint, blue water footprint, and grey water footprint are equal to 3,592 m^3/ton, 850 m^3/ton, 1,134 m^3/ton, and 1,608 m^3/ton, respectively. Since before harvesting period durian will not produce any yield, this factor is an important variable in water footprint calculation. It can be said that water footprint is inversely proportional with production yield, as shown in Figure 1.

When comparing green water footprint and blue water footprint in every stage of Durian Monthong plantation in Rayong province, blue water footprint is higher than green water footprint. It can be interpreted that the effective rainfall in Rayong province is not sufficient for Durian Monthong plantations and leads to high water usage of surface water or irrigation water, which in this study is blue water footprint.

Moreover, grey water footprint in every stage of Durian Monthong plantation is very high, as shown in Figure 1. This resulted from the intense use of organic and chemical fertilizers through out the plantation stages including branches development stage, flower inducement stage, fruiting stage, young fruit development stage, fruit maturation stage, until ripening stage of fruit. From this reason, the crop cannot use all the mineral which in this case is nitrogen in fertilizer. So, the calculated grey water footprint is like the amount of water used to dilute chemicals before release into water resources without exceeding the environmental standard of 5 mg/L. Nevertheless, over fertilization can cause nitrogen to remain in the area and lead to water pollution if it gets washed by the rain.

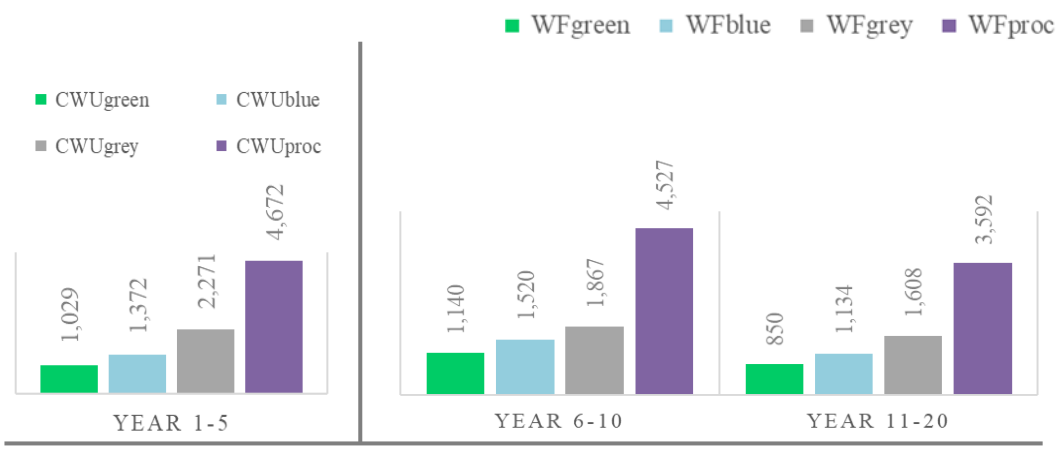

Figure 1. Comparison graph of water footprint of Durian Monthong plantation before harvesting and the harvesting period in Rayong province.

When comparing water footprint of durian plantation in a large scale agricultural extension in Trat province by the Office of Agricultural Economics 6 (2015), the total water footprint in crop plantation is equal to 868 m^3/ton, green water footprint is equal to 417 m^3/ton, and blue water footprint is equal to 452 m^3/ton while grey water footprint was not calculated in the study. Fom this information, it causes a difference in calculated Water Footprint Process values. However, Blue Water footprints trends of both studies are similar. They showed that the Blue water footprints are higher than the Green water footprints.

From the comparison, the resulting values show significant difference due to the different constant values used and different calculation method, for example, the data collection process of this research. The data collection process of this research was divided into two groups which were before harvesting (year 1-5) and harvesting period (year 6-10 and 11-20). On the other hand, the research from the Office of Agricultural Economics 6 did not mention about the age of the durian trees nor the breed of durian which is different from this research study that focus on durian Monthong plantation only.

Moreover, the Crop coefficient (K_c) value used in Water Footprints calculations did not vary according to the age of durian tree and could affect the calculated value. By using Crop coefficient (K_c) value according to the age of durian tree as well as the breeds, the calculated Water Footprints value would be more accurate.

The study of Soytong et al. (2017) shows that industrial development process has rapidly increased in the Eastern part of Thailand under the Eastern Sea Board development project and causes changes in land use. This correlated with field surveys that show an increased rate of land use change from agricultural land use in orchard type (durian) to industrial and urban area such as in Nikhom Phatthana district, Pluak Daeng district, and Ban Chang district.

According to the study of Soytong et al. (2017), a change in land use can generate higher water needs and can lead to water resource conflict in the area. Furthermore, climate change is also a major factor that affects water resources. Some areas face flood problems while others face drought. These problems directly affect agricultural production. From the study, “Effect of Climate Change on Durian Production” (Chanthaburi Horticultural Research Center, 2015), fluctuations of climate affect durian plantation in all stages, such as flowering, flowering inducement, flowers development, fruiting, fruit development, and harvesting stage as well as the quality of the product. This information is correlated with an interview with farmers of durian Monthong plantation in Rayong province. From the interview, the farmer indicated that durian Monthong production was reduced in 2019 due to prolonged drought period. The effect from durian Monthong production and in accordance with higher demand for durian Monthong lead to higher selling price of durian. Due to the aforementioned problems,

organizations related with agriculture should rasie awareness about affects from climate change, educate and communicate warnings about climate change, provide appropriate mitigation measures for the farmer in order to plan for their proper production, as well as set up policies on the development of production technology to reduce the impact of an increasing climate change in the future.

In addition, a study of Hoekstra et al. (2003) found that, during 1995-1999, Thailand was the third in net virtual water export in the world. Virtual water trade is the trade of water in the form of product or goods that had high water consumption in the production process since trading actual water is not possible due to high cost and transportation difficulty. From the interview with farmers, the majority of durian production in 2019 was sold to a middle man at the farm gate before selling to an agricultural product export company that exports them to China. This can be compared to vitual water trade of water resources in the area. In the future, the water resources availability in the area needs to be taken into consideration since the need for water consumption of both agricultural and industrial sectors has increased.

5. Conclusions

The water footprint of Durian Monthong plantations in Rayong province was assessed by field survey and in-depth interview with the key informants. The topics of the questionaire included crop water use and chemical use in every crop length stage, starting from land preparation, branches development, flower inducement, flower development, fruiting, young fruit development, fruit maturation, until the fruit ripening stage. Moreover, this study also included climatological data in the past 30 years (1989-2019) of Rayong province along with crop coefficient (Kc).

The studied and analyzed data were calculated in CROPWAT 8.0 program. The results show that before harvesting period (year 1-5) has a total crop water use in plantation process, green, blue, and grey crop water use of 4,672 m^3/rai, 1,029 m^3/rai, 1,372 m^3/rai, and 2,271 m^3/rai For the plantation of Durian Monthong during harvesting period year 6-10, the total water footprint, green water footprint, blue water footprint, and grey water footprint are equal to 4,527 m^3/ton, 1,140 m^3/ton, 1,520 m^3/ton, and 1,867 m^3/ton, respectively. During the harvesting period year 11-20, the total water footprint, green water footprint, blue water footprint, and grey water footprint are equal to 3,592 m^3/ton, 850 m^3/ton, 1,134 m^3/ton, and 1,608 m^3/ton, respectively. Since before harvesting period durian will not produce any yield, this factor is an important variable in water footprint calculation. It can be said that water footprint is inversely proportional with production yield. Regarding the water scarcity footprint of Durian Monthong before harvesting and the harvesting period year 6-10 and year 11-20 in Rayong province, the value is equal to 20.6 $m^3 H_2O$eq, 22.8 $m^3 H_2O$eq, and 17.0 $m^3 H_2O$eq respectively.

Moreover, the comparison of the results of water economic valuation and economic return shows that the production cost of Durian Monthong plantation, including the cost of water before harvesting and the harvesting period year 6-10 and 11-20, in Rayong province has a value of 35,928 baht/rai, 36,829 baht/rai, and 28,420 baht/rai, respectively. The profit from Durian Monthong during the harvesting period year 6-10 and year 11-20 is 107,810 baht/rai and 166,379 baht/rai respectively. This shows that the economic returns obtained are worth the cost of production.

Acknowledgement

Firstly, I sincerely thank my major advisor, Assoc. Prof. Nathsuda Pumijumnong, and also my co-advisors, Asst. Prof. Achara Ussawarujikulchai and Asst. Prof. Noppol Arunrat, for their highly valuable guidance, encouragement, and supervision. I appreciate the kind and invaluable advice from them, indeed.

Moreover, I would like to thank many agriculturists, who are the owners of the durian orchard in Rayong province for all their assistance, constant help, and support during my thesis. I also wish to thank all the lecturers, staffs and professors in the Faculty of Environmental and Resource Studies, Mahidol University for support and supplies during my study.

I wish to thank Dr. Thomas Neal Stewart for sharing, recommending, and helping correct my grammar in this thesis.

Last but not least, this researcher would like to show gratitude to her family which always encourages and attentively cares for her until her completion of both thesis and education.

All mistakes and misconceptions of the thesis are completely under the researcher's responsibility.

References

Agricultural Development Policy and Planning, Office of Agricultural Economic. Management Guidelines for Regional Economic Zones. Bangkok: n.d.; 2019.

Allen RG, Pereira LS, Raes D, Smith M. Crop evapotranspiration-Guidelines for computing crop water requirements-FAO Irrigation and drainage paper 56. Fao Rome 1998; 300(9):D05109.

Allen RG, Pruitt WO, Wright JL, Howell TA, Ventura F, Snyder R, Smith M. A recommendation on standardized surface resistance for hourly calculation of reference ETo by the FAO56 Penman-Monteith method. Agricultural Water Management 2006; 81(1-2):1-22.

Arnell NW. Climate change and global water resources: SRES emissions and socio-economic scenarios. Global environmental change 2004;14(1):31-52.

Centre for Agricultural Information, Office of Agricultural Economics. Trade Statistics of Thai Agricultural Products with Foreign Countries 2018. Bangkok n.d.; 2019.

Chapagain AK, Hoekstra AY, Savenije HH. Gautam R. The water footprint of cotton consumption: An assessment of the impact of worldwide consumption of cotton products on the water resources in the cotton producing countries. Ecological economics 2006; 60(1):186-203.

Climatological Center, Thailand Meteorological Department.Rayong Climate; 2019.

Department of Agricultural Extension. Good and suitable quality durian production guide. Bangkok: The Agricultural Co-operative Federation of Thailand; 2000.

Department of Mineral Resources. Area Classification for Geological and Mineral Resource Management in Rayong Province. Bangkok: Advance Vision Service Co., Ltd.; 2008.

Direk Tongara et al. Plant Watering Design and Technology (Revised Edition).2nd Publication. Bangkok: Than Printing; 2002.

Gheewala SH, Silalertruksa T, Nilsalab P, Mungkung R, Perret SR, Chaiyawannakarn N. Water footprint and impact of water consumption for food, feed, fuel crops production in Thailand.Water 2014;6(6):1698-1718.

Hiran Hiranpradi, Sookwat Chandraparnik, Sermsuk Salakpetch. Durian Production Technology 3rd Publication. Bangkok: Kasetsart University Publisher; 2003.

Hoekstra AY, Chapagain AK., Mekonnen MM, Aldaya MM, editors. The water footprint assessment manual: Setting the global standard. Cornwall: TJ International Ltd; 2011.

Hoekstra AY, & Hung, PQ. Virtual water trade. In Proceedings of the international expert meeting on virtual water trade 2003; 12:1-244.

Johnny Sawangsrisakulpon. A Study of the Relationship among Durian Farmers, Durian Buyers, and Middle Men in Chanthaburi Province. (Thesis) Chonburi: Burapha University;2017. Page 50-52.

Keerati Leewatchanakul. Hydrology. Pathum Thani: Rangsit University Publisher; 2009.

Land Development Department. [Retrieved April 30th, 2020]. From: http://www1.ldd.go.th/ WEB_OLP/Lu_61 /Lu61_E/RYG61.htm.

Nisa Pakwilai, Samart Porncharoen, Warin Weingra. Water Footprint Analysis Using by CROPWAT 8.0 of Marian Plum: Case Study in Paka Subdistrict, Ban Na District, Nakornnayok Province. VRU Research and Development Journal Science and Technology 2019; 14(1):100-109.

Office of Agricultural Economics 6. Study of Durian Water Footprint in Large Scale Agricultural Extension Area, Trat Province. Bangkok: n.d.; 2015.

Office of Agricultural Economics 7. Study of Durian Water Footprint in Large Scale Agricultural Extension Area, Lopburi Province. Bangkok: n.d.; 2016.

Office of Agricultural Research Development Agency (public organization). [Retrieved May 11th, 2020]. from: http://www.arda.or.th/kasetinfo/south/durian/used/01-02.php

Pairat Aurama, Narong Pleerux, Parin Lopittayakorn, and Narumon Intarawichian. Water Footprint of Mangosteen: Case Study of Trok Nong subdistrict community enterprise, Khlung district, Chantaburi province. The 11th National and International "Global Goals, Local Actions: Looking Back and Moving Forward 2020". Bangkok: Graduate School Suan Sunandha University; 2020. Page 1079-1089.

Plantations International and Durian Harvests. Durian Global Market Report 2017. [Retrieved May 11th, 2020]. Available from: http://www.plantationsinternational. com/docs/durian-market.pdf.

Rapeepong Lapatpakanu, Bittawat Wichaidist, Peerayuth Chanpenngam, and Chaisri Suksaroj. Water Footprint Assessment of Pathumthani Rice 1 in Alternated Wet/Dry Plot and Flooded Plot. Confernce 11th THAICID National Symposium with Topic of "Innovative and Sustainable Agri-water Management: Alternative Strategies for Irrigation infrastructure development". Bangkok: Thai National Committee on Irrigation and Drainage (THAICID); 2018. Page 109-121.

Rayong Provincial Office, Strategic and Information Division for Provincial Development. Summary of Rayong Province 2019. N.d.; 2019.

Shrestha S, Pandey VP, Chanamai C, Ghosh DK. Green, blue and grey water footprints of primary crops production in Nepal. Water resources management 2013; 27(15):5223-5243.

Soytong, P., Janchidfa, K., Phengphit, N., Chayhard, S., & Perera, R. (2016). The effects of land use change and

climate change on water resources in the eastern region of Thailand. Int J Agri Technol, 12(7.1), 1695-722.

Thai customs; 2 0 1 5 [Retrieved May 11th, 202] from: http://www.customs.go.th/statistic_report.php?tab=by_statistic_code.

Thai Encyclopedia for Youth by the Royal Whishes of His Majesty the King Rama IX. Thai Encyclopedia for Youth vol. 28 Thai Encyclopedia for Youth by the Royal Whishes of His Majesty the King Rama IX. Bangkok: Darnsutha Press; 2010.

Varawoot Vudhivanich. Thailand ET0 Calculation by Penmann-Montieth Method. Faculty of Engineering, Kasetsart University 1996; 10(9).

Vörösmarty CJ, Green P, Salisbury J, Lammers RB. Global water resources: vulnerability from climate change and population growth. Science 2000; 289(5477):284-288.

Wallace JS. Increasing agricultural water use efficiency to meet future food production. Agriculture, ecosystems & environment 2000; 82(1).

Restoring Seaweed Beds by Changing Sea Urchin Foraging Behavior

Dominic F.C. Belleza[a*], Takeshi Urae[a], Shinichiro Tanimae[a], Hiroto Tateishi[a], Makoto Kabeyama[a], Shigetaka Matsumuro[a], and Gregory N. Nishihara[b]

[a]Graduate School of Fisheries and Environmental Sciences, Nagasaki University, 1-14 Bunkyo-machi, Nagasaki City, Nagasaki, Japan
[b]Institute for East China Sea Research, Organization for Marine Science and Technology, Nagasaki University, 1551-7, Taira-machi, Nagasaki City, Nagasaki, Japan

ABSTRACT

Alarm cues from dead conspecific urchins are known to evoke a fear response in the purple urchin, *Heliocidaris crassispina*. The disruption of their normal foraging patterns through behavioral change is an important step in the conservation of seaweed beds throughout Japan. Although guidelines have been put in place to counteract the declining seaweed ecosystems because of overgrazing, the management practices often involve installing net barriers and periodic urchin culling which are not only expensive and labor-intensive to implement but also unsustainable in the long-term as urchin populations rapidly recover due to the overfishing of natural predators. This study examined the possibility of using urchin alarm cues to prevent overgrazing of seaweed ecosystems and how this can be introduced as a new tool for seaweed ecosystem restoration. In laboratory experiments, we exposed purple urchins to fresh extracts taken from different conspecific urchin body tissues and results show that all extracts potentially have a repellent effect. Field trials using fresh extracts embedded in agar show urchins limiting their movement and are less likely to forage outside their burrows. The method presented would involve less personnel and equipment and would be a cheaper alternative for coastal communities aiming to help restore seaweed forest ecosystems.

Keyword: Seaweed ecosystem/ Purple urchins/ Overgrazing/ Fear response

---

*Corresponding Author: Dominic F.C. Belleza, Tel: +81-095-850-4588; Fax: +81-095-840-1881
E-mail address: dfcbelleza@gmail.com

The Comparative Compressive Strength Study between Hand Cut Waste PET Bottles Fiber Concrete and Standard Concrete

Surada Chundasutathanakul[a] and Norlabodee Supatchapichai[b*]

[a]Suan Dusit University, 145/9 Sukothai Road, Dusit, Dusit, Bangkok 10300, Thaland
[b]KIS International School, 123-124 Pracha Uthit Rd, Samsen Nok, Huai Khwang, Bangkok 10310, Thailand

ABSTRACT

This research aims to portray Khok Nong Na sustainable farming model, both in theory and its practice in reality. The objective of the research is to scrutinize Khok Nong Na models practiced in Nong Khai province, Thailand, to portray success and obstacles the relevant agents face. The research is qualitative by nature as the researchers use semi-structure interviews and focus groups to gather the data. The informants are farmers who practice Khok Nong Na models in Nong Khai province, local administrative agents and subdistrict administrative organizations, academics and practitioners. As well, the researchers use social capital and human security theories to study the cases.

The findings are that even if the Khok Nong Na model is widely publicized in Thailand, it is still difficult for farmers to access governmental assistance, especially in term of financial help. Therefore, unfortunately, to achieve the full potential of the model, the farmers must invest personal budget along the process. Also, since the model is quite new, the local agents are not well informed about the model which leads to confusion and highly time-consuming processes. Furthermore, many organizations have used Khok Nong Na model as public relation scheme, rather to practice the model for actual sustainable development.

The researchers conclude that Khok Nong Na model is actually crucial for sustainable development and will greatly benefit the community if it is well-practiced. Moreover, it is suggested that the model should be more accessible because that will enhance food security and sustainable development in the country.

Keyword: Sustainable development/ Food security

---

*Corresponding Author: Norlabodee Supatchapichai, Tel.: +66 95-195-5456
E-mail address: csurada@gmail.com

Is Species Richness of Macroalgae Related to Wave Exposure and Water Temperature in Arikawa Bay?

Shinichiro Tanimae[a], Dominic F.C. Belleza[b], and Gregory N. Nishihara[a,b,c*]

[a]Graduate School of Fisheries and Environmental Sciences, Nagasaki University, Nagasaki City, 851-8521, Japan
[b]Organization for Marine Science and Technology, Nagasaki University, Nagasaki City, 851-8521, Japan
[c]Institute for East China Sea Research, Nagasaki University, Nagasaki City, 851-2213, Japan

ABSTRACT

With ongoing changes in the global climate, seaweed communities are in transition and a number of studies have been reported from various sites. Water temperature and wave exposure are some of many important environmental factors determining the structure of seaweed communities. This is because these environmental factors affect the photosynthetic rate, induce physical stress in the thallus, and can also play a role in reproduction. As a result, only those seaweed species that have appropriately adapted can remain in certain types of environments. The relationships between these environmental factors and seaweed communities have been examined by many investigators on relatively large spatial scales. However, how does water temperature and wave exposure vary within small spatial scales, and will such variation affect the structure of seaweed communities? We are studying how small variations in water temperature and wave exposure affect the structure of seaweed communities on a small spatial scale. Seven stations within a 200 m distance were established in Arikawa Bay, Nagasaki, Japan. We identified seaweed species found at each site, and measured the water temperature, wave exposure, sedimentation rates, and depth at each station. Then, we developed a model to describe how species richness is related to each environmental factor and hypothesized that species richness and environmental factors are related. Thus far, our observations support the hypothesis even within a small spatial scale.

Keyword: Seaweed/ Species richness/ Wave exposure/ Water temperature/ Nagasaki/ Japan

---

*Corresponding Author: Gregory N. Nishihara, Tel.: +81-95-850-7311
E-mail address: greg@nagasaki-u.ac.jp

The Evolution of Hybrid Modes in Water and Agriculture: Case Study of Vietnamese Mekong Delta

Linh Nguyen[a*], Keichiro Iguchi[a], Hironori Hamasaki[a], and Dang Kieu Nhan[b]

[a]Nagasaki University, 1-14 Bunkyomachi, Nagasaki, 852-8521, Japan
[b]Can Tho University, 3/2 Street, Xuan Khanh Ward, Ninh Kieu, Can Tho, 94000, Vietnam

ABSTRACT

The Mekong Delta plays an important role in water and food security of Vietnam and the world. With diverse water zones and complex hydrological system, balancing economic prosperity, water conservation and sustainable agriculture in this region is challenging. Extensive literature has focused on analyzing the dominant control approach in irrigation and rice policy. However, little is understood about the evolution of hybrid modes in the transformation towards sustainable water and agriculture in this region. This paper reviews evolution of hybrid mode in legal framework of Mekong Delta's water governance from 1970s to present and analyze the interaction of different modes in case study of integrated rice-shrimp model. The paper uses coding scheme, desk review and in-depth interviews with farmers, government officers, researchers, and international organization. Results from coding highlight a significant increase of market mode from 2010s and more balanced hybrid modes in period 2010s to present. Case study analysis of integrated rice-shrimp shows the importance of combined three modes for sustainability of the model. Specifically, there are changes to hierarchy and emergence of market and network mode. Furthermore, conflict between hierarchy and network during 1990s and conflict among market, network and hierarchy during 2000s have been transformed to synergies among three modes since 2010s. Still, stability and scale of hybrid mode needs to be further improved. The findings help increase our understanding on empirical knowledge of hybrid mode and inform other farmers and policy makers about sustainable rice-aquaculture policy and practices.

Keyword: Hybrid mode/ Water/ Agriculture/ Rice-Shrimp/ Mekong Delta

---

*Corresponding Author: Linh Nguyen, Tel: +81-080-3971-4441
E-mail address: dieulinh1186@gmail.com

Community Structure of Meiofauna in Coral Reefs at Mu Ko Similan National Park, the Andaman Sea

Nachaphon Sangmanee[a*], Makamas Sutthacheep[a], Laongdow Jungrak[a], Sirirat Jaihan[a], Suphakarn Paoduang[a], Prarop Plangngan[b], and Thamasak Yeemin[a]

[a]Marine Biodiversity Research Group, Department of Biology, Faculty of Science, Ramkhamhaeng University, Huamark, Bangkok, Thailand
[b]Phuket Marine National Park Operation Center 2, Department of National Parks, Wildlife and Plant Conservation, Phuket, Thailand

ABSTRACT

Coral reefs are complex ecosystems bearing the high biological diversity of the oceans. Assessing biodiversity and ecosystem functions is an essential step to predict the consequences of biodiversity loss. Soft bottom habitats in the coral reefs, such as sand and rubble, are an important component of coral reef communities. Meiofauna are the primary food source for various marine organisms, particularly economically important species in coral reef ecosystems. Even though a lot of small invertebrates, such as meiofauna, can live in the soft-bottoms of coral reefs, but only few researches have focused on the community of meiofauna in coral communities. This study examined the abundance and composition of meiofauna in coral communities at Haad Lek (8-9 m in depth) and Hin Muan Deaw (19-20 m in depth), Mu Ko Similan National Park, the Andaman Sea in February 2021. The results showed that the average density of meiofauna at Haad Lek was 61.00±2.89 inds. 10 cm^{-2}, while that at Hin Muan Deaw was 19.93±2.48 inds. 10 cm^{-2}. Foramminifera and Copepoda were the major groups at both study sites. Ostracoda was an abundant group at Haad Lek, whereas Nematoda was a major group at Hin Muan Deaw. Tardigrada was found only at Hin Muan Deaw. Our results showed the difference in community structure of meiofauna between different depths. The habitat types in coral communities at Mu Ko Similan appear to be affected by different wave motions, current exposure and food supply with different depths that can influence the community structure of meiofauna in that area.

Keyword: Meiofauna/ Coral reef/ Andaman Sea/ Mu Ko Similan

---

*Corresponding Author: Nachaphon Sangmanee, Tel: +668-2332-3409; Fax: +662-310-8415
E-mail address: nachaphon.sangmanee@gmail.com

Rhizo-mineralization of Manganese Oxides by a Halophyte *Salicornia europaea*

Pulla Kaothien-Nakayama[a], Yoshiki Ohgi[a], Yu-Shan Wu[a,b], and Hideki Nakayama[a*]

[a]*Department of Environmental Science, Graduate School of Fisheries and Environmental Sciences, Nagasaki University, 1-14 Bunkyo-machi, Nagasaki City, Nagasaki 852-8521, Japan*
[b]*Department of Aquaculture, College of Hydrosphere Science, National Kaohsiung University of Science and Technology, No.142, Haizhuan Rd., Nanzi Dist., Kaohsiung City 811, Taiwan (R.O.C.)*

Abstract

As a result of simultaneous concentration of salts and heavy metals in environment and crosstalk between stress-responsive signal transduction pathways, bacteria and plants living in high-salinity environments (halophiles and halophytes) usually also show high tolerance to heavy metals. In our laboratory, we study these bacteria and plants to better our understanding of mechanisms used by them to survive in high-salinity environment as well as the nature of their interactions with various heavy metals. Our goal is to develop better bacterial strains and plants for industrial, agricultural, and bioremediation applications. One of the plants we have been working with is *Salicornia europaea*, a halophyte known not only for its ability to remove salts and heavy metals from environment, but also for its use in food, pharmaceutical, cosmetic, and bioenergy industries. In this study, ability of *S. europaea* to accumulate Mn, which is one of the important elements for both the ecosystem and the industries, were characterized using *Spinacia oleracea* as a comparative control. Both species were cultivated in hydroponic nutrient solution containing 0.2 M NaCl and 0.2 mM $MnCl_2$, which is roughly the highest concentration of Mn allowed in drainage water according to Japanese government guideline (10 ppm Mn), for 21 days and the amount of Mn accumulated by the plants were analyzed by Inductively Coupled Plasma-Optical Emission Spectrometry (ICP-OES). Although *S. oleracea* obtained greater biomass than *S. europaea* through the course of the experiment, the result from ICP-OES analysis shows that *S. europaea* accumulated nearly 3 times more Mn per gram fresh weight than *S. oleracea*. Furthermore, staining of the roots of the tested plants with Leucoberbelin blue I (LBB) shows that *S. europaea*, but not *S. oleracea*, could generate Mn oxides in its rhizosphere. As these biologically derived Mn oxides (biogenic Mn oxides) are known to function as very effective metal scavengers in nature, ability to fix Mn oxides in its rhizosphere could, therefore, be an important factor for survival of *S. europaea* in its wild habitats, which usually have low availability of essential trace metals.

Keyword: *Salicornia europaea*/ Manganese/ Rhizo-mineralization/ Manganese oxides/ Biogenic Manganese oxides

---

*Corresponding Author: Hideki Nakayama
E-mail address: nakayamah@nagasaki-u.ac.jp

1. Introduction

Salicornia (common names include sea asparagus, glass wort, or marsh samphire) is a genus of succulent halophytes, which grow on coastal salt marshes and some inland salty habitats of Europe, North America, Africa, and Asia. *Salicarnia* has become well known after researchers found that the plant could be useful in pharmaceutical, agricultural, and ecological fields dues to its ability to grow in high salinity environment, produce various bioactive compounds, and tolerate/accumulate several toxic metals (*Cardenas-Perez et al.*, 2021). Other than being an up-and-coming model plant for research, *Salicornia europaea* used in this work is also edible. Natural saltiness of *S. europaea* (raw or cooked) pairs well with seafood and a field of *Salicornia* also looks beautiful in autumn. Figure 1 shows *Salicornia europaea* growing in an abandon salt field in Okayama, Japan.

In plants, Manganese (Mn) is important for activity of many enzymes including those crucial for photosynthetic activity. Excess amount of Mn, however, is toxic--making it 1of the 3 toxic essential elements alongsides Copper (Cu) and Zinc (Zn). Despite the importance of Mn homeostasis in plant cells, study of uptake, transport, compartmentation, and accumulation

of Mn in plant is still underrated (Alejandro *et al*, 2020). Here, we set out to study the ability of *S. europaea* to accumulate Mn and ended up discovering that the root of *S. europaea* could mineralize Mn, forming biogenic Mn oxides (Tebo et al., 2004), which potentially function as metal scavengers to help the plant survive in its trace-element-deprived wild habitats.

Figure 1. *Salicornia europaea* plants in abandon salt field, Bizen, Okayama, Japan.

2. Methodology

2.1 Plant growth and Mn treatment

Salicornia europaea (sea asparagus) and *Spinacia oleracea* (spinach) seeds were vernalized at 4°C for 24 hours before they were sown on filter paper soaked with tap water. After germination, seedlings were transplanted to perlite medium supplemented with 1/10 Hoagland's nutrient solution containing 0.2 M NaCl with or without 0.2 mM $MnCl_2$ (semi-hydroponic culture). Seedlings were grown in 25°C growth chamber with a relative humidity of 50 to 60% and a photoperiod of 16 light/8 dark hours. Seedlings grown in this chamber for 21 days were harvested for experiments.

2.2 Analysis of Mn content in plant tissues by Inductively Coupled Plasma-Optical Emission Spectrometry (ICP-OES)

The harvested seedlings were rinsed with 0.2 M NaCl solution and dabbed on paper towel to remove any remain solution. To reduce the solid MnO_2 into the soluble Mn^{2+} ion, the seedlings were transferred to 50 mL Polypropylene tubes containing 15 mL of 20 mM vitamin C (ascorbic acid) solution. These tubes were then covered with watch glasses lid (DigiTUBE, SCP Science, Quebec, Canada) and set on a digestion heat block (DigiPREP jr., SCP Science, Quebec, Canada). Acid digestion was done by adding 10 mL of Milli-Q water and 5 mL of 70% HNO_3 (Nacalai Tesque Inc., Kyoto, Japan) to each sample and heated the mixtures to 65°C for 15 min followed by the second heat-up to 105°C and for 120 min before letting the mixture cool down to room temperature. After cooling down, 0.5 mL of 30% H_2O_2 (Fujifilm Wako Pure Chemical, Ltd., Osaka, Japan) were added to the mixtures and the digestion block was re-heated to 105°C and maintained at this temperature for 60 min. After cooling down, acid-digested samples were filtered through 0.45 µm-pore-size Teflon® membrane filter (DigiFILTER, SCP Science, Quebec, Canada). After flushing the filter with Milli-Q water, volume of each filtered samples was adjusted to 25 mL by adding Milli-Q water. Measurements were conducted on an ICP-OES (ICPS-7500,

Shimadzu Corporation, Kyoto, Japan) following the instruction provided by the manufacturer (Nakayama et al., 2019).

2.3 Leucoberbelin blue I (LBB) analysis

To detect Mn oxides, seedling samples were sprayed with colorless Leucoberbelin blue I (LBB), which turns blue when reacts with Mn(III/IV) oxides (Krumbein and Altmann, 1973).

3. Results and Discussion

3.1 Mn accumulation in S. europaea and S. oleracea.

To test ability of *S. europaea* to accumulate Mn, seedlings of *S. europaea* and the control *S. oleracea* were grown in hydroponic nutrient solution with or without the addition of 0.2 mM $MnCl_2$ for 21 days before the plants were harvested for ICP-OES analysis. As shown in Figure 2a and b., when compared with *S. oleracea*, *S. europaea* could accumulate almost 3 times higher Mn per gram fresh weight. Although *S. europaea* and other *Salicornia* species have been found to accumulate copper (Cu), zinc (Zn), and cadmium (Cd) (Cardenas-Perez et al., 2021), as far as we know, this work is the first to show the potential of *S. europaea* as a tool for phytotemediation of Mn.

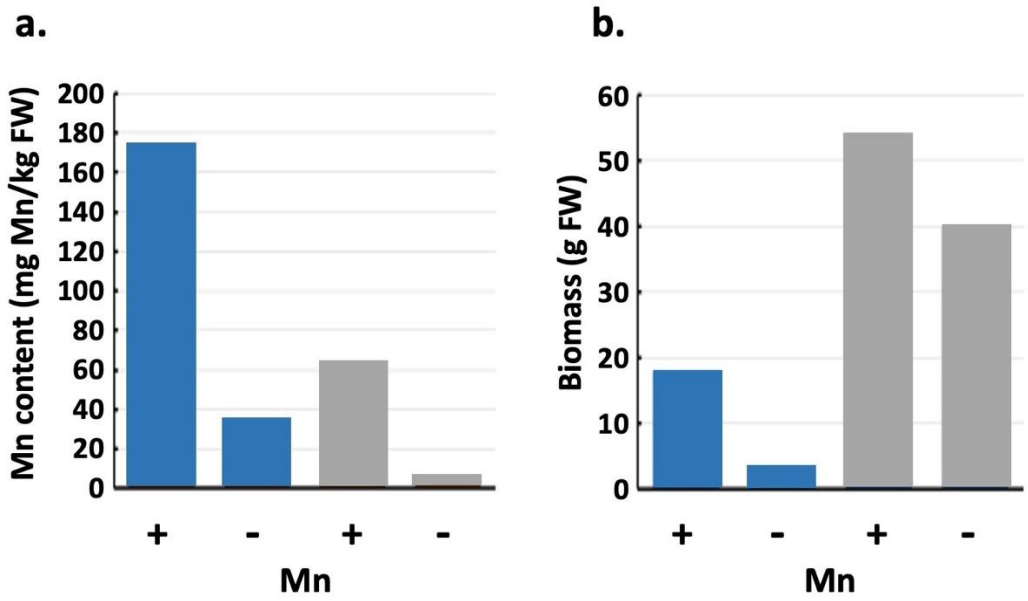

Figure 2. *Mn accumulation in Salicornia europaea and Spinacea oleracea grown for 21 days in hydroponic nutrient solution with or without 0.2 mM $MnCl_2$. a) Graph showing Mn content in and around the tissues of S. europaea and S. oleracea. The amount of Mn accumulated were shown as mg Mn per kg fresh weight of the tested plant tissues. b) Graph showing biomass of S. europaea and S. oleracea used in ICP-OES analysis. S. europaea (Blue bar) and S. oleracea (Gray bar). 0.2 mM $MnCl_2$ were added in, or omitted from, hydroponic nutrient solution as indicated (+ Mn or -Mn).*

3.2 Detection of Mn oxides in the rhizosphere of S. europaea

As showed in Figure 3a., dark brown substance similar in color to that of MnO_2 was visible on the root of *S. europaea* grown for 21 days in hydroponic nutrient solution containing 0.2 mM $MnCl_2$. This observation prompted us to perform Leucoberbelin blue I (LBB) analysis on the root to verify the identity of the dark brown substance. LBB is a colorless dye, which turns blue when oxidized by Mn oxides. As expected, *S. europaea* root treated with LBB turned blue, confirming that Mn oxides were form in its rhizosphere. In contrast, white root of *S. oleracea* remained white after LBB treatment (Figure 3c and d).This finding is significant because Mn oxides has multiple geochemical functions including working as an oxidation catalyst and metal scavenger (Nakayama et al., 2019, Tebo et al., 2004).

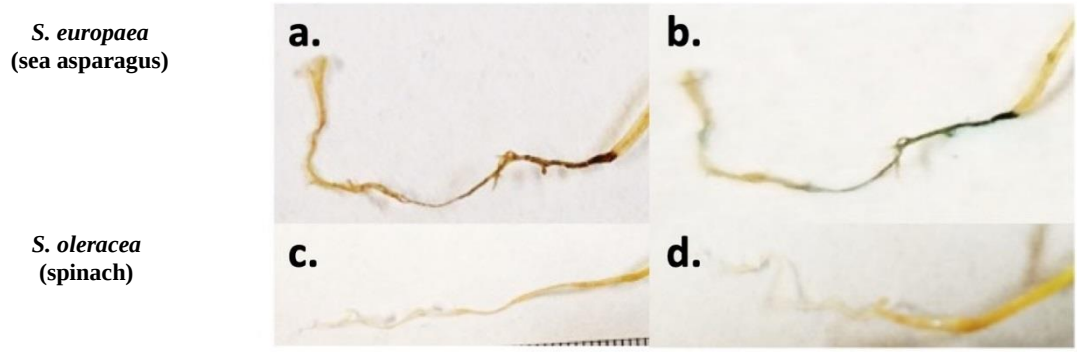

Figure 3. Leucoberbelin blue I (LBB) analysis of Mn oxides production in rhizosphere of *Salicornia europaea* and *Spinacea oleracea* grown for 21 days in hydroponic nutrient solution containing 0.2 mM $MnCl_2$. a) Photo of *S. europaea* root before LBB treatment. b) Photo of *S. europaea* root after LBB treatment. c) Photo of *S. oleracea* root before LBB treatment. d) Photo of *S. oleracea* root after LBB treatment.

4. Conclusions

Important findings obtained from this work are 1. *S. europaea* could accumulate nearly 3 times more Mn per gram fresh weight than *S. oleracea*, and 2. *S. europaea*'s root could mineralized Mn(II) into biogenic Mn oxides. The first finding suggested that *S. europaea* could probably be useful as a tool for phytoremediation of Mn in wastewater. Additional experiment to expose *S. europaea* to a higher concentration of Mn than the current work, however, should be done to better determine the real extent of Mn accumulation potential of *S. europaea*. The second finding further explains the first finding, *i.e.* most Mn detected in *S. europaea* samples by ICP-OES analysis probably were derived from Mn oxides generated in its rhizosphere. The second finding also gave us evidence of mechanism used by *S. europaea* to survive in their low trace-element habitats and provided important clue of the mechanisms underlying the ability of *S. europaea* to accumulate heavy metals--as Biogenic Mn oxides has ability to bind varieties of them (Figure 4). Research with emphasis on finding key factors important for this rhizo-mineralization reaction would further our understanding of heavy-metal sequestration mechanism and benefit future phytoremediation research.

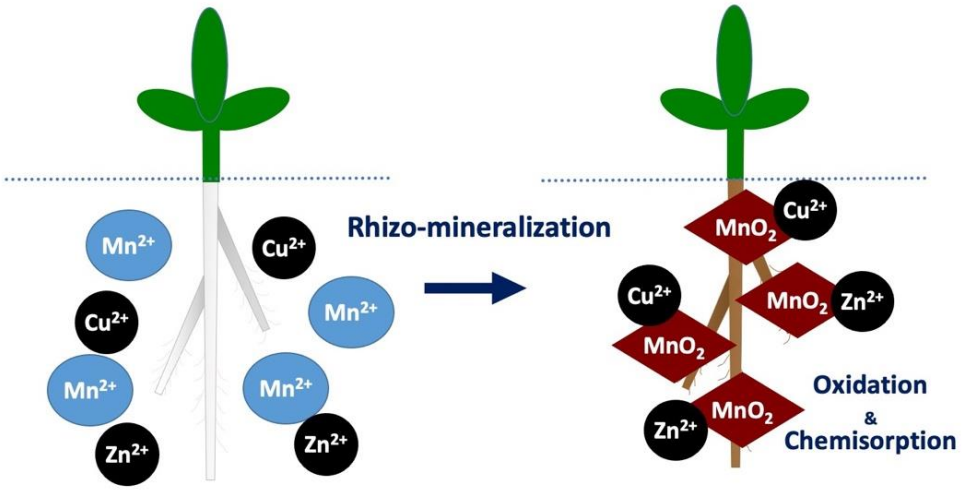

Figure 4. Role of Mn Rhizo-mineralization and chemisorption in phytoremediation.

Acknowledgement

We thank Dr. Kazuya Urata and Prof. Yasuyuki Ikegami of Institute of Ocean Energy, Saga University for technical support during ICP-OES analysis.

References

Alejandro, S., Holler, S., Meier, B., & Peiter, E. 2020. Manganese in plants: From acquisition to subcellular allocation. Frontiers in Plant Science, 11, 300.

Cardenas-Perez, S., Piernik, A., Chanona-Perez, J.J., Grigore, M.N., & Perea-Flores, M.J. 2021. An overview of the emerging trends of the *Salicornia* L. genus as a sustainable crop. Environmental and Experimental Botany, 191, 104606.

Krumbein, W., Altmann, H. 1973. A new method for the detection and enumeration of manganese oxidizing and reducing microorganisms. Helgoland Marine Research, 25, 347-56.

Nakayama, H., Shin, Y., Sumita, T., Urata, K., & Ikegami, Y. 2019. Characterization of manganese oxide-biomineralization by the psychrophilic marine bacterium, *Arthrobacter* sp. strain NI-2 and its spontaneous mutant strain NI-2'. Environment and Natural Resources Journal, 17(4), 68-77.

Tebo, B.M., Bargar, J.R., Clement, B.G., Dick, G.J., Murray, K.J., Parker, D., Verity, R., & Webb, S.M. 2004. Biogenic Manganese Oxides: Properties and mechanisms of formation. Annual Review of Earth and Planetary Sciences, 32, 287-328.

Color Removal of Pulp and Paper Mill Wastewater by the Residual Eucalyptus Wood

Kanjana Yupin[a,b], Thanakrit Neamhom[a,b], Chatchawal Singhakant[a,b], Sirenee Sreesai[a,b], and Supawadee Polprasert[a,b*]

[a]Department of Environmental Health Sciences, Faculty of Public Health, Mahidol University, 420/1 Rajvithi Rd., Rajchathawee, Bangkok 10400, Thailand

[b]Center of Excellence on Environmental Health and Toxicology (EHT) and Science & Technology Postgraduate Education and Research Development Office (PERDO), Faculty of Science, Mahidol University,272 Rama VI Road, Ratchathewi, Bangkok 10400, Thailand

Abstract

The purpose of this study was to investigate the color removal efficiency of pulp and paper mill wastewater using residual eucalyptus wood, and also to minimize the solid wastes generated from pulp and paper processes. The activated carbon used in this study as the color adsorbent was produced from residual eucalyptus wood. The carbon was activated with phosphoric acid and carbonized in the furnace at a temperature of 500°C for 60 minutes. Effects of types and amounts of activated carbon on color removal efficiency were evaluated. Three types of solid wastes consist of wood chip, bark, and mixed wood (wood chip and bark ratio 1:1) were investigated at a loading of 1, 3, 5, and 7 g/100 mL under contact times of 30, 60, 90, and 120 minutes. The results showed that 7 g/100 mL loading of wood chip activated carbon under all contact times gave high color removal efficiency of about 94-97%. However, the highest adsorption capacity of 216 ADMI/g occurred at 1 g of adsorbent used. Freundlich isotherms were supposed to be satisfactorily fitted to experimental data for the best condition because of high correlation coefficients. The color removal efficiency depended on surface area, pore volume, structure and characteristic of the activated carbon.

Keyword: Pulp and paper mill wastewater/ Color removal/ Activated carbon/ Residual eucalyptus wood

---

*Corresponding Author: Supawadee Polprasert
E-mail address: supawadee.pol@mahidol.ac.th

1. Introduction

At present, Thai people have a quite high rate of paper usage lead to increasing in the paper industry. The paper industry requires large volumes of process water of high purity and generate large amount of wastewater from digestion, lignin extraction, and bleaching process, which is highly colored. Approximately 20 m^3 of fresh water are required to process 1 ton of eucalyptus wood for producing pulp and paper. Moreover, one ton of eucalyptus wood can produce about 0.534 tons of paper and also generated the solid waste such as bask, wood chip and dust of about 0.074 tons, 0.43 tons, and 0.018 tons respectively. The pulp and paper production generates a significantly large amount of pollutants characterized by this high concentration of suspended solids (SS), COD, toxicity and biochemical oxygen demand (BOD) (Pokhrel, 2004). Pulp and paper mill wastewater is a dark brown colored liquid known as 'black liquor'. The pulp and paper mill effluent color is largely due to lignin derivatives and polymerized tannins removed during pulping and bleaching processes, which are resistant to degradation due to the presence of carbon-to-carbon biphenyl linkages (El-Bestawy et al., 2008). The color of paper mill wastewater is one of the major environmental problems, because of the difficulty of treating by conventional methods. Production of various paper has been defined as a business that is harmful to health because it produces color and toxic substances from the production process (Ngernyen, 2014). Color not only cause the bad aesthetical effect but also reduce the self-purification capacity of rivers by inhibiting photosynthetic production of oxygen and direct destruction of aquatic communities (Chooaksorn, 2012). Due to these risks, department of industrial works of Thailand

provides the water quality standard value for controlling the color of effluent from the industry. The effluent standard of color is 600 ADMI for pulp production and 350 ADMI for paper production (The Ministry of Natural Resources and Environment Subject, 2018). Meeting the regulatory discharge standards for pulp and paper mill wastewater has become more difficult because of its recalcitrant and colored dissolved organic matter (DOM) (Shi et al., 2016). The effluent is normally treated by biological process such as aerated lagoon and activated sludge processes. The biological processes are very effective for removing the non-settleable colloidal solids and to stabilize the organic matter, but are not suitable for removing the color (Yadav, 2012).

There are many processes for the color removal of pulp and paper wastewater. It is well known that activated carbon has a high adsorption capacity and can absorb color and odor as well. The activated carbon can remove the color of pulp and paper wastewater by 70% (Ngernyen, 2014). Moreover, a maximum reduction of dyeing effluent in color and COD of 91.84% and 75.21% was observed by using bamboo-based activated carbon (Ahmad, 2009). Besides, the performance of oat hulls activated carbon was studied by the results showed that COD and color removal from landfill leachate were up to 90% (Ferraz, 2020). Therefore, the color removal efficiency of pulp and paper effluent using the residual eucalyptus wood as activated carbon absorbent was investigated in this study.

2. Methodology

The pulp and paper wastewater was collected from the effluent of wastewater treatment plants at the mixed tank after being treated with the secondary clarifier process by grab sampling. The parameters of pH, color, COD, TSS, TDS, and TKN were investigated. The residual eucalyptus wood generated from pulp and paper processes was used as activated carbon for the color adsorbent. The characteristics of pulp and paper wastewater used in the study were described in Table 1. The BOD and COD ratio was pretty low of about 0.15 because the effluent was already treated with biological processes. Therefore, adsorption is an attractive alternative process to treat the color of the effluent after biological treatment. The activated carbon was activated with phosphoric acid at concentrations of 85 % (ratio 1:1) and soak for 60 minutes. After that activated carbon was washed with deionized water several times until pH return to neutral and dried at 105°C for 4 hours (Patnukao, 2008; Kongsuwan, 2009). Carbonized in the furnace at a temperature of 500°C for 60 minutes (Kongsuwan, 2009). The activated carbon was crushed and filtered with sieve to particle size of 0.71 mm. (Chuyingsakuntip, 2013). The physical characteristics of the residual eucalyptus wood and activated carbon were shown in Figure 1, 2, and 3.

Table 1. The characteristics of pulp and paper effluent used in the study

Parameter	Unit	Value
pH	-	7.8-8.2
BOD	(mg/l)	13-17
COD	(mg/l)	96-102
TSS	(mg/l)	10-13
TDS	(mg/l)	1,362-1,370
Color	ADMI (pH-Original)	379-384
	ADMI (pH-Adjust)	338-345
Conductivity	(µs/cm)	2,560-2,620
TKN	(mg/l)	3.24-3.86

The experiments were carried out to investigate the color removal efficiency in batch experiments. The experimental design is 3×4×4 factorial design with 4 replications. The studied factors including the type of eucalyptus wood (wood chip, bark, and mixed wood), amount of

activated carbon (1, 3, 5, 7 grams), and contact times (30, 60, 90, 120 mins) were determined to explore the optimum condition of color removal efficiency. The 250 mL Erlenmeyer flask was used as an adsorption reactor with 100 mL working volume. Then, the amount of each type of activated carbon was added according to the experimental design, and the sample was shaken at 120 rpm for 30, 60, 90, and 120 minutes. The color concentration was analyzed by using a spectrophotometer following ADMI method. The isotherms of Langmuir and Freundlich adsorption were also studied to evaluate the adsorption pattern.

3. Results and Discussion

3.1 The Effect of type and amount of activated carbon

Regarding the three types of activated carbon investigated, the maximum color removal efficiency was obtained from wood chips due to their physical properties such as porosity and surface area. The bark differs from wood chips in terms of its anatomical structure, properties, and chemical composition as shown in Figure 1. The physical structure of wood and bark AC were illustrated in Figure 2 and 3, respectively. The pore size of wood chip AC was larger than bark AC and had non uniform pore size from 3.597 µm to 49.48 µm, while bark AC had similar pore size between 8.467 µm to14.75 µm as shown in Figure 4. The fixed carbon in the bark is higher than in the wood chips, which had 13.10% in the bark and 16.42% in the wood chips. The volatile matter content of wood chips and bark was 83.23% and 75.05% respectively. The ash in the bark was higher than approximately 4 times of others, which has 0.5% in the wood and 1.35% in the bark. (Kiatgrajai, 1994; Kongsuwan, 2009; Borgesa, 2019). Moreover, the results showed that when using wood chipsof 7g/100mL the highest color removal efficiency of 97%was obtained as shown in Figure5(a). Moreover, TDS decreased from 1,370 mg/L to 713 mg/L and conductivity also decreased from 2,620 µs/cm to 1,220 µs/cm as illustrated in Table 2. However, the highest adsorption capacity of 196 ADMI/ g occurred at 1 g of adsorbent used. When using bark and mix wood of 7g/100 mL the highest color removal efficiency of 84% and 89% were obtained as shown in Figure 5(b) and 5(c), respectively.

Figure 1. (a) Eucalyptus wood chips; (b) Eucalyptus Bark; (c) Eucalyptus wood chips after carbonization; and (d) Eucalyptus Bark after carbonization

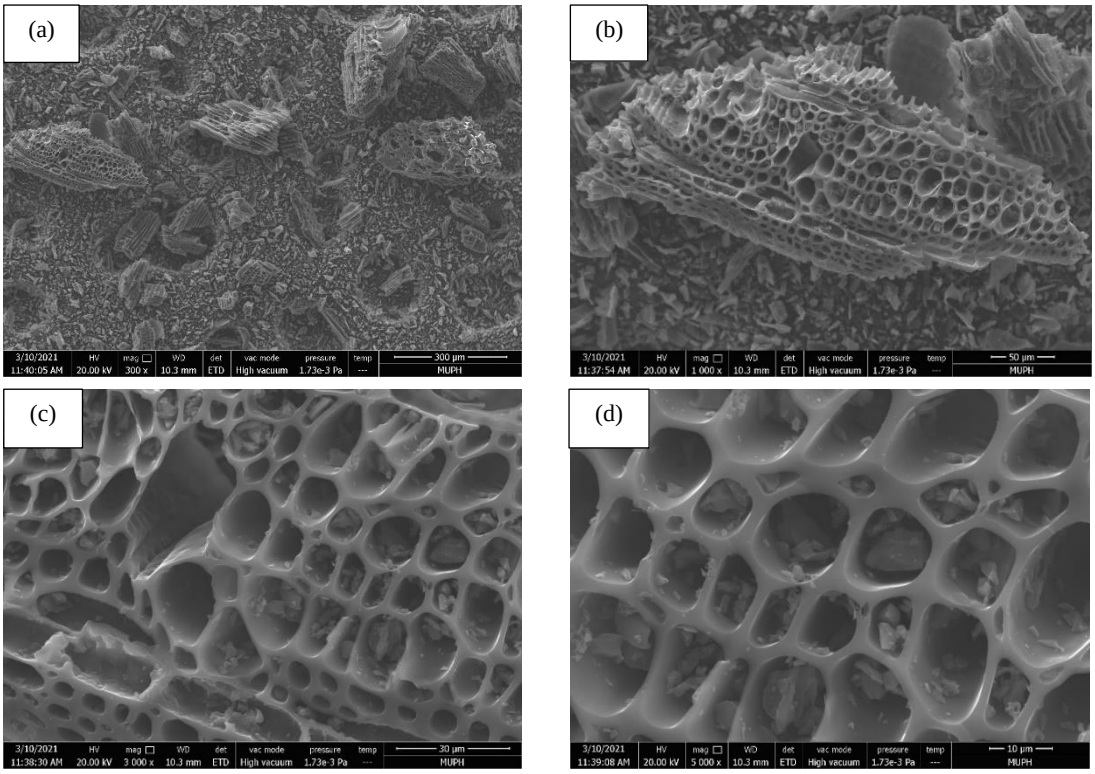

Figure 2. Physical characterization of wood chip activated carbon with SEM Photographs of wood chips activated carbon. (a) Wood chips 500X, (b) Wood chips 1000X, (c) Wood chips 3000X, and (d) Wood chips 5000X

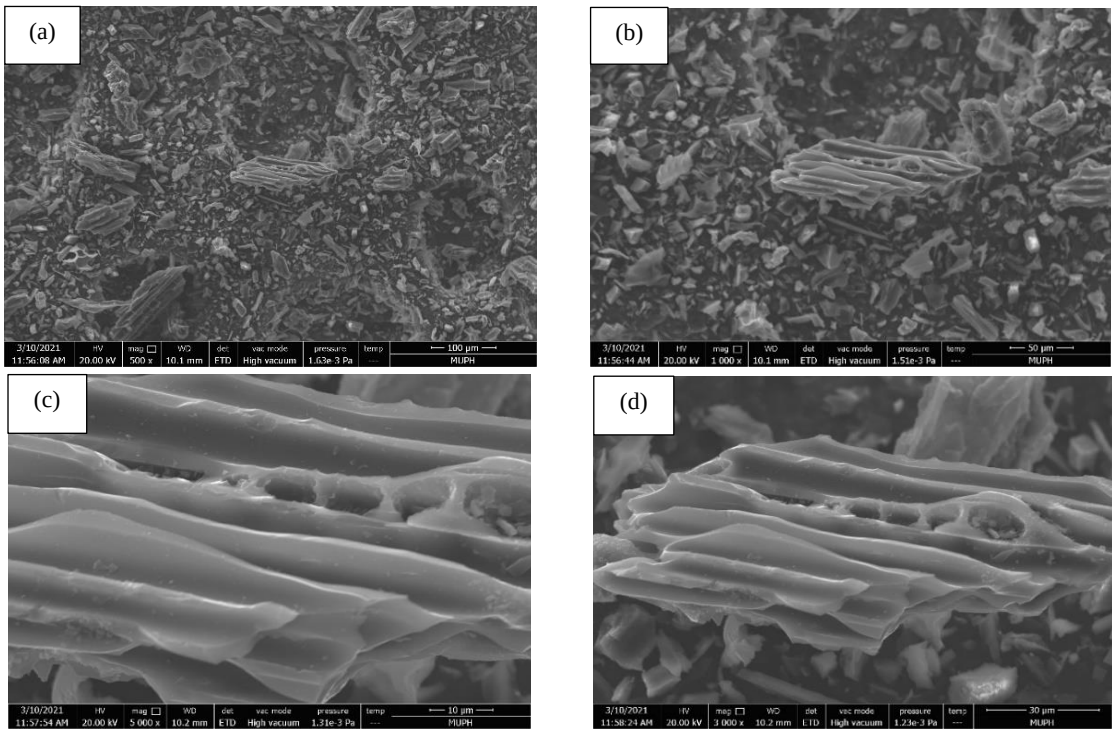

Figure 3. Physical characterization of bark activated carbon with SEM Photographs of Bark activated carbon (a) Bark 500X, (b) Bark 1000X, (c) Bark 3000X, and (d) Bark 5000X

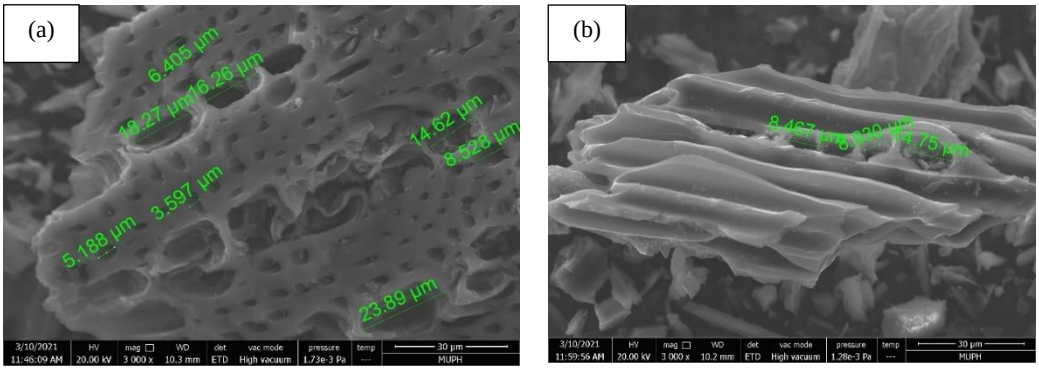

Figure 4. Pore size of wood chip AC (a), and bark AC (b)

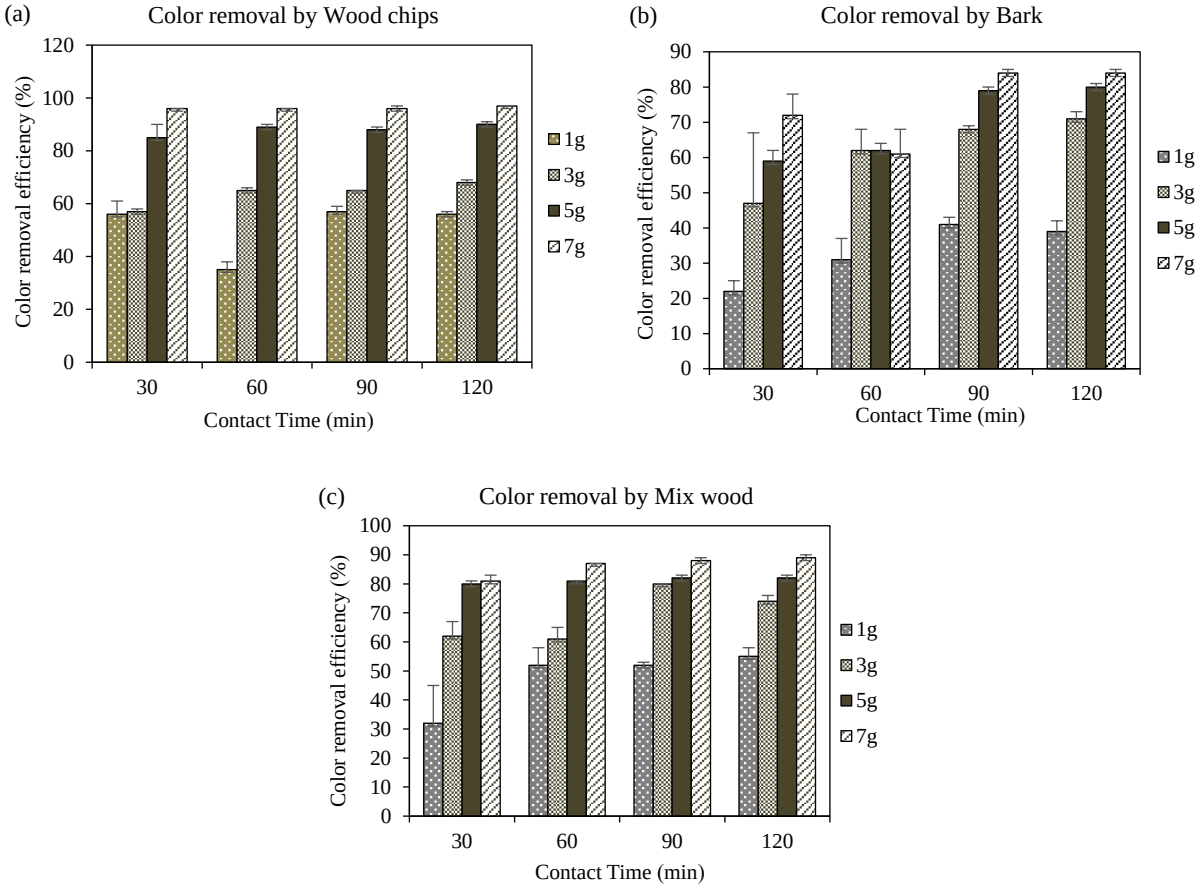

Figure 5. Color removal efficiency using eucalyptus wood chips (a); using eucalyptus bark (b); and using mix wood (c) at activated carbon loading 1, 3, 5, and 7 grams for contact times of 30, 60, 90, and 120 minutes

3.2 The effect of contact time

The effect of contact time was determined on color removal in batch experiments. Regarding the three types of activated carbon from loading at 1, 3, 5, and 7 g/100 mL for a contact time of 30, 60, 90, and 120 minutes, results indicated that the efficiency of adsorption is increased with increasing of contact time. However, color adsorption was rapidly increased in the first period. After that, the color adsorption was gradually decreased.

In addition, the results showed that the highest color removal efficiency of 97% was obtained from wood chips loading at 7g/100 mL for contact times of 120 minutes. It's also obvious that a period is desired for a high amount of wood chip activated carbon used. If the contact time increasing to 120 minutes, the

color removal efficiency was significantly different from 30 minutes. However, the highest color removal efficiency of 84% was observed when using 7 g/100 mL of bark-activated carbon as an adsorbent for 90 minutes. Whereas, the highest color removal efficiency of about 89% was achieved when using 7 g of mixed wood for 120 minutes as shown in Figure 5(a), 5(b), and 5(c), respectively. The effluent after adsorption had characteristic within the effluent standard of color according to the notification of Ministry of Industry. Freundlich isotherms were supposed to be satisfactorily fitted to experimental data for the best condition because of high correlation coefficients as shown in Figure 6.

Table 2. Characteristics of pulp and paper effluents after adsorption using wood chips AC for 120 min

Parameter	Unit	Amount of wood chips AC (g)			
		1 g	3 g	5 g	7 g
pH	-	7.5-7.6±0.03	5.7-5.9±0.10	3.5-3.8±0.17	2.8-3.0±0.04
COD	(mg/L)	84-91±2.94	73-80±2.94	45-56±4.79	28-37±4.11
TSS	(mg/L)	7.6-8.2±0.30	5.8-6.6±0.38	5.6-6.4±0.37	4.6-5.4±0.37
TDS	(mg/L)	1,320-1,360±17.1	1,190-1,210±12.7	984-998±6.80	698-728±12.3
Color	ADMI (pH-Original)	158-171±5.0	117-128±5.0	35-43±4.0	10-11±1.0
	ADMI (pH-Adjust)	138-151±6.0	71-78±3.0	39-58±9.0	15-30±7.0
Conductivity	(µs/cm)	2,140-2,160±8.16	1,910-1,940±12.6	1,620-1,680±25.0	1,220-1,280±25.0

4. Discussion

When contact time increasing, the ability of adsorption was also increased until the equilibrium situation occurred. In the first period, the fast initial adsorption has occurred since the concentration gradient in the solution and the space on the surface of the adsorbent was still plentiful. After that, the ability of adsorption was reduced until equilibrium was attained because the spaces have fully absorbed with color and other substances (Srimoon, 2016). The fixed carbon contents and pore size of activated carbon are factors which could influence the color removal efficiency (Okeola et al., 2012). Moreover, TDS concentration and conductivity decreased with increasing amount of adsorbent and contact time. In order to predict the mechanism of the color adsorption process on the different type of eucalyptus wood activated carbon, it was observed that the Freundlich isotherm model described the adsorption process with high coefficient of determination R^2 (R^2>0.9) better than the Langmuir isotherm model.

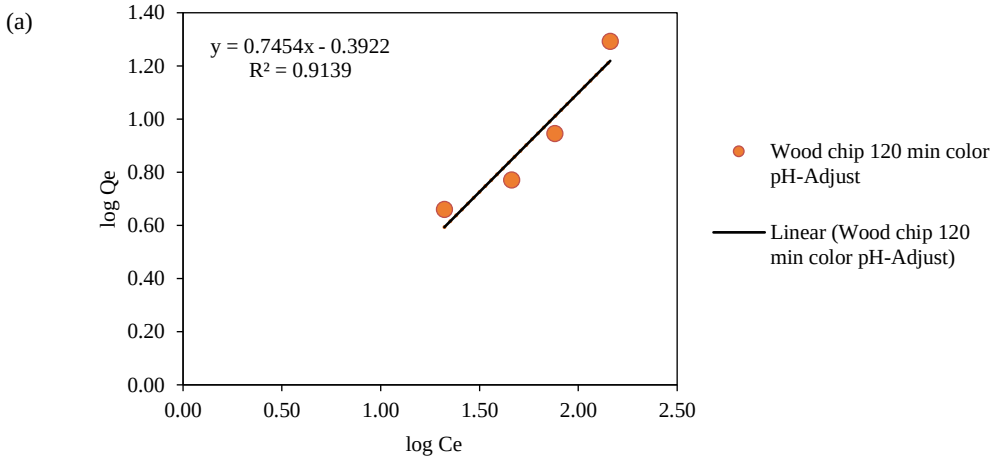

Figure 6. Freundlich isotherms of eucalyptus wood (a) and bark AC; (b) for 120 min contact time

(b)

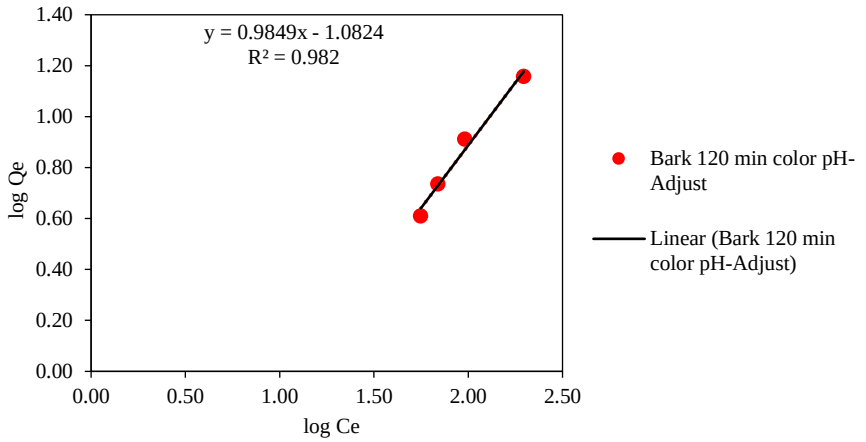

Figure 6. Freundlich isotherms of eucalyptus wood (a) and bark AC; (b) for 120 min contact time (cont.)

5. Conclusions

The adsorption efficiency and amount of activated carbon were direct variations. The color removal efficiencies were slightly increased by increasing amount of activated carbon from 1 to 7 grams for wastewater of 100 mL. The adsorption process occurred very quickly on the surface of the adsorbent when using a large amount of the adsorbent since more surface area of the adsorbent were obtained. Moreover, the ability of absorbent was increased with increasing the contact time from 30 to 120 minutes. When contact time increased, the ability of adsorption was also increased until the equilibrium occurred. Therefore, a shorter contact time was required when using the higher amount of adsorbent. Regarding the experimental data, the eucalyptus wood chip activated carbon gave the highest color removal efficiency due to higher fixed carbon content and non-uniform pore sizes.

Acknowledgement

This research was partially supported by internal grants at the Department of Environmental Health Sciences, Mahidol University, provided by the Center of Excellence on Environmental Health and Toxicology (EHT) under the Science and Technology Postgraduate Education and Research Development Office (PERDO) of the Ministry of Education, Bangkok, Thailand. The researchers also thank the staff at the Environmental Health Sciences Laboratory, Department of Environmental Health Sciences, Faculty of Public Health, Mahidol University, for their excellent technical assistance.

References

Ahmad A.A., Hameed B.H. (2009). Reduction of COD and color of dyeing effluent from a cotton textile mill by adsorption onto bamboo-based activated carbon. Journal of Hazardous Materials, 172, 1538-1543.

Announcement of the Ministry of Natural Resources and Environment Subject: Establishing standards for controlling the drainage of pulp and paper factories. (2018), (135), 13-16.

Borgesa A.C.P., Onwudilib J.A., Andradec H.M.C., Alves C.T., Ingram A., S.A.B. Vieira de Melo S.A.B., Torres E.A. (2019). Catalytic supercritical water gasification of eucalyptus wood chips in a batch reactor. Journal of Fuel, 255, 115804.

Chooaksorn W. (2012). Color removal technology in industrial wastewater. Burapha Science Journal, 17, 181-191.

Chuyingsakuntip S., Tangsathitkulchi C. (2013). Adsorption of natural aluminium dye complex from silk-dyeing effluent using eucalyptus wood activated carbon. American Journal of Analytical Chemistry, 4, 379-386.

El-Bestawy E. El-Sokkary I., Hussein H. Farouk Abu Keela A. (2008). Pollution control in pulp and paper industrial effuents using integrated chemical-biological treatment sequences. J Ind Microbiol Biotechnol, 35,1517-1529.

Ferraz F.M., Yuan Q. (2020). Performance of oat hulls activated carbon for COD and color removal from landfill leachate. Journal of Water Process Engineering, 33, 101040.

Kiatgrajai P., Laohathai B., Sangkul S. (1994). Charcoal Briquette from river red gum. Thai Journal Forestry, 13, 38-49.

Kongsuwan A., Patnukao P., Pavasant P. (2009). Binary component sorption of Cu (II) and Pb (II) with activated carbon from *Eucalyptus camaldulensis* Dehn bark. Journal of Industrial and Engineering Chemistry,15, 465-470.

Ngernyen Y., Khamwilaisak K., Chano S., Iamdamrong P. (2014). Color removal of wastewater from pulp and paper industry by activated carbon. [Thesis], Khon Kaen University, 1-10.

OkeolaO., Odebunmi E., Ameen O. (2012). Comparison of sorption capacity and surface area of activated carbon prepared from prepared from *Jatropha Curcas* fruit pericarp and seed coat. Chemical Society of Ethiopia, 26(2), 171-180.

Patnukao P, Pavasant P. (2008). Activated carbon from *Eucalyptus camaldulensis* Dehnbark using phosphoric acid activation. Journal of Bioresource Technology, 99, 8540-8543.

Pokhrel, D.; Viraraghavan, T. (2004). Treatment of pulp and paper mill wastewater. A review. Sci. Total. Environ, 333, 37-58.

Srimoon R. (2016). Dyes treatment in wastewater using adsorption processes. Khon Kaen University Science Journal, 44(3), 419-434.

Shi X., Xu C., Hu H., Tang F., Sun L., (2016). Characterization of dissolved organic matter in the secondary effluent of pulp and paper mill wastewater before and after coagulation treatment. Water Science and Technology, 74(6), 1346-1353.

Yadav R., Upadhyay K., Maru S. (2012). Colour removal from paper mill effluent using activated carbon. Journal of Industrial Pollution Control, 28(1), 45-50.

Phosphorus Recovery and Bioavailability from Chemical Extraction of Municipal Wastewater Treatment's Waste Activated Sludge: A Case of Bangkok Metropolis, Thailand

Kay Thi Khaing [a,b] and Chongchin Polprasert [a,b,*]

[a]*Department of Sanitary Engineering Faculty of Public Health, Mahidol University, Bangkok 10400, Thailand*
[b]*Center of Excellence on Environmental Health and Toxicology, Bangkok 10400, Thailand*

Abstract

The aim of this study was to evaluate the extractability and bioavailability of Phosphorus (P) recovered from Waste Activated Sludge (WAS) so as to reduce dependence on the import of non-renewable P resources. P extraction was carried out with sulfuric acid (H_2SO_4) concentrations. A response surface methodology was used to optimize conditions for the chemical leaching of WAS. The result of this study showed the optimum condition for leaching WAS with 0.1 M H_2SO_4 occurred at 30 min, resulting in 97% P released. The efficiency of P recovery for P precipitation was improved in the association of pH value and Mg:P. At pH 7, 9, and 11, P was recovered 92, 92, and 91% with uncontrolled Mg and 93, 93, and 92% with sea salt added (Mg:P, 2:1), respectively. However, the yield of the produced struvite was much lower as compared to that of sea salt added. From elemental analysis, struvite of about 26% was precipitated at pH 9 of Mg:P, 2:1, and the total P content of the precipitate was 12%. P available was almost 80% after 35 days of operation, which was higher than that of the commercial fertilizer. Results of this study are expected to provide fully comprehensive information regarding the suitability of P-composite matter recovered from WAS in order to encourage decision-makers for its implementation. This will also help close the loop of the P cycle for food cultivation in the human ecosystem.

Keyword: Waste activated sludge/ Phosphorus extraction/ P recovery/ P-bioavailability

---

*Corresponding Author: Chongchin Polprasert
E-mail address: chongchin.pol@mahidol.ac.th

1. Introduction

Phosphorus (P) is an essential element for all living organisms and plays an important role as a fertilizing nutrient in agriculture. Moreover, P is one of the limited and non-renewable resources and is required for food production (Wither et al., 2015). More than 85% of the mined phosphate rock (PR), is used to produce P fertilizer (Geissler, 2015). It has been noted that the demand for P fertilizer for food production will increase significantly due to the growing world population, which will reach 9 billion people in 2050, who need food to live (M. Chen & Graedel, 2016; Geissler, 2015). PR is rapidly depleting and is available in some geographical areas of the world such as Morocco, China and the USA (Van Vuuren et al., 2010). PR reserves are expected to dwindle in the next 50-100 years (Cordell & White, 2014). Consequently, P recovery from any P-rich residues has attracted considerable attention.

Among P-composite residues, domestic wastewater contains 5-20 g of P (in ortho-phosphates and organic compounds) in one cubic (Li et al., 2015). Biological nutrient removal is the most widely used technique to treat domestic wastewater, phosphates are uptake in excess of normal metabolic requirement and then stored as the intracellular biopolymer polyphosphate (poly-P) within poly-P accumulating organisms (PAOs) (Chen et al., 2012; Wang et al., 2017). In the intervening time, PAOs are enriched by recirculating the waste activated sludge (WAS) (Kodera et al., 2013). Consequently, WAS, as a major byproduct derived from biological WWTP, accumulates a substantial amount of P causing P removal, in which over 90% of P is transferred to WAS (Balmer, 2004). Considering continuous production of WAS in large amounts during biological nutrient removal (Wang et al., 2018; Xu et al., 2018; Zhao et al., 2017), P

recovery from plentiful inexpensive WAS has received increasing attention.

According to the work of Thitanuwat et al. (2016), P at the end of pipe in Bangkok Metropolitan Administration (BMA) was reported to come from domestic wastewater, septage sludge, and green garbage. Only 4% was recycled in public parks. In Bangkok, most of solid wastes go directly to landfills, which are sinks for P resource and can potentially be used for P recycling. This constitutes 81% of P discarded. Meanwhile, annual average of 2116.7 t P was generated from domestic wastewater in BMA. WAS is a major by-product from WWTP in BMA with 16.3 g P/kg or about 63% (456.1 t P/year) to is disposed of in landfill. In addition, it also contains considerable amounts of phosphorus about 356 mg P/L together with components valuable for potential fertilizers such as Mg and Ca. WAS, on the other hand, is polluted with human diseases such as feces-borne coliform bacteria, viable helminth eggs, and active parasite cysts. Hence, fresh sewage sludge should not be disposed on land unless it has experienced pathogen diminishment (Sreesai et al., 2013). Therefore, direct application of WAS on agricultural field is prohibited.

Recently, P recovery from wastewaters by chemical precipitation has been widely investigated. Struvite is a crystalline substance obtained from the input of chemicals including an alkali source for pH adjustment and an Mg source needed to achieve at least equimolar concentrations (1:1) of Mg^{2+} and PO_4^{3-} in the alkali pH solution. It can be used as P fertilizer or as a raw material for P-composite fertilizers (Rahman et al., 2014; Vaneeckhaute et al., 2017). Regardless of the total amount of P in the compost, the origin of the organic waste influences the type and fractions of P forms, which might alter P-bioavailability (Frossard et al., 2002). Due to the existence of low-solubility P, struvite has been considered an excellent P fertilizer and is frequently described as a slow-release fertilizer.(Ackerman et al., 2013; Talboys et al., 2016).

The aforementioned wastes comprise recoverable P, in which pre-treatment is needed to concentrate P from wastes prior to recovery process. However, very few studies in Thailand have been carried out to recover P before landfilling and/or incineration. These therefore necessitate the need to find appropriate method to recover P from such the wastes as to close the loop of P cycle for production in the human ecosystem. Successful results of this study are expected to pave the way for the implementation of engineering process for P recovery nationwide. These will help not only save the money from the cost of imported fertilizer, but also protect the environment from eutrophication, due to excessive P discharge. The objectives of this study are (i) to evaluate the efficiency of chemical P extraction from WAS using sulfuric acid and study the feasibility of engineering and economic of P recovery processes (ii) to investigate speciation of P-composite materials obtained from precipitation of P-containing supernatants produced from chemical P extraction processes (iii) to investigate the P-bioavailability from the recovered P product, in comparison with commercial fertilizers.

2. Methodology

2.1 Source Waste activated Sludge (WAS)

The WAS used in this study was collected from the secondary sedimentation tank of Nong Khaem water quality control WWTP, BMA, Thailand. After collecting, the characteristics of WAS were measured, and it was stored in closed plastic containers at 4°C, prior to use. The main characteristics of WAS are shown in Table 1, which demonstrates that the sample contains P, Ca, and Mg as the major elements. The total solids (TS) content of WAS were diluted with distilled water to 3% of solids content, (w/v) which is the average TS content found in general WAS (Zhang et al., 2020), in order to ensure consistency before acid leaching.

2.2 Soil

The soil selected for this study was taken from the upper layer of an agricultural field in Nakhon Pathom, Thailand. The soil was sieved to obtain the fraction ≥1 cm. It had a total P content of 0.005 mg/g.

Table 1. Characteristics of waste activated sludge (WAS).

Parameter	Unit	Values
Total phosphorus (TP)	mg/L	356 ± 12.47
Soluble phosphorus	mg/L	48.05 ± 0.37
Chemical oxygen demand (COD)	mg/L	16304 ± 10.3
Magnesium (Mg)	mg/L	155.37 ± 0.06
Ammonia (NH_3)	mg/L	168.7 ± 17.03
Calcium (Ca)	mg/L	226.93 ± 2.00
Total solid (TS)	mg/L	35100 ± 24.30
Percentage of volatile solid of total solid (VS)	%	52.28 ± 3.4
Total suspended solid (TSS)	mg/L	31000 ± 23.21
Percentage of volatile suspended solid of total suspended solid (VSS)	%	53.72 ± 2.27

2.3 Chemical leaching tests

In chemical leaching tests, 500 mL of WAS (3% of solids content) was mixed with concentration H_2SO_4, in order to prepare four different concentrations of H_2SO_4 (0.01, 0.05, 0.1, and 0.5 M). The mixture was stirred at 200 rpm using Jar tester at ambient temperature (20-25°C). For P extraction, the experiments were conducted in triplicate by varying reaction times (15, 30, 45, 60, 90, and 120 mins). After leaching treatment, the mixture was separated using 10 µm filter paper (Whatman No. 93). Subsequently, the filtrates were determined PO_4^{3-}, Mg, and Ca. The sludge residue was dried at 105°C for 24 h. After drying, for it was used to analyze to the remaining P.

2.4 Optimization and prediction model

The response surface methodology (RSM) of Design Expert 13 software licensed to the faculty of graduate studies, Mahidol University was used to determine the optimum condition for leaching process, which can be used for optimizing the factors including reaction time and acid concentration (Anderson et al., 2009; Coetzer et al., 2018). An I-optimally with 16 runs were used. The interactions among the variables and responses P extraction were determined from the analysis of variance (ANOVA). In order to quantify the quality of the quadratic prediction models, model terms statistical significance, coefficient of determination (R^2), probability (P-value) with 95% confidence level, and (t-test) at 5% significance level (Prob<0.05) were determined. Moreover, the 3D surface was created to identify the optimum region. Thus, a mathematical model was developed following a second order polynomial shown in Equation (1).

$$Y = \beta_0 + \beta_i A + \beta_j B + \beta_{ii} A^2 + \beta_{jj} B^2 + \beta_{ij} AB \quad (1)$$

Where; Y is percentage of P extraction responded, β_0, β_i, β_j, β_{ii}, β_{jj} and β_{ij} are constant, linear effect, quadratic effect, and interaction effect coefficients, respectively; A and B represents the independent variables, viz., reaction time and acid concentration.

2.5 Phosphorus precipitation

The precipitation tests were conducted for P recovery. The leachate obtained from the optimum condition of leaching process was used as the P-stock solution. In the experiment, two different Mg^{2+}:PO_4^{3-} molar ratios (1.07:1 (uncontrolled) and 2:1 (sea salt addition)) were used. For Mg/P=2, sea salt was added as the external source of Mg. The pH of all cases were controlled at 7, 9, and 11 by dropwise addition of sodium hydroxide solution (12 N) at the beginning of each experiment. These experiments were done three times at ambient temperature. The stirring velocity were initially set at 200 rpm for 15 min, slow mixing at rpm 75 for 30 min and were followed by settling for 1 h. After settling, the mixture was separated by 10 µm filter (Whatman No. 93). Finally, the precipitates formed during this process were separated by filtration and oven dried at 103°C for 24 h. After that, the dried solids precipitates were determined P containing solid.

2.6 Phosphorus bioavailability procedures

The pot experiment was carried out to compare P-bioavailability of P-solids precipitates (PSP) obtained from this study with that of commercial fertilizers such as Mono-phosphate (MP) and Diammonium phosphate (DAP). The experiments were conducted in plastic pots (with pots size 0.11 m × 0.005 m^2) in triplicates for each experiment. Those three fertilizers were measured to 100 mg P per pot (150 kg P ha^{-1}). The fertilizers in each pot were dissolved with pH6 tap of 90 mL per day equivalent to the amount of rainfall per year of the country. The experiments were generated until 35-day test duration. Samples were collected every day to analyze the P content.

2.7 Analysis and Calculations

The total Kjeldahl nitrogen (TKN), TS, VS, TSS, VSS, COD, total ammonia nitrogen concentrations were measured according to standards methods (APHA, 2012). Mg and Ca were measured with AAS (atomic adsorption spectrophotometer). The data were expressed using mean value and standard deviations (S.D.). Independent T test and One-way analysis of variance (ANOVA) were used to determine whether there were statistically significant differences among the leaching experiments, 16 runs for acid leaching of P recovery, P-bioavailability and percentage P content in solid and liquids. All tests were performed by using SPSS statistics 18.0 for windows licensed to Mahidol University.

Phosphorus recovery: The P recovery efficiency defined in Equation (2) was determined by the difference of initial and final PO_4^{3-}concentrations in experiments, as shown in Equation (2).

$$(\%)\ P_{recovery} = \left[\frac{[PO_4^{3-}-P]_{initial}-[PO_4^{3-}-P]_{final}}{[PO_4^{3-}-P]_{initial}}\right] \times 100 \quad (2)$$

Where; $[PO_4^{3-}-P]_{initial}$is the initial phosphate concentrations, mg/L and $[PO_4^{3-}-P]_{final}$is final phosphate concentrations, mg/L.

Phosphorus crystal content: It is calculated, following Equation (3).

$$\text{P crystal content } (\%) = \left[\frac{C_s \times MW \text{ of P crystal}}{M}\right] \times 100 \quad (3)$$

Where; C_s is the molar concentration of limiting ions (mol/L), the molecular weight of P crystal formed (g/mol) and M is the number of solids formed in the precipitation experiment (g/L).

P bioavailability: It is computed, as shown in Equation (4).

$$\%\ \text{P release efficiency} = \frac{P_{mix,t} - Blank_t}{P_{m,0} - Blank_0} \times 100 \quad (4)$$

Where $P_{mix,t}$ is the mix phosphate concentrations at day, mg/L, $P_{m,0}$ is start phosphate concentrations (mg/g), $Blank_t$ is soil concentrations at day and $Blank_0$ is start soil concentrations.

3. Results and Discussion

3.1 Optimization of the extraction parameters by response surface methodology (RSM) and analysis of variance (ANOVA)

The results collected from these experiments were fitted into a quadratic polynomial model and regression coefficients obtained. To determine the best model for the response (%P extraction), standard deviations, the predicted sum of squares, and R-squared values were compared (Cornell et al., 2011; Iweka et al., 2021).

The resulting ANOVA (analysis of variance) data is shown in Table 2. It can be seen that the significant model terms in this model are time (A), acid concentration (B), the two-level interactions of time and acid concentration (A*B), and the quadratic effect of acid concentration (B^2) which indicate that those terms have the great influence on %P extraction. Based on the mathematical calculations for a good-fit model the amount of the variation in the response must be close to one (Onsekizoglu et al., 2010). According to the correlation coefficients (R^2) values obtained in this study for P extraction is 0.9889, it can be concluded that there is a good fit between models and experimental data. Moreover, the adjusted correlation coefficients, R^2 (adj) were 0.9833. F-tests for 'lack of fit' were used to assess the model's suitability. The 'lack of

fit' in P extraction, was not significant, with F-values of 0.7080 and p-values of 0.6430, respectively. This means that the model's suitability for explaining this process (Falowo et al., 2019). In order to make predictions about the response for given levels of each factor, an equation in terms of coded factors can be used. In other words, this equation is useful where identification of the relative influence of a factor is important and is done through comparing the factor coefficients against one another. Effective mathematical models as functions of the coded variables for P extraction are proposed as shown in Equation (5):

$$\%P\ extraction = +121.25 + 32.20A + 2.85B - 1.38AB - 53.25A^2 - 1.61B^2 \quad (5)$$

Where; A is the reaction time (min), B is the acid concentration for chemical leaching (M), for extraction P (min). This equation describes the created model and gives solutions for the dependent variable based on the independent variable combinations, whether they are significant in the response. Optimization of the reaction parameters by response surface methodology (RSM) described by the regression model in Figure 1. Based on the above discussed, both time and acid concentration are important factors for the leaching efficiency of P. The Figure also shows that increasing acid concentration and time affected into increased %P extraction efficiency. However, the leaching efficiency decreases slightly when acid concentration increased above 0.45 M. As can be seen, this model forecast that optimum values to obtain the highest value of P extraction are: 30 min of reaction time and 0.1 M of acid concentration.

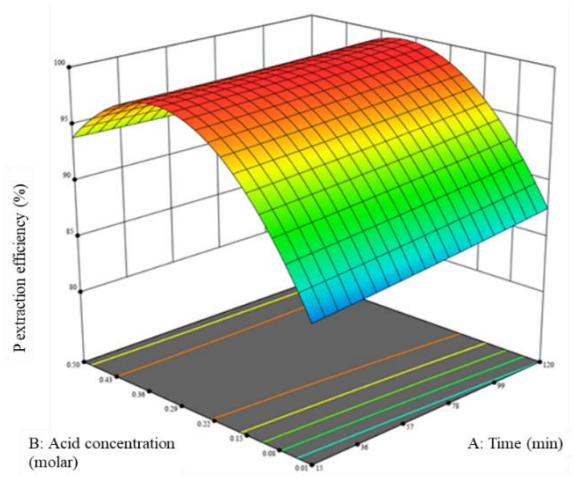

Figure 1. 3D-surface plot for P-extraction in respect to the most influential parameters, i.e., Time and acid concentration (ambient temperature).

Table 2. Analysis of variance table for P extraction

Source	Sum of Squares	df	Mean Square	F-value	p-value	
Model	6463.56	5	1292.71	177.39	<0.0001	significant
A-Time	171.37	1	171.37	23.52	0.0007	
B-Acid concentration	5036.23	1	5036.23	691.10	<0.0001	
AB	39.54	1	39.54	5.43	0.0421	
A^2	9.25	1	9.25	1.27	0.2861	
B^2	3854.31	1	3854.31	528.91	<0.0001	
Residual	72.87	10	7.29			
Lack of Fit	30.21	5	6.04	0.7080	0.6430	not significant
Pure Error	42.67	5	8.53			
Cor Total	6536.44	15				
			R^2	0.9889		
Std. Dev.	2.70		**Adjusted R^2**	0.9833		
Mean	83.81		**Predicted R^2**	0.9783		
C.V. %	3.22		**Adeq Precision**	35.1792		

3.2 P recovery via precipitation and P-containing solids speciation

To confirm the feasibility of P recovery from WAS as magnesium ammonium phosphate (MAP) and hydroxyapatite (HAP), P crystallization from the leachate obtained from the optimum condition (0.1 M, 30 min) followed by speciation of precipitates formed were conducted. The reactions of MAP and HAP and their solubility product constants are presented in Equation (6) and (7), respectively.

$$MgNH_4PO_4(s) \rightleftharpoons Mg^{2+}(aq) + NH_4^{+}(aq) + PO_4^{3-}(aq) \quad (6)$$

$$Ca_3(PO4)_2\,(s) \rightleftharpoons 3Ca^{2+}(aq) + 2PO_4^{3-}(aq) \quad (7)$$

As illustrated in Figure 2 the efficiencies of P recovery from the WAS leachate under uncontrolled magnesium (Mg/P=1.07) were 92, 92, and 91% at pH 7, 9, and 11, respectively. Similarly, for sea salt addition (Mg/P=2), the P recovery efficiencies at pH 7, 9, and 11 were 93, 93, and 92%, respectively. These results indicate that both pH and molar ratio of Mg/P are not affected into the %P extraction. However, it is obvious that efficiencies of P recovery for all cases decreased when using pH=11. Previous studies found that a wide range of molar ratios of Mg/P can be used for struvite precipitation (Khaita & Polprasert, 2019; Pinatha et al., 2020), Perera et al. (2007) reported that increasing the molar ratio of Mg/P increases supersaturation, resulting in more nucleation and crystal growth, but the final pH limits any further precipitation. The different finding may be that the different type of supernatants used in P recovery.

The percentage of various types P-containing solids generated from this experiment also was calculated based on the proportion of P in each compound detected. Based on the results, the %MAP increased when sea salt addition was applied. The higher MAP% was found with sea salt addition (Mg/P=2) while the percentage of MAP were only 2 to 5% for uncontrolled Mg (Mg/P=1.07) at pH 7, 9, and 11. The highest MAP of 26% was found at pH 9 under addition of sea salt (Mg/P=2). This would mean that molar ratio of Mg/P affected to the formation of MAP in this study. In case of %HAP, the results also show that %HAP under sea salt addition was higher than uncontrolled Mg condition, 8-12% of HAP for Mg/P=2 and 3-5% of HAP for Mg/P=1.07. As discussed above, pH 9 with the addition of sea salt was chosen to be an optimum condition for production of P-containing solids which was used in the P-bioavailability.

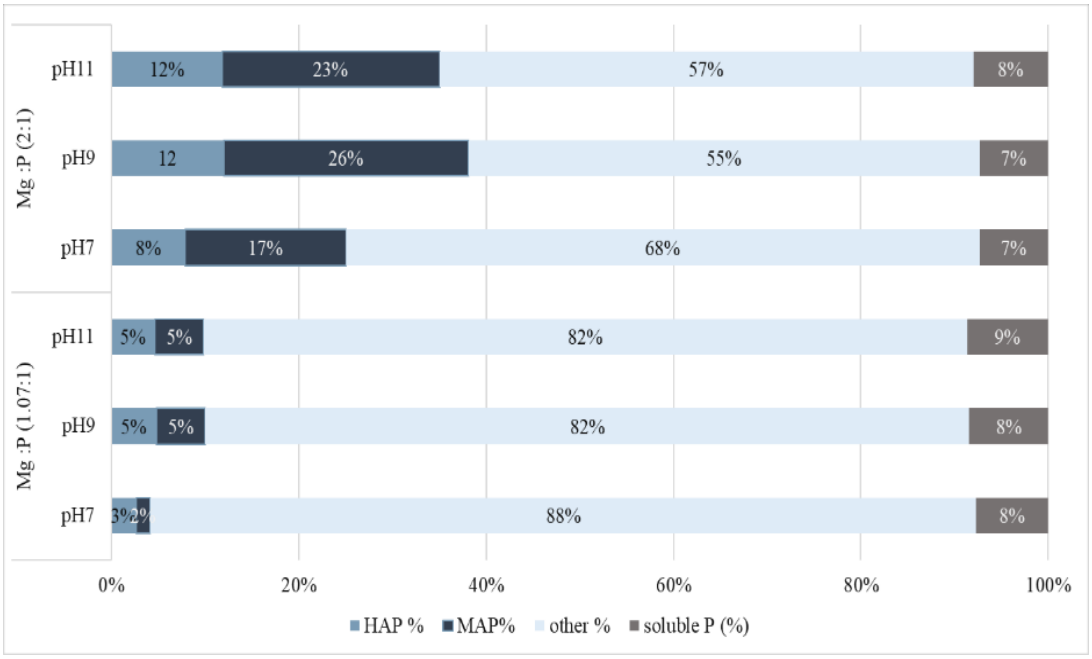

Figure 2. Speciation of P-composite precipitates recovered from WAS under different experimental conditions.

3.3 P recovery as different P fertilizer

The percentage of P content in the solids precipitates is an important measure for developing an alternative P fertilizer. Table 3 shows a comparison of the percent P content in the solids precipitated from this study and the commercial P fertilizers. The percent P content in the solid precipitates was in the range of 7-12% for both uncontrolled magnesium (Mg/P=1.07) and sea salt addition (Mg/P=2) with pH from 7 to 11. The highest %P in solids for all cases were found at pH 9, 11% P in solids for Mg/P=1.07 and 12% P in solids for Mg/P=2, which were higher than that of commercial superphosphate (SSP) fertilizer (8.8% P). Therefore, the P-containing solids obtained from both experiments can be used as an alternative P fertilizer. In addition, the precipitates from other experiments with P content less than 8.80% can be used as soil conditioner due to their good nutrient qualities, especially P (Lind et al., 2000). Hence, P-solids precipitates obtained from WAS can be effectively used to produce fertilizer for agricultural crops to achieve the sustainable P management helps to strengthen Thailand's food security.

Table 3. A comparison of P content in solid precipitate of this study and commercial P fertilizers.

P recovery from WAS (This study)			Commercial P fertilizer			
Mg/P ratios	pH	% P content in solid precipitate (% dry wt.)	P fertilizer	Formula	% P_2O_5	% P
1.07	pH 7	8	Superphosphate	0-20-0	20	8.80
	pH 9	11	Triple super- phosphate	0-46-0	46	20.24
	pH 11	7	Diammonium phosphate	18-46-0	46	20.24
2	pH 7	11	Monoammonium phosphate	11-52-0	52	22.88
	pH 9	12				
	pH 11	9				

3.4 P bioavailability from WAS recovered product

Comparison of P-bioavailability of P-solids precipitates (PSP) obtained from WAS and commercial fertilizers including Di-ammonium phosphate (DAP) and Mono-phosphate (MP) was determined by solubility of P compounds in water at pH 6. 150 kg ha^{-1} of these P-fertilizers was dissolved in 90 mL of water for 35-day. The DAP, MAP and P-precipitating solid were 47%, 31% and 20% soluble in water after 35 days, respectively, as shown in Figure 3. The amount of P remaining in the soil is 79.20 kg P ha^{-1} of DAP, 103.23 kg P ha^{-1} of MP and 118.09 kg P ha^{-1} of PSP which means that about 53%, 69%, and 80% of P in commercial fertilizers (DAP and MP) and PSP were remained in the soil, respectively, indicating that PSP are highest bioavailable for plant uptake.

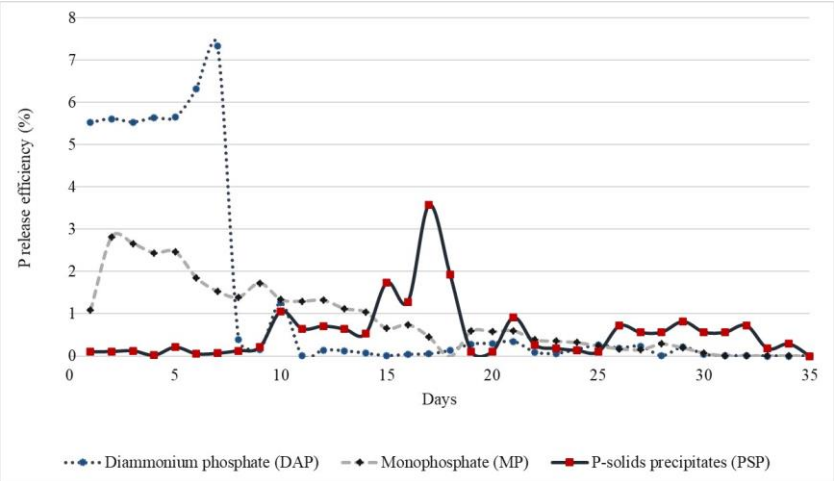

Figure 3. Percentage of P release efficiency for P-bioavailability test (%)

3.5 Economic assessment

Finally, to complete the results of this study, the analysis of the costs of P recovery process and the possible gains from the sale of the resulting product have been calculated based on the method by Pinatha et al. (2020). Table 4 depicts the potential economic savings for P recovery from the leachate obtained at the optimum condition. Chemical additions, especially sulfuric acid, is the major costs of the process due to the extraction of P (pH lower than 1). This also resulted in the large amount of 50% NaOH used to adjust pH in the step of precipitation at pH 7 to 11. Therefore, when average costs in the unit of USD/kg P were compared with the market price of commercial fertilizers, the lowest average costs were found with the addition of sea salt at pH 9. This indicates that sea salt addition can reduce the total costs that mostly came from acid addition by increasing of both the production of precipitates and %P in solids. Thus, additional economic savings could also be possible when the market fertilizer prize in the future is higher than the average costs obtained.

Table 4. Cost analysis of P recovery process using different pH and molar ratio of Mg/P.

Parameters	pH 7		pH 9		pH 11	
	(1.07:1)	(2:1)	(1.07:1)	(2:1)	(1.07:1)	(2:1)
Chemical additions (kg/m^3)						
Acid H_2SO_4	10.30	10.30	10.30	10.30	10.30	10.30
NaOH 50%	1.44	1.44	1.52	1.52	2.28	2.28
Sea salt	0	0.33	0	0.33	0	0.33
Material costs (USD/kg)						
Mg source (sea salt)[a]	0.06	0.06	0.06	0.06	0.06	0.06
50% NaOH[b]	0.20	0.20	0.20	0.20	0.20	0.20
Acid H_2SO_4[c]	0.18	0.18	0.18	0.18	0.18	0.18
Waste activated sludge	0	0	0	0	0	0
Energy consumption (kWh/m^3)						
Rapid Mixing (15 min)	0.0626	0.0626	0.0626	0.0626	0.0626	0.0626
Slow mixing (30 min)	0.0013	0.0013	0.0013	0.0013	0.0013	0.0013
Electricity cost per unit (USD kW/h)[d]	0.12	0.12	0.12	0.12	0.12	0.12
Product produced (kg/m^3)						
Obtained solids from precipitation	1.03	1.3	1.11	1.88	1.2	1.6
%P content in solids precipitate	8.00	11.00	11.00	12.00	7.00	9.00
P content in solid precipitate (kg P/m^3)	0.082	0.15	0.12	0.23	0.09	0.14
Total costs (USD/kg P)						
[1] Average costs	25.78	14.17	17.40	9.56	26.53	16.03
[2] Market fertilizer prize[e]	3.52±5	3.52±5	3.52±5	3.52±5	3.52±5	3.52±5
[2]-[1] Profit margin	-22±-21	-11±-9	-14±-12	-6±-5	-23±-22	-13±-11

± Standard division; [a] https://oae.go.th/view/1/TH-TH; [b] https://www.alibaba.com/premium/sodium;
[c] https://www.alibaba.com/premium/acid; [d] Thailand's electricity cost from Metropolitan Electricity Authority (www.mea.or.th);
[e] OAE.go.th (Lowest price for N-P-K formula 18-46-0 and highest price for formula 16-16-8; P as P_2O5 and K as K_2O).

4. Conclusions

P recovery from WAS, using chemical leaching and precipitation with sea salt addition, appears to be a promising method for recovering the limiting nutrient P. The optimum condition for P leaching (0.1 M H_2SO_4, 30 min) found from RSM could achieved nearly 100% P extraction efficiency. The highest P recovery efficiency (%) was found at pH 9 with sea salt addition, resulting in 26% MAP formed. The precipitating solids contained about 12% P. Moreover, the percentage bioavailability of P uptake from WAS-recovered solid P was about 80%, which is much better than those of commercial fertilizers. This indicate that recovered P-solids from WAS is technically

feasible to be utilized as fertilizing compound for plant cultivation. Therefore, the results found in this study will help understand P leaching and precipitating from WAS and guide decision-makers for its implementation. Consequently, this will lead to closing the loop of P-for-food management in the human ecosystem.

Acknowledgement

This research was financially supported by the Mahidol-Norway Capacity Building Initiative for Myanmar Phase 2.

References

Ackerman, J. N., Zvomuya, F., Cicek, N., & Flaten, D. (2013). Evaluation of manure-derived struvite as a phosphorus source for canola. Canadian Journal of Plant Science, 93(3), 419-424.

Anderson-Cook, C. M., Borror, C. M., & Montgomery, D. C. (2009). Response surface design evaluation and comparison. Journal of Statistical Planning and Inference, 139(2), 629-641.

Balmer, P. (2004). Phosphorus recovery-an overview of potentials and possibilities. Water science and technology, 49(10), 185-190.

Chen, M., & Graedel, T. J. (2016). A half-century of global phosphorus flows, stocks, production, consumption, recycling, and environmental impacts. Global Environmental Change, 36, 139-152.

Chen, Y., Wang, D., Zhu, X., Zheng, X., & Feng, L. (2012). Long-term effects of copper nanoparticles on wastewater biological nutrient removal and N2O generation in the activated sludge process. Environmental science & technology, 46(22), 12452-12458.

Coetzer, R., Joubert, T., Viljoen, C., Nel, R., & Strydom, C. (2018). Response surface models for synthetic jet fuel properties. Applied Petrochemical Research, 8(1), 39-53.

Cordell, D., & White, S. (2014). Life's Bottleneck: Sustaining the World's Phosphorus for a Food Secure Future. Annual Review of Environment and Resources, 39(1), 161-188.

Cornell, J. A. (2011). Experiments with mixtures: designs, models, and the analysis of mixture data (Vol. 403): John Wiley & Sons.

Falowo, O. A., Oloko-Oba, M. I., & Betiku, E. (2019). Biodiesel production intensification via microwave irradiation-assisted transesterification of oil blend using nanoparticles from elephant-ear tree pod husk as a base heterogeneous catalyst. Chemical Engineering and Processing-Process Intensification, 140, 157-170.

Frossard, E., Skrabal, P., Sinaj, S., Bangerter, F., & Traore, O. (2002). Forms and exchangeability of inorganic phosphate in composted solid organic wastes. Nutrient Cycling in Agroecosystems, 62(2), 103-113.

Geissler, P. W. (2015). Para-states and medical science: Making African global health: Duke University Press.

Iweka, S. C., Owuama, K. C., Chukwuneke, J. L., & Falowo, O. A. (2021). Optimization of Biogas yield from anaerobic co-digestion of Corn-Chaff and Cow Dung Digestate: RSM and Python Approach. Heliyon, E08255.

Khaita, C., & Polprasert, C. (2019). Effect of Organic Matter on Struvite Precipitation of Phosphorus Contained in Tapioca-starch Wastewater. Thai Environmental Engineering Journal, 33(1), 31-39.

Kodera, H., Hatamoto, M., Abe, K., Kindaichi, T., Ozaki, N., & Ohashi, A. (2013). Phosphate recovery as concentrated solution from treated wastewater by a PAO-enriched biofilm reactor. Water Research, 47(6), 2025-2032.

Li, W.W., Yu, H.Q., & Rittmann, B. E. (2015). Chemistry: Reuse water pollutants. Nature News, *528*(7580), 29.

Onsekizoglu, P., Bahceci, K. S., & Acar, J. (2010). The use of factorial design for modeling membrane distillation. Journal of Membrane Science, 349(1-2), 225-230.

Perera, P., Han, Z.Y., Chen, Y.X., & Wu, W.X. (2007). Recovery of nitrogen and phosphorous as struvite from swine waste biogas digester effluent. Biomed. Environ. Sci, 20(5), 343-350.

Pinatha, Y., Polprasert, C., & Englande Jr, A. J. (2020). Product and cost perspectives of phosphorus recovery from human urine using solid waste ash and sea salt addition–A case of Thailand. Science of the Total Environment, 713, 136514.

Rahman, M. M., Salleh, M. A. M., Rashid, U., Ahsan, A., Hossain, M. M., & Ra, C. S. (2014). Production of slow release crystal fertilizer from wastewaters through struvite crystallization-A review. Arabian journal of chemistry, 7(1), 139-155.

Sreesai, S., Peapueng, P., Tippayamongkonkun, T., Sthiannopkao, S. J. (2013). Assessment of a potential agricultural application of Bangkok-digested sewage sludge and finished compost products. Waste Management & Research, 31(9), 925-936.

Talboys, P. J., Heppell, J., Roose, T., Healey, J. R., Jones, D. L., & Withers, P. J. (2016). Struvite: a slow-release fertiliser for sustainable phosphorus management? Plant and soil, 401(1-2), 109-123.

Thitanuwat, B., Polprasert, C., & Englande, A. J. (2016). Quantification of phosphorus flows throughout the consumption system of Bangkok Metropolis, Thailand. Science of The Total Environment, 542, 1106-1116.

Van Vuuren, D. P., Bouwman, A. F., & Beusen, A. H. W. (2010). Phosphorus demand for the 1970–2100 period: A scenario analysis of resource depletion. Global Environmental Change, 20(3), 428-439.

Vaneeckhaute, C., Lebuf, V., Michels, E., Belia, E., Vanrolleghem, P. A., Tack, F. M., & Meers, E. (2017). Nutrient recovery from digestate: systematic technology review and product classification. Waste and Biomass Valorization, 8(1), 21-40.

Wang, D., Duan, Y., Yang, Q., Liu, Y., Ni, B.J., Wang, Q., Zeng, G., Li, X., Yuan, Z. (2018). Free ammonia enhances dark fermentative hydrogen production from waste activated sludge. Water Research, 133, 272-281.

Wang, D., Fu, Q., Xu, Q., Liu, Y., Ngo, H. H., Yang, Q., Zeng, G., Li, X., Ni, B.J. (2017). Free nitrous acid-

based nitrifying sludge treatment in a two-sludge system enhances nutrient removal from low-carbon wastewater. Bioresource Technology, 244, 920-928.

Withers, P. J. A., Elser, J.J., Hilton, J., Ohtake, H., Schipper, W.J., van Dijk, K.C. (2015). Greening the global phosphorus cycle: how green chemistry can help achieve planetary P sustainability. Green Chem., 17(4), 2087-2099.

Xu, D.C., Zhong, C.Q., Yin, K.H., Peng, S.H., Zhu, T.T., Cheng, G. (2018). Alkaline solubilization of excess mixed sludge and the recovery of released phosphorus as magnesium ammonium phosphate. Bioresource Technology, 249, 783-790.

Zhang, L., Chen, Y., Ma, C., Liu, L., Pan, J., Li, B., Wang, Q. (2020). Improving heavy metals removal, dewaterability and pathogen removal of waste activated sludge using enhanced chemical leaching. Journal of Cleaner Production, 271, 122512.

Zhao, J., Gui, L., Wang, Q., Liu, Y., Wang, D., Ni, B.J., Li, X., Xu, R., Zeng, G.,Yang, Q. (2017). Aged refuse enhances anaerobic digestion of waste activated sludge. Water Research, 123, 724-733.

Regeneration Heat Duty of Novel AMP–MPDL Solvent for CO_2 capture

Rattanaporn Apaiyakul[a], Ratana Jiraratananon[b], Paitoon Tontiwachwuthikul[c], and Teerawat Sema[a,d*]

[a]Department of Chemical Technology, Faculty of Science, Chulalongkorn University, Thailand
[b]Department of Chemical Engineering, Faculty of Engineering, King Mongkut's University of Technology Thonburi, Thailand
[c]Clean Energy Technologies Research Institute (CETRi), Faculty of Engineering and Applied Science, University of Regina, Canada
[d]Center of Excellence on Petrochemical and Materials Technology, Chulalongkorn University, Thailand

ABSTRACT

In the present work, high potential novel 2-amino-2-methyl-1-propanol (AMP)-*N*-methyl-4-piperidinol (MPDL) solvent was experimentally investigated as an alternative solvent for capturing CO_2 in terms of regeneration heat duty (Q_{reg}, kJ/mol CO_2). Generally, Q_{reg} composes of three heat components including heat of desorption (Q_{des}), heat of vaporization (Q_{vap}), and sensible heat (Q_{sen}). The three heat components were determined based on a solvent regeneration experiment and a specific heat capacity (C_p) measurement. The experiment was conducted in a laboratory scale regeneration reactor at total amine concentration of 30%wt. (5/25, 10/20, and 15/15 %wt. AMP/MPDL) and 363 K, which are typical total amine concentration and regeneration temperature used in the industry. C_p of the solvent was analyzed by differential scanning calorimeter (DSC). The results showed that a major contributor of Q_{reg} was Q_{sen} then Q_{des}, while Q_{vap} was rarely changed for the studied AMP/MPDL blended ratios. Even though an increasing of AMP/MPDL blended ratio resulted in (i) an increasing of Q_{des} and (ii) a decreasing of Q_{sen}, Q_{reg} was found to be reduced. This dues to the fact that Q_{sen} is the main heat component and a reduction of Q_{sen} is larger than a raising of Q_{des}. In comparison with industrially used benchmarking 30%wt. monoethanolamine (MEA) solvent, the proposed novel AMP-MPDL solvent required 60-63% less regeneration heat duty. This is expecting to be very beneficial for an operating cost of CO_2 capture process.

Keyword: CO_2 capture/ Regeneration heat duty/ Novel solvent/ *N*-methyl-4-piperidinol

---

*Corresponding Author: Dr. Teerawat Sema
E-mail: teerawat.se@chula.ac.th

1. Introduction

Global warming, which dues to an increasing amount of greenhouse gases in the atmosphere, is considered as a main challenge in the likely future scenario of increasing the demand for energy because of the continued increases in population and industry. Carbon dioxide (CO_2) has been considered as a major greenhouse gas contributing to the global warming issue (J.G.J and J.A.H.W, 2020). It is produced mainly due to the combustion of fossil fuel for power generation (Knuutila et al., 2009). One of the most mature technologies for capturing CO_2 from industrial CO_2 emission sources (including fossil fuel fired power generation plant) is an absorption using reactive amine solvent (Mukherjee et al., 2019). This is because of its capability to handle a large volume of flue gas, regenerate the solvent, operate at reasonable cost, and remove over 90% of CO_2 (Tontiwachwuthikul et al., 2011; Wang et al., 2011).

Typical amines used for capturing CO_2 are primary monoethanolamine (MEA), secondary diethanolamine (DEA), tertiary triethanolamine (TEA), and sterically hindered primary 2-amino-2-methyl-1-propanol (AMP) (Chowdhury et al., 2013; Nwaoha et al., 2016). MEA has been industrially used as a benchmarking amine for capturing CO_2 because of its high reactivity with CO_2 and high mass transfer rate. However, the major drawbacks of MEA are limited absorption capacity and high regeneration heat duty (Shen and Li, 1992). Since conventional amine has its own advantages and disadvantages, the novel

promising amines should have lower regeneration heat duty, much higher absorption capacity and cyclic capacity, and faster absorption rate than the conventional amines (Singto et al., 2016; Wai et al., 2018). A utilization of high effective amine is one of the most important solutions to improve overall performance of CO_2 absorption. Recently, numbers of researchers are searching and developing novel amines that can perform better than the conventional amines (Sema et al., 2019; Xiao et al., 2017). It is reported that the novel cyclical tertiary amine, *N*-methyl-4-piperidinol (MPDL), shows great potential for capturing CO_2. MPDL possesses higher absorption capacity and lower regeneration heat duty comparing with conventional MEA. Even though MPDL performs much better than conventional MEA solvent, it cannot be used as a single solvent due to its major drawback of slow reaction with CO_2. To improve its overall reaction kinetics, MPDL should be blended with AMP because AMP has convincible reactivity with CO_2 (Chowdhury et al., 2011). Sema and co-workers reported that an addition of AMP into MPDL solvent can enhance the overall reaction kinetics of the AMP-MPDL solvent (Sema et al., 2020).

Regeneration heat duty (kJ/mol CO_2) is one of the most important performance indicating parameters for regeneration tower since over 70% of CO_2 capture operating cost is used for regenerating the solvent. Therefore, a reduction of the regeneration heat duty will greatly lead to a lower cost for capturing CO_2 (Nwaoha et al., 2017). The major goals of this study are to experimentally determine regeneration heat duty of novel AMP-MPDL solvent and to evaluate its potential for capturing CO_2 in terms of regeneration heat duty in comparison with the conventional MEA. In this study, the regeneration experiment was conducted in a regeneration reactor at total amine concentration of 30%wt. (blended ratios of 5/25, 10/20, and 15/15 %wt. AMP/MPDL) and regeneration temperature of 363 K.

2. Methodology

2.1 Chemicals and materials

AMP and MPDL with a purity of 98% were purchased from Sigma-Aldrich, Switzerland. MEA with a purity of 98% was obtained from Merck, Germany. Chemical structure of three amines used in this study are presented in Table 1. Standard solution of 1.0 M HCl was supplied by QRec, New Zealand. CO_2 and Nitrogen (N_2) with a purity of 99.5% were purchased from Thai-Japan Gas Co., Ltd, Thailand. The materials were used without any additional purification.

2.2 Operating concentrations and temperature

In this study, total amine concentration was fixed at 30% wt., which is a typical concentration used in the industry. The blended ratios were also varied at 5/25, 10/20, and 15/15 %wt. AMP/MPDL for 30%wt. total amine concentration. Regeneration heat duty was experimentally measured at 363 K, which is a regeneration temperature.

Table 1. Chemical structure of amines used in the present work.

Amine	CAS. No.	Molecular weight (g/mol)	Amine classification	Chemical structure
MEA	141-43-5	61.08	Primary amine	
AMP	124-68-5	89.14	Primary sterically hindered amine	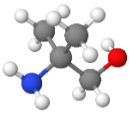
MPDL	106-52-5	115.17	Cyclical tertiary amine	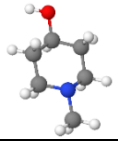

2.3 Regeneration heat duty

Regeneration heat duty (Q_{reg}, kJ/mol CO_2) composes of three heat components including heat of desorption (Q_{des}, kJ/mol CO_2), heat of vaporization (Q_{vap}, kJ/mol CO_2), and sensible heat (Q_{sen}, kJ/mol CO_2) as shown in Eq. (1) (Nwaoha et al., 2016; Nwaoha et al., 2017).

$$Q_{reg} = Q_{des} + Q_{vap} + Q_{sen} \quad (1)$$

Based on Eq. (1), heat of desorption (Q_{des}) of blended amine solvent is an amount of energy required for amine-CO_2 desorption reaction, which is equivalent to the heat of CO_2 absorption reaction (Nwaoha et al., 2017). Q_{des} can be calculated from a summation of mole fraction weighted of the heat of desorption of each amine component in blended amine solvent as shown in Eq. (2) (Wai et al., 2018).

$$Q_{des} = \sum \frac{C_i}{C_T} \Delta H_{des\_i} \quad (2)$$

Where Q_{des} is heat of desorption of blended amine solvent (kJ/mol CO_2), C_i is concentration of the i^{th} amine in blended amine solvent (kmol/m^3), C_T is total amine concentration in blended amine solvent (kmol/m^3), and ΔH_{des_i} is heat of desorption of the i^{th} amine in blended amine solvent (kJ/mol CO_2).

Heat of vaporization (Q_{vap}) of blended amine solvent is an amount of energy to evaporate liquid solvent during the regeneration process (Nwaoha et al., 2016). In this study, the experimental regeneration temperature is 363 K. At this temperature, it is assumed that only water was vaporized (no amine vaporization). Thus, Q_{vap} can be calculated from the amount of water in the blended amine solvent after the regeneration experiment as shown in Eqs. (3)-(5) (Nwaoha et al., 2017).

$$Q_{vap} = \Delta H_{vap\_H_2O} \frac{P_{H_2O}}{P_{CO_2}} \quad (3)$$

$$P_{H_2O} = (P^{sat}) x_{H_2O\_lean} \quad (4)$$

$$P_{CO_2} = 101.3 - P_{H_2O} \quad (5)$$

Where; Q_{vap} is heat of vaporization of blended amine solvent (kJ/mol CO_2), $\Delta H_{vap\_H_2O}$ is latent heat of water vaporization at 363 K (41 kJ/mol H_2O), P_{H_2O} and P_{CO_2} are partial pressures of water and CO_2, respectively (kPa), P^{sat} is saturation pressure of water at 363 K (kPa), and $x_{H_2O\_lean}$ is mole fraction of water in the CO_2 lean blended amine solvent.

Lastly, sensible heat (Q_{sen}) of blended amine solvent is an energy needed to raise temperature of the blended amine solvent (313 K) to the regeneration temperature (363 K) (Nwaoha et al., 2016). It can be calculated from the measured specific heat capacity (C_p) of blended amine solvent by differential scanning calorimeter (DSC) as presented in Eq. (6) (Nwaoha et al., 2017).

$$Q_{sen} = \frac{mC_p\Delta T}{[(\alpha_{CO_2\_rich} - \alpha_{CO_2\_lean})]mol_{amine}} \quad (6)$$

Where; Q_{sen} is sensible heat of blended amine solvent (kJ/mol CO_2), m is weight of amine solvent in the regeneration reactor (g), C_p is specific heat capacity of amine solvent (kJ/g·K), ΔT is temperature difference between absorption temperature (313 K) and regeneration temperature (363 K) (K), $\alpha_{CO_2\_rich}$ and $\alpha_{CO_2\_lean}$ are CO_2 loading of rich amine solvent and lean amine solvent, respectively (mol CO_2/mol amine), and mol_{amine} is mole amine in the solvent (mol amine).

It should be noted that C_p of blended amine solvent at various temperatures (293-363 K) was analyzed by differential scanning calorimeter or DSC (METTER TOLEDO DSC-822e) using C_p by sapphire (DIN 51007 standard test method). To confirm an accuracy and a reliability of the measurement of C_p, pure water and pure MEA were used to validate the measurement of C_p over a temperature range of 293-363 K. It was found that the measured C_p values were well corresponding with the literature data with %AADs of 6.15% and 5.35%, respectively (Chiu et al., 1999; Lee, 1994; Osborne et al., 1939). Thus, the experimental measurement of C_p is accurate and

reliable. Then, the experimentally obtained C_p can be used for determining Q_{sen} of amine solvent that required for elevating solvent temperature from 313 to 363 K was calculated from Eq. (6).

2.4 Solvent regeneration experiment

Experimental set-up for solvent regeneration is similar to that described by Nwaoha and colleagues (Nwaoha et al., 2017). To obtain the desired concentration of amine solvent at corresponding equilibrium CO_2 loading with 10.1 kPa partial pressure of CO_2 and 313 K (which was reported in our previous work of Apaiyakul et al. (2021a) and Apaiyakul et al. (2021b) was firstly prepared. 100 mL of the rich amine solvent was poured into the regeneration reactor, which was immersed in oil bath at temperature of 363 K and atmospheric pressure. Thermometer was immersed inside the regeneration reactor to confirm the regeneration temperature. As regeneration proceeds, 1 mL liquid sample was taken from the regeneration reactor for measuring total amine concentration and CO_2 loading (mol CO_2/mol amine) by acidification technique (Horwitz, 1975) every 10 min (for 80 min).

3. Results and Discussion

3.1 Compressive Strength Test result

Regeneration heat duty (Q_{reg}) of AMP-MPDL solvent was measured at various AMP/MPDL blended ratios of 5/25, 10/20, and 15/15 %wt. and temperature of 363 K in the regeneration reactor are presented in Figure 1 as a summation of three heat components (i.e., Q_{des}, Q_{vap}, and Q_{sen}). The results were reported in kJ/mol CO_2. According to Eq. (2), Q_{des} of 30%wt. AMP-MPDL was calculated. It was observed that Q_{des} increased as AMP/MPDL blended ratio increased as shown in Figure 1. This well corresponded with the fact that AMP has higher heat of desorption (ΔH_{des}) than MPDL (Nwaoha et al., 2017). As a result, Q_{des} of the blended solvent increased as AMP/MPDL blended ratio increased. Figure 1 shows that Q_{des} of AMP-MPDL solvent is lower than that of 30%wt. MEA. This is because ΔH_{des} of MPDL is lower than that of AMP and MEA, respectively (Nwaoha et al., 2017; Xiao et al., 2017).

Q_{vap} of AMP-MPDL solvent was determined based on solvent regeneration experiment (which can be calculated from Eqs. (3)-(5)) with a main assumption that only water in the blended solvent was vaporized. In this study, the total amine concentration of regenerated solvent was obtained from titrating with 1.0 M HCl standard solution. Then, $x_{H_2O\_lean}$ can be calculated from the regeneration experiment as shown in Table 2. As a result, Q_{vap} of AMP-MPDL solvent are presented in Figure 1. By considering the results at 5/25, 10/20, and 15/15 %wt. AMP-MPDL (30%wt.), it was observed that Q_{vap} was constant at 74.27 kJ/mol CO_2. Additionally, Q_{vap} of AMP-MPDL was slightly higher than that of 30%wt. MEA (as shown in Figure 1). It is because $x_{H_2O\_lean}$ of AMP-MPDL (i) were rarely changed for the three blended ratios and (ii) has higher water content than of 30%wt. MEA as can be seen in Table 2.

The last heat component, Q_{sen}, can be calculated from Eq. (6), which is associated with the experimentally measured solvent of C_p. Regarding the experimental data presented in Table 3. The results showed that C_p of AMP-MPDL solvent slightly increased as temperature increased, which was in good agreement with the literature data (Chiu et al., 1999; Lee, 1994; Osborne et al., 1939). It can also be seen that C_p of the blended solvent increased as AMP/MPDL blended ratio increased. As a result, the calculation of heat requirement for increasing 100 mL of the regenerated solvent was increased (shown in Table 2), which is a numerator of Eq. (6). According to the Q_{sen} calculation, a denominator of Eq. (6) represents mole of desorbed CO_2 (given in Table 2). It is well accepted that moles of desorbed CO_2 (or moles of CO_2 produced) increase as AMP/MPDL blended ratio increases. Even though, an increasing of AMP/MPDL blended ratio resulted in an increasing of heat requirement for raising the solvent temperature (because of an increasing of C_p), the mole of CO_2 produced was found to increase. The results showed that Q_{sen}

of AMP-MPDL solvent (i) decreased as AMP/MPDL blended ratio increased and (ii) was much lower than that of 30%wt. MEA as presented in Figure 1. This dues to the fact that C_p of 30%wt. MEA was higher than that of AMP-MPDL solvent (as shown in Table 3). Thus, the heat requirement for raising solvent temperature of 30%wt. MEA was higher than that of AMP-MPDL solvent. Additionally, tertiary MPDL and sterically hindered AMP can release CO_2 more easily than primary MEA (Nwaoha et al., 2017; Xiao et al., 2017). As a result, a much lower amount of CO_2 was desorbed from 30%wt. MEA compared with AMP-MPDL solvent as shown in Table 2. Lastly, cyclic capacity of AMP-MPDL solvent was much higher than that of 30%wt. MEA as reported by our previous study (Apaiyakul et al., 2021b).

As a summation of three heat components, Q_{reg} of AMP–MPDL solvent are presented in Figure 1. The main contribution on a reduction of Q_{reg} is Q_{sen}, which contributing of 54-61% of Q_{reg}, follows by Q_{vap} (22-24% of Q_{reg}) and Q_{des} (17-22% of Q_{reg}) for 30%wt. AMP-MPDL solvent. Therefore, it can be concluded that an increasing of AMP/MPDL blended ratio resulted in (i) a decreasing of Q_{sen}, (ii) an increasing of Q_{des}, and (iii) Q_{vap} remained unchanged. Thus, Q_{reg} was found to be reduced. In summary, Figure 1 also shows that Q_{reg} of 30%wt. AMP-MPDL was 60-63% lower than that of 30%wt. MEA and can be ranked as: 30 %wt. MEA>5/25 %wt. AMP/MPDL>10/20 %wt. AMP/MPDL>15/15 %wt. AMP/MPDL.

Table 2. Mole fraction of H_2O, heat requirement for increasing solvent temperature, and CO_2 produced of 30%wt. AMP-MPDL at various blended ratios.

Amine solvent	Total amine concentration	$x_{H_2O\_lean}$	Heat requirement for increasing solvent temperature (kJ)	CO_2 produced (mol CO_2)
30%wt. MEA	30%wt.	0.886	19.77	0.029
5/25%wt. AMP/MPDL	30%wt.	0.931	17.15	0.084
10/20%wt. AMP/MPDL		0.929	17.30	0.098
15/15%wt. AMP/MPDL		0.927	17.53	0.106

Table 3. Heat capacity of 30%wt. AMP–MPDL at various blended ratios and temperatures.

Temperature (K)	Heat capacity (J/g°C)			
	30 %wt. MEA	AMP/MPDL		
		30%wt.		
		5/25 %wt.	10/20 %wt.	15/15 %wt.
298	3.605	3.261	3.410	3.476
303	3.697	3.303	3.419	3.490
308	3.757	3.336	3.432	3.502
313	3.805	3.367	3.444	3.509
318	3.842	3.402	3.455	3.515
323	3.871	3.417	3.463	3.517
328	3.909	3.422	3.478	3.524
333	3.943	3.469	3.498	3.528
338	3.920	3.472	3.507	3.535
343	3.936	3.483	3.517	3.541
348	3.951	3.492	3.533	3.548
353	3.967	3.496	3.548	3.556
358	3.982	3.534	3.563	3.564
363	3.998	3.553	3.568	3.572

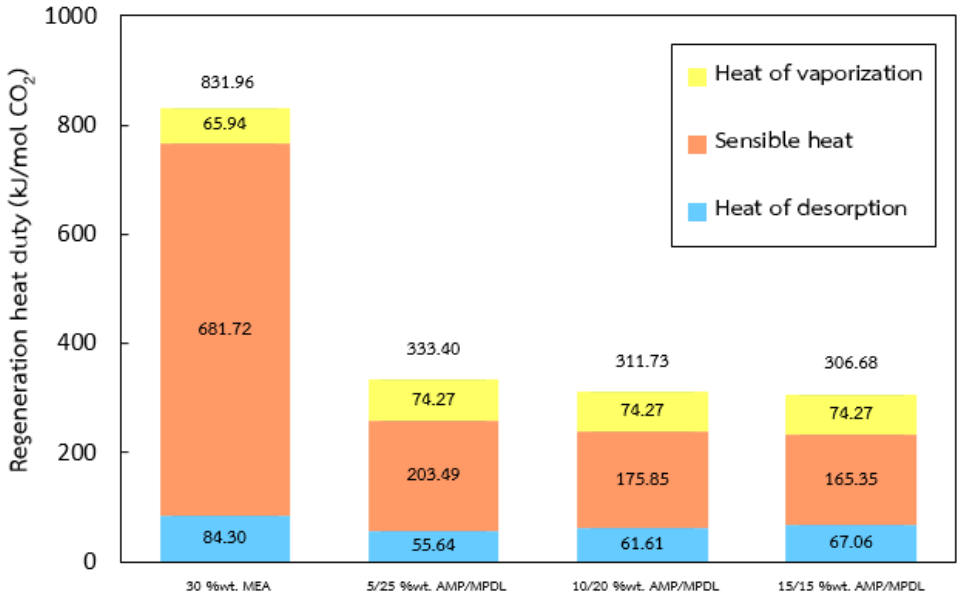

Figure 1: Regeneration heat duty of 30%wt. AMP-MPDL at various blended ratios.

3.2 Comprehensive perspective

This study is an extension of our previous works (Apaiyakul et al., 2021a; Apaiyakul et al., 2021b; Sema et al., 2020), which reported that AMP-MPDL solvent showed promising the absorption performance and can potentially be used in substitution of conventional 30%wt. MEA. In the previous works (Apaiyakul et al., 2021a; Apaiyakul et al., 2021b; Sema et al., 2020), 30%wt. AMP-MPDL (5/25, 10/20, and 15/15 %wt. AMP/MPDL) solvent was investigated. It was reported that CO_2 absorption capacity (at 313 K and 363 K), cyclic capacity, and absorption kinetics increased as AMP/MPDL blended ratio increased. The three blended AMP-MPDL solvents showed 39-48% higher CO_2 absorption capacity (at 313 K and CO_2 partial pressure 10.1 kPa) and 3.3-3.9 times larger cyclic capacity than those of 30%wt. MEA. Additionally, an elevation of AMP/MPDL blended ratio in the amine solvent resulted in an increasing of solvent absorption kinetics as reported by Sema and co-workers (Sema et al. 2020). However, the regeneration performance of AMP-MPDL solvent has not yet been reported in the open literature. Thus, the present work then focuses on the regeneration heat duty (Q_{reg}), which well represents the regeneration performance of the amine solvent. By comparing 30%wt. AMP-MPDL (5/25, 10/20, and 15/15 %wt. AMP-MPDL) and conventional 30%wt. MEA, it can be observed that the Q_{reg} of 30%wt. AMP-MPDL was 60-63% lower than that of MEA. Additionally, Q_{reg} of 30%wt. AMP-MPDL decreased as AMP/MPDL blended ratio increased. These indicate that an increasing of AMP/MPDL blended ratio is preferable. As a result, 15/15 %wt. AMP/MPDL solvent should be considered as the best concentration (within a range of studied concentration) in terms of CO_2 absorption capacity, cyclic capacity, absorption kinetics, and regeneration heat duty. Hence, 15/15 %wt. AMP/MPDL solvent shows a great potential to be used as an alternative solvent for capturing CO_2. However, its comprehensive investigation on mass transfer performance, solvent corrosiveness, and solvent stability should be further studied for an effectively utilization of this blended solvent.

4. Conclusions

Novel 30%wt. AMP-MPDL (5/25, 10/20, and 15/15 %wt. AMP/MPDL) solvent can be considered as an alternative promising solvent for capturing CO_2 in substitution of conventional 30%wt. MEA in terms of regeneration heat duty. An experiment of the regeneration heat duty determination was conducted at 363 K. The results showed that as AMP/MPDL blended

ratio increased, regeneration heat duty decreased, especially sensible heat. In comparison with a benchmarking 30%wt. MEA, 60-63% reduction of regeneration heat duty was observed for 30%wt. AMP-MPDL solvent. Based on these results, 15/15 %wt. AMP/MPDL solvent was suggested as a high potential alternative solvent. However, further investigation of AMP-MPDL solvent on the mass transfer, solvent corrosiveness and solvent stability should be conducted before being used as an alternative solvent for CO_2 capture application.

Acknowledgement

Fundamental Fund (FF) through Chulalongkorn University was gratefully acknowledged. This research was also supported by Grants for Development of New Faculty Staff, Ratchadaphiseksomphot Endowment Fund, Chulalongkorn University, Thailand.

References

Apaiyakul, R., et al.,. (2021a). CO_2 absorption capacity of novel AMP-MPDL solvent. 15th International Conference on Greenhouse Gas Control Technologies (GHGT-15), 1-6.

Apaiyakul, R., T. Sema, and R. Jiraratananon. (2021b). Carbon dioxide absorption capacity and cyclic capacity of novel AMP-MPDL solvent. In GNRU Conference 2021 (pp. 211-221). Kamphaeng Phet Rajabhat University.

Chiu, L.-F., H.-F. Liu, and M.H. Li. (1999, November). Heat capacity of alkanolamine aqueous solutions. Journal of Chemical and Engineering Data, 44, 1396-1401.

Chowdhury, F.A., et al.,. (2011). Synthesis and selection of hindered new amine absorbents for CO_2 capture. Energy Procedia, 4, 201-208.

Chowdhury, F.A., et al.,. (2013). CO_2 Capture by tertiary amine absorbents: A performance comparison study. Industrial and Engineering Chemistry Research, 52, 8323-8331.

Horwitz, W. (1975, April) Official methods of analysis of AOAC. Menasha, WI, USA: George Banta Co.

J.G.J, O. and P. J.A.H.W. (2020). Trends in global CO_2 and total greenhouse gas emissions: 2019 report. The Hague, the Netherlands: PBL Publishers.

Knuutila, H., H.F. Svendsen, and M. Anttila. (2009). CO_2 capture from coal-fired power plants based on sodium carbonate slurry; a systems feasibility and sensitivity study. International Journal of Greenhouse Gas Control, 3, 143-151.

Lee, L.L. (1994). Thermodynamic models for natural gas sweetening fluids: annual report to gas research institute. University of Oklahoma: Norman, OK.

Mukherjee, A., et al.,. (2019). Review of post-combustion carbon dioxide capture technologies using activated carbon. Journal of Environmental Sciences, 83, 46-63.

Nwaoha, C., et al.,. (2016). Carbon dioxide (CO_2) capture: Absorption-desorption capabilities of 2-amino-2-methyl-1-propanol (AMP), piperazine (PZ) and monoethanolamine (MEA) tri-solvent blends. Journal of Natural Gas Science and Engineering, 33, 742-750.

Nwaoha, C., et al.,. (2017). Heat duty, heat of absorption, sensible heat and heat of vaporization of 2-Amino-2-Methyl-1-Propanol (AMP), Piperazine (PZ) and Monoethanolamine (MEA) tri-solvent blend for carbon dioxide (CO_2) capture. Chemical Engineering Science, 170, 26-35.

Osborne, N.S., H.F. Stimson, and D.C. Ginnings. (1939, August). Measurements of heat capacity and heat of vaporization of water in the range 0ºC to 100ºC. Journal of Research of the National Bureau of Standards, 23, 197-260.

Sema, T., W. Khuenkaew, and O. Sirirathomsud. (2019). Kinetics of CO_2 absorption in novel tertiary *N*-methyl-4-piperidinol solvent. International Journal of Greenhouse Gas Control, 90.

Sema, T., et al.,. (2020). Absorption kinetics of CO_2 in novel formulated 2-amino-2-methyl-1-propanol and *N*-methyl-4-piperidinol solvent. Energy Reports, 6, 143-150.

Shen, K.P. and M.H. Li. (1992, January). Solubility of carbon dioxide in aqueous mixtures of monoethanolamine with methyldiethanolamine. Journal of Chemical and Engineering Data, 37, 96-100.

Singto, S., et al.,. (2016). Synthesis of new amines for enhanced carbon dioxide (CO_2) capture performance: The effect of chemical structure on equilibrium solubility, cyclic capacity, kinetics of absorption and regeneration, and heats of absorption and regeneration. Separation and Purification Technology, 167, 97-107.

Tontiwachwuthikul, P., et al.,. (2011). Recent progress and new development of post-combustion carbon-capture technology using reactive solvents. Carbon Management, 2(3), 261-263.

Wai, S.K., et al.,. (2018). Absorption heat, solubility, absorption and desorption rates, cyclic capacity, heat duty, and absorption kinetic modeling of AMP-DETA blend for post-combustion CO_2 capture. Separation and Purification Technology, 194, 89-95.

Wang, M., et al., (2011). Post-combustion CO_2 capture with chemical absorption: A state-of-the-art review. Chemical Engineering Research and Design, 89(9), 1609-1624.

Xiao, M., et al.,. (2017). A new model for correlation and prediction of equilibrium CO_2 solubility in *N*-methyl-4-piperidinol solvent. AIChE Journal, 63(8), 3395-3403.

Effects of Steam Activated Chars from Bamboo and Palm Kernel Shell on Biocrude Production from Bagasse by Hydrothermal Liquefaction

Natchanon Nilon[a,b] and Prapan Kuchonthara[a,b,c*]

[a]*Center of Excellence on Petrochemical and Materials Technology,Chulalongkorn University, Bangkok 10330, Thailand*
[b]*Department of Chemical Technology, Faculty of Science, Chulalongkorn University, Bangkok 10330, Thailand,*
[c]*Center of Excellence in Catalysis for Bioenergy and Renewable Chemicals (CBRC), and Department of Chemical Technology, Faculty of Science, Chulalongkorn University, Bangkok 10330, Thailand*

Abstract

Nowadays, the main sources of energy are natural gas and crude oil from the Earth's oil drilling process. Using the above materials produces a large amount of carbon dioxide (CO_2) and is the main factor contributing to global warming. Reducing CO_2 emissions can be achieved by the use of biomass as an energy source instead of drilling for oil. Hydrothermal liquefaction (HTL) is an interesting process that can convert biomass into liquid or biocrude products. Adding a catalyst into the process helps improve the quality and yield of liquid products from the HTL. Char could act as a catalyst in the process. The char is inexpensive and easily produced from biomass. Catalytic activity of char could be enhanced by the steam activation which increases the char porosity and surface area. In this research, the effects of steam- activated chars from palm kernel shell (PKS) and bamboo (BB) on biocrude yield and quality from bagasse (BA) by HTL were studied. The experiments were carried out in a high- pressure batch reactor at temperatures of 300-350°C with a reaction time of 60 min. Chars were activated by steam at a temperature range of 800-900°C with a reaction time of 120 min. The results indicated that the presence of either char or activated char in HTL process can improve yield of bio-crude oil. The best condition is BA+PKS at 300°C had yield of bio-crude oil 26.9 wt.%. In addition, when using activated char in the HTL process improve the quality of biocrude oil as higher heating value.

Keyword: Hydrothermal Liquefaction/ Activated carbon/ Biomass/ Biochar catalyst/ Steam activation

---

*Corresponding Author: Prapan Kuchonthara
E-mail address: prapan.k@chula.ac.th

1. Introduction

Currently, the main sources of energy are natural gas and crude oil from the earth's oil drilling process. Using the above materials produces a large amount of carbon dioxide (CO_2) and is the main factor contributing to global warming. Therefore, one of the best ways to reduce CO_2 emissions is the use of biomass as an energy source instead of drilling for oil. The resulting products can be used in a variety of applications such as fuel, heat, etc. and interested in liquefaction process, which provides the most liquid products, has many advantages over other forms of fuel. Thailand has a large amount of agricultural waste. One of them is bagasse. This research was thus interested in the conversion of bagasse to liquid fuel by hydrothermal liquidation (HTL). In such a thermochemical process, it is supposed that adding of a catalyst could improve the quality and yield of liquid products from the HTL. Char is one of carbonaceous materials that is a promising catalyst for the process because it is inexpensive and can be easily produced from biomass. Moreover, the activation of char can enhance its porosity and surface area, promoting the reactivity of char as the catalyst.

2. Methodology

2.1 Preparation of material

Bagasse was grinded and sieved to particle size in range of 150-250 μm and dried in oven at 60°C for 24 h before use.

Chars from palm kernel shell (PKS) and bamboo (BB) were ground and sieved to particle size in range of 2-5 mm after that washed with distilled water and dried at 105°C for 24 hours and stored in a desiccator.

2.2 Activation of char

Steam activation was employed to produce activated char. 30 g of char was placed in the fixed-bed reactor. The reactor was heated up to a desired temperature either 800°C or 900°C in a vertical heating furnace. The steam was fed from the bottom of the reactor. The activation reaction was held for 2 h. Afterward, the reactor was cooled down to room temperature. The activated carbon was washed with distilled water and was dried at temperature 105°C for 24 h.

2.3 Hydrothermal liquefaction

The hydrothermal liquefaction (HTL) was carried out in a 250-mL Parr reactor. 10 g of bagasse and 100 ml of distilled water was loaded in the reactor. The oxygen in the reactor was purged out with N_2 a couple time, afterward the reactor was pressurized to the initial pressure of 2 MPa with N_2. The reactor was stirred at the rotation speed of 300 rpm and then heated up to the reaction temperatures of either 300°C or 350°C. After the reactor was held that the given temperature for an hour, it was cooled down to around 35°C. Gas products was collected and the liquid-solid mixture was washed out by acetone. The liquid product was separated from the solid residue by the vacuum filtration. The solid product was dried at 110°C for 24 h and weighed for the yield calculation. The liquid phase was evaporated at 80°C under a reduced pressure of 400 mbar, stirring speed 30 rpm for 2 h in a rotary evaporator. The remaining was weight and defined as bio-crude.

2.4 Characterization techniques

2.4.1 Analysis of raw materials

Proximate analysis and ultimate analysis was performed using standard method and the CHN elemental analyzer, respectively. N_2 adsorption-desorption isotherms was used to determine the surface area of chars and activated chars. The mineral matter was also analyzed using X-Ray Fluorescence Spectrometer (XRF).

2.4.2 Products analysis

All yields were determined on a dry ash-free basis. The HHV (Higher heating value) of bio-oil and solid residue as well as the raw material were determined based on the Dulong correlation.

3. Results and Discussion

3.1 Characterization of raw materials

The proximate analysis of bagasse and different types of char, including bamboo char (BB), palm kernel shell char (PKS) is shown in Table 1. Bagasse as the raw biomass has high portion of volatile matter, while both types of char have high fixed carbon content and low ash. The volatile in the raw biomass is typically reduced during the carbonization for char production. Furthermore, during the decomposition char is structured into a disordered crystal structure, along with the breakdown of the structure in volatile matter or tar to cover the surface or pores.

Table 1. Proximate analysis of feedstock

Feedstock	Moisture	Ash	Volatile	Fixed carbon
Bagasse (BA)	8.33	3.99	76.63	11.05
Palm kernel shell (PKS)	2.11	3.74	44.7	49.46
Bamboo (BB)	1.32	6.26	24.74	67.68

Table 2 shows the ultimate analysis of bagasse and different types of chars, BB and PKS. Both types of char contain the most carbon elements followed by oxygen, hydrogen, and nitrogen, respectively. Decomposition during carbonization causes a fragmentation of organic compounds to carbon dioxide (CO_2), methane (CH_4) as well as other small compounds. In addition, tar and volatile matter were removed. As a result, higher carbon but lower oxygen contents were found in biomass-derived chars. (Yek et al., 2019).

Table 2. Ultimate analysis of feedstock

Feedstock	C	H	N	S	O
BA	41.850	6.105	0.700	2.850	48.500
PKS	65.200	4.540	0.6100	1.100	28.550
BB	76.230	3.380	0.670	0.820	18.910

Table 3 show the surface area of biochar and steam activated char. The steam activated bamboo char (SABB) at 800°C and 900°C have surface area of 432.66 m^2/g and 534.49 m^2/g, respectively. Steam activated palm kernel shell char (SAPKS) at 800°C and 900°C have surface area of 617.78 m^2/g and 833.34 m^2/g respectively. It was clear that the steam activation can significantly increase porosity and surface area of biomass-derived char. In addition, it was observed that the surface area was increased with increasing activation temperature.

Table 3. Surface area of biochar and steam activated char at different temperature.

Biochar	Temp (°C)	Surface area (m^2/g)
BB	25	2.28
SABB_800	800	432.66
SABB_900	900	534.49
PKS	25	141.07
SAPKS_800	800	617.78
SAPKS_900	900	833.34

It was found that palm kernel shell char (PKS) has Fe_2O_3 and K_2O higher than bamboo char (BB) as shown in Table 4. Moreover, steam activated palm kernel shell char (SAPKS) and steam activated bamboo char (SABB) had higher contents of Fe_2O_3 and K_2O compared with PKS and BB.

3.2 Characterization of Products

The HTL of bagasse (BA) mixed with palm kernel shell char (PKS) (BA+PKS) and BA mixed with steam activated palm kernel shell char at 800°C (SAPKS (800)) (BA+SAPKS (800)) was carried out at the reaction temperature of 300°C. The weight ratio of 1:1 was employed for the mixing between biomass and char or activated char. The yield of bio-crude from BA+PKS and BA+SAPKS (800) were 26.9 wt% and 15.6 wt%, respectively, as can be seen in Figure 1. When comparing the values obtained from the experiment and the predicted values which is determined from the weight-average value. This indicated that there is interaction between bagasse and PKS char during the HTL. The PKS char could play a catalytic role in depolymerization. This results in greater thermal depolymerization and may lead to greater bio-crude yield. Moreover, it was found that the bio-crude yield from BA+SAPKS (800) was lower than the predicted value. Due to the amount of Fe_2O_3 of SAPKS was higher than PKS from Table 4. For this reason, Fe_2O_3 compounds was dehydrogenation catalysts, decarboxylation, and carbonization. Hence, the further thermal decomposition of bio-crude was supposed to take place, resulting in the decrease in yield of bio-crude.

Table 4. Element of char and activated char

Feedstock	Fe_2O_3	K_2O
PKS	16.2	19.8
SAPKS	18.9	20.1
BB	12.3	15.7
SABB	15.4	18.5

Figure 2 illustrates the yield of bio-crude from BA+BB and BA+SABB (800). The result was similar to that obtained in case of BA+PKS or SAPKS. The yield were 27.7% and 18.6% for BA+BB and BA+SABB (800), respectively. It indicated that the BB or SABB could play the same role during the HTL with BA.

It was deduced from Table 5 that the contents of carbon in the bio-crude increased and oxygen decreased with the presence of either char or activated char. Char can promote deoxygenation in liquid and the quantity of oxygen in liquid was reduced. If the oxygen content decreases, the oil quality was improved in terms of heating value.

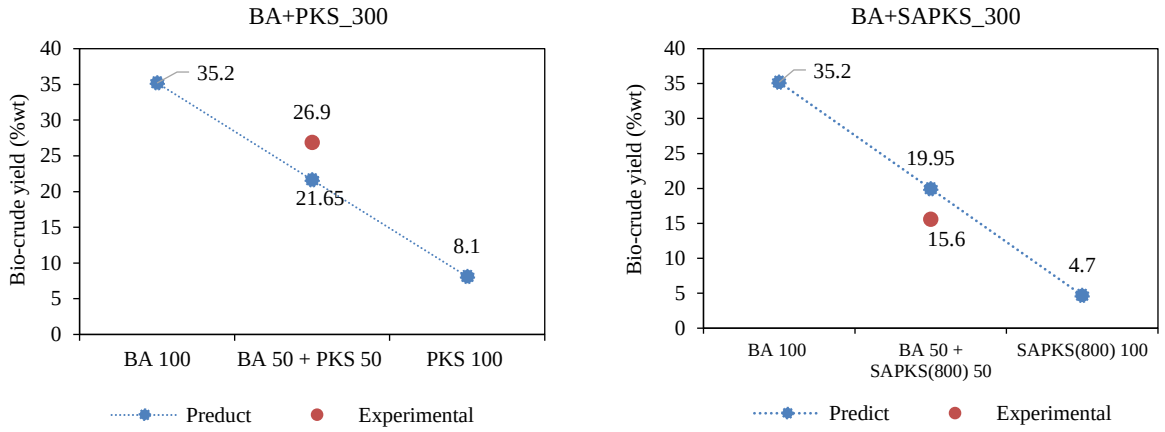

Figure 1. Bio-crude yield from HTL of (a) BA+PKS and (b) BA+SAPKS (800) at temperature of 300°C

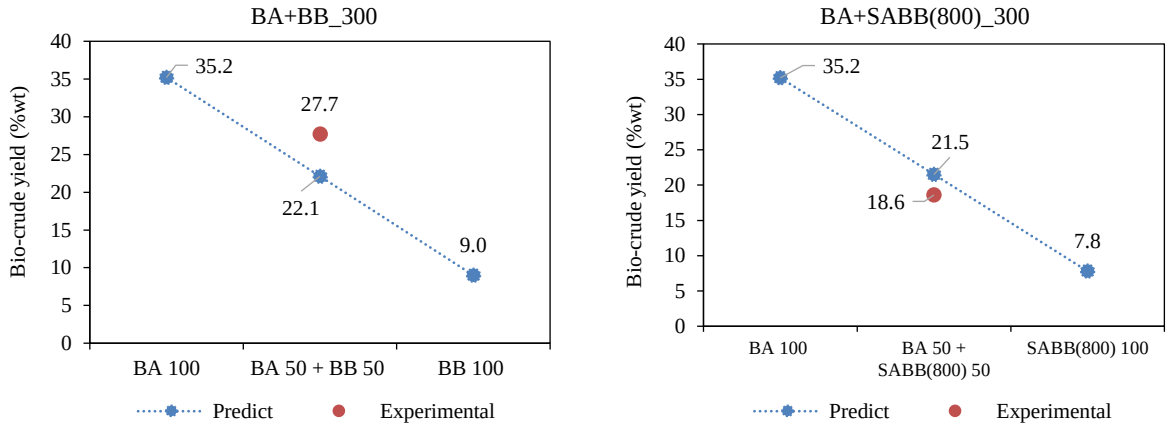

Figure 2. Bio-crude yield from HTL of (a) BA+BB and (b) BA+SABB (800) at temperature of 300°C

Table 5. Element of bio-crude oil

Bio-crude oil	C	H	N	S	O
BA_300	59.58	5.74	1.13	0.655	32.895
BA+PKS_300	60.87	6.495	1.045	0.695	30.895
BA+SAPKS (800)_300	66.29	6.945	2.605	0.73	23.43
BA+BB_300	34.935	4.32	0.95	0.905	58.89
BA+SABB(800)_300	55.675	6.62	1.83	1.11	34.765

4. Conclusions

Palm kernel shell (PKS) and Bamboo (BB) char had the high constants fixed carbon content and low ash. The surface area of PKS and BB char was obviously increased by steam activation. The higher temperature in the activation could contribute to the larger surface area. Yield and quality of bio-crude oil was found to be improved when char/activated char was employed in HTL. The optimum condition was BA+PKS at 300°C have yield of bio-crude oil 26.9% wt.

Acknowledgement

This project is funded by Department of Chemical Technology, Faculty of Science, Chulalongkorn University.

References

J. Chen, Bio-oil production from hydrothermal liquefaction of *Pteris vittata L.*: Effects of operating temperatures and energy recovery, Bioresource Technology, vol. 265, p. 320-327, 2018.

L. Nazari, Z. Yuan, S. Souzanchi, M. B. Ray, and C. Xu, Hydrothermal liquefaction of woody biomass in hot-

compressed water: Catalyst screening and comprehensive characterization of bio-crude oils, Fuel, vol. 162, p. 74-83, 2015.

L. Yang, Q. He, P. Havard, K. Corscadden, C. Xu, and X. Wang, Co-liquefaction of spent

coffee grounds and lignocellulosic feedstocks, Bioresource Technology, vol. 237, p. 108-121, 2017.

T. Muppaneni, Hydrothermal liquefaction of *Cyanidioschyzon merolae* and the influence of catalysts on products, Bioresource Technology, vol. 223, p. 91-97, 2017.

W. Chen, K. Li, M. Xia, Catalytic deoxygenation co-pyrolysis of bamboo wastes and microalgae with biochar catalyst, Energy, vol 157, p. 472-482, 2018.

Y. Rae, Preparation and characterization of mesoporous activated carbons from nonporous hard carbon *via* enhanced steam activation strategy, Materials Chemistry and Physics, vol 242, p. 256-267, 2018.

Y. Fu, Activated bio-chars derived from rice husk via one- and two-step KOH-catalyzed pyrolysis for phenol adsorption, Science of the Total Environment, vol. 646, p. 1567-1577, 2019.

Yek, P.N.Y., et al., Microwave steam activation, an innovative pyrolysis approach to convert waste palm shell into highly microporous activated carbon, Journal of Environmental Management, 2019. 236: p. 245-253.

Indoor Air Quality in Public Health Centers: A Case Study of Public Health Centers Located on Main and Secondary Roadside, Bangkok

Natlada Boonphikham, Chatchawal Singhakant*, Suwimon Kanchanasuta, Withida Patthanaissaranukool, and Tawach Prechthai

Department of Environmental Health Sciences, Faculty of Public Health, Mahidol University, Thailand

Abstract

Public health center (PHC) had role and responsibility to provide health services cover the primary health care needs of the local people in Bangkok. Currently, there were 69 PHCs distributed in 50 district areas in Bangkok to support the convenient health service and reduce the crowded patients in hospitals. Therefore, indoor air quality(IAQ) was an important issue in order to protect health risk in the personals and the sensitive patients. This cross-sectional study aimed to investigate the IAQ of PHCs located on the main and secondary roadside in Bangkok. Three air pollutants; $PM_{2.5,}$ CO_2, and CO were measured in 3 sampling areas (Medical records department (MRD), Outpatient department (OPD), and Examination room (EXR)) of total 6 PHCs located on 2 different locations (Main roadside and secondary roadside). The results showed that the average levels of $PM_{2.5}$, CO_2, and CO in the PHCs located on main roadside (10.4±5.1 μg/m^3, 777.0±290.1 ppm, and 2.5±1.4 ppm, respectively) were higher than those located on secondary roadside (9.0±3.0 μg/m^3, 668.4±119.4 ppm, and 1.6±0.8 ppm, respectively). Among these parameters, only CO was a parameter that found significant different between the PHCs on 2 locations indicating the result of vehicles and traffic source toward the indoor CO level. Furthermore, all the parameters were compared among the sampling areas with different ventilations; natural ventilation, air conditioner without ventilation fan, and air conditioner with ventilation fan. The results showed that the average levels of $PM_{2.5}$ and CO_2 were found the highest in sampling area with air conditioner without ventilation fan (10.5±4.7 μg/m^3 and 793.1±253.6 ppm, respectively), while the level of CO was found the highest in area with natural ventilation(2.5±0.9 ppm). However, all the measured levels of $PM_{2.5,}$ CO_2, and CO in all sampling areas were found below the recommended values in the related standards, indicating the safe IAQ for people who are working and getting service in PHCs.

Keyword: Indoor air quality/ Public health centers/ Carbon monoxide (CO)/ Carbon dioxide (CO_2)/ Particulate matter of less than 2.5 μm diameter ($PM_{2.5}$)

---

*Corresponding Author: Chatchawal Singhakant, Tel: 0-2354-8525; Fax: 0-2354-8525
E-mail address: chatchawal.sin@mahidol.ac.th

1. Introduction

Indoor air quality (IAQ) was one of the environmental risks on the people's health, it could affect to their health, comfort, and well-being when they lives in a building (Luksamijarulkul et al., 2018). Nowadays, most people always spend more than 90% of their times for various activities in indoor environment such as in office, school, and in their home (Giulio et al., 2010). Thus, the IAQ became an important environment especially in workplaces. The poor IAQ could lead to discomfort and sickness, and result in work performance drop and absenteeism problems in the workplace (Environmental Protection Department, 2019). Some equipment in building such as heater, ventilation system, and air conditioner, could cause higher accumulation of the air pollutants resulting in the low IAQ (Brickus et al., 1998).

Public Health Center (PHC) had role and responsibility to provide health services cover the primary health care needs of the local people in Bangkok. Currently, there were 69 public health centers distributed in 50 district areas in Bangkok to support the convenient health service and reduce the crowded patients in hospitals. In 2019, the average patients per month had been reported at about 2,423 people (~80 people per day) depending on the service area of each center (Health Department Bangkok Metropolitan Administration, 2020). Moreover,

PHC was a workplace which had a strict requirement about the IAQ due to these places had patients with communicable diseases who could spread pathogen via air transmission, and also these places always had to use disinfectants inside the building (Hellgren et al., 2008). Thus, control of the IAQ was an important role in order to prevent the spread of infectious diseases and protect the hospital personals and the sensitive patients (Leung et al., 2006).

The location of the PHC was an important factor for patients to receive services, especially, the PHCs in midtown which located on main roadside, easy to approach, and always had many people come to get services. However, the location was related to the potential sources of pollutants such as busy roads, which could affect the IAQ (Karner et al., 2010). Some previous study reported that people who live, work, or attend school near the major roads appeared to be more at risk for a variety of short- and long-term health effects (Mullen et al., 2011). In Bangkok, the major sources of air pollution were the large number of vehicles, the construction of buildings and sky train, and the open burning especially grilled food cooking. Vehicle was indicated to be a main cause of air pollution problems in 2018, it generated high concentrations of pollutants including black smoke, nitrogen dioxide (NO_2), ozone gas (O_3), particulate matter with a diameter of 2.5 micrometers or less ($PM_{2.5}$) and particulate matter with a diameter of 10 micrometers or less (PM_{10}) which was problem in area around the roadside (PCD, 2020).

Previous research of the IAQ in 9 Advance-level hospitals from 11 provinces in 2014 revealed that the air quality parameters in the examination rooms from all hospitals which exceeded the maximum permissible levels were including CO_2 (15.59%), relative humidity (43.48%), temperature (87.68%), $PM_{2.5}$ (1.70%), formaldehyde (19.51%), bacteria (50.00%), and mold (25.75%) (Chokwinyou et al., 2014). Consequently, the result from a research that had measured IAQ in Thailand, it could be concluded that the most problematic parameters were temperature, relative humidity and dust (PM_{10}, $PM_{2.5}$) due to the activities of building users and insufficient ventilation (Bureau of Occupational and Environmental Diseases (BOED), 2018). In addition Environmental Sanitation Office, Bangkok Metropolitan Administration had conducted a survey to measure air quality in 27 buildings of the PHCs in 2019 and found that some IAQ parameters in waiting room, OPD, and nursing laboratory of several PHCs were above the maximum permissible levels including; $PM_{2.5}$ (18.52% of total survey), PM_{10} (16.05% of total survey), and CO_2 (12.35% of total survey) which exceeded the Singapore recommended values of less than 35 $\mu g/m^3$, 50 $\mu g/m^3$ and less than 1,000 ppm, respectively (Health Department BMA, 2020).

This study was conducted to reveal the IAQ of PHCs (including 3 main parameters; $PM_{2.5}$, CO_2, and CO) which located in different location (on the main roadside and secondary roadside). Comparisons of the results among different indoor area were also conducted to reveal effect on IAQ from ventilation. The results can provide information to set up guideline or suggestion to improve the IAQ minimizing the health risk of the patient and staffs in the PHCs.

2. Methodology

2.1 Study area

This cross-sectional study was conducted in 6 from total 69 PHCs in Bangkok during May to July, 2021. These 6 sampling sites were selected from purposive sampling method and dividing into 2 groups; 3 PHCs (PHC_A, PHC_B, and PHC_C) located on main roadside, and other 3 PHCs (PHC_D, PHC_E, and PHC_F) located on secondary roadside (small street with 2 lanes) (Figure 1).

2.2 Data collection

In each PHCs, the samples were collected at 3 different areas including medical records department (MRD), outpatient department (OPD), and examination room (EXR) which had different activities, number of people, and ventilation. Each sampling point was collected at 2 different service time intervals; 8.00-11.30 am and 12.30-16.00 pm, the triplicate samples were collected from 3 different weekdays; Monday, Thursday, and Friday. Each time of sampling, total 3 main parameters were

collected including $PM_{2.5}$, CO_2, and CO, and ventilation in the area was also recorded during sampling. The sample sizes were 108 samples per parameter.

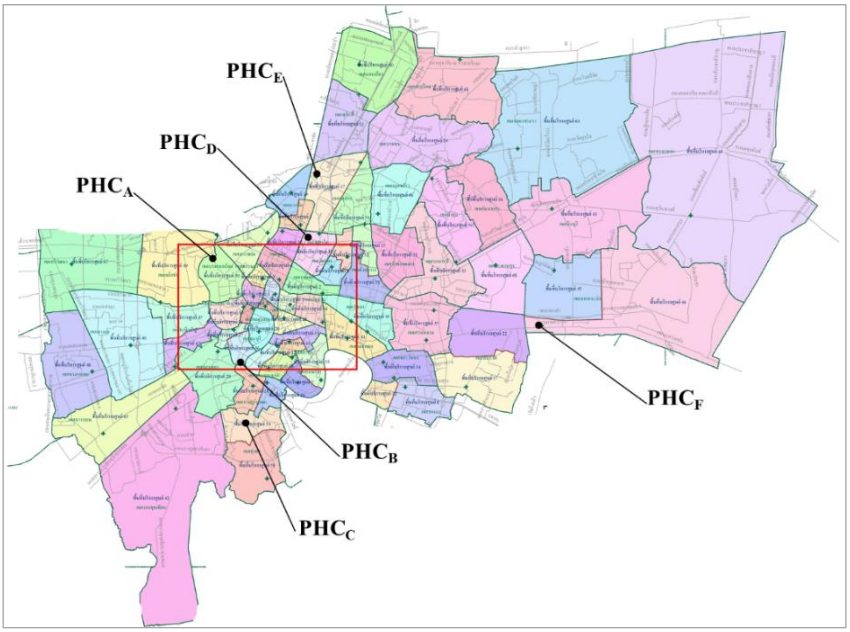

Figure 1. Sampling sites

2.3 Indoor air quality measurement

The level of $PM_{2.5}$ was determined by a particle measurement instrument (DustTrak™ II Aerosol Monitor 8530). The instrument was real-time aerosol mass readings with gravimetric sampling and zero calibration was performed with the Zero (HEPA) filter, before starting the sampling. The measurement range was 0.001 to 400 mg/m^{3}and particle size range approximately 0.1 to 10 µm. Meanwhile, the CO and CO_2 were measured using an indoor air quality meter (HD37AB1347). The measurement range was 0 to 5,000 ppm for CO_2 and 0 to 500 ppm for CO. Both instruments were calibrated before initiation of this study. Each measurement, the instruments were placed at the breathing zone with a height of 90 to 100 cm above the floor and in the middle of the room.

2.4 Statistical analysis

Descriptive statistics were used to illustrate the PHC characteristics. The normal distribution of the results was checked by the Kolmogorov-Smirnov test, it was assumed that each sample was drawn from a non-normal distribution. The results obtained for IAQ parameters ($PM_{2.5}$, CO_2, and CO) were compared by Mann-Whitney U test for different location (main and secondary roadside). Kruskal-Wallis Test was used to compare the results of all measurement between different ventilations (natural ventilation, air conditioner without ventilation fan, and air conditioner with ventilation fan).The critical level for statistical significance was used as $p<0.05$ and all data were analyzed using SPSS 18.0.

3. Results

3.1 Ventilation of the sampling areas in PHCs

In the selected PHCs, all the buildings were old with the age up to 30 years. The sampling areas had different ventilations during sampling although they were the same type of sampling area; MRD, OPD, or EXR. Most of them had air conditioner (83.3%) but some area in some PHCs had natural ventilation via window and door (16.7%). Ventilation of the sampling area could be divided into 3 types; natural ventilation, air conditioner without ventilation fan, and air conditioner with ventilation fan as shown in Table 1.

Table 1. Ventilation of the area during sampling (N=108)

Types of ventilation	Sampling Areas			Total (%)
	MRD	OPD	EXR	
Natural ventilation	0	7	11	18 (16.7%)
Air conditioner without ventilation fan	31	14	22	67 (62.0%)
Air conditioner with ventilation fan	5	15	3	23 (21.3%)
Total	36	36	36	108 (100%)

3.2 Comparison of IAQ between groups of PHCs with different locations

The IAQ in 2 groups of PHCs, located on main roadside and on secondary roadside, were compared to investigate the effect between those locations on IAQ in PHCs. The $PM_{2.5}$ in group of PHCs on the main roadside were found in range of 1-34 μg/m^3 with the average of 10.4±5.1 μg/m^3 higher than those in group of the PHCs on the secondary roadside with range of 5-20 μg/m^3 with the average of 9.0±3.0 μg/m^3. The CO_2 in group of PHCs on the main roadside were found in range of 421-1,708 ppm with the average of 777.0±290.1 ppm higher than those in group of the PHCs on the secondary roadside with range of 461-1,181 ppm with the average of 668.4±119.4 ppm. While the CO in group of PHCs on the main roadside were found in range of 0.1-5.1 ppm with the average of 2.5±1.4 ppm higher than those in group of the PHCs on the secondary roadside with range of 0.6-4.9 ppm and the average of 1.6±0.8 ppm. The comparison of all IAQ parameters in PHCs between the group located on the main roadside and on secondary roadside was shown in Table 2, only the CO was found significant different between these 2 groups ($p<0.001$).

Table 2. Comparison of IAQ parameters in PHCs between the groups located on the main roadside and on secondary roadside

IAQ Parameters	Location of PHCs		p-value
	Main roadside, (n=54)	Secondary roadside, (n=54)	
$PM_{2.5}$ (μg/m^3)	10.4±5.1	9.0±3.0	0.12
CO_2 (ppm)	777.0±290.1	668.4±119.4	0.13
CO (ppm)	2.5±1.4	1.6±0.8	<0.001*

*: Mann-Whitney U test

3.3 *Comparison of IAQ among the sampling area with different ventilation*

In order to investigate the effect of the ventilation on the IAQ, the results of $PM_{2.5}$, CO_2, and CO measurement in each sampling area among 3 different ventilations were compared. For the $PM_{2.5}$, the highest average level was found in area with air conditioner without ventilation (10.5±4.7 μg/m^3), following by natural ventilation (9.4±3.3 μg/m^3) and air conditioner with ventilation fan (7.7±2.6 μg/m^3), respectively. While the CO_2 was found the highest average level in area with air conditioner without ventilation fan (793.1±253.6 ppm), following by air conditioner with ventilation fan (662.0±94.8 ppm) and natural ventilation (538.3±62.0 ppm), respectively. Finally, the CO, it was found the highest average level in area with natural ventilation (2.5±0.9 ppm), following by air conditioner without ventilation fan (2.2±1.4 ppm) and air conditioner with ventilation fan (1.2±0.6 ppm), respectively. The comparison of IAQ parameters among the sampling area in PHCs with different ventilations was shown in Table 3, all the parameters in the area with different ventilation were found significantly different.

Table 3. Comparison of IAQ parameters among the sampling area in PHCs with different ventilation

IAQ parameters	Types of ventilation			p-value
	Natural ventilation, (n=18)	Air conditioner without ventilation fan, (n=67)	Air conditioner with ventilation fan, (n=23)	
$PM_{2.5}$ (µg/m^3)	9.4±3.3	10.5±4.7	7.7±2.6	0.034*
CO_2 (ppm)	538.3±62.0	793.1±253.6	662.0±94.8	<0.001*
CO (ppm)	2.5±0.9	2.2±1.4	1.2±0.6	0.001*

*: Kruskal- Wallis Test

4. Discussion

This cross-sectional study was a short-term assessment of IAQ in PHCs which had compared the IAQ parameters among the group of PHCs with different locations and the sampling areas with different ventilations to determine the effect of the locations and ventilations. As the results showed that the average levels of $PM_{2.5}$, CO_2, and CO in the PHCs located on main roadside were higher than those located on secondary roadside which proved that these different locations had some effect on the IAQ in PHCs (Table 2). However, only the CO was found significant different between these 2 groups ($p<0.001$), the CO in PHCs on the main roadside was higher due to the higher traffic volume which was the main source of CO from the road. Babayiğit et al. (2012) reported a case study of IAQ at primary schools in Turkey that the higher level of CO in the schools located on a main street and close to heavy traffic which significantly different from the level in the schools far from heavy traffic. While, Chamseddine et al. (2019) studied the indoor CO level from 3 hospitals in Beirut, Lebanon and found that the CO level at the lower floor was slightly higher than those at the upper floor which was primarily from the result of outdoor vehicle induced emission.

In comparison of the IAQ among the sampling areas with different ventilations (Table 3), the results of all $PM_{2.5}$, CO_2, and CO were found significantly different in each area with different ventilations indicating effect of ventilations on these indoor pollutants. For the $PM_{2.5}$, the highest average level (10.5±4.7 µg/m^3) was found in area with air conditioner without ventilation fan, it was due to the accumulation of the fine particles from outdoor sources such as diesel vehicles which no or less ventilation to the outside. Lomboy et al. (2015) studied the characterization of $PM_{2.5}$ in an urban tertiary care hospital in the Philippines and found that the level of $PM_{2.5}$ in the mechanically ventilated wards were predominantly affected by the air conditioning system, human activities, and the infiltration of contaminated outdoor air. Furthermore, a case study in Bangkok about the relationship between indoor and outdoor $PM_{2.5}$ concentrations in different conditions (open and closed ventilation systems) reported the $PM_{2.5}$ concentrations in the closed ventilation area each place in term of Indoor/Ambient ratio (I/A ratio) were in range of 0.37 to 3.57, indicating that the outdoor $PM_{2.5}$ can enter the buildings through ventilation system and infiltration (Sompornratanaphan et al., 2018). In addition, this highest average level of $PM_{2.5}$ at 10.5±4.7 µg/m^3 was still below 15 µg/m^3 (24-hour) following the new WHO air quality guidelines (WHO, 2021) indicating the safety for people health from $PM_{2.5}$ inside the PHC building.

For the CO_2, the highest average level (793.1±253.6 ppm) was found in the area with air condition without ventilation fan. There were high levels of CO_2 detected in some areas, the maximum level at 1,708 ppm, which were higher than 1,000 ppm indicating the inadequate ventilation in the building (NIOSH, 1987). It was due to the source of indoor CO_2, was from people inside the building, both patients and staffs, and under inadequate ventilation of the area resulting in indoor CO_2 accumulation. A previous study of the indoor CO_2 in a hospital in Naijing, China, found that the cause of indoor CO_2 level related to the patient habit in order to maintain thermal comfort including close-open the windows or doors andturning air-conditioner on-off. The increasing indoor CO_2 level was from the close room which the indoor air could

not be diluted by the fresh air from outside (Zhou et al., 2015). Similarly, Argunhan and Avci (2018) evaluated IAQ of the university's classrooms in Turkey and found that the increased CO_2 levels were associated with number of people in the area together with the doors and windows closing. While, Zuraimi et al. (2007) studied the effect of ventilation strategies of child care centers on IAQ in Singapore and found that the ventilation rate of the air conditioner was significantly lower than those of the natural ventilation resulting in the higher levels of occupant-related pollutant as CO_2. In addition, this highest average level of CO_2 at 793.1±253.6 ppm was still below the threshold limit value of 5,000 ppm as the American Conference of Governmental Industrial Hygienists (ACGIH) standard (ACGIH, 2013) indicating the safety for people health from CO_2 inside the PHC_s building.

For the CO, it was found the highest average level (2.5±0.9 ppm) in area with natural ventilation which was due to the IAQ were affected by the outdoor source. Mendes et al. (2013) studied the IAQ in elderly care centers in Portugal and found that maximum CO level in the room with an open window next to a heavy traffic road. Similarly, Synnefa et al. (2003) investigated the IAQ in fifteen school buildings in Athens, Greece and found that the CO level in several classrooms higher than the recommended limits which due to insufficient natural ventilation and lack of mechanical ventilation. However, the highest average level of CO at 2.5±0.9 ppm was still below 4 ppm (24-hours) following the new WHO air quality guidelines (WHO, 2021) indicating the safety for people health from CO inside the PHC building.

Finally, overview of the results in Table 3 revealed that the better ventilation could provide the better IAQ by reducing the indoor air pollutants. The area with air conditioner with ventilation fan had the lower level of all $PM_{2.5}$, CO_2, and CO. Thus the ventilation fan opening in the room under air conditioner should be done to reduce the health risk from indoor air pollutants.

5. Conclusions

The safety for health of staffs and patients from indoor air pollutants during working and getting service in PHCs was ensured by the results in this study. Although, these results showed that the average levels of $PM_{2.5}$, CO_2, and CO at the PHCs located on main roadside were higher than those located on secondary roadside, only CO was found significantly different between both locations however it could indicate the increasing indoor air pollutant from the outdoor sources, especially, the CO from vehicles and traffic source.

The average levels of $PM_{2.5}$, CO_2, and CO in the areas with different ventilations were found different indicating the effect of ventilation on the indoor air pollutants. The ventilation was proved to be a key measure to improve IAQ. For this reason, the PHCs should consider the ventilation efficacy to improve the IAQ including the window opening to dilute indoor pollutants before providing the service and using ventilation fan in the room under air conditioner during service time. These measures should be done to reduce the health risk from indoor air pollutants which could be a suggestion for PHCs to perform routinely.

Acknowledgement

The authors gratefully acknowledge the support provided by the Health Department, Bangkok Metropolitan Administration for their support to the measured and instruments for measurements from Department of Environmental Health Sciences, Faculty of Public Health, Mahidol University.

References

American Conference of Governmental Industrial Hygienists (ACGIH). TLVs and BEIs. Cincinnati: ACGIH; 2016.

Argunhan Z, Avci AS. Statistical evaluation of indoor air quality parameters in classrooms of a university. Advances in Meteorology 2018; 2018:1-10.

Babayiğit MA, Bakir B, TEKBAŞ ÖF, Oğur R, Kilic A, Ulus S. Indoor air quality in primary schools in Keçiören, Ankara. Turkish journal of medical sciences 2014; 44(1):137-44.

Brickus LS, Cardoso JN, Aquino Neto FR. Distributions of indoor and outdoor air pollutants in Rio de Janeiro, Brazil: implications to indoor air quality in bayside

offices. Environmental science & technology 1998; 32(22):3485-90.

Bureau of Occupational and Environmental Diseases (BOED). Guide to measuring indoor air quality for Entrance and exit channels. 1st ed. Bangkok: Aksorn graphic and design Bangkok; 2018. p. 9-10.

Chamseddine A, Alameddine I, Hatzopoulou M, El-Fadel M. Seasonal variation of air quality in hospitals with indoor–outdoor correlations. Building and Environment 2019; 148:689-700.

Chokwinyou P, Pensuk C, Paweenkitiporn W. Indoor air quality in hospitals and hotels, Thailand. Environmental Health Journal2014; 16:51-66.

Di Giulio M, Grande R, Di Campli E, Di Bartolomeo S, Cellini L. Indoor air quality in university environments. Environmental monitoring and assessment 2010; 170(1): 509-17.

Environmental Protection Department. Guidance Notes for the Management of Indoor Air Quality in Offices and Public Places. [Internet]. 2019 [cited 2021 Sep 11]. Available from: https://www.iaq.gov.hk/media/82253/gn_officeandpublicplace_eng-2019.pdf.

Hellgren UM, Palomaki E, Lahtinen M, Riuttala H, Reijula K. Complaints and symptoms among hospital staff in relation to indoor air and the condition and need for repairs in hospital buildings. Scandinavian Journal of Work Environment and Health 2008; 34(4): 58-63.

Karner AA, Eisinger DS, Niemeier DA. Near-roadway air quality: synthesizing the findings from real-world data. Environmental science & technology 2010; 44(14): 5334-44.

Leung M, Chan AH. Control and management of hospital indoor air quality. Medical science monitor 2006; 12(3): 17-23.

Lomboy MFTC, Quirit LL, Molina VB, Dalmacion GV, Schwartz JD, Suh HH, et al. Characterization of particulate matter 2.5 in an urban tertiary care hospital in the Philippines. Building and Environment 2015; 92: 432-39.

Luksamijarulkul P, Somjai N, Nankongnap N, Pataitiemthong A, Kongtip P, Woskie S. Indoor air quality at different sites of a governmental hospital, Thailand. Nursing and Palliative Care 2019; 4: 1-5.

Mendes A, Pereira C, Mendes D, Aguiar L, Neves P, Silva S, et al. Indoor air quality and thermal comfort-Results of a pilot study in elderly care centers in Portugal. Journal of Toxicology and Environmental Health 2013; 76(4-5): 333-44.

Mullen NA, Bhangar S, Hering SV, Kreisberg NM, Nazaroff WW. Ultrafine particle concentrations and exposures in six elementary school classrooms in northern California. Indoor Air 2011; 21(1): 77-87.

Office of public health system Development, Health Department, Bangkok Metropolitan Administration. Annual reports and key statistics 2019 Bangkok. [Internet]. 2020 [cited 2021 Sep 11]. Available from:https://webportal.bangkok.go.th/health/Annual-reports-and-key-statistics.

Pollution Control Department, Ministry of Natural Resources and Environment. Booklet on Thailand State of Pollution 2018.1st ed. Bangkok: S.Mongkon Press Limited Partnership; 2019. p. 20-5.

Sompornrattanaphan M, Thongngarm T, Tantilipikorn P, Kreetapirom P, Foo J. The Contribution of Outdoor Fine Particulate Matter to Indoor Air Quality in Bangkok Metropolitan Region, Thailand–Are Indoor Dwellers Safe? Siriraj Medical Journal 2018; 70(4): 265-71.

Synnefa A, Polichronaki E, Papagiannopoulou E, Santamouris M, Mihalakakou G, Doukas P, et al. An experimental investigation of the indoor air quality in fifteen school buildings in Athens, Greece. International Journal of Ventilation 2003; 2(3): 185-201

National Institute for Occupational Safety and Health (NIOSH). Guidance for Indoor Air Quality Investigations. Cincinnati: NIOSH; 1987.

World Health Organization (WHO). WHO global air quality guidelines: Particulate matter ($PM_{2.5}$ and PM_{10}), ozone, nitrogendioxide, sulfur dioxide and carbon monoxide.Geneva: World Health Organization; 2021.

Zhou Q, Lyu Z, Qian H, Song J, Möbs VC. Field-measurement of CO_2 level in general hospital wards in Nanjing. Procedia Engineering2015; 121: 52-8.

Zuraimi MS, Tham KW, Chew FT, Ooi PL. The effect of ventilation strategies of child care centers on indoor air quality and respiratory health of children in Singapore. Indoor air 2017; 17(4): 317-27.

Enhancement of Sulfate Removal Efficiency Using Ettringite Precipitation at High Temperature

Pullop Treerasaeng[a,b], Yothin Chimupala[c], and Pimluck Kijjanapanich[a*]

[a]Department of Environmental Engineering, Faculty of Engineering, Chiang Mai University, Chiang Mai 50200, Thailand
[b]Graduate School, Chiang Mai University, Chiang Mai 50200, Thailand
[c]Research Laboratory of Pollution Treatment and Environmental Materials, Department of Industrial Chemistry, Faculty of Science, Chiang Mai University, Chiang Mai 50200, Thailand

Abstract

Ettringite precipitation has been recognized as one of the most promising treatment technology for remediation of mine drainage. With this treatment, the enormous amount of mine drainage (>2 million m^3) could be treated and utilized for agriculture, etc. However, a long reaction time is normally required for this treatment (at least 6 h to remain productive), which in turn require the large size of the reactor. Therefore, the aims of this research are to enhance the sulfate removal efficiency of mine drainage treatment and reduce the reaction time through the increase of the reaction temperature. The effects of the reaction temperature, reaction time, and aluminium/sulfate (Al/S) ratio (mole basis) on the sulfate removal efficiency were investigated using full factorial design. From the statistical analysis, it was shown that the Al/S ratio and reaction temperature had a significant effect on sulfate removal efficiency. This study showed that the sulfate removal efficiencies of Lamphun mine drainage increased when the Al/S ratio and reaction temperature were increased. The highest sulfate removal efficiency of 82.5% was achieved from the designed experiment when reaction temperature, reaction time, and Al/S ratio of 60 °C, 2.5 h, and 2.5 were used, respectively. The sulfate concentration of the treated water on this condition was 152.67 mg/L, which is lower than the drinking water standard. In addition, the precipitates of ettringite could be utilized as material for Calcium sulfoaluminate-belite cement production or as a sorbent for heavy metal or arsenate removal.

Keyword: Ettringite precipitation/ Full factorial design/ Mine drainage/ Sulfate removal

---

*Corresponding Author: Pimluck Kijjanapanich, +6-653-944-192 ext. 107
E-mail address: pimluck@eng.cmu.ac.th

1. Introduction

A large quantity of wastewater (>2 million m^3), namely as mine drainage, is created during mining activities. The mine drainage from lignite coal mines normally contains high total dissolved solids (TDS), high concentrations of sulfate and sometime toxic trace metals (iron, manganese, zinc, copper and cadmium), which in turn, inhibit the utilization of this mine drainage. The ettringite precipitation process has been recognized as one of the most promising treatment technology for remediation of mine drainage. With this treatment, the heavy metals can precipitate as metal hydroxide (Equation 1), while sulfate and calcium precipitate as ettringite ($Ca_6Al_2(SO_4)_3(OH)_{12}\cdot 26H_2O$) by additional of aluminium ions (Equation 2). Then, treated mine drainage could be utilized for agriculture, etc. This precipitation method can reduce sulfate concentration in the water to less than 200 mg/L (Dou et al. 2017; Pratinthong et al. 2021; Tolonen et al. 2016), which is lower than the drinking water guideline (WHO 2004; Department of Health-Ministry of Public Health 2020). In addition, the precipitates of ettringite could be utilized as material for Calcium sulfoaluminate-belite cement production or as a sorbent for heavy metal or arsenate removal (Rungchet et al. 2016; Tolonen et al. 2016). However, a long reaction time is required for this treatment (6 h), which in turn require the large size of the reactor (Pratinthong et al. 2021). Therefore, the aims of this research are to determine the optimum conditions and study the effects of the temperature, reaction time, and aluminium/sulfate (Al/S) ratio (mole basis) for sulfate removal from Thai mine drainage by ettringite precipitation.

$$M^{2+} + 2OH^- \rightarrow M(OH)_2 \quad (1)$$

$$3Ca^{2+} + 2Al(OH)_4^- + 3CaSO_4 + 4OH^- + 26H_2O \rightarrow Ca_6Al_2(SO_4)_3(OH)_{12} + 26H_2O \quad (2)$$

2. Methodology

2.1 Experimental design

MINITAB 17 software was used for the statistical design of the experiments and data analysis. In this study, Full Factorial Design (2^k) was used for optimize the three important variable. The independent variables, including, reaction temperature, reaction time, and Al/S ratio, used in this experiment were in the range of 45-75 °C, 1.5-3.5 h, and 1.5-3.5, respectively (Table1), while calcium/sulfate (Ca/S) ratio (mole basis) was fixed at 4:1 for all experiments (Pratinthong et al. 2021). The experiments were employed with eight factorial points and six replicates at the center point (14 experiments) as shown in Table 2.

Table 1. Range of Process Parameters Tested in the Experiment.

Parameter	-1	0	+1
Temperature(°C)	45	60	75
Reaction time (h)	1.5	2.5	3.5
Al/S	1.5	2.5	3.5

2.2 Experimental procedure

The experiment was conducted at difference temperature (Table1) using the mine drainage from Lamphun, Thailand, which is an abandoned open pit coal mine. The initial pH of mine drainage was acid (pH around 4 (Kijjanapanich et al. 2012)). However, the pre-treatment had been done by the mine owner by adding lime and limestone dust in order to increase the pH before closing the mine. Thus, the pH of mine drainage from Lamphun was neutral when water sampling was done. The main characteristics of this mine drainage were as follows: pH = 7.85 ± 0.05, sulfate = 925.29 ± 8.13 mg/L, TDS = 1527 ± 7.55 mg/L, calcium = 317.80 ± 5.40 mg/L and magnesium = 43.86 ± 4.12 mg/L.

First, the mine drainage 500 mL was filled into the tall beaker 1 L. The temperature of mine drainage was then increased to the desired temperature (Table 1) using a controlled temperature C-MAG HS7 IKA hotplate, Germany. After that, calcium hydroxide ($Ca(OH)_2$–95%; Loba Chemie Pvt. Ltd., India) 1.23 g and aluminium hydroxide ($Al(OH)_3$–90%; QReC, New Zealand) at the desire amount (Table 1) were added to the mine drainage. Then, the mine drainage were stirred rapidly at 150 rpm for 5 min. The beaker was then leave in a controlled temperature Digital Heat water bath until the selected reaction time was reached as shown in Table 1. Finally, the samples were then left to settle for 30 min at ambient temperature. The pH was measured and the supernatant was filtered through a glass microfiber filter GF/C and was taken to determine sulfate concentration according to the Standard Methods for the Examination of Water and Wastewater (APHA et al. 2017). Then, the effects of the three variable factors on the sulfate removal efficiency at the 95% confidence limit were analyzed using MINITAB 17 software to obtain the optimum conditions from the prediction equation.

3. Results and Discussion

This study showed that the highest sulfate removal efficiency of 82.5% could be achieved from the designed experiment when temperature, reaction time, and Al/S ratio of 60 °C, 2.5 h, and 2.5 were used, respectively. The sulfate concentration decreased from 925.29 (initial concentration) to 152.67 mg/L. This is lower than the quality standard of drinking water in Thailand and the WHO, which is 250 mg/L (WHO 2004; Department of Health-Ministry of Public Health 2020). Moreover, previous studies have proven that using ettringite precipitation is an efficient method up to 90% for sulfate removal, depending on the treatment (Dou et al. 2017; Pratinthong et al. 2021; Tolonen et al. 2016). Although, sulfates can kill aquatic plants while feeding algal blooms, causing severe disruptions to ecosystems (Kijjanapanich et al. 2014). There is no sulfate discharge standard of wastewater for Thailand. These limits are often dependent on hardness; in British Columbia, Canada, for example,

maximum sulfate limits typically range from 128–429 mg/L (Saltworks Technologies 2021). From Table 2, it can be seen that using a low Al/S ratio, the sulfate removal efficiency at high temperature is better than the other one at low temperature. This is due to the solubility of aluminum hydroxide is increased at high temperature (Moller et al. 2006). Thus, the limitation of the chemical solubility is eliminated. The study of Alvarez et al. (2005) found that the optimum condition for ettringite precipitation was at 60 °C, reaction time 4 h and pH 12. Pratinthong et al. (2021) also found that sulfate removal efficiencies sharply increased from 33.3-42.3 to 81.8-89.9%, when the temperature was increased from 25 to 80 °C during a 3 h reaction time at the constant Ca/S and Al/S ratio. Moreover, the giant polyaluminium species, which sulfate ions take part in coordination of the aluminium polycation, could be generated at high temperature. This in turn would increase sulfate removal efficiency (Sun et al. 2011). However, the formation of polyaluminium also depends on the aluminium concentration.

Table 2. Respond of Full Factorial Design in the Experiments.

Experiment points	No	Temperature (°C)	Reaction Time (h)	Al/S ratio	Sulfate Removal (%)
Factorial points	1	45	1.5	1.5	59.35
	2	45	1.5	3.5	76.23
	3	45	3.5	1.5	60.50
	4	45	3.5	3.5	80.59
	5	75	1.5	1.5	72.11
	6	75	1.5	3.5	71.93
	7	75	3.5	1.5	72.66
	8	75	3.5	3.5	74.56
Center point	9	60	2.5	2.5	82.82
	10	60	2.5	2.5	83.48
	11	60	2.5	2.5	83.24
	12	60	2.5	2.5	82.21
	13	60	2.5	2.5	83.30
	14	60	2.5	2.5	80.22

In contrast, Fang et al. (2018) found that sulfate removal efficiency decreased when the reaction temperature was increased from 25 to 80 °C, where the low aluminum ratio (Al/S: 1) was used. However, in this present study, using a high Al/S ratio, the sulfate removal efficiency at low temperatures is better than the other one at high temperatures. It might be due to the formation of other type of precipitates at high temperature, such as monosulfate, instead of ettringite. From previous study, it was found that increasing the aluminium dose resulted in an increase in monosulfate precipitation (Lothenbach et al. 2008; Almasri et al. 2015). In addition, solubility of aluminum hydroxide might not be improved at high temperature due to a high Al/S ratio had been used.

The factorial responses were studied using the analysis of variance (ANOVA) of MINITAB 17 software. It was found that Al/S and temperature had a significant effect on sulfate removal efficiency. On the other hand, the reaction time had little effect on increasing of the sulfate removal efficiency at high temperature (Table 3). From the Pareto chart (Figure 1) indicated that three main effects, including, the reaction time, reaction temperature and Al/S ratio, and one interaction effect, which is the Temperature x Al/S, had a significant effect on sulfate removal efficiency ($\alpha = 0.05$). Figure 2 showed that the sulfate removal efficiency increases when reaction temperature, reaction time and Al/S ratio are raised to the optimum value (center point) then the sulfate removal efficiency had decreased after the center point. The equation for predicting the relationship between the sulfate removal efficiency and main and interaction effects in coded value for sulfate removal is shown in Equation 3, which is obtained for statistical analysis by the MINITAB 17 software where Ct Pt is center point.

$$\text{Sulfate Removal Efficiency (\%)} = 70.991 + 1.086\ \text{Reaction time} + 1.824\ \text{Temperature} + 4.836\ \text{Al/S} - 4.406\ \text{Temperature*Al/S} + 11.554\ \text{Ct Pt} \quad (3)$$

Table 3. ANOVA of the Sulfate Removal Efficiency Using Full Factorials Design.

Source	DF	Adj SS	Adj MS	F-Value	P-Value
Model	5	836.160	167.232	112.83	0.000
Linear	3	223.163	74.388	50.19	0.000
Reaction time	1	9.440	9.440	6.37	0.036
Reaction temperature	1	26.609	26.609	17.95	0.003
Al/S	1	187.115	187.115	126.25	0.000
2-Way Interactions	1	155.320	155.320	104.80	0.000
Temperature* Al/S	1	457.677	457.677	104.80	0.000
Curvature	1	11.857	1.482	308.80	0.000
Error	8	4.336	1.445		
Lack-of-Fit	3	7.521	1.504	0.96	0.479
Pure Error	5	848.017			
Total	13	848.017			
Model Summary					
	S	R-sq	R-sq (adj)	R-sq (pred)	
	1.21742	98.60%	97.73%	95.09%	

Figure 3 shows that the comparison curve of predicted sulfate removal (%) versus experimental sulfate removal (%). It was found that the predicted sulfate removal efficiency close to the values achieved from the experiments only at the condition of the center point. In addition, the p-value of curvature was significant (p-value = 0.000), which implies that the factors have a curved relationship with the responses. Thus, further experiments are required for optimization of the prediction equation.

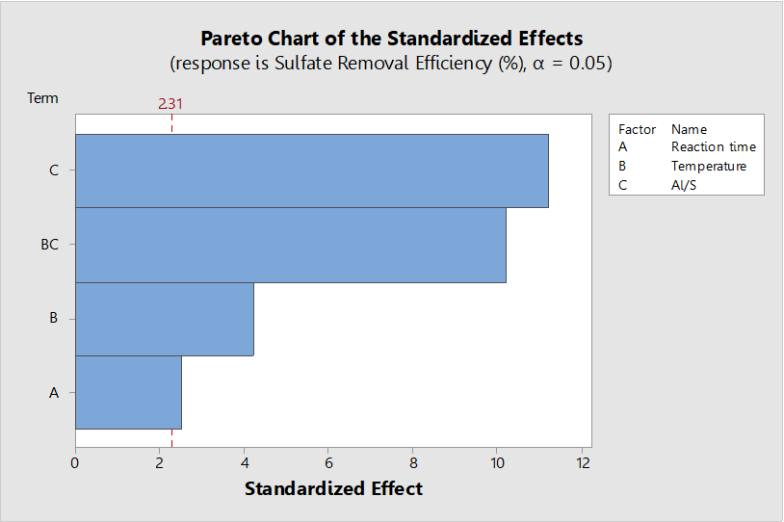

Figure 1. The Pareto Chart of the Standardized Effects

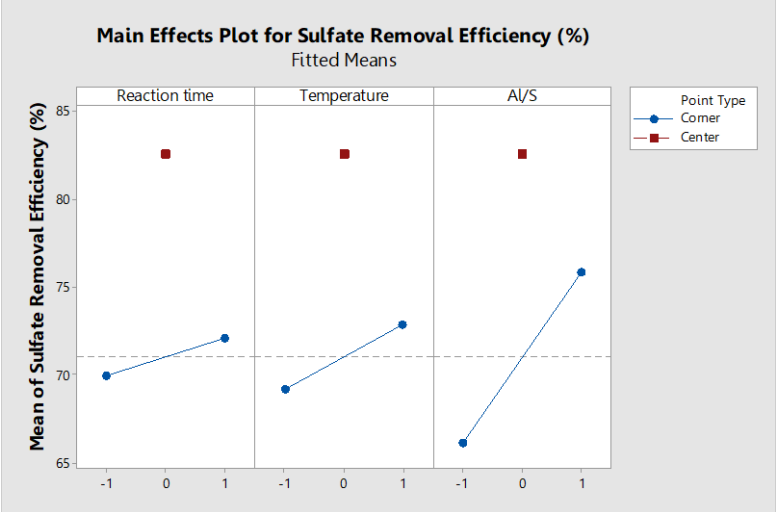

Figure 2. Main Effect Plot for Sulfate Removal Efficiency (%)

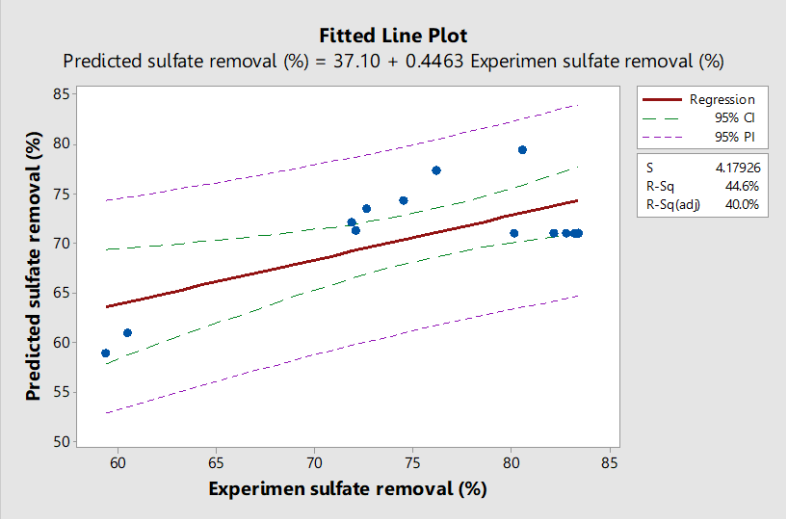

Figure 3. Predicted vs Experiment Sulfate Removal (%)

The precipitates of ettringite that were obtained from this study could be utilized as material for Calcium sulfoaluminate-belite cement production (Rungchet et al. 2016). Calcium sulfoaluminate-belite cement has shown good dimensional stability, low alkalinity, low permeability, compressive strength comparable to Portland cement concrete and high resistance to chemical attack (for example by seawater, sulfates, chloride) due to its dense structure (Rungchet et al. 2016). All of the phases in the production of Calcium sulfoaluminate-belite cement, which has ettringite as an intermediate in the production process, are stable at a temperature of approximately 1250 °C, which is about 200 °C lower than the temperature used for Portland cement production, and thus has lower energy consumption and lower carbon dioxide emissions. In addition, the study of Tolonen et al. (2016) indicate that the precipitate produced during sulfate removal from mine water by precipitation as ettringite could be further used as a sorbent for arsenate removal. The removal efficiency of 86-96% had been achieved from the initial arsenate of 1.5 mg/L when using 1 g/L of ettringite precipitate.

4. Conclusions

This study showed that the highest sulfate removal efficiency of 82.5% could be achieved from the designed experiment when temperature, reaction time, and Al/S ratio of 60 °C, 2.5 h, and

2.5 were used, respectively. It was found that Al/S and temperature had a significant effect on sulfate removal efficiency. On the other hand, the reaction time had little effect on increasing of the sulfate removal efficiency at high temperature. In addition, the p-value of curvature was significant, which implies that the factors have a curved relationship with the responses. Thus, further experiments are required for optimization of the prediction equation.

Acknowledgement

The authors acknowledge the Graduate School of Chiang Mai University, for financial support under a Teacher Assistant and Research Assistant scholarship (TA/RA). This research was also supported through The Murata Science Foundation 2020.

References

Almasri, Dema, Khaled A. Mahmoud, and Ahmed Abdel-Wahab. 2015. Two-stage sulfate removal from reject brine in inland desalination with zero-liquid discharge, Desalination, 362: 52-58.

Alvarez-Ayuso, E., and H. W. Nugteren. 2005. Synthesis of ettringite: a way to deal with the acid wastewaters of aluminium anodising industry, Water Research, 39: 65-72.

APHA, AWWA, and WEF. 2017. Standard Methods for the Examination of Water and Wastewater. in 23rd (ed.) (American Public Health Association: Washington,DC).

Department of Health-Ministry of Public Health. 2020. Water Supply Standard of Thailand Accessed 10 November.

Dou, W., Z. Zhou, L. M. Jiang, A. Jiang, R. Huang, X. Tian, W. Zhang, and D. Chen. 2017. Sulfate removal from wastewater using ettringite precipitation: Magnesium ion inhibition and process optimization, Journal of Environment Management, 196: 518-26.

Fang, Ping, Zi-jun Tang, Xiong-bo Chen, Jian-hang Huang, Zhi-xiong Tang, and Chao-ping Cen. 2018. Removal of High-Concentration Sulfate Ions from the Sodium Alkali FGD Wastewater Using Ettringite Precipitation Method: Factor Assessment, Feasibility, and Prospect, Journal of Chemistry, 2018: 1-8.

Kijjanapanich, P., K. Pakdeerattanamint, P. N. Lens, and A. P. Annachhatre. 2012. Organic substrates as electron donors in permeable reactive barriers for removal of heavy metals from acid mine drainage, Environmental Technology, 33: 2635-44.

Kijjanapanich, Pimluck, Ajit P. Annachhatre, and Piet N. L. Lens. 2014. Biological Sulfate Reduction for Treatment of Gypsum Contaminated Soils, Sediments, and Solid Wastes, Critical Reviews in Environmental Science and Technology, 44: 1037-70.

Lothenbach, Barbara, Thomas Matschei, Göril Möschner, and Fred P. Glasser. 2008. Thermodynamic modelling of the effect of temperature on the hydration and porosity of Portland cement, Cement and Concrete Research, 38: 1-18.

Moller, Nancy, Christomir Christov, and John. Weare. 2006. Thermodynamic Models of Aluminium Silicate Mineral Solubility for Application to Enchanced Geothermal System, Thirty-First Workshop on Geothermal Reservoir Engineering: pp. 1-8.

Pratinthong, N., S. Sangchan, Y. Chimupala, and P. Kijjanapanich. 2021. Sulfate removal from lignite coal mine drainage in Thailand using ettringite precipitation, Chemosphere, 285: 131357.

Rungchet, A., P. Chindaprasirt, S. Wansom, and K. Pimraksa. 2016. Hydrothermal synthesis of calcium sulfoaluminate–belite cement from industrial waste materials, Journal of Cleaner Production, 115: 273-83.

Saltworks Technologies. 2021. Sulfate Discharge: Measurement and cost-optimized removal, Accessed 27 November.

Sun, Z., H. Wang, H. Tong, and S. Sun. 2011. A giant polyaluminum species S-Al32 and two aluminum polyoxocations involving coordination by sulfate ions S-Al32 and S-K-Al13, Inorganic Chemistry, 50: 559-64.

Tolonen, E. T., T. Hu, J. Ramo, and U. Lassi. 2016. The removal of sulphate from mine water by precipitation as ettringite and the utilisation of the precipitate as a sorbent for arsenate removal, Journal of Environment Management, 181: 856-62.

WHO. 2004. Sulfate in drinking-water. in, Background document for development of WHO Guidelines for Drinking-water Quality (World Health Organization: Geneva).

Ambient Noise Levels at an Urban Recreational Lake Park: A Case Study of Ampang Hilir Lake Park

Nazatul Syadia Zainordin*, Muhammad Adib Azahar, Nur Izzati Zulkifli, Nurshahira Osmadi and Nur Aina Kamilia Othman

Department of Environment, Faculty of Forestry and Environment, Universiti Putra Malaysia, 43400 UPM Serdang, Selangor, Malaysia

Abstract

Urban lake park plays an important role in urban planning and one of its purposes is as a recreational space for fitness activities and social engagements. However, the significant increase in urbanization can lead to undesirable sound perception, able to cause annoyance and disturbance among park visitors. The focus of the study was to determine the ambient noise level at Ampang Hilir Lake Park, located in the city centre of Kuala Lumpur, Malaysia. The noise levels (L_{Aeq}) were monitored by using sound level meter for 12-hour at three monitoring points during weekdays and weekend. Descriptive statistics and independent t-test analysis were conducted to indicate the variations and to identify the significant different of the noise levels between weekdays and weekends, respectively. Results showed L_{Aeq} were highest at P2 during weekdays with average of 68dBA, exceeding the standard limit 65dBA, while both average values on weekend at P2 and weekdays at P3 were on the limit threshold. Noise levels were higher at P2 as it is located at the park main entrance and near the busy road. Significant differences were also found between weekdays and weekend ($p<0.05$) at all monitoring points where the noise levels were higher during weekdays as there were more anthropogenic sources due to higher traffic volume caused by people commuting to/from work, construction activities which are allowed only on weekdays, etc. These findings give an insight of the ambient noise level of the study area and consolidated the knowledge on further environmental management for the urban planning.

Keyword: Environmental noise/ daily variation/ public urban space/ urbanization/ anthropogenic sources/ urban noise

---

*Corresponding Author: Nazatul Syadia Zainordin, Tel: +60134310247; Fax: +60397693768
E-mail address: nazatulsyadia@upm.edu.my

1. Introduction

The growing public support and interest in health and fitness lead to various outdoor and nature-based activities for improvement in quality of life. Urban recreational lake parks have been suitable venues especially for the urbanites to enjoy an array of recreational or leisure activities, ranging from participatory in activities such as jogging, children's playgrounds, fishing, bird watching, to indulgence in the tranquil of the natural environment (Othman and Jafari, 2019). Hence, this kind of public space area is considered as an essential element of urban areas to fulfil the urbanites daily needs. However, due to the urbanization, these areas are not excluded from the urban noise pollution associated with increased of ground transportations, constructions, road and public maintenances, commercial activities, etc. Urban noise has been reported as major environmental health threats in overall Europe where the main source is contributed from the traffic (European Environment Agency, 2014). Health effects considered by the World Health Organization (2011) related to urban noise includes annoyance, sleep disturbance, hearing loss, psychological stress, and cardiovascular diseases.

This paper is aimed to determine the ambient noise levels at Ampang Hilir Lake Park during weekdays and weekends in order to investigate the noise exposure towards the visitors of the recreational park. The noise levels at selected monitoring points were also compared with the permissible noise limits set by the Malaysian Department of Environment. The permissible noise level varies considering

the sensitivity of the area, land use category and the population density of the area. Based on the Guidelines for Environmental Noise Limits and Control (Malaysian Department of Environment, 2019), by taking into consideration the characteristics of the study area, the recommended permissible noise level that was referring to is based on the existing built-up area for urban residential and mixed development, which should not exceed 65 (dBA) during daytime and 60 (dBA) during nighttime.

2. Methodology

2.1 Study area This study was conducted at Ampang Hilir Lake Park, an urban park with an average area of 40 acres and located in the city centre of Kuala Lumpur, Malaysia (Said, Othman & Ahmad, 2012). This study area is surrounded mainly by residential areas, commercial areas, international embassies, and main roads. This urban lake park is provided with various facilities for both outdoor and indoor recreational activities that can meet the need for all age groups. There is also a multi-purpose hall that can be used by the public as a gathering venue for any social activities. Three monitoring points were selected around the park as shown in Figure 1, and the details are shown as in Table 1.

Figure 1. Location of the selected monitoring points at Ampang Hilir Lake Park

Table 1. Details of the selected monitoring points

Monitoring Points	Coordinates	Details
P1	3°9'20.77"N 101°44'48.86"E	Near to second entrance, main road and residential area
P2	3°9'11.28"N 101°44'46.30"E	Near to main entrance, multi-purpose hall, main road and commercial area
P3	3°9'11.50"N 101°44'34.21"E	Near to international embassies and residential area

2.2 Data Collection

Monitoring data were collected in order to determine the ambient noise levels that were exposed to the visitors of the lake park. The parameters measured were L_{Aeq}, L_{max}, L_{min}, L_{10} and L_{90}. The monitoring was conducted for 12 hours during daytime starting from 6:30 a.m. to 6:30 p.m. Every point was monitored for a week including weekdays and weekend. The noise level was measured by using sound level meter (SLM) which complies with the IEC 61672 Class 1 Standard, meanwhile the meteorological parameters were measured by using Kestrel 5500 Pocket Weather Meter. SLM was setup 1.5m above the ground and at least 1m from any objects such as walls, buildings or other sound reflecting structures.

2.3 Data Analysis

Data analysis was performed to organize, transform and discover useful information from the monitoring data to determine the ambient noise levels at Ampang Hilir Lake Park. The information related to distribution of the parameters were determined by performing the descriptive analysis. This analysis was used to illustrate the characteristics and provide the description of the data set in an organize manner in order to answer the research question of the study (Marshall and Jonker, 2010). Meanwhile, independent t-test was conducted to compare the noise levels between weekdays and weekends at selected monitoring points. Independent t-test is an inferential statistical test which able to determine whether there is a statistically significant difference between the means in two unrelated groups (Laerd Statistics, 2013).

3. Results and Discussion

3.1 Results 1

The average noise levels at each of selected monitoring points on weekdays and weekends are presented in Table 2. From the analysis, the results revealed that the highest average of measured equivalent continuous noise levels (L_{Aeq}) on weekdays and weekend were both recorded at P2 with the values of 68 dBA and 65 dBA, respectively. According to the Guidelines for Environmental Noise Limits and Control (Malaysian Department of Environment, 2019), the permissible noise level for existing built-up area for urban residential and mixed development should not exceed 65 (dBA) during daytime. The average noise level on weekdays exceeded the permissible limit, while on weekend, the value was just on the threshold. This shows that the noise level may give significant effects to the health and comfortableness of the park visitors.

Table 2. Descriptive statistics of noise levels at selected monitoring points

Monitoring points	Session of monitoring	L_{Aeq} (dBA)	L_{max} (dBA)	L_{min} (dBA)	L_{10} (dBA)	L_{90} (dBA)
P1	Weekdays	56	58	54	57	56
	Weekend	54	56	53	56	54
P2	Weekdays	68	70	66	69	68
	Weekend	65	71	63	69	65
P3	Weekdays	65	72	61	69	64
	Weekend	63	68	51	68	63

Average noise level was monitored the highest at P2 because of the location which is near to the main entrance and parking areas of the recreational park, in a close proximity with construction areas and also nearby to the main road and commercial areas. Increase in these dominating human sounds will affects the noise levels in the recreational park (Nitidara et al., 2018). Payne (2008) also reported higher noise levels at monitoring point which located at the entrance, and as it goes to the middle of the park, the levels were reduced. Highest average noise levels were also recorded on weekend at P2 due to the gathering activities around the lake and the wedding event which took place in the multi-purpose hall located in the recreational park. The multi-purpose hall is open to the public based on the reserve basis as a venue for any social activities and events. A similar result was also recorded by Nitidara et al. (2018) where the “event noise” leads to higher noise level during weekend. However, it was noticeable that the L_{max} was recorded the highest at P3. This was contributed from the blower machine that was used to clean and maintain the recreational park.

Based on the independent t-test analysis in Table 3, it showed that there was significant difference between noise levels on weekdays and weekends for all monitoring points at Ampang Hilir Lake Park since the p-value for P1 and P2 are $p<0.001$, while P3 is .022. Noise levels were always recorded higher during weekdays compared to weekends as illustrated

in Figure 2. It was visible at the study area that the dominant noise source was from the traffic. The total amount of vehicles that passed by the study area were high especially during the peak hours where people commuting to/from work. The loudness of the traffic noise occurred mainly from the frictional effect between road surface and tires, heavier traffic volumes, driving in high speed and higher numbers of trucks on road, which can cause negative impacts to the urban communities and the surrounding environment (Hayden, 1971; Zulkepli et al., 2000; Segaran et al. 2020).

Table 3. Comparison of noise levels between weekdays and weekend at Ampang Hilir Lake Park based on independent t-test analysis

Monitoring points	P1	P2	P3
t	9.451	9.650	2.335
df	94.000	61.103	76.876
p-value	<0.001	<0.001	0.022

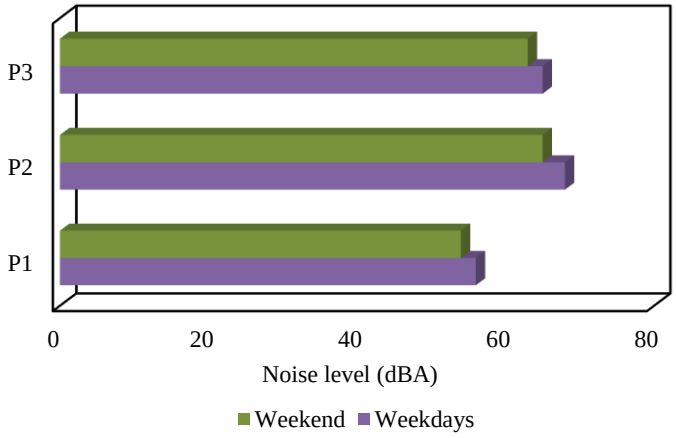

Figure 2: Average Noise Level (L_{Aeq}) at selected monitoring points on weekdays and weekend at Ampang Hilir Lake Park

5. Conclusions

This study aimed to determine the ambient noise levels at Ampang Hilir Lake Park during weekdays and weekends in order to investigate the noise exposure towards the visitors of the recreational park. The results of this study showed that there is a significant difference ($p<0.05$) between both sessions where weekdays were always recorded higher noise levels compared to weekends. Based on the Malaysian Guidelines for Environmental Noise Limits and Control, the average L_{Aeq} on weekdays was exceeding the permissible limit of 65dBA during daytime and both average values on weekend at P2 and weekdays at P3 were barely on the threshold of the limit. Further research is suggested to be carried out by also considering the qualitative elements in order to gain the public point overview related to the exposure of urban noise at public park. More detailed studies in the future are necessary to identify the extent of daily exposure risks to high noise levels especially in urban recreational park while consolidating the knowledge on further environmental management for the urban planning.

Acknowledgements

This research did not receive any specific grant from funding agencies in the public, commercial, or not-for-profit sectors. However, the authors would like to thank Kuala Lumpur City Hall for the research collaboration and permission related to the monitoring and data collection at Ampang Hilir Lake Park, Kuala Lumpur, Malaysia.

References

European Environment Agency (EEA) (2014). Noise in Europe in 2014. Luxembourg: European Union, pp 6-55

Hayden, R. E. (1971). Roadside noise from the interaction of a rolling tire with the road surface. The Journal of the Acoustical Society of America, 50(1A), 113-113.

Laerd Statistics (2013). Independent t-test using SPSS statistics [Online].Available:https://statistics.laerd.com/statistical-guides/independent-t-test-statistical-guide.php [Accessed on 13 November 2021].

Malaysian Department of Environment (2019). Guidelines for Environmental Noise Limits and Control (3rd Ed).

Said, K. S., Othman, M. S. & Ahmad, A. K. (2012). The determination of water quality and metal concentrations of Ampang Hilir Lake, Selangor, Peninsular Malaysia. Pakistan Journal of Biological Sciences: PJBS, 15(9), 437-447.

Segaran, V. C., Tong, Y. G., Abas, N. H., Daniel, B. D., Nagapan, S., & Kelundapyan, R. (2020). Traffic noise assessment among residential environment in Batu Pahat, Johor, Malaysia. In IOP Conference Series: Materials Science and Engineering (Vol. 713, No. 1, p. 012049). IOP Publishing.

Nitidara, N. P. A., Sudarsono, A. S., & Sarwono, J. (2018). The Soundscape Assessment of Three Urban Parks in Bandung Based on the Relationship Between Noise Level and Activities in Urban Park. 25th International Congress on Sound and Vibration.

Othman, J., & Jafari, Y. (2019). Economic valuation of an urban lake recreational park: case of taman tasik cempaka in bandar baru bangi, Malaysia. Sustainability, 11(11), 3023.

Payne, S. R. (2008). Are perceived soundscapes within urban parks restorative. Journal of the Acoustical Society of America, 123(5), 3809-3809.

World Health Organization (WHO) (2011). Burden of Disease from Environmental Noise: Quantification of Healthy Life Years Lost in Europe. World Health Organization, Geneve.

Zulkepli, H. I., Hazel, M. & Richard, K. (2000). Noise Pollution at School Environment Located in Residential Area. Malaysian Journal of Civil Engineering, 12 (2) 47-62.

Analysis of Microplastics (MPs) Pollution in Wastewater Treatment Plant (WWTP) and Study on Microplastics Removal Efficiency

Chutinat Boonwattana[a*], Pumis Tubtimdang[a,b], and Alice Sharp[a]

[a]Master's Degree Program in Environmental Science, Environmental Science Research Center, Faculty of Science, Chiang Mai University, Chiang Mai 50200, Thailand
[b]Department of Chemistry, Faculty of Science, Chiang Mai University, Chiang Mai 50200, Thailand

Abstract

Plastic pollution has become common as a result of improper disposal of plastic waste. Microplastics are polymers with a particle size <5 mm (MPs). Wastewater treatment plants (WWTPs) are one of the sources of MPs in the environment, although the treatment process can remove some MPs before being discharged. Therefore, this study aims to understand MPs' characteristics and the treatment process's removal efficiency by analyzing MPs' physical and chemical characteristics, the level of contamination, and the removal efficiency of the wastewater treatment process. Wastewater and sludge samples were obtained from the WWTP influent, treated effluent, and sludge bed at the Wastewater Control and Treatment Division, Chiang Mai University. The average MPs detected in the influent, effluent, and sludge were 56.01±5.0 particle/L, 5.78±1.1 particle/L, and 734±107.01 particle/kgWW (wet weight), respectively. Thus, the MPs removal efficiency was almost 90%. Most MPs were in the size range of >2.5 m (fibers) and 0.1-0.5mm (irregular shape). Among these MPs, fibers were the main shape found in wastewater influent and treated effluent. However, irregular-shaped MPs were found mainly in the sludge. PE has been the dominant polymer type in this WWTP, according to FTIR analysis. The results indicate that the removal of fiber MPs may need additional removal treatment. This study confirms that WWTP can remove most MPs; however, the contamination in the sludge is of concern as it will be applied as a soil amendment. Therefore, further study on the toxicity of MPs or toxic chemicals attached to the surface of MPs on living organisms is needed.

Keyword: Microplastics (MPs)/ Wastewater treatment plant (WWTP)/ Removal efficiency

---

*Corresponding Author: Chutinat Boonwattana, Tel: +66-99-143-5599
E-mail address: chanikan_boonw@cmu.ac.th.

1. Introduction

In addition to the problem of large-size plastic waste contamination in the environment, microplastics (MPs) contamination is becoming increasingly common. MPs are defined as plastics with particle sizes ranging from 50 µm to 5 µm (0.05-5 mm.) (Andrady, 2011). They can be classified into two categories based on the nature of their particles and their origins. The first category is called primary MPs, and it includes MPs manufactured into small plastics for direct use, such as microbeads (Napper et al., 2015). Primary MPs can be found in various cosmetic and pharmaceutical products, including soaps, facial cleansers, body scrubs, and toothpaste. The second type of MPs is formed when large plastics accumulate in the environment and are eroded over time by water, wind, and sunlight (Galgani et al., 2013). Finally, they disintegrate into tiny particles of various shapes and sizes, including synthetic fibers from textile garments that peel off during washing (Browne, 2015; Napper & Thompson, 2016).

MPs, particularly those with particle sizes smaller than 5 mm, can potentially contaminate the environment and enter the food chain of organisms. Furthermore, because MP particles can absorb contaminants on their surface, they facilitate the accumulation of persistent bio-accumulative and toxic substances (PBTs). These are Persistent Organic Pollutants (POPs), chlorinated hydrocarbons such as Polychlorinated Biphenyls (PCBs), and other substances (Bakir et al., 2012; Browne et al., 2013; Rios et al., 2010). Thus, the combination of MP particles and toxic substances impacts the quality of water resources and the food chain, and it may pose a risk to human health in the future.

One of the significant sources of MPs in the environment is wastewater treatment plants (WWTP). As MPs are small, light, and floatable particles, they can eventually pass-through water bodies and the environment via wastewater treatment plants. Additionally, MP particles in biofilms in the wastewater treatment systems precipitate and accumulate in the sludge (Carr et al., 2016). The majority of the sludge is transferred to the agricultural area as organic fertilizer. As a result, sludge becomes another critical intermediate in wastewater treatment systems that disperse MPs into adjacent ecosystems, not exclusively in the aquatic environment.

This study aims to assess the level of MPs contamination in the wastewater treatment plant and determine the characteristics of those MPs. In addition, this study provides a baseline for MPs contamination in wastewater treatment plants to suggest other MPs removal techniques.

2. Methodology

2.1 Description of WWTP

All samples were collected at Chiang Mai University's wastewater treatment plant in Chiang Mai Province. The WWTP is responsible for the treatment of wastewater generated from the daily activities of Chiang Mai University. The plant has a 50-kilometer-long separate sewer pipeline receiving system that excludes rainwater. The wastewater treatment plant employs a conventional activated sludge wastewater treatment system and treats sludge by anaerobic digestion. It can treat 8,500 cubic meters of wastewater and 36 cubic meters of sludge per day. Figure 1 depicts an overview of the wastewater treatment system. This system comprises the following components: a bar screening system, a sewage tank, a grit chamber, sludge aeration, a sedimentation tank, and a disinfection system. Treated wastewater is discharged into the Chiang Mai Municipality's drainage channel, which flows into the Mae Kha Canal. A portion of the sludge is delivered to the fermentation tank to reduce its volume. The digested sludge is transferred to the drying bed, where it is dried, and the water is drained to be used as compost for agricultural applications.

2.2 Sample collection and pretreatment

2.2.1 Water samples

Samples were collected from the influent and the effluent of the WWTP. Samples were collected three times at two weeks intervals. Each time, a five-replications of 5 liters of influent and 30 liters of effluent were collected. First, the wastewater was filtered using a metal sieve with a 1 mm, 0.25mm, and 0.125 mm mesh size. The samples were then rinsed to collect the remaining material on the sieve with distilled water into a glass bottle for further laboratory analysis. A method from Xu et al. (2019) was modified for the wastewater MPs separation process. For each sample, the collected materials were washed with distilled water into a 250 ml beaker and dried for 24 hours at 90°C. Dried samples were treated with 30 ml of 30% hydrogen peroxide (H_2O_2) and Fe (III) solutions to digest organic matter contaminated on the MPs' surface. The mixture was stirred with a magnetic stirrer at 60°C and 120 rpm until the H_2O_2 completely evaporated. Repeat until all organic matter contaminants have been digested completely. The digested MPs suspension was allowed to settle overnight before filtered using a vacuum pump through a glass sand core Buchner filter funnel with cellulose membrane (diameter 47mm, pore size 5µm). The obtained filter paper was then dried at room temperature for further investigation of MPs.

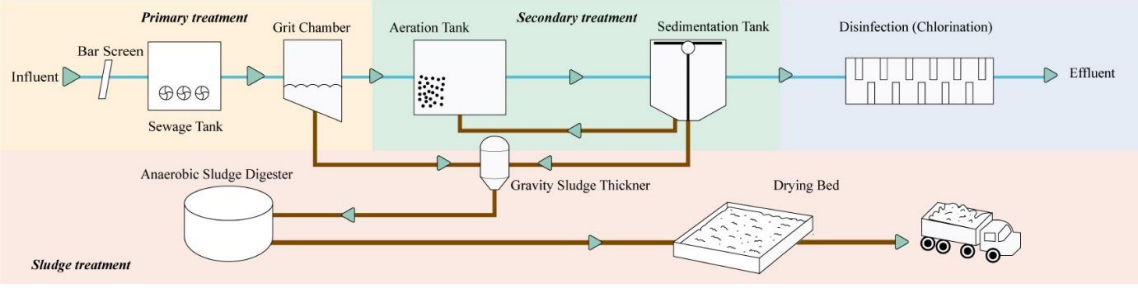

Figure 1. An overview of the wastewater treatment plant system.

2.2.2 Sludge samples

At the same time as the wastewater samples, 500 grams of dried sewage sludge to be used as fertilizer were collected in glass jars. The samples were returned to the laboratory to be analyzed for microplastics. The separation of microplastics from sludge was modified from Masura et al. (2015). The collected samples were divided into five sub-samples, each weighing 100 g, and dried for 72 hours at 90°C in 250 ml beakers. The dried sample was mixed with 200 ml of a 5M NaCl solution and stirred for 1 hour at a moderate speed, allowing for overnight settling. The suspension was then filtered through a metal sieve with 1 mm, 0.25 mm, 0.125 mm mesh sizes. The remainder of the sample material on the sieve was rinsed in a 250 ml beaker with distilled water. The samples extracted from the sludge were dried in a 90°C oven for 24 hours. The dried samples were then treated with 30 ml of 30 percent hydrogen peroxide (H_2O_2) and Fe (III) solutions to aid in the digestion of microplastic-contaminated organic matter. It was stirred with a magnetic stirrer at 60 °C and 120 rpm until the H_2O_2 completely evaporated. Rep this procedure until all organic contaminants have been completely digested. The digested solution was allowed to settle overnight before being vacuum-filtered through a glass sand core filter with a cellulose filter membrane (diameter 47mm, pore size 5µm). Take the filter paper and allow it to dry at room temperature before checking for microplastics.

2.3 Examination and identification of microplastics

2.3.1 Optical microscopy

Using an Olympus compound light microscope, all suspected MPs on the surface of each dried filter were observed at magnifications of 40–100 times. An ocular micrometer was used to determine sample sizes. Visual separation was used to count and record the abundance, type, and size of MPs in each sample.

2.3.2 FTIR spectroscopy

In each sample, MPs were counted and classified based on their shape. To characterize suspected microplastic furthers, Fourier Transform Infrared Spectroscopy (FTIR) was used. The measurement was carried out using attenuated total reflection FTIR spectroscopy. Because there were so many samples, some representative samples were chosen for identification. In this study, thirty samples were chosen at random and analyzed. In single-point transmission mode, the MPs were individually exposed to infrared radiation with a wavelength of 4,000-500 cm^{-1} and a time acquisition of 3s. The obtained spectra were compared to spectra libraries for all polymers to confirm the polymer composition of the microplastic sample.

3. Results and discussion

3.1 Abundance and characterization of MPs

3.1.1 Abundance of MPs

In this study, the abundance of MPs in the influent, effluent, and sludge contained an average of 56.01 (±5.0) particle/L, 5.78 (±1.1) particle/L, and 734.67 (±107.1) particle/kg WW (wet weight), respectively (Table 1). It can be seen that the amount of MPs contamination in the sludge is higher than in the wastewater samples. The abundance of MPs reported in the effluent of other WWTPs varies from 0 to 81 particle/L (Table 1). Additionally, (Leslie et al., 2017) reported MPs in sludge ranging from 501 to 760 particle/kg WW (wet weight), consistent with our study, which found the average MPs in sludge to be 734.67 (±107.1) particle/kg WW (wet weight). Microplastics were found in sludge from other WWTPs in various abundance from 400 to 7000 particles per kilogram wet weight and possibly up to 1,500-170,000 particles per kilogram dry weight (Sun et al., 2019). The majority of MPs in wastewater treatment plants enter the sewage sludge at various treatment units. Talvitie et al. (2017) estimate that 20% of activated sludge (including microplastics) is returned to the wastewater flow. Approximately 80% of the activated sludge is retained in the dry sludge, which will be disposed of later. However, because each study had its scope and methodology, detailed results could not be compared directly. Other studies' data could only confirm the current study's trends.

Table 1. Reported average abundance and removal efficiency of MPs in influent, effluent, and sludge of WWTPs from different counties.

Reference	Influent particle/L	Effluent particle/L	Removal (%)	Sludge particle/kg	Treatment process	Country
This study	56.1	5.78	89.68	734.67 (WW)	Primary, secondary, sludge	Thailand
(Carr et al., 2016)	1	8.8×10^{-4}	99.9	50 (WW)	Primary, secondary, tertiary, returned activated sludge	USA
(Dris et al., 2015)	293	35	88.1	na	Primary, secondary (biofilter)	France
(Lares et al., 2018)	57.6	1	98.3	170900 (DW)	Primary, secondary, digested sludge	Finland
(Leslie et al., 2017)	68-910	55-81	11-94	501-760 (WW)	Primary, secondary, sludge	Netherland
(Magnusson & Norén, 2014)	15.1	0.00825	99.9	720 (WW)	Primary, secondary	Sweden
(Michielssen et al., 2016)	133	5.9	95.6	na	Primary, secondary	USA
(Murphy et al., 2016)	15.7	0.25	98.4	1200 (WW)	Primary, secondary	Scotland
(Talvitie et al., 2017)	610	13.5	97.8	na	Primary, secondary, tertiary (BAF)	Finland

Note: WW mean the concentration was presented based on wet weight of the sludge.; DW means that the concentration was presented based on dry weight of the sludge.; Na: not applicable; Treatment processes: Secondary treatment: conventional activated sludge process.; BAF: biological aerated filter

3.1.2 Shape distribution

According to their shape, microplastics are classified into two broad categories: fibers and irregular shapes (Fig.2). The irregular shapes include flakes, films, and fragments of MPs. Fibers are the most prevalent component of pretreated wastewater at 73.16%. (Sun et al., 2019) concluded on the relative abundance of MPs of various shapes found in WWTPs that fibers accounted for the highest proportion of MPs observed in wastewater, accounting for an average of 52.7%. The high number of fibers in the wastewater may be explained by the substantial amount of fibers released via domestic washing machine discharges (Browne et al., 2011; Napper & Thompson, 2016; Pirc et al., 2016). Likewise, the high proportion of fibers in wastewater are due to the difficulty of distinguishing synthetic from natural fibers, and some studies also accounted for natural fibers. While according to (Talvitie et al., 2017), natural fibers such as cotton and linen maybe account for more than half of the fibers in wastewater samples. Therefore, a practical investigation method to distinguish effectively synthetic and natural fibers is critical for accurate MPs measurements of WWTP in the future.

Effluent contained slightly more fibers (53.26%) than irregular shapes (46.74%). (Fig 3a). Previous researches have found that fibers predominate over irregular shapes in wastewater (Lares et al., 2018; Leslie et al., 2017; Talvitie et al., 2015; Ziajahromi et al., 2017). In the case of sludge samples, irregular shapes accounted for the greatest proportion, accounting for 77.22 percent. The degradation of everyday plastic products could cause MPs with irregular shapes. Most MPs found in films, granules, and foams,

for example, are derived from the decomposition of plastic bags and packaging products, as well as plastic beads from personal care products (Carr et al., 2016). Numerous fibers in influent and effluent demonstrate that conventional wastewater treatment systems cannot effectively remove fibers. Furthermore, the presence of a high number of irregularly shaped microplastics in the sludge explains how well the sedimentation process isolates these microplastics in wastewater treatment plants.

3.1.3 Size distribution

The size range distribution of microplastics in a WWTP (Figure 3b) can be classified as follows: 0.1-0.5 mm, >0.5-1 mm, >1-2.5 mm, >2.5 mm. MPs with a particle size of >2.5 mm are the majority in the influent, accounting for 55.36%. In addition, this study examined fiber size, resulting in a high proportion of MPs with a particle size greater than 2.5 mm. In previous studies, microplastics larger than 0.5 mm were observed at 70% in influent (Dris et al., 2015; Lares et al., 2018). The particle size distribution of effluent and sludge was mainly between 0.1 and 0.5 mm, accounting for 35.39% and 49.94%, respectively. Most prominent MPs were disposed of by grit chamber, mechanical agitation, biological treatment, and sludge settling. Moreover, sedimentation results in the cracking and deterioration of their particle size. As a result, the number of MPs with small particle sizes in effluent and sludge was relatively high (Xu et al., 2019). However, a number description of the MPs size distribution may be insufficient due to the irregular shape of MPs. Future studies on their size should employ standardized colloidal science parameters to obtain comparable data on the actual size of microplastic particles in a normalized manner (Filella, 2015).

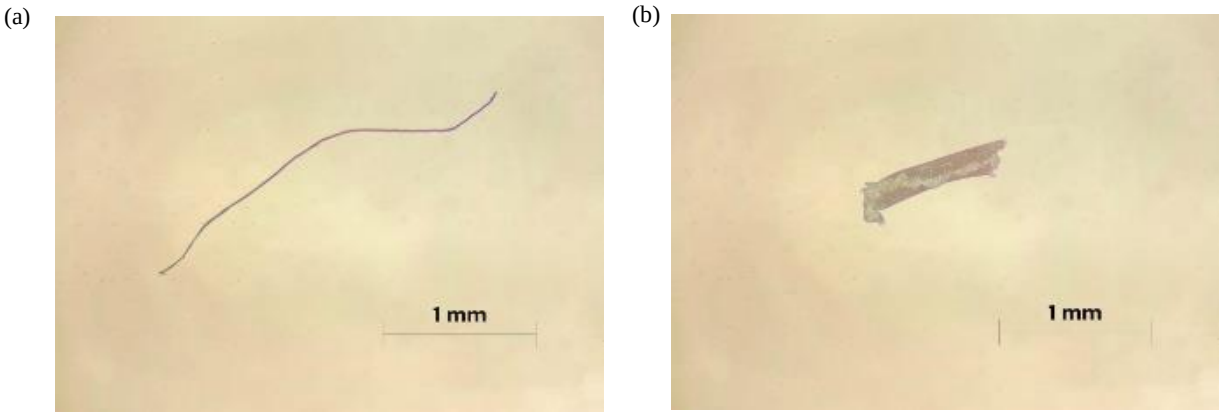

Figure 2. MPs under a microscope, (a) fiber shape MPs; MPs. (b) irregular shape

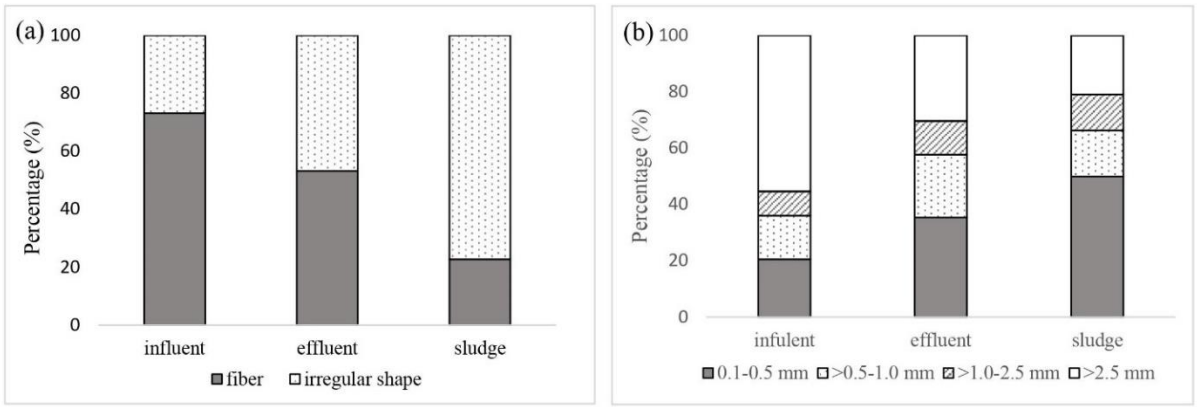

Figure 3. Distribution of MPs in a WWTP, (a) represents the percentage of shape distribution; (b) represents the percentage of size distribution.

3.1.2 Polymer types

Further confirmation of polymer type was done using Fourier Transform Infrared Spectroscopy (FTIR). The analysis of MPs revealed that only 18 of the 30 polymer samples could be examined for the polymer types, representing 60% of the total samples. Polyester (PES), low-density polyethylene (LDPE), polyvinyl chloride (PVC), and alkyd were discovered in a wastewater treatment plant (WWTP) (Figure 4). PES, widely used in synthetic clothing, and LDPE, widely used in food packaging, were two of the most common polymers discovered. Wood coatings chemicals add other polymers, such as alkyd, to the results. The presence of microplastic materials in wastewater detected at WWTPs indicates that most MPs in wastewater originate in our daily lives. Although the origins and routes by which MPs enter WWTPs are unknown, such information can help control MPs sources and prevent related pollution. As a result, polymer types and contamination sources should be thoroughly investigated in the future (Sun et al., 2019). Although physical characteristics such as shape and color make MP identification simple, the chemical composition is complicated in the analytical process. The smaller the size of the MPs particle, the more difficult it is to identify. Because it can analyze samples in small quantities, micro-FTIR spectroscopy is required for MP analysis. One of the limitations of many MPs studies, including the current study, is a lack of appropriate equipment. Furthermore, the discovered fuzzy particles may appear plastic, making accurate identification of microplastics difficult (Song et al., 2015).

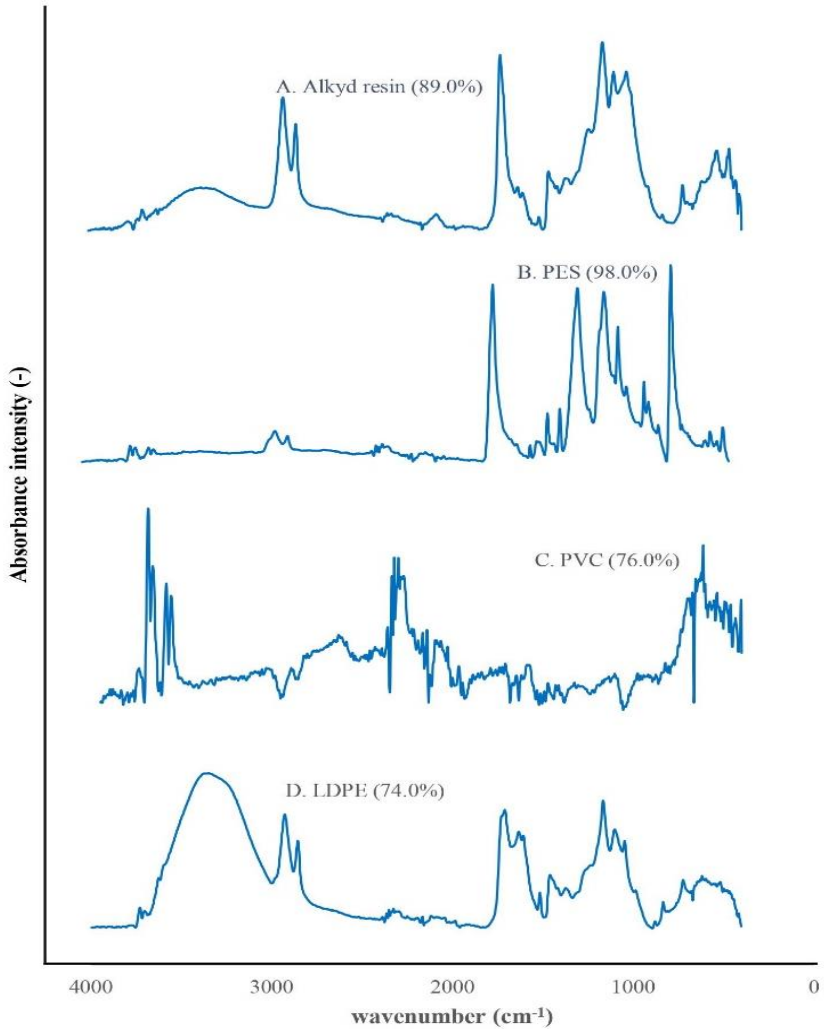

Figure 4. Analysis of MPs with ATR-FTIR spectroscopy, Abbreviations: alkyd resin; PES, polyester; PVC, polyvinylchloride; LDPE, polyethylene low density polymer.

3.2 Removal efficiency

The current study found that this wastewater treatment plant had an MPs removal efficiency of 89.68% (Table 1), consistent with other studies such as (Dris et al., 2015), which found the MPs removal efficiency 88.1 %. The comparative efficacy study conducted in seven wastewater treatment plants in the Netherlands discovered an average MPs removal efficiency of 72%. (Leslie et al., 2017). While the removal efficiency in Sweden was at 99.9% (Magnusson & Norén, 2014), US 99.9% (Carr et al., 2016), UK 98.4% (Murphy et al., 2016). Another study in China found that 11 WWTPs studied in China had efficiency above 90% (Xu et al., 2019). Thus, MPs' removal efficiency in most WWTPs was in the range of 90% to 99.9%. The removal efficiency varies depending on the wastewater treatment process and method used to collect, separate, and identify water samples in a WWTP (Mason et al., 2016). The data could be used as a baseline for future operations because of differences in study methods (e.g., filter mesh size and sample volume).

4. Conclusions

This study aimed to as certain the presence of microplastics at this wastewater treatment plant and validate microplastics' discharge into the environment. The average abundance of MPs in influent was 49.64±6.7-65.80±11.1 particle/L in the effluent, it was 3.66±0.5-7.11±0.8 particle/L, and in sludge was 532±66.1-896±83.9 particle/kg WW (wet weight). According to the result, a high concentration of MPs in sludge is another primary source of MPs entering the environment. It's because MPs released via sludge have the potential to spread to non-aquatic ecosystems. The results confirm that this wastewater treatment plant has a microplastics removal efficiency is 89.68 %, which is classified as acceptable. It is sufficient compared to research on the efficacy of microplastic removal (Carr et al., 2016; Dris et al., 2015; Magnusson & Norén, 2014; Murphy et al., 2016; Xu et al., 2019). However, fiber MPs are the primary shape in wastewater, while irregular shape MPs are the most encountered in sludge.

Additionally, MPs in effluent and sludge are smaller than those in influent. Microplastics extracted from this WWTP include PES, LDPE, PVC, and alkyd resin derived from apparel, food packaging, and polymer applications in daily life. Due to their microparticles and surface texture, MPs are a critical substrate for accumulating toxicity for heavy metals and POPs. Regarding methodology, due to the variation in the collection, separation, and the limitations of the tools used to identify MPs, the outcomes of studies vary. However, the data indicate microplastics' contamination load and disposal efficiency in this WWTP. The information can be helpful in the future of plastic waste management to limit MPs'

Acknowledgement

The authors would like to thank Chiang Mai University's wastewater treatment plant and WWTP staff for their practical and information help during the sampling campaign.

References

Andrady, A. L. (2011). Microplastics in the marine environment. *Marine pollution bulletin, 62*(8), 1596-1605.

Bakir, A., Rowland, S. J., & Thompson, R. C. (2012). Competitive sorption of persistent organic pollutants onto microplastics in the marine environment. *Marine pollution bulletin, 64*(12), 2782-2789.

Browne, M. A. (2015). Sources and pathways of microplastics to habitats. *Marine anthropogenic litter*, 229-244.

Browne, M. A., Crump, P., Niven, S. J., Teuten, E., Tonkin, A., Galloway, T., & Thompson, R. (2011). Accumulation of microplastic on shorelines woldwide: sources and sinks. *Environmental science & technology, 45*(21), 9175-9179.

Browne, M. A., Niven, S. J., Galloway, T. S., Rowland, S. J., & Thompson, R. C. (2013). Microplastic moves pollutants and additives to worms, reducing functions linked to health and biodiversity. *Current biology, 23*(23), 2388-2392.

A., Liu, J., & Tesoro, A. G. (2016). Transport and fate of microplastic particles in wastewater treatment plants. *Water research, 91*, 174-182.

Dris, R., Gasperi, J., Rocher, V., Saad, M., Renault, N., & Tassin, B. (2015). Microplastic contamination in an urban area: a case study in Greater Paris. *Environmental Chemistry, 12*(5), 592-599.

Filella, M. (2015). Questions of size and numbers in environmental research on microplastics: methodological and conceptual aspects. *Environmental Chemistry, 12*(5), 527-538.

Galgani, F., Hanke, G., Werner, S., & De Vrees, L. (2013). Marine litter within the European marine strategy

framework directive. *ICES Journal of Marine Science*, *70*(6), 1055-1064.

Lares, M., Ncibi, M. C., Sillanpää, M., & Sillanpää, M. (2018). Occurrence, identification and removal of microplastic particles and fibers in conventional activated sludge process and advanced MBR technology. *Water research*, *133*, 236-246.

Leslie, H., Brandsma, S., Van Velzen, M., & Vethaak, A. (2017). Microplastics en route: Field measurements in the Dutch river delta and Amsterdam canals, wastewater treatment plants, North Sea sediments and biota. *Environment international*, *101*, 133-142. [Record #13 is using a reference type undefined in this output style.]

Mason, S. A., Garneau, D., Sutton, R., Chu, Y., Ehmann, K., Barnes, J., Fink, P., Papazissimos, D., & Rogers, D. L. (2016). Microplastic pollution is widely detected in US municipal wastewater treatment plant effluent. *Environmental pollution*, *218*, 1045-1054.

Masura, J., Baker, J., Foster, G., & Arthur, C. (2015). Laboratory Methods for the Analysis of Microplastics in the Marine Environment: Recommendations for quantifying synthetic particles in waters and sediments.

Michielssen, M. R., Michielssen, E. R., Ni, J., & Duhaime, M. B. (2016). Fate of microplastics and other small anthropogenic litter (SAL) in wastewater treatment plants depends on unit processes employed. *Environmental Science: Water Research & Technology*, *2*(6), 1064-1073.

Murphy, F., Ewins, C., Carbonnier, F., & Quinn, B. (2016). Wastewater treatment works (WwTW) as a source of microplastics in the aquatic environment. *Environmental science & technology*, *50*(11), 5800-5808.

Napper, I. E., Bakir, A., Rowland, S. J., & Thompson, R. C. (2015). Characterisation, quantity and sorptive properties of microplastics extracted from cosmetics. *Marine pollution bulletin*, *99*(1-2), 178-185.

Napper, I. E., & Thompson, R. C. (2016). Release of synthetic microplastic plastic fibres from domestic washing machines: Effects of fabric type and washing conditions. *Marine pollution bulletin*, *112*(1-2), 39-45.

Pirc, U., Vidmar, M., Mozer, A., & Kržan, A. (2016). Emissions of microplastic fibers from microfiber fleece during domestic washing. *Environmental Science and Pollution Research*, *23*(21), 22206-22211.

Rios, L. M., Jones, P. R., Moore, C., & Narayan, U. V. (2010). Quantitation of persistent organic pollutants adsorbed on plastic debris from the Northern Pacific Gyre's "eastern garbage patch". *Journal of Environmental Monitoring*, *12*(12), 2226-2236.

Song, Y. K., Hong, S. H., Jang, M., Han, G. M., Rani, M., Lee, J., & Shim, W. J. (2015). A comparison of microscopic and spectroscopic identification methods for analysis of microplastics in environmental samples. *Marine pollution bulletin*, *93*(1-2), 202-209.

Sun, J., Dai, X., Wang, Q., van Loosdrecht, M. C., & Ni, B.-J. (2019). Microplastics in wastewater treatment plants: Detection, occurrence and removal. *Water research*, *152*, 21-37.

Talvitie, J., Heinonen, M., Pääkkönen, J.-P., Vahtera, E., Mikola, A., Setälä, O., & Vahala, R. (2015). Do wastewater treatment plants act as a potential point source of microplastics? Preliminary study in the coastal Gulf of Finland, Baltic Sea. *Water Science and Technology*, *72*(9), 1495-1504.

Talvitie, J., Mikola, A., Setälä, O., Heinonen, M., & Koistinen, A. (2017). How well is microlitter purified from wastewater?–A detailed study on the stepwise removal of microlitter in a tertiary level wastewater treatment plant. *Water research*, *109*, 164-172.

Xu, X., Jian, Y., Xue, Y., Hou, Q., & Wang, L. (2019). Microplastics in the wastewater treatment plants (WWTPs): Occurrence and removal. *Chemosphere*, *235*, 1089-1096.

Ziajahromi, S., Neale, P. A., Rintoul, L., & Leusch, F. D. (2017). Wastewater treatment plants as a pathway for microplastics: development of a new approach to sample wastewater-based microplastics. *Water research*, *112*, 93-99.

Decolorization of Reactive Red 239 by Activated Sludge Immobilized in Calcium Alginate Beads

Sitanan Norkaew[a,b], Kulapa Chanawanno[b,c], and Pumis Thuptimdang[b,c*]

[a]*Master's Degree Program in Environmental Science, Environmental Science Research Center, Faculty of Science, Chiang Mai University, Chiang Mai 50200, Thailand*
[b]*Environmental Science Research Center (ESRC), Faculty of Science, Chiang Mai University, Chiang Mai 50200, Thailand*
[c]*Department of Chemistry, Faculty of Science, Chiang Mai University, Chiang Mai 50200, Thailand*

Abstract

As Thailand's community-scale textile industries are growing, Reactive Red 239 (RR 239) is one of the synthetic azo dyes increasingly used in the dyeing process, resulting in the release of the dyes into the wastewater. Without proper treatment, the dye released with wastewater can be harmful to the environment. Bacteria in community wastewater normally have an ability to degrade various pollutants including the dye; however, high salt concentration used in the dyeing process can adversely affect the cells and reduce the degradation efficiency. Immobilization is one of the methods used to protect the cells from harsh condition. Therefore, the purpose of this research is to investigate the efficacy of immobilized sludge in the treatment of RR 239 under salt condition. The sludge was collected from the wastewater treatment plant of Chiang Mai University, and the immobilization was conducted using calcium alginate beads. The results showed that the 100 mg/L sludge and immobilized sludge were able to treat 80.38 and 72.89% of RR 239, respectively, within 24 hours. Under 40 g/L salt concentration conditions, the immobilized sludge showed better RR 239 decolorization efficiency (66.63%) compared with the sludge (4.29%). The reusability of the immobilized sludge was tested, and the results showed that the immobilized sludge still retained more than 80% of the treatment efficiency after 8 times of the reuse. The findings from this study showed that the immobilized activated sludge from wastewater treatment plant might be an alternative for low-cost textile wastewater treatment system.

Keyword: Sludge/ Immobilization/ Azo dye/ Reactive Red 239/ Biodegradation

---

*Corresponding Author: Pumis Thuptimdang
E-mail address: pumis.th@cmu.ac.th

1. Introduction

Thailand's textile industry, especially on the community level, has been continuously expanded. This can lead to more industrial activities including the dyeing process, which requires a lot of water and chemical uses. At least 10-15% of the dyes from the dyeing process are released in the wastewater and further into the environment (Wang et al., 2013). This is because most community-level dyehouses still lack adequate wastewater treatment methods. Azo dyes are among the most popular synthetic dyes, which takes up approximately 70% of the textile dyes used worldwide (Wang et al., 2013). Azo dyes consist of one or more azo groups containing two nitrogen atoms joined by a double bond (-N=N-) (Lim et al., 2014). The contamination of the azo dye molecules in environment can lead to mutagenicity, carcinogenicity, and the dysfunction of organs, reproductive system, and central nervous system of an organism (Zhou et al., 2019).

Several methods can be used to treat wastewater from the dyeing process. Physicochemical methods such as coagulation, adsorption, and membrane filtration have been used for the treatment of dye in wastewater, however, these technologies have the disadvantage of containing a lot of sludge and being costly (Wang et al., 2013). In contrast, biological methods using wastewater bacteria have shown environmental and economic advantages, producing less sludge and yielding less-toxic end products or even having complete mineralization (Saratale et al., 2011). Under oxygen limiting conditions, bacterial decolorization process is initiated by the production of the azoreductase enzymes, leading

to the cleavage of dyes azo linages and formation of aromatic amines resulting in a decrease in color concentration (Elfarash et al., 2017).

Microorganisms in activated sludge are widely recognized for their degradation roles in wastewater treatment (Han et al., 2021). Using of the activated sludge for the azo dye decolorization might be the solution to the community-based dye wastewater treatment system. However, sodium chloride is a common salt used in the dyeing process to improve the combination between dyes and cellulose fibers (Liu et al., 2017). The salt concentration of 0.5–5% can affect the efficiency of biological treatment in wastewater treatment plants because saline loads reduce the metabolic functions of activated sludge microorganisms**.** (Mirbolooki et al., 2017).

Immobilization of bacterial cells in sodium alginate has several advantages such as the protection of cells from external stresses including temperature, pH, or toxic compounds, the enhancement of degradation capability **(**Kurade et al., 2018**),** the enhancement of biological and physical stabilities of cells, and the prolonged reusability of cells (Wadhawan et al., 2010.). Therefore, immobilization of the activated sludge should not only improve the dye decolorization efficiency but also allow the multiple uses for dye wastewater treatment. However, it is uncertain that the immobilized sludge will be able to tolerate salt in dye wastewater; therefore, the effect of salt such as sodium chloride (NaCl) on the azo dye decolorization efficiency by the immobilized sludge should be investigated.

This study aimed to determine the effect of NaCl on the efficiency of the azo dye, Reactive Red 239 (RR 239), decolorization using immobilized sludge. The activated sludge from wastewater treatment plant was immobilized using calcium alginate beads. The study was conducted under oxygen limitation (no shaking condition), and the effect of salt concentrations on the decolorization efficiency was investigated compared with the non-immobilized sludge. In addition, the reusability of the immobilized sludge was also observed.

2. Methodology

2.1 Sludge sample and RR 239 dye

The sludge was collected from the wastewater treatment plant of Chiang Mai University and kept at 4 °C before use. The RR 239 dye was supplied by DyStar Thai Ltd. in the powder form. The RR 239 is a mono-azo dye, which has a molecular weight of 1026 g/mol and a molecular formula of $C_{31}H_{24}ClN_7O_{19}S_6$. The structure of the dye is shown in Figure 1. Before each experiment, the dye was dissolved in de-ionized (DI) water to a concentration of 1000 mg/L. The RR 239 solution was filtered through a 0.22-μm sterile syringe filter (Masterflex®) and kept as a stock solution at room temperature.

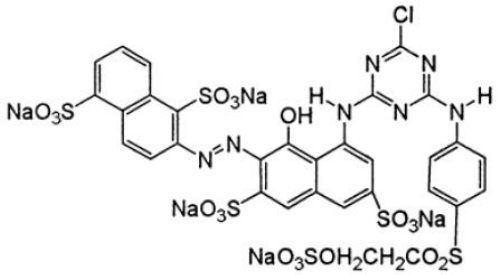

Figure 1. Structure of RR 239

2.2 Preparation of the immobilized sludge

Half grams of wet sludge were mixed with 60 mL of 2% sodium alginate (SA) in a 100-mL bottle. This mixture was then added dropwise into 100 mL of 2% $CaCl_2$ solution in a 250-mL Erlenmeyer flask using a dropper. After the calcium alginate beads were formed, they were left in the solution overnight (18 -24 h). The immobilized sludge beads were washed three times with normal saline solution (0.8%) before immediately used for the experiment.

2.3 Dye decolorization experiments

Half grams of the immobilized sludge or the non-immobilized was added to 50 mL of sterile Luria Bertani (LB) broth containing RR 239 and/or NaCl at required concentrations in a 100-mL bottle. The bottles were incubated at room conditions (25-33 °C) with the cap tightly closed and no shaking to limit oxygen intake. Three milliliters of sample were collected every 6 h for the total time of 48 h. Each experiment was performed in triplicate using three bottles for

one sampling time. The dye concentration was measured by UV-VIS Spectrophotometer at a wavelength of 540 nm. The concentration of RR 239 dye was determined from a standard curve of the dye stock solution. Dye removal was calculated using the following equation:

$$\text{Dye removal (\%)} = \frac{C_0 - C_t}{C_0}$$

Where; C_0 is the initial concentration of dye, and C_t is the concentration of dye at the sampling time.

The experiments were divided into three parts: the effect of dye concentrations (0, 50, 100, 300 and 500 mg/L), the effect of NaCl concentrations (0, 20, 40, 60 and 100 g/L), and the reusability of the immobilized sludge. For the experiment to determine the reusability of the immobilized sludge, 100 mg/L of RR 239 was fixed. Once the decolorization efficiency reached 80%, the immobilized sludge beads were transferred to a fresh LB media containing the same concentration of RR 239. This was repeated until the beads were disintegrated and could not be obtained from the solution.

3. Results and Discussion

3.1 RR 239 decolorization by the immobilized activated sludge

The decolorization of RR239 at various concentrations by wastewater sludge and immobilized sludge was evaluated (Figure 2). It can be observed that RR239 was rapidly removed by both the sludge and immobilized sludge at the highest efficiency of 80.38 and 72.89% within 24 h, respectively. When the concentration was increased, the decolorization rate seemed to be slower according to the slope of the graphs. However, highest efficiency of RR 239 decolorization by both sludge and immobilized sludge were obtained at 500 mg/L of RR 239 in 48 hours, which are 96.48 and 89.92%, respectively. reported that *S. xiamenensis* G5-03 isolated from contaminated landfill soil was able to remove RR239 48.8% of RR 239 after 3 h (Cossolin et al., 2019). And, azoreductase emzyme derived from Bacillus sp. strain YZU1 that anaerobic condition was able to remove Reactive Black 5 (Wang et al., 2013). The reason for the lower removal efficiency by the immobilized sludge may be from the fact that the calcium alginate beads might allow the dye and media to slowly move into the beads, resulting in slower decolorization. However, at the end of the experiments, the decolorization efficiency by the immobilized sludge was still comparable with the non-immobilized sludge.

It should be noted that the calcium alginate beads alone were able to remove 8.36% of RR 239 (data not shown) while the sterile sludge alone could remove 0.61% of RR 239 (data not shown). Since the calcium alginate beads contain porous surface, they can act as an absorbent to reduce dye concentration in wastewater (Bao-e et al., 2006). Therefore, the decolorization of RR 239 observed in Figure 2 was mainly from the biological activity of the sludge rather than the adsorption by the calcium alginate beads or the sludge.

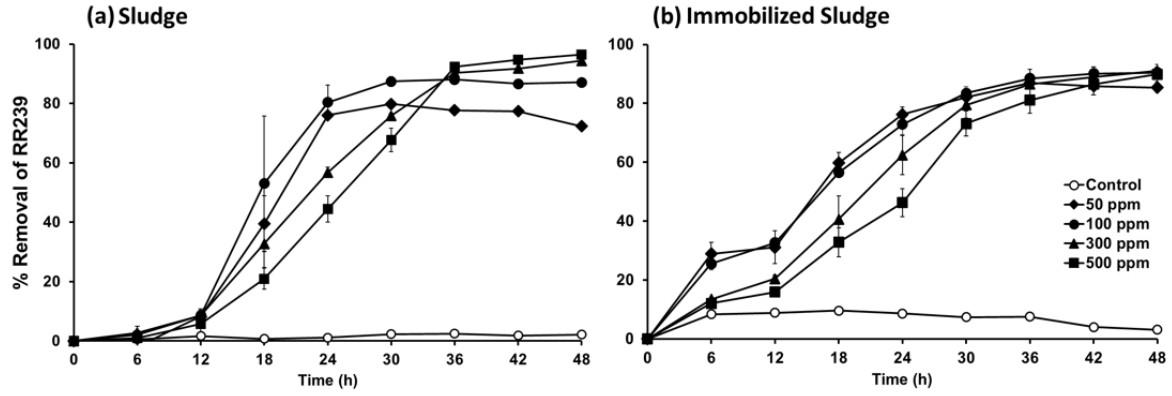

Figure 2. Decolorization of RR 239 by sludge (a) and immobilized sludge (b) at the concentrations of 0, 50, 100, 300, and 500 mg/L.

3.2 Effect of NaCl on RR 239 decolorization

The effect of NaCl on the decolorization of RR239 by sludge and immobilized sludge was evaluated, and the results are presented in Figure 3. The results show that while the non-immobilized sludge was able to remove 81.99% of RR 239 under NaCl concentration up to 40 g/L (Figure 3(a)), 4.52% removal was observed at the NaCl concentrations of 60 g/L. No decolorization was observed at 100 g/L of NaCl. On the other hand, the immobilized sludge was able to remove 80.26% and 16.02% of RR 239 at 60 g/L and 100 g/L of NaCl, respectively (Figure3(b)).

The results from Figure 3 shows that the immobilization was able to protect the microorganisms in the activate sludge from high salt concentrations, resulting in better RR 239 decolorization efficiency. It has been found that the immobilization technique can prevent microbial cells from the osmotic stress caused by salinity (Xue et al., 2019, Liu et al., 2017).

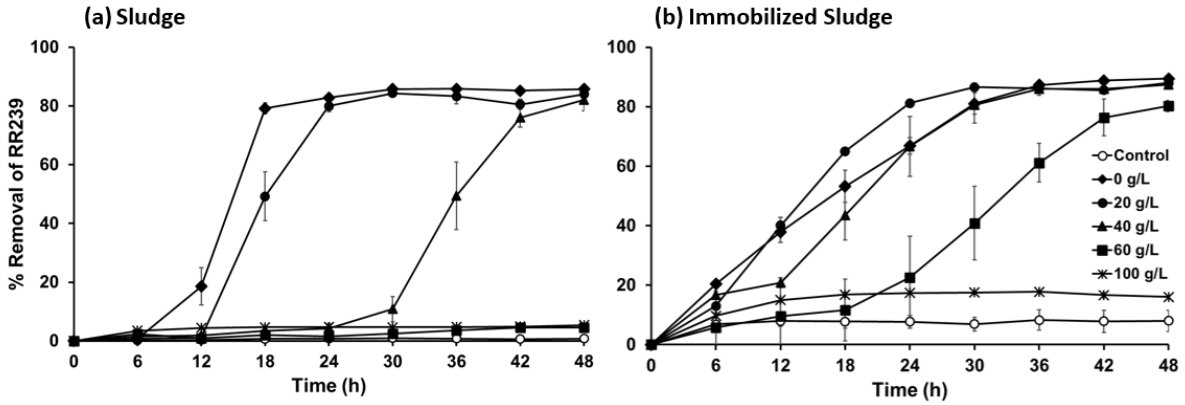

Figure 3. Decolorization of RR 239 by sludge (a) and immobilized sludge (b) at NaCl concentrations of 0, 20, 40, 60, and 100 g/L.

3.3 Reusability of the immobilized activated sludge

The immobilized activated sludge beads were investigated for their reusability. The decolorization experiments were conducted in the same manner with previous experiments using 100 mg/L of RR 239. After the decolorization efficiency reached 80% or above, the beads were reused for another decolorization experiment. This step was repeated until the beads were disintegrated and could not be used anymore. The results are depicted in Figure 4.

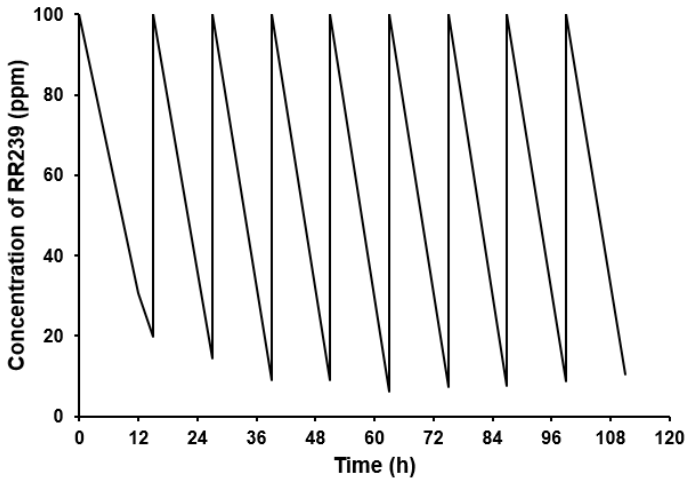

Figure 4. Reusability of the immobilized activated sludge.

From Figure 4, it was revealed that the immobilized sludge was able to remove RR 239 with the efficiency more than 80% up to 8 cycles. The average decolorization efficiency was at 89.80%. After the fourth cycle of decolorization, the immobilized beads began to release the sludge according to visual inspection. However, the beads were still able to be obtained, and the efficacy was still greater than 80% within 12 h. At the end of the eighth cycle, it was found that more than half of the beads were disintegrated to slimy substance. It should be noted that these polymer beads are safe and environment-friendly material (Leea et al., 2012); therefore, the waste of the polymer beads should not be a concern if released into the wastewater.

4. Conclusions

This study showed that the immobilized activated sludge was able to remove RR 239 at the concentration up to 500 mg/L with the decolorization efficiency of 89.92%. Under high NaCl concentration (60 g/L), the immobilized sludge showed better removal efficiency of 80.26% at 100 mg/L of RR 239 compared with the non-immobilized sludge (4.52% removal). In addition, the immobilized sludge could also be reused up to 8 times with the decolorization efficiency higher than 80% within 24 h of each reuse. Therefore, immobilization technique of the activated sludge might be a suitable technique to be used as a dye wastewater treatment system for local dyehouses.

References

Bao-e, W., Yong-you, H. (2006). Comparison of four supports for adsorption of reactive dyes by immobilized *Aspergillus fumigatus* beads. Journal of Environmental Sciences, 451–457

Cossolin, A., Reis, H., Castro, K., Santos, B., Marques, M., Parizotto, C., Oglio, E., Vasconcelos, L. (2019). Decolorization of textile azo dye Reactive Red 239 by the novel strain *Shewanella xiamenensis* G5-03 isolated from contaminated soil. Journal of Applied Science, (14)6, 1-11

Elfarash, A., Mawad, A., Yousef, N., Shoreit, A. (2017). Azoreductase kinetics and gene expression in the synthetic dyes- degrading Pseudomonas. Egyptian Journal of Basic and Applied Sciences, (4)4, 315-322

Han, T., Zheng, J., Han, Y., Xu, X., Li, M., Schwarz, C., Zhu, L. (2021). Comprehensive insights into core microbial assemblages in activated sludge exposed to textile-dyeing wastewater stress. Science of the Total Environment, 791, 148145

Kurade, M.B., Waghmode, T.R., Xiong, J.Q., Govindwar, S.P. and Jeon, B.H. (2018). Decolorization of textile industry effluent using immobilized consortium cells in upflow fixed bed reactor. Journal of Cleaner Production, 213, 884-891

Leea, k., Mooney, D. (2012). Alginate: Properties and biomedical applications. Progress in Polymer Science, 37(1), 106-126

Lim, C.K., Aris, A., Neoh, C.H., Lam, C.Y., Majid, Z.A., Ibrahim, Z. (2014). Evaluation of macrocomposite based sequencing batch biofilm reactor (MC-SBBR) for decolorization and biodegradation of azo dye Acid Orange 7. International Biodeterioration & Biodegradation, 87, 9-17

Liu, W., Liu, C., Liu, L., You, y., Jiang, J., Zhou Z. and Dong, Z. (2017). Simultaneous decolorization of sulfonated azo dyes and reduction of hexavalent chromium under high salt condition by a newly isolated salt-tolerant strain *Bacillus circulans* BWL1061. Ecotoxicology and Environmental Safety, 141, 9-16

Mirbolooki, H., Amirnezhad, R., Pendashteh, A. (2017). Treatment of high saline textile wastewater by activated sludge microorganisms. Journal of Applied Research and Technology, 15(2), 167-172

Saratale, R.G., Saratale, G.D., Chang, J.S., Govindwar, S.P. (2011). Bacterial decolorization and degradation of azo dyes: A review. Journal of the Taiwan Institute of Chemical Engineers, 42(1), 138-157

Wadhawan, T., McEvoy, J. Prüβ B.H. and Khana, E. (2010). Assessing tetrazolium and ATP assays for rapid in situ viability quantification of bacterial cells entrapped in hydrogel beads. Enzyme and Microbial Technology, 47(4), 166-173

Wang, Z. W., Liang, J. S., Liang, Y. (2013). Decolorization of Reactive Black 5 by a newly isolated bacterium Bacillus sp. YZU1. International Biodeterioration & Biodegradation, 76, 41-48.

Xue, J., liang, J., Wu, Y., Shi, K., Xiao, X., Gao, Y., Li, L., Qiao, Y. (2019). Study on the degradation performance and kinetics of immobilized cells in straw-alginate beads in marine environment. Bioresource Technology, 280, 88-94

Zhou, Y., Lu, J., Zhou, Y., Liu, Y. (2019). Recent advances for dyes removal using novel adsorbents: A review. Environmental Pollution, 252, 352-365.

Effect of Sludge Addition on the Biodegradation Efficiency of Diclofenac in Wastewater from Chiang Mai University Wastewater Treatment Plant

Piriyakorn Injai[a], Kullapa Chanawanno[b,c], Pumis Thuptimdang[b,c*]

[a]Master's Degree Program in Environmental Science, Environmental Science Research Center, Faculty of Science, Chiang Mai University, Chiang Mai 50200, Thailand
[b]Environmental Science Research Center (ESRC), Faculty of Science, Chiang Mai University, Chiang Mai 50200, Thailand
[c]Department of Chemistry, Faculty of Science, Chiang Mai University, Chiang Mai 50200, Thailand

Abstract

Diclofenac (DFN) is one of the non-steroidal anti-inflammatory drugs (NSAIDs) widely used in households, which leads to its contamination in wastewater. Because the pathway of DFN degradation in wastewater has not been clearly understood, there is a possibility that DFN may not be completely degraded in the conventional wastewater treatment plant. The objective of this research was to study the biodegradation efficiency of DFN in wastewater from a wastewater treatment plant of Chiang Mai University with the addition of the sludge from the plant to improve DFN biodegradation. Batch experiments were conducted with DFN at the concentrations of 0, 0.1, 0.5, 1, 5, and 10 mg/L in the wastewater with and without the sludge (1 g). The flasks were shaken for 5 days under dark condition at room temperature (25-35 °C). Degradation of DFN was measured by High-Performance liquid chromatography (HPLC). It was found that DFN in wastewater showed no degradation over 5 days of the experiment. On the other hand, more than 90% degradation of 0.1 and 0.5 mg/L DFN was observed in wastewater with 1 g of sludge. The increase in DFN concentrations led to lower degradation efficiency. Findings from this research showed that DFN in community wastewater may not be biodegradable, but it should be by the activated sludge system once it reached the wastewater treatment plant.

Keyword: Diclofenac/ Biodegradation/ Wastewater treatment/ Sludge

---

*Corresponding Author: Pumis Thuptimdang
E-mail address: pumis.th@cmu.ac.th

1. Introduction

Recently, contamination of drugs in aquatic environment is an important concern. Due to their wide applications and daily uses, certain amount of the drugs is excreted from human's body in the urine and feces, either in the original form or its metabolites, causing their residues in wastewater. Diclofenac or DFN (2-[2-(2,6-dichlorphenyl)amino] benzene acetic acid) is a regularly used antirheumatic non-steroidal anti-inflammatory drug. The global consumption of DFN can reach as high as 940 tons per year (Domaradzka et al., 2015). DFN has been found in wastewater treatment plant effluents in various countries such as Germany (Stülten et al., 2008), Spain (Rosal et al., 2010) and Canada (Lishman et al., 2006). DFN is considered an emerging contaminant because its effects and treatment methods are unclear. It is toxic even at the low levels (µg/L) to different organisms like fish and mussels (Vasquez et al. 2016).

Because most wastewater treatment plants were not designed to remove emerging contaminants, the untreated DFN has then been detected in groundwater, surface water, and wastewater effluents, and drinking water at the concentrations ranging between ng/L and µg/L (Chen et al., 2014), (Memmert et al., 2013) and (Inderfurth et al., 2013) DFN in environment could adversely affected the nature of a river bacterial community at the 10-100 µg/L range (Backhaus et al., 2011). To prevent the environmental effects from untreated DFN, the DFN removal efficiency of the conventional wastewater treatment system should be assessed. It has been found that DFN in a wastewater treatment system at the concentration as low as 50 pg/L can cause a permanent change the

microbial community composition (Kosjek et al., 2007); therefore, it is likely that the biological wastewater treatment system may not be able to remove DFN.

A common municipal wastewater treatment plant relies on the biological system. In Thailand, it is still unclear whether DFN in the wastewater going to the treatment plant can be degraded by microorganisms in wastewater. Therefore, the objective of this study is to determine the biodegradation efficiency of DFN in wastewater collected from a wastewater treatment plant of Chiang Mai University as a representative of the municipal wastewater treatment plant. Batch experiments were conducted at room conditions with DFN at the concentrations of 0, 0.1, 0.5, 1, 5, and 10 mg/L. To improve DFN biodegradation in wastewater, the experiments were also conducted with the addition of the sludge from the plant, which should serve as a source of microorganisms for DFN biodegradation.

2. Methodology

2.1 Wastewater and sludge samples

Wastewater and sludge samples were taken from the wastewater treatment plant, Chiang Mai University (Figure 1). Wastewater was collected from the influent and the sludge was collected from the sludge dewatering machine. Both wastewater and sludge samples were kept at 4°C to maintain the sample condition before used in further experiments. Same samples were used throughout all experiments within one month to ensure the same microbial activity in the samples.

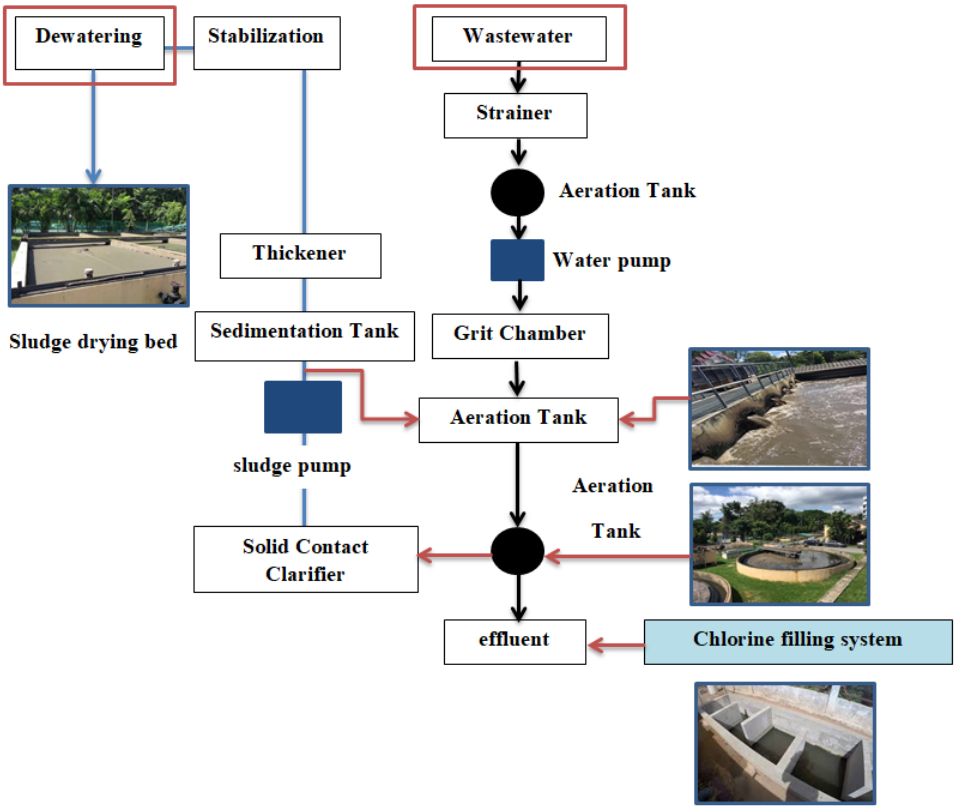

Figure 1. Schematic diagram of the wastewater treatment plant, Chiang Mai University.

2.2 DFN removal experiments

The experiments were divided into three groups: the control to determine abiotic degradation of DFN (de-ionized (DI) water+DFN), the biodegradation by wastewater (WW+DFN), and the biodegradation by wastewater and sludge (WW+Sludge+DFN). DFN was purchased as 2-[2-(2,6-dichlorphenyl) amino] benzene acetic acid sodium salt in powder form (HPLC grade, purity >98.5%, Sigma-Aldrich). DI water was added to the DFN vial to prepare a stock solution of 1,000 mg/L. The DFN

stock solution was kept in dark at 4°C before use. The solution was diluted with DI water to the desired concentrations to be used in the experiments.

In each experimental group, the experiment was conducted in 250-mL Erlenmeyer flasks wrapped in aluminum foil to prevent DFN degradation by light during the experiment. Each flask consists of 100 mL of sterile DI water or wastewater added with DFN to the final concentrations of 0, 0.1, 0.5, 1, 5 and 10 mg/L. Sludge was weighed for 3.3 g (wet weight) before added into the flasks of the experiments requiring the sludge. The flasks were then shaken at 100 rpm at room conditions (25-33°C) for 5 days. Two milliliters of sample were taken at day 0, 1, 2, 3, 4, and 5 for the measurement of DFN concentration by the High-performance liquid chromatography (HPLC), in which the methods are described below. Each experiment was replicated with two flasks, and two samples were taken from each flask. The data were then averaged from those four samples.

To determine the DFN removal by the biomass of the sludge, the adsorption experiment was conducted. The sludge was autoclaved (121°C, 30 min, 15 psi) before used in the experiment. The sterile sludge was added to the wastewater containing DFN (WW + Sludge (sterile) + DFN). The experiment was done in the same manner as the biodegradation by wastewater and sludge mentioned above.

2.3 Determination of diclofenac by HPLC

The 2-mL sample obtained from the experiments was filtered through a nylon syringe filter (0.2 µm of the pore size). The filtered sample was analyzed for DFN by HPLC with the UV detector (Agilent 1100 VWD). The conditions used in the HPLC are as follows: Hypersil ODS reverse phase column (125 × 4.0 mm, 5 µm), the mobile phase of acetonitrile:DI water: formic acid (25 mM) (55:40:5, %v/v), the flow rate of 0.5 mL/min, and the wavelength for DFN detection at 276 nm. The stock solution of DFN diluted to various concentrations was analyzed and the data were used to conduct a standard curve to find the remaining concentration of DFN. The results of DFN removal were described as a C/C_0 curve, where C is the diclofenac concentration at the sampling day and C_0 is the concentration of diclofenac at day 0.

3. Results and Discussion

DFN in DI water at low concentrations were degraded or decomposed around 10-20% (Figure 2(a)). However, higher concentrations of DFN (1, 5, and 10 mg/L) showed no decomposition in DI water, which means that any removal of DFN at these concentrations in further experiments should be from wastewater or sludge.

Interestingly, DFN in wastewater showed low to no degradation within 5 days of the experiments (Figure 2(b)). At the DFN concentrations of 0.1 and 0.5 mg/L, the removal efficiencies at day 5 were 31.26% and 46.18%, respectively. When the DFN concentrations were increased to 1, 5 and 10 mg/L, no degradation occurred. Higher degradation of DFN in wastewater than in DI water could be from the biodegradation of microorganisms in wastewater; however, the microbial activity might not be sufficient for complete biodegradation to occur.

Interestingly, when the sludge was added with wastewater, DFN degradations at day 5 were increased to 96.93% and 100% for 0.1 and 0.5 mg/L of DFN, respectively (Figure 2(c)). It was found that DFN degradation efficiency decreased as the concentrations increased. Comparing day 5 data, the degradation efficiencies decreased to 87.92, 66.59%, and 51.43% for 1, 5, and 10 mg/L of DFN, respectively. It should be noted that most of the degradation occurred within the first day of the experiment. This shows the effectiveness of the sludge to remove DFN from wastewater. Since the sludge can contain numerous species of microorganisms, biodegradation of DFN is possible to occur. A previous study showed that environmental bacteria were able to degrade DFN through hydroxylation reactions with almost complete mineralization (Stylianou et al., 2018). Therefore, relying on diverse microorganisms in sludge should be the approach to obtain a complete DFN degradation in wastewater.

To prove that the sludge removed DFN by biodegradation, the adsorption of DFN by the sterile sludge was observed, and the results are described in Figure 3.

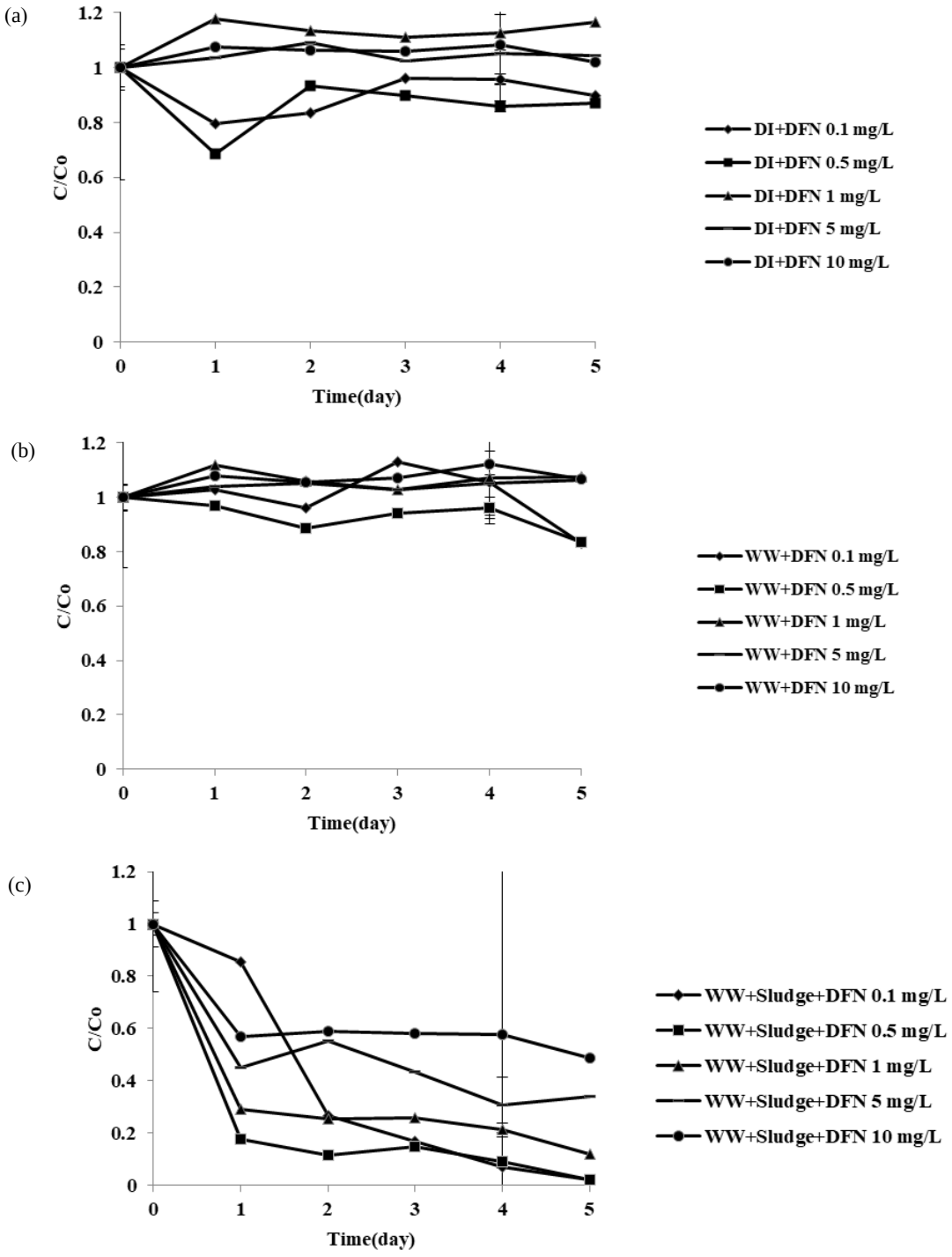

Figure 2. DFN degradation by wastewater and sludge: (a) control (DI + DFN), (b) wastewater (WW + DFN), and (c) wastewater and sludge (WW + Sludge + DFN).

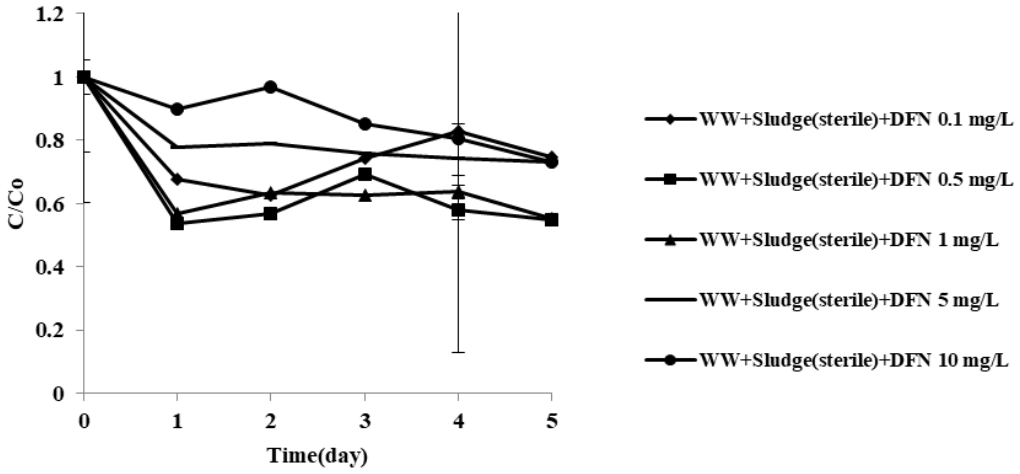

Figure 3. DFN adsorption by sludge

It was found that highest DFN removal efficiencies were as follows: 37.42% at day 2 for 0.1 mg/L, 46.14% at day 1 for 0.5 mg/L, 44.70% at day 1 for 1 mg/L, 26.76% at day 5 for 5 mg/L, and 26.99% at day 5 for 10 mg/L. The removal efficiencies were higher than those in the wastewater alone (Figure 2(b)), which means that DFN could be adsorbed onto the biomass of the sludge. However, the removal efficiencies were still lower than those in the active sludge (Figure 2(c)), proving that DFN was largely removed by the biodegradation process. The data of the DFN removal efficiencies from all experiments are summarized in Table 1. It is obvious that the activated sludge will play an important role in the wastewater treatment system in order to remove the emerging contaminant such as DFN.

Table 1. DFN removal efficiencies at day 1 and day 5 of all experiments.

Experiment	DFN concentration (mg/L)	% Removal at day 1	% Removal at day 5
DI+DFN	0.1	5.11 ± 0.01	5.92 ± 0.00
	0.5	0.00 ± 0.02	0.00 ± 0.02
	1	0.00 ± 0.06	0.00 ± 0.06
	5	0.00 ± 0.19	0.00 ± 0.17
	10	0.00 ± 0.14	0.00 ± 0.51
WW + DFN	0.1	0.00 ± 0.00	0.00 ± 0.00
	0.5	0.00 ± 0.03	0.00 ± 0.02
	1	0.00 ± 0.01	0.00 ± 0.02
	5	0.00 ± 0.11	0.00 ± 0.05
	10	0.00 ± 0.21	0.00 ± 0.12
WW + Sludge + DFN	0.1	31.22 ± 0.00	96.93 ± 0.00
	0.5	85.02 ± 0.00	100 ± 0.00
	1	70.89 ± 0.02	87.92 ± 0.01
	5	55.97 ± 0.10	66.59 ± 0.31
	10	50.81 ± 1.36	51.43 ± 0.33
WW + Sludge (sterile) + DFN	0.1	32.15 ± 0.02	25.34 ± 0.00
	0.5	46.14 ± 0.03	45.18 ± 0.02
	1	43.31 ± 0.04	44.70 ± 0.16
	5	22.10 ± 0.08	26.75 ± 0.06
	10	10.25 ± 0.67	26.99 ± 0.20

4. Conclusions

This study observed the biodegradation efficiency of DFN in wastewater from a wastewater treatment plant of Chiang Mai University. The addition of the activated sludge from the plant along with wastewater was also conducted to improve DFN biodegradation. Results showed that DFN in wastewater was not biodegraded over 5 days of the experiment. In contrast, when 1 g of activated sludge was added, 96.93 and 100% of the degradation were observed at 0.1 and 0.5 mg/L of DFN, respectively. It was found that increasing the DFN concentrations resulted in lower degradation efficiency. In conclusion, DFN should not be biodegraded in wastewater; however, it should be degraded by the activated sludge system in the wastewater treatment plant.

Acknowledgement

This research was supported by CMU Junior Research Fellowship Program, Chiang Mai University.

References

Backhaus, T., Porsbring, T., Arrhenius, A., Brosche, S., Johansson, P., Blanck, H. (2011). Single-substance and mixture toxicity of five pharmaceuticals and personal care products to marine periphyton communities. Environmental Toxicology. 30(9), 2030-2040

Chen, JB., Gao, HW., Zhang, YL., Zhang, Y., Zhou, XF., Li, CQ., Gao, HP. (2014). Developmental Toxicity of Diclofenac and Elucidation of Gene Regulation in zebrafish (Danio rerio). Ecological Environmental Sciences. Rep. 4, 4841

Deng, Y., Ezyske, C.M.(2011). Sulfate radical-advanced oxidation process (SR-AOP) for simultaneous removal of refractory organic contaminants and ammonia in landfill leachate. Water Research, 45(18), 6189-6194.

Domaradzka, D., Guzik, U., Wojcieszyńska, D. (2015). Biodegradation and biotransformation of polycyclic non-steroidal anti-inflammatory drug. Environ Sci Biotechnol, 229-239.

Inderfurth, N., Veuskens, T., Schraa, G., Blokland, M., Kujawa-Roeleveld, K., Rijnaarts, H. (2013). Microbial Removal of the Pharmaceutical Compounds Ibuprofen and Diclofenac from Wastewater. Research Article. ID 325806, 9

Kosjek, T., Heath, E., Kompare, B. (2007). Removal of pharmaceutical residues in a pilot wastewater treatment plant. Analytical and Bioanalytical Chemistry. 387, 1379–1387

Li,W., Nanaboina, V., Zhou, Q., Korshin, G.V. (2012). Effects of Fenton treatment on the properties of effluent organic matter and their relationships with the degradation of pharmaceuticals and personal care products. Water Research. 46(2), 403-412.

Lishman, L., Smyth, SA., Sarafin, K., Kleywegt, S., Toito, J., Peart, T., Lee, B., Servos, M., Beland, M.,Seto, P. (2006). Occurrence and reductions of pharmaceuticals and personal care products and estrogens by municipal wastewater treatment plants in Ontario, Canada. Science of The Total Environment.367(2-3), 544-558.

Memmert, U., Peither, A., Burri, R., Weber, K.,Schmidt, T., Sumpter, JP., Hartmann, A. (2013). Diclofenac: New data on chronic toxicity and bioconcentration in fish. Environmental Toxicology. 32(2), 442-452

Stylianou, K., Hapeshi, E., Vasquez, M., Despo Fatta-Kassinos., & Vyrides, I. (2018). Diclofenac biodegradation by newly isolated Klebsiella sp. KSC: Microbial intermediates and ecotoxicological assessment, Microbial intermediates and ecotoxicological assessment, Journal of Environmental Chemical Engineering. 6(2), 3242-3248

Song, W., Cooper, W.J., Peake, B.M., Mezyk, S.P., Nickelsen, M.G., O'Shea, K.E. (2009). Free-radical-induced oxidative and reductive degradation of N, N0 - diethyl-m-toluamide (DEET): Kinetic studies and degradation pathway. Water Research. 43, 635-642.

Stülten, D., Zühlke, S., Lamshöft, M., Spiteller, M., (2008). Occurrence of diclofenac and selected metabolites in sewage effluents. Science of The Total Environment. 405(1–3), 310-316

Rosal, R., Rodríguez, A., Perdigón-Melón, JA., Petre, A., García-Calvo, E., Gómez, MJ., Agüera, A., Fernández-Alba, AR. (2010). Occurrence of emerging pollutants in urban wastewater and their removal through biological treatment followed by ozonation. Water Research. 44(2), 578-588

Vasquez, MI., Michael, I., Kümmerer, K., Fatta-Kassinos, D. (2016). Bioassays Currently Available for Evaluating the Biological Potency of Pharmaceuticals in Treated Wastewater. Wastewater Reuse and Current Challenges. 49-80

Yu, H., Nie, E., Xu, J., Yan, S., J. Cooper, W., Song, W. (2013). Degradation of Diclofenac by Advanced Oxidation and Reduction Processes: Kinetic Studies, Degradation Pathways and Toxicity Assessments, Water Research. 47 (5), 1909-1918.

Potential of Ethanol-to-jet (ETJ) in Accordance with Carbon Offsetting and Reduction Scheme for International Aviation (CORSIA)

Tadpong Ratanasoponchai[a*], Weerin Wangjiraniran[b]

[a]Energy Technology and Management, Graduate School, Chulalongkorn University, Chaloem Rajakumari 60 Building (Chamchuri 10 Building), M1 Floor, Soi Chula 12, Phayathai Road, Phatumwan, Bangkok 10330, Thailand
[b]Energy Research Institute, Chulalongkorn University, 12th Floor Institute Building III, Phayathai Road Pathumwan Bangkok 10330, Thailand

Abstract

The purposes of this study were to evaluate and determine economic and technical potential of ethanol used for the biojet fuels from Ethanol-to-jet (ETJ) technology, which has been enlisted from 2021 to 2035, whether this can be worth developing to serve the carbon offsetting for CORSIA. The international aviation data were used to determine the overall the biojet's ethanol demand from fuel quantities, ICAO maximum blending ratio acceptance and carbon emission using sensitivity analysis, the total ethanol consumption to determine annually overall ethanol demand excluding biojet fuels, and the quantities of ethanol production in Thailand. The stock from ethanol producer was additionally applied for the investigation of the supply potential of ethanol. The result of this study has revealed that the economic potential under the normal scenario has the potential to develop the technology to serve biojet fuels. Similarly, under the COVID-19 scenario, has also shown the potential to develop this technology to serve this biojet fuels. Regarding the technical potential, under the normal scenario, it was appeared the possibility of the ethanol insufficiency on the long run even including the stock of ethanol producer until the post-period of CORSIA timeframe. Meanwhile, under the COVID-19 scenario revealed that Thailand was possibly produce sufficient ethanol demand after the mid-period of CORSIA timeframe. However, on year 2025-2027 shows that there was a possibility of ethanol shortage due to excessive demand.

Keyword: CORSIA/ Biojet Fuels/ Ethanol/ Ethanol-to-jet pathway/ Sensitivity Analysis/ International Aviation

---

*Corresponding Author: Tadpong Ratanasoponchai
E-mail address: 6282006420@student.chula.ac.th

1. Introduction

Ethanol-to-jet biofuels, does Thailand have potential or worth to invest on or develop Ethanol-to-jet pathway technology to serve Carbon offsetting from International aviation under the Carbon Offsetting and Reduction Scheme for International Aviation (CORSIA)? And does Thailand have sufficient Ethanol production to serve Biojet fuels?

CORSIA or Carbon Offsetting and Reduction Scheme for International Aviation is the mechanism accepted by United Nations Framework Convention on Climate Change (UNFCCC) for global aviation carbon emission, developed by the International Civil Aviation Organization (ICAO) and adopted in October 2016. Its goal is to have a carbon neutral growth from 2020. CORSIA uses Market-based environmental policy instruments to offset CO_2 emissions: aircraft operators have to purchase carbon credits from the carbon market. Starting the Pilot phase in 2021, the scheme is voluntary for all countries until 2027, and Thailand was voluntarily attending this scheme during the Baseline phase since year 2019.

The International Civil Aviation Organization (ICAO) has set ambitious goals for reducing greenhouse gas emissions (GHG) in the aviation sector (ICAO, 2016). These have been managed by the Carbon Offsetting and Reduction Scheme for International Aviation (CORSIA) (ICAO, 2020), and the use of Alternative Jet Fuels (AJF) is one strategic way to achieve these goals (ICAO, 2017). (Rafael S. Capaz, 2021)

Biojet fuel production is the process of producing renewable liquid fuel for aviation applications. The renewable fuel can be produced from various biomass from plants, animals, wastes, and residues (Cheng Tung Chong, Jo-Han Ng, 2021).

The objective of this study was to analyze the potential of Ethanol in Thailand by evaluating the feasibility of Alcohol-to-jet, Ethanol-to-jet pathway technology along with the sufficiency of Total Ethanol demand, Ethanol production, Ethanol stock and biojet demand. To determine whether the Ethanol supply in Thailand was potentially sufficient to uphold Total Ethanol demand and biojet demand.

2. Methodology

2.1 CORSIA Carbon Offsetting Requirements

The State shall calculate, for each of the operators attributed to it, the amount of CO_2 emissions required to be offset in a given year prior to consideration of the CORSIA eligible fuels: (Annex 16 Vol. IV Part II Chapter 3, 3.2)

$$OR_y = \%S_y * (OE_y * SGF_y) + \%O_y * (OE_y * OGF_y)$$

Where; OR_y=Offsetting requirements in year y; OE_y=CO_2 emissions covered by CORSIA in year y; SGF_y=Sector's Growth Factor; OGF_y = Individual growth factor; $\%S_y$=Percent sectoral in year y; $\%O_y$=Percent individual in year y.

In this study, due to the confidentiality issues, we are assuming the total summation of all international aviation data as 1 operator (1 sector). Thus, the operator's requirement for year y (from 2021) could be written as below:

$$OR_y = OE_y \times \frac{(SE_y - SE_{B,y})^*}{SE_y}$$

Where; OR_y=Offsetting requirements for Operator in year y; OE_y=Operator's CO_2 emissions covered by CORSIA in year y; SE_y=Sectoral emissions, with route-coverage by CORSIA in year y; $SE_{B,y}$=Sectoral emissions in baseline (av. 2019/2020) with route-coverage by CORSIA in year y; *We assumed $\frac{(SE_y - SE_{B,y})}{SE_y}$ as sectoral growth factor (SGF).

For the baseline of CO_2 emissions (the average emission of year 2019 and 2020), the international emission data given by CAAT was used on year 2019 and assumed the growth from year 2019 to 2020 to 4.15% (Kasetsart University, Mechanical Engineering Dpt., Executive Summary, February 2020). The scenario for aviation industry has been predicted that the situation of aviation industry might be recovered to the situation as year 2019 on year 2024**.** Then, calculated the average emission by finding the average emission of year 2019 and year 2020 as the ceiling of CO_2 emission on year 2021 to the end of CORSIA timeframe (year 2035) (Krungsri Research, Industry outlook: Aviation industry year 2021-2023).

2.2 Ethanol Potential Analysis

In this study, the Potential analysis consists of 2 parts, Economic and Technical Potential Analysis.

For Economic Potential Analysis, there were 2 scenarios, normal and COVID-19 scenario to determine whether the Ethanol-to-jet fuels worth/feasible to develop in Thailand under the CORSIA. The input data for Economic Potential Analysis are:

- Jet-fuel price.
- Carbon Credit Price (CDM-based).
- Ethanol-to-jet Technology cost.
- Maximum Blending Ratio for Ethanol-to-jet.
- International Aviation Carbon Emission.

For Technical Potential Analysis, there were also 2 scenarios, normal and COVID-19 scenario to determine whether Thailand Ethanol production is potentially sufficient to serve all Ethanol-to-jet fuels under the CORSIA. The input data for Technical Potential Analysis are:

- Ethanol consumption demand, stock and producer supply.
- Biofuels (ULG) consumption projection.
- Maximum Blending Ratio for Ethanol-to-jet.
- International Aviation Carbon Emission.

2.3 Sensitivity Analysis/Scenario Analysis

Sensitivity analysis is the tool to gauge how the inference originating from a model is dependent upon the assumptions and parameters feeding into it.

Scenario analysis is a qualitative method to analyze future events by considering possible outcomes (Duinker & Greig, 2007).

The usage of scenario analysis is not limited by hypotheses, so it is flexible enough to analyze and forecast uncertain development.

Scenario analysis considers potential conditions and emergencies as many as possible and provides evidence for decision-makers as much as possible (Fan Zhang, 2021).

In this study, there were 2 scenarios for Economic Potential Analysis, normal and COVID-19 scenarios and 2 scenarios for Technical Potential Analysis, Clear and Cloud scenarios. These scenarios explained as follow:

Normal scenario (N), indicates the International Carbon Emission normally without COVID-19 pandemics involved. This scenario determines Total Ethanol from biojet and International aviation emission under Normal situation without COVID-19 influenced.

COVID-19 scenario (C), indicates the International Carbon Emission under the COVID-19 pandemics concurrent. This scenario determines Total Ethanol from biojet and International aviation emission under the COVID-19 pandemics concurrent.

Clear scenario (1), indicates energy consumption behavior which people is changing their lifestyle with seriously concern on environment. Digitalization becomes indispensable. Self-sustain & prosumer are the majority of transformation. Economic is driven mainly by new S-curve. Bio & Circular economies are growing. Energy business is moving toward market competition. Sustainability & 2DC target become the priority for national policy. (ERI & PTT, Thailand Energy Scenario towards Sustainability 2050)

In other words, this scenario was written based on E20 ethanol blending ratio on gasoline demand based. (ERI & PTT, Thailand Energy Scenario towards Sustainability 2050)

Cloud scenario (2), indicates energy consumption behavior which people lifestyle is changing gradually in accordance to digitalization trend. Clean & potential tech disruption are growing so fast, but still cannot take the majority. No significant structural changes in economy, industry, energy business. Impact on pollution & GHG emission is getting worst.International regulation with environment concern come in force. Current policies on clean & smart energy come in place based on energy security. (ERI & PTT, Thailand Energy Scenario towards Sustainability 2050)

In other words, this scenario was written based on ethanol-target based as mentioned on AEDP2018. (Ministry of Energy, AEDP2018, Oct 2020)

In this study we have a total of 4 scenarios, N1, N2, C1 and C2. We called N1 as Normal-clear scenario, which means the Emission and biojet demand were based on Normal Scenario and Total ethanol consumption was based on Clear Scenario. And the other scenarios were following the same.

Each of the input parameters will be varied as follow:

- Jet-fuel price, considered on Flat price rate and US-EIA Jet-fuel price projection rate.
- Carbon Credit Price (CDM-based), considered on Max. and Min. price per tCO_2e.
- Ethanol-to-jet Technology cost, considered on Max. and Min. technology cost per liter.
- Maximum Blending Ratio for Ethanol-to-jet and International Aviation Carbon Emission, considered on normal and COVID-19 scenario to predict the total jet fuels under the CORSIA, then using Maximum Blending Ratio for Ethanol-to-jet from ICAO to calculate back to Maximum Ethanol quantities.
- Ethanol consumption demand, calculated by using the production target on year 2035, published by OCSB.
- Ethanol stock and producer supply, after year 2020, the stock was assumed to be remained the same as year 2020 until 2035.
- Biofuels (ULG) consumption projection, calculated by using the ratio of Ethanol consumption in ULG on each scenario, and total ethanol demand on year 2018 to July 2021. Then, find the average ratio of each case. The calculated ratio will be used as divisor for each respective case and scenario.

3. Results and Discussion

3.1 The Prediction of Carbon Offsetting Requirements with Maximum Ethanol demand for biojet fuels.

The Prediction of Carbon Offsetting Requirements indicates the amount of Carbon Emission under the CORSIA from year 2021 to 2035, and the baseline emission, which calculated by the average of the summation of the emission on year 2019 and predicted emission on year 2020. The emissions on each year which exceed the baseline emission must be offsetting using Carbon Credit scheme accepted by the ICAO.

The Predicted Carbon Emission considered in 2 scenarios, under the Normal scenario, and under the COVID-19 scenario.

Under these scenarios, assuming the constant aviation growth of 4.15% until year 2035 for Normal scenario, and assuming the aviation industry status to be recovered as year 2019 on year 2024 given the constant aviation growth of 4.15% for COVID-19 scenario. The emission for each scenario and baseline emissions have been predicted as shown on Figure A and B.

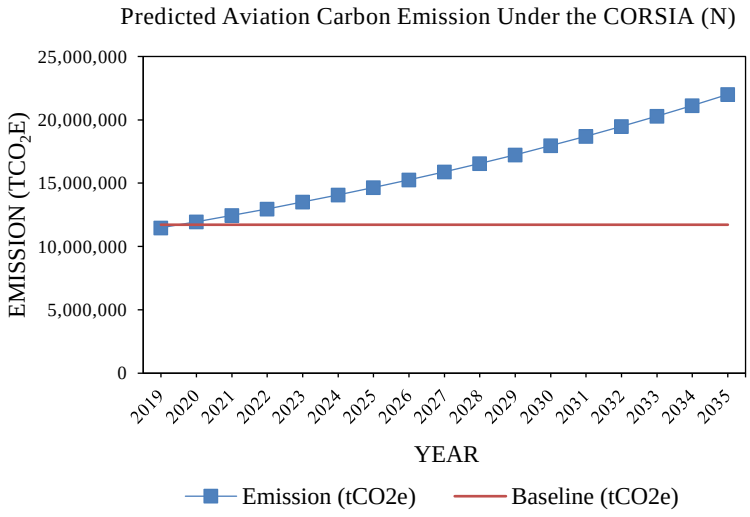

Figure A. The predicted amount of Carbon Offsetting Requirements and Baseline Emission under the CORSIA (N)

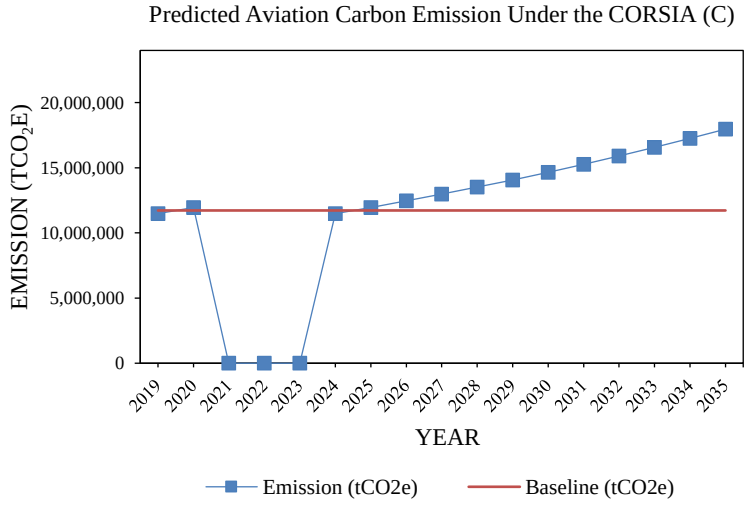

Figure B. The predicted amount of Carbon Offsetting Requirements and Baseline Emission under the CORSIA (C)

3.2 Prediction of overall Ethanol consumption

The Prediction of overall Ethanol consumption indicates overall demand excluded Ethanol-to-jet fuels in order to evaluate the sufficiency of Ethanol in Thailand. In this study, there are 2 assumptions for prediction, using the ratios to be predicted as follow:

- The Ethanol from ULG Simulation (Clear scenario (1)) : Total Ethanol consumption ratio
- The Ethanol from ULG Simulation (Cloud scenario (2)) : Total Ethanol consumption ratio

The overall Ethanol consumption was predicted by using the average ratio from each assumption from January 2018 to July 2021. These ratios were used as divisor for each assumption in order to calculate total overall Ethanol consumption. The Total ethanol consumption based on Clear scenario on Y2035 was 2,530 Million Litres and 2,580 Million Litres on Cloud Scenario.

3.3 The Economic Potential of Ethanol

The Economic Potential of Ethanol was considered on various dimensions. In this study, the Economic Potential was focused on the Jet-fuel price, the Ethanol-to-jet (ETJ) Technology cost, and the Carbon Credit price. By varying ETJ Technology cost and Carbon Credit Price compared with Jet-fuel Flat-rate price and Jet-fuel with US-EIA Projection rate price to determine whether the Ethanol-to-jet fuels was worth developing or investing. The conclusion of Economic Potential of Ethanol has been summarized as shown on Figure C and D.

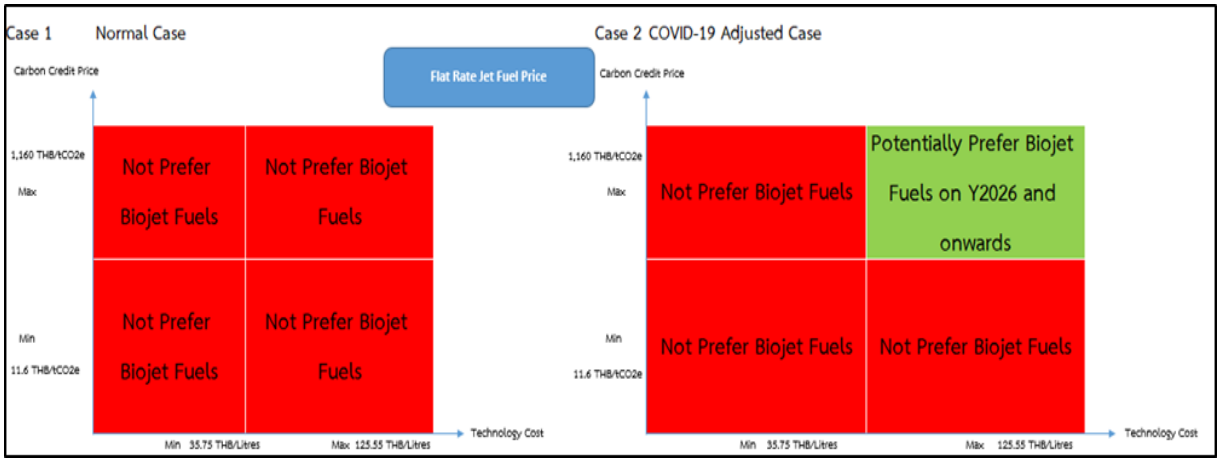

Figure C. The Economic Potential of Ethanol under each scenario by considering Flat Rate Jet fuel Price.

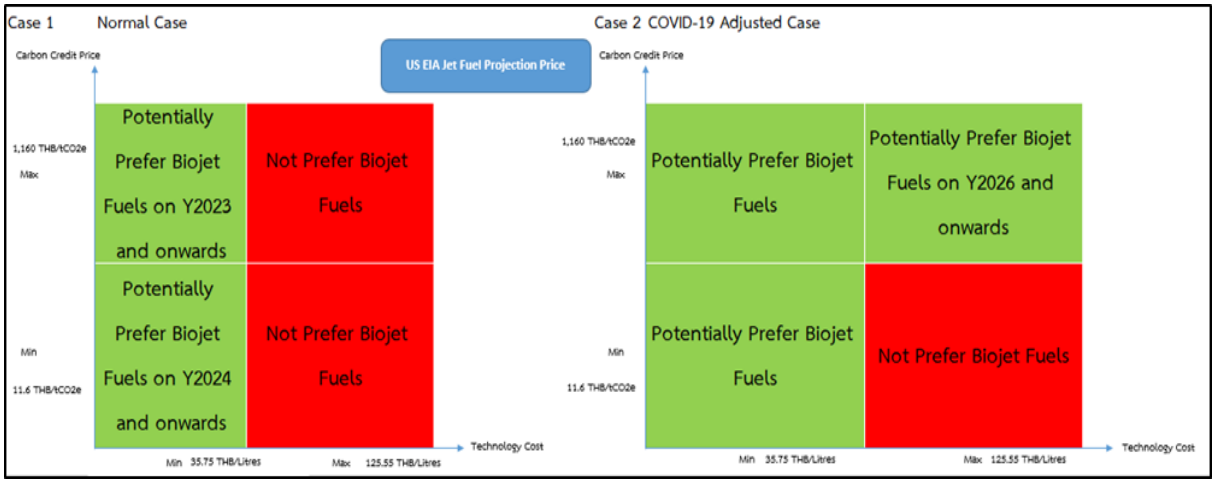

Figure D. The Economic Potential of Ethanol under each scenario by considering US EIA Jet fuel Projection Price.

3.4 The Technical Potential of Ethanol

The Technical Potential of Ethanol was considered on the sufficiency of Ethanol demand and Ethanol production, ethanol supply and stock. By comparing the Ethanol supply (from Ethanol Production and Producer Stock) and Total Ethanol demand (from overall Ethanol consumption and Total Ethanol for Biojet), the results was shown on Figure E to H.

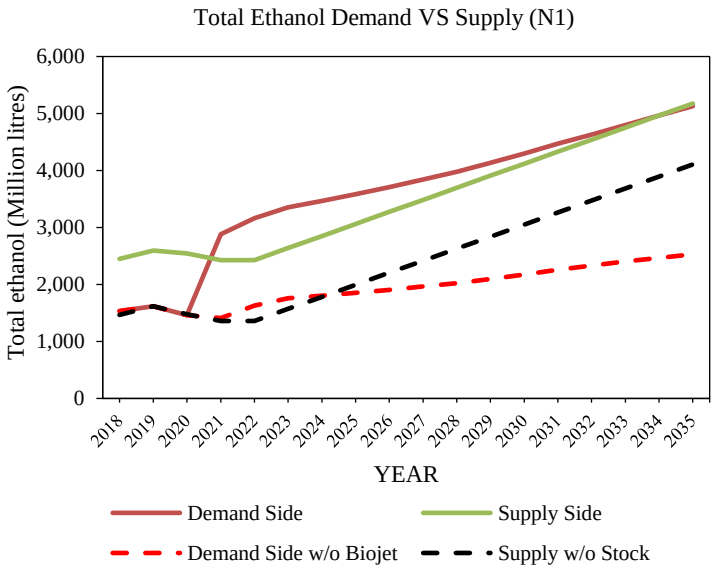

Figure E. The Technical Potential of Ethanol with the consumption prediction under Ethanol use in ULG and Total Ethanol consumption Ratio (N1)

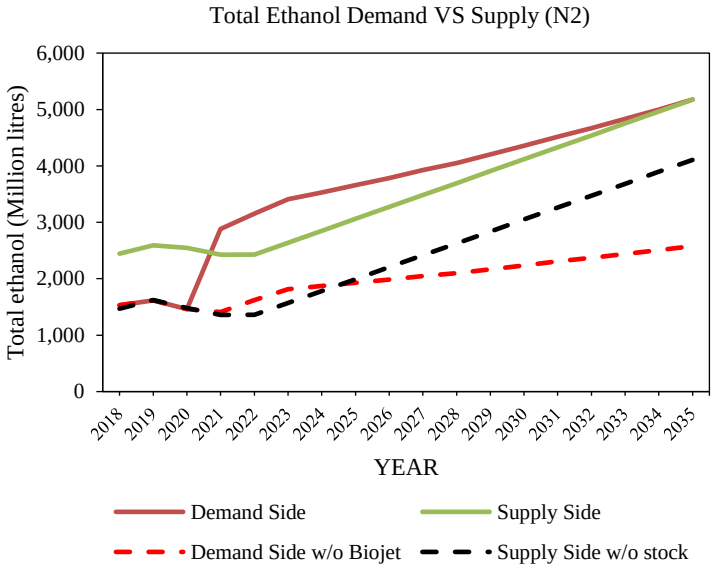

Figure F. The Technical Potential of Ethanol with the consumption prediction under Ethanol use in ULG and Total Ethanol consumption Ratio (N2)

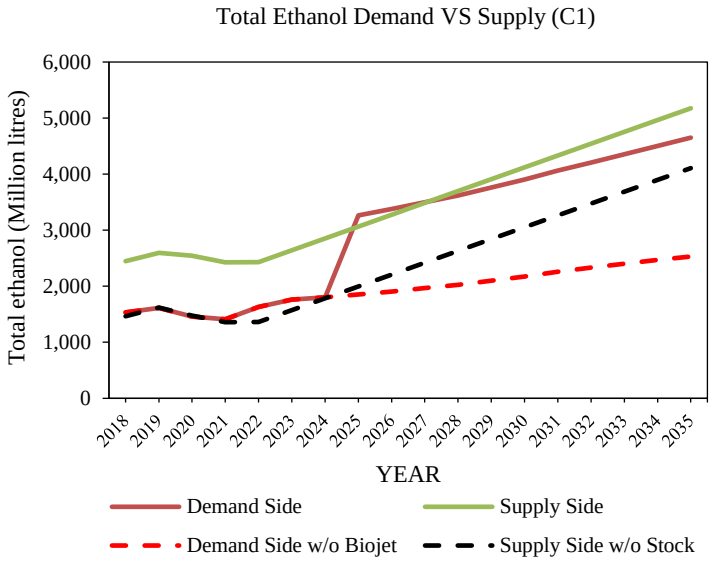

Figure G. The Technical Potential of Ethanol with the consumption prediction under Ethanol use in ULG and Total Ethanol consumption Ratio. (C1)

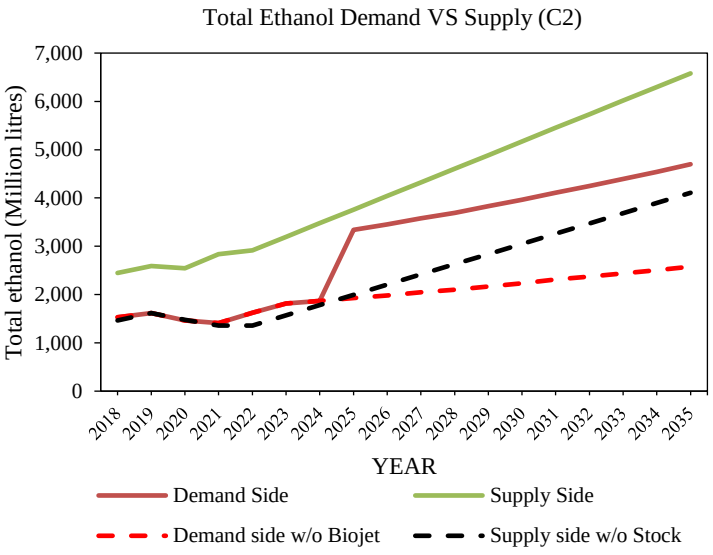

Figure H. The Technical Potential of Ethanol with the consumption prediction under Ethanol use in ULG and Total Ethanol consumption Ratio. (C2)

4. Conclusions

In this study, the Potential of Ethanol was evaluated by considering the Economic Potential of Ethanol, and the Technical Potential of Ethanol. The conclusions upon the scenarios could be as follows:

CDM Carbon credit price (1,160 THB/tCO_2e) on year 2023 and onwards. There were cases that the Ethanol supply cannot hold upon overall Ethanol demand on the post period

Normal Scenario Perspective (N-Perspective) – The Ethanol-to-jet Technology was potentially preferred upon the possibly lowest technology cost (35.75 THB/Litre) on year 2024 at the Minimum CDM Carbon credit price (11.6 THB/tCO_2e) and at the Maximum of CORSIA timeframe, the ethanol supply might not be sufficiently served overall ethanol demand.

COVID-19 Scenario Perspective (C-Perspective)-The Ethanol-to-jet Technology was potentially preferred upon the possibly lowest technology cost (35.75 THB/Litre) with Minimum and Maximum Carbon Credit Price (CDM) (11.6-1,160 THB/tCO_2e) and preferred upon the highest technology cost (125.55 THB/Litre) and Maximum Carbon Credit Price (CDM) (1,160 THB/tCO_2e). There was some case that show ethanol supply might be shortage. However, the ethanol supply can hold upon overall Ethanol demand when passing the mid-CORSIA timeframe period.

Acknowledgements

I would like to give my gratitude to CAAT for providing us the International Aviation data, as well as DEDE whose publish the ethanol production data. This study could not have done without these data.

References

CAAT, Aviation Fuel consumption and Emission Data Year 2019, 18 February 2021.

Cheng Tung Chong, Jo-Han Ng, Biojet Fuel in Aviation Applications, Chapter 2 - Biojet fuel production pathways, 2021.

Department of Alternate Energy Development and Efficiency, Monthly Ethanol Database, year 2018 to July2021.Available:https://www.dede.go.th/ewt_news.php?nid=55608&filename=index [Accessed on 16 September 2021]

Department of Mechanical Engineering, Kasetsart University, Executive Summary, Sustainable Aviation Biofuel Study, February 2020. Available:http://e-lib.dede.go.th/mm-data/BibA11646_%E0%B8%A3%E0%B8%B2%E0%B8%A2%E0%B8%87%E0%B8%B2%E0%B8%99%E0%B8%89%E0%B8%9A%E0%B8%B1%E0%B8%9A%E0%B8%AA%E0%B8%B8%E0%B8%94%E0%B8%97%E0%B9%89%E0%B8%B2%E0%B8%A2.pdf. [Accessed on 16 September 2021]

EASA, Carbon Offsetting and Reduction Scheme for International Aviation (CORSIA), Available: https://www.easa.europa.eu/eaer/topics/market-based-measures/corsia [Accessed on 16 September 2021]

Energy Research Institute & PTT, Thailand Energy Scenario towards Sustainability 2050, Diesels and ULG consumption model and scenarios, 15 July 2020.

ICAO Secretariat, ICAO Regional Workshop on CORSIA, Session 6: CORSIA Offsetting Requirements.

ICAO. Annex 16 Vol.4 SARPs Oct 2018, CO2 offsetting requirements Part 2 Chapter 3.2 (p. II-3-2).

Krungsri Research, Industry Outlook: Aviation Industry Year 2021 to 2023, Available: https://www.krungsri.com/th/research/industry/industry-outlook/logistics/air-transport/IO/io-Air-Transport-21 [Accessed on 16 September 2021]

Ministry of Energy, Alternate Energy Developing Plan 2018 (AEDP2018), October 2020.

Office of the Cane and Sugar Board, Ministry of Industry, Ethanol situation (September 2018)

Rafael S. Capaz, The carbon footprint of alternative jet fuels produced in Brazil: exploring different approaches, 2021.

Thailand Greenhouse gas Organization, Carbon Market, Carbon Credit Price (CDM) Available: http://carbonmarket.tgo.or.th/index.php?lang=TH&mod=Y2hhcnQ=&action=bGlzdA== [Accessed on 16 September 2021]

US Energy Information Administrative, Annual Energy Outlook 2021, Table 3. Energy Prices by Sector and Source, Jet Fuel Price Projection. Available: https://www.eia.gov/outlooks/aeo/data/browser/#/?id=3-AEO2021&region=1-0&cases=ref2021~aeo2020ref&start=2019&end=2050&f=A&linechart=~~ref2021-d113020a.29-3-AEO2021.1-0~aeo2020ref-d112119a.29-3-AEO2021.1-0&map=aeo2020ref-d112119a.3-3-AEO2021.1-0&sourcekey=0 [Accessed on 16 September 2021].

Site Selection for Feasibility Study of Pump-Storage Hydropower Project in the Philippines

Sornsawan Utthakrue[a*] and Thitisak Boonpramote[b]

[a]Energy Technology and Management, Chulalongkorn University, Bangkok, Thailand
[b]Department of Mining and Petroleum Engineering, Faculty of Engineering, Chulalongkorn University, Thailand

Abstract

Pumped-storage hydropower project (PSP) is a technology for hydroelectric energy storage. It is a design of two water reservoirs at different elevations that can create electricity as water flows from one to the other via a turbine. Additionally, the system requires electricity to pump water back into the top reservoir. The PSP system is similar to a huge battery, even though it can store and then release energy as needed. The Philippines is a country with a wide range of altitudes and a frequent occurrence of natural disasters, making it challenging to build any structure. A massive structure with long life and the ability to generate a large amount of energy at a high price. Therefore, this research will concentrate on the initial stage of identifying areas suitable for PSP by means of a distant investigation of two significant conditions: geography and geology. The feasibility of PSP also includes economic and financial models.

There are three research areas located throughout the region's islands: Luzon (L), Visayas (V), and Mindanao (M). The result shows only the upper reservoir, the lower is natural water; (L), Lat: 14.395 N and Lon: 121.388 E; (V), Lat: 10.368 N and Lon: 123.743 E; and (M), Lat: 8.142 N and Lon: 123.658 E. To analyze PSP, we use a DCF model with a 25-year concession period. The results of this research show that the net present value is 541 (L), 430 (V), and 1,337 (M) million USD, the internal rate of return is 13.26% (L), 12.98% (V), and 18.83% (M), respectively, and the benefit-cost ratio is perhaps 1.56 (L), 1.53 (V), and 2.27 (M). The payback project will last 8 (L), 8 (V), and 6 (M) years. Therefore, the project is feasible for economic and financial.

Keyword: Feasible study/ Geography/ Geology/ PSP/ Pump-storage hydropower project/ Site selection/ Electricity/ Financial model/ Philippines

---

*Corresponding Author: Sornsawan Utthakrue, Tel: +66-974-199-822
E-mail address: sornsawan.ut@gmail.com

1. Introduction

The hydroelectric power plant is a technology ability to produce high energy. On the other hand, this technology requires analysis in a variety of technical, environmental, and financial sectors, including hydraulics, civil construction, environmental and social, and so on. However, this research focuses on the preliminary stage before proceeding to the next step, which is a desk study analysis of feasible sites for a pump-storage hydropower project (PSP). When this stage is completed, the developer and owner of the project can continue to the next stage.

A pump-storage hydropower project is a type of hydropower electric plant in which the technology may provide a large amount of energy over a long period of time at a cheap cost. As shown in Figure 1, hydropower has a lower levelized cost of energy (LCOE) than other energy sources (0.04 USD/kWh). PSP is a technology that began in the 1890s in Switzerland and Italy and has since spread worldwide, especially to high-tech countries like Germany, the United States, Japan, and China. As shown in Figure 1, In comparison to the other sources of electricity in Figure 2, PSP is the most efficient method of storing capacity electricity (batteries).

Water is important on a worldwide scale because of its impact on the population and economy. Figure 3 depicts a study on GDP and the economy by seasonality. Agriculture and GDP are related to the percentage of rainfall, and hydropower plants are also related to the percentage of potential to expand the country.

However, because water does not exist in many areas, PSP is the best choice of technology for drought areas to keep water and create power at the same time. In Switzerland, for example, this technology stores water in reservoirs during the summer and generates power during the winter.

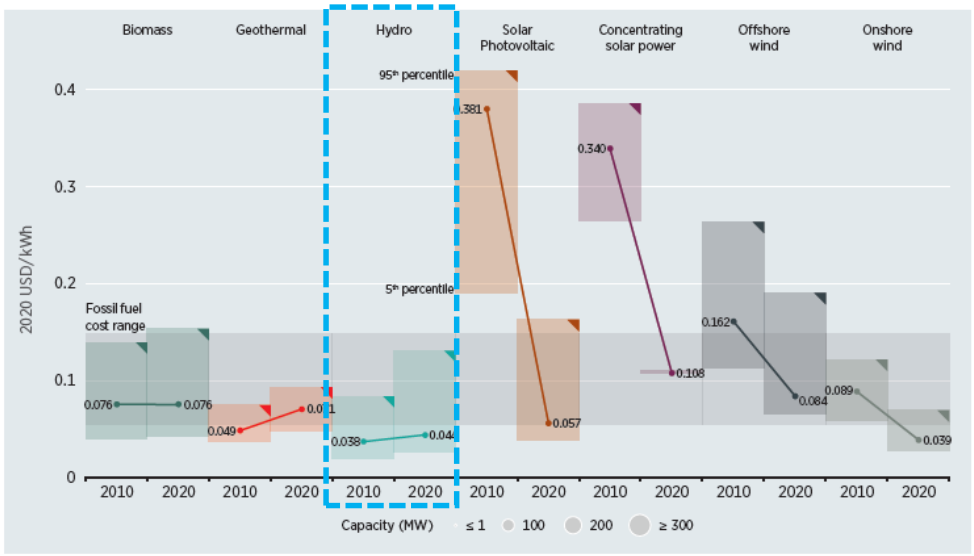

Source: IRENA Renewable Cost Database

Figure 1. Global LCOEs from newly commissioned, utility-scale renewable power generation technologies, 2010-2020. (IRENA 2020 report) [6]

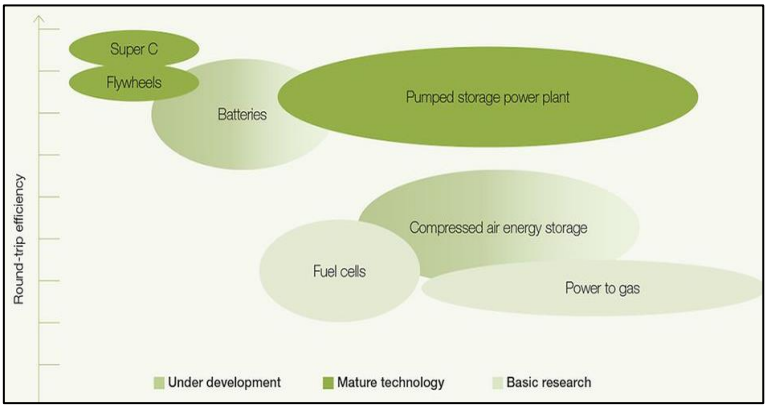

Figure 2. Electricity storage technology source capacity comparison. (*Andritz).*

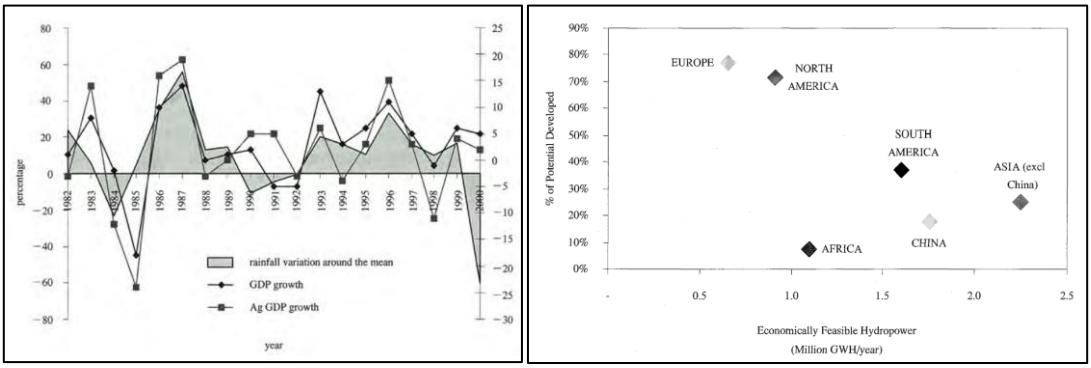

Figure 3. Left = the amount of rainfall and its impact on GDP growth and agricultural GDP growth, Right = Economically Feasible Hydropower. [7]

According to a 2019 population survey, the Philippines has a population of roughly 108 million people, which is expanding each year. As a result, the rapid growth of the population has an impact on excessive energy consumption [3]. However, PSP can store enough energy to meet the peak demand of the Philippines in a variety of circumstances.

The significance of location in relation to PSP is that reservoirs with upper-lower locations serve as a repository for gravitational potential energy, as shown in Figure 4. During times of peak demand, water will flow from the upper reservoir into the lower reservoir, through a turbine (at the powerhouse), generating expensive electricity. Although pumping water between reservoirs uses between 15% and 30% of the energy supplied, it nonetheless generates revenue for each project.

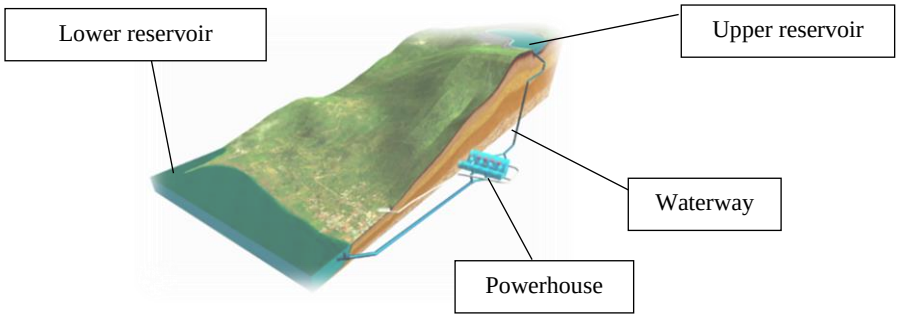

Figure 4. An example of a 3D model of a PSP's primary component. [9]

The cost-effectiveness analysis project necessitates economic management and finance; an analysis technique is followed by the selection of the project site. The Discount Cash Flow Model (DCF) was computed using the following assumptions: construction spending, project costs, project operations, the annual power sales price, and estimated annual power output. This research is preliminary in nature because it collects and analyzes data in order to discover prospective areas for developing a PSP project that will be included in the financial model. Following that, the data analysis results for each location will be compared to a financial model. To predict future development costs, this research will divide the study area into three regional areas: Luzon, Visayas, and Mindanao.

2. Methodology

The research examines the viability of developing a PSP with a capacity of more than 500 MW. The methodology is designed with a focus on the initial phase of desk research. Whereas, the Philippines is a large country with islands separating it from the mainland. As a result, the research will be divided into three study areas, one for each of the islands indicated in Figure 5. Then start research as the step in the flowchart of Figure 6.

- Study area 1 = Luzon
- Study area 2 = Visayas
- Study area 3 = Mindanao

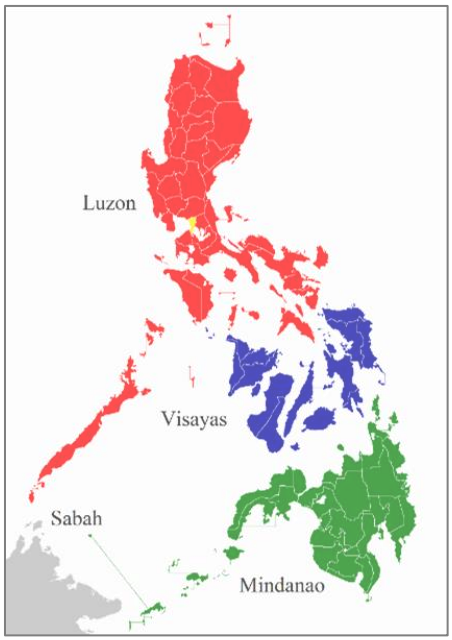

Figure 5. Regional map of the Philippines

Main Parameters Given:

1. The capacity of PSP = > 500 MW.
2. Construction period = 4-5 years (2021-2026)
3. Concession operated period = 25 years (2026-2050)
4. Exchange rate PHP to USD the 4th quarter of 2021 = 50.67 PHP/USD

2.1 Data Collection

This process will utilize a GIS program to overlay vector data such as point, line, and polygon in order to generate a map related to Figure 7.

2.1.1 Geographic Information:

In the beginning, it is critical to collect geographic information systems (GIS) data; this stage must involve the collection of elevation contours and basin water data. Because the research is still in its initial phases, information can be gathered from publicly available sources at this time (Website: USGS, OSM, DIVA, etc.). For example, topography, elevation, reservoir catchment area (inland water area), roads, population, transmission lines, and administrative borders are only a few of the characteristics to consider.

2.1.2 Regional geological setting and disaster:

The second step for research is regional geology, which provides information on the tectonic setting, geology rock units, and disaster evidence (Volcanic eruption, active fault, landslide). Data is collected from PHIVOLCS and the USGS.

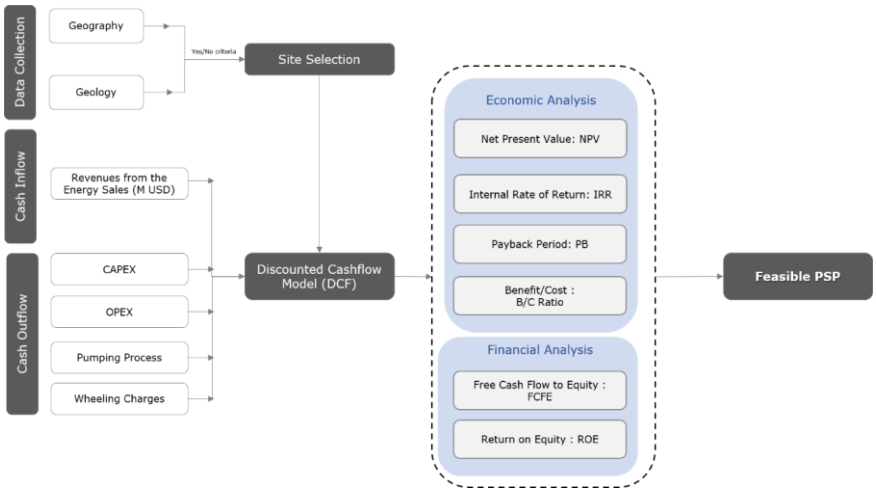

Figure 6. A flowchart of the main methodology by the author

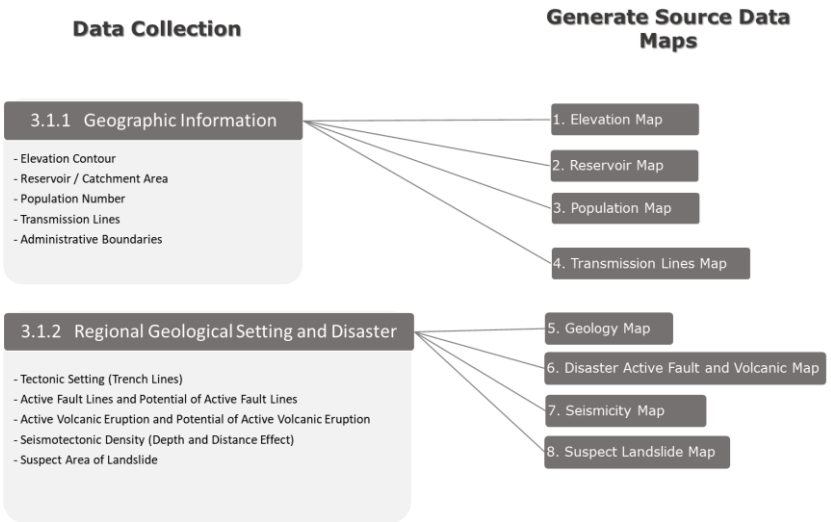

Figure 7. A list of mappings derived from the data collecting process.

2.2 Site Selection Analysis

The PSP site's potential should be properly evaluated on a stage-by-stage basis. The primary components of the chosen procedure are topography and geology. In the event of morphology and hazard detection, the site can be changed. Mapping data might provide an overview of alternate areas. The first phase in the analysis process is to generate maps in compliance with the list in Figure 7, followed by the selection of an analysis location using the Yes/No criteria in Figure 8. There are more conditions as follows;

2.2.1 Topography and General Analysis

➢ Topographic elevation (m.): An indicator of L/H is used as a reference index for site selection. [7] Where; L: Horizontal length of waterway from intake to tailrace (m); H: Difference of riverbed elevation between both dam sites (m) **The L/H is 4 to 6 times or less. These calculations may be used as a benchmark for the research if local conditions allow for the building of a tunnel at a reasonable cost.*

➢ General spatial and geographic data were obtained from publicly available databases such as OpenStreetMap and NASA, as well as the Department of Energy.

- Population density = energy demand. transmission
- Line, substation and main generator. = Low construction transportation costs
- Information such as main roads and secondary roads. = Low cost of construction.
- Geospatial and boundary data for provinces, districts, villages and other relevant areas.
- Inland water line and boundary.

2.2.2 Regional Geological Setting and Geo-hazard

Geological understanding is critical even before operators select or build a hydropower plant. Geology is critical because it illustrates how a reservoir's rock composition might leak water or how a high-quality rock can serve as an effective foundation for construction. Operators are required to conduct a thorough geological investigation. Additionally, the area should be safe from geohazards, which may be identified using publicly available information such as regional geology, seismicity records, and maps of active fault locations. However, if a company invests in PSP, additional steps may involve borehole drilling and geophysical surveys. This project's objective is to implement preliminary site assessments. The proceeds are as follows:

- Analyzing the general geomorphology's structural organization
- Tectonic analysis of the experiment region: Plate boundary structure and active faults.
- The primary geology of the experiment region is determined by utilizing geological mapping data. The experimental zone must be defined in terms of rock types. Additionally, a site is specified for the use of that rock as a construction material.
- The importance of any construction must be concerned with geo-hazards. The map has collected data on disaster-prone areas, such as those affected by landslides, earthquakes, and active volcanic eruptions. Secondly, determine the distance between the experimental area and the disaster region.

2.3 Economic and Financial Model Analysis

This stage can be examined after the finalization of the location selection. The estimated energy capacity of each PSP is based on an expected reservoir volume. The PSP is feasible through a discounted cash flow model (DCF), which can be used to generate electricity by simulated sales, a scenario in which electricity is generated during peak and off-peak hours. Furthermore, expected costs or outcomes such as capital expenditures, operational expenses, pumping charges, and transmission line fees are included.

The final step of economic and financial analysis is DCF, and this step will be carried out by an excel program utilizing the input parameters presented in Table 1.

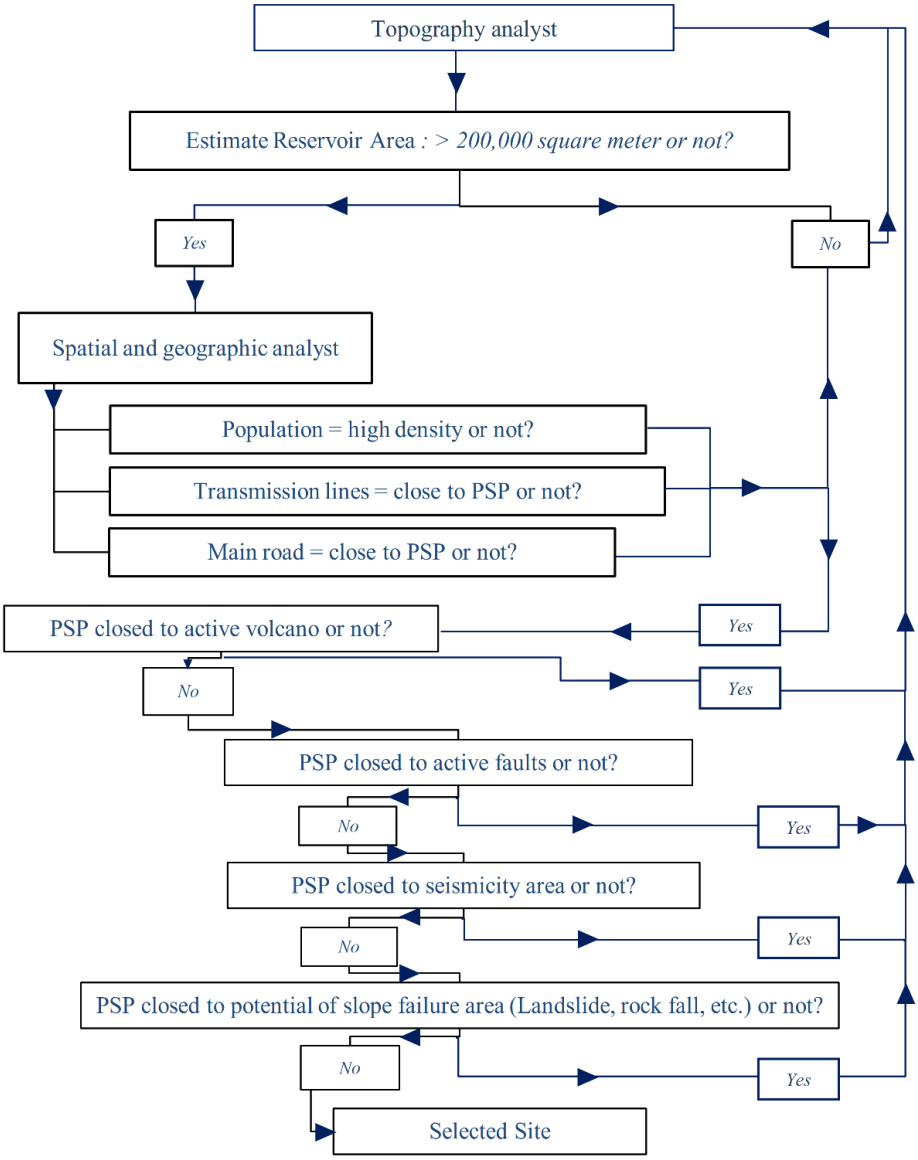

Figure 8. Flowchart of the Yes/No criterion analysis used to define site selection.

Table 1. Conclusion of financial parameters given

1. Equity	=	30%
2. Debt	=	70%
3.Discount Rate	=	9%
4. Interest on Loan	=	6%
5. Financing Charges	=	1%
6. Loan Maturity	=	10 years
7. Construction Time	=	4.5-5 years (2021-2026)
8. Depreciation and Concession Period	=	25 years (2026-2050)
9. Corporate Income Taxes	=	30%
10. VAT	=	Not included
11. Tariff Wheeling Charges	=	0.0197 USD/kWh
12. Losses	=	Availability = 98% and Own Consumption = 1.5%
13. Inflation in USD	=	2%

2.3.1 Annual Revenue

The revenue generated by the operation pattern (hours of pumping and generation each day) must be determined using the daily electricity price projection; that is, for each day of this time, the prices have been assessed (day-ahead pricing), and the daily operation pattern defined. The energy consumption/generation numbers for each day are derived using the pricing and operating pattern, as well as the pumping expenses and money generated by generation. The study will be conducted using the Belisama PSP simulation [9]. This offered historical data on which to anticipate scenario revenue for the years 2026-2050 based on the most likely market outcomes for WESM without ancillary services.

The graphs in Figure 9 and Figure 10 give an indication of the average daily profile of prices and how they change over time with growth in demand and the addition of capacity. The year 2023 represents the year when Belisama PSP [9] starts its operation, and the year 2035 represents a forecast long-term view. The National power corporation unbundled rates (NPC charges only) the average NPC effective rate by grid of each region from January to October, 2021, with Luzon=4.39, Visayas=3.74, and Mindanao=2.85. (https://www.psalm.gov.ph/home/ercrates) estimated annual expenditure and revenue by using Table 2. This data will be used to calculate a simulation of the revenue of PSP.

Table 2. Average price per region (PHP/kWh)

		Non Peak hour (10.00 pm.-9.00 am.)	Peak hour (9.00 am.-10.00 pm.)
Luzon	Monday - Saturday	2.591	6.222
	Sunday/Holiday	2.295	3.071
Visayas	Monday - Saturday	2.658	4.572
	Sunday/Holiday	2.463	3.624
Mindanao	Monday - Saturday	2.533	3.054
	Sunday/Holiday	2.470	2.946

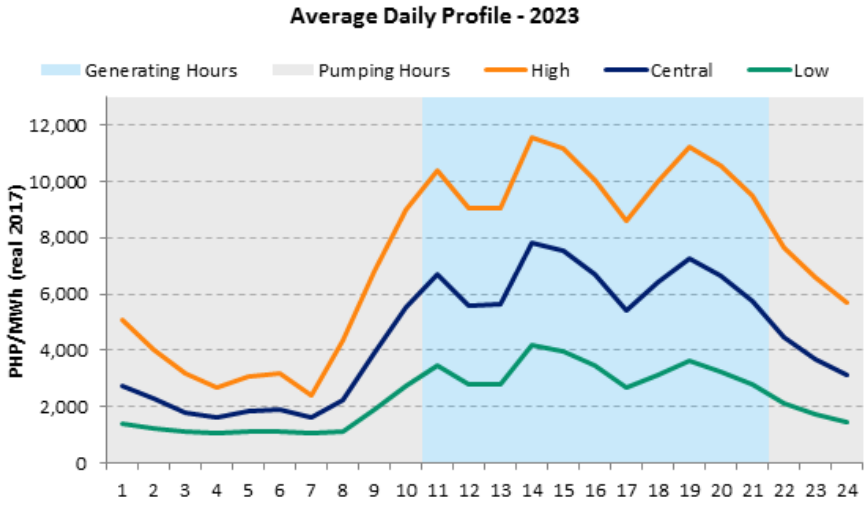

Figure 9. Average Daily Profile for the Year 2023 [9]

2.3.2 Cost Estimate

2.3.2.1 CAPEX (Construction Cost Estimate)

The construction necessitates a variety of methodologies for cost estimation. The majority of construction costs were estimated from first principles, with the resources required for various activities identified and costed using current prices, supplemented by obtaining cost estimates for various items from suppliers and

subcontractors. This included the supply and installation of the electro-mechanical equipment, with these major costs also being evaluated against historical data and current industry rates.

The cost estimate is for both direct and indirect construction costs and allows for the following main sections and components in Table 3.

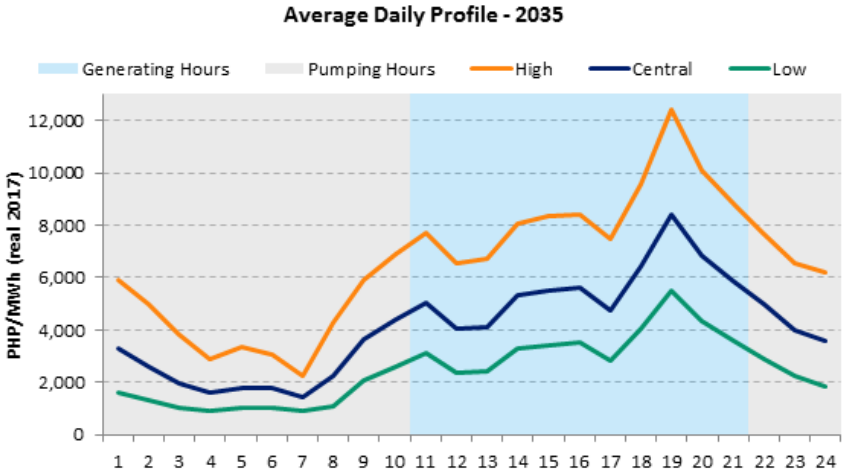

Figure 10. Average Daily Profile for the Year 2035 [9]

Table 3. CAPEX Including.

Type of CAPEX	Group of Work	Description
Direct Cost	Civil Works	Site Development
		Upper Pond
		Pressure tunnel
		Tailrace Tunnel
		Intake Lower Reservoir
		Power Cavern
		Contingencies
	Hydromechanical Works	HM in Gate chamber
		Penstock and steel liner
		Gates and trash rack lower intake
		Contingency
	Electromechanical Works	Generating equipment E&M
		Switchyard
		Transmission line (TL)
		Contingency EM
Indirect Cost	Client Administration (5% of total direct costs)	
	Engineering, Site Supervision (5% of total direct costs)	
	Detailed Design (3% of total direct costs)	
	Land Acquisition and EIA Cost (EIA ; Environmental Impact Assessment)	
	Project Development Cost	
	Insurance (2% of total direct costs)	
	Other Business Expenses (2% of total direct costs)	
	Interest during Construction (IDC) (17.52% of total direct costs)	

2.3.2.2 OPEX (Costs during operation and maintenance)

Operation and Maintenance (O&M) costs comprise the total annual expenditure incurred during the operation of the project. O&M costs are split into:

- Fixed O&M costs: Fixed operating expenses related to the type and size of the plant only, but not related to the output.
- Variable O&M costs: Expenses depend on the output of the plant.

For hydropower plants the variable O&M costs are rather small compared to fixed O&M costs. O&M costs typically include cost components for regular operation and maintenance, overhauls, staff, management and administration and insurance and fees, shown in Table 4.

Table 4. OPEX Including

Type of OPEX	Description
Cost Item	• Cost of O&M (without overhauls) • Staff Cost • Administration and Management • Insurances and Fees
Cost for overhauls (Maintenance)	Major overhaul (every 6 years) = 1.3% of CAPEX for Generating E&M Equipment
	Major overhaul (every 12 years) = 3.7% of CAPEX for E&M Equipment

*O&M=Operation and Maintenance; *E&M=Electrical and Mechanical

2.3.3 Feasible Study by Discount Cash Flow Model (DCF)

The economic and financial analysis for the PSP is discussed at this stage. The economic analysis focuses on the project's expenses and advantages. The economic cash flow definition allows for the definition of three economic indicators: IRR, NPV, and payback time. The indicators of the financial model are FCFE and ROE, as follows:

2.3.3.1 Net Present Value (NPV) measures the added value of the project in present terms.

$$NPV = \left(\sum_{t=1}^{n} \frac{C_t}{(1+r)^t}\right) - I$$

Where; I=The first investment; C=Annual cash flow; r=Discount Rate; t=Project life; n=Number of interest periods

By considering investments from the results of NPV as follows: NPV>0 : Able to invest the return on investment is greater. NPV=0: Just enough breakeven, should consider other factors besides money. NPV<0: Should be avoided The return on investment is less.

2.3.3.2 Internal Rate of Return (IRR) measures the profitability (overall rate of return) of the project (the discount rate at which the NPV of costs equals the NPV of the benefits).

$$I - \left(\sum_{t=1}^{n} \frac{C_t}{(1+r)^t}\right) = 0$$

Where; I=The first investment; C=Annual cash flow; r=Discount Rate; t=Project life; n=Number of interest periods By considering investments from the results of IRR as follows: IRR>r: Investment in that project should be made, IRR<r: investment in that project should be rejected.

2.3.3.3 Payback period measures how long the investment takes to 'pay for itself' (to reach the break-even); the time value of money is not taken into account.

2.3.3.4 B/C Ratio is an indicator showing the relationship between the relative costs and benefits of a proposed project. If a project has a B/C Ratio greater than 1.0, the project is expected to deliver a positive net present value to a firm and its investors.

B/C Ratio = Total Cash Flow Discounted ÷ Total Costs (with IDC)

2.3.3.5 Free Cash Flow to Equity (FCFE), IRR after financing; determine if dividend payments and stock repurchases are paid for with free cash flow to equity or some other form of financing. Investors want to see a dividend payment and share repurchase that is fully paid by FCFE. The free cash flow to equity (FCFE) is calculated as shown below:

FCFE = Net Income + Depreciation - Capital Costs - Payoff Loan + New Debt Issued

2.3.3.6 Return on Equity (ROE) shows how well the investment of the sponsors is used to generate profits.

$$ROE = \frac{\text{Net Income}}{\text{Equity}}$$

Where; ROE>0: Able to invest the return on investment is greater.

3. Results and Discussion

The potential area is present as the stars that are indicated in Figure 12, Figure 15 and Figure 17 are all located near natural reservoirs, indicating that they are part of the open system PSP. Because the reservoir is supplied by natural water and is located near transmission lines, construction costs can be reduced. According to the population density, this location is in high demand among consumers.

As a result, there is no risk of water leaking in the geology rock unit identified by the rock type symbol. Luzon is indicated by the QVP and R, Visayas by the IK, Pgl, and SN1, and Mindanao by the R, QVP, QV, and N3+Q1. Table 5 contains a description of each case study. Rock is a type of volcanic rock, which is an excellent choice for building foundations because of its strength and resistance to erosion. However, this is only the initial level of the desk study. In the second process of work, they must identify it through site inspection and subsurface study. This location may be relocated if a karst zone or a zone of high permeability is discovered. If we do not relocate the location, the geotechnical engineer will have to mitigate the risk by extending the excavation depth to a high quality of rock for a strong reservoir foundation.

From the result, site selection of feasibility PSPs is possible in areas far from active faults, active volcanic eruptions, and landslide susceptibility zones. Significant parameters such as seismicity were not impacted by the earthquake that was more than 5 mg. Therefore, these locations are accepted for the first step of desk study to be PSP potential.

Table 5. Regional geology, rock units

Rock Unit	Description
R	Recent alluvial, lacustrine or beach deposits.
QV	Pliocene-Quaternary, Non-active cone (general pyroxene andesite) with dacite or andesitic plugs.
QVP	Pliocene-Quaternary, Volcano plain or piedmont pyroclastic deposits.
N3-Q1	Pliocene-Quaternary, Marine and terrestrial sediments.
Pg1	Mostly quartz diorite
SN1	Oligocene-Miocene, Thick, transgressive mixed self-marine deposits: wackes, shales and reef limestone. Underlain by conglomerate and/or paralic coal.
IK	Cretaceous-Paleocene (Igneous Rocks)

3.1 Result of Study area 1; Luzon

The island's first potential PSP is located in Laguna province, near the settlement of "Dambo" and surrounded by the "Laguna de Bay" reservoir. The coordinates of the location of the lower reservoir are Lat: 14.392 N/Lon: 121.405 E and the upper reservoir are Lat: 14.395 N/Lon: 121.388 E. And from Figure 11, the upper reservoir is approximately 490 m above sea level, while the lower reservoir is around 2 m above sea level. The tunnel length is estimated to be 1800 meters. Figure 12 will

provide the location indicated in the star symbol of each map as the high potential of the selected site in Luzon. The Laguna provinces have a population density of around 3 million (3.1% of the total population).

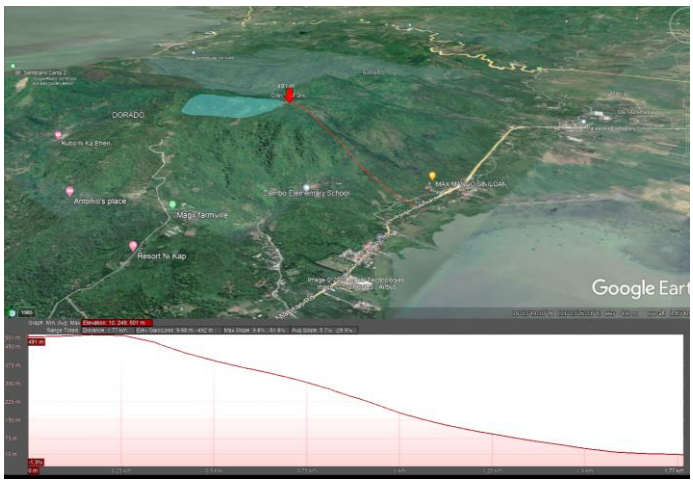

Figure 11. A satellite image of Luzon in a 3D terrain view, along with a cross-section along an estimated tunnel line. The red line represented the elevation of the terrain along the tunnel. Source: Google Earth.

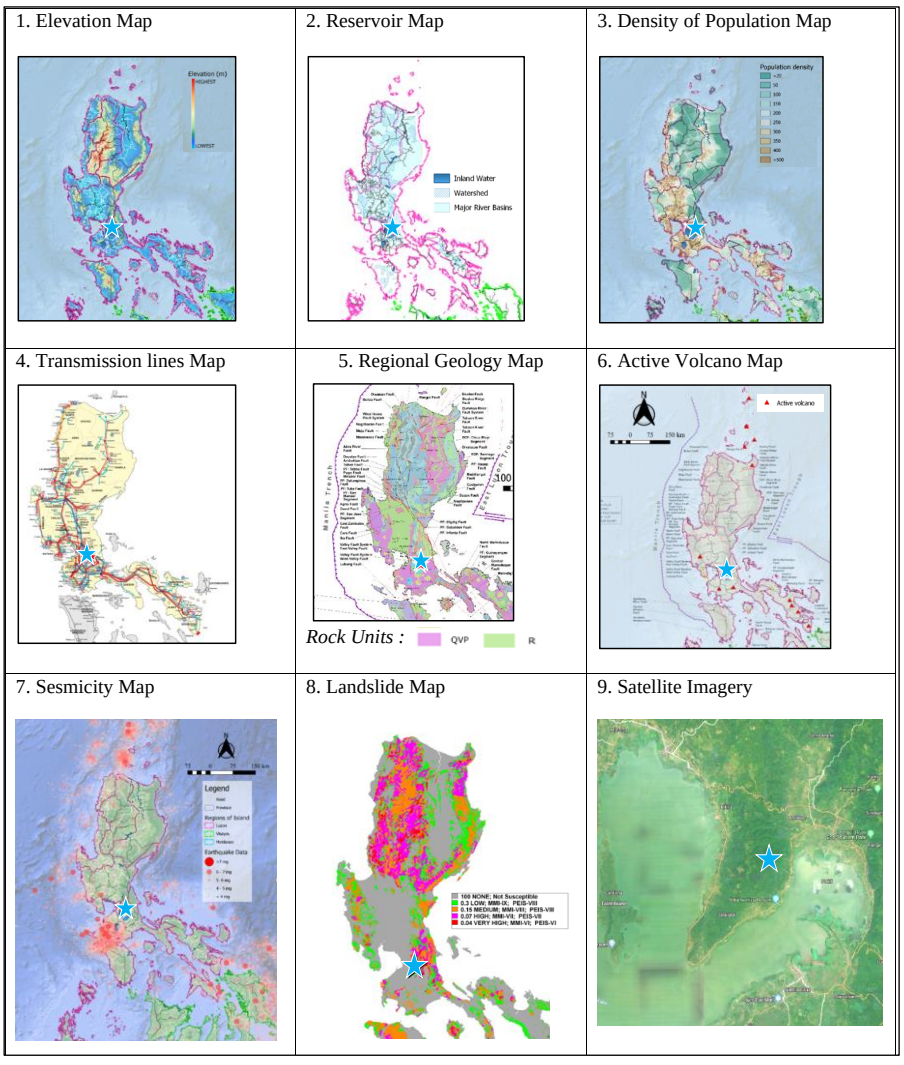

Figure 12. Comparison Maps Analysis for Luzon Area

3.2 Result of Study area 2; Visayas

The island's second potential PSP is located in Cebu province, near the settlement of "Bagakay" and closed to the "Malubog" lake. The coordinates of the location of the lower reservoir are Lat: 10.369 N/Lon: 123.726 E and the upper reservoir are Lat: 10.368 N/Lon: 123.743 E. And from Figure 13, the upper reservoir is approximately 450 m above sea level, while the lower reservoir is around 150 m above sea level. The tunnel length is estimated to be 1900 meters. Figure 15 will provide the location indicated in the star symbol of each map as the high potential of the selected site in Visayas. The Laguna provinces have a population density of around 5 million (4.72 % of the total population). This PSP has less capacity because the lower reservoir has a limited supply of water. It is incomparable to Luzon and Mindanao, which are connected to the bay with a high volume of reservoir supply.

The special feature of this location is its approach to an open-pit mine that has the potential to expand to the upper reservoir, as seen in Figure 14, assuming no operations occur in the future. The advantageous usage of this technology can result in significant cost savings associated with the excavation phase of the construction process.

This technology is already in use in the development of gold mines in Australia. The building of the Kidston Pumped Storage Hydro Project at the Kidston Clean Energy Hub in Queensland will create over 500 direct jobs and will support remote and regional businesses and communities during these difficult economic times.

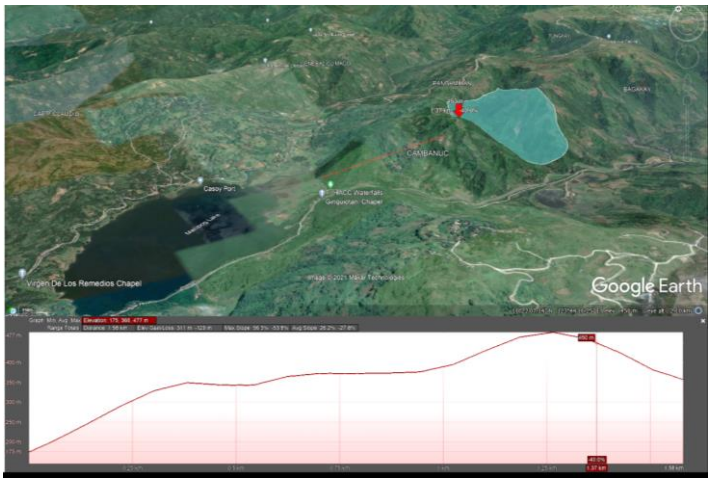

Figure 13. A satellite image of Visayas in a 3D terrain view, along with a cross-section along an estimated tunnel line. The red line represented the elevation of the terrain along the tunnel. Source: Google Earth

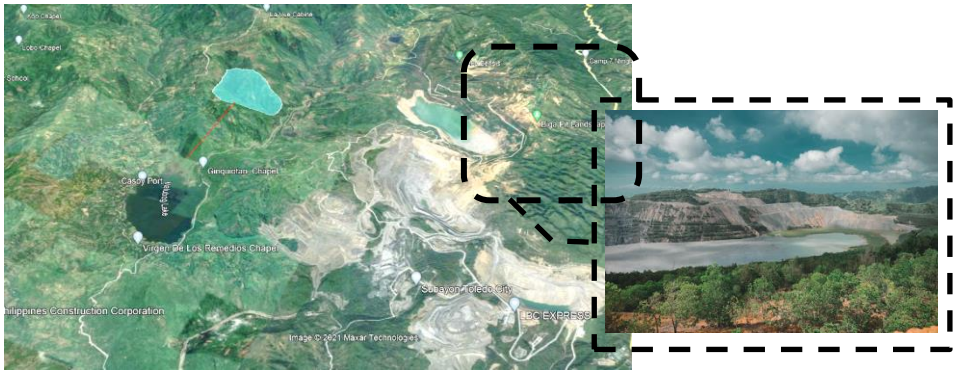

Figure 14. Another potential location with cheaper excavation costs is the upper reservoir, which is located in an open-pit mine at the same elevation. Source; Google Earth

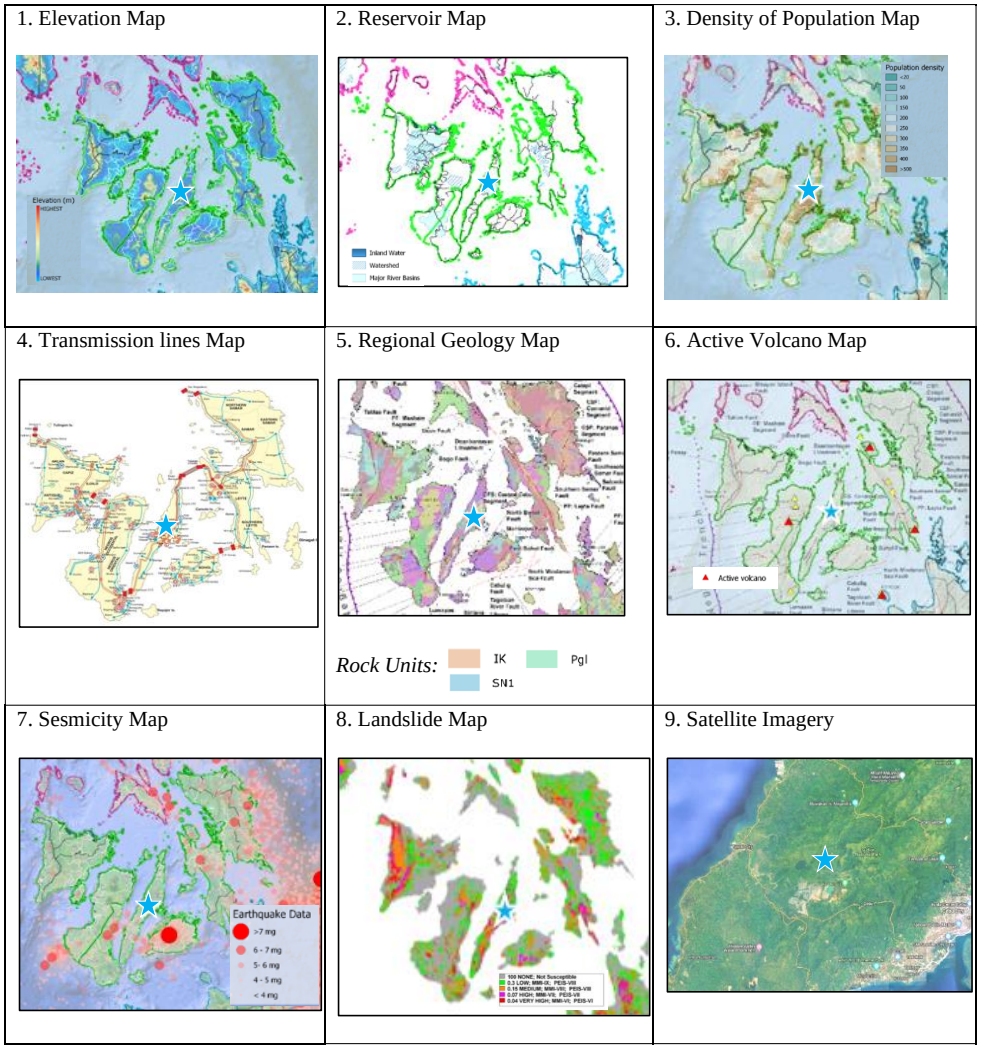

Figure 15. Comparison Maps Analysis for Visayas Area

3.3 Result of Study area 3; Mindanao

The island's first potential PSP is located in Misamis Oriental province, near the settlement of "Gala" and “San Antonio” and closed to the "Panguil Bay" reservoir. The coordinates of the location of the lower reservoir are Lat: 8.054 N/Lon: 123.711 E and the upper reservoir are Lat: 8.142 N/Lon: 123.658 E. And from Figure 16, the upper reservoir is approximately 1260 m above sea level, while the lower reservoir is around 2 m above sea level. The tunnel length is estimated to be 10,000 meters. Figure 17 will provide the location indicated in the star symbol of each map as the high potential of the selected site in Mindanao. The Misamis Oriental provinces have a population density of around 1.6 million (1.55% of the total population).

3.4 Result of Economic and Financial Model Analysis

The 21project feasibility can be assumed to be an expected capacity size for economic and financial considerations, as shown in Table 6.

3.4.1 Result of Cost Estimate

CAPEX and OPEX are the cost estimation principles. The computation assumes starting with Luzon and applying the value to Visayas (-17%) and Mindanao (+60%) of Luzon. This approximate design for a similar design is currently under construction. It consists of an upper reservoir, a waterway, and various other infrastructure components. The result is presented in Table 7.

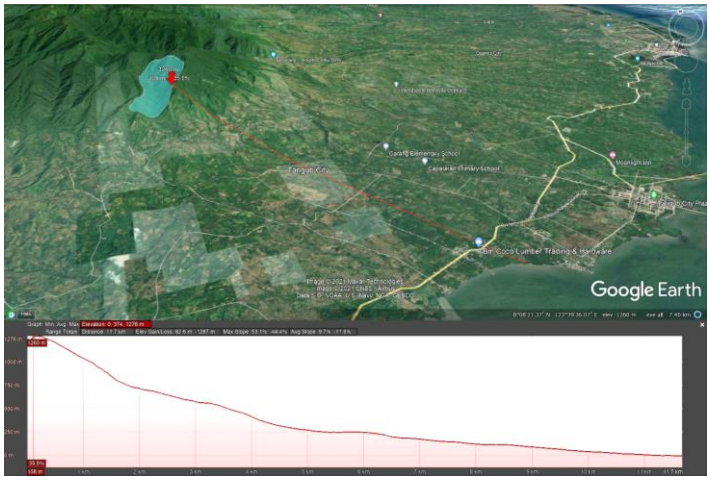

Figure 16. A satellite image of Mindanao in a 3D terrain view, along with a cross-section along an estimated tunnel line. The red line represented the elevation of the terrain along the tunnel. Source: Google Earth

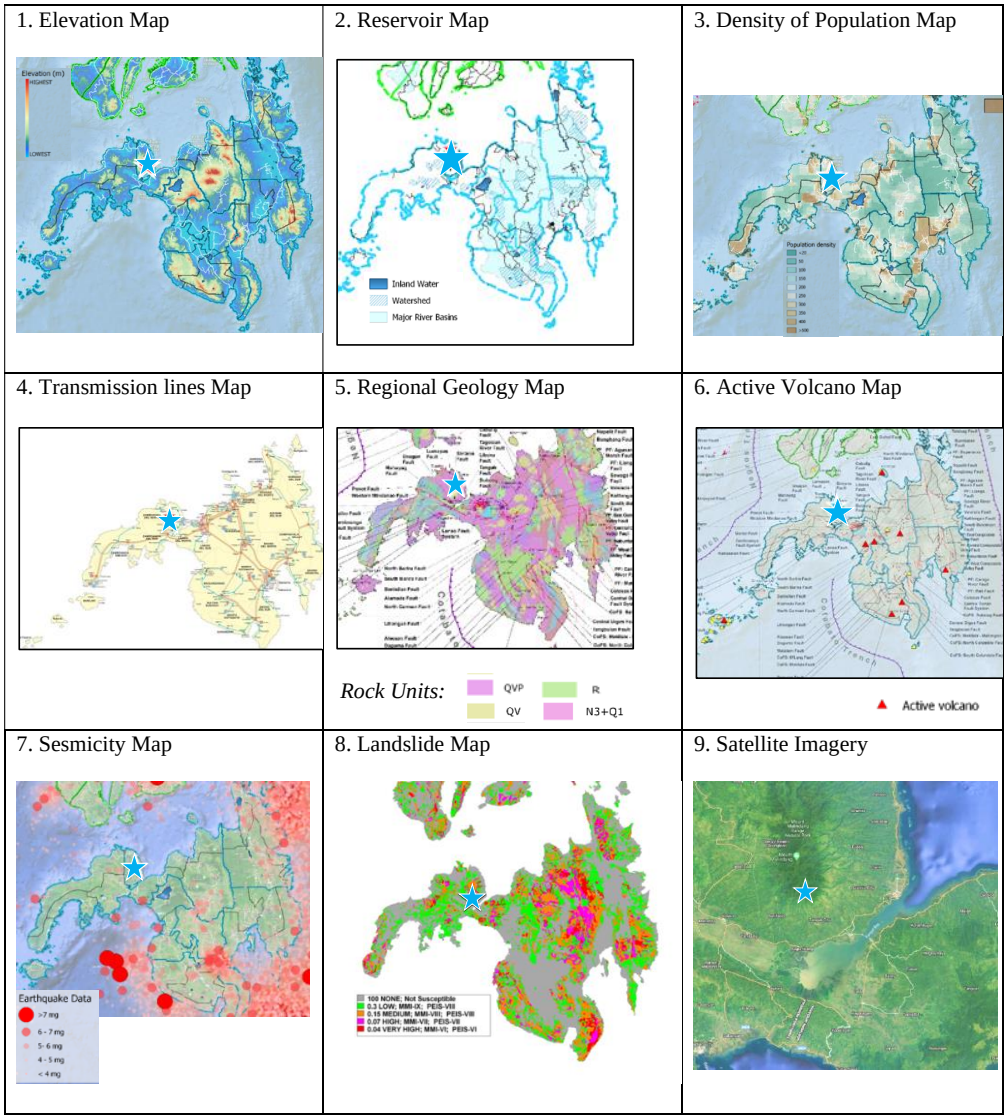

Figure 17. Comparison Maps Analysis for Mindanao Area

Table 6. Assumptions of capacity for PSP

	Installed capacity (MW)	Turbine Unit	Pump turbines per unit
Study Area : Luzon	800	4	200 MW
Study Area : Visayas	660	3	220 MW
Study Area : Mindanao	2500	5	500 MW

Table 7. The result of the CAPEX and OPEX.

Cost estimated (USD)		Luzon	Visayas	Mindanao
CAPEX	Total Civil Works	464,588,600	385,608,538	743,341,760
	Total Hydromechanical Works	40,493,913	33,609,947	64,790,260
	Total Electromechanical Works	151,480,800	125,729,064	242,369,280
	Contingencies	68,741,149	57,055,154	109,985,838
	Total Direct Costs	656,563,313	558,078,816	558,078,816
	Total Indirect Costs	241,645,656	200,565,894	386,633,049
	Total Project Costs	898,208,968	758,644,710	944,711,865
	Indirect Costs (without IDC)	126,615,763	105,091,083	202,585,221
	Indirect Costs (including IDC)	241,645,656	200,565,894	386,633,049
	Total Project Costs (without IDC)	851,920,225	720,225,053	870,649,875
	Total Project Costs (including IDC)	**966,950,117**	**815,699,864**	**1,054,697,703**
OPEX	Cost of O&M (without overhauls)	2,890,000	2,385,500	8,650,000
	Staff Cost	2,437,580	2,403,580	2,557,580
	Administration and Management	1,379,240	1,345,240	1,499,240
	Insurances and Fees	1,725,000	1,431,750	2,760,000
	Total OPEX	**8,431,820**	**7,566,070**	**15,466,820**

Another price spent during the operational phase is wheeling costs. They are calculated based on the gross of pumping (GWh/a) and output losses (percent), with 98.6% availability and an annual price of 0.0197 USD/kWh. The final cost of the process will be presented in Table 8. It includes self-consumption as well as the operation and maintenance process, which loses time due to dam maintenance.

3.4.2 Result of Economic and Financial Analysis

Table 9 shows the result of the feasibility PSP calculation of DCF indicators using Excel.

Table 8. The result of the wheeling and lossed during operation.

	Total Other Cost		Total Other Losses		
	Pumping Costs	Wheeling Charges	Own Consumption	O&M Losses	Total
Luzon	3195.70	884.25	175.92	128.65	4384.52
Visayas	2652.43	733.93	146.01	106.78	3639.15
Mindanao	5113.11	1414.80	281.47	205.84	7015.23

Table 9. The result of the DCF criteria for economic and financial analysis.

		Luzon	Visayas	Mindanao
Economic	NPV	541.32	430.09	1,337.38
	IRR	13.26%	12.98%	18.83%
	Payback period	8 years	8 years	6 years
	B/C Ratio	1.56	1.53	2.27
Financial	FCFE	12.60%	12.18%	20.66%
	ROE	29.06%	28.08%	49.77%

4. Conclusions and Recommendation

This investigation, as noted by the author in the introduction, is the preliminary stage in establishing the viable placement of PSP. However, hydropower project feasibility requires further information, such as hydraulics, power electric scenarios, civil design, and so on. The feasibility study location is chosen from among those that require a field site for more detailed data collection.

Mindanao, in particular, the location has the ability to produce a large amount of energy while also delivering advantages. This region does not have the same amount of energy consumption as Luzon. As a result, if we need to create this PSP in the future, other considerations such as infrastructure planning and city density will need to be extensively investigated. And additional research on the cost of purifying seawater for the purpose of producing electricity is necessary.

The economic and financial research analysis for three PSPs is based on the Belisama PSP [9] which includes all parameters as well as a fully simulated energy and revenue model using 2018 data. The figures may vary in the future, depending on the market share price of LCOE.

The author's contribution to this work is to give options for "Water Management" in developed countries. Numerous benefits from this research could have a positive impact on the environment, promoting clean energy and preserving the country's energy stability.

The final suggestion is that not only can this research produce the best PSP, but there are several dimensions that require in deep-learning prior to beginning the project, such as topography survey with high resolution (centimeter), investigation geology, electro-mechanical and hydro-mechanical equipment, civil design, risk assessment, and simulation of operation aspects.

The operation process will be less expensive due to "Hybrid" technology; at this time, pump-storage hydropower projects can use another technology to assist generated electricity in the pumping stage, such as solar and wind technology. This is the future energy-saving technology in combination.

Acknowledgement

This independent study was conducted effectively with the support of Mr. Braunshofer, the project manager, who provided significant advice and perspectives throughout the research process. This includes advising me on the most effective strategy for obtaining high-quality research for my project. I'm quite grateful for your support. Additionally, I would like to express my gratitude to AFRY, Thailand for giving me an abundance of information and experience.

In appreciation to my adviser, Prof. Thitisak Boonpramote (Ph.D.) for giving guidance and recommending other research techniques. Appreciate TPI Polene (Public) Co., Ltd. for providing scholarships to support students in completing full course requirements.

Finally, I would like to thank you my family for their support in the study. And it has fueled my desire to study throughout my life. Furthermore to serve as a motivation for my continued self-improvement.

References

Brandi A. Antal, B.S., University of Colorado – Boulder. (2004). Pumped Storage Hydropower: A Technical Review, May 2014, Master, Department of Civil Engineering University of Colorado Denver. Ref [1].

Department of Energy (DOE). Power Situation Report 2019. [Online]

Available : https://www.doe.gov.ph/electric-power/2019-power-situation-report. Ref [2].

Electricity Market Corporation Philippines. Annual Market Assessment Report 26 November 2019 to 25 November 2020, July 2021. Document ID: CPC.TMP.11, Version No.: 2.0, Effective Date: 05-Aug-2020, (pp. 21-22). Ref [3].

Goldsmith, K. Economic and Financial Analysis of Hydropower Projects. Norwegian Institute of Technology. Division of Hydraulic Engineering, 1993. Ref [4].

Guillaume Hennequin, Hydro, Tidal and Wave Energy in Japan. Tokyo, September 2016, Business, Research and Technological Opportunities for European Companies. Ref [5].

IRENA (International Renewable Energy Agency), (2021). Renewable Power Generation Costs in 2020, Abu Dhabi. ISBN 978-92-9260-348-9. (pp. 15). Ref [6].

Japan International Cooperation Agency, Guideline and Manual for Hydropower Development Vol. 1 Conventional Hydropower and Pumped Storage Hydropower, March 2011. (Part 1). (pp. 1-1 to 3-10). Ref [7].

National Hydropower Association. 2018 Pumped Storage Report (202), [2018]. Ref [8].

Robert Braunshofer (PM). ARFY, Thailand. (2018). 800 MW Belisama Pump-Storage Project. Addendum to the Feasibility Study, [Publish on December 2018]. Ref [9].

SEMİH ÇETİNKAYA. Capacity Determination of Pumped Storage Projects using Market Electricity Prices, Master, The Graduate School of Natural and Applied Sciences Middle East Technical University, January 2014. Ref [10].

NGCP. Transmission Development Plan 2014-2015. 2016. Ref [11].

Ashraf, U., Zhang, H., Anees, A., Mangi, H. N., Ali, M., Zhang, X., Imraz, M., Abbasi, S., Abbas, A., Ullah, Z., and Tan, S. (2021). A Core Logging, Machine Learning and Geostatistical Modeling Interactive Approach for Subsurface Imaging of Lenticular Geobodies in a Clastic Depositional System, SE Pakistan. Natural Resources Research, 30, 2087-2830.

Ashraf, U., Zhu, P., Yasin, Q., Anees, A., Imraz, M., Mangi, H. N., & Shakeel, S. (2019). Classification of reservoir facies using well log and 3D seismic attributes for prospect evaluation and field development: A case study of Sawan gas field, Pakistan. Journal of Petroleum Science and Engineering, 175, 338-351.

Bunopas, S., and Vella, P. (1983). Opening of the gulf of Thailand: rifting of continental S.E. Asia and Late Cenozoic Tectonics; Journal of Geological Society. Thailand, 6, 1-12.

Charoensrisomboon, S., and Jankaew, K. (2009). Lithostratigraphy of Mae Sod Formation, Fang Basin, Changwat Chaing Mai. BEST, 2, 87-89.

Foopatthanakamol, A., Ratanasthien, B., Petersen, H. I., Wongpornchai, P., and Utamo, W. (2008). Composition and petroleum potential of lake facies in the FA-MA-48-73 well Mae Soon structure, Fang oilfield, Northern Thailand. Journal of Petroleum Geology, 31, 317-326.

Kongurai, P. 2013. Sedimentary facies and evolution of San Sai Oil Field, Fang Basin. M.S. dissertation, Suranaree University of Technology.

Larionov, V.V. 1969. Borehole radiometry. Moscow: Nedra.

Nuntajun, R. (2009). Seismic Stratigraphy of the Fang Basin, Chiang Mai, Thailand. Chiang Mai Journal of Science, 36, 77-82.

Petersen, H.I., Nytoft, H.P., Ratanasthien, B., and Foopatthanakamol, A. (2007). Oils from Cenozoic rift-basins in central and northern Thailand. Journal of Petroleum Geology, 40, 59-78.

Settakul, N. (2009). Fang Oilfield Development. Walailak Journal of Science and Technology, 6, 1-15.

Ammonia Effects on Reproductivity of the Marine Rotifer *Brachionus rotundiformis*

Chengyan Han[a*], Hee-Jin Kim[a], Yoshitaka Sakakura[a, b], and Atsushi Hagiwara[a, b]

[a]Graduate School of Fisheries and Environmental Sciences, Nagasaki University, Bunkyo 1-14, Nagasaki, 852-8521, Japan
[b]Organization for Marine Science and Technology, Nagasaki University, Bunkyo 1-14, Nagasaki, 852-8521, Japan

ABSTRACT

Unionized ammonia (NH_3-N), a major stress factor in aquaculture facilities, rises with the expansion of species, causing culture collapse. Rotifer *Brachionus* spp. is a widely used live food for larval rearing, as well as an effective model organismfor toxicant tests. Among the marine *Brachionus* species, *B. rotundiformis* exhibits active population growth even under higher concentrations of NH_3-N during mass culture. To explain this phenomenon, we investigated the reproductive responses of *B. rotundiformis* under NH_3-N stressful conditions. Rotifers were subjected to 0-40 mg/L of NH_3-N for acute and chronic toxicity tests. The following parameters were investigated: (1) rotifer mortality after 24-h acute exposure; (2) the life history [i.e., survival, generation time, fecundity, and intrinsic growth rate (*r*)] and reproductive (i.e., the population growth rate for asexual reproduction, mixis, fertilization, and resting egg production for sexual reproduction) parameters in the chronic exposure. Finally, the median lethal concentration (24-h LC_{50}) and effective concentration (EC_{50}) on reproductive parameters were computed by probit analysis and sigmoid dose-response regression, respectively. The tested 24-h LC_{50} of NH_3-N was 26.9 mg/L. During chronic exposure, NH_3-N>17.0 mg/L suppressed rotifer population growth, as evidenced by a delayed generation time and reduced fecundity of one individual. While the sexual mixis and resting egg production were inhibited at NH_3-N≥1.1 mg/L, indicating that rotifer sexual reproduction is less tolerant to ammonia stress than asexual reproduction. The differences in sexual and asexual NH_3-N sensitivity suggest that rotifer may devote more energy to asexual reproduction to maintain their population under stressed environments.

Keyword: Rotifer/ Ammonia stress/ Reproductive patterns

---

*Corresponding Author: Chengyan Han, Tel.: +81-95-819-2830
E-mail address: bb53419803@ms.nagasaki-u.ac.jp

Carbon Footprint in the Faculty of Public Health, Mahidol University During Lockdown and Non-Lockdown Periods

N. Chareonwimonruk[a,b], W. Patthanaissaranukool[a,b], T. Neamhom[a,b], and S. Polprasert[a,b*]

[a]Department of Environmental Health Sciences, Faculty of Public Health, Mahidol University
420/1 Ratchawithi Rd., Rajchathewi, Bangkok 10400, Thailand
[b]Center of Excellence on Environmental Health and Toxicology (EHT), Bangkok 10400, Thailand

Abstract

Climate change and its effect caused by excessive anthropogenic greenhouse gas emission is a major crisis that is affecting to be severely environmental problems economic and social development around the world. Furthermore, from the end of 2019 (Dec, 2019), the COVID-19 pandemic is impacting human activities, particularly energy use and carbon dioxide (CO_2) emissions. Carbon footprint for the organization is the method used to identify direct and indirect carbon emissions from various activities of the organization and is considered as the first step towards sustainability. This study aimed to compare the carbon footprint of the Faculty of Public Health Mahidol University in the 2020 fiscal year (October 2019 – September 2020) between non-Lockdown period (196 business days: 1 October 2019 – 22 March 2020, and 1 June – 30 September 2020) and Lockdown period (47 business days: 23 March – 31 May 2020). The study covered three categories of emissions including direct carbon emission (fuel consumptions, fertilizer use and wastewater treatment process), indirect carbon emission from purchased energy (including work/study from home while Lockdown period) and other indirect emissions (water consumption, paper use, LPG and plastic bag use in cafeteria and market, waste management and commuting) related to the energy and resources used. The results showed that the carbon footprints during non-Lockdown and Lockdown periods in the Faculty of Public Health, Mahidol University were 20,594.32 $kgCO_2e$/day/period equivalent to 19.78 $kgCO_2e$/capita/day, and 15,151.03 $kgCO_2e$/day/period equivalent to 14.55 $kgCO_2e$/capita/day, respectively. The main carbon emission source in both periods was electricity consumption followed by commuting and waste management respectively. The effectively alternative implementation for minimizing the carbon footprint of this organization is energy conservation. The use of high energy-efficient appliances such as air conditioning and lighting as well as energy-saving campaigns to reduce the power consumption such as turning off the appliance when not use were introduced. The overall carbon footprint achieved during Lockdown period was lower than that of the prior.

Keyword: Carbon Footprint for Organization/ Faculty of Public Health/ Mahidol University/ Non-Lockdown period, and Lockdown period

---

*Corresponding Author: Supawadee Polprasert
E-mail address: supawadee.pol@mahidol.ac.th

1. Introduction

Greenhouse gas emissions continue to rise and accumulate in the atmosphere, causing the increasing global average temperature of at least 1°C warmer than pre-industrial level. The climate change situation is a major crisis that is affecting to be severely environmental problems such as biodiversity loss, extreme weathers events, causing severe impacts on economic and social development around the world. Furthermore, the coronavirus COVID-19 pandemic is the defining global health crisis of this time. The COVID-19 pandemic is impacting human activities, and in turn energy use and carbon dioxide (CO_2) emissions. The COVID-19 pandemic has imposed a number of dramatic impacts on all sectors of the global economy (Filimonau et al., 2020). The sector of higher education is also affected from government Lockdown in part of teaching and learning and administrative system. All campuses are closed and prohibited student and staff mobility, coupled with teaching, and learning system delivered completely online.

Thailand as a party to the UNFCCC intends to cooperate through various national plans and policies on the climate change dimension by encouraged all Thai sectors into a low-carbon society (NESDB, 2020). In its

Nationally Determined Contribution (NDC), Thailand committed to reducing 20-25% of emissions from the energy, transport, waste, and industry sectors by 2030 below business as usual. (ONEP, 2019). In the same way, all types of organizations are significant contributors to international greenhouse gas emissions including academic institutions.

Mahidol University has established a strategy for sustainable management by creating a policy to promote the creation of an Eco University. Accordingly, the evaluation of the Carbon Footprint Organization has been introduced as a method that can be used for identifying directly and indirectly carbon emissions from various activities of the organization. Furthermore, it can identify the main significant source of carbon emission from an organization's activities and their relevant mitigation schemes to minimize the carbon emission. However, during Lockdown situation, the teaching and other relevant activities in the faculty was changed to online. Therefore, the carbon emission is also altered. The comparative of carbon emission of online and face-to-face education was evaluated for discovery the appropriate practice to reduce the carbon emission. The carbon footprint can also expand its role to promote a low-carbon concept for the organization by improving its facilities and practice as well as carbon offsetting. Accordingly, it can be considered as the first step towards sustainability and can be suggested as the guideline for the management of carbon emission reduction (TGO, 2020). Additionally, the results of this study can be revealing the main activities of the faculty with the highest carbon emissions. This leads to appropriate and effective measures to minimize greenhouse gas emissions, also being a guideline for other academic institutions. Also served the country's target of Paris agreement in reducing 20-25% of emissions by 2030 below business as usual, as previously ratified with the UNFCCC.

2. Methodology

2.1 Faculty of Public Health, Mahidol University

Located at Mahidol University Phayathai Campus, Bangkok Thailand. Consists of 13 departments with 9 buildings. In addition to learning/teaching, there are also other role such as center of health and public health and environmental services for general health promotion service and environmental health promotion including safety in work job and industrial hygiene. The faculty has a health promotion center that provides health promotion and patients' screening diseases prevention for people and being the practice center on promotion of students' health. Moreover, also being the academic leader for country development, provide academic assistance, academic services, and short training for Asia Pacific countries. In terms of academic services, the faculty has operated in urban, rural, and industrial areas. (Mahidol University, 2020)

In the academic year 2019, the Faculty of Public Health has graduates in several majors from bachelor, master, and doctoral degrees 361, 299 and 66 students respectively, and 315 academic and support staffs (updated 31 January 2019). (Mahidol University, 2019)

2.2 Mahidol University Lockdown

The Bangkok Lockdown was ordered on 22 March 2020. As a part of the order, the Faculty of Public Health, Mahidol University had moved all learning working and operation to online system and not allowed to access University facilities since 23 March - 31 May 2020 (47 business days). While 172 support staff remained on campuses for administrative, security, and maintenance only as necessary.

2.3 Study design

This study was designed as analytical survey research to evaluate the carbon footprint of the Faculty of Public Health, Mahidol University under two periods including non-Lockdown and during Lockdown period. The carbon emission was analyzed following the carbon footprint organization guidelines of Thailand Greenhouse Gas Management Organization (TGO), which is based on the ISO 14064-1 (2006), GHG Protocol (2001 and 2004) and some examples from ISO/PDTR 14069 (2013) adopt to the Thai context.

2.3.1 Setting Organization/Operational Boundaries

The system boundaries were set up based on an operational control approach for the department which is able to response for their emissions and control. Consist of 9 buildings and common areas such as garden and car parking. Therefore, the carbon footprint of non-Lockdown period was compared with during Lockdown period due to the most of activities changed. Carbon emission of all resources collected in both direct and indirect sources was identified. The activity data was divided into 3 scopes due to the resources and energy used in the faculty and data availability, according to TGO guidelines as follows: direct carbon emission, indirect carbon emission from purchased energy, and other indirect emissions. (TGO, 2018)

2.3.2 Data Collection

The Resources and energy data were collected in the 2020 fiscal year (October 2019 – September 2020) separated into non-Lockdown period (196 business days: 1 October 2019 – 22 March 2020, and 1 June – 30 September 2020) and during Lockdown period (47 business days: 23 March – 31 May 2020) from both in primary and secondary data. The methods and sources of data collection were showed in Table 1.

Table 1. Summary of data collection methods and sources

Activities	Unit	Collection method	Source
Non-Lockdown period			
Scope 1 Direct carbon emission			
1.1 Fuel consumption	L	Receipt	Division of finance, supplies and property
1.2 Fertilizer use	kg	Report	Division of finance, supplies and property
1.3 Wastewater treatment process	m^3	Lab Report	Division of physical, environment and safety
Scope 2 Indirect carbon emission from purchased energy			
2.1 Electricity consumption	kWh	Receipt	Division of physical, environment and safety
Scope 3 Other indirect emissions			
3.1 Water consumption	m^3	Receipt	Division of physical, environment and safety
3.2 Paper use	kg	Report	Division of finance, supplies and property
3.3 LPG use in cafeteria and market	kg	Questionnaire	Seller
3.4 Plastic bag use in cafeteria and market	kg	Questionnaire	Seller
3.5 Waste management	kg	Report	Department of Environmental Health Sciences
3.6 Commuting	L	Questionnaire	Staff and students
Work/Study from home during Lockdown period			
- Air condition (8 hr.)			
- Light bulb (8 hr.)			
- Laptop (8 hr.)			
- Smartphone (charge) (1 hr.)	kWh	Estimation	Estimation
- Electric rice cooker (40 mins.)			
- Microwave (15 mins.)			
- Kettle (15 mins.)			

A random sampling method will be used in this study for the questionnaire collection. This study will be focused on the student and staff of 1,041 mans (66 doctoral degree's students, 299 master degree's students, 361 bachelor degree's student, and 315 academic and support staffs (updated in January, 2019). Therefore, the sample size in this study will be calculated following the Krejcie and Morgan's equation.

$$n = \frac{x^2 Np(1-p)}{e^2(N-1) + x^2 p(1-p)}$$

Where, n is the required sample size, x^2 is the value of chi-square where the df = 1 (2.71),

N is the population, p is the population proportion (assumed to be 0.5), e is the degree of accuracy expressed as proportion (0.1)

2.3.3 Calculations of carbon emissions

Carbon emission was calculated based on the Process–Analysis (PA) or Bottom–Up, the calculation method referring to each step or process of activity, which is suitable for medium scale scope such as an organization or building level. The emission values gain from multiplying a quantity measurement with the relevant emission factor, which is mostly from TGO guidelines. The data were interpreted in the form of unit measurement of mass carbon dioxide equivalent (CO_2e).

$$CO_2 \text{ emission} = AD \times EF$$

Where,CO_2 emission is the amount of carbon emission (kg/tones CO_2e), AD is the activities that cause carbon emission., EF is the constant value for changing the activity data into the amount of carbon emission

2.3.4 Uncertainty analysis

The uncertainty arising from the preparation of the greenhouse gas accounting demonstrate quality of carbon emission data collected. The uncertainty can be estimated by multiplying the data quality level from the data collection method with the data quality level from the source of emission factor used. The data quality level from the data collection method, the data quality level from the source of emission factor used, and the uncertainty analysis descriptions of the score ranging as described in Table 3, 4, and 5 respectively.

Uncertainty analysis = A x B

Where, A is the data quality level from the data collection method, B is the data quality level from the source of emission factor used

3. Results and Discussion

The average activity data of resources and energy used occurred in the Faculty of Public Health, Mahidol University in non-Lockdown and Lockdown period per day illustrated in table 6.

Table 2. The emission factor used in this study

Resources	Unit	Emission factor ($kgCO_2e$/unit)	Reference
Diesel	L	2.74	TGO, 2020
Gasohol 95	L	2.24	TGO, 2020
Fertilizer	kg	1.51	TGO, 2020
Electricity	kWh	0.49	TGO, 2020
Paper	kg	2.10	TGO, 2021
Water	m^3	0.79	TGO, 2020
LPG	kg	3.11	TGO, 2020
HDPE	kg	6.71	TGO, 2021
PP	kg	1.81	TGO, 2021
Waste management (Open dump)			
Food waste	kg	2.53	TGO, 2020
Paper	kg	2.93	TGO, 2020
Plastic	kg	2.32	TGO, 2020

Table 3. The data quality level from the data collection method.

Data collection method (A)	A = 6 point	A = 3 point	A= 1 point
	Data collected by CEMs	Data collected by meter or receipt	Data collected by estimation

Table 4. The data quality level from the source of emission factor used.

Emission factor source (EF) (B)	B = 4 point	B = 3 point	B = 2 point	B = 1 point
	Measurement EF	National EF	Regional EF	International EF

Table 5. The uncertainty analysis description of the score ranging.

Level	Range point	Description
1	1 – 6	High uncertainty/Low data quality
2	7 – 12	Medium uncertainty/Medium data quality
3	13 – 18	Low uncertainty/Good data quality
4	19 - 24	Low uncertainty/Very good data quality

Table 6. The average activity data of resources and energy used in the Faculty of Public Health, Mahidol University during non-Lockdown and Lockdown period.

Activity	Unit/Day	Average Activity Data (Day)	
		Non-Lockdown period	Lockdown period
Scope 1 Direct carbon emission			
1.1 Fuel consumption			
1.1.1 Diesel	L	69.799	9.842
1.1.2 Gasohol 95	L	2.546	1.012
1.2 Fertilizer use	Kg	0.936	0.638
1.3 Wastewater treatment process			
1.3.1 Flow rate	m^3	197.920	32.701
1.3.2 Average BOD_{inf}	mg/L	105.250	17.390
1.3.3 Average BOD_{eff}	mg/L	10.000	1.652
Scope 2 Indirect carbon emission from purchased energy			
2.1 Electricity consumption	kWh	20,660.494	10,290.574
Scope 3 Other indirect emissions			
3.1 Water consumption	m^3	168.992	97.340
3.2 Paper use	Kg	4.108	2.809
3.3 LPG use in cafeteria and market	Kg	46.089	7.605
3.4 Plastic bag use in cafeteria and market			
3.4.1 Poly propylene	Kg	5.738	0.947
3.4.2 High density polyethylene	Kg	13.707	2.262
3.5 Waste management			
3.5.1 Food waste	Kg	128.870	21.264
3.5.2 Paper	Kg	33.968	5.605
3.5.3 Plastic	Kg	66.899	11.038
3.6 Commuting			
3.6.1 Diesel	L	1,812.767	236.150
3.6.2 Gasohol 95	L	1,845.096	315.835
Work/Study from home (869 mans)			
Air condition (8 hr.)	kWh	-	15,642.000
Light bulb (8 hr.)	kWh	-	111.232
Laptop (8 hr.)	kWh	-	364.980
Smartphone (1 hr.)	kWh	-	5.214
Electric rice cooker (40 mins.)	kWh	-	430.155
Microwave (15 mins.)	kWh	-	119.488
Kettle (15 mins.)	kWh	-	135.781

3.1 Scope 1 direct carbon emission

Scope 1 emissions are direct greenhouse (GHG) emissions that occur from sources that are controlled or owned by an organization. The carbon emissions in scope 1 are generated from the fuel consumption by Faculty's vehicles which held the largest share in this scope, followed by wastewater treatment process of the faculty, and the fertilizer uses in garden care.

3.2 Scope 2 indirect carbon emission from purchased energy

Scope 2 emissions are indirect GHG emissions associated with the purchase of electricity and energy. The highest carbon emission of this scope under non-Lockdown period caused by purchased energy for education, academic services, research, administrative, and others activities in the faculty.

3.3 Scope 3 other indirect carbon emission

Other indirect carbon emission of the faculty also focuses on this scope including water consumption, paper use, waste management, student and stuff commuting, and the LPG and plastic bag use in cafeteria and market under the supervision of the faculty.

Since scope 3 (indirect emissions) held almost half of overall carbon footprint emissions of the faculty (48.87%) and decreased 38.49% during the Lockdown period, this information may assist organizations to pursue emissions mitigation projects not only within the organization but also across indirect emission activities (Awanthi and Navaratne, 2018).

3.4 Carbon emission from work/study from home

During lockdown period, student and staff work/study from home by using their own electricity appliances considered with the following pattern: worked/study from home 08.30 am - 05.30 pm, 5 days a week, from Monday to Friday. As the Lockdown period (March-May) in Thailand is characterized by hot weathers. An air condition, light bulb, and laptop was in constant use 8 hours a day. Smartphone also included for the communication. Lunch was included so the electric rice cooker, microwave, and kettle were assumed to preparation with 40 mins., 15 mins., and 15 mins. a day respectively. Other activities at home were excluded due to not related to the faculty business and the data availability. The results showed that the electricity used for air condition was the largest amount of carbon emission (93.06%).

This result indicated that the overall carbon footprint occurred during Lockdown was lower than the non-Lockdown period. The main sources of carbon emission under non-Lockdown period in descending order are the electricity consumption, followed by commuting and waste management, respectively. Whereas the key source of carbon emission during COVID-19 Lockdown period was the electricity use at home for online teaching/learning and work operation. From COVID-19 situation, work/study from home is the alternative way to reduce overall carbon emission due to no commuting of staffs and students. The results showed that all activities occurred during work/study from home generates lower carbon footprint than only University commuting. As part of an eco-university drive, finding measures to minimize carbon emissions from these main activities will help resource conservation of the country and reduce the effect form global warming. Reduce greenhouse gas emissions from the energy sector, support national policies aimed at a low-carbon society. Filimonau et al. (2020) reported that a large share of the carbon savings achieved by moving education online to avoided student and staff mobility. Additionally, work/study from home can be a reasonable option for local institutions of higher education. Not only non-commuting can contribute to the reduction of air pollution in these areas, but it will also save time for staff/students due to avoid traffic crowding.

Overall carbon emission during lockdown period was decreased by around 26.43% compared with non-Lockdown. This was mainly due to a significant reduction in the fuel consumption and electricity used. Rugani and Caro (2020) reported that the CF in the Lockdown period is about 20% lower than the mean CF calculated for the past in Italy. The higher reduction in carbon emissions found in our study may be due to the changing of working scheme to work/study from home operation.

The results showed that the carbon footprints during non-Lockdown and Lockdown period in the Faculty of Public Health, Mahidol University were 20,594.32 $kgCO_2e$/day/period equivalent to 19.78 $kgCO_2e$/capita/day, and 15,151.03 $kgCO_2e$/day/period equivalent to 14.55 $kgCO_2e$/capita/day, respectively. The main carbon emission source in both periods was electricity consumption followed by commuting and waste management respectively as presented in Table 7 and figure 2

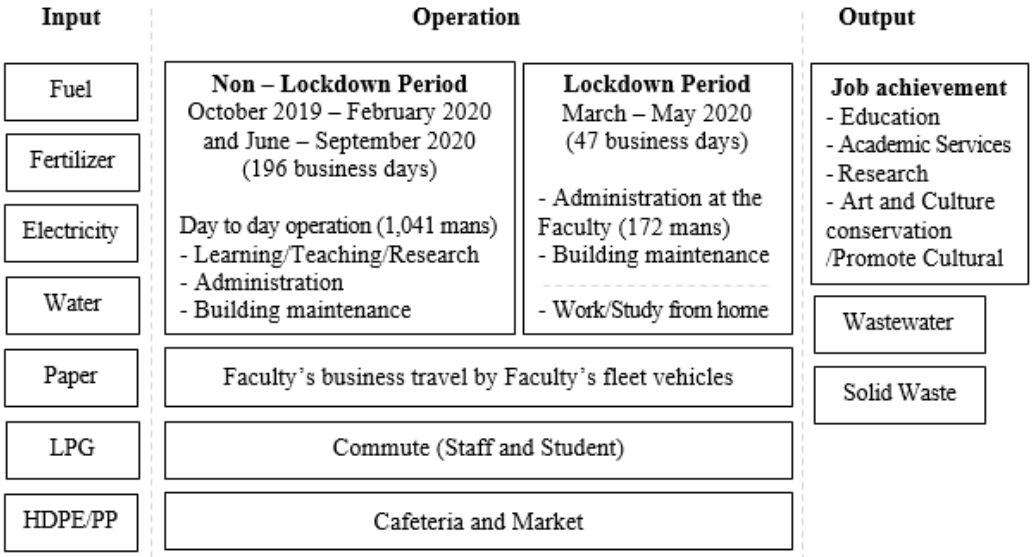

Figure 1. Operational boundaries of the Faculty of Public Health, Mahidol University

Table 7. Carbon footprint of the Faculty of Public Health, Mahidol University

Activities	Carbon footprint ($kgCO_2e$/day)	
	Non-Lockdown period	During Lockdown period
Scope 1 Direct carbon emission		
1.1 Fuel consumption		
1.1.1 Diesel	191.27	26.97
1.1.2 Gasohol 95	5.70	2.26
1.2 Fertilizer use	1.41	0.96
1.3 Wastewater treatment process	2.67	0.44
Scope 2 Indirect carbon emission from purchased energy		
2.1 Electricity consumption	10,328.18	5,144.26
Scope 3 Other indirect emissions		
3.1 Water consumption	134.31	77.37
3.2 Paper use	8.64	5.90
3.3 LPG use in cafeteria and market	143.49	23.68
3.4 Plastic bag use in market		
3.4.1 Poly propylene	10.38	1.71
3.4.2 High density polyethylene	91.93	15.17
3.5 Waste management	580.78	95.83
3.6 Commuting	9,095.55	1,353.74
Work/Study from home (869 mans)		
Air condition (8 hr.)	0	7,819.44
Light bulb (8 hr.)	0	55.60

Table 7. Carbon footprint of the Faculty of Public Health, Mahidol University

Activities	Carbon footprint ($kgCO_2e$/day)	
	Non-Lockdown period	During Lockdown period
Laptop (8 hr.)	0	182.45
Smartphone (1 hr.)	0	2.61
Electric rice cooker (40 mins.)	0	215.03
Microwave (15 mins.)	0	59.73
Kettle (15 mins.)	0	67.88
Total ($kgCO_2e$/day/period)	20,594.32	15,151.03
Carbon footprint ($kgCO_2e$/capita/day) (1,041 mans)	19.78	14.55

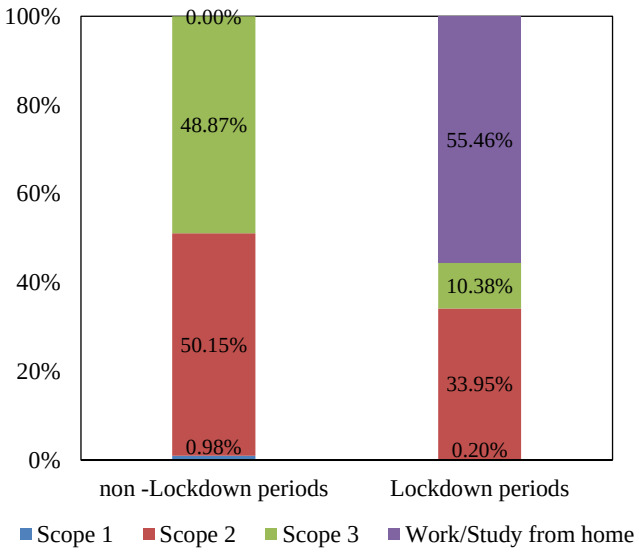

Figure 2: Carbon emissions comparison between non-Lockdown and Lockdown period.

As part of an eco-university drive, finding measures to minimize carbon emissions from these three main activities will be most effective and help the country conserve resources. Reduce greenhouse gas emissions from the energy sector, support national policies aimed at a low-carbon society. From COVID-19 situation, the teaching and learning online was the alternative way to reduce overall carbon emission.

For assessing the uncertainty, most activities were at a high uncertainty/low data quality because of the data collected by receipt and the estimation by questionnaires. To have low uncertainty with high quality of information, it is necessary to collect activity data with a continuous emission monitoring system (CEMS). The uncertainty data was illustrated in Table 8.

Table 8. Uncertainty data analysis

Activities	Data collection method (A)	Emission factor source (B)	Result (AxB)	Data quality
Scope 1 Direct carbon emission				
Fuel consumption	3	3	9	Medium uncertainty/medium data quality
Fertilizer use	1	3	3	High uncertainty/Low data quality
Wastewater treatment process	6	1	6	High uncertainty/Low data quality
Scope 2 Indirect carbon emission from purchased energy				
Electricity consumption	3	3	9	Medium uncertainty/medium data quality

Table 8. Uncertainty data analysis

Activities	Data collection method (A)	Emission factor source (B)	Result (AxB)	Data quality
Scope 3 Other indirect emissions				
Water consumption	3	3	9	Medium uncertainty/medium data quality
Paper use	1	3	3	High uncertainty/Low data quality
LPG use in cafeteria and market	1	3	3	
Plastic bag use in cafeteria and market	1	3	3	
Waste management	1	3	3	
Commuting	1	3	3	
Work/Study from home	1	3	3	

4. Conclusions

The results indicated that the carbon footprints in the Faculty of Public Health, Mahidol University decreased by almost 26.43% during the Lockdown period. The main sources of carbon emission under non-Lockdown period in descending order are the electricity consumption, followed by commuting and waste management, respectively. The highest carbon emission represents the electricity use because many activities need to use electricity, reduction strategies should be highly focused on this issue. Additionally, the key source of carbon emission during COVID-19 Lockdown period was the electricity use at home for online teaching/learning and work operation. Therefore, the use of high energy-efficient appliances such as air conditioning and lighting equipment as well as energy-saving campaigns to reduce the power consumption such as turning off the appliance when not use were introduced. However, the commuting during non-lockdown also generated the high amount of carbon emission similar to the electricity use. Thus, the carbon savings by moving working and education online to avoided student and staff mobility should be considered.

Acknowledgements

This research was partially supported by internal grants at the Department of Environmental Health Sciences, Mahidol University, provided by the Center of Excellence on Environmental Health and Toxicology (EHT) under the Science & Technology Postgraduate Education and Research Development Office (PERDO) of the Ministry of Education, Bangkok, Thailand.

References

Kulkarni SD. A bottom up approach to evaluate the carbon footprints of a higher educational institute in India for sustainable existence. (2019) Journal of Cleaner Production, 633-641.

Ma, X., Longley, I., Gao, J., Salmond, J., 2020. Assessing schoolchildren's exposure to air pollution during the daily commute-a systematic review. Sci. Total Environ. 737, 140389.

Mahidol University. (2020). History [Online]. Available: https://www.ph.mahidol.ac.th/ [Accessed 14 February 2020]

Mahidol University. (2020). Statistic [Online]. Available: https://www.ph.mahidol.ac.th//ed/statistics/ [Accessed 20 February 2020]

M.G.G. Awanthia, C.M. Navaratne. (2018) Carbon Footprint of an Organization: a Tool for Monitoring Impacts on Global Warming. Procedia Engineering, 212, 729–735.

Oliver J. Robinson, Adam Tewkesbury, Simon Kemp, Ian D. Williams. (2018) Towards a universal carbon footprint standard: A case study of carbon management at universities. Journal of Cleaner Production, 172, 4435e4455

ONEP (Office of Natural Resources and Environmental Policy and Planning). (2019). Paris Agreement [Online]. Available: https://climate.onep.go.th. [Accessed on 12 October 2021]

Sun, C., Luo, Y., Li, J. (2018). Urban traffic infrastructure investment and air pollution: evidence from the 83 cities in China. J. Clean. Prod. 172, 488–496.

TGO (Thailand Greenhouse Gas Management Organization (Public Organization)). (2018). Carbon Footprint for Organization [Online]. Available: http://www.tgo.or.th/. [Accessed on 12 October 2021]

V. Filimonau, D. Archer, L. Bellamy, et al. (2021). The carbon footprint of a UK University during the COVID-19 lockdown, Science of the Total Environment, 756, 143964.

Slope Stability Analysis to Evaluate Slope Failure in Northern Thailand by Standard Penetration Test

Patthranit Payaksiri[a*], Sayam Aroonsrimorakot[a], Pet Pakchotanon[b], and Bunlur Emaruchi[c]

[a]Faculty of Environment and Resource Studies, Mahidol University, Thailand
[b]Faculty of Engineering, Chulalongkorn University, Thailand
[c]Faculty of Engineering, Mahidol University, Thailand

Abstract

Highway embankments constructed on high mountain areas usually have a problem of slope stability in the rainy season that can have a great impact on road users because it is often limited in terms of boundaries. The purpose of this study was to analyze the stability of slope by using the Standard Penetration Test (SPT). The SPT is an in-situ of soil testing that can be collected data while boring. N-Value from SPT gives shear strength parameters of soil that can analyze the factor of safety. A total of 30 samples were collected from slope failure locations along the highway in Northern Thailand that had boring data in the area or nearby distance between slope failure area and borehole, not more than 30 km. N-Value can compare the relationship with the effective friction angle of coarse grains (sand) or the cohesion of fine gains (clay). Friction angle and cohesion have analyzed the factor of safety under a critical period of rain and normal traffic volume. The factor of safety is between 0.108-1.471 and displayed the results of the analysis in "Factor of Safety Map in Northern Thailand".

Keyword: Slope stability/ Standard penetration test/ Factor of safety

---

*Corresponding Author: Tel: +6-698-896-1594
E-mail address: patthranit.pay@student.mahidol.ac.th

1. Introduction

The problem of landslide or slope failure along the roads constructed in a mountainous area is often found frequently when entering the rainy season. Because the construction in these areas is often limited space constraints. The terrain has steep slopes and land use. Damage caused by the failure of the slope will affect the road user and people who live nearby. This requires budget and staff to solve problems and manage areas after a disaster. Therefore, if there is a way to assess the stability of slope before a disaster occurs, responsible agency will be prepared to prevent damage or mitigate any damage that may occur can alert the people who use to route as well as coordinating with people in the management of land use area or even pre-construction planning such as road expansion or construct a new road.

The evaluation of slope stability can be done in a number of methods [1]. This research is studied by the geotechnical method. Studying the factor affecting the failure of slope using data from soil drilling with the Standard Penetration Test (SPT) method to analyze the factor of safety (F.S.) of the area along the road. The Standard Penetration Test is one of the popular methods of testing soil properties in the field (In-situ test) and gives shear strength parameters without using more laboratory [2]. It is used widely because of its simplicity and is not expensive [2].

Assessment of the slope stability, a factor of safety will be taken into consideration [3]. For stable slope embankment, a factor of safety is greater than 1.5 and critical when F.S. is equal to 1 [4]. N-Value from SPT is a blow count. The tester will count the number of times the cylinder is hammered into the ground at a distance of 15 cm in 3 intervals. The value of the Standard Penetration Test (N-Value) is the number of hammer times to achieve a distance of 30 cm (2 times after). The first 15 centimeters are not taken into account because the soil in this period is considered to be disturbed by the drilling process. In general, the SPT is not suitable for soils with an N value less than 4 [4]. N-Value have been used to the shear strength parameter are cohesion and friction angle of soil that can be calculate to factor of safety. In this research, the relationship

between N-Value and factor of safety have been discussed to ensure that N-Value affect to factor of safety.

2. Previous work

In mountainous areas, highways construction in these areas is often damaged in the rainy season. Because when it rains, rainwater will seep through the soil layer, which will increase the moisture in the soil mass. It makes the attraction between a grain of soil loosening. The shear strength is reduced by moisture. As a result, the stability of slope embankment is decreasing, and there is an increased likelihood of landslide or slope failure [5]. Several methods of assessment of slope stability have been studied by many researchers. One of them is the method of studying the geotechnical factors by analyzing the shear strength parameter of soils. Obtaining shear strength parameters can be done in many methods both in the field (in-situ test) and in the laboratory.

Dechpatungwesa and Chairatanangamdaj, 2019 studied and analyzed the cause of slope failure of highway embankment no.1194 Mae Sariang - Mae Samlaep route sta.21+150 [6]. And Muntathong et. al., 2017 studied the cause of slope failure of highway embankment no.1349 Samoeng – Wat Chan route sta.34+450 [7]. The research has collected soil samples to test shear strength by the Direct Shear Test method under normal moisture and high moisture conditions. The data analysis is base on the principle of Limit Equilibrium. Analysis factor of safety of the soil in the study area. In normal moisture conditions, the slope will be stable. But in high moisture conditions and earthquakes, the slope will be unstable.

Yousof and Zabidi, 2018 [2] studied the reliability of using standard penetration test (SPT) in predicting properties of soil. SPT is one of the methods that can be done with the shear strength parameters. It is used widely because of its simplicity, inexpensively, and gives a chance to obtain these parameters without using laboratory tests. The research had studied the reliability of SPT in predicting Atterberg limits and shear strength parameters; cohesion, and angle of friction in the State of Pahang, Malay. The simple correlation between SPT and soil parameters is performed by using a simple regression method. The results show the shear strength of the soils affects the SPT number.

Marques and Lukiantchuki, 2015 [8] evaluated of the stability of a highway slope through numerical modeling in Sao Paulo, Brazil. This research is to assess the stability of the slope from the factor of safety. N-value from Standard Penetration Test was used in this study for estimation of shear strength parameter of soil. Stability analysis based on Morgenstern-Price method and 20 kPa of surcharge load. The result shows a factor of safety of 1.16 that is below the minimum recommended by the Brazilian Technical Standard. After that, the stability of the slopes was analyzed during the critical period. The result shows the factor of safety of 0.78 that a decrease of 33% from normal conditions. Then, the reliability of the analysis results was determined. The factor of safety can vary between 0.74 and 1.59. The standard deviation was 0.11 and the reliability index 1.44, resulting in a probability of failure of 7.7%. From the analysis, the stability of the section to be unsatisfactory.

3. Present Work

The efficient method in geotechnical engineering for analyzing slope stability is the Direct Shear Test but it is very difficult to collect samples, test in the laboratory, and people who test samples should a specialist in geotechnical engineer. So in this research, the Standard Penetration Test is an interesting method because it is easier than the Direct Shear Test. Standard Penetration Test can test in the field and people who test samples are not required to the specialist in geotechnical engineering. However, this research wants to analyze the factor of safety for evaluating the stability of slope in an easy method but the accuracy of analysis results must be within acceptable criteria or not very inaccurate.

The purpose of this study was to analyze the stability of slope along with the road construction in a mountain area of Northern Thailand by using the N-Value obtained from the Standard Penetration Test.

4. Methodology

4.1 Data preparation

Preparing data for this research use of secondary data from the Bureau of Materials, Analysis, and Inspection, Department of Highways, and related other agencies for analyzing the Factor of Safety (FS). The data used are as follows:

4.1.1 Boring data in 2016 – 2020.

4.1.2 Cross-section of landslide or slope failure embankment in each location along the mountainous roads in 2016 – 2021.

4.1.3 Shape file: Boundary of Province (in Northern Thailand), Highway route, Geology and etc.

Boring data in 2016-2020, In the soil survey, there will be a Standard Penetration Test which is following the Standard Test Method for Standard Penetration Test (SPT) and Split-Barrel Sampling of Soils D1586-11 [9]. The test drives the weight to transfer the force to the hollow inside the slitting cylinder to penetrate the layer where the soil sample will be collected. The tester will count the number of times the cylinder is hammered into the ground at a distance of 15 cm in 3 intervals. The value of the standard penetration test is the number of hammer times to achieve a distance of 30 cm (2 blocks). The first 15 centimeters are not taken into account because the soil in this period is considered to disturb by the drilling process. But in general, the SPT test is not suitable for soils with an N value less than 4 [4]. However, the conditions for stopping hammering depend on the type of foundation work to be constructed. The results of this drilling survey were shallow foundation surveys. So stop hammering at N = 50. The N-value obtained from the test must be revised to N with a standard energy efficiency of 60%. Because soil parameters that interpreted from SPT testing and the geotechnical engineering knowledge database was developed based on the N_{60} value. However, these adjustments are not welcome because of difficulties and complexity. In practice, it is assumed that the value of N measured in the field is equal to N_{60}.

The sample drilling results (Boring Log and Field Log) will contain various information that can compare to the relationship between the N value and the shear strength parameter. This can apply in the analysis of the factor of safety. An example of the boring data and field log are shown in Figure 1 and Figure 2.

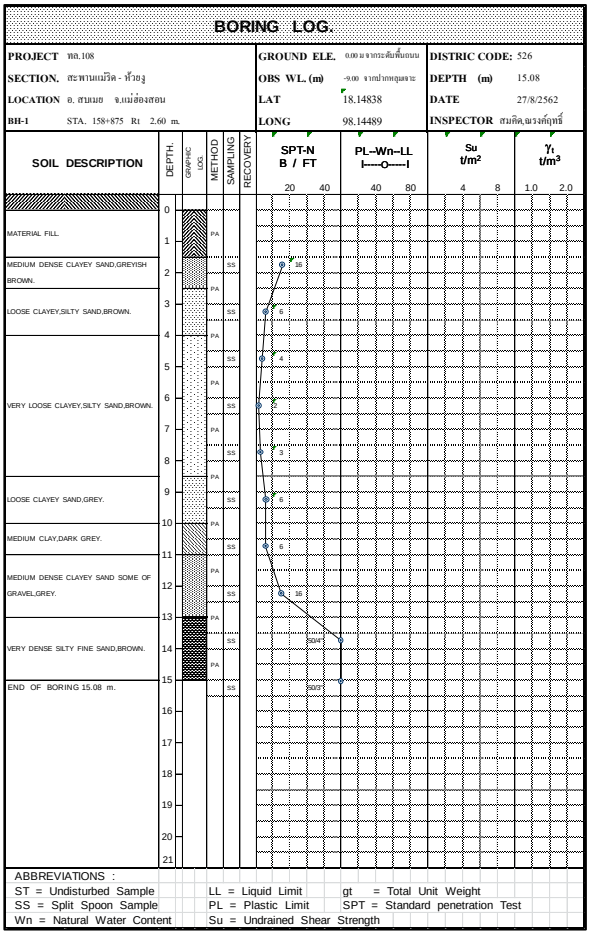

Figure 1. Boring log results show the depth and N values in each soil type.

The relationship between N-value and soil parameters was used to calculate the safety factor are:

- *Effective Friction Angle, Ø*

The relationship between N and the effective friction angle has been shown in the form of a comparative table in several studies. For this research, the relationship between N-values and the effective friction angle of coarse-grained soils of Wisutmethanukul, 2015 as shown in Table 1.

FIELD LOG

PROJECT.	ทล.108	**DATE.**	27/8/2562
SECTION	สะพานแม่ริด - ห้วยงู	**DISTRIC CODE:**	526
LOCATION	อ.สบเมย จ.แม่ฮ่องสอน	**INSPECTOR.**	สมคิด,ฉรังค์ฤทธิ์
COOR.	LAT = 18.14838 LONG = 98.14489	**GROUND ELE.**	0.00 ม. จากระดับพื้นถนน
BH-1	STA. 158+875 Rt 2.60 m.	**OBS WL.**	-9.00 ม

NO.	DEPTH. FROM (M.)	DEPTH. TO (M.)	METHOD	STANDARD PENETRATION TEST 6"	6"	6"	N	SAMPLING SOIL DESCRIPTION
1	0.00	1.50	PA					
2	1.50	1.95	SS	7	9	7	16	MEDIUM DENSE CLAYEY SAND,GREYISH BROWN.
3	1.95	3.00	PA					
4	3.00	3.45	SS	2	3	3	6	LOOSE CLAYEY,SILTY SAND,BROWN.
5	3.45	4.50	PA					
6	4.50	4.95	SS	2	2	2	4	VERY LOOSE CLAYEY,SILTY SAND,BROWN.
7	4.95	6.00	PA					
8	6.00	6.45	SS	1	1	1	2	-DITTO.-
9	6.45	7.50	PA					
10	7.50	7.95	SS	1	1	2	3	-DITTO.-
11	7.95	9.00	PA					
12	9.00	9.45	SS	3	3	3	6	LOOSE CLAYEY SAND,GREY.
13	9.45	10.50	PA					
14	10.50	10.95	SS	2	3	3	6	MEDIUM CLAY,DARK GREY.
15	10.95	12.00	PA					
16	12.00	12.45	SS	3	7	9	16	MEDIUM DENSE CLAYEY SAND SOME OF GRAVEL
17	12.45	13.50	PA					GREY.
18	13.50	13.95	SS	33	50/4"	-	50/4"	VERY DENSE SILTY FINE SAND,BROWN.
19	13.95	15.00	PA					
20	15.00	15.45	SS	503"	-	-	50/3"	-DITTO.-
								END OF BORING. (15.08 m.)

PA= POWER AUGER ST=SHELBY TUBE SS=SPLIT SPOON WO=WASH OUT

Figure 2. The number of times that the hammer was hammered into each interval of 15 cm in 3 test intervals.

Table 1. The relationship between N-values and the effective friction angle of coarse-grained soils. (Wisutmethanukul, 2015)

N	N_{60}	Describe	γ_t (kN/m³)	D_r (%)	ø' (degree)	X (degree)
0 – 5	0 – 3	Very Loose	11 – 16	0 – 15	26 – 28	0
5 – 10	3 – 9	Loose	14 – 18	16 – 35	29 – 34	0
10 – 30	9 – 25	Medium	17 – 20	36 – 65	35 – 40[a]	$\phi'_p - \phi'_{cs}$
30 – 50	25 – 45	Dense	19 – 22	66 – 85	40 – 45[a]	$\phi'_p - \phi'_{cs}$
> 50	> 45	Very Dense	> 20	86 – 100	> 45[a]	$\phi'_p - \phi'_{cs}$

- Estimation of undrained shear strength of fine-grained soils

The determination of the undrained shear strength of clays (C_u) is usually tested in a laboratory. However, Cu can be estimated from the SPT test that has adjusted the incident energy N60: as shown in Table 2.

In this research, N-value had converted to the effective friction angle in the soil or the undrained shear strength by the rule of three in arithmetic. Using the N-value data obtained from the SPT test, it is necessary to classify the soil type: clay or sand. Because of the selection of a comparison table, only one of the tables will be used. But in reality, there will be silt soil, which is soil whose grain size is between clay and sand. In selecting the table, the relationship of coarse-grained soil was used. Together with the cohesion cost of soil grains in the rainy season, that is the average value in the engineering soil group of Thailand (Sornralump et al., 2018) [10], as shown in Figure 3. The type of rock or soil origin can be determined by overlapping the coordinates of the slope failure location with the geology map shapefile as shown in Figure 4.

Table 2. The relationship between the N60 value and the undraining shear strength of clay soils. (Visutmethanukul, 2015)

N_{60}	Describe	γ_t (kN/m^3)	C_u (kPa)	Pressed with the thumb
0 - 2	Very Soft	< 15.7	< 10	Sink more than 1 inch (2.5 cm.)
3 - 5	Soft	15.7 – 18.8	10 - 25	Sink about 1 inch
6 - 9	Medium	15.7 – 20.4	25 - 50	Sink when using moderate force
10 - 15	Stiff	18.8 – 20.4	50 - 100	It is about 0.8 cm deep.
15 - 30	Very Stiff	18.8 – 22.0	100 - 200	Not a deep mark but you can use your fingernail to press it to make a mark.
30 - 50	Hard	> 20.4	200 - 300	Not a deep mark when using a fingernail, it is still difficult to scratch.

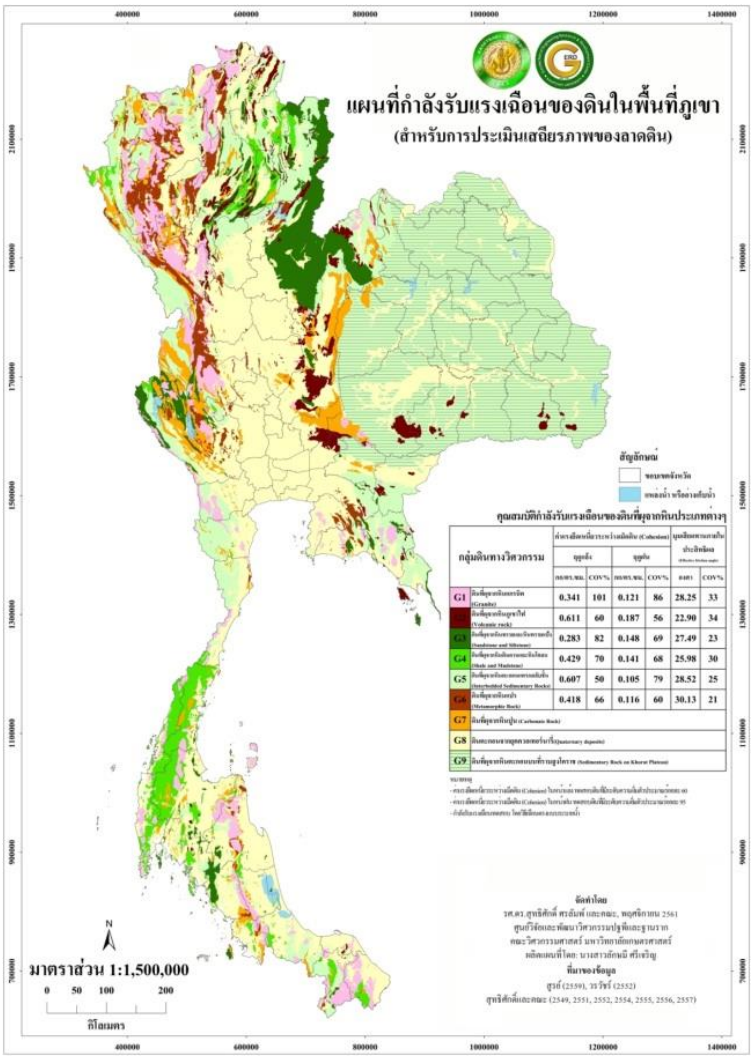

Figure 3. Map of soil shear strength in mountainous areas (for evaluating slope stability) (Sorralump et al., 2018)

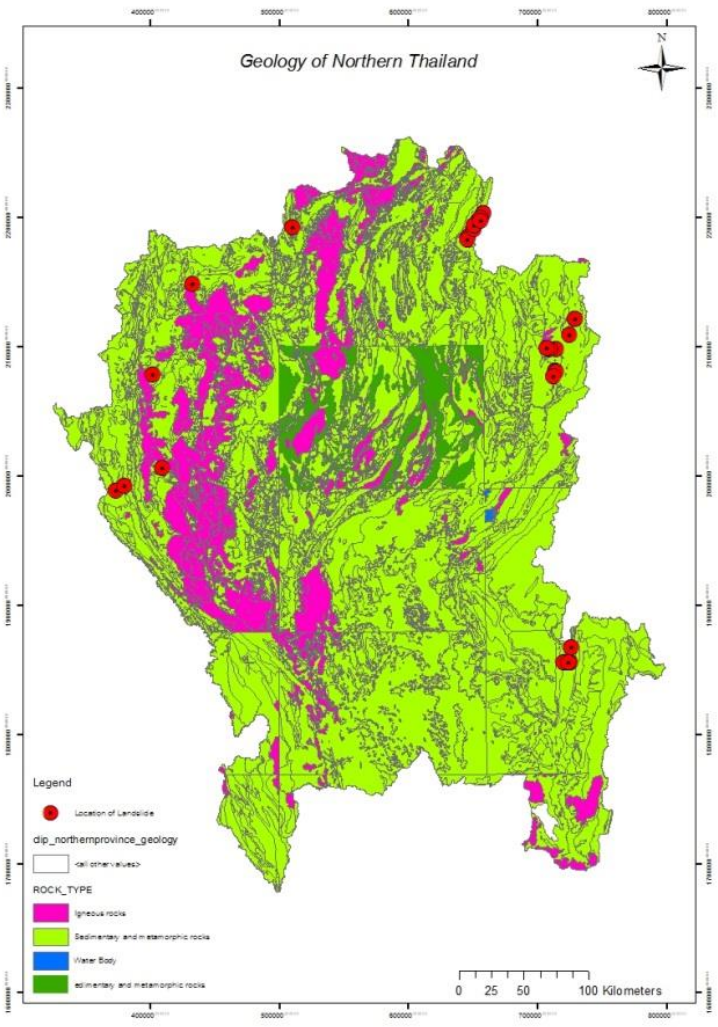

Figure 4. The location of slope failure in different rock types

The location and cross section of slope failure in 2016-2021, cross-section data will know the slope angle that failed. Cross section data as shown in Figure 5. Slope Angle is one of the factors used to calculate the factor of safety and can also take distances both horizontally and vertically to be plotted in the Geo Studio 2007 program to create a sloped model as well.

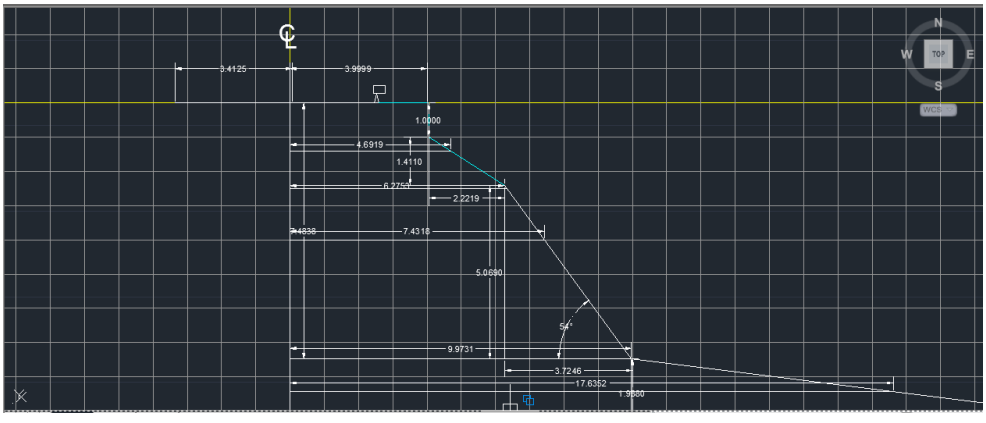

Figure 5. The example of cross section at the site of the slope collapse.

When the data is collected, boring data is taken into account together with the location of the slope failure. The courtesy of the drilling data, there are many objectives of exploration. In this research, the study only the borehole data corresponding to the failure site or nearby area was selected from 30 areas as shown in Figure 6. (In the distance between the borehole and the site of the failure, not more than 30 kilometers because the greater distance, the more information will be inaccurate at that location.).

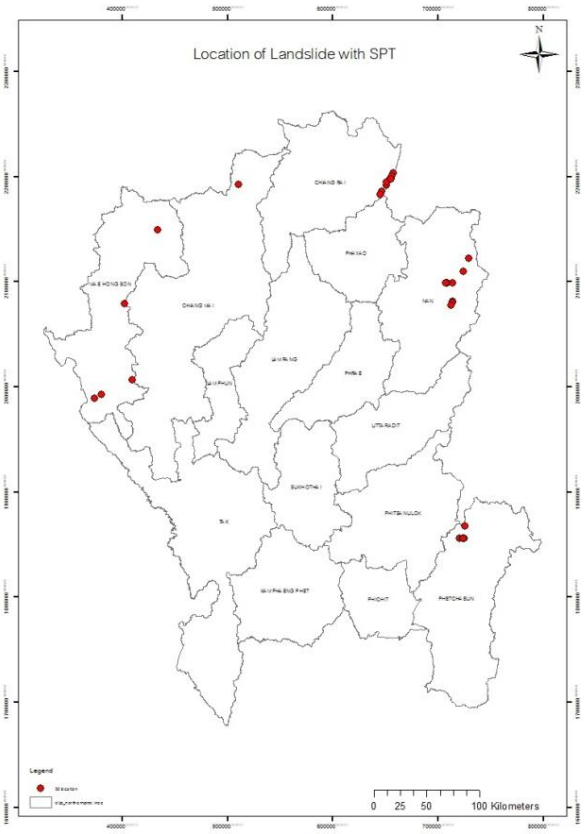

Figure 6. Slope failure location with nearby borehole data

4.2 Classified type of slope failure

There are several formulas in the factor of safety analysis according to the erosion characteristics of the slopes. Therefore, it is appropriate to choose a formula for calculating the factor of safety. This research classifies the characteristics of failure into two major types:

4.2.1 Erosion failures as shown in Figure 7 are based on the Infinite Slope stability analysis equation.

$$F.S.= \frac{c\prime}{\gamma z \sin\alpha \cos\alpha} + \left[\frac{\tan\emptyset\prime}{\tan\alpha} - m\left(\frac{\gamma_w \tan\emptyset\prime}{\gamma \tan\alpha}\right)\right]$$

Figure 7. Show the area and nature of the failure of a slopes in Highway No.1263, section Khun Yuam - Pang Ung, at about 18+580 km LT.

4.2.2 Circular failure as shown in Figure 8 using Bishop's Simplified Method slope stability analysis equation.

$$F.S. = \frac{\sum_{n=1}^{n=p}(cb_n + W_n \tan\emptyset + \Delta T \tan\emptyset)\frac{1}{m_{\alpha(n)}}}{\sum_{n=1}^{n=p} W_n \sin\alpha_n}$$

Figure 8. Show the area and nature of the failure of a slopes in Highway no. 108, section Mae Rid Bridge-Huai Ngu at km. 158+865 - km.158+923 RT.

4.3 Slope stability analysis

Once the erosion characteristics have been classified, the above two equations have been applied appropriately. Substituting variables were obtained by comparing the relationship of the N-Value with the effective friction angle and undrained shear strength in combination with the slope angle obtained from cross-section data. For substituting other variables as follows:

- The unit weight of soil was determined at approximately 18 kN/m^3 [11].
- The weight of the backfill according to the report data from the Bureau of Materials,

Analysis, and Inspection, Department of Highways at approximately 20 kN/m^3.

• Moisture condition based on the highest moisture conditions (m = 1) (Saturated Soils).

• The external force is the weight of the vehicle being transferred into the pavement, which may increase the forces causing the embankment slide down recommended by Standard Truck and Lane Loads according to AASHTO: Standard Specification for Highways Bridge is 9.3 kN/m^2 (this research uses 10 kN/m^2) [12].

Because Bishop's Simplified Method is a rather detailed and complex computational method, Geo Studio ver.2007 was used for stability analysis as shown in Figure 9.

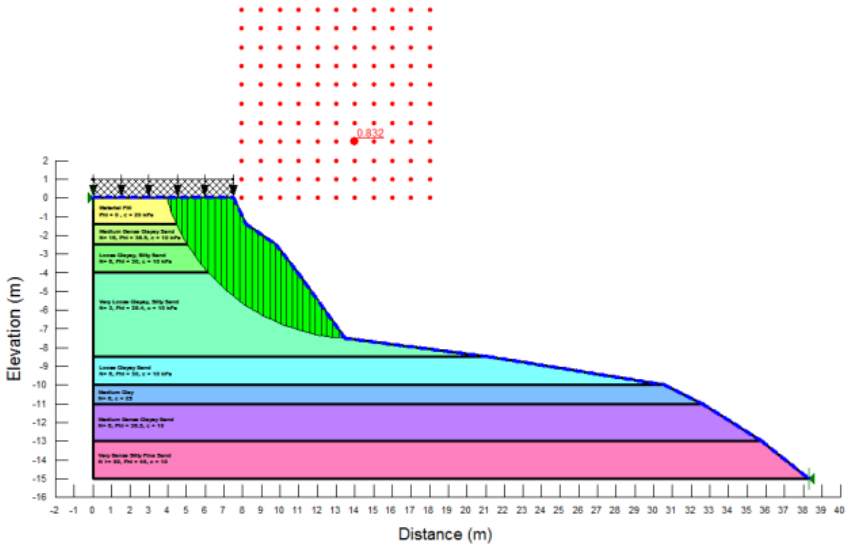

Figure 9. Model of failure characteristics and factor of safety results in Highway no. 108 at km. 158+865-km.158+923 RT.

Then the values of these variables are calculated for slope stability in the form of factor of safety, which is the factor of safety is the comparative ratio between soil power to the unit of resistance while balancing. The safety ratio was used to assess the stability of the sliding slope. as shown in Table 3.

Factor of Safety = (Shear Strength)/(Shear Stress)

5. Result

After analysis, the type of slope can be classified into 2 major types. Erosion slope in 8 areas and circular failure in 22 areas. And type of country rock as shown in Table 4.

Table 3. Factor of Safety for the stability of sliding slopes. (Visutmethanukul, 2015)

Stability	Analysis	Factor of Safety
Temporary excavation work and embankment	Analyzed with non-drained shear strength. (C_u)	1.1 - 1.3
Permanent excavation work	Critical Friction Angle Analysis (ϕ'_{cs})	1.2 - 1.4
Foundation of the embankment	C_u or ϕ'	1.2 - 1.5
Embankment (or compacted soil)	ϕ'	1.2 - 1.4
Soil filling on the old disaster plane	Analyzed by the angle of residual friction (ϕ'_r)	Natural value

Table 4. The location of the slope failure, type of slope failure, and country rock

No.	High way no.	Section	Km. – Km.	Lane	Location		Type of failure	Country rock
					X	Y		
1	1249	Mae Ngon – Nong Tao	Km.14+620.000 - Km.15+050.000	RT	510441.6020	2192928.501	Circular failure	Shale/Sandstone
2	108	Mae Rid Bridge – Huai Ngu	Km.158+865.000 - Km.158+923.000	RT	409740.4321	2006780.649	Circular failure	Shale/Metamorphic rock
3	2331	Jowo – Phu Hin Rong Kla Nation Park	Km.8+300.000 - Km.11+000.000	LT, RT	725880.7811	1868081.261	Infinite slope	Sandstone
4	1095	Mae Na – Tha Krai	Km.112+007.000 - Km.112+035.000	RT	433359.8463	2149395.779	Circular failure	Granite
5	1263	Khun Yaum – Pang Oung	Km.18+580.000	LT	402360.7991	2079167.396	Infinite slope	Granite
6	1093	Khun Huai Krai – Pha Tung	Km.48+650.000 - Km.48+675.000	LT	646527.7069	2186278.469	Circular failure	Phyllite
7	1093	Khun Huai Krai – Pha Tung	Km.44+250.000 - Km.44+280.000	RT	645471.0827	2183520.320	Infinite slope	Phyllite
8	1093	Khun Huai Krai – Pha Tung	Km.59+300.000 - Km.59+500.000	LT, RT	651024.1710	2192067.360	Infinite slope	Phyllite
9	1093	Khun Huai Krai – Pha Tung	Km.72+687.500 - Km.72+787.500	LT	654071.0426	2197577.897	Circular failure	Phyllite
10	1225	Pang Chang – Na Bua	Km.19+500.000 - Km.19+785.000	RT	714020.7632	2081848.327	Circular failure	Tuff
11	1225	Pang Chang – Na Bua	Km.20+290.000 - Km.20+325.000	RT	714192.9263	2081230.692	Circular failure	Tuff
12	1225	Pang Chang – Na Bua	Km.25+135.000 - Km.25+325.000	LT	712334.3665	2077796.603	Circular failure	Sandstone
13	12	Wang Thong – Kek Noi	Km.110+330.000 - Km.110+405.000	LT	725098.0616	1856120.143	Circular failure	Sandstone/ Shale
14	1081	Don Moon – Lak Lai	Km.37+025.000 - Km.37+095.000	LT	714095.7693	2099171.977	Circular failure	Shale
15	1081	Don Moon – Lak Lai	Km.30+900.000 - Km.30+970.000	LT	709047.9233	2099010.546	Infinite slope	Shale
16	1081	Don Moon – Lak Lai	Km.28+650.000 - Km.28+725.000	RT	707129.3827	2099390.562	Circular failure	Shale
17	1194	Mae Sariang – Mae Samlaep	Km.37+700.000 - Km.37+750.000	RT	373988.6972	1989716.407	Circular failure	Sandstone/Shale
18	1194	Mae Sariang – Mae Samlaep	Km.26+775.000 - Km.26+900.000	LT	380361.3980	1993211.504	Circular failure	Sandstone/Shale
19	1081	Lak Lai – Bo Kluea	Km.62+090.000 - Km.62+350.000	RT	724413.2560	2110316.617	Infinite slope	Sandstone/Shale
20	1093	Khun Huai Krai – Pha Tung	Km.64+215.000 - Km.64+250.000	LT	651064.1253	2195039.456	Circular failure	Phyllite
21	1093	Khun Huai Krai – Pha Tung	Km.80+800.000 - Km.80+900.000	LT	656381.0114	2200871.125	Circular failure	Phyllite
22	1093	Khun Huai Krai – Pha Tung	Km.88+720.000 - Km.88+760.000	LT	657915.9465	2204127.663	Circular failure	Phyllite
23	1093	Khun Huai Krai – Pha Tung	Km.88+742.000 - Km.88+777.000	RT	657916.4104	2204145.954	Infinite slope	Phyllite
24	1093	Khun Huai Krai – Pha Tung	Km.80+270.000 - Km.80+410.000	RT	656031.5364	2200637.095	Circular failure	Phyllite
25	1093	Khun Huai Krai – Pha Tung	Km.74+800.000 - Km.75+200.000	LT	655648.2625	2198084.994	Circular failure	Phyllite
26	1081	Lak Lai – Bo Kluea	Km.78+523.000 - Km.78+533.000	LT	728960.5745	2122457.578	Circular failure	Sandstone/Shale
27	1081	Lak Lai – Bo Kluea	Km.78+475.000 - Km.78+505.000	RT	728941.8534	2122426.736	Infinite slope	Sandstone/Shale
28	12	Wang Thong – Kek Noi	Km.103+880.000 - Km.103+960.000	LT	720630.5130	1856061.568	Circular failure	Sandstone/Shale
29	12	Wang Thong – Kek Noi	Km.108+570.000 - Km.108+635.000	LT	723611.4762	1856466.669	Circular failure	Sandstone/Shale
30	12	Wang Thong – Kek Noi	Km.108+890.000 - Km.108+940.000	LT	723839.9794	1856426.495	Circular failure	Sandstone/Shale

5.1 The result of factor of safety

From the analysis of the factor of safety totaling 30 areas in the northern region of Thailand. Both with Erosion and Circular Failure models. The result of the factor of safety totaling 30 areas in the northern region of Thailand was approximately 0.108-1.471, as shown in Table 5.

Table 5. The result of factor of safety

no.	Highway no.	Section	Km. - Km.	Lane	Factor of Safety
1	1249	Mae Ngon – Nong Tao	Km.14+620.000 – Km.15+050.000	RT	0.923
2	108	Mae Rid Bridge – Huai Ngu	Km.158+865.000 - Km.158+923.000	RT	0.832
3	2331	Jowo – Phu Hin Rong Kla Nation Park	Km.8+300.000 - Km.11+000.000	LT, RT	0.500
4	1095	Mae Na – Tha Krai	Km.112+007.000 - Km.112+035.000	RT	0.195
5	1263	Khun Yaum – Pang Oung	Km.18+580.000	LT	0.430
6	1093	Khun Huai Krai – Pha Tung	Km.48+650.000 - Km.48+675.000	LT	0.874
7	1093	Khun Huai Krai – Pha Tung	Km.44+250.000 - Km.44+280.000	RT	0.600
8	1093	Khun Huai Krai – Pha Tung	Km.59+300.000 - Km.59+500.000	LT, RT	0.444
9	1093	Khun Huai Krai – Pha Tung	Km.72+687.500 - Km.72+787.500	LT	0.917
10	1225	Pang Chang – Na Bua	Km.19+500.000 - Km.19+785.000	RT	1.471
11	1225	Pang Chang – Na Bua	Km.20+290.000 - Km.20+325.000	RT	0.767
12	1225	Pang Chang – Na Bua	Km.25+135.000 - Km.25+325.000	LT	0.398
13	12	Wang Thong – Kek Noi	Km.110+330.000 - Km.110+405.000	LT	0.549
14	1081	Don Moon – Lak Lai	Km.37+025.000 - Km.37+095.000	LT	0.286
15	1081	Don Moon – Lak Lai	Km.30+900.000 - Km.30+970.000	LT	0.326
16	1081	Don Moon – Lak Lai	Km.28+650.000 - Km.28+725.000	RT	0.349
17	1194	Mae Sariang – Mae Samlaep	Km.37+700.000 - Km.37+750.000	RT	0.849
18	1194	Mae Sariang – Mae Samlaep	Km.26+775.000 - Km.26+900.000	LT	1.287
19	1081	Lak Lai – Bo Kluea	Km.62+090.000 - Km.62+350.000	RT	0.755
20	1093	Khun Huai Krai – Pha Tung	Km.64+215.000 - Km.64+250.000	LT	0.908
21	1093	Khun Huai Krai – Pha Tung	Km.80+800.000 - Km.80+900.000	LT	0.949
22	1093	Khun Huai Krai – Pha Tung	Km.88+720.000 - Km.88+760.000	LT	0.915
23	1093	Khun Huai Krai – Pha Tung	Km.88+742.000 - Km.88+777.000	RT	1.330
24	1093	Khun Huai Krai – Pha Tung	Km.80+270.000 - Km.80+410.000	RT	0.953
25	1093	Khun Huai Krai – Pha Tung	Km.74+800.000 - Km.75+200.000	LT	0.976
26	1081	Lak Lai – Bo Kluea	Km.78+523.000 - Km.78+533.000	LT	0.957
27	1081	Lak Lai – Bo Kluea	Km.78+475.000 - Km.78+505.000	RT	0.600
28	12	Wang Thong – Kek Noi	Km.103+880.000 - Km.103+960.000	LT	0.514
29	12	Wang Thong – Kek Noi	Km.108+570.000 - Km.108+635.000	LT	0.491
30	12	Wang Thong – Kek Noi	Km.108+890.000 - Km.108+940.000	LT	0.108

5.2 Slope stability map

From the result, this research will be presents the slope stability assessment in "Factor of Safety Map in Northern Thailand". The results of a factor of safety have been interpolated to evaluate the stability of the area. Levels of a factor of safety are classified into 15 levels. The map is shown in Figure 10.

6. Discussion

Slope stability analysis in this research is the N-Value from the Standard Penetration Test in the slope failure area (or nearby at a distance of not more than 30 kilometers). The N-Value can compare to correlate the shear strength of soil (effective friction angle and cohesion), but N-Value should change to N_{60} (Bowles, 1997 and Aggour, 2001) before being calculated.

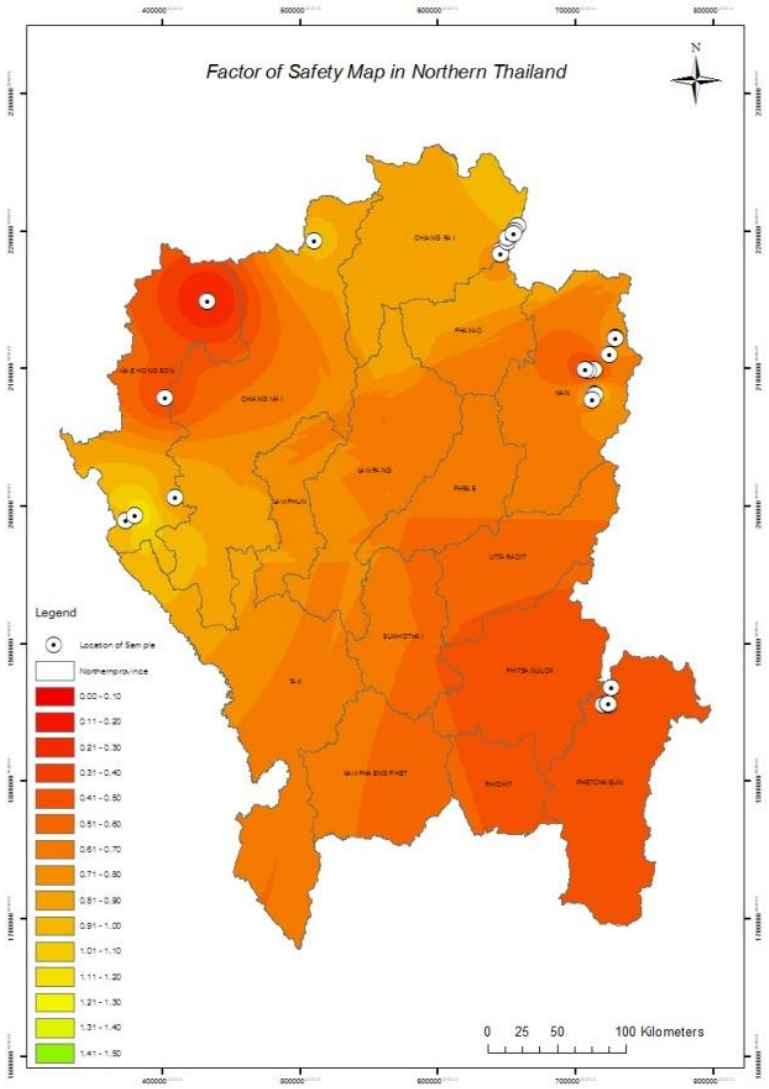

Figure 10. Factor of Safety Map in Northern Thailand

This research analyzes the effective friction angle and cohesion of soil from the Standard Penetration Test and calculates a factor of safety. According to research by Dechpatungwesa and Chairatanangamdaj (2019) studied and analyzed the cause of slope failure of Highway embankment No.1194 Mae Sariang - Mae Samlaep route sta.21+150 with is located theclosest to Study area no.18 (Highway No.1194 km.26+775-km.26+900 LT). Dechpatungwesa and Chairatanangamdaj analyzed the engineering properties of soil from the Direct Shear Test at normal humidity and high humidity. This research compared with the test at high humidity conditions. The factor of safety in high humidity is 1.10 (in normal conditions is 1.547), which similar to the calculation in this research is 1.287. However, the factor of safety is still different. In addition, there are different methods of obtaining the factor of safety. This may because this research focuses only on engineering properties in high moisture conditions (m=1), but Dechpatungwesa and Chairatanangamdaj were studied other properties as well because Mae Hong Sorn Province has an active fault. So, in areas with active fault, the earthquake force should be considered, and analysis of the factor of safety in each area should consider other natural factors as well.

7. Conclusions

This research focuses on the factor of safety from the Standard Penetration Test. Because a factor of safety is one of the indicators for evaluating slope stability by back-calculation analysis to calculate the factor of safety in slope failure area. N-value from the Standard Penetration Test can be compared to shear strength parameters: cohesion and friction angle. The result of calculating the factor of safety is approximately 0.108-1.471.

Acknowledgements

The authors would like to thank the Bureau of Materials, Analysis, and Inspection, Department of Highways for giving boring data, field data of slope failure sites along highways, and supporting Geo Studio 2007.

References

AASHTO: Standard Specification for Highway Bridges. American Association of State Highway and Transportation Officials. 1996. [12]

Baginska I. Estimating and Verifying Soil Unit Weight Determinated on the basis of SCPTu Test. Annals of Warsaw University of Life Science -SGGW. 2016; Land Reclamation No. 48(3) : p.233-42. [11]

Dechpatungwesa P., Chairatanangamdaj G., Poungchompu P. Study on Slope Failure of Highway Embankment No.1194 Mae Sariang-Mae Samlaep Route Sta.21+150. KKU Research Journal (Graduate Studies). 2019; 19 No.4: p. 127-38. [In Thai] [6]

Department of Mineral Resources. Geology of Northern and Western, Thailand. 2016. [Cited 2021 April 13]. Available from: http://www.dmr.go.th/ewtadmin/ewt/dmr_web/main.php?filename=nw_geo#b [21]

Devkata K.C., Regmi A.D., Pourghasemi H.R., Yoshida K., Pradhan b., Ryu I. C., et al. Landslide Susceptibility Mapping Using Certainty Factor, Index of Entropy and Logistic Regression Model in GIS and Their Comparison at Mugling-Narayanghat Road Section in Nepal Himalaya. Natural Hazard. 2012; 65: p. 135-65. [22]

Haapanen A.B., Stabilizing the Landslide on Road E87 Burgas-Malko Tornovo, Bulgaria. Procedia Engineering. 2016; Vol 43: p.650-57. [19]

Kaewsong R., Soicha T. and Boonsungnoen W. Study of Landslide Geo-Engineering: Hang Thang Luang Village Tumbol Phu Fah Aumphoe Bo Kluae, Nan. 2010. Bangkok. Bureau of Geo-Technical. Department of Mineral Resources. 63 pages. [In Thai] [16]

Mairaing W. Landslide : A Recent Natural Disaster. The Engineering Institute of Thailand Under H.M. The King's Patronage (EIT). 2006; Year 59th Vol. 4: p.51-65. [In Thai] [1]

Marques G.S. and Lukiantchuki J.A. Evaluation of the Stability of a highway slope through numerical modeling. DYNA. 2017; Vol.84, no.200: p.121-28. [8]

Mooltathong C., Chairatanangamdej G. and Poungchoompu P. Study on Slope Failure of Highway Embankment No.1349 Samoeng-Wat Chan Route. The 22nd National Convention on Civil Engineering. 18-20 July. 2017. Nakorn Ratchasima. Thailand.. [In Thai] [7]

Oh H. J., Saro L., Chotikasathien W., Kim C.H., Kwon J. H., Predictive Landslide Susceptibility Mapping Using Spatial Information in the Petchabun Area of Thailand. Environmental Geology. 2009; 57: p. 641-51. [18]

Porlila V., Thaiyuenyong S., Ongsuphankul S. and Thepwong R. Effect of Volume Change on Shear Strength of Unsaturated Soil. Rattanakosin Journal of Science and Technology (RJST). 2019; Vol. 1 Issue 3: p.22-32. [In Thai] [5]

Prothong S., Carling P. A., Leyland j. Climate Change and Landslide Risk Assessment in Uttaradit Province, Thailand. Engineering Journal. Vol.22 Issue 1; 2018: p.243-55. [17]

Rujajaratwong S. Department of Mineral Resources and Problem Solving of Landslide in Thailand. Bureau of Environmental Geology. Department of Mineral Resources. Academic Conference of Department of Mineral Resources. p. 238-44. [20]

Salunkhe D.P., Chvan G., Bartakke R.N. and Kothavale P.R. An Overview on Method for Slope Stability Analysis. International Journal of Engineering Research and Technology (IJERT). 2017; Vol. 6 Issue 03: p.528-35. [3]

Soralump S., Thowiwat W. Shear Strength-Moisture Behavior of Residual Soils of Landslide Sensitive Rocks Group in Thailand. The 15th National Convention on Civil Engineering. 12-14 May. 2010. Ubon Ratchathani. Thailand. [In Thai] [13]

Soralump S., Thowiwat W., Mairaing W. Shear Strength Testing of Soil Using for Warning Heavy Rainfall-Induced Landslide. The 12th National Convention on Civil Engineering. 2-4 May 2007. Pitsanulok. Thailand. [In Thai] [14]

Sorralum S. et al. Map of soil shear strength in mountainous areas (for evaluating slope stability) [Internet]. Geotechnical Engineering Research and Development Center (GERD). Bangkok: Kasetsart University; 2019. [Cited 2019 June 9]. Available from: http://www.gerd.eng.ku.ac.th/Map/Map.html [10]

Standard Test Method for Standard Penetration Test (SPT) and Split-Barrel Sampling of Soils: D1586-11. American Society for Testing and Materials (ASTM). 2011. [9]

Visutmethanukul P. Foundation Engineering Manual. Bangkok: Se-Ed Education. 2015. 792 pages. [In Thai] [4]

Yusof N.Q.A.M and Zabidi H. Reliability of Using Standard Penetration Test (SPT) in Predicting Properties of Soil. Journal of Physics. 2018; 1082: p.1-6. [2]

Yuth Kaiyawan. Principle and Using Analysis of Logistic Regression for Research. Journal of Research. Rajamangala University of Technology Srivijaya. 4(1); 2555: p.1-12. [In Thai] [1

Study of Using Natural Rubber Latex as a Filtrate Loss Prevention Additive for API Class G Cement

Pattariya Aksornnarong[a*] and Akkapun Wannnakomol[b*]

School of Geotechnology, Institute of Engineering, Suranaree University of Technology, Nakhon Ratchasima, 30000, Thailand

Abstract

The main objective of this research is to study the probability of using natural rubber latex (NRL), inexpensive and ecological friendly biopolymer and easily affordable in Thailand, as a fluid loss prevention additive for the API Class G Cement. In this study the API class G cement had been prepared as cement slurry at water/cement ratio (W/C) of 0.5 wt.% and were mixed with natural rubber latex (60% concentrated Latex - High Ammonia) at polymer (NRL) /cement ratio (P/C) of 0.05, 0.10, 0.15, 0.20 and 0.25 The cement slurry samples were casted in the cylindrical mold, moist cured for 7 days, and air cured for 28 days at room temperature, respectively.

The porosity and permeability test were conducted under the Overburden poro-perm cell unit, and results of the tests showed that the porosity and permeability values of the cement samples decreased until the P/C ratio reach 10 wt.% and then they increased steadily. This is because if the P/C ratio is greater than 10 wt.%, the hydration reaction of the mixed cement will take place rather than the polymer coalescence reaction and resulted in the higher polymer flocculant and dispersion. Therefore, the optimal P/C ratio for using the natural rubber latex as a fluid loss prevention additive for the API Class G Cement is 10 wt.%.

Keyword: API class G cement/ Natural rubber latex/ Latex modified cement/ Porosity/ Permeability

---

*Corresponding Author: Tel: +6680-333-0843[a], +6689-722-5234[b]
E-mail address: m6040352@g.sut.ac.th[a]; akkhapun@sut.ac.th[b]

1. Introduction

Primary cementing is the process of placing cement in the annulus between the casing and the formations exposed to the wellbore. Since its inception in 1903, the major objective of primary cementing has always been to provide zonal isolation in the wellbore of oil, gas, and water wells (Smith, 1984), e.g., to exclude fluids such as water or gas in one zone from oil in another zone. To achieve this objective, a hydraulic seal must be obtained between the casing and the cement, and between the cement and the formations, while at the same time preventing fluid channels in the cement sheath (Figure 1).

Fluid loss control agents have been added to well cement slurries for more than 20 years, and it is now recognized that the quality of cement jobs has improved significantly. Indeed, it is generally acknowledged that insufficient fluid-loss control is often responsible for primary cementing failures, because of excessive increases in slurry density or annulus bridging. In addition, formation invasion by cement filtrate may be very damaging and deleterious to production (Bannister and Lawson, 1985; Economides and Nolte, 1987). With respect to remedial cementing, the problem is to adjust the fluid-loss rate to the perforation size and the nature of the formation (Binkley et al., 1957; Cook and Cunningham, 1977). However, for both primary and remedial cementing, very little has been written to justify the level of fluid-loss control required to achieve a good cement job [1].

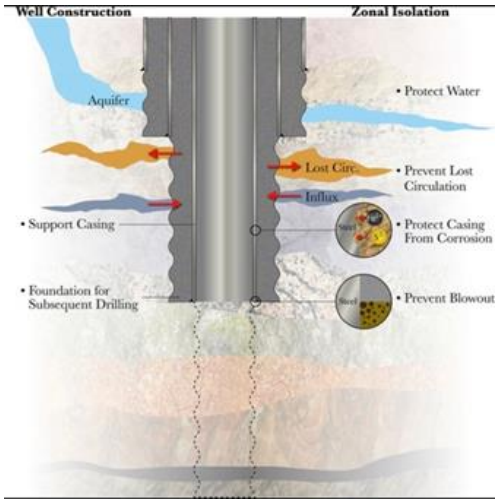

Figure 1. Illustrates the reasons why we cement wells

Nowadays cement mix may be used a chemical as an additive to provide the suitable cement. For example, using polymer as an additive to reduce fluid loss and reduce permeability. However, these chemicals are expensive and to reduce costs, this study is to find replacement materials.

polymer-modified (or polymer- cement) mortar or concrete, which is made by the modifying ordinary cement mortar or concrete with polymer additives such as latexes, redispersible polymer powders, water-soluble polymers, liquid resins, and monomers. Polymer-modified mortars and concretes have a monolithic co-matrix in which the organic polymer matrix and the cement gel matrix are homogenized. The properties of polymer modified mortar and concrete are characterized by such a co-matrix. In the systems modified with the latexes, redispersible polymer powders, and water-soluble polymers, the drainage of water from the systems along with the cement hydration leads to film or membrane formation. In the systems modified with the liquid resins and monomers, the addition of water induces the hydration of the cement and the polymerization of the liquid resins or monomers [2].

In 2020, the total value of intermediate rubber production in Thailand came to around THB140 billion, including goods sold on both domestic and export markets. Thailand is in the fortunate position of its production being overwhelmingly of fresh rubber (92% of upstream production is of fresh latex rubber).

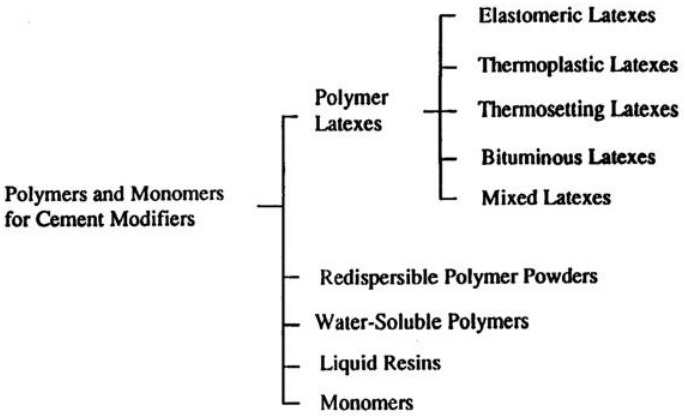

Figure 2. Polymers and monomers for cement modifiers

Over the years 2004 to 2011, the price of rubber rose to historic highs because Global demand for rubber rose sharply through this period, especially from China and India, following this boom period, though, demand slackened substantially and world commodity markets deflated as speculative pressure had faded, leaving global stocks of rubber at around 3.0 - 3.1 million tones at the end of 2018-2019. Nowadays the price of rubber is very low. Therefore, this study, in finding replacement materials, also wanted to increase the value of rubber latex as well [3].

Natural Rubber Latex (NRL) is a natural renewable resource, which can be employed for modification of cement [4]. Natural Rubber latex obtained from *Heveabrasiliensis* tree by natural polymerization process and is a dispersion of polyisoprene [5].

Natural Rubber Latex represents an eco-friendly, sustainable and non-petroleum based material. Low cost, increasing availability and the ecological aspect as a renewable material make natural rubber attractive for new applications [6].

Natural rubber latex is a good choice to use in cement mix because it is a natural polymer, not harmful to the environment, low costs and easy to provide locally. However, the appropriate mixing ratio of cement, Natural rubber latex, and other binder materials is not well studied and determined.

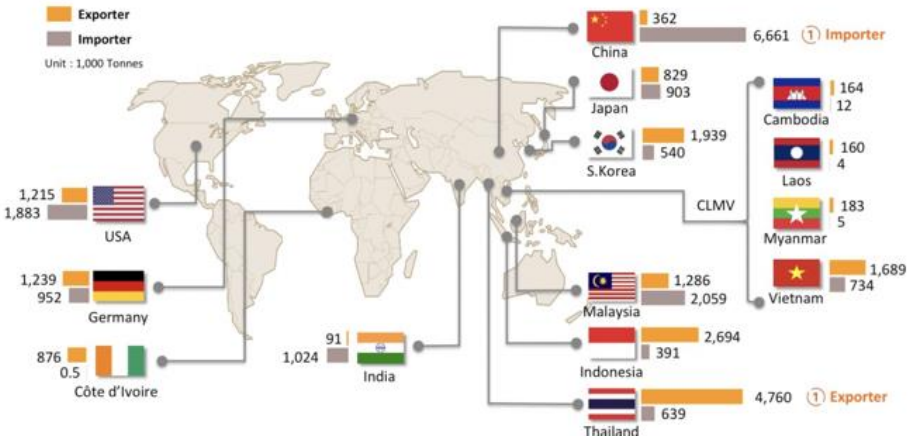

Figure 3. Major Natural Rubber Exporters and Importers (2019)

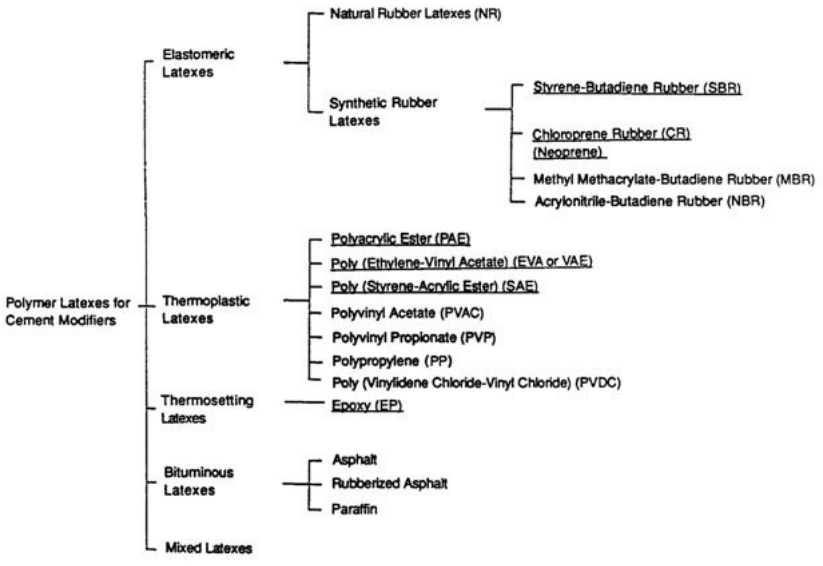

Figure 4. Commercially available polymer latex for cement modifiers

2. Literature review

Brief description of the various past studies conducted on the effect of natural rubber latex modification of concrete is presented below.

Bala M., Ismail M. (2012) discovered the concrete with natural rubber latex improves the plain concrete from porous to an impermeable structure by forming a lining of latex film across voids pores and micro cracks [7]. Muhammed Ijas M. et al. (2016) investigated effect of natural rubber latex (NRL) – clay power mixture on the strength of Portland concrete. The strength of concrete mainly depends upon the porosity. Concrete has high compressive strength and low tensile strength. Earlier natural rubber latex was added to the concrete, which were able to reduce the porosity that a polymer latex added to concrete can reduce the porosity and improve the strength of the test concrete [8]. Thanarit R. (2011) studied filtration properties of Natural Rubber Latex containing mud and found that Natural Rubber Latex in bentonite could reduce the fluid filtration loss volume. He also found that the thermal stability of the Natural Rubber Latex mud could be used in subterranean well formation having downhole temperature up to 80°C [17]. Therefore, this study aims to determine the optimum material mixing ratio in order to improve the compressive strength of the mixed API class G cement.

3. Methodology

3.1 Principles of latex modification

Latex modification of cement mortar and concrete is governed by both cement hydration and polymer film formation processes in their binder phase. The cement hydration process generally precedes the polymer formation process. In due course, a co-matrix phase is formed by both cement hydration and polymer film formation processes [2].

3.2 Mechanism of Polymer-Cement Co-matrix Formation

It is believed that a co-matrix phase which consists of cement gel and polymer films is generally formed as a binder according to a three-step simplified model shown in Figure 5 and Figure 6

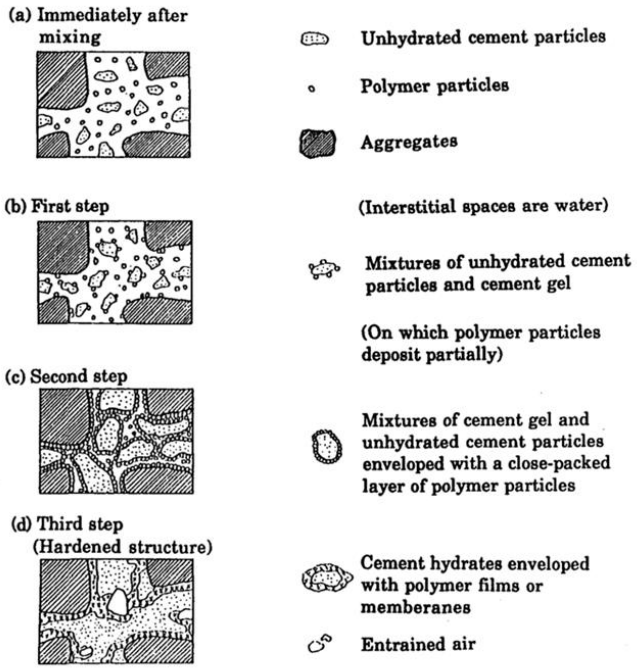

Figure 5. Simplified model of formation of polymer -cement co-matrix

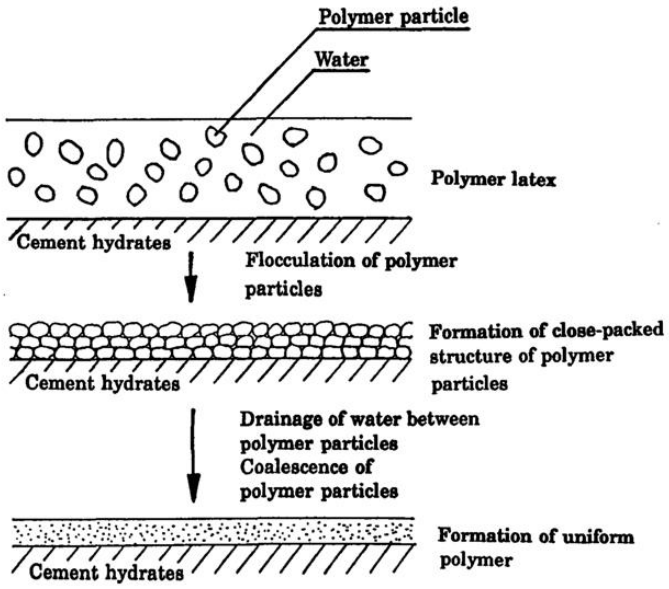

Figure 6. Simplified model of process of polymer film formation on cement hydrates

Grosskurth proposed a similar model indicating the formation of the polymer cement co-matric. Sugita et al., have recently investigated the microstructures and composite mechanism of latex-modified pastes and mortars, and found the interfacial layer of cement hydrates with a large amount of polymer particles on the aggregates and cement particles. As a result, both the particle dispersion of the polymer and the formation of polymer films are necessary for explaining the composite mechanism of the latex-modified systems [2].

3.3 Material

3.3.1 API Class G Cement

API Class G (HSR) cements are used in the production and exploration of oil and gas onshore and in deep water offshore wells to depths of up to 10,000 feet (3,048 meters). A typical well can be thousands of meters deep, less than a meter wide, and is constructed by using a metal casing surrounded by a special cement slurry mix that fills the annulus between the outer face of the tubing and the wall formation of the hole.

3.3.2 Natural Rubber Latex

Natural Rubber latex in Hevea Brasiliensis is located in latex vessels to be founded in various parts of the tree. The lowest occurring is in the wood and the highest in the secondary phloem. There are the vessels aligned to spirals in concentric circles close to cambium. It is obtained from them by tapping based on cutting of the tree bark by special knife under approximate angle of 30°. It is collected into special bowls. In this study used natural rubber latex (60% Concentrated Latex - High Ammonia)

3.3.3 Water

Water is an important ingredient of concrete as it actively participates in the Chemical reaction with cement. The quantity and quality of water is to be carefully selected for the test conducted for the investigation.

3.3.4 Surfactants

Polymer latex is a colloidal dispersion of small polymer particles in water, which is generally produced by the emulsion polymerization of monomers with surfactants. Surfactants are a large group of surface-active substances with numerous applications because of their relatively complex behaviors [10-13]. Surfactants have a hydrophobic part and a hydrophilic part. depending on the nature of the hydrophilic part the sur- factants are classified as anionic, nonionic, cationic, and zwitterionic [14]. Ouyang et al. (2008) studied the effect of the synthetic surfactant combining nonionic and anionic surfactant on the compressive strength of

cement mortar. The results indicated that the suitable dosage of this surfactant could improve not only the fluidity but also the compressive strength of mortar. On the other hand, an excess amount of surfactant may have an adverse effect on the strength of the latex modified mortar and concrete because of the reduced latex film strength [16]. Siriphun S. et al. (2005) Mixed concrete with natural rubber latex Can be mixed with a mixer like general concrete Importantly, water must be mixed with non-ionic surfactants [9].In this study used Lutensol XL 80 at a ratio of 4% by weight of the total cement. When the concrete is well blended, the natural latex is then mixed in the last order.

3.4 Cement Preparation

In this study the API class G cement had been prepared as cement slurry at water/cement ratio (W/C) of 0.5 wt.% and were mixed with natural rubber latex (60% concentrated Latex - High Ammonia) at polymer (NRL) /cement ratio (P/C) of 0, 0.05, 0.10, 0.15, 0.20 and 0.25 by Cement mixer equipment

The cement slurry samples were casted in the cylindrical mold and cut in size 1.46”x2”, moist cured for 7 days, and air cured for 28 days at room temperature, respectively. The formulations of the cement are shown in Table 1.

Table 1. Compositions of cement sample.

Sample	API class G cement (g.)	Water (g.)	NRL (g.)	Surfactant (g.)
No.1	1500	750	0	0
No.2	1500	750	75	60
No.3	1500	750	150	60
No.4	1500	750	225	60
No.5	1500	750	300	60
No.6	1500	750	375	60

3.5 Testing

All of cement sample was tested in the Suranaree University of Technology laboratory. Base on API (American Petroleum Institute) RP 10B-2, Recommended Practice for Testing Well Cements [18].

3.5.1 Porosity

Porosity is define as the ratio of void-space volume (ie. Pore volume) to bulk volume of a material. Porosity in clean and dried core samples is determinate by a combination of two of the following three physical properties such as Grain volume, Pore volume, and Bulk volume Grain volume and pore volume can be determined from Helium injection and the application of Boyle’s Law. Bulk volume measured by the summation of pore volume and grain volume [19].

3.5.2 Pemeability

To determine the permeability (using Overburden poro-perme cell) of a core sample air (or nitrogen) at a known initial pressure (upstream pressure) is made to flow through the length of the sample. The sample is sealed along its length so that no air may bypass the sample. The flow rate of air from the other end of the sample is measured. The permeability for that sample is then calculated using Darcy’s Law through knowledge of the upstream pressure and flow rate during the test, the atmospheric pressure, the viscosity of air (or nitrogen), and the length and cross sectional area of the sample [19].

Figure 7. Cement sample

4. Result and Discussion

4.1 Porosity Test

Porosity test results of cement samples by using a Porosimeter (Figure 8). In this testing, including the use of principles Boyle's Law for determining porosity is shown in Table 2 and Figure 10

Figure 8. Porosimeter

4.2 Permeability Test

Permeability Test Results of the cement sample using a permeameter (Figure 9) for testing and Darcy's Law Principle of Coefficient Calculation in the permeability of cement. This test used an external pressure (Overburden pressure) of 600 psi and the pressure that flows through the sample 40 psi as shown in Table 3 and Figure 11.

Based on the porosity measurement results of a set of natural rubber latex cement samples. It was found that the porosity of all samples tended to improve with the addition of natural rubber latex, (%porosity are decrease), When natural latex was not added, the result was 18.01. When adding up to 10%wt., the porosity was continuously decreasing. But if adding more than 10% wt., founded the porosity will gradually increase. However, the porosity was still less than when natural latex was not added.

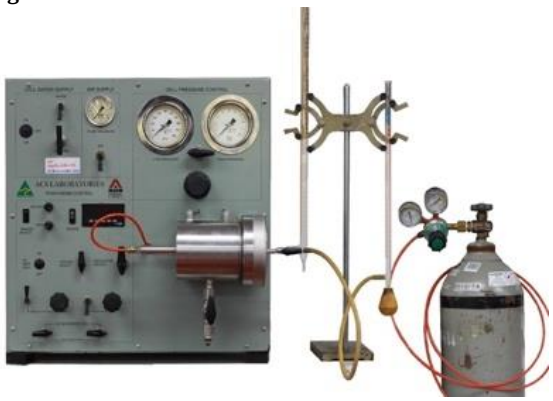

Figure 9. Permeameter

Table 2. Porosity results of cement samples

Ratio	Sample	Diameter (mm)	Length (mm)	P_{os} (psi)	P_s (psi)	Porosity (%) Result	Average
0.00	1/1	37.3	51.1	50.01	12.01	17.91	18.01
	1/2	37.4	49.8	50.08	11.81	18.11	
0.05	2/1	37.3	50.6	50.01	12.39	13.96	15.34
	2/2	37.3	51.7	50.04	12.28	16.72	

Table 2. Porosity results of cement samples (cont.)

Ratio	Sample	Diameter (mm)	Length (mm)	P_{os} (psi)	P_s (psi)	Porosity (%) Result	Average
0.10	3/1	37.5	53.8	50.01	13.44	12.73	11.44
	3/2	37.4	51.9	50.06	13.29	10.14	
0.15	4/1	37.3	50.6	50.02	12.44	13.58	12.50
	4/2	376	50.7	50.05	12.94	11.43	
0.20	5/1	37.4	53.2	50.01	12.86	15.17	14.09
	5/2	37.8	52.7	50.04	13.2	13.01	
0.25	6/1	37.8	49.2	50.08	12.10	15.46	16.28
	6/2	37.8	50.1	50.05	12.08	17.09	

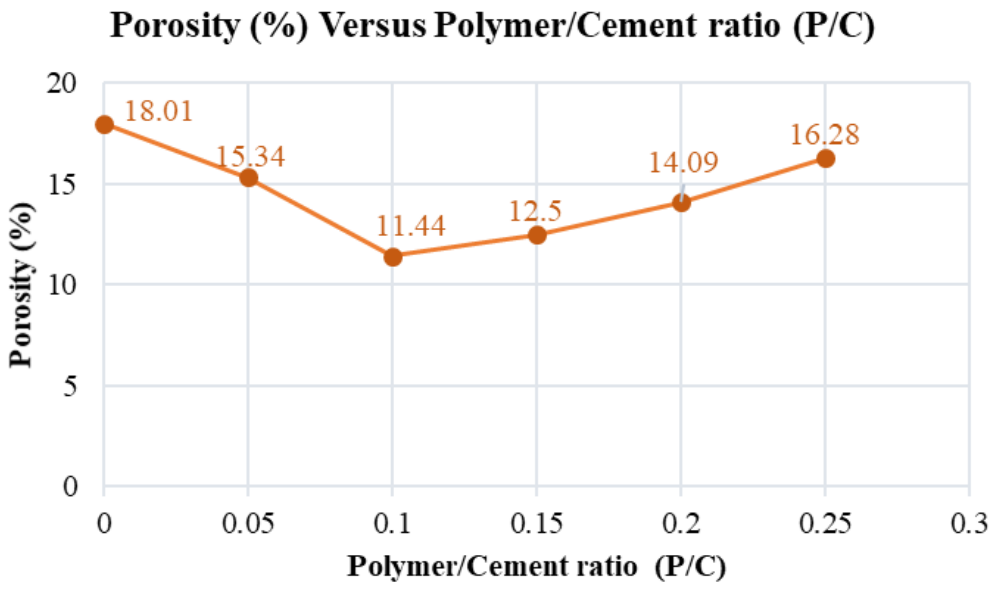

Figure 10. Porosity (%) Versus Polymer/Cement ratio (P/C)

Table 3. Permeability results of cement samples

Ratio	Sample	Diameter (mm)	Length (mm)	P_c psi	P_1 psi	V cm^3	Time sec	Q cm^3/sec	k (millidarcy) Result	Average
0.00	1/1	37.3	51.1	600	40	10	27.58	0.363	0.446	0.471
	1/2	37.4	49.8	600	40	10	24.05	0.416	0.496	
0.05	2/1	37.3	50.6	600	40	10	20.5	0.049	0.062	0.064
	2/2	37.3	51.7	600	40	10	19.0	0.053	0.066	
0.10	3/1	37.5	53.8	600	40	10	35.0	0.029	0.035	0.027
	3/2	37.4	51.9	600	40	10	26.3	0.038	0.047	
0.15	4/1	37.3	50.6	600	40	10	25.4	0.039	0.048	0.048
	4/2	376	50.7	600	40	10	24.8	0.040	0.048	
0.20	5/1	37.4	53.2	600	40	10	15.7	0.064	0.081	0.077
	5/2	37.8	52.7	600	40	10	17.0	0.059	0.073	
0.25	6/1	37.8	49.2	600	40	10	9.1	0.110	0.127	0.124
	6/2	37.8	50.1	600	40	10	9.6	0.104	0.122	

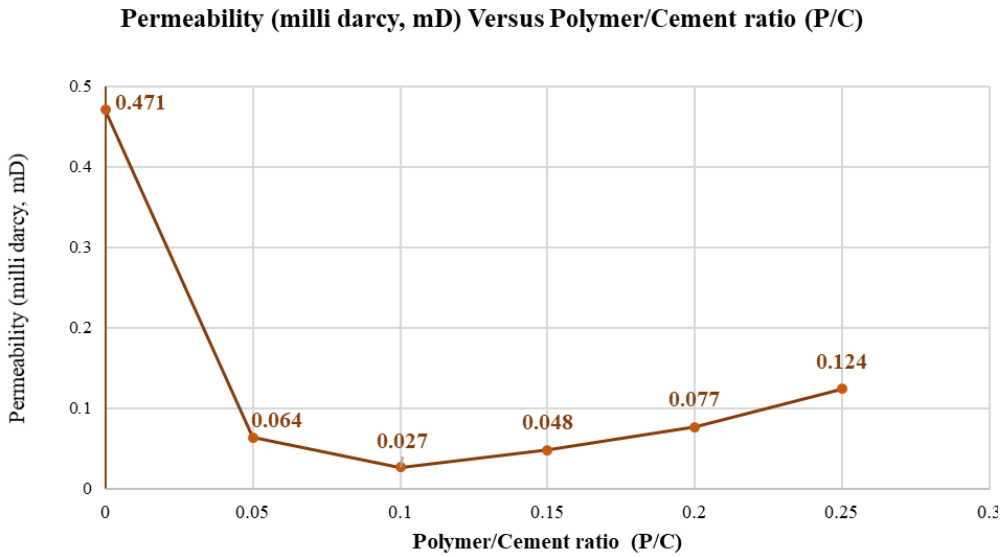

Figure 11. Permeability (milli darcy, mD) Versus Polymer/Cement ratio (P/C)

Based on the permeability measurement results of a set of natural rubber latex cement samples. It was found that the permeability decreased sharply when natural rubber latex was added. It shown that adding natural rubber latex and cement had formation of polymer films.

Results of the tests showed natural rubber latex cement decrease porosity and permeability by forming a lining of latex film across voids pores and micro cracks. the porosity and permeability values of the cement samples decreased until the P/C ratio reach 10 wt.% and then they increased steadily.the porosity and permeability values began to increase again after adding more than 10% wt. because if the P/C ratio is greater than 10 %wt., the hydration reaction of the mixed cement will take place rather than the polymer coalescence reaction and resulted in the higher polymer flocculant and dispersion. Therefore, the optimal P/C ratio for using the natural rubber latex as a fluid loss prevention additive for the API Class G Cement is 10 % wt.

5. Conclusions

Based on laboratory experiments and data analysis in this study. Some conclusions were drawn as follows:

1. Natural latex can be used as an additive for class G cement in terms of its use as a protective loss fluid.
2. From the test of cement added with natural rubber latex. It was found that natural latex binds to cement, has better porosity and better permeability.
3. The optimum ratio for use is P/C = 0.10 because it is low porosity and permeability.

Acknowledgement

This research has been supported by Suranaree University of Technology (SUT). The author is also thankful to all of the staff of SUT laboratory for allowing using analyzes equipment and their advice. This thesis cannot be completed without the effort from Miss Supharapon Sakulpakdee, Mr. Sakchai Glumglomjit, and other people for suggestions and all their help.

References

API RP 10B, Recommended Practice for Testing Well Cements (22nd ed.). (1997). Washington, DC: API.

Asst Prof. Ahana K Reji, Athira Ajithan B, Fouzia Hussain M, Alfiya J, Minsurya Shajahan (2018). Latex Modified high performance concrete. Internationnal Journal of engineering Research & Tecnology (IJERT).

Bala M., Ismail M. (2012). “Performance of Natural rubber latex modified concrete in acidic and sulfated environments”, ELSEVIER Journal of Constuction and Building Material, Vol.31, pp.129-134

Crook, R. (2006). Petroleum Engineering Handbook (Volume II- Drilling Engineering). Richardson, TX: Society of Petroleum.

D. M. Bloor, Y. Li, and E. Wyn-Jones (1995). “Binding of sodium alkyl sulfates to a polymer labeled with a covalently bonded solvatochromic probe,” Langmuir, vol. 11, no. 10, pp. 3778–3781,

Erik B. Nelson (1990). Well Cementing. Texas: Schlumberger Educational Services.

G. Wang and G. Olofsson (1995). "Ethyl (hydroxyethyl) cellulose and ionic surfactants in dilute solution. Calorimetric and viscosity study of the interaction with SDS and some cationic surfactants," Journal of Physical Chemistry, vol. 99, no. 15, pp. 5588– 5596.

Kohiya s., Ikeda Y. (2014). Chemistry, Manufacture and Applications of Natural Rubber. United Kingdom: Woodhead Publishing.

M. Cappellari, A. Daubresse, and M. Chaouche (2013). "Influence of organic thickening admixtures on the rheological properties of mortars: relationship with water-retention," Construction and Building Materials, vol. 38, pp. 950–961,

M. U. K. Afridi, Y. Ohama, K. Demura, and M. Z. Iqbal (2003). "Development of polymer films by the coalescence of polymer particles in powdered and aqueous polymer-modified mortars," Cement and Concrete Research, vol. 33, no. 11, pp. 1715–1721

Mohammed Ijas M, Bifin Johns M.T., Shehinshad T.P., Nuayim E., Dr A.S. Abdul Rasheed & Fazil A. (2016). Effect of Natural Rubber Latex (NRL)-Clay powder mixture on The Strenght Of portland Concrete.Imperial Journal of Interdisciplinary Research (IJIR), (pp 12-16).

Nagraj T, S., Iyengar R., Rao K. (2010). "Super plasticized natural rubber latex modified concrete", Cement and Concrete Research, Vol 18 (1), pp 138-144

Ohama Yoshihiko (1995). Handbook of polymer-modified concrete and motar. New Jersey: Noyes Publications.

Siriphun S., Bunnun P., Loha K., Gamnerdvam A. (2005). "Using natural rubber for development of concrete works".

Sowcharoensuk C. (2021). "Natural rubber processing". Thailand industry outlook 2021-23., pp.1-11.

Thanarit Riyapan (2011). Using Natural Rubber Latex as Drilling. pp 46-52.

W. P. Seng, K. C. Tam, R. D. Jenkins, and D. R. Bassett (2000). "Calori- metric studies of model hydrophobically modified alkali- soluble emulsion polymers with varying spacer chain length in ionic surfactant solutions," Macromolecules, vol. 33, no. 5, pp. 1727–1733.

W. P. Seng, K. C. Tam, R. D. Jenkins, and D. R. Bassett(2000). "Model alkali-soluble associative (HASE) polymers and ionic surfactant interactions examined by isothermal titration calorimetry," Langmuir, vol. 16, no. 5, pp. 2151–2156.

X. Ouyang, Y. Guo, and X. Qiu (2008). "The feasibility of synthetic surfactant as an air entraining agent for the cement matrix," Construction and Building Materials, vol. 22, no. 8, pp. 1774– 1779,

A Study on the Coupling Coordination Between Tourism Economy and Ecological Environment

Yiming Liu[a], Taro Nishizawa[a], Yanning Cai[a], Shanshan Wang[b], and Sunhee Suk[a*]

[a]Graduate School of Fisheries and Environmental Sciences, Nagasaki University, Nagasaki 852-8521, Japan
[b]Heihe University, Heihe 164300, China

Abstract

Tourism environment is the basis of sustainable development of tourism economy. Exploring the coupling relationship between tourism economy and ecological environment system can not only promote the construction of tourism ecological civilization, but also contribute to the sustainable development of tourism economy. Based on data from Nagasaki Prefecture, Japan, from 2010-2019, this paper aims to introduce an indicator system and develop an integrated approach to assess the coupling and coordination between the tourism economy and the environment. The indicator system consists of 2 levels, 6 aspects, and 18 indicators, weighted by Entropy method. Based on the development status of Nagasaki Prefecture in Japan the PSR model framework of the coupling and coordination mechanism of tourism economy and ecological environment is constructed. Then, the coupled coordination degree of its tourism economy and ecological environment is evaluated, and the comprehensive evaluation index of the system is derived. Finally, suggestions for promoting the sustainable development of tourism and environment in Nagasaki Prefecture, Japan, are proposed.

Keyword: PSR model/ Tourism development/ Ecological environment/ Coupled and coordinated development

---

*Corresponding Author: Sunhee Suk
E-mail address: suksunhee@nagasaki-u.ac.jp

1. Introduction

As a resource-dependent and environment-dependent industry, tourism development and the ecological environment are inextricably linked. On the one hand, the ecological environment is the guarantee and source of the development of the tourism economy, which in turn will promote the improvement of the ecological environment. On the other hand, excessive pursuit of economic benefits will lead to the deterioration of the ecological environment, which in turn will affect the sustainability of tourism economic development. Therefore, the study of the coupled and coordinated development of tourism and the ecological environment has become a hot spot for academic research. This has important theoretical and guiding values.

Researchers have studied the relationship between the environment and tourism as far back as 1920 (Lutz, H. J.,1945). In this initial phase, scholars began to study the ecological impacts of tourism activities. Most of the studies are general observations and qualitative descriptions (Akoglu, T., 1971 and Budowski, G., 1976). With the rapid development of tourism, researchers have begun to pay attention to the issues of tourism capacity and tourism carrying capacity (Ovington, J. D., Groves, K. W., Stevens, P. R., & Tanton, M. T., 1974 and Sutcliffe, C. M., & Sinclair, M. T., 1980). In the 21st century, as research continues to intensify, researchers have gradually become more interested in studying the relationship between ecological environment and tourism. Studies of the relationship between tourism and the ecological environment have become more specific and diverse, especially in tourism ecological security (Nie, N., Wang, H., & Xiong, J. X., 2011 and Wang, Y., Wu, C., Wang, F., Sun, Q., Wang, X., & Guo, S., 2021), the development of tourism resources and the protection of the ecological environment (Bo, Q. I. N., 2007), and the impact of climate warming on tourism development (Wang, S., He, Y., & Song, X.,2010 and Shi-Jin, W., & Lan-Yue, Z., 2019). Researchers have introduced a large number of models and quantitative methods, which have provided new research ideas for the study of the coordinated development of tourism

and the environment. In the study of coupled and coordinated development, most scholars have conducted research on tourism and the environment (Tang, Z., 2015 and GENG, S., & XIE, Y.,2013). Many researchers have studied its coupling and coordination with tourism from the perspective of tourism traffic (Wang, Y. M., & MA, Y. F., 2011 and Zeng, J., Rong, Q., Yue, W., Dai, X., & Su, M.,2020, March), urbanization (Liu, J., Li, C., Tao, J., Ma, Y., & Wen, X., 2019 and Nan, C. A. O., Yaofeng, M., Tianshun, L., & Kai, B. A. I., 2013) and air environment (Geng, Y., Wei, Z., Zhang, H., & Maimaituerxun, M., 2020 and Geng, Y., Maimaituerxun, M., & Zhang, H., 2020).

In summary, research methods on the relationship between the ecological environment and the tourism economy have gradually changed from qualitative to quantitative research. Among them, coupled coordination models have been more widely applied (Geng, Y., Wang, R., Wei, Z., & Zhai, Q., 2021 and Li, Y., Li, Y., Zhou, Y., Shi, Y., & Zhu, X., 2012 and Chen, J., Li, Z., Dong, Y., Song, M., Shahbaz, M., & Xie, Q., 2020). However, existing studies are mainly limited to large cities with mature tourism development and the whole country, while small and medium-sized cities are neglected as the basic units of the interaction between ecological environment and tourism economy (Huang, J., Shen, J., & Miao, L. , 2021 and Cheng, X., Long, R., Chen, H., & Li, Q., 2019). Therefore, this research takes Nagasaki Prefecture in Japan as the research object and constructs an evaluation index system for ecological environment and tourism economy.

2. Methodology

2.1 Study area

The study area was Nagasaki Prefecture, which is located at the southernmost tip of Japan and the westernmost of Kyushu Island. Nagasaki Prefecture is located close to the Korean Peninsula and mainland China, making it the closest place in Japan to mainland Asia. There are 13 cities under Nagasaki Prefecture, and the seat of the prefectural office is Nagasaki City. The climate in Nagasaki Prefecture is typically maritime, with an average annual temperature of 18.0°C and an annual precipitation of 1,464 mm. Nagasaki Prefecture has the 2nd longest coastline in Japan at 4,203 km. Nagasaki Prefecture has the largest fishery resources in Japan, with a variety of natural fish species. The location of Nagasaki Prefecture is shown in Figure 1.

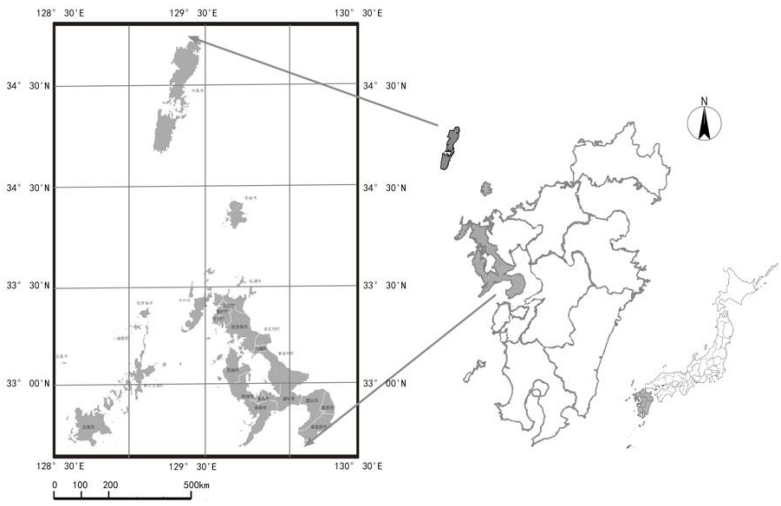

Figure 1. The location of Nagasaki Prefecture

2.2 Date resource

This paper used panel data (2010, 2013, 2016, and 2019) in Nagasaki Prefecture. Among them, tourism economic data was obtained from the Nagasaki Prefectural Tourism Trends Survey and Nagasaki Prefectural Tourism Statistics. The ecological environment data were derived from the Ministry of the Environment's official

website, the e-Stat statistics website and the website of the National Institute for Environmental Studies of Japan.

3. Methods

3.1 Assessment index system

At present, there is no uniform standard for the construction an evaluation index system of tourism economy and ecological environment system. Therefore, this research has selected the indicators that exist to study the relationship between tourism economy and ecological environment with high frequency of use. In order to analyze the coupling development process of tourism economy and ecological environment more objectively and systematically in Nagasaki Prefecture. This research combines the actual situation of Nagasaki Prefecture and constructs an evaluation index system for the tourism economy and ecological environment system (Table 1). Among them, the tourism economic system selects 9 indicators from the three dimensions of ecological resources, ecological environment and development potential to comprehensively evaluate the development level of the tourism economy. According to the "pressure (P)-state (S)-response (R)" model, the ecological environment system selects 10 indicators in three dimensions to comprehensively evaluate the development level of the ecological environment.

Table 1. Index system used for evaluation of the relationship between tourism economy and eco-environment

Subsystem	First-class index	Second-class index	Unit
Tourism economy	Economic benefit	Total tourism revenue	Billion yen/year
		The proportion of total tourism revenue in the tertiary industry	%
		Total tourism revenue as a proportion of GDP	%
	Scale of development	Total number of tourist reception	Ten thousand people
		Total number of foreign tourists received	Ten thousand people
		Total number of tourist reception accounts for the proportion of the permanent population	%
	Tourism supply	Number of main tourist facilities	place
		Number of places of interest	place
		Number of accommodation facilities	place
Eco-environment	Pressure	Discharge of domestic waste per person per day	g/person·day
		Water pollutant discharge	Thousand tons/year
		Waste discharge	Thousand tons/year
		Garbage discharge per person per day	g/person·day
	State	Dam impoundment rate	%
		Forestry rate	%
		Park green area per capita	Hectares
	Response	Waste treatment rate	%
		Population penetration rate of sewage treatment	%
		Waste recycling rate	%

3.2 data standardization

The tourism economy and eco-environmental system contains several index layers. The dimensions of each index are different, and the direction of the force is also different. Therefore, the value of each index needs to be standardized for comprehensive evaluation (Fan, Y., Fang, C., & Zhang, Q., 2019). Assuming that the m-th index value of the n-th year in a certain place is x_{nm}, the maximum value of index j is x_{max} and the minimum value is x_{min}. According to the positive and negative properties of the index, the normalized value of x_{nm} can be obtained.

Positive index (larger value for a useful parameter):

$$\chi'_{nm} = \frac{\chi_{nm} - \chi_{min}}{\chi_{max} - \chi_{min}} \quad (1)$$

Negative index (smaller value for a useful parameter):

$$\chi'_{nm} = \frac{\chi_{max} - \chi_{nm}}{\chi_{max} - \chi_{min}} \quad (2)$$

3.3 Index weight calculation

Since the entropy method is more objective than the subjective analysis method, this study uses the entropy method to determine the weight of the index and avoid the influence of subjective factors. This study follows the calculation process of the entropy method. First, calculate the normalized index proportion S_{nm} of index m (Equation 3); second, calculate the entropy value h_m of index m (Equation 4); third, calculate the difference coefficient α_m of index m (Equation 5); fourth, determine the weight of the indicator w_m (Equation 6).

$$S_{nm} = \chi'_{nm} / \sum_{n=1}^{p} \chi_{nm} \quad (3)$$

$$h_m = \frac{1}{In\, p} / \sum_{n=1}^{p} \chi_{nm} \quad (4)$$

$$\alpha_m = 1 - h_m \quad (5)$$

$$w_m = \alpha_m / \sum_{m=1}^{q} \alpha_m \quad (6)$$

3.4 Sub-system development index calculate on

This research uses the weighting method to calculate the development level index P_n of a certain subsystem in a certain place in the *i* year.

$$P_n = \sum_{m=1}^{q} w_m \chi'_{nm} \quad (7)$$

3.5 Development of the CCD model

The coupling degree can only reflect the degree of interaction between the birth tourism economic system and the ecological environment system, but cannot really measure the synergistic effect of their overall development. Therefore, this study builds a coupling coordination model between the two based on the coupling degree model. This can judge the coordinated development of tourism economy and ecological environment more scientifically. The calculation formula is:

$$D(P_{TE}, P_{EE}) = \sqrt{C \times T} \quad (8)$$

$$C = \sqrt{\frac{P_{TE} \times P_{EE}}{(P_{TE} + P_{EE})^2}} \quad (9)$$

$$T = \alpha P_{TE} + \beta P_{EE} \quad (10)$$

Where; D denotes degree of coupling coordination; C is the coupling degree of the two systems; T is the comprehensive coordination index of the two systems; P_{TE} and P_{EE} are the comprehensive evaluation indexes of the tourism economic system and the ecological environment system respectively; α and β are undetermined coefficients. Since the tourism economic system and the ecological environment system are of equal importance, the values of α and β are both 0.5 in the actual calculations of this research.

3.6 Grade division of the coordinated development

On the one hand, the calculation of the coupling coordination D for the two systems in 2010-2019 is mainly in the smaller range of 0.3-0.6. On the other hand, in order to more clearly distinguish the coupling and coordination relationship between tourism economy and ecological environment. Therefore, this research uses the tenth method of coupling coordination degree to classify the coordinated development level. The specific classification criteria are shown in Table 2.

Table 2. The classification of the coupling coordination degree

Category	Coupling coordination degree	Subclass
Disorder (zone of unacceptable)	0.00-0.09	Extreme disorder
	0.10-0.19	Serious disorder
	0.20-0.29	Moderate disorder
	0.30-0.39	Light disorder
Transition (zone of reluctantly accept)	0.40-0.49	Near disorder
	0.50-0.59	Reluctance coordination

Table 2. The classification of the coupling coordination degree (cont.)

Category	Coupling coordination degree	Subclass
Coordination (zone of tolerance)	0.60-0.69	Primary coordination
	0.70-0.79	Middle coordination
	0.80-0.89	Well coordination
	0.90-1.00	High coordination

4. Results and Discussion

4.1 The characteristics of comprehensive development of tourism economy and ecological environment

According to the coupling degree model and the coupling coordination degree model, this research obtained the comprehensive development index P_{TE} and P_{EE}, the coupling degree C, the integrated evaluation index T of tourism economic system and ecological environment system, and the coupling coordination degree D for Nagasaki County from 2010 to 2019. According to the classification basis in Table 2, the specific results of this study are shown in Table 3 and Figure 2. It can be seen from Table 3 and Figure 2:

Table 3. Coupling degree and coordination degree between tourism economy and ecological environment in Nagasaki Prefecture

	P_{TE}	P_{EE}	C	T	D
2010	0.084	0.245	0.436	0.164	0.268
2013	0.191	0.298	0.488	0.245	0.345
2016	0.301	0.083	0.412	0.192	0.282
2019	0.424	0.133	0.426	0.279	0.345

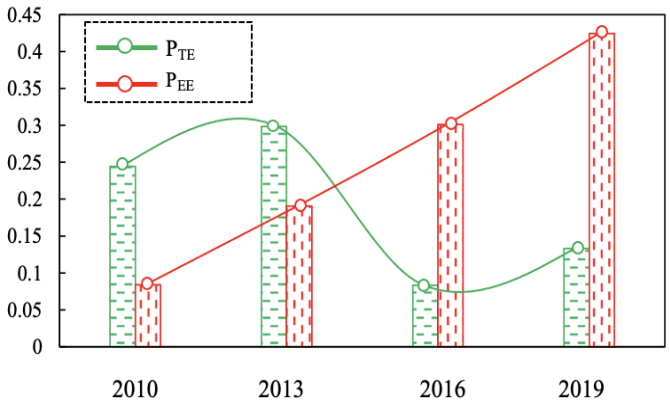

Figure 2. Comprehensive development index of tourism economy and eco-environment

(1) From the perspective of the comprehensive development index of the ecological environment, the ecological environment development index of Nagasaki Prefecture from 2010 to 2019 showed a fluctuating decline (0.245 to 0.133). Among them, 2013-2016 showed a sharp downward trend, with the remaining years showed a slight increase. This indicates that although the ecological status of Nagasaki Prefecture is good and the ecological pressure is decreasing year by year, the response to the ecological environment is insufficient. Obviously, the waste treatment rate, sewage treatment rate and waste recycling rate in Nagasaki Prefecture have all been greatly reduced, all of which have contributed to a negative increase in the overall ecological environment.

(2) From the perspective of the comprehensive tourism economic development index, the tourism economic development index of Nagasaki Prefecture from 2010 to 2019 has shown an increasing trend (from 0.084 to 0.424), and its rate of development has increased year by year. This is mainly due to the following three points:

- In 2013, Nagasaki Prefecture was certified as one of the world's three new night scenes, and night tourism is growing rapidly.

- In 2015, Nagasaki Prefecture was registered as a World Heritage Site for its "Industrial Revolution Heritage of Meiji Japan Steelmaking/Steelmaking, Shipbuilding and Coal Industry", and tourism in Nagasaki Prefecture is gaining attention.
- In 2018, Nagasaki Prefecture was affected by the world cultural heritage "Christian Hidden Heritage", and the number of cruise ship tourists and visitors to surrounding facilities increased significantly.

(3) From an overall perspective, Nagasaki Prefecture's P_{TE} was less than its P_{EE} from 2010 to 2013, meaning that Nagasaki Prefecture's the comprehensive development index of tourism economy is lower than the comprehensive development index of ecological environment at this stage, which belongs to the lagging development stage of tourism industry. This shows that, on the one hand, tourism activities are still within the controllable range of the ecological environment. On the other hand, there is also a relatively large room for progress in the development of tourism. The P_{TE} of Nagasaki Prefecture in 2016-2019 is greater than the P_{EE}. The tourism economic development index exceeds the ecological environment development index. This shows that the level of tourism economic development has been rapidly improved on the original basis, but the level of ecological environment has shown a significant downward trend. This also reflects that the development of tourism in Nagasaki Prefecture has brought a certain pressure or has begun to coerce the ecological environment.

4.2 The characteristics of the coordinated evolution of tourism economy and ecological environment coupling

According to the data obtained in Table 3 and formula 8-10, the coupling degree and coordinated development degree of the tourism economy and ecological environment system of Nagasaki Prefecture from 2010 to 2019 can be calculated. From the results in Figure 3 and the metric based on the coupling degree (Table 4), it can be seen that the coupling degree index of the tourism economy and eco-environment system of Nagasaki Prefecture has been developing steadily since 2010, a, with the coordination degree index showing an overall fluctuating upward trend. The degree of coupling between tourism economy and ecological environment in Nagasaki Prefecture was mainly in the antagonistic stage, i.e., C was between [0.3, 0.5].

Table 4. Coupling measurement standard (Li Shujuan, & Wang Tong., 2017)

C	Stage
[0,0.3]	Low-level coupling
[0.3,0.5]	Antagonistic stage
[0.5,0.8]	Run-in stage
[0.8,1]	High level of coupling

The above showed that the coordination effect of various factors between the tourism economy and ecological environment system of Nagasaki Prefecture was not obvious enough. The coupling between the tourism economy and the ecological environment was at a low level of coupling, and the negative effects of the growing tourism industry on the ecological system were becoming apparent. This was mainly due to the immature development of the tourism industry in Nagasaki Prefecture, and the structure of the tourism industry still needs to be optimized. This means that if tourism in Nagasaki Prefecture continues to develop at such a rapid pace, it is bound to have a negative impact on the ecological environment. For the entire study period, the coupling between tourism and the ecological environment in Nagasaki Prefecture was at an increasing stage (0.164 to 0.279), which indicated that the mutual influence and interaction between the two was gradually increasing. This showed not only that ecological conservation in Nagasaki Prefecture drives the development of tourism, but also that the development of tourism promoted ecological conservation.

4.3 Coupling and coordinated development

According to Figure 3 and the coordination degree measurement standard (Table 2), it can be seen that from 2010 to 2019, the coupling coordination degree of the tourism industry and the ecological environment in

Nagasaki Prefecture showed a fluctuating upward trend (0.268 to 0.345), from a moderate disorder to a light disorder. Among them, the coupling coordination degree was the worst in 2010, only 0.268, which was a moderate disorder. This was due to the lowest comprehensive development index of the tourism economic system of Nagasaki Prefecture in 2010, and the development of tourism is in its infancy. In addition, P_{EE} was much larger than P_{TE}, and the comprehensive development level of the tourism economic system and the ecological environment system itself was relatively low, resulting in poor coupling coordination. There was a slight downward trend in the coupling degree from 2013 to 2016, which was mainly due to the impact of the significant decrease in P_{EE}. From 2016 to 2019, the coupling coordination degree of the tourism economy and the ecological environment system of Nagasaki Prefecture has been continuously improved, and finally rose to the highest coordination degree during the research period in 2019, which was in the development stage of mild imbalance.

The above showed that although Nagasaki Prefecture has adopted a series of measures to make it develop in a good manner, the coordination between the tourism economic system and the ecological environment system of Nagasaki Prefecture was not high. With the emergence of other new tourism methods such as ecotourism, health tourism, and green tourism, the comprehensive development level of the tourism economy and ecological environment of Nagasaki Prefecture has been continuously improved. This has further promoted the improvement of the coupling and coordination between the tourism economic system and the ecological environment system in Nagasaki Prefecture.

5. Suggestions

(1) The level of tourism development in Nagasaki Prefecture has been growing year on year, and its tourism infrastructure development, tourism capital investment and tourism policies are relatively stable. Therefore, in the future, Nagasaki Prefecture's tourism industry should focus on optimising the structure of the tourism industry. Nagasaki Prefecture should not only pay attention to land use planning, environmental protection planning, urban and rural development planning, forest land protection planning, and cultural relics protection planning, but also strengthen the protection and management of tourism resources.

(2) The overall development level of the ecological environment system in Nagasaki Prefecture is in a declining stage. Therefore, Nagasaki Prefecture should pay more attention to the protection of the ecological environment while paying attention to the development of tourism economy. First of all, Nagasaki Prefecture should increase citizens' awareness of environmental protection and allow more citizens to receive environmental protection education. Secondly, Nagasaki Prefecture should reasonably control the discharge of waste gas, waste, and wastewater from enterprises, and promote the use of clean energy. Thirdly, Nagasaki Prefecture should strengthen the supervision and enforcement of environmental protection, and improve relevant laws on environmental protection.

(3) Nagasaki Prefecture maintains a good coordination between the development of tourism and the ecological environment, which is the key to the sustainable development of the tourism economic system and the ecological environment system. Therefore, Nagasaki Prefecture should vigorously develop eco-tourism. On the one hand, Nagasaki County should increase its support for the eco-tourism industry and provide it with some preferential policies and tax reduction and exemption policies. On the other hand, Nagasaki Prefecture should strictly implement environmental protection measures to achieve the coordinated and sustainable development of tourism and the ecological environment.

6. Conclusions

Based on the pressure-state-correspondence framework and taking into account the characteristics of the ecological environment of Nagasaki Prefecture, this research constructs a PSR model of the direct coupling and coordination extremes between the tourism economy and the ecological environment. In this

research, the coupling degree model and the coupling coordination degree model were introduced to measure the comprehensive development index of the tourism economic system and the ecological environment system in Nagasaki Prefecture. Then, this research analyses the state of coupled and coordinated development of the tourism economy and the ecosystem in Nagasaki Prefecture and the evolution of the trend. The results show that:

(1) Nagasaki Prefecture's tourism economic development index showed an increasing trend from 2010 to 2019, but the Nagasaki Prefecture's ecological environment development index showed a fluctuating decline;

(2) From 2010 to 2019, the coupling degree between the tourism economic system and the ecological environment system of Nagasaki Prefecture is mainly in the antagonistic stage, and the coupling degree between the two needs to be improved;

(3) From 2010 to 2019, the coupling coordination degree of the tourism economy and ecological environment system of Nagasaki Prefecture has changed from a moderate disorder to a light disorder.

(4) This research covers the period from 2010 to 2019, and the statistical data are all from official Japanese websites. As some indicator data cannot be obtained continuously, this research only selects data for 2010, 2013, 2016, and 2019. This leads to certain limitations in the research results. If the research timeline can be extended, and the spatial dimension analysis based on the data of each city in Nagasaki Prefecture, the research will more clearly reflect the evolution process of the coupling and coordination of the tourism industry and the ecological environment system in Nagasaki Prefecture.

Acknowledgement

This research was funded by Nagasaki University “Doctoral Program for World-leading Innovative and Smart Education” for Global Health, KENKYU SHIDO KEIHI (“the Research Grant”)

References

Lutz, H. J. (1945). Soil conditions of picnic grounds in public forest parks. *Journal of Forestry*, *43*(2), 121-127.

Akoglu, T. (1971). Tourism and the problem of environment: Relations between environment, nature and tourism. *The Tourist Review*.

Budowski, G. (1976). Tourism and environmental conservation: conflict, coexistence, or symbiosis? *Environmental conservation*, *3*(1), 27-31.

Ovington, J. D., Groves, K. W., Stevens, P. R., & Tanton, M. T. (1974). Changing scenic values and tourist carrying capacity of national parks. An Australian example. *Landscape Planning*, *1*, 35-50.

Sutcliffe, C. M., & Sinclair, M. T. (1980). The measurement of seasonality within the tourist industry: an application to tourist arrivals in Spain. *Applied Economics*, *12*(4), 429-441.

Nie, N., Wang, H., & Xiong, J. X. (2011). Research on tourism ecological security of Lake in Dongting Lake. In *Applied Mechanics and Materials* (Vol. 71, pp. 2657-2660). Trans Tech Publications Ltd.

Wang, Y., Wu, C., Wang, F., Sun, Q., Wang, X., & Guo, S. (2021). Comprehensive evaluation and prediction of tourism ecological security in droughty area national parks—a case study of Qilian Mountain of Zhangye section, China. *Environmental Science and Pollution Research*, *28*(13), 16816-16829.

Bo, Q. I. N. (2007). Tourism Resource Development and Eco-logical Environment Protection of Guangxi Dayao Mountain Nature Reserve [J]. *Environmental Science Survey*, *3*.

Wang, S., He, Y., & Song, X. (2010). Impacts of climate warming on alpine glacier tourism and adaptive measures: A case study of Baishui Glacier No. 1 in Yulong Snow Mountain, Southwestern China. *Journal of Earth Science*, *21*(2), 166-178.

Shi-Jin, W., & Lan-Yue, Z. (2019). Integrated impacts of climate change on glacier tourism. *Advances in Climate Change Research*, *10*(2), 71-79.

Tang, Z. (2015). An integrated approach to evaluating the coupling coordination between tourism and the environment. *Tourism Management*, *46*, 11-19.

GENG, S., & XIE, Y. (2013). Research on Coupling Relation between Tourism Economy and Ecological Environment of China's Sub-provincial Cities. *Urban Development*, 01.

Wang, Y. M., & MA, Y. F. (2011). Analysis of coupling coordination between urban tourism economy and transport system development—A case study of Xi′ an city [J]. *Journal of Shaanxi Normal University (Natural Science Edition)*, *1*.

Zeng, J., Rong, Q., Yue, W., Dai, X., & Su, M. (2020, March). Coupling relationship between transportation and tourism systems—a case study in the Huizhou City, China. In *IOP Conference* Series: Materials Science and Engineering (Vol. 787, No. 1, p. 012009). IOP Publishing.

Liu, J., Li, C., Tao, J., Ma, Y., & Wen, X. (2019). Spatiotemporal coupling factors and mode of tourism industry, urbanization and ecological environment: a case study of Shaanxi, China. Sustainability, 11(18), 4923.

Nan, C. A. O., Yaofeng, M., Tianshun, L., & Kai, B. A. I. (2013). Study on the Coordinative Development between Tourism Industry and Urbanization Based on Coupling Model: A Case Study of Xi'an. Tourism Tribune/Lvyou Xuekan, 28(1).

Geng, Y., Wei, Z., Zhang, H., & Maimaituerxun, M. (2020). Analysis and prediction of the coupling coordination relationship between tourism and air environment: Yangtze River economic zone in China as example. Discrete Dynamics in Nature and Society, 2020.

Geng, Y., Maimaituerxun, M., & Zhang, H. (2020). Coupling coordination of water governance and tourism: measurement and prediction. Discrete Dynamics in Nature and Society, 2020.

Geng, Y., Wang, R., Wei, Z., & Zhai, Q. (2021). Temporal-spatial measurement and prediction between air environment and inbound tourism: Case of China. Journal of Cleaner Production, 287, 125486.

Li, Y., Li, Y., Zhou, Y., Shi, Y., & Zhu, X. (2012). Investigation of a coupling model of coordination between urbanization and the environment. Journal of environmental management, 98, 127-133.

Chen, J., Li, Z., Dong, Y., Song, M., Shahbaz, M., & Xie, Q. (2020). Coupling coordination between carbon emissions and the eco-environment in China. Journal of Cleaner Production, 276, 123848.

Huang, J., Shen, J., & Miao, L. (2021). Carbon emissions trading and sustainable development in China: empirical analysis based on the coupling coordination degree model. International Journal of Environmental Research and Public Health, 18(1), 89.

Cheng, X., Long, R., Chen, H., & Li, Q. (2019). Coupling coordination degree and spatial dynamic evolution of a regional green competitiveness system–a case study from China. Ecological indicators, 104, 489-500.

Yang, Y., Bao, W., & Liu, Y. (2020). Coupling coordination analysis of rural production-living-ecological space in the Beijing-Tianjin-Hebei region. Ecological Indicators, 117, 106512.

Fan, Y., Fang, C., & Zhang, Q. (2019). Coupling coordinated development between social economy and ecological environment in Chinese provincial capital cities-assessment and policy implications. Journal of Cleaner Production, 229, 289-298.

Li Shujuan, & Wang Tong. (2017). An empirical study on the coordinated development of tourism-economy-eco-environment coupling in coastal cities. Journal of Ocean University of China: Social Sciences Edition, (6), 43-49.

Citizen-led Renewable Energy Implementation: A case study of Nagasaki Prefecture in Japan

Taro Nishizawa and Sunhee Suk*

Faculty of Environment Science, Nagasaki University, Japan

Abstract

In Japan, since the Great East Japan Earthquake (March 2011), renewable energy has been positioned as a major energy source in maintaining self-sufficient energy schemes and realizing a low-carbon society. As a follow-up measure, the FIT (Feed-in Tariff) was introduced in July 2012. Under this scheme, regionally distributed energy was promoted, resulting in expanding the installed capacity of renewable energy by four times compared to before the scheme. Following this trend, Nagasaki Prefecture formulated the Nagasaki Comprehensive Plan and took steps to enact or amend ordinance to promote the introduction of renewable energy sources. Focusing on the resident-led renewable energy implementation strategies of Nagasaki Prefecture, this study aims to review its policy and identify the characteristics of its solar power projects and compare such with cases in other municipalities. It also discusses the challenges and obstacles for further expansion of renewable energy and the means to increase the participation of residents. While its achievements in terms of regional revitalization were recognized, several challenges were also revealed, such as the limited installation locations for solar panels in Nagasaki, the curtailment of solar PV generation in the Kyushu area without compensation, the uncertainty of securing profits due to FIT revision, etc. This study provides a reference to strengthen citizen-participatory energy projects at the local level in the midst of relevant policies that affect the economic feasibility of such projects, which keep changing.

Keyword: Citizen-led business/ FIT (feed-in tariff)/ Iida City/ Nagasaki prefecture/ Solar power generation

---

*Corresponding Author: Sunhee Suk
E-mail address: suksunhee@nagasaki-u.ac.jp

1. Introduction

Since the Great East Japan Earthquake that occurred in March 2011, Japan has promoted the government's policy of securing sustainable energy and realizing a low-carbon society. In July 2012, the renewable energy FIT (Feed-in Tariff) system was introduced, and entry into the renewable energy field expanded (Agency for Natural Resources and Energy, 2021a). Nagasaki Prefecture formulated its Environmental Basic Plan" and has enacted or amended ordinances to promote the introduction of renewable energy (Nagasaki Prefecture. 2021a). In recent, the “Fourth Nagasaki Prefecture Environmental Basic Plan” was formulated with the aim of providing guidelines for various policies, including the promotion of introduction of renewable energy (Nagasaki Prefecture, 2021a). The purpose of this study was to provide an understanding of Nagasaki prefecture based on local comparison, using case studies. One of these is Iida City, Nagano Prefecture in Japan, which was chosen as a noteworthy example of a local renewable energy dissemination project, for comparison with projects in Nagasaki Prefecture. This research proposes mechanisms and systems that can be used to promote the introduction of renewable energy led by citizens in Nagasaki Prefecture. Furthermore, it proposes recommendations for future introduction in local areas that face similar issues. This paper is structured as follows. The research method is first described in section 2, the results of the survey are described in section 3, and section 4 provides recommendations to overcome issues related to renewable energy in Nagasaki Prefecture. Section 5 concludes the paper with a summary.

2. Methodology

This study was mainly conducted based on a literature review as well as interviews with relevant actors in Nagasaki prefecture. Literature searches were conducted using the Internet, newspaper articles, and previous studies. (1)

First, the current situation in Nagasaki Prefecture, especially as regards energy policy, and (2) the current situation and problems of renewable energy introduction projects led by citizens were investigated. (3) Next, of the renewable energy introduction projects that are currently unfolding throughout Japan, Iida City, Nagano Prefecture, was chosen as the subject for case study due to its citing in several studies conducted to date. (4) The characteristics of local industry, awareness of local residents, natural environment, and structure were next investigated.

3. Results

3.1 Brief overview of renewable energy policy of Japan and Nagasaki Prefecture

The Japanese government has been forced to reconsider its energy policy, in the light of the domestic and international situation. Other issues that affect various regions of the country include declining birth rates, reduced state of industrial activity, aging population, as well as competition from emerging economies. Regarding foreign factors, the Paris Agreement and the adoption of the 2030 Agenda for Sustainable Development in 2015 can be mentioned. In this relation, the Government of Japan has released the 5th Basic Environmental Plan (Ministry of Environment, 2018) and the 6th Basic Energy Plan (Ministry of Economy, Trade and Industry, 2021).In which, renewable energy is positioned as a major energy source in the mid- to long-term. Nagasaki Prefecture formulated the "Fourth Nagasaki Prefecture Environmental Basic Plan" following such trends of the Japanese government. This aims of preparing for disasters and the related damage, which have been on the rise in recent years, and has achieved the GHG reduction targets declared in the Paris Agreement, and has provided direction to Nagasaki residents, companies and organizations in the prefecture. In particular, it shows four basic goals (Creating a carbon-free society, creating a community where people and nature coexist, and creating a sound material-cycle society, and creating a safe, secure and comfortable environment) and the measures for them. The solar panel installation project dealt with in this research is classified under "Creating a carbon-free society" in the first goal.

3.2 Issues of introducing renewable energy in the region

The introduction of renewable energy in the region can be tackled by local residents and local actors with the aim of raising the level of acceptability through smooth dissemination (Toyoda, 2016). In addition, since most of the renewable energy can be acquired from the natural environment, it is possible to generate electricity by solar power generation provided appropriate sunlit land can be secured. Therefore, as well as protecting the global environment and involving sustainable economic activities and coexistence with nature, it has the potential to lead to regional revitalization (Kobayashi, 2019). In addition, Japan is surrounded on all sides by the sea, and most of the energy used to generate electricity domestically currently depends on imports from overseas (Agency for Natural Resources and Energy, 2021b). If the introduction of renewable energy in the region can be promoted, it has the potential to solve several problems in Japan simultaneously. However, various challenges act as barriers to introducing renewable energy in the region. First of all, since certain natural resources in the area are used, the understanding of local residents and local governments is essential, so care needs to be exercised when introducing it. Many problems resulting from reflected light have been reported in the prefecture due to the installation of solar panels. Second, relying on businesses outside the region for the introduction of renewable energy makes it difficult for the region to benefit economically [10]. In reality, many of the domestic renewable energy suppliers and investors are outsiders headquartered in the metropolitan area. Only a small number of cases (22%) are based on local businesses (Shirai, 2018). Since feed-in tariffs were introduced, the adoption of renewable energy in the region has been implemented in many locations across the country. although there are differences in the mechanism and scale. However, there are certain commonalities, such as: (1) enhancement of regional autonomy, (2) the need for good relationships between the project and local residents and investors, and (3) establishment of a system of local return and circulation of profits from energy business. Of these, the case of Iida

City, Nagano Prefecture has been reported in various studies. Iida City, Nagano Prefecture has a track record of self-government systems since the 1950s, and from 1994, the "Renewable Energy Ordinance" was enacted to promote higher awareness of the residents that the benefits of commercial use of the local environment by residents should be attributed to the residents. The city has received much praise for its integrated environmental conservation activities (Tokei station Nagano, 2021). This research compares the renewable energy introduction project in Nagasaki Prefecture with the project in Iida City, Nagano Prefecture, which is considered a noteworthy example, and proposes future related business opportunities for Nagasaki Prefecture.

3.3 Practice example: a case of Iida City, Nagano Prefecture, Japan

Iida City, Nagano Prefecture, Japan is located in the southern part of Nagano Prefecture (Figure1), with a total area of 658.66 km^2 and a population of approximately 95,000 (as of October 2021). Nagano is a well-known winter tourist destination due to its heavy snowfall, and attracts many skiers, .However, since Iida city is located on a southern slope, the amount of snowfall is less, making it suitable for solar power generation. Solar panels were first installed there in the 1990s, ahead of Japan's first basic environmental plan.

The regional characteristics of Iida City include the multi-layered nature of environmental efforts and the activity of local government activities, as represented by district community center activities (Tokei station Nagano, 2021). Iida City established the "Iida City Basic Environmental Ordinance" in 1996, aiming to harmonize all activities from daily life to business activities with nature, which led to the "Iida Environmental Plan", the basic environmental plan of Iida City. The plan has undergone five revisions to date (Minami Shinshu Ohisama Shinpo homepage). However, Iida City's renewable energy efforts are evaluated not only in the above-mentioned efforts centered on local governments, but also in various aspects such as the history of self-government activities and awareness of local industries and the environment of residents (Tokei station Nagano, 2021). This study focuses on a comparison of projects led by Ohisama Progress Energy Co., Ltd., established by an NPO corporation, a citizen group of Iida City, which became the model for projects in Nagasaki Prefecture.

The project in Iida City began with the establishment of Ohisama Progress Shinpo Co., Ltd., led by an NPO, Minami Shinshu Ohisama Shinpo. This project consists of a civic group organized by local residents who invested in Ohisama Progressive Energy, which itself invested in solar panel installation companies and roof providers, as well as sale of the generated power to electric power companies.

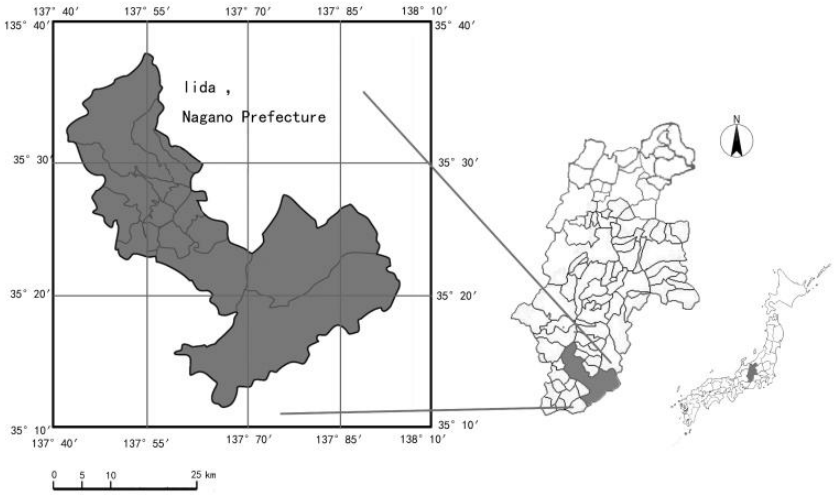

Figure 1. Location of Iida City

The characteristics of the project in Iida City, Nagano Prefecture are (1) a long history of self-government for energy policy, (2) business involvement of local companies, and (3) the residents' awareness and participating, (4) local governments supporting citizens' businesses. First of all, regarding self-government activities, Iida City has practiced this since the 1950s, and while there are other municipalities that advocate energy autonomy, Iida City has established and put into practice a mechanism for promoting renewable energy projects in which local autonomy organizations play a leading role. Local public halls and other public building earn income from selling electricity by installing solar panels, as well as use it as an emergency power source. Further, the profits obtained can be used in support of the district's activities to help local residents. Another factor is increased receptivity towards solar power. Shirai (2018) points out that the utilization of electricity sales revenue at the stage of installing solar panels or after installation has the effect of enlightening the interest and knowledge of local residents in introducing renewable energy (Shirai, 2018). Ohisama Progress Energy Co., Ltd. is the parent organization of NPO Minami Shinshu Ohisama Progress. This NPO not only promotes environmental conservation, but also manages organizations that share such objectives as well as community development and education, and contacts related organizations (Minami Shinshu Ohisama Shinpo homepage) (Figure 2). The NPO comprises not only people involved in Iida City but also participants from outside, which greatly increases awareness that the community can take the initiative. Furthermore, Iida City, the regional local government, introduced the 'Ordinance on Sustainable Community Development by Introducing Iida City Renewable Energy'. This ordinance supports projects to earn income from selling electricity using local resources, and provides support to struggling companies if their aim is to support local citizens. In so doing, the Ordinance became a mechanism to support businesses that invest in projects aimed at benefitting society or the environment (Iida City Web Site).

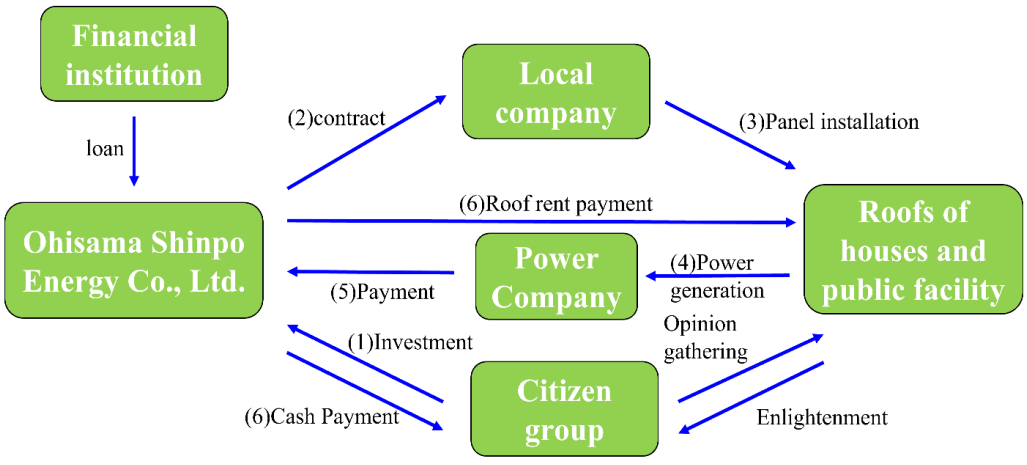

Figure 2. Iida City Project Structure (Image source from: depicted by author based on below web. https://ohisama-energy.co.jp/business/energy-creation/mega-sunpo/)

3.4 Nagasaki Prefecture

3.4.1 Basic information of Nagasaki Prefecture in Japan

Nagasaki Prefecture is located to the west of Japan and has a relatively warmer climate than other regions in Japan and provides sufficient daylight hours for solar power generation. It has a population of about 1.3 million and an area of 4,131km^2 (Nagasaki Prefecture. 2021b). The prefecture has prospered as a port city since ancient times and was used as a base for foreign trade before the modern era. It developed as a coal producing area until the 1970s, during which the country underwent an energy revolution. As a symbolic site, within the prefecture is an island, shaped like a warship, or Gunkan-jima, which supported Japan's economic growth. Nagasaki itself is closely linked with Japan's the shipping

industry and has numerous shipyards. Nagasaki Prefecture has tourist destinations such as the Peace Park and Dejima, an island that was used as a trading hub before modern times and was experiencing a rise in tourist numbers prior to the Corona crisis (Nagasaki newspaper, 2021). Currently, the local economy is in a state of exhaustion due to factors such as the change of domestic industry, the rise of emerging economies in the region since the latter half of the 1990s, and the declining birthrate and aging population that began in the first half of the 2000–2010 decade. The creation of new industries has therefore become an urgent issue.

3.4.2 Citizen-led renewable energy project in Nagasaki Prefecture

As mentioned in the previous section, the introduction of renewable energy in the region requires consensus building between actors in the local community, but it is unclear what form such consensus building should take in Nagasaki. Environmental Counseling Association Nagasaki, an NPO mainly ran by the prefecture started a business to install solar panels on the roofs of public halls and elementary schools in May 2013. However, it is currently difficult to earn an income from selling electricity due to the increased amount of power generated by renewable energy in the Kyushu Electric Power jurisdiction, and many plans to install solar panels have had to be cancelled.

3.4.3 Comparative analysis with the case of Iida city in the Nagano Prefecture

(1) Prior to commencement of projects

The project conducted in Iida City, Nagano Prefecture, has been pointed out as a good example of a citizen-led solar panel installation project in previous research. Preparations for the project were well underway before the project had actually started, owing to the extent of self-governance activities carried out by citizens based in public halls and efforts by local governments ahead of the national environmental basic plan. Thus there was a high level of public awareness, which meant the enabling conditions for environmental efforts were already present.

According to Shirai (2018), self-governing activities concerning the environment have taken place in Iida City since the 1950s, which were to assist in aspects of business promotion carried out at later. Such activities have included social education conducted in public halls based on the concept of 'problem-solving learning', puppet shows and seminars – all of which have promoted an environment for learning in support of the city's self-development.

On the other hand, in Nagasaki Prefecture, there are many questions about the history of public hall activities. This may be due to the prefecture's focus on development of industry in support of the growth of Japan's economy, such as shipbuilding and coal mines. The prefecture's basic environmental plan has already undergone four revisions, and while it might appear awareness of the environment was low, due to the nature of the work that the residents were engaged in but This fact may differentiate it from Iida City.

(2) Involvement of companies in related businesses

Projects in both cities were led by citizens; however, differences exist in the way companies became involved in the projects. The project in Iida City, Nagano Prefecture began with the establishment of Ohisama Shinpo Energy by the NPO, Minami Shinshu Ohisama Shinpo, which is composed of citizens aiming to popularize solar power generation together with members of a restaurant association in Iida City (Ohisama Shinpo Energy Website). Its parallel in terms of purpose in Nagasaki Prefecture, is Ohisama NET Nagasaki, which aimed at promoting renewable energy through an NPO, Environmental Counseling Association Nagasaki, through citizen-led dissemination.

However, the difference from the project in Nagasaki Prefecture is that the companies that cooperated with the project in Iida City were not limited to those related to the project, and that the project was rooted in the city and initiated by it through proposing cooperation (Shirai, 2018).

(3) Citizen's awareness of projects

There is no doubt that awareness of the environment has changed in Japan, due to factors such as the adoption of the Paris Agreement as well as the increasing prevalence of abnormal weather caused by global warming in recent years, the effects of which occur on a global

scale. However, it is possible that differences in environmental awareness exist between Iida City and Nagasaki Prefecture due to the histories and industries associated with each city. According to Shirai (2016), in Iida City, Nagano Prefecture, awareness of the environment has historically been high, and installation of solar panels has proceeded smoothly. Further, public sentiment towards installing solar panels has been maintained along with development of the business side of it, with the knowledge that it returns profits, which has deepened public awareness of the business and environmental conservation (Shirai, 2016).

Toyoda (2016) states that one of the conditions for a 'citizen-regional joint power plant' is to be able to contribute to the community, such as through returning a certain portion of profits to citizens and the community in some form. In the case of the project in Nagasaki Prefecture dealt with in this study, the project started in very similar way to that of Iida City, but the returned profits are much lower, and no events related to the project took place.

(4) Types of system

A difference also exists in the concepts behind the overall systems, in that the government directed the system related to Iida City with the aim of further promoting a project that was started based on a citizen-led initiative, while in Nagasaki Prefecture the project and the system existed independently and involved rice fields.

Yatsuki (2014) states that the formation of a small-scale decentralized energy system requires the establishment of a region-specific system. In the case of Iida City, Nagano Prefecture, a system was established to maintain promotion of the project as well as return profits to the region during its development, while in Nagasaki Prefecture the prefecture established a basic environmental plan prior to the project, in which various ordinances resulted based on the plan. However, the system did not support the project per se, thus the project and the ordinance existed independently of each other.

Furthermore, Shirai (2016) points out that the Renewable Energy Ordinance enacted by Iida City has led to the linkage of multi-layered environmental efforts and local citizenship activities, which cannot be said to have occurred in relation to the self-governance activities in Nagasaki Prefecture to such extent.

4. Discussion and Conclusion

Citizen-led renewable energy not only contributes to conservation of the global environment, but also greatly helps in the expansion of local industry based on a model in which profits are returned to residents and local governments. This survey targeted renewable energy introduction projects carried out in Nagasaki Prefecture and compared them to those in Iida City, Nagano Prefecture in terms of the flow leading up to the start of the projects, company involvement in the business, and citizens' awareness of the business. Several points of insufficiency were found with regard the system used in Nagasaki Prefecture. With Iida City, the results of self-government activities have accumulated since the 1950s, and the hurdles were low to inception of the project. Various events were held in the city related to the city's self-governance activities, and the level of citizen participation was very high. On the other hand, it is unclear how the public facilities in Nagasaki Prefecture were used by the residents. In Iida City, the public hall is regularly used not only for environmental conservation activities but also other events, making it a familiar gathering place for citizens. In addition, the Renewable Energy Ordinance enacted by the city has ensured activities it carried out through self-governance were consistent with environmental conservation activities, further raising awareness among residents. Therefore, it could be concluded that Nagasaki Prefecture needs to take measures such as establishing a system that allows residents to actively use public facilities such as public halls, carry out environmental conservation activities, and hold regular events. In addition, with regard to residents voluntarily setting up companies aiming to contribute to the community, the government should not only encourage participation of residents by providing coordination in self-governance activities, but also support the self-governance activities that provide benefits to the community. While the introduction of renewable energy in the region is based on citizen participation, further projects

can be expected to appear if local businesses and governments support residents in such endeavours. Efforts to introduce renewable energy into local regions are being carried out by various local governments in Japan, which if seen in a broader context can help solve the problems currently faced by Japan and at the same time help the country with regards to meeting its international obligations. However, as a precondition for introducing renewable energy in each region, it is necessary to understand the ways in which businesses are connected with local residents, build up a series of activities through self-governance, develop related local businesses through investment by residents, and support resident-led activities.

Acknowledgement

There is no special grant for this study. The authors would like to express their gratitude to those involved in the interview, especially the person in charge at the Nagasaki Environmental Counseling Association.

References

Agency for Natural Resources and Energy. 2021a. Now I understand! Renewable energy [Online]. Available: https://www.enecho.meti.go.jp/category/saving_and_new/saiene/ [Accessed on 12 November 2021]

Agency for Natural Resources and Energy. 2021b. Japan's Energy 2018 "10 Things to Know About Energy Now" [Online]. Available: https://www.enecho.meti.go.jp/about/pamphlet/energy2018/html/001/ [Accessed on 12 November 2021]

Fujii, K., Yamashita, H., 2015. Actual conditions and issues of renewable energy use in local regions – From the results of a national municipal questionnaire [Online]. Available: http://hermes-ir.lib.hit-u.ac.jp/rs/bitstream/10086/27059/1/keizai0080100270.pdf [Accessed on 12 November 2021]

Iida City Web Site. About "Iida City Ordinance on Sustainable Community Development by Introducing Renewable Energy" [Online].https://www.city.iida.lg.jp/site/ecomodel/project-79.html [Accessed on 12 November 2021]

Kobayashi, Y., 2019. Citizen's windmill with the area [Online]. Available: https://www.jstage.jst.go.jp/article/jwea/43/1/43_51/_article/-char/ja/ [Accessed on 12 November 2021]

Minami Shinshu Ohisama Shinpo. Group information [Online].http://www.ohisama-shinpo.or.jp/group [Accessed on 12 November 2021]

Ministry of Economy, Trade and Industry. Cabinet approval received for the 6th Basic Energy Plan [Online]. Available: https://www.meti.go.jp/press/2021/10/20211022005/20211022005.html [Accessed on 12 November 2021]

Ministry of Environment. About Cabinet decision of the fifth environmental basic plan [Online]. https://www.env.go.jp/press/files/jp/108981.pdf [Accessed on 12 November 2021]

Nagasaki newspaper. The largest number of tourists is 35.5 million. In 2018, Nagasaki Prefecture Statistics World Heritage registration boosts [Online]. https://www.nagasaki-np.co.jp/kijis/?kijiid=516623696 660186209 [Accessed on 12 November 2021]

Nagasaki Prefecture. 2021a. 4th Nagasaki Environmental Basic Plan [Online]. https://www.pref.nagasaki.jp/shared/uploads/2021/03/1616995022.pdf [Accessed on 12 November 2021]

Nagasaki Prefecture. 2021b. 67th Edition Nagasaki Prefecture Statistical Yearbook [Online]. https://www.pref.nagasaki.jp/bunrui/kenseijoho/toukeijoho/kankoubutsu/nenkan/488846.html#shihyo [Accessed on 12 November 2021]

Ohisama Shinpo Energy Co., Ltd. Birth Story [Online]. https://ohisama-energy.co.jp/about/origin/ [Accessed on 27 November 2021]

Shirai, N., (2018). Community Development with Renewable Energy: The Road to Transformation into an Independent and Symbiotic Society, 56-76

Tokei station Nagano. Monthly Population Change Survey (October 2021) Statistical Table [Online]. Available: https://tokei.pref.nagano.lg.jp/statistics/20260.html [Accessed on 12 November 2021]

Toyoda, Y., 2016. TRENDS AND DEVELOPMENTS OF Citizen's Co-owned Renewable Energy Power Plants, Sustainability Study, 6, 87-100, Hosei University Repository [Online]. Available: https://hosei.repo.nii.ac.jp/?action=repository_action_common_download&item_id=13017&item_no=1&attribute_id=22&file_no=1 [Accessed on 12 November 2021]

Yatsuki, S., 2014. The Building of Local Autonomy System toward the Spread of Natural Energy : A Case Study on Iida City in Nagano Prefecture, Japan, 81, 4, 351-367, Society of Political Economy, Kyushu University [Online]. Available: https://doi.org/10.15017/1515794 [Accessed on 27 November 2021]

An Innovative Toxic Heavy Metals Monitoring Product Development for a Sustainable Industry: A Case Study of Smartphone-Based Electrochemical Analytical Device

Wasapon Thanabodypath[a*], Kingkan Pungjunun[a,b], Sudkate Chaiyo[c], Achara Chandrachai[d], and Orawon Chailapakul[b]

[a]Technopreneurship and Innovation Management Program, Graduate School, Chulalongkorn University, Bangkok 10330, Thailand
[b]Electrochemistry and Optical Spectroscopy Center of Excellence (EOSCE), Department of Chemistry, Faculty of Science, Chulalongkorn University, Bangkok 10330, Thailand
[c]The Institute of Biotechnology and Genetic Engineering, Chulalongkorn University, Thailand
[d]Chulalongkorn Business School, Chulalongkorn University, Thailand

Abstract

The understanding of Smartphone-Based Electrochemical Analytical Device (SEAD) development for monitoring heavy metal contaminants in wastewaters from industrial manufacturers contributes to environmental sustainability. The herewith-presented applied research of six case studies in Thailand is aimed to preliminarily scrutinize the industrial user's willingness to adopt the novel SEAD technology for monitoring a sustainable environment. This research employs the practical application of scientific methods and the concurrent triangulation strategy of integrating Quality Function Deployment (QFD) with a qualitative approach based on in-depth interviews. SEAD prototype was developed to test with lead and extreme users to assess their adoption determinants as well as the product's performance. The proposed SEAD was successfully applied to the determination of As(III), Cd(II), Pb(II) and Hg(II) in standard samples. A real wastewater sample from a battery manufacturer exemplified an effective detection of four metals. The results demonstrated rapid, economical, reproducible, and reliable analytical capabilities of SEAD, which will be useful for sustainable industrial wastewater screening. Analysis of data from industrial user interviews revealed that industrial buyer innovation adoption (IBIA) determinants, which are seller, buyer organization, individual user, technological innovation and external environments impact SEAD adoption. This research contributes to the understanding of SEAD's transition from scientific knowledge into sustainable technology and diffusible innovation.

Keyword: Smartphone-based electrochemical device/ Toxic heavy metals quantification/ Industrial buyer innovation adoption/ Environmental waters/ Industrial sustainability

---

*Corresponding Author: Wasapon Thanabodypath
E-mail address: wasapon@gmail.com

1. Introduction

The World Health Organization (WHO) has called for an urgent need in managing ten chemicals of major public health concern, including four heavy metals, which are arsenic, cadmium, lead and mercury (WHO, 2010). With the global concerns on toxic heavy metals screening and management, electrochemical analytical paper-based devices (ePADs) have gained significant attention among researchers during the past decade for their capabilities in environmental monitoring (Atide et al., 2020). The smartphone-based electrochemical analytical devices (SEAD) are developed from the integration of ePADs and smartphone communicating technologies, simplifying sophisticated electrochemical experiments on handheld devices. The potentiometric methods using selective electrodes on ePADs can quantify toxic heavy metals instantly, accurately and portably with the aid of wireless technologies (e.g., Bluetooth, Near-Field Communication (NFC), Wi-Fi) on smartphones (Steinberg et al., 2015, Krorakai, 2021). However, SEADs are still struggling from transforming R&D research into comercializable and sustainable innovation.

By understanding the insights of stakeholders, we will be able to develop new

product strategies for assessing the risk of toxic chemicals in the environment. The challenges of new product development are not only user's satisfaction in innovative quality, but are also strict industrial standards and environmental legislations. SEAD innovation is targeted to support sustainable digital transitions of our economy and society for monitoring contaminated water, which is aligned with the European Commission's Chemicals Strategy for Sustainability Towards a Toxic-Free Environment (2020). The ultimate goal of SEAD is not about saving money or time, but it is about saving lives in global communities as well as supporting four UN Sustainable Development Goals (UN SDG), which are (1) clean water and sanitation, (2) industry, innovation and infrastructure, (3) life on land and (4) life below water.

1.1 SEADs and smartphone communicating technologies

The concept of SEAD is developed from ePADs with the integration of smartphone communicating technologies. The electrochemical analytical methods are suitable for environmental monitoring due to their selectivity, reproducibility, speed, and reliable analytical capability (Ataide et al., 2020, Shamkhalichenar et al., 2020). ePADs quantify heavy metal ions by redox reactions, which selectively measure the electron transfer in the microvolume of an electrochemical cell with voltammetric techniques between modified electrodes (i.e., reference electrode, working electrode and auxiliary electrode) (Aragay et al., 2011, Skoog et al., 2017). Previously developed ePADs' limits of detection were compliant with the international guidelines in Table 1. For instance, Kim and Kim (2017) demonstrated ePAD determining 0.1 µg L^{-1} of As(III). Chaiyo et al., (2016) developed ePAD to detect 0.1 µg L^{-1} of Cd(II) and Pb(II). Sánchez-Calvo et al., (2019) introduced ePAD measuring 0.0012 µg L^{-1} of Hg(II). Although these ePADs were miniaturized, they were still required to work with bulky workstations and potentiostats.

Table 1. Water quality guidelines for heavy metals (µg L^{-1} or ppb) (Lace & Cleary, 2021, Industrial Effluent Standards, 2017)

Heavy Metal	Drinking water				Wastewaters
	Oxidation States	WHO	European Union	US Environmental Protection Agency (US EPA)	Department of Industrial Works (DIW, Thailand)
Arsenic (As)	III, V	10	10	10	250
Cadmium (Cd)	II	3	5	5	30
Lead (Pb)	II	10	10	15	200
Mercury (Hg)	I, II	1	1	2	5

Smartphone wireless communication technologies can be integrated with SEADs as an application of portable electrochemical impedance spectroscopy (EIS). Electrochemical analysis requires modified electrodes, which are connected to an electronic instrument (i.e., potentiostat or galvanostat) to control the voltage difference between a working electrode and a reference electrode. The experiments of former EIS systems were difficult as they relied on wired computers. Nevertheless, wireless communication technologies available in smartphones can replace wired computers and connections with Wi-Fi, Bluetooth or NFC. To illustrate, Steinberg et al. (2015) has previously demonstrated the proof of concept of a credit card-sized wireless NFC potentiostat with an electrochemical sensor to measure blood glucose with smartphones. Each wireless technology has advantages and disadvantages as shown in Table 2. Distinctly, the most suitable technology for SEADs is NFC as it can draw power from a smartphone's battery, making the devices portable, wireless and powerless.

Table 2. Comparison of smartphone wireless technologies (Khorov et al., 2018, Woolley & Schmidt, 2017, NFC Technology, n.d.)

Wireless technology	Wi-Fi 802.11ax	Bluetooth 5.0	NFC
Signals	Ultra-High Frequency (UHF), Super High Frequency (SHF), Industrial, Scientific and Medical band (ISM)	UHF, ISM	Radio Frequency Identification (RFID)
Frequency range	1-6 GHz	2.402-2.480 GHz	13.56 MHz
Propagation distance	>100 meters	40-500 meters	<10 centimeter
speed	10 Mbit/s	2 Mbit/s	424 Mbit/s
Power source	Required active batteries	Required active batteries	Operated from passive electromagnetic induction

1.2 Quality Function Deployment (QFD)

QFD is a systematic technique that helps organizations to design, improve and develop new products based on the identification of customers' needs, which are linked and aligned with the organizational processes, functions and goals (Akao, 1997). The method has also been applied widely in various industries to develop sustainable technologies. For instance, Vinodh & Chintha (2011) provided evidence of the QFD approach for ensuring a sustainable manufacturing practice. QFD successfully improved volatile organic compounds abatement in aluminium foil surface coating (Gupta & Modi, 2018). The user's needs and perception in substituting petrochemical plastic for bioplastic adoption were scrutinized by QFD (bin Ahmad Shamsuddin et al., 2015). Moreover, other strategic quality management tools (e.g. TRIZ, AHP, Value Engineering, SERVQUAL) were also combined with QFD to create innovative products in various industries such as automobiles, healthcare, electronics, software, and utilities (Thawesaengskulthai, 2019).

QFD matrix or the House of Quality (HOQ) shows the relationship between the customer's requirements and the product's attributes, which will be useful to enhance new product development, especially the SEAD technology as the framework is a structured customer-focused approach.

1.3 Sustainable industrial dynamics

Features of sustainability rely on interconnected three pillars, which are environmental, economic and social (Barbier, 1987). Technological development has also been considered a sub-domain of sustainable development (Magee et al., 2013) as science, technology and innovation improve economic growth and social well-being (Schumpeter & Opie, 1934, OECD, 2000). However, developed technology capabilities and trajectories could potentially exceed users' needs, exploiting resources and time. The economic and institutional factors play a pivotal role in selecting radical and incremental innovators, who will survive in the competitive environment by taking risks in trial-and-error processes (Dosi, 1982). To minimize business failures, Rothwell (1994) proposed an innovation coupling model, which suggests sellers understand the market's needs, and also internally and externally communicate and assess their technological innovation. The coupling strategy between seller and buyer can be viewed as an integration of Technology Acceptance Models (TAM) and consumer behavior theories. The seller's and buyer's objectives should be aligned to develop and implement sustainable new products in the industry. From buyers' perspectives, TAMs analyze users' intention to use from attitudes that are influenced by external variables, perceived usefulness and perceived ease of use (Davis, 1989). Similarly, Kotler (1997) suggested that the buying process starts from communication with the target audience through various channels, which results in a purchasing decision. The process involves the environment, the organization, sellers, and individual participants who play different roles as users,

influencers, decision-makers, buyers and gatekeepers (Webster and Wind, 1972). As this study focuses on identifying user's determinants with the adoption of the novel SEAD technology for monitoring sustainable environment, we propose that there are five factors (seller, buyer organization, individual user, technological innovation and external environments) that impact SEAD adoption for the sustainable heavy metal-free environment as summarized in Table 3.

Table 3. Determinants influencing SEAD adoption for sustainable heavy metal-free environment (Adapted from Thanabodypath et al. (2021)

Determinants	Description
1. Seller	A new solution or technology offered by sellers is a key to improving sustainability by aligning their strategies to support users' targets and UN SDGs. The seller stimulus interactions help users to identify their needs effectively through communication channels and influencers, which will result in an adoption intention.
2. Buyer organization	Sustainable sourcing practices ensure supply chain operations. Buyers enhance their sustainability with suppliers by assessments and certifications. A network of trusting relationships will assist a decision on new technology adoption based on a mutual goal and a shared appreciation of innovation development.
3. Individual user	Organizations require internal people to assess new solutions. Perceived usefulness, perceived ease of use and internal people characteristics impact users' attitudes, intentions and behaviors. Individual-level and group-level actions impact an organization's dynamic capabilities from adopting environmentally sustainable innovation.
4. Technological innovation	Relative advantage, complexity, and compatibility lead to adoption in the innovation-decision process. Perceived superior technological advantages with less spent resources will make users more likely to adopt new technology. Additional attributes (e.g., standards, cost, and accuracy) of new technology are taken to benchmark against existing rivals. If a new technology is more advantageous and sustainable, users will be more likely to adopt it.
5. External environments	Environmentally beneficial technologies in the chemical-related industries are more likely to diffuse earlier than technologies that are contrary to directions of external environment trends. Sustainable challenges imposed by external environments impact users' adoption decisions, especially in aspects of regulations, economics, society, culture and technological infrastructure.

In brief, SEAD technology capabilities should be scrutinized holistically from users' and researchers' perspectives to address industrial adoption barriers for monitoring a sustainable environment. QFD and determinants influencing SEAD adoption will be assessed by instruments and methods in the next section.

2. Methodology

2.1 SEAD materials and methods

Although the electrochemical technologies and wireless potentiostats are available for research and development, a commercial product using such techniques for industrial heavy metals monitoring in the environment is still absent on the market. They were made and intended to be experimented in laboratories by skilled technicians only. Our newly developed SEAD concept for industrial users comprises of four components, which are (1) nanomaterials modified screen-printed graphene electrodes (SPGEs) or sensors, (2) supporting electrolyte, (3) customized NFC potentiostat, and (4) NFC enabled Andriod smartphone. The system is designed to detect arsenic(III), cadmium(II), lead(II) and mercury(II), which are chemicals of major public health concern specified by WHO (2010).

Standards for four metal assays were prepared from sodium arsenite, cadmium(II), lead(II) and mercury(II) standard solution for AAS (Sigma-Aldrich, Missouri, USA). Potential interferences were prepared from iron(III) chloride hexahydrate, nickel(II) sulfate hexahydrate, potassium dichromate, magnesium chloride, iron(II) sulfate, sodium chloride,

potassium chloride, calcium chloride, aluminium, chromium(VI), zinc(II) and copper(II) standard solution for AAS (Merck, Darmstadt, Germany). Silver/silver chloride ink was purchased from the Gwent group (Gwent Electronic Materials, UK). Carbon ink was purchased from Acheson (California, USA). Bismuth(III) for AAS was purchased from Sigma-Aldrich (Missouri, USA). Copper phthalocyanine was purchased from Sigma-Aldrich (Missouri, USA). All solutions were prepared with deionized water (18.2 MΩ.cm) from a Milli-Q system (Millipore, UK). A stock solution of arsenic(III), and mercury(II) were prepared by dissolving in 0.1 mol L^{-1} HCl, and stock solution of cadmium(II), lead(II) were dissolved in 0.2 mol L^{-1}.

The screen-printed electrodes were fabricated on a polyvinyl chloride sheet to make sensors for electrochemical detection using techniques from our previously published methods with a modification as summarized in Table 4. Additionally, the shelf life of sensors was tested by a laminated film and stored in a re-sealable zipper storage plastic with silica gel.

Table 4. Modification of screen-printed graphene electrodes (SPGEs) or sensors used in SEAD for sustainable heavy metal-free environment

Referenced methods	Proposed modified electrodes and supporting electrolytes in this work			
Analyte	Working electrode	Reference electrode	Counter electrode	Supporting electrolyte
As(III) (Pungjunun et al., 2018)	SPGE	Screen-printed Ag/AgCl	SPGE	HCl + Au(III)
Cd(II) and Pb(II) (Chaiyo et al., 2016)	Bi(III) in-situ/SPGE	Screen-printed Ag/AgCl	SPGE	HCl
Hg(II) (Chaiyo et al., 2014)	Copper phthalocyanine (CuPc)/SPGE	Screen-printed Ag/AgCl	SPGE	HCl

The differential pulse voltammetric electrochemical measurements were performed by using a customized credit-card sized NFC potentiostat with SIC4341 microchip (Silicon Craft Technology PLC, Bangkok, Thailand), which acquired energy from the electromagnetic induction emitted from Motorola One Smartphone (Motorola, IL, USA). iQuan Andriod mobile application was newly developed to control the NFC potentiostat for this SEAD system.

The quantification of SEAD hinges on three steps (Figure 1). The first step is sample preparation. A standard sample of each heavy metal is mixed with a supporting electrolyte at a specified ratio. The second step is sensor calibration by connecting a specified heavy metal sensor with NFC potentiostat, which is controlled by iQuan application. Then, an Andriod smartphone is tagged over the NFC potentiostat. Thirdly, the application will ask a user to drop the mixed solution on a sensor covering all electrodes. The mobile device will automatically quantify and display the test result.

2.2 Participants

Purposive sampling was used as the basis of interviewees selection. Lead and extreme users from 40 industrial corporations in Thailand that regularly monitored heavy metal contaminants in water were offered to test the SEAD prototype in person at their factories. Potential participants were approached by telephone calls to explain the study objectives and methods. After that the official letters were sent to them by email and post. Six industrial leaders volunteered to test provided SEAD system with standard samples and participate in the interview. The interviewees were managers and experts, who were familiar with the environmental heavy metal analysis. Their internal test methods included colorimetry, atomic absorption spectrometry (AAS), inductively coupled plasma mass spectrometry (ICP-MS) and portable photometers (Table 5).

To understand SEAD adoption drivers, data sources were triangulated through the convergence of interviewees' qualitative information as explained in section 3.3. QFD was also used to quantitatively synergize SEAD users' needs and the product's technical features.

Step 1. Sample preparation | Step 2. Sensor calibration | Step 3. Heavy metal quantification

Figure 1. The system of SEADs for environmental toxic heavy metal quantification with an NFC-enabled smartphone.

Table 5. Interviewees profile

Code	Job role	Industry	Internal Heavy metal test method	Test frequency
No.1	Factory manager	Semiconductor	Colorimetry	1 time/weekly
No.2	Factory manager	Waste treatment	ICP-MS	1 time/daily
No.3	Environmental manager	Industrial estate developer	Colorimetry	1 time/daily
No.4	Technical expert	Chemical manufacturer	ICP-MS	1 time/daily
No.5	Technical expert	Water treatment	AAS	1 time/daily
No.6	Technical expert	Batteries manufacturer	Colorimetry, portable Bluetooth photometer	3 times/daily

2.3 Technology acceptance determinants

The data were collected from face-to-face semi-structured interviews at participant's organizations. The duration of the interview was between 40 and 80 minutes. Interview questions were designed to assess five adoption determinants of SEAD technology for a sustainable heavy metal-free environment, which are sellers, buyer's organizations, individual users, technological innovations and external environments. Probing questions in each determinant were used to obtain detailed insights from real users. Since this is an exploratory research, the researchers aimed to examine how these five determinants and their sub-factors influence sustainable technology adoption. The content analysis was used to construct a novel industrial buyer innovation adoption model (IBIA) from the literature review and the collected emerging primary data.

2.4 QFD

QFD processes quantify and benchmark the user's requirements against the developer's targeted technical specifications as shown in Figure 2 and Table 6. The QFD tool can be early applied in the product life cycle and be reiterated in four phases from product planning (engineering characteristics), product designing (part characteristics), process planning (process parameters) and process controlling (production operations) (Moubachir & Bouami, 2015). The QFD assessment played a significant role in this study as the researcher aimed to bring the new SEAD for heavy metals quantification to the market for the first time. Innovations failed from technology-push approaches. Thus, the development of new technological products also heavily relies on customers' needs. The QFD process was completed in a single iteration of the product planning stage. The assessment

criteria in the QFD matrix were agreed and made by the SEAD developer team based on primary and secondary data. To explore industrial users' hesitation with the adoption of the novel SEAD technology for monitoring sustainable environment, interviewers were asked a series of questions to scrutinize their needs and ratings on SEAD attributes.

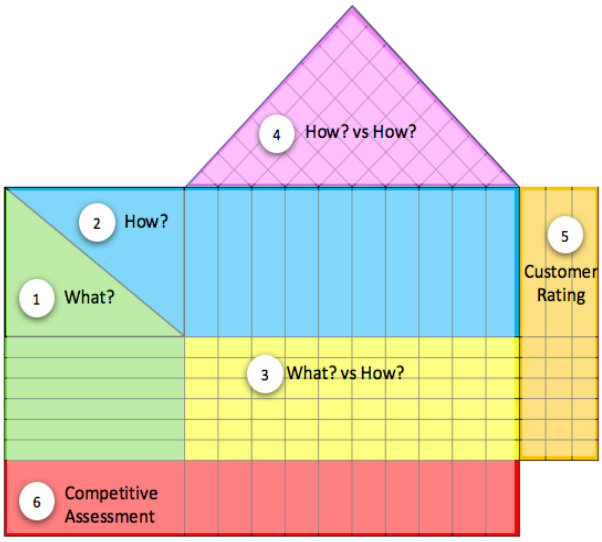

Figure 2. QFD Matrix or the House of Quality (HOQ)

Table 6. QFD Processes and Actions Adapted from Dehe & Bamford (2017)

QFD Processes	Actions
1. What?	Defining customer's requirements or the voice of customers (VOC) with a weight of importance
2. How?	Establishing product's technical features or the voice of business (VOB)
3. What? vs How?	Analyzing relationships between VOC and VOB
4. How? vs How?	Analyzing correlations and trade-offs between each technical feature
5. Customer Rating	Comparing the new product's quality with competitors' by customers
6. Competitive Assessment	Benchmarking the new product's quality with competitors' within an organization based on technical targets and objectives

3. Results and Discussion

3.1 SEAD performance

The analytical performance of SEAD under the optimized condition is summarized in Table 7. The differential pulse voltammetry (DPV) was chosen to develop with the NFC potentiostat as this electrochemical method was simple with a distinct peak current compared to the linear scan and square-wave methods (Nigović & Šimunić, 2003). The limits of detection (LOD) were 7.54 µg L^{-1}, 3.95 µg L^{-1}, 1.90 µg $L^{-}1$ and 32.80 µg L^{-1} for As(III), Cd(II), Pb(II) and Hg(II), respectively. Our SEAD's LODs (except mercury) were compatible with EU, US EPA and DIW standards in Table 1. Ten sensors and ten NFC potentiostats were prepared under the same conditions. The relative standard deviations were ≤10%, respectively, indicating high sensor-to-sensor reproducibility.

To verify the precision and accuracy, results obtained from our method were compared with the inductively coupled plasma atomic emission spectroscopy (ICP-OES) method by using a battery manufacturer's real wastewater samples. The experiments were performed and evaluated using samples spiked with three levels as shown in Table 8. No As(III), Cd(II), and Hg(II) were found in the real samples. The %RSD and %recoveries values were in the ranges of 0.1-6.5% and 83.40-109.4% for the proposed method, respectively. These results showed good agreement with the results obtained from the ICP-OES method. Paired samples t-tests were used to compare

means of results from both methods. The calculated p-values were below 0.05 threshold, confirming that there was no significant difference between the two methods.

Table 7. SEAD analytical performance

Analyte	Linear range (µg L^{-1}, ppb)	Regression	LOD (µg L^{-1}, ppb)	RSD (%)	Deposition potential (v)	Deposition time (s)
As(III)	20-1,000	y = 0.0374x + 1.5564 (R^2 = 0.9936)	7.54	6.2-8.8	-0.5	160
Cd(II)	50 – 1,500	y = 0.0566x - 1.4592 (R^2 = 0.9971)	3.95	3.8-10.4	-1.1	180
Pb(II)	50 – 1,500	y = 0.0436x - 1.1305 (R^2 = 0.9908)	1.90	2.2-3.8	-1.1	180
Hg(II)	100-3,000	y = 5.1604x + 0.5767 (R^2 = 0.9977)	32.80	3.0-5.2	-0.8	60

Table 8. The comparison of SEAD and ICP-OES results

As(III)							
Samples		Proposed method			ICP-OES		
	Spiked (µg L^{-1})	Found			Found		
		$\bar{X}$±SD (µg L^{-1})	%RSD	%recovery	$\bar{X}$±SD (µg L^{-1})	%RSD	%recovery
Pre-treatment	non-spike	ND	-	-	ND	-	-
	200.0	166.9±9.1	5.5	83.4	168.7±2.6	1.5	84.3
	400.0	374.4±24.3	6.5	93.6	389.4±1.7	0.4	97.4
Post-treatment	non-spike	ND	-	-	ND	-	-
	200.0	172.0±8.8	5.1	86.0	170.8±3.3	1.9	85.4
	400.0	379.0±20.1	5.3	94.8	383.8±3.2	0.8	95.9

Cd(II)							
Samples		Proposed method			ICP-OES		
	Spiked (µg L^{-1})	Found			Found		
		$\bar{X}$±SD (µg L^{-1})	%RSD	%recovery	$\bar{X}$±SD (µg L^{-1})	%RSD	%recovery
Pre-treatment	non-spike	ND	-	-	ND	-	-
	300.0	265.2±8.6	3.2	88.4	279.2±0.5	0.2	93.1
	500.0	430.9±21.6	5.0	86.2	485.1±0.6	0.1	97.0
Post-treatment	non-spike	ND	-	-	ND	-	-
	300.0	320.4±2.7	0.9	106.8	260.3±0.9	0.3	86.8
	500.0	474.8±0.4	0.1	95.0	442.9±0.9	0.1	88.6

Pb(II)							
Samples		Proposed method			ICP-OES		
	Spiked (µg L^{-1})	Found			Found		
		$\bar{X}$±SD (µg L^{-1})	%RSD	%recovery	$\bar{X}$±SD (µg L^{-1})	%RSD	%recovery
Pre-treatment	non-spike	3437.7±106.1	3.1	-	3,530.4±0.8	0.02	-
	300.0	3739.3±154.4	4.1	100.5	3,840.1±3.3	0.09	103.3
	500.0	3878.3±137.4	3.5	88.1	4,030.0±5.9	0.15	99.93
Post-treatment	non-spike	80.1±1.1	1.3	-	79.8±1.7	2.2	-
	300.0	387.6±10.4	2.7	109.4	343.2±2.9	0.9	87.8
	500.0	580.1±27.9	4.8	99.9	594.0±5.1	0.9	102.9

Table 8. The comparison of SEAD and ICP-OES results (cont.)

Hg(II)							
Samples		Proposed method			ICP-OES		
	Spiked ($\mu g\ L^{-1}$)	Found			Found		
		$\bar{X}$±SD ($\mu g\ L^{-1}$)	%RSD	%recovery	$\bar{X}$±SD ($\mu g\ L^{-1}$)	%RSD	%recovery
Pre-treatment	non-spike	ND	-	-	ND	-	-
	500.0	510.9±14.1	2.8	102.2	505.9±0.3	0.1	101.2
	1,000.0	891.5±43.2	4.9	89.2	1,026±0.0	0.0	102.6
Post-treatment	non-spike	ND	-	-	ND	-	-
	500.0	498.1±19.2	3.9	99.6	492.5±1.9	0.4	98.5
	1,000.0	934.5±9.4	1.0	93.4	952.7±1.4	0.1	95.3

ND: Not detected

The interference study was performed by adding metal ions that were also found in environmental waters and wastewaters into a standard solution. The tolerance ratio of interference for a signal change for 0.5 $\mu g\ mL^{-1}$ As(III), 1 $\mu g\ mL^{-1}$ Cd(II), 1 $\mu g\ mL^{-1}$ Pb(II) and 1 $mg\ mL^{-1}$ Hg(II) are listed in Table 9. The results illustrated SEAD offered outstanding selectivity in the detection of As(III), Cd(II), Pb(II) and Hg(II) with the percent deviation of all interfering environmental metals were less than ±5.0%. However, a presence of Cu(II) in samples competed against signals and peaks of As(III), Cd(II), Pb(II) and Hg(II). Therefore, Cu(II) should be eliminated to improve SEAD for environmental heavy metal detection capabilities. To improve the peak signal and reduce the interference of Cu(II), ferricyanide will be added in electrode fabrication in future development.

The screen-printed electrodes were stored in four different environments, including Ziplock bag, plastic wrap and silica gel as displayed in Figure 3. The shelf life of sensors in all environments still performed similar results with only ±5% deviation after 60 days from the manufactured date.

Table 9. SEAD environmental metals interference

		Interference and tolerance ratio							
		Ca(II)	Mg(II)	K(I)	Fe(II)	Zn(II)	Na(I)	Cd(II)	Ni(II)
Analyte	As(III)	1,000	1,000	1,000	1,000	1,000	1,000	500	500
	Cd(II)	250	500	500	2.5	25	500		25
	Pb(II)	1,000	1,000	1,000	500	50	1,000		500
	Hg(II)	1,000	1,000	1,000	100	10	1,000	500	10

		Interference and tolerance ratio						
		Al(III)	Fe(III)	Cr(VI)	Pb(II)	Hg(II)	As(III)	Cu(II)
Analyte	As(III)	500	100	10	10	10		1
	Cd(II)	25	25	2.5		1	1	0
	Pb(II)	50	500	2.5		10	1,000	0
	Hg(II)	500	10	10	100		0	0

3.2 QFD result

QFD was used to assess the industrial users' key elements in adopting SEAD for toxic heavy metal quantification. SEAD was intended to be tested with environmental and industrial wastewaters, but many water sources were highly contaminated with Cu(II), which interfered SEAD system. As a result, the SEAD prototype was tested with standard samples by six lead and extreme users in their actual work

environment. A six-step QFD process from Table 6 was used to analyze SEAD attributes.

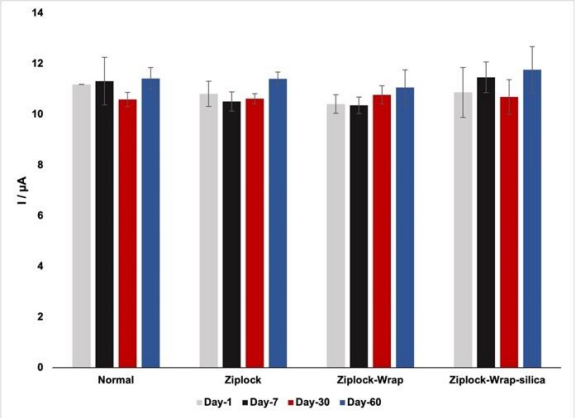

Figure 3. Sensors shelf life in different storage environments

Firstly, interviewees were asked to rate the importance of 10 user's demanded qualities in usage, cost and standard perspectives. A five-point rating scale was used for all measurement items (1=extremely unimportant, 2=unimportant, 3=neutral, 4=very important, 5=extremely important). The weight/importance scores in Figure 4 were averaged scores from 6 interviewees. 'Ease of use in organization and environment', 'fast and instant test results', 'reducing test expenses' and 'device accuracy' were the most demanded SEAD attributes. 'Low equipment maintenance', 'cleaning time and procedure after use', 'portability' and 'environmental-friendly equipment and methods' were very important while 'smartphone integration' attribute received the lowest score (3.8), yet still above neutral.

Secondly, decision-makers established a set of 10 product characteristics. These technical features allowed SEAD developers to define the measurable functional and operational requirements of the system.

Secondly, decision-makers established a set of 10 product characteristics. These technical features allowed SEAD developers to define the measurable functional and operational requirements of the system.

Thirdly, the relationships between the user's demanded qualities and the developer's technical requirements were agreed by decision-makers in 3 intensities (1 or ▲=weak relationship; 3 or O=moderate relationship; 9 or Ꝋ=strong relationship). Although ePAD and SEAD technologies were widely adopted in research laboratories, they are still new to the industry with no certified international standard. Hence, 'device standards and certifications' had weak relation to almost all quality characteristics. The decision-makers deemed that 'setup and report time', 'user hardware and software compatibility' and future 'R&D' would moderately increase user's attention as these attributes enhanced usability in internal and external environments. Users would be able to acquire accurate heavy metal monitoring results with low maintenance costs by utilizing environmentally responsible testing equipment and methods. Compatible limits of detections for As(III), Cd(II), Pb(II) and Hg(II) with international regulations encouraged users to shift to new technology. A smartphone integration with four-metal-analysis in one device also helped users to reduce testing expenses. Therefore, the detection limit qualities were agreed to have strong relationships with 'fast and instant test results' and 'device accuracy' attributes.

Fourthly, the decision-makers analyzed correlations and trade-offs between each technical feature. 'Cadmium LOD' and 'lead LOD' had a positive strong correlation since the developed sensor could simultaneously detect both metals. 'Accuracy' and 'reproducibility' were also strongly correlated as SEAD results should be able to be repeated and compared with conventional test methods. The 'user hardware and software compatibility' had a positive correlation with 'setup and report time' and 'accuracy'. SEAD system should be hassle-free for users in syncing NFC potentiostats with sensors and smartphones to monitor environmental contaminants timely and accurately. However, negative correlations between four metals and interfering Cu(II) should be minimized in future research and development.

Fifthly, QFD compared SEAD capabilities against market competitors, specifically colorimetric (e.g., test strips) and conventional methods (e.g., ICP-MS, AAS) by allocating a score ranging between 0 (worst) and 5 (best).

From the user's perspective, SEAD was exceptional in its ease of use, instant test report and portability with smartphone integration. However, its accuracy and certification method should be improved to meet targeted international and industrial standards in the final step.

Finally, SEAD attributes were benchmarked the new product's quality with competitors' within an organization based on technical targets and objectives as seen in the bottom section of Figure 4. The priority was to eliminate Cu(II) interference in the system and improve all four metals detection limits to meet the industrial effluent standards of the Department of Industrial Works in Thailand. Clearly, accuracy, reproducibility and future product upgrade and development were also crucial for SEAD improvement in order to be adopted and replace conventional technologies.

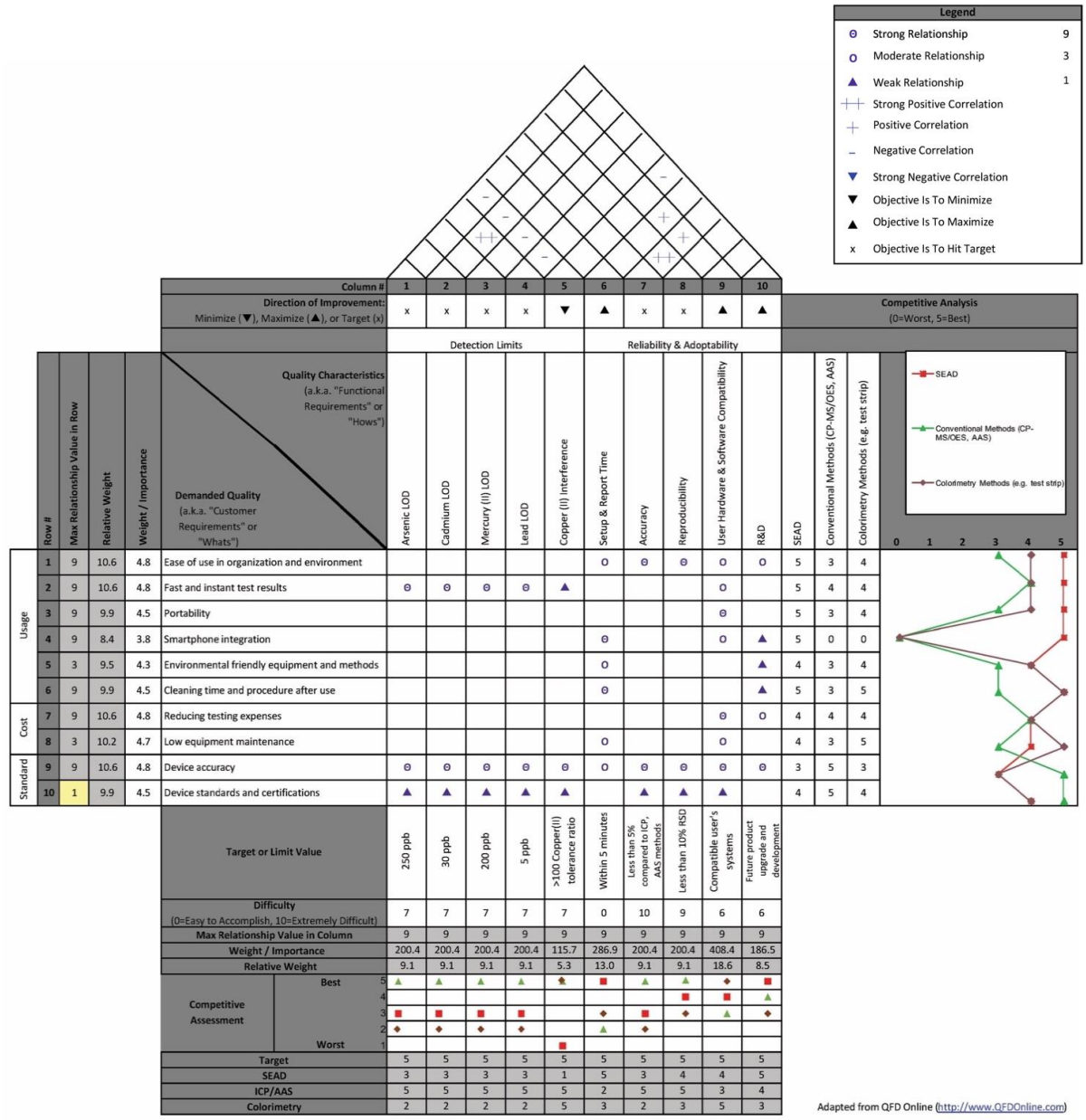

Figure 4. QFD of SEAD for Sustainable Heavy Metal-Free Environment

3.3 SEAD innovation adoption determinants

The interview data were analyzed based on content analysis from the transcripts. Keywords relating to SEAD innovation adoption determinants were identified, which are seller, buyer organization, individual user,

technological innovation and external environments. Six interviewees admitted that all industrial buyer innovation adoption (IBIA) factors played an essential role in the innovation-decision process for monitoring heavy metal-free environments.

Sellers' actions influenced users' needs, reflected their directions in supporting users' sustainable targets, and supported their adoption intention. For example, interviewee No. 1 asserted that "*information exchange is vital as this would help users to proactively solve existing and potential problems. The seller should enhance the product lifecycle and shelf life of heavy-metal monitoring techniques. They should be environmentally disposable and storable. Some products that we purchased expired within 7 months, and these are financial and environmental wastes that we had to throw them away.*" Correspondingly, interviewee No. 3 experienced the same shelf life problem, stating that "*the reliable colorimetric test strips were difficult to find in the market and it took months to import from overseas. Colorimetric devices that we stored in our lab did not react in any color changes when we were assessing environmental waters. We could not get an assured result and also had to throw them away while the seller did not show any responsibility. We need to have a shared goal. Innovative technologies should provide multiple benefits to users, communities and the environment.*"

In the aspect of buyers and their internal organization, sustainable sourcing practices ensure the supply chain operations as well as enhance supplier's performances through assessments, certifications and networking. Interviewee No. 6 exemplified that *"the commitment in responsible procurement in a joint platform or a collaboration with suppliers promotes a decision on new technology adoption based on a shared appreciation of innovation development. The Headquarters establishes a single organizational standard that applies to all of branches in every country in order to fulfill customer's requirements with minimized risks from intra- and inter-organizational feedbacks."* Furthermore, *"if the new product can be customized for our uses in quantifying zinc oxide, we will be more likely to consider purchasing it. We seek resources integrity. The values of a heavy metal detection device are not only from its practical usability, but also from a sustainable return on investment."* – Interviewee No. 4

Individual users impact the organization's resources and capabilities by adopting environmentally sustainable innovation. Interviewee No. 1 affirmed that *"internal people characteristics impact personal's intention and behaviors in using any technology. Although our current heavy metal monitoring by a colorimetric method is very easy, sometimes the responsible employee neglected using the purchased devices in their routine inspections. Conversely, they used their own experience in estimating light blueish green colors of copper contaminants in wastewaters with bare eyes. We need to encourage our staff to collaborate with us. So, the new heavy metal detection technology should make users feel at ease. What we are concerned about SEAD is how the frontline users would take care of a smartphone and the NFC potentiostat. If the system is waterproof and could be immersed in water, that might be a good option."* In contrast, Interviewee No.3 was against colorimetric methods. *"Inspectors were afraid to make a judgment from unclear color variants when comparing the result with the device's color chart. Results can be biased from people's eyes and lights. Users have to take risks when reporting from color ranges, and sometimes we are not quite positive about the device's accuracy."*

SEAD technological innovations help users to reduce leakages and exposure to contaminants of toxic heavy metals in wastewaters. Relative advantage, simplicity, and compatibility lead to adoption in the innovation-decision process. According to Interviewee No. 5, *"we would switch to an alternative product, if a new heavy metal quantification device had a better technological quality, a competitive price and a certified standard. SEAD is great for rapid screening results, but it would be costly to find compatible smartphones, if it only operates with Andriod systems and specific potentiostats. For the electrochemical sensors, if each sensor could be reused 10 times, this would make us save more costs. Another thing to point out is*

the device calibration and standard. Apart from accurateness, we perceive that innovations, which are in compliance with international standards would help us maintain and attain a better industrial ecosystem. New technology should be calibrated to meet American Water Works Association (AWWA) or US EPA standards." After testing the SEAD prototype, 5 of 6 interviewees showed their intention to purchase the device when it is completely developed. Its detection limit, reliability, reproducibility still need improvements to meet the targeted standard as advised by experts and guided by QFD assessment.

External environments place immense pressure to improve sustainability practices. All interviewees admitted that they strictly conform with their community and government regulations. Stakeholders have influences on interviewees' preferences in choosing heavy metal monitoring devices and techniques. Interviewee No. 2 claimed that *"the economic situation drives us to control costs. We consider technologies that are the most economical and in line with industrial standards."* In addition, innovations can be developed with society. Interviewee No.3 explained that *"we engage with a local engineering institute to provide opportunities for students to learn about wastewater management while the corporate also learned from them. We plan to become a smart industrial estate. For a more sustainable approach, we are using automated technology to help quantify and benchmark BOD and COD results from the database. This system also reports to the Department of Industrial Works. It would be advantageous, if SEAD could offer a real-time monitoring result. We are vigilant in monitoring wastewater qualities and we are ready for any surveillance audit."*

Findings from the proposed SEAD innovation adoption determinants concur with the literature. Firstly, the seller context had effects on new product adoption, and information exchange and feedback are keys to resolving conflicts (Rothwell 1994; Kotler, 1997). SEAD technology for toxic heavy metals contamination is new to consumers, therefore choosing communication channels to stimulate awareness should focus on understanding and having a mutual goal between sellers and buyers. Secondly, the buyer organization had effects on innovation adopting in terms of collaboration and networking. Unsuccessful technology integration jeopardized organization resources and reputations (Smith, 2013). Uncertain return on investment (Bierman et al., 2011), and technological threats (Yao et al., 2012) are barriers to RFID adoption in healthcare and wireless environmental monitoring systems. However, the successful resources sharing in R&D projects have proved sustainability in promoting RFID adoption in the healthcare industry (Katz & Shapiro, 1985). Thirdly, although, internal people characteristics may hinder technology adoption when users have negative attitudes (Venkatesh et al., 2003), if employees are familiar and become experienced with RFID technology, they will be more inclined to adopt it (Wang et al., 2010). Fourthly, superior, practical and valuable new technological attributes will lead to adoption. If a new technology is more advantageous and sustainable, users will be more likely to adopt it. The availability of compatible technologies impacts the potential adopter's interest in new technologies (Pham & Ho, 2015). Important technological attributes required from SEAD potential users are accuracy, standardization, sustainability, convenience, compatibility, minimized costs and simplicity. Lastly, the external environment plays a decisive role in adoption and sustainability. The findings concur with previous studies on NFC and RFID adoption (Museli & Navimipour, 2018; Wang et al., 2010). Technology adoption is a consequence of regulations, economic pressures, and societies that encourage sustainability in products and businesses. In short, it is vivid that seller, buyer organization, internal people, new technological innovation and external environment impact the diffusion of SEAD for heavy metal quantification. This study contributes to the understanding of sustainable industrial buyer innovation adoption (IBIA), which is influenced by related stakeholders. IBIA framework is an alternative hands-on navigator for understanding, creating and analyzing industrial innovations that reflect all fundamental foundations of sustainability, which

are society (people), the environment (planet), and the economy (profit) (Thanabodypath et al., 2021).

4. Conclusions

The objective of this applied research was to preliminarily explore industrial users' hesitation with the adoption of the novel SEAD technology for monitoring sustainable environment from leading industry experts in Thailand. SEAD prototype was developed to assess user's adoption determinants as well as the product's performance.

The results demonstrated the practical application of SEAD for the determination of As(III), Cd(II), Pb(II) and Hg(II) from standard and real samples, which were in satisfactory agreement for ICP-OES determination. SEAD was developed and expected to analyze industrial wastewaters. SEAD's limits of detection (LOD) were 7.54 µg L^{-1}, 3.95 µg L^{-1}, 1.90 µg L^{-1} and 32.80 µg L^{-1} for As(III), Cd(II), Pb(II) and Hg(II), respectively. Whilst prospective users showed their intention to adopt SEAD, the future development of SEAD innovation relies on its performance improvements, especially in terms of interference elimination, detection limit, reproducibility and reliability. Once the targeted specifications are achieved, SEAD could potentially be benchmarked with conventional heavy metal determination methods using real industrial wastewaters.

Analysis of data from industrial user interviews revealed that five industrial buyer adoption (IBIA) determinants, which are seller, buyer organization, individual user, technological innovation and external environments impact SEAD adoption. This research contributes to the understanding of SEAD transition from scientific knowledge into sustainable technology and diffusible innovation, which aligns with UN SDG in monitoring clean water and sanitation, promoting industrial innovation and infrastructure, and ensuring the safety of life on land and below water.

Acknowledgement

This research was supported by the 90th Anniversary of Chulalongkorn University Fund (Ratchadaphiseksomphot Endowment Fund), the Ministry of Higher Education, Science, Research and Innovation, the National Research Council of Thailand (NRCT Grant No. N41A640073) as well as Technopreneurship and Innovation Management Program, Graduate School, Chulalongkorn University, Thailand. The authors would like to thank Silicon Craft Technology PLC for developing the NFC potentiostat to use in this study.

References

Akao, Y. (1997, October). QFD: Past, present, and future. In *International Symposium on QFD*(Vol. 97, No. 2, pp. 1-12).

Aragay, G., Pons, J., & Merkoçi, A. (2011). Recent trends in macro-, micro-, and nanomaterial-based tools and strategies for heavy-metal detection. *Chemical reviews*, *111*(5), 3433-3458.

Ataide, V. N., Mendes, L. F., Gama, L. I., de Araujo, W. R., & Paixao, T. R. (2020). Electrochemical paper-based analytical devices: ten years of development. *Analytical Methods*, *12*(8), 1030-1054.

Barbier, E. B. (1987). The concept of sustainable economic development. *Environmental conservation*, *14*(2), 101-110.

Bierman, P., Lewis, M., Ostendorf, B., & Tanner, J. (2011). A review of methods for analysing spatial and temporal patterns in coastal water quality. *Ecological Indicators*, *11*(1), 103-114.

bin Ahmad Shamsuddin, D. M., Chew, B. C., & Shin, L. H. (2015). Quality function deployment for bio plastics adoption in Malaysian industry. *Journal of Technology Management and Business*, *2*(2).

Chaiyo, S., Chailapakul, O., & Siangproh, W. (2014). Highly sensitive determination of mercury using copper enhancer by diamond electrode coupled with sequential injection–anodic stripping voltammetry. *Analytica chimica acta*, *852*, 55-62.

Chaiyo, S., Apiluk, A., Siangproh, W., & Chailapakul, O. (2016). High sensitivity and specificity simultaneous determination of lead, cadmium and copper using µPAD with dual electrochemical and colorimetric detection. *Sensors and Actuators B: Chemical*, *233*, 540-549.

Davis, F. D. (1989). Perceived usefulness, perceived ease of use, and user acceptance of information technology. *MIS quarterly*, 319-340.

Dehe, B., & Bamford, D. (2017). Quality Function Deployment and operational design decisions–a healthcare infrastructure development case study. *Production Planning & Control*, *28*(14), 1177-1192.

Dosi, G. (1982). Technological paradigms and technological trajectories: a suggested interpretation of the determinants and directions of technical change. *Research policy*,*11*(3), 147-162.

European Commission. (2020). *Chemicals Strategy for Sustainability Towards a Toxic-Free Environment*.

European Commission. Retrieved 1 July 2021, from https://ec.europa.eu/environment/pdf/chemicals/2020/10/Strategy.pdf

Gupta, A. K., & Modi, B. A. (2018). Selection of sustainable technology for VOC abatement in an industry: an integrated AHP–QFD approach. *Journal of The Institution of Engineers (India): Series A*, *99*(3), 565-578.

Industrial Effluent Standards. Department of Industrial Works by the Minister of Industry in the Government Gazette. (2021). Retrieved 1 July 2021, from https://www.diw.go.th/hawk/news/11.PDF.

Katz, M. L., & Shapiro, C. (1985). *Network externalities, competition, and compatibility*. *The American economic review*, *75(3)*, 424-440

Kim, J., Han, S., & Kim, Y. (2017). Electrochemical detection of arsenic (III) using porous gold via square wave voltammetry. *Korean Journal of Chemical Engineering*, *34*(7), 2096-2098.

Kotler, P. (1997). *Marketing management, analysis, planning, implementation, and control, Philip Kotler*. London: Prentice-Hall International.

Khorov, E., Kiryanov, A., Lyakhov, A., & Bianchi, G. (2018). A tutorial on IEEE 802.11 ax high efficiency WLANs. *IEEE Communications Surveys & Tutorials*, *21*(1), 197-216.

Krorakai, K., Klangphukhiew, S., Kulchat, S., & Patramanon, R. (2021). Smartphone-Based NFC Potentiostat for Wireless Electrochemical Sensing. *Applied Sciences*, *11*(1), 392.

Lace, A., & Cleary, J. (2021). A Review of Microfluidic Detection Strategies for Heavy Metals in Water. *Chemosensors*, *9*(4), 60.

Langmuir, D., Chrostowski, P., Chaney, R. L., & Vigneault, B. (2004). *Issue paper on the environmental chemistry of metals*. US Environmental Protection Agency.

Magee, L., Scerri, A., James, P., Thom, J. A., Padgham, L., Hickmott, S., ... & Cahill, F. (2013). Reframing social sustainability reporting: Towards an engaged approach. *Environment, development and sustainability*, *15*(1), 225-243.

Moubachir, Y., & Bouami, D. (2015). A new approach for the transition between QFD phases. *Procedia Cirp*, *26*, 82-86.

Museli, A., & Jafari Navimipour, N. (2018). A model for examining the factors impacting the near field communication technology adoption in the organizations. *Kybernetes*, *47*(7), 1378-1400.

NFC Technology. (n.d.). NFC Forum. Retrieved September 1, 2020, from https://nfc-forum.org/what-is-nfc/about-the-technology/

Nigović, B., & Šimunić, B. (2003). Determination of 5-aminosalicylic acid in pharmaceutical formulation by differential pulse voltammetry. *Journal of pharmaceutical and biomedical analysis*, *31*(1), 169-174.

OECD. (2000). Science, technology and innovation in the new economy. *Policy Brief, OECD, September*.

Pham, T. T. T., & Ho, J. C. (2015). The effects of product-related, personal-related factors and attractiveness of alternatives on consumer adoption of NFC-based mobile payments. *Technology in society*, *43*, 159-172.

Pungjunun, K., Chaiyo, S., Jantrahong, I., Nantaphol, S., Siangproh, W., & Chailapakul, O. (2018). Anodic stripping voltammetric determination of total arsenic using a gold nanoparticle-modified boron-doped diamond electrode on a paper-based device. *Microchimica Acta*, *185(7)*, 324.

Rothwell, R. (1994). Towards the fifth-generation innovation process. *International marketing review*.

Sánchez-Calvo, A., Fernández-Abedul, M. T., Blanco-López, M. D. C., & Costa-García, A. (2019). based electrochemical transducer modified with nanomaterials for mercury determination in environmental waters. *Sensors and Actuators B: Chemical*, *290*, 87-92.

Schumpeter, J. A., & Opie, R. (1934). *The theory of economic development: An inquiry into profits, capital, credit, interest, and the business cycle*. Cambridge, Mass: Harvard University Press.

Shamkhalichenar, H., Bueche, C. J., & Choi, J. W. (2020). Printed Circuit Board (PCB) Technology for Electrochemical Sensors and Sensing Platforms. *Biosensors*, *10*(11), 159.

Skoog, D. A., Holler, F. J., & Crouch, S. R. (2017). *Principles of instrumental analysis*. Cengage Learning.

Smith, A. M. (2013). The value co-destruction process: a customer resource perspective. *European Journal of Marketing*.

Steinberg, M. D., Kassal, P., Kereković, I., & Steinberg, I. M. (2015). A wireless potentiostat for mobile chemical sensing and biosensing. *Talanta*, *143*, 178-183.

Thanabodypath, W., Chandrachai, A., Chaiyo, S., & Chailapakul, O. (2021). Industrial Buyer Innovation Adoption Model: A Focus on a Smartphone-Based Electrochemical Analytical Device for Toxic Heavy Metal Detection. *Sustainability*, *13*(21), 11718.

Thawesaengskulthai, N. (2019). *Quality engineering and management guide to continual improvement and innovation creation*. Chulalongkorn University Press.

Tornatzky, L. G., & Klein, K. J. (1982). Innovation characteristics and innovation adoption-implementation: A meta-analysis of findings. *IEEE Transactions on Engineering Management*, (1), 28-45.

Venkatesh, V., Morris, M. G., Davis, G. B., & Davis, F. D. (2003). User acceptance of information technology: Toward a unified view. *MIS Quarterly*, 425-478.

Vinodh, S., & Chintha, S. K. (2011). Application of fuzzy QFD for enabling sustainability. *International Journal of Sustainable Engineering*, *4*(4), 313-322.

Wang, Y. M., Wang, Y. S., & Yang, Y. F. (2010). Understanding the determinants of RFID adoption in the manufacturing industry. *Technological Forecasting and Social Change*, *77*(5), 803-815.

Webster, F. E., & Wind, Y. (1972). *Organizational buying behavior*. Prentice Hall.

Woolley, M., & Schmidt, S. (2017). Bluetooth 5 Go Faster. Go Further. *Bluetooth SIG*, *1*(1), 1-25.

World Health Organization (WHO). (2010) Action is Needed on Chemicals of Major Public Health Concern.

Retrieved 1 July 2021, from https://www.who.int/ipcs/features/10chemicals_en.pdf.

Yao, W., Chu, C. H., & Li, Z. (2012). The adoption and implementation of RFID technologies in healthcare: a literature review. *Journal of Medical Systems*, *36*(6), 3507-3525.Nuntajun, R. (2009). Seismic Stratigraphy of the Fang Basin, Chiang Mai, Thailand. Chiang Mai Journal of Science, 36, 77-82.

Petersen, H.I., Nytoft, H.P., Ratanasthien, B., and Foopatthanakamol, A. (2007). Oils from Cenozoic rift-basins in central and northern Thailand. Journal of Petroleum Geology, 40, 59-78.

Settakul, N. (2009). Fang Oilfield Development. Walailak Journal of Science and Technology, 6, 1-15.

Nanomechanical Property of Podoviruses for Biocontrol Agents of Bacterial Wilt Disease

Udom Sae-Ueng*

National Center for Genetic Engineering and Biotechnology (BIOTEC), National Science and Technology Development Agency (NSTDA), 113 Thailand Science Park, Phahonyothin Road, Khlong Nueng, Pathum Thani 12120, Thailand

ABSTRACT

Bacteriophages (phages) are viruses that are capable of eradicating bacteria. Despite already being commercialized, phage usage for preventing and controlling crop bacterial pathogen in agriculture is still low compared to other antagonistic biocontrol agents. One of the major contributing causes is its variable efficacy originated from poor understanding of how phages survive under environmental duress i.e. phage stability. An emerging platforms to investigate the phage stability is atomic force microscopy (AFM). In this study, we applied AFM-based imaging technique and nano-indentation to extract nanomechanical property namely stiffness of two podoviruses. Both phages isolated from soil samples in Thailand are capable of lysing *Ralstonia solanacearum* causing bacterial wilt disease in chili and tomato. The stiffness of the podoviruses was examined under variation of two external factors of pH and ionic strength. The specific range of the stiffness of the podoviruses were shown to be associated with the highly retained phage infectivity quantified by plaque-based assay during storage period. This work offers a complementary understanding of phage stability which can be correlated to how phages stabilize under fluctuating conditions. Improving multidisciplinary knowledge will pave for a way for effective utilization of phage in biocontrol for agriculture.

Keyword: Bacteriophage/ Podovirus/ Nanomechanical property/ Phage stiffness/ Atomic force microscope

---

*Corresponding Author: Udom Sae-Ueng, Tel.: +66-2-564-6700
E-mail address: udom.sae@biotec.or.th

Operationalizing One Health for the Survival of the Planet and Humanities

Boripat Siriaroonrat*

Faculty of Environment and Resource Studies, Mahidol University, Salaya, Putthamonthon, Nakhonpathom 73170

ABSTRACT

Southeast Asia is home to terrestrial and marine ecosystems, including species and genetic diversity of plants, animals and microbes. Biodiversity values clearly serve human well-being for utilitarian, esthetic, ecological and moral purposes. However, recent reports from international organization and committees are all pointing at the 2 major issues, Climate change and biodiversity loss. UNEP added the existing environmental pollutions and called it 'the triple planetary crisis. There are clear scientific evidences cited in recent reports that the global population will reach 9.5 billion in 2050, and human have been putting extreme pressure on the planet and caused severe consequences such as degradation of landscape and sea scape, extinction of species, disease emergence, and global warming. The Living Planet Report 2020 by WWF addressed how humanity's destruction of nature is having catastrophic impacts not only on wildlife populations, but also human health, economics and well-being. UNESCAP is calling out for safeguarding the ecosystems' health for the sustainable future development and environment. IPBES-IPCC report, UNESCAP Policy Brief, UNEP report are all recommending us that human must make peace with nature and forge a new relationship with the planet. If the planet survives, humanities survive, too. One Health approach has been suggested as a guiding principle to be operationalized at all level, for scientific community, policy-making community as well as general public and individual citizens.

Keyword: One Health/ Climate change/ Biodiversity/ Environment

---

*Corresponding Author: Boripat Siriaroonrat
E-mail address: boripat.sir@mahidol.ac.th

Sponsors of the ENRIC 2021 Conference

	Mahidol University
PTTEP	IRPC Public Company Limited
IRPC Public Company Limited	IRPC Public Company Limited
	Industrial Estate Authority of Thailand
Human Resources Tipco	Tipco Foods Public Company Limited
Esso	Esso (Thailand) Public Company Limited

The 4 Environment and Natural Resources International Conference

Mahidol University
Faculty of Environment and Resource Studies

PTTEP

Tipco Human Resources

IRPC
Shape What's Good for Tomorrow

Esso

Faculty of Environment and Resource Studies, Mahidol University